LDRD

ANNUAL REPORT

2014

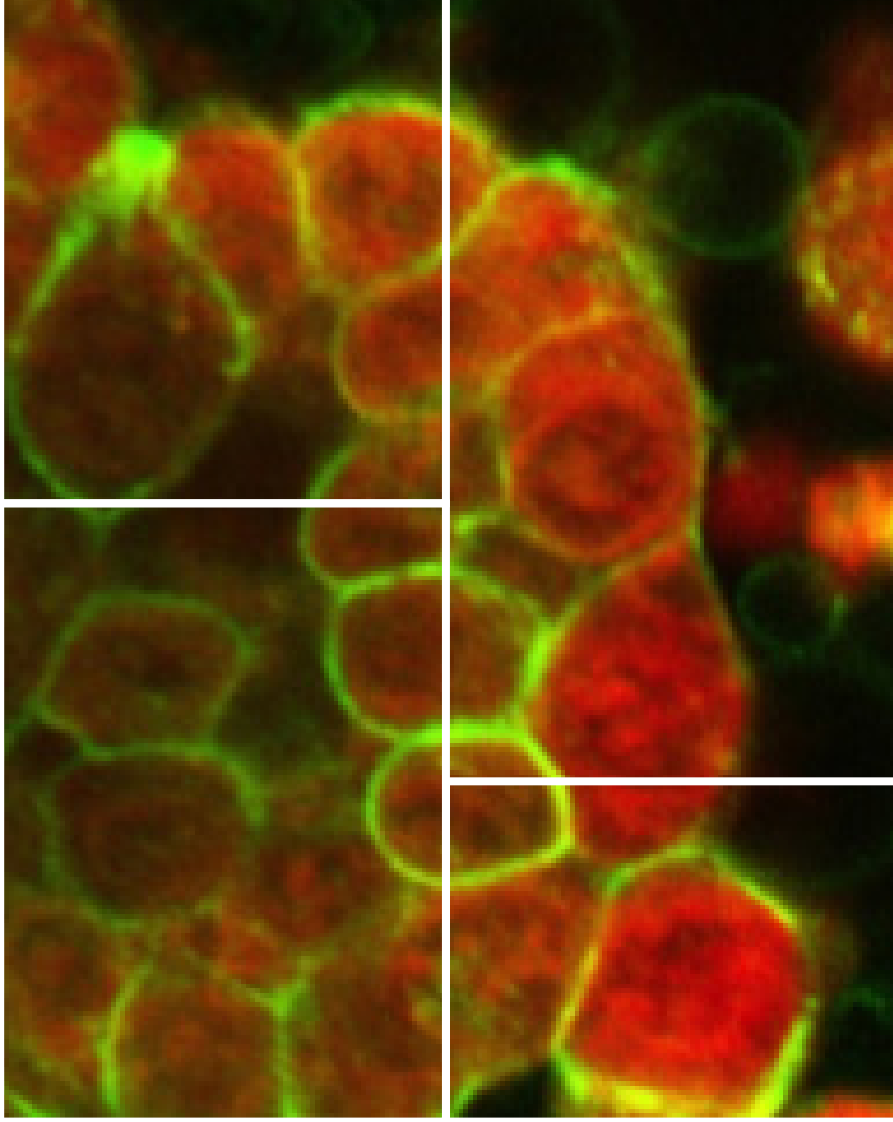

ANL-15/05

Laboratory Directed Research and Development Program Activities

Office of the Director
March 2015

Argonne NATIONAL LABORATORY

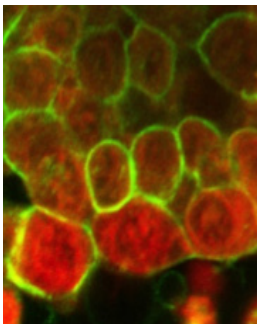

ON THE COVER

The image on the cover depicts HCT116 cells treated with TiDoL (TiO_2-DOPAC-luciferase) after TiDoL activation with luciferin. For more information, see project report "Curing Cancer with the Power of Fireflies" (2012-181-R2).

ABOUT ARGONNE NATIONAL LABORATORY

Argonne is a U.S. Department of Energy Laboratory managed by UChicago Argonne, LLC, under contract DE-AC02-06CH11357. The Laboratory's main facility is outside Chicago at 9700 South Cass Avenue, Argonne, Illinois 60439. For information about Argonne and its pioneering science and technology programs, see www.anl.gov.

DISCLAIMER

This report was prepared as an account of work sponsored by an agency of the United States Government. Neither the United States Government nor any agency thereof, nor UChicago Argonne, LLC, nor any of their employees or officers, makes any warranty, express or implied, or assumes any legal liability or responsibility for the accuracy, completeness, or usefulness of any information, apparatus, product, or process disclosed, or represents that its use would not infringe privately owned rights. Reference herein to any specific commercial product, process, or service by trade name, trademark, manufacturer, or otherwise, does not necessarily constitute or imply its endorsement, recommendation, or favoring by the United States Government or any agency thereof. The views and opinions of document authors expressed herein do not necessarily state or reflect those of the United States Government or any agency thereof, Argonne National Laboratory, or UChicago Argonne, LLC.

Every day, scientists and engineers at Argonne National Laboratory make important discoveries that translate into a real difference in the world, working towards the Lab's mission to develop energy solutions, preserve the environment, protect the nation, and help the economy thrive.

Argonne's Laboratory Directed Research and Development (LDRD) program is key to advancing our leadership in science and technology and enables us to explore new ideas, build new capabilities, and address emerging research opportunities.

LDRD is an invaluable resource for contributing to the future science and technology needs of DOE and the nation. It helps us investigate new directions for Department programs while being able to adapt to new opportunities in a changing environment. Equally crucially, it serves to maintain and enhance the capabilities of both our staff and our R&D facilities.

In fact, investment by Argonne's LDRD program has, over time, made crucial contributions to the realization of many achievements, including:

- Advancing in energy storage and battery technologies, combined with materials synthesis and characterization capabilities;
- Paving the path to exascale computing and addressing issues related to power consumption, performance, and reliability;
- Driving accelerator technologies to improve in both energy and brightness, enabling x-rays to penetrate deeper inside materials to reveal crucial information about structure and function;
- Leading the Center for Electrochemical Energy Science, an Energy Frontier Research Center, and participating in five others as a primary partner with other national laboratories and universities; and
- Earning many awards and recognition for our research and staff, from a wide variety of professional societies, government, and industry.

The Director's Grand Challenge LDRD project on "big data" continues to leverage Argonne's Mira supercomputer and our computational expertise. This research is part of a data science strategy designed to propel and expand the results of data gathered at Argonne's Advanced Photon Source, enabling inverse simulation and accelerating imaging processes; the initiative, which leverages our computational expertise and capabilities, will help us continue to map the future of computing.

I can attest that in managing Argonne's LDRD program, we have adhered without exception to the requirements of DOE Order 413.2b and associated guidelines. Our program management continually strives to be more efficient. In addition to meeting all reporting requirements during FY 2014, our LDRD Program Office continues to implement intranet-based process enhancements that better serve all LDRD stakeholders, from our researchers and managers to our DOE Site Office colleagues.

The individual project reports that follow demonstrate that Argonne staff have pursued projects at the forefront of their fields and contributed significantly to the advancement of Argonne's major initiatives. Evidence of the continuing strength of this program is found in follow-on sponsorship garnered in many cases as well as in the numbers of publications, invited presentations, inventions, and new staff hires that are direct results of LDRD.

It is with great pride in our researchers' accomplishments that I present Argonne National Laboratory's Annual Report on its Laboratory Directed Research and Development (LDRD) activities for fiscal year 2014.

Peter B. Littlewood
Laboratory Director

Table of Contents

Research Reports – by Components vi

Acknowledgments xi

Laboratory Overview xii

Program Assessment xiv
- Program Overview xiv
- LDRD Management Process xiv

FY 2014 LDRD Program Components xvi
- Strategic Initiatives xvi
- Director's Grand Challenge xviii
- Director's Competitive Grants (DCG) xix

FY 2014 LDRD Project Characteristics xix
- Categories of Work xix
- Mission Relevance xx
- Distribution of Funding xx
- Level of Funding xxi
- LDRD Investigators xxii

FY 2015 Update xxii

Peer Review Experience in FY 2014 xxiii

Performance Metrics xxiii

LDRD Five-Year Funding Summary ($ in thousands) for Projects Active in FY 2014 xxvi

Research Reports 1
Director's Competitive Grants 2
Advanced Computing 47
Applied Energy and Sustainable Transportation 69
Biological and Environmental Systems 80
Director's Grand Challenge 103
Hard X-ray Sciences 107
Materials for Energy 120
National Security 149
Nuclear Energy 157
Sustainable Energy Production and Use 164
Other Novel R&D 166

Appendix 170
Intellectual Property Events Occurring in FY 2014 171
Publications and Presentations I 177
Publications and Presentations II 209
Index by Project Number 220
Author Index 223
FY 2015 New Start Projects 230
Argonne Organizations – Abbreviations 233

Research Reports – by Components

Director's Competitive Grants

2012-012-R2 New High Energy Rechargeable Li Batteries Based on Selenium and Selenium-Sulfur Composite (Se_xS_y) Electrodes 3

2012-061-R2 Revealing Lithium-Based Battery Performance by *in situ* Characterization 4

2012-072-R2 Graphene-Enabled Superlubricity: Vanishing Friction and Wear in Static and Sliding Contacts 5

2012-087-R2 Rechargeable Nanofluids Technology for Electrical Energy Storage 7

2012-180-R2 Novel Non-Carbon Catalyst Support for Polymer Electrolyte Fuel Cells 9

2012-181-R2 Curing Cancer with the Power of Fireflies 11

2013-013-R1 Improving the Stability of Rubisco Activase, the Weak-Link, in the Biological CO_2 Fixation Machinery 12

2013-016-R1 Spin-Based Thermal Power Generation 13

2013-022-R1 Superlubricious Carbon Films Derived from Natural Gas for Home-Refueling Applications 15

2013-035-R1 Extreme Optomechanics 16

2013-036-R1 Development of Near-Field-Enhanced Terahertz Pump X-ray Probe Techniques for Ultrafast Control of Strongly Correlated Materials 18

2013-063-R1 Visualization of Stress-Induced Polarization Switching in Electromechanically Coupled Ferroelectric Polymers 19

2013-070-R1 Imaging Ecological Engineers: A Novel Quantum Dots Approach to Map Microbes in Complex Soil Structures with X-rays 21

2013-080-R1 Ultra-Low Loss Superconducting Microstrip for Multi-Chroic Cosmic Microwave Background Detectors 22

2013-096-R1 Graphene Windows for Advancing Electron RF Guns 24

2013-100-R1 3-D Compositional Control of Intermediate-Band Solar Cells 25

2013-116-R1 Nanolaminate Coatings for Improved Nuclear Fuel Cladding Performance 26

2014-004-N0 Magnetic Separation of Rare Earth Elements 28

2014-018-N0 Dynamics of Spin Ice 29

2014-019-N0 Exploring the Universe with Full-Sky Simulations of the Cosmic Microwave Background 30

2014-023-N0 Development of Large-Area Vacuum Ultraviolet Microchannel Plate Photodetectors for Use in Large Liquid Argon and Xenon Time Projection Chambers 31

2014-025-N0 New Paradigms for High T_c Superconductivity in Acene-Based Materials 32

2014-034-N0 Exploring the Direct Observation of the ^{229m}Th Isomeric Decay 34

2014-046-N0 Plastic Artificial Leaves for Water Splitting 35

2014-051-N0 Carbon Nano-Network as Next Generation Support for Catalysis and Electrocatalysis 37

2014-054-N0 Thin Film Skyrmion Spin Textures 38

2014-077-N0 Directly Probing Nanoscale Dynamics in Shear Thickening Complex Fluids 39

2014-081-N0 Pb-Assisted Corrosion/Cracking Mechanisms at the Interface between Pb-Containing Solution and Nickel Oxide 40

2014-084-N0 Probing the Chemistry of Atmospheric Dust Particles Using X-ray Spectromicroscopy: Implications for Climate Science 42

2014-095-N0 Tuning the Transport Properties of Coupled Majorana 43

2014-108-N0 Single Cell Structural Genomics of Uncultured Sediment Archaea: On the Trail for Novel Proteases 45

Advanced Computing

2011-213-R3* Towards the Exascale Sky 48

2011-214-R3* Mobile Device Vulnerability Research 49

2012-114-R2 Extreme-Scale Electromagnetic Modeling with Nanoscience Applications 50

2012-202-R2* A Future for Energy-Efficient General-Purpose Computing Based on Heterogeneity 51

2013-199-R1 MADNESS for Materials 53

2013-206-R1 Mathematical Techniques to Model Urban Data 54

2013-208-R1 General-Purpose Technical Cloud Platforms 56

2013-212-R1 Multiscale Materials Modeling Using Accurate *ab initio* Approaches (M^3A^3) 57

2013-213-R1 X-PECT: Performance Framework to Characterize and Transform Applications and Architectures at Extreme Scales 59

2013-218-R1* Urban Systems Integration Modeling and Analysis 60

2014-160-N0 Developing an Integrated Sensor Network for Science 61

2014-163-N0 Emerging Compute and Data Infrastructure 62

2014-166-N0 Scalable Stochastic Algorithms for Exascale Computational Mesoscience 63

2014-167-N0 Improving and Validating Models of the Urban-Climate Connection with Dense Sensor Networks 64

2014-174-N0 Advanced Pipeline for High-Throughput Digitization of Large-Scale Collections 65

2014-181-N0* PARIS: Data Knowledge-Based Extreme-Scale Resilience 66

2014-182-N0 Dynamic Data Mirroring for Data-Intensive Science 67

Applied Energy and Sustainable Transportation

2012-208-R2 20-kV/10-A 4H-SiC Vertical Trench Field-Controlled Thyristor (VTFCT) 70

2013-148-R1 Development of Predictive Multi-Dimensional Combustion Modeling Capability with Detailed Chemistry 72

2013-154-R1 Atomic Layer Deposition System for Continuous, High-Speed Thin-Film Processing 74

2013-156-R1 Fast High-Efficiency Process to Fabricate Aligned Nanotubes in Nano-Composite Membranes for High-Performance Filtration Applications 75

** Some projects topically associated with a strategic initiative area, as well as other innovative projects, were reviewed and selected by the Laboratory Director outside the normal annual LDRD call for proposals and review cycle.*

2014-120-N0 Grid Level Energy Storage for Integration of Renewable Energy 77

2014-169-N0 Magneto-Dielectric Composite Substrates Comprised of High Aspect-Ratio Magnetic Nanofibers for Smart Antennas Operating at Microwave Frequency 78

Biological and Environmental Systems

2012-016-R2 Knowledge Discovery in Microbial Community Composition and Metabolite Turnover Using Satellite Remote Sensing Data 81

2012-074-R2 Carbon Flux from Thawing Permafrost: Development of a Predictive Model Linking Microbial Activity and Biogeochemistry with Carbon Metabolism 82

2012-205-R2* Modeling the Interactions of Biophysical, Biogeochemical, and Microbial Dynamics in Permafrost-Affected Soils: From Pore Scale to Regional Scale 83

2012-206-R2* Developing, Improving, and Testing Methods for Predicting Spatial and Vertical Distributions of Soil Organic Carbon at Regional Scales 85

2013-177-R1 Identifying Novel Pathways for Anaerobic Microbial Oxidation of Methane 86

2013-194-R1 Annotating, Modeling, and Exploring Enzyme Promiscuity 88

2014-132-N0 Identifying Patterns and Association among Hyperspectral Data and Meteorological and Biological Measurements for Investigating Near-Surface Atmosphere-Biosphere Interactions 90

2014-141-N0 Minimizing Environmental Microbial Community Complexity at the Bench: Isolating and Characterizing Minimal Stable Communities (MSCs) over Time 91

2014-145-N0 Developing Remote Automated Sensors to Direct Sampling of Aerobic-Anaerobic Switching in Floodplain Ecosystems to Characterize the Response of Microbial Carbon Metabolism at High Temporal Resolution 93

2014-157-N0 Biology@speed: D-Factory, a Novel Experimental Framework 94

2014-162-N0 Soft X-ray Scanning Transmission X-ray Microscopy: Giving Argonne a Nanoscale Picture of Carbon in Soils and in Energy Materials 95

2014-183-N0 Impact of Radiation and Surface Turbulent Fluxes on the Transition from Stratocumulus to Cumulus Cloud Regime 96

2014-187-N0* Self-Assembled Functional Membranes for Filtration and Photocatalytic Water Treatment 97

2014-188-N0* Timescale of Groundwater Transport: A Prerequisite for Developing and Maintaining Groundwater Reservoirs 99

2014-189-N0* Membrane-Biofilm Nexus: Advanced Membrane Autopsy as a Tool for Revealing Membrane Biofouling and Development of New Membrane Materials and Structures 100

2014-193-N0* Turbulent Transports in Cumulus Topped Boundary Layers 101

Director's Grand Challenge

2013-165-R1 Integrating Simulation and Observation: Discovery Engines for Big Data 104

** Some projects topically associated with a strategic initiative area, as well as other innovative projects, were reviewed and selected by the Laboratory Director outside the normal annual LDRD call for proposals and review cycle.*

Hard X-ray Sciences

2013-111-R1 Feasibility Study of Applying Thin-Film High-Temperature Superconducting Films on Copper or Niobium-Sputtered-on-Copper for the Purpose of Achieving Helium-Free Operation with Cryocoolers 108

2013-168-R1* The Tao of Fusion: Pathways for Big-Data Analysis of Energy Materials at Work 109

2014-122-N0 Superconducting Radio Frequency Cavities for Hard X-ray Science 111

2014-127-N0 Development of a Novel Analyzer System for Resonant Inelastic X-ray Scattering with Better Than 10-meV Resolution 113

2014-134-N0 Three-Dimensional Coherent Diffraction Imaging Using Polychromatic Hard X-rays 114

2014-137-N0 $YBa_2Cu_3O_7$ High-Temperature Superconducting Prototype Undulator 115

2014-175-N0 Automation of *in situ* Crystallization Plate Screening and Data Collection at Room Temperature 117

2014-184-N0 Long SCU Magnet 118

Materials for Energy

2011-217-R3* Polyelectrolyte Brushes in Multi-Valent Ionic Media 121

2012-015-R2 Mesoscale Elastic Problems 122

2012-204-R2* Membrane-Bound, Broad-Spectrum, Photo-Driven Protein Devices 124

2012-209-R2 Atomistically Informed Mesoscale Modeling for Advanced Electrical Energy Storage Systems 125

2013-184-R1 Hierarchical Modeling of Self-Assembly in Nanostructured Soft Materials at Equilibrium and Far from Equilibrium 127

2013-202-R1 Computational Molecular Science 128

2013-215-R1* Mesoscale Materials by Design from Assemblies of Ionic Polymers and Nanoparticles 130

2013-216-R1* Directed Self-Assembly and Three-Dimensional Characterization of Block Copolymers in Semi-Thick Films 131

2013-219-R1* Transition Edge Sensors for Fundamental Physics 132

2014-121-N0 Integration of Scalable Microwave Reactor with High-Energy X-ray Beamline for High-Throughput Screening Energetic Nanomaterial Synthesis 133

2014-128-N0 Length-Scale Bridging Computational Scheme for Structure and Transport 135

2014-129-N0 The Design and Synthesis of Novel Oxides: Coupling Materials Informatics with a Next-Generation Deposition System Employing *in situ* X-ray Scattering and Photoemission Spectroscopy 136

2014-130-N0 New Materials for Natural Gas Storage and Conversion Technologies 138

2014-133-N0 *In-situ* X-ray Characterization of Doped Materials by Atomic Layer Deposition for Energy Applications 139

2014-139-N0 Fast Electronic Structure Methods for Rapid Reaction Screening for Inorganic Materials Synthesis and Particle Formation 141

** Some projects topically associated with a strategic initiative area, as well as other innovative projects, were reviewed and selected by the Laboratory Director outside the normal annual LDRD call for proposals and review cycle.*

2014-151-N0 Developing Predictive Models of Wide Bandgap Semiconductor Synthesis and Processing 142

2014-161-N0 Bridging the Electronic and Atomistic Scales: Force Field Development for Reactive Interfaces from First Principles 144

2014-191-N0* Defect-Localized Spins in Semiconductors for Quantum Optoelectronics 145

2014-192-N0* Computational Spectroscopy of Heterogeneous Interfaces 147

National Security

2013-171-R1 Unconventional Signatures for Characterizing Culture Conditions 150

2013-173-R1 Ratiometric Semiconductor Nanocrystal-Based Sensors for Threat Reduction Applications 151

2013-178-R1 Uranium and Plutonium Detection by Plasmonic Graphene-Based Nanosensors 153

2014-194-N0* Crime on the Urban Edge: Simulating the Interface between Transitional and Local Crime 155

Nuclear Energy

2013-152-R1 Nanolaminate Materials for Extreme Environments: A Demonstration of Argonne Capabilities for Design, Synthesis, and Accelerated Testing of Radiation-Tolerant NE Materials 158

2014-177-N0 Development of a Computational Fluid Dynamics Multiphase Boiling Capability to Predict the Critical Heat Flux in Nuclear Reactor Fuel Assemblies 160

2014-190-N0* Feasibility Study of a Fast Reactor for Isotope Production 162

Sustainable Energy Production and Use

2011-210-R3* Improved Catalytic Performance by Applying Electrochemical Control 165

Other Novel R&D

2014-185-N0* Enabling Sodium-Ion Batteries for Grid Storage....167

** Some projects topically associated with a strategic initiative area, as well as other innovative projects, were reviewed and selected by the Laboratory Director outside the normal annual LDRD call for proposals and review cycle.*

Acknowledgments

Argonne's LDRD Program Office comprises the Associate Chief Scientist for LDRD, Dr. Kawtar Hafidi; LDRD Program Manager, Rebecca R. Rank; Administrative Specialist, Marianne I. Lohr-Dietz; and Web Designer (graduate student), Sean M. Sullivan. The program as a whole reports to the Laboratory Director, Dr. Peter B. Littlewood, through the Director for Strategy and Innovation, Gregory S. Morin. Those of us in the program's management are grateful for the critical support received throughout the year, particularly while preparing this Annual Report. Special appreciation and thanks are due to the many research staff members who execute research projects that strive to build new programs; to the technical and administrative management of Argonne's programmatic divisions, within which the research and development are pursued; to the peer-review panels that evaluate LDRD proposals; and to the strategic initiative leaders, whose vision helps guide and refine Argonne's LDRD portfolio. In particular, the following individuals provided key support for this document:

Computing and Information Systems Division
Jason Boggs
Fred Moszur
Ross Pallan

Legal Department
Mark Hilliard
Debbie Krakowski

Office of the Chief Financial Officer
Richard Crowley
Luba Zholents

Communications, Education, and Public Affairs
Kevin A. Brown (Project Manager)
Linda Conlin (Lead, Document Production)
Joseph Harmon (Editor)
Andrea Manning (Editor)
Marita Moniger (Lead Editor)
Michele Nelson (Lead, Design and Layout)
Katherine Obmascik (Editor)
Lorenza Salinas (Production)
Carolyn Steele (Editor)
Elizabeth Stefanski (Editor)
Else Tennessen (Editor)

Laboratory Overview

Argonne National Laboratory is a multidisciplinary science and engineering research center, managed by UChicago Argonne, LLC, for the U.S. Department of Energy (DOE), Office of Science (SC). Argonne staff work along with experts from industry, academia, and other government laboratories to address vital national challenges in the areas of clean energy, the environment, technology, and national security. Through collaborations involving researchers both here at Argonne and around the world, the Laboratory strives to discover and develop solutions to energy-related challenges through its scientific work; create novel materials, molecule by molecule; and develop a deeper understanding of our planet, our climate, and the cosmos.

Argonne works to accelerate innovation in science and technology not only for its primary research sponsor, DOE SC, but also for DOE's Office of Energy Efficiency and Renewable Energy (EERE) and National Nuclear Security Administration (NNSA), and for a variety of other federal agencies. Argonne designs, builds, and operates unique national scientific user facilities that enhance its research capabilities and serve a broad community of researchers from educational institutions, industry, and government laboratories.

As a national laboratory, Argonne concentrates on scientific and technological challenges that can be addressed only through a sustained, interdisciplinary focus at a national scale. Argonne's eight major initiatives, as enumerated in its Strategic Plan, are *Hard X-ray Sciences, Leadership Computing, Materials for Energy, Energy Storage, Sustainable Transportation, Nuclear Energy, Biological* and *Environmental Systems*, and *National Security*. They are organized around the following core capabilities:

Fundamental Sciences
Accelerator Science and Technology
Advanced Computer Science, Visualization, and Data
Applied Mathematics
Biological Systems Science
Chemical and Molecular Science
Computational Science
Condensed Matter Physics and Materials Science
Environmental Subsurface Science
Nuclear Physics
Particle Physics

Applied Sciences and Engineering
Applied Materials Science and Engineering
Applied Nuclear Science and Technology
Chemical Engineering
Climate Change Science
Large-Scale User Facilities/Advanced Instrumentation
Systems Engineering and Integration

User Facilities

- The Advanced Photon Source (APS) provides a high-brightness, high-energy electron beam. This unique source of high-energy x-rays for scattering, spectroscopic, and imaging studies has a timing structure that enables time-resolved research from picoseconds to seconds. The planned APS upgrade project will result in an improved world-class source of high-brightness, high-energy, tunable x-rays for scientific research.
- The Center for Nanoscale Materials (CNM), one of five DOE Nanoscale Science Research Centers, combines advanced scanning probes (including an x-ray nanoprobe; organic, inorganic, and digital synthesis; and nanofabrication), all of which are coupled with theory and modeling.
- The Electron Microscopy Center (EMC) provides state-of-the-art aberration-corrected electron microscopy (e.g., TEAM, the Transmission Electron Aberration-Corrected Microscope) with applications to three-dimensional elemental imaging and *in situ* environmental studies of catalysts and other nanoscale materials.
- The Argonne Tandem Linac Accelerator System (ATLAS) is a scientific user facility based on a superconducting linear accelerator. It provides heavy ions in the energy domain best suited for studying the properties of the nucleus, the core of matter, and the fuel of stars.
- The Argonne Leadership Computing Facility (ALCF) offers users access to petascale computing for research on energy systems and catalysis and research in the life, environmental, and basic sciences.
- The Transportation Research Analysis and Computing Center (TRACC) operates the largest high-performance computing cluster available to U.S. transportation researchers. It performs targeted research to foster technology transfer from the national laboratory's energy research complex to the transportation research community.
- The DOE Atmospheric Radiation Measurement (ARM) Climate Research Facility provides the world's most comprehensive capabilities for continuous observations of atmospheric data specifically for climate change research.

In addition to these facilities, Argonne hosts a Transportation Technology Research and Development Center, Theory and Computing Sciences (TCS) Building, Materials Engineering Research Facility (MERF), and the University of Chicago's Howard T. Ricketts Laboratory and Institute for Molecular Engineering (IME).

Program Assessment

Program Overview

Argonne's Laboratory-Directed Research and Development (LDRD) program strives to encourage the development of novel technical concepts, enhance the Laboratory's research and development (R&D) capabilities, and enable pursuit of laboratory strategic goals.

Argonne's LDRD projects are proposal-based and peer-reviewed for ideas that require advanced exploration before being sufficiently developed for support through normal programmatic channels. Among the aims of the projects supported by the LDRD program are the establishment of engineering proofs of principle, assessment of design feasibility for prospective facilities, development of instrumentation or computational methods or systems, and discoveries in fundamental science and exploratory development.

The projects supported by the LDRD program are distributed across the major mission areas at Argonne, as indicated in the Laboratory's LDRD Plan for fiscal year (FY) 2014. All LDRD projects have demonstrable ties to one or more of the science, energy, environment, and national security missions of the U.S. Department of Energy (DOE), and many are also relevant to the missions of other federal agencies that sponsor work at Argonne. A natural consequence of the more "applied" type projects is their concurrent relevance to industry.

In addition to their relevance to strategic and programmatic activities, LDRD projects naturally fall under one or more areas of science and technology corresponding to the disciplines and fields in which Argonne's technical staff are trained and excel in supporting existing programs. The project reports in this document demonstrate that more often than not, expertise is drawn from several technical areas to pursue the goals of any given project. Quite often, theory and computational work are integrated with experiments in these projects. This multidisciplinary approach is a hallmark of Argonne as a multiprogram national laboratory and reflects the synergistic manner in which both LDRD and programmatic work are pursued.

The FY 2014 DOE-approved funding cap for LDRD was $30.0 million, or about 3.8% of Argonne's estimated FY 2014 operating plus capital budgets. Actual expenditures amounted to $29.2 million, which includes an overhead levy of approximately 30.6%. A table of planned or actual funding profiles for each project active in FY 2014 is provided on pages xxvi-xxviii. Individual brief project reports for FY 2014 make up the bulk of this document. A list, by title, of new projects begun to date in FY 2015 is provided in the appendix.

LDRD Management Process

Argonne's R&D activities are organized under four associate laboratory directors (ALDs), who oversee the research conducted in some 15 programmatic divisions. Responsibility for management and oversight lie with the Laboratory Director, who has delegated the management task to the Deputy Laboratory Director for Operations and the Director for Strategy and Innovation. This senior management group makes final recommendations concerning the LDRD program investment and management.

Argonne's LDRD program consists of four components: the Strategic Initiatives, the Director's Grand Challenge, the Director's Competitive Grants (DCG), and the Director's Strategic Reserve (a portion of the total allowed expenditure temporarily reserved to handle mid-year opportunities, strategic hires for LDRD projects, and LDRD collaborative arrangements). The Strategic Initiatives, Director's Grand Challenge, and Director's Strategic Reserve components fund R&D projects that are aligned with the Laboratory initiatives consistent with Argonne's Strategic Plan, while the DCG component supports exploratory research aligned with DOE mission areas and core competencies of the Laboratory. Annually, the Laboratory Director determines the appropriate balance of funding among the four components. All final decisions concerning Argonne's LDRD program reside with the Laboratory Director. Certain responsibilities regarding funding, oversight, proposal evaluation, and project direction are delegated.

The LDRD Program Office reviews all proposals to ensure their adherence to DOE Order 413.2b and associated guidelines, as well as to Laboratory administrative procedures. The flowchart in Figure 1 illustrates the relationships of the management and review processes for two of the components of the FY 2014 program.

Argonne LDRD Selection Process Schematic

(Applies to Review and Selection Process for FY 2014 Proposals)

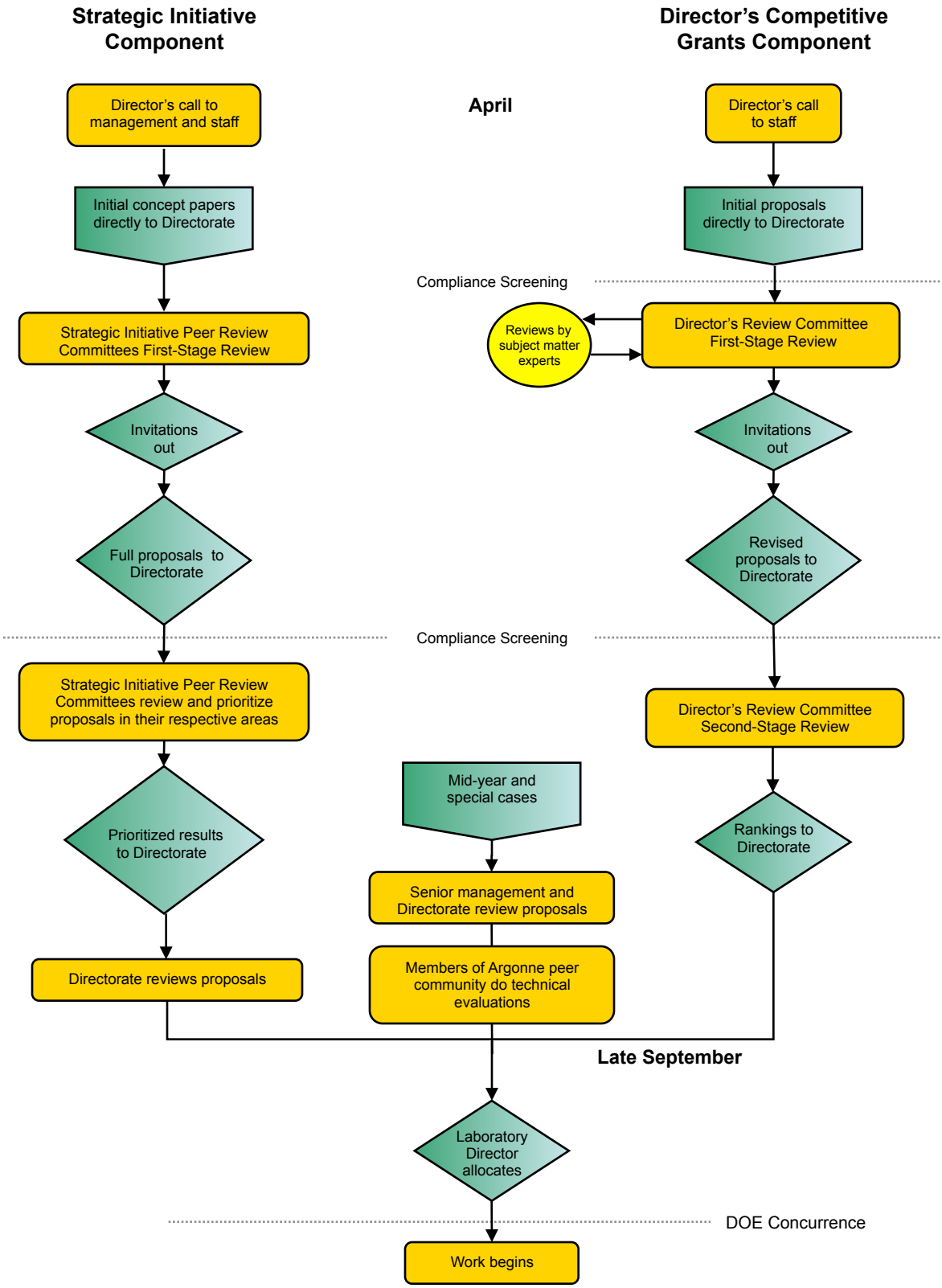

Figure 1. Argonne LDRD Selection Process Schematic

The LDRD program is funded lab-wide through the Laboratory's indirect budget, which derives from a levy against all program operating and equipment budgets. Although two- or three-year durations are proposed for many projects, funding levels and project selection are determined annually and based on technical progress and the Laboratory's strategic goals and resources.

LDRD funds may be used in collaborative arrangements with third parties to enhance the application or scope of the research, with attendant beneficial interactions. To effect these arrangements, the Laboratory has in place DOE-approved procedures and instruments, such as Cooperative Research and Development Agreements (CRADAs), subcontracts, and site access Guest Agreements. These instruments and procedures enable the application of LDRD funds while ensuring that appropriate terms and conditions are applied thereto, including those related to intellectual property rights.

Line managers in Argonne's programmatic divisions are responsible for monitoring the progress and performance of LDRD research during execution. Strategic Initiative coordinators and line managers confirm that mid-year progress reviews have occurred and indicate whether any remedial action or advice is needed. The responsibility for the actual conduct of all LDRD projects, including associated environmental safety and health requirements, resides with the ALDs and their line managers.

During FY 2014, all program management requirements were satisfied. Reports required by DOE, including the Annual Report for FY 2013, the LDRD Program Plan for FY 2015, and project data uploaded to the DOE/CFO (Office of the Chief Financial Officer) database, were submitted completely in a timely fashion.

Concurrence request forms (also referred to as "data sheets" in relevant guidance documents) were submitted electronically, on a project-by-project basis, to the DOE Argonne Site Office (ASO) to obtain the DOE Site Manager's concurrence before work on the FY 2014 LDRD projects proceeded.

FY 2014 LDRD Program Components

Strategic Initiatives

This larger component of LDRD emphasizes R&D explicitly aligned with Laboratory and Department missions as reflected in Strategic Initiatives proposed by senior management and consistent with Argonne's Strategic Plan. Strategic goals are revised periodically and reevaluated as necessary. The choice of initiative areas reflects an evaluation of the state of development of the relevant technical fields, the potential value to the Department and the nation of advancing those fields, and, of course, the compatibility and synergy that these fields have with existing facilities, capabilities, and staff expertise at Argonne.

In FY 2014, leadership of the Strategic Initiative areas and of the Laboratory's major initiative areas as delineated in Argonne's Strategic Plan were focused under respective Associate Laboratory Director-led teams. Under this model, there were seven Strategic Initiative areas in which proposals could be submitted. The FY 2014 review procedures continued to ensure that all individual proposals identified as fitting under a Strategic Initiative were reviewed for their scientific quality, innovativeness, and value to each respective mission-related initiative.

The review of proposals with regard to the Strategic Initiatives component relies on a combination of peer and management reviews within initiative areas. The appropriate ALD appoints Strategic Initiative coordinators for each of the respective Strategic Initiatives to evaluate and recommend projects for funding. The Strategic Initiative coordinator selects internal and external subject matter experts (SMEs) to serve on review panels to assist in reviewing the proposals that have been submitted. Results are reported to the Laboratory Director, who makes final selections and approves the content and aggregate budget.

The seven FY 2014 Strategic Initiative areas are as follows:

Advanced Computing

The key elements of this initiative fall under the following general areas: next generation architectures, programming models and software stacks; data-intensive computing infrastructure and systems; computational science application code development; and novel computing applications and over-the-horizon technologies.

Applied Energy and Sustainable Transportation

The key elements of this initiative fall under the following areas: sustainable transportation, including (a) computational combustion, (b) materials for transportation, and (c) methane for transportation; advanced manufacturing, including (a) nanomaterials for manufacturing systems, (b) advanced manufacturing processes, (c) biomanufacturing, and (d) integrated computational materials engineering; and renewable energy, including (a) high-fidelity weather forecasting, (b) statistical and uncertainty analysis for renewables, and (c) power grid modeling and simulation.

Biological and Environmental Systems

The key elements of this initiative fall under the following general areas: miniaturization and automation of high-throughput laboratory and field sampling and monitoring processes; microbial ecosystems and community processes; accelerating the understanding of protein/DNA sequence–structure–function relationships; and climate and biosphere interactions.

Hard X-ray Sciences

Three key focus areas for projects under this initiative area are as follows: research and development in support of the Advanced Photon Source upgrade project (including production of short pulses, novel insertion devices, and advanced beamline instrumentation), science enablers, and future hard x-ray sources (including, high-repetition-rate free-electron lasers, free-electron oscillators, and/or ultimate storage rings).

Materials for Energy

Two research focus themes were selected for this initiative on the basis of how much they represent core areas of expertise and provide an opportunity for future scientific growth: molecular materials design and discovery (M2D2) and computational chemistry and materials (C2M). The M2D2 theme focuses on accelerated design, discovery, and creation of functional energy materials and chemistries through advances in synthesis science and on linking *in situ* probes of growth and function with theory, modeling, and simulation to close the feedback loop. The C2M theme focuses on the development of methods and algorithms for the accelerated discovery of materials structures and functionalities, suitable for the challenges of synthesis and design, by using high-performance computing for large-scale simulations and data-driven science as it pertains to model discovery, verification, and validation. In addition to these thematic topics, the Materials for Energy Strategic Initiative will solicit proposals for "mini-challenges:" projects designed to integrate all the components of the Materials for Energy strategy (computation, synthesis, imaging/characterization) into an integrated project that addresses a well-defined materials or chemical challenge in the energy realm. The topical areas for these mini-challenges include wide-band-gap semiconductors, low-power electronics, and thermoelectric materials.

National Security

The national security initiative has two major focus areas: weapons of mass destruction (WMD) (including chemical, biological, radiological, and nuclear threat areas) and global resource security and resiliency. Topics to be considered under the WMD focus area are sensor systems including sensors/detectors, forensics/attribution, nonproliferation/safeguards, and data/modeling. Topics to be considered under the global resource security and resiliency focus area are energy security, environmental security, and critical materials security.

Nuclear Energy

The key elements of this initiative fall under the following areas: (1) nuclear energy science, including (a) material science for nuclear energy, (b) *in situ* studies of nuclear energy materials irradiation under challenging service conditions or extreme environments, and (c) the design and synthesis of materials that can enhance the performance, safety, and economics of nuclear energy systems; (2) engineering and technology demonstration, including (a) reactor and fuel cycle technologies or concepts that meet the goals for future systems in the areas of economics, resource utilization, safety assurance, proliferation resistance, and waste management, (b) materials, operating concepts, and diagnostic capabilities to improve light water reactor (LWR) plant performance, enhance safety assurance, and extend operating lifetimes, (c) technical solutions to improve the management of used nuclear fuel, and (d) U.S. safety, security, and nonproliferation goals related to the international use of nuclear energy; and (3) nuclear energy modeling and simulation, including the (a) design and operation of nuclear engineering (NE) systems by reducing uncertainty in predictions of performance and safety characteristics, (b) enhancement of nuclear safety and improved response to potential accidents, (c) prototyping of advanced NE technologies and systems, and (d) design of and licensing processes for advanced systems and technologies.

Figure 2 illustrates the distribution of funding among the seven strategic initiative areas.

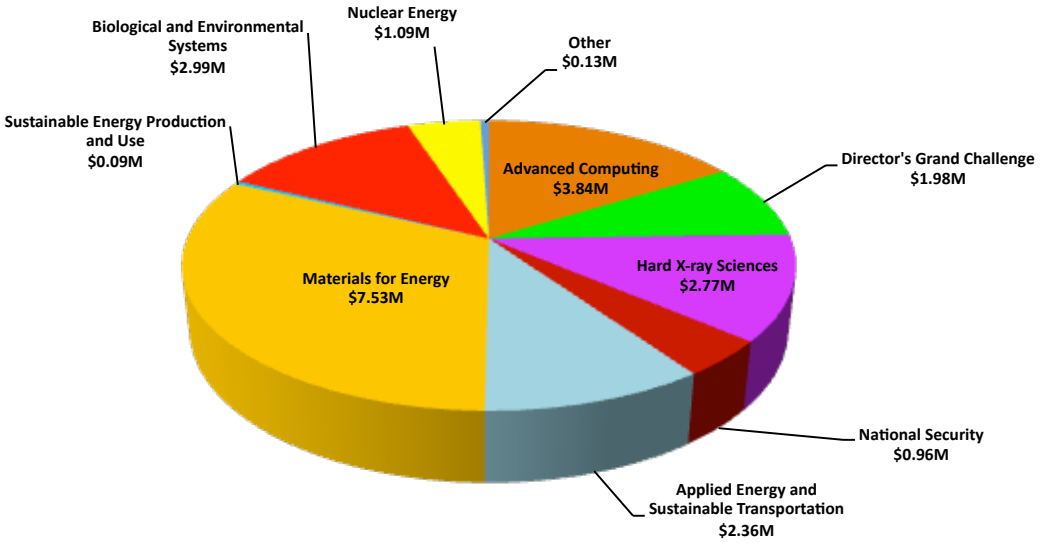

Figure 2. Distribution of Funding among Strategic Initiative Areas

Director's Grand Challenge

The Director's Grand Challenge component of the LDRD portfolio may be included in the LDRD program of any given fiscal year by the Laboratory Director. Also at the discretion of the Laboratory Director is the schedule for the call for proposals and for the review and selection of projects for this component, which does not need to match the schedules for the Strategic Initiatives or Director's Competitive Grants components. For a Grand Challenge project, sufficient talent and resources are devoted to a specific technical topic within an area that is of substantial strategic value to the Laboratory and to DOE, in order to allow major strides to be made toward achieving its R&D goals. The emphasis is on cross-cutting initiatives that synergistically draw on Argonne's core competencies.

As a precursor to formal LDRD proposal submissions, brief "white papers" are solicited. The white papers are evaluated by a Grand Challenge Review and Oversight Panel composed of four to ten internal and external SMEs. The panel members recommend which white paper authors should be invited to submit more extensive formal proposals. The latter are reviewed and ranked on the basis of their expected impact, creativity, degree of cross-cutting utilization of Argonne core capabilities and staff, and potential for success. The successful Grand Challenge LDRD project is expected to target a specific outcome, enabled by a specific innovative approach, with a well-coordinated team. The awarded project is formally reviewed by the Grand Challenge Review and Oversight Panel semiannually to evaluate progress.

In FY 2014, there were no new Director's Grand Challenge topics funded. However, the data-driven science-related project from FY 2013 was continued. The project was awarded $1.98M in FY 2014, with funding expected to be minimally decreased in FY 2015.

Director's Competitive Grants (DCG)

The DCG component invests in a full spectrum of investigator-initiated proposals across the Laboratory in DOE-mission-related science and engineering areas. This component provides an avenue for R&D staff to propose highly innovative projects directly to the Laboratory Director. Proposals are subjected to peer review by the Director's Review Committee to assess their scientific and technical quality. The Committee is composed of nonmanagerial scientists and engineers selected by the Laboratory Director. The Committee currently comprises 23 members who have substantial expertise in their technical fields, are familiar with the peer review process, and represent a broad cross section of the Laboratory. The Director's Review Committee conducts an initial peer review that results in a smaller number of proposals being retained for further review by the Committee. The products of the review procedure are a rank-ordered list of proposals given to the Laboratory Director and brief critiques of proposals sent to the proposing investigators.

The DCG review process is augmented by the recruitment of members of the Laboratory's research community who serve as volunteer SMEs to help the Director's Review Committee review proposals. Approximately 275 researchers volunteered, and their assistance made it possible for the Director's Review Committee to recommend the highest-quality proposals for funding in FY 2014.

FY 2014 LDRD Project Characteristics

Categories of Work

The distribution of LDRD projects across the DOE-defined categories of work, as shown in Figure 3, reflects the types of actual "hands-on" work performed by our LDRD-supported investigators. However, a better indication of the ultimate purpose(s) of the work and therefore of the potential future benefits to specific programs (for example, using high-performance computation to simulate biological or catalytic processes) can be found in the description of the research itself in the body of this report.

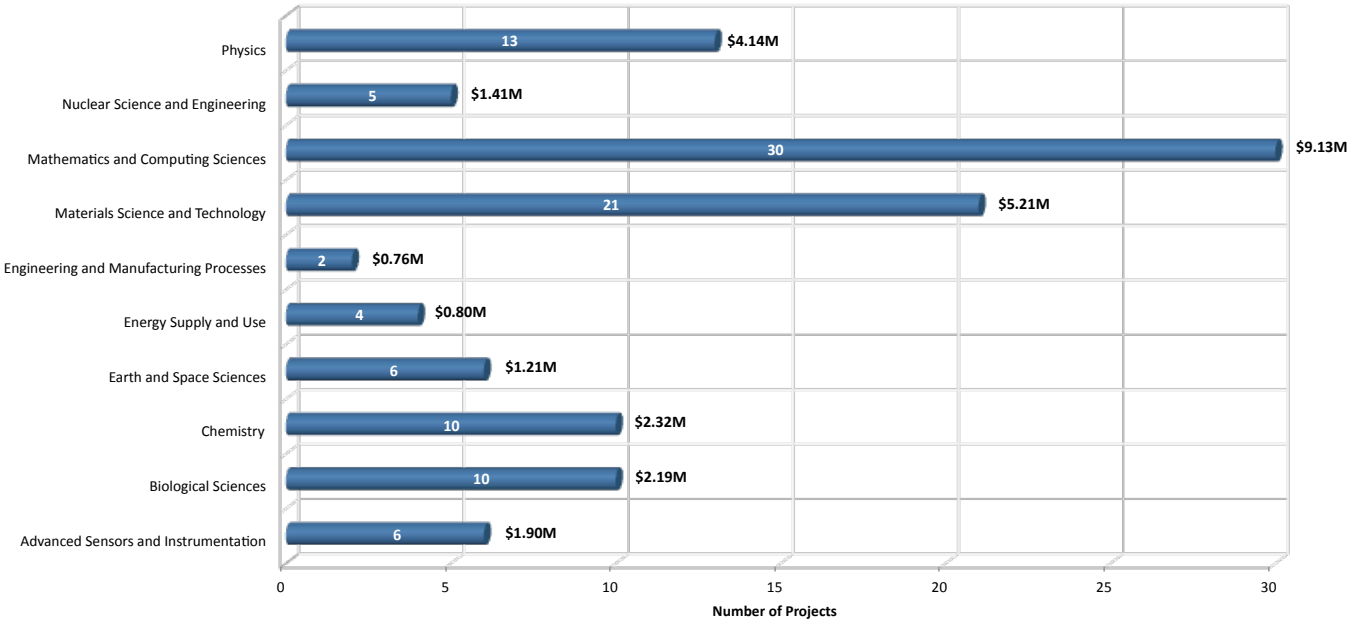

Figure 3. Number and Dollar Values of LDRD Projects across the DOE-Defined "Categories of Work"

Mission Relevance

Evaluating the relevance of LDRD projects with respect to DOE mission areas is of utmost importance during the review and selection process. All LDRD projects have demonstrable ties to one or more of the science, energy, environment, and national security missions of DOE, and many are also relevant to the missions of other federal agencies that sponsor work at Argonne. Figure 4 represents the number of FY 2014 LDRD projects supporting the four DOE mission areas.

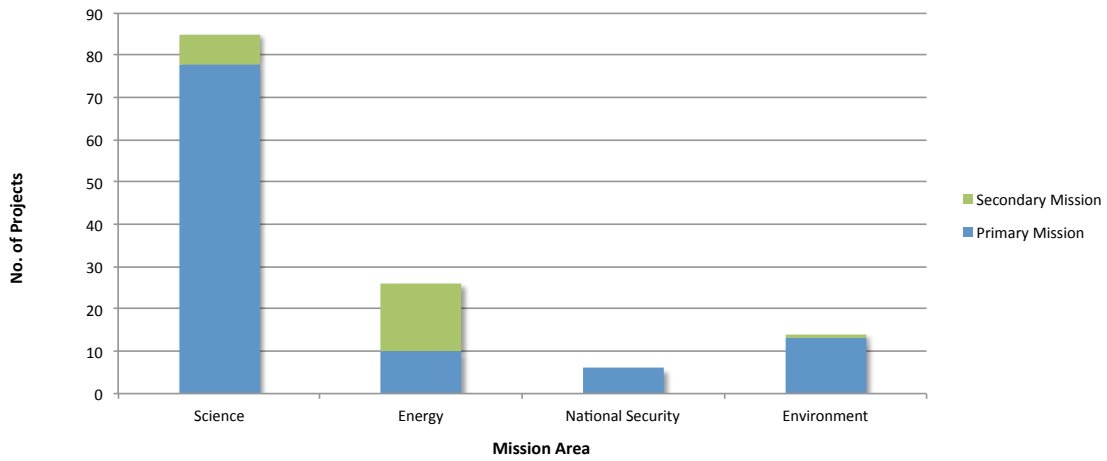

Figure 4. Number of LDRD Projects Supporting the DOE Mission Areas

Distribution of Funding

In FY 2014, the LDRD Program funded 107 projects with a total budget of $29.1M. The distribution of funding among the LDRD components is shown in Figure 5.

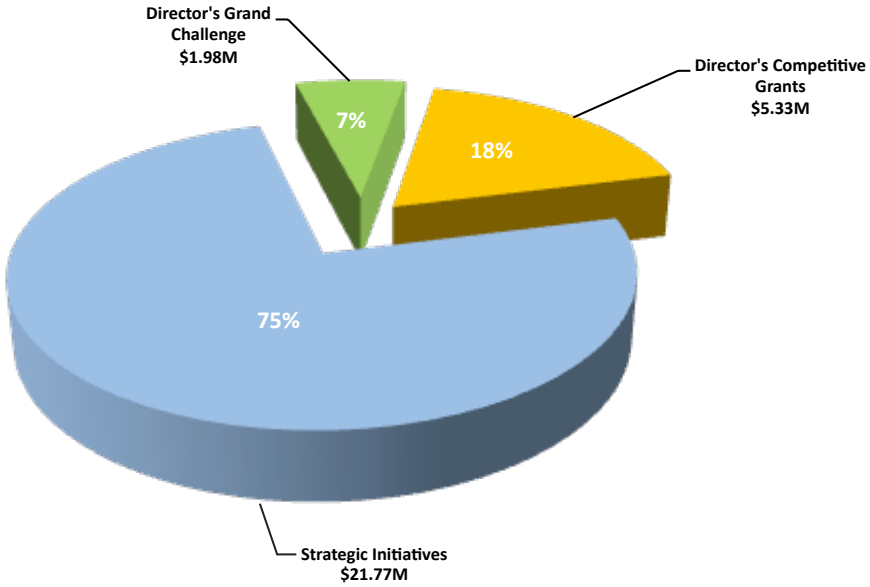

Figure 5. Distribution of Funding among the LDRD Project Components. (Total funding for FY 2014 was $29.1M.)

Strategic Initiatives

In FY 2014, 38 new projects and 35 continuing projects in the seven Strategic Initiative areas listed in a previous section were funded at an aggregate level of $21.6M. Some additional mid-year and strategic-hire projects, selected by the Laboratory Director, are included in these figures. Also in FY 2014, one continuing strategic project totaling $85.4K represented the completion of a former Sustainable Energy Production and Use initiative project. And, one new strategic project totaling $130K represented an R&D research opportunity that fell outside our strategic initiative areas. The overall FY 2014 funding level for the Strategic Initiative component equaled $21.8M, which is 75.0% of the overall budget. The 75 projects funded under the Strategic Initiative areas were 70% of all projects funded in FY 2014.

Director's Grand Challenge

In FY 2014, one continuing Director's Grand Challenge project was funded at just under $2.0M. This project represented about 7% of the total FY 2014 LDRD Program budget.

Director's Competitive Grants

Under the Director's Competitive Grants component of LDRD, 14 new projects and 17 continuing projects were funded at a total level of $5.3M, which represents 18.0% of the Laboratory's LDRD budget. The 31 DCG projects accounted for 29% of the LDRD projects funded in FY 2014.

Level of Funding

Figure 6 depicts the funding distribution for the 107 projects funded in FY 2014. Around 54% of the projects were in the $101K to $250K range, with a little more than 11% receiving $100K or less. Around 25% of the projects received between $251K and $500K, while only 7% of projects were in the range of $501K to $1M. Just under 2% of projects received more than $1M. The average funding level of a project in FY 2014 was about $272K.

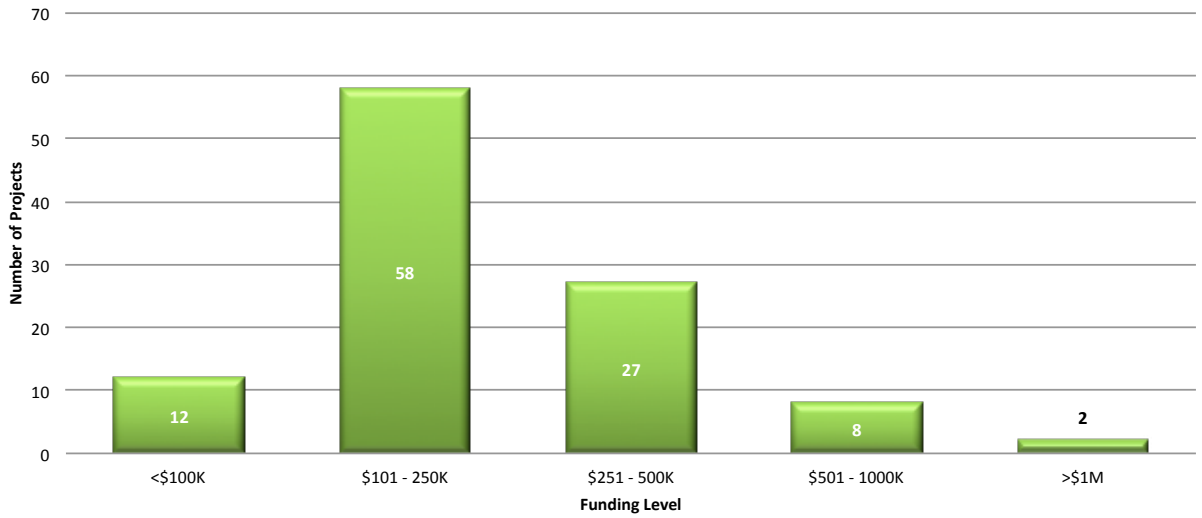

Figure 6. Number of Projects and Levels of Funding (The average funding level for an LDRD project in FY 2014 was about $272K.)

LDRD Investigators

By nature, LDRD projects fall under one or more areas of science and technology. Argonne's diverse pool of technical staff members represents a vast array of technical expertise that can ensure the success of any given project. The multidisciplinary aspect of Argonne's LDRD program is reflected in Figure 7.

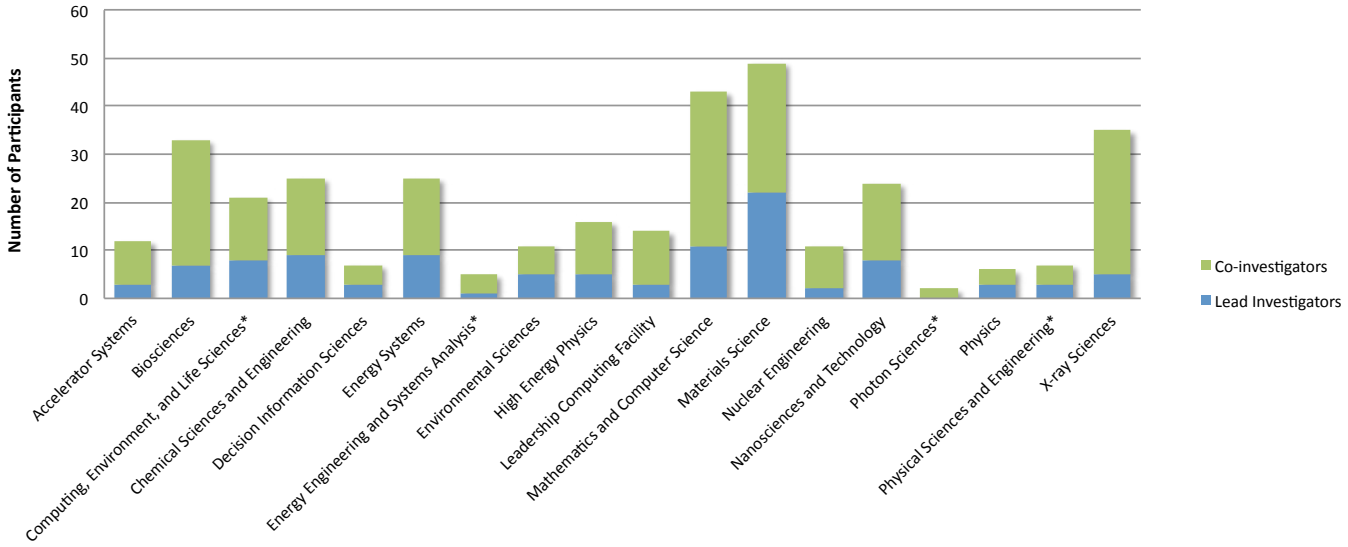

Figure 7. LDRD Investigators across Programmatic Divisions and Directorates

FY 2015 Update

DOE approved Argonne's FY 2015 LDRD Plan and program expenditures not to exceed $32.0M. A list of projects begun so far in FY 2015, by title, is provided in the appendix to this report.

For the 2015 fiscal year, we have restructured our mid-year review process for the Director's Competitive Grants component of our Program. In the enhanced review procedure, volunteer internal SMEs will be called upon to evaluate appropriate projects. Evaluation topics will include the current state of the project, future plans, and any obstacles that may have arisen since the start of the project and/or start of the fiscal year. These SME evaluations will be used by the Director's Review Committee in the review of renewal proposal submissions for FY 2016. If this method of mid-year review is effective, we plan to extend the process to the Strategic Initiative component of the Program in FY 2016.

In FY 2015, we will also continue to refine our use of electronic tools to communicate with investigators and reviewers and to collect and document performance information on LDRD projects. Based on user feedback and other forms of input, we are continuing to refine our existing web-based applications and creating new tools as necessary. One such example was the modification to our peer review application. The enhancements made to the system allow us to better track SME volunteers, make review assignments more efficiently, and follow up on outstanding reviews in a timelier manner. Another recent example is the creation of a web-based document directory for our review committee members. This is a repository of proposal and other review-related documents that can be downloaded as individual or multiple files. This new system also eliminates the need to transfer files via e-mail. A more general maintenance of IT applications that support the management of the LDRD Program is also ongoing.

Peer Review Experience in FY 2014

The pursuit of LDRD is managed and its performance is reviewed as an integral part of the activities of the respective technical divisions in which the work resides. Periodic peer reviews of each division's programs and research are conducted by committees empanelled by Argonne's management and operations (M&O) contractor, UChicago Argonne, LLC. The quality of the science and technology performed under LDRD funding within a division cannot be distinguished from that reflected in the division's performance of programmatic R&D. By and large, the same research personnel and the same facilities are applied to both, and no discernible qualitative differences have been observed. LDRD is therefore not reviewed separately; however, results and plans relevant to LDRD projects are routinely exposed to Review Committee scrutiny. A tabulation of such reviews for FY 2014 is provided here in Table 1, along with an aggregate accounting of the number of LDRD projects exposed to committee review and their total dollar values. The LDRD Program Office also requires principal investigators to report all other relevant external reviews of their work. LDRD projects from the Accelerator Systems (ASD), Chemical Sciences and Engineering (CSE), Decision and Information Sciences (DIS,), High-Energy Physics (HEP), Mathematics and Computer Sciences (MCS), and X-ray Sciences (XSD) divisions; the Leadership Computing Facility (LCF); and the Computer, Environment, and Life Sciences (CELS) ALD area were reviewed as part of an overall contractor-chartered review.

Table 1. Summary of Peer Review History by Organization

Programmatic Organization	Date of Review	Number of LDRD Presentations	Number of LDRD Projects	Dollar Value of Projects ($ in thousands)
ASD	5/28/14	1	2	$781.6
CELS	9/9/14	2	1	$3,469.4
CSE	8/25/14	5	4	$5,875.4
DIS	1/29/14	6	14	$5,431.1
HEP	9/9/14	1	2	$6,624.2
LCF	9/9/14	1	2	$297.3
MCS	9/9/14	1	1	$3,469.4
XSD	5/28/14	13	13	$8,139.1
Totals		**30**	**39**	**$34,087.5**

Performance Metrics

The LDRD Program Office collects statistical data on current and completed LDRD projects. Such data cover various items; examples include publications (see citations in appendix to this report), inventions (see appendix to this report), follow-on sponsorship, and the enhancement of staff by post-doctoral appointees and new hires. Although these data are of little value on a project-by-project basis, in aggregate, they do provide a picture of overall program productivity. The management processes employed to collect these data include surveys of current and former investigators, analyses of project annual reports, and validation against records of the Office of Technology Development and Commercialization (TDC); the Legal Department (LEG); and the Publications and Record Services section of the Computing and Information Systems (CIS) division. Summaries of the most recently collected data are provided here in Tables 2 and 3. The first table displays project outcomes realized only during FY 2014 but derived from projects active in any year or years from FY 2011 forward. For the same prior and currently active projects, the second table displays those metrics for which cumulative results are monitored, with no restriction as to when the accomplishments occurred.

Table 2. Aggregate FY 2014 Outcomes for Recently Completed and Current Projects

LDRD Component	Number of Refereed Publications	Number of Students/ Postdocs Supported	Number of New Staff Hires	Number of Non-Publication Copyrights	Number of Invention Disclosures	Number of Patents Issued/ Pending
2011						
Competitive Grants	4	0	1	0	0	1
Strategic Initiatives	3	0	0	0	0	1
2012						
Competitive Grants	4	0	1	0	2	3
Strategic Initiatives	12	0	0	0	3	5
2013						
Competitive Grants	8	0	0	0	1	5
Strategic Initiatives	48	0	3	2	2	0
2014						
Competitive Grants	18	40	2	0	5	3
Strategic Initiatives	91	135	12	1	5	0
Grand Totals: 239 Projects	**188**	**175**	**19**	**3**	**18**	**18**

Table 3. Aggregate Outcomes for All Years of Recently Completed and Current Projects (2011–2014)

Most Recent Project Year	Number of Projects Receiving Follow-on Funds	Number of Proposals Submitted To Sponsors	Number of External Reviews
2011	9	86	10 DOE 3 Other 26 UofC
			39 Total
2012	15	112	19 DOE 6 Other 44 UofC
			69 Total
2013	29	154	10 DOE 4 Other 82 UofC
			96 Total
2014	20	132	12 DOE 3 Oher 36 UofC
			51 Total
Totals: 239 Projects	**73**	**484**	51 DOE 16 Other 188 UofC
			255 Total

LDRD Five-Year Funding Summary ($ in thousands) for Projects Active in FY 2014

Project Number	FY 2012	FY 2013	FY 2014	FY 2015 (a)	FY 2016 (b)	Total (c)
2011-210-R3	146.5	135.6	85.4			426.6
2011-213-R3	1,023.6	1,021.9	754.6			3,154.8
2011-214-R3	477.8	204.6	150.3			971.2
2011-217-R3	334.4	374.2	264.5			1,024.8
2012-012-R2	173.9	197.7	215.6			587.2
2012-015-R2	266.3	205.0	196.9			668.2
2012-016-R2	125.4	94.0	104.2			323.6
2012-061-R2	210.0	133.3	150.0			493.3
2012-072-R2	149.7	161.7	190.3			501.7
2012-074-R2	448.6	419.5	400.7			1,268.8
2012-087-R2	117.0	149.8	150.3			417.1
2012-114-R2	202.5	149.5	131.1			483.1
2012-180-R2	217.8	253.0	104.7			575.5
2012-181-R2	158.8	140.4	155.1			454.3
2012-202-R2	155.2	143.1	149.4			447.7
2012-204-R2	69.0	95.7	121.8			286.5
2012-205-R2	159.6	298.5	301.3	150.0		909.4
2012-206-R2	114.1	288.1	284.1	189.0		875.3
2012-208-R2	285.2	518.0	398.8			1,202.0
2012-209-R2	10.0	122.1	418.8	320.0		870.9
2013-013-R1		223.4	222.0	216.0		661.4
2013-016-R1		172.0	189.5	193.0		554.5
2013-022-R1		128.4	141.5	145.0		414.9
2013-035-R1		216.5	198.0	200.8		615.3
2013-036-R1		213.2	234.3	255.0		702.5
2013-063-R1		148.6	192.5	207.6		548.7
2013-070-R1		211.1	217.2	234.0		662.3
2013-080-R1		235.3	246.5	204.8		686.6
2013-096-R1		79.4	93.1			172.5
2013-100-R1		153.8	212.6	225.0		591.4
2013-111-R1		173.2	370.7	300.0		843.9
2013-116-R1		105.6	130.5	160.0		396.1
2013-148-R1		466.0	608.4	400.0		1,474.4
2013-152-R1		508.1	593.2	500.0		1,601.3
2013-154-R1		231.7	296.6	245.0		773.3
2013-156-R1		526.9	501.9	400.0		1,428.8
2013-165-R1		1,486.3	1,983.1	1,600.0	495.9	5,565.3
2013-168-R1		474.3	499.8	400.0		1,374.1
2013-171-R1		170.8	177.2	150.0		498.0
2013-173-R1		484.0	504.2	400.0		1,388.2
2013-177-R1		249.5	252.5	185.0		687.0
2013-178-R1		124.3	140.6	100.0		364.9
2013-184-R1		352.2	300.3	300.0	361.0	1,313.5
2013-194-R1		116.1	183.7	200.0		499.8
2013-199-R1		49.0	99.6	100.0		248.6

LDRD Five-Year Funding Summary ($ in thousands) for Projects Active in FY 2014

Project Number	FY 2012	FY 2013	FY 2014	FY 2015 (a)	FY 2016 (b)	Total (c)
2013-202-R1		283.4	306.1	120.0		709.5
2013-206-R1		126.1	390.8	155.0		671.9
2013-208-R1		199.6	185.7	185.0		570.3
2013-212-R1		49.1	99.6	100.0		248.7
2013-213-R1		99.1	198.3	155.0		452.4
2013-215-R1		386.8	453.0			839.8
2013-216-R1		197.7	419.8	428.0	116.3	1,161.8
2013-218-R1		7.4	98.7			106.1
2013-219-R1		514.0	2,044.1	900.0	163.2	3,621.3
2014-004-N0			119.8	125.0		244.8
2014-018-N0			107.5	188.0	191.6	487.1
2014-019-N0			130.0	140.0	134.0	404.0
2014-023-N0			199.5	200.0		399.5
2014-025-N0			201.8	190.0	210.0	601.8
2014-034-N0			138.7			138.7
2014-046-N0			196.8	198.0	225.0	619.8
2014-051-N0			165.4	173.5	215.0	553.9
2014-054-N0			159.8	166.0	190.0	515.8
2014-077-N0			160.6	178.0	185.0	523.6
2014-081-N0			191.7	198.0	210.0	599.7
2014-084-N0			190.7	180.0	200.0	570.7
2014-095-N0			158.2	165.0	175.0	498.2
2014-108-N0			161.8	211.1	192.0	564.9
2014-120-N0			303.5	300.0	300.0	903.5
2014-121-N0			302.7	300.0	320.0	922.7
2014-122-N0			266.4			266.4
2014-127-N0			174.6	100.0	80.0	354.6
2014-128-N0			110.1	300.0	325.0	735.1
2014-129-N0			300.0	300.0	300.0	900.0
2014-130-N0			346.4			346.4
2014-132-N0			127.0	150.0	160.0	437.0
2014-133-N0			329.7	300.0	340.0	969.7
2014-134-N0			269.7	292.0	301.7	863.4
2014-137-N0			182.3	230.0	207.0	619.3
2014-139-N0			213.8	200.0	202.0	615.8
2014-141-N0			196.4	400.0	528.4	1,124.8
2014-145-N0			199.4	300.0	546.8	1,046.2
2014-151-N0			762.8	750.0	932.4	2,445.2
2014-157-N0			279.6	300.0	300.0	879.6
2014-160-N0			217.3	175.0	250.0	642.3
2014-161-N0			312.3	300.0	500.8	1,113.1
2014-162-N0			303.2			303.2
2014-163-N0			94.9	100.0	200.0	394.9
2014-166-N0			200.0	155.0	260.0	615.0
2014-167-N0			217.9	155.0	350.0	722.9
2014-169-N0			253.9	250.0	250.0	753.9

LDRD Five-Year Funding Summary ($ in thousands) for Projects Active in FY 2014

Project Number	FY 2012	FY 2013	FY 2014	FY 2015 (a)	FY 2016 (b)	Total (c)
2014-174-N0			100.1	100.0	177.0	377.1
2014-175-N0			80.2	213.0	205.6	498.8
2014-177-N0			298.5	400.0	415.0	1,113.5
2014-181-N0			561.0	574.0	597.0	1,732.0
2014-182-N0			192.2	155.0	350.0	697.2
2014-183-N0			88.5	85.0	90.0	263.5
2014-184-N0			930.0	80.0	350.0	1,360.0
2014-185-N0			127.9	130.0	130.0	387.9
2014-187-N0			70.5	125.0		195.5
2014-188-N0			76.2	75.0		151.2
2014-189-N0			31.6	35.0		66.6
2014-190-N0			200.4			200.4
2014-191-N0*			171.0	347.4	350.6	869.0
2014-192-N0*			154.1	304.0	313.6	771.7
2014-193-N0			92.7	300.0	300.0	692.7
2014-194-N0			141.3	400.0	300.0	841.3
Totals	**4,845.4**	**14,268.6**	**29,075.9**	**21,016.2**	**13,496.9**	**83,307.0**

(a) FY 2015 figures represent allocations rather than actual expenditures.
(b) FY 2016 figures represent projections assuming the project continues into FY 2015.
(c) Totals for FY 2011 projects include funding from 2011 not shown in the table.
* FY 2014 late start projects may incur costs in FY 2017 that are not shown in the table.

LDRD

Research Reports

ANNUAL REPORT

2014

LDRD

Director's Competitive Grants

ANNUAL REPORT

2014

New High Energy Rechargeable Li Batteries Based on Selenium and Selenium-Sulfur Composite (Se_xS_y) Electrodes

2012-012-R2

Ali Abouimrane and Khalil Amine

Project Description

The objective of this project is to develop novel cathode materials for high-energy-density, rechargeable lithium batteries. An advanced energy storage system with high energy density, low cost, and great safety is the ultimate goal of current research. High-energy-density batteries are essential, especially for electric vehicles or plug-in hybrid electric vehicles. Achieving this goal requires breakthroughs in the area of novel electrode materials, since commercial batteries with typical capacities of 120–160 $mAhg^{-1}$ are far below what is demanded for these applications. In terms of high-energy-density batteries, Li/S and Li/O_2 batteries are attractive because they have the potential of providing 2–5 times the energy density of the lithium-ion batteries currently on the market. However, they all have some limitations, such as poor cycle performance, large cell polarization, and low conductivity of sulfur (S).

We are exploring the potential of selenium (Se), a d-electron-containing member of group 16 with higher electrical conductivity than S, as an electrode material for rechargeable batteries. Our focus is on the electrochemical performance testing of a series of new Se-containing materials, as well as understanding the mechanism of electrochemical behavior through the high-energy x-ray scattering technique (pair distribution function [PDF]), *in situ* battery x-ray diffraction (XRD), and x-ray absorption spectroscopy (XAS).

Mission Relevance

This project is relevant to DOE's mission in energy security and fundamental science. Warning signs of a new energy crisis necessitate our development of an alternative energy source that can reduce our overwhelming dependence on fossil fuel. Developing the best energy storage technique is a key challenge in achieving efficient renewable energy applications. This project's objective is to develop new energy storage materials with the high energy density needed for electric vehicle and large-scale smart grid applications. In addition, understanding electrochemical processes and improving battery performance are fundamental objectives of this work.

FY 2014 Results and Accomplishments

In FY 2012, Se and carbon composites were successfully tested as cathode materials for lithium (Li) batteries at room temperature and 55°C. Unlike the widely studied Li/S system, Li/Se batteries can be cycled to high voltages (up to 4.6 V) without failure. Extension of the cycling potential up to 4.6 V did not adversely impact the electrochemical performance of Li/Se-C, which sustains a capacity of 280 $mAhg^{-1}$ over 80 cycles (100 mAg^{-1}, ~C/6). In addition, preliminary investigation of a mixed chalcogenide system, SeS_2 and carbon composite, demonstrates that Se_xS_y-based electrodes can offer higher theoretical capacities than Se alone.

In FY 2013, we made significant progress in our focus area: screening electrolytes and understanding the mechanism. Discharge capacities of 350, 571, and 833 mAh/g for the Li/Se, Li/SeS_2, and Li/SeS_7 cells, respectively, were maintained for more than 50 cycles. The mechanism of Li insertion in Se for Li/Se battery in ether-based electrolyte was proposed, so that Se would be reduced into Li_2Se with the formation of multiple soluble polyselenides, which would cause the shuttle effect and energy decay.

In FY 2014, the lithiation mechanism of the Li–Se cell in a carbonate-based electrolyte was further investigated. It was found that Se was directly reduced to Li_2Se in discharge, with no intermediate phases detected by *in situ* XRD or XAS (Figure 1). The reason is that the redox products Se and Li_2Se, as well as lithium polyselenides, were insoluble in the carbonate-base electrolyte. Therefore no shuttle effect is expected. The key to further enhancing Li–Se battery performance is to improve the lithium ion and electron transport property and intensify the interaction between Se and conductive matrixes. This work demonstrated another advantage of the Li–Se cell over the Li–S cell — that the absence of soluble polyselenides with the less expensive carbonate-based electrolyte avoids the need to prevent the shuttle effect.

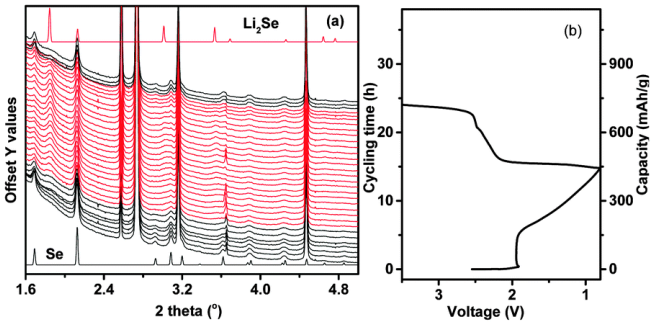

Figure 1. In situ *high-energy XRD characterization of Li–Se cell in GenII electrolyte cycled between 0.8 and 3.5 V with a charging rate of 30 mA g^{-1}: (a) XRD pattern of the cell during cycling and the reference material Se and Li_2Se, and (b) voltage profile.*

Revealing Lithium-Based Battery Performance by *in situ* Characterization

2012-061-R2

Dean Miller

Project Description

The project is designed to improve our understanding of lithium battery operation by bridging the gap between macroscale diagnostics and nanoscale characterization. In particular, this research focuses on characterizing isolated single particles, providing a direct correlation between electrochemical performance and microstructural evolution. Our approach uses *in situ* and *ex situ* characterization of microscale and nanoscale batteries in operation to help determine what makes them work and, perhaps more importantly, what makes them stop working.

Mission Relevance

This project directly addresses the DOE mission to transform the nation's energy system, particularly in the area of electric vehicle technology, by illuminating the underlying mechanisms of performance degradation in lithium (Li)-based batteries.

FY 2014 Results and Accomplishments

In the first two years of this project, we developed a novel approach for carrying out electrochemical cycling of single Li-ion battery cathode particles that allows a direct measurement of electrochemical performance for a single particle. We focused on a scanning-electron microscopy-based imaging approach that proved useful in characterizing mesoscale phenomena in oxide cathode materials during electrochemical cycling. *In operando* characterization of single $LiNi_{0.8}Co_{0.15}Al_{0.05}O_2$ particles provided an example of the new insight this approach could provide by revealing the early onset of particle cracking and the progression of cracking as a function of electrochemical cycle. This observation led to a new model for performance degradation in batteries made from this material.

In FY 2014, we focused on exploiting our new approach for *in situ* and *in operando* characterization of single Li-ion battery cathode particles. Each single particle can be characterized in detail by electron and x-ray approaches, providing a better correlation between performance and microstructural evolution.

We focused on a different class of Li-battery high-capacity cathode materials, which have a graded composition with a nickel (Ni) -rich core (composition in the general range of $LiNi_{0.8}Co_{0.1}Mn_{0.1}O_2$) and a manganese (Mn) -rich periphery (composition in the general range of $LiNi_{0.5}Co_{0.2}Mn_{0.3}O_2$). The concept for these materials is that the Ni-rich core offers high capacity, while the Mn-rich periphery minimizes detrimental interactions with the electrolyte. However, it has also been found that these materials exhibit much better long-term performance, with less "fade" in capacity over many cycles. This behavior is a significant improvement over that of $LiNi_{0.8}Co_{0.15}Al_{0.05}O_2$ (i.e., NCA), which shows much more significant capacity fade. Because our *in situ* studies suggest one of the mechanisms for capacity fade in NCA is the particle fracture that occurs during cycling, we applied our approach to the graded materials to see if this was an important factor in their improved performance.

An example of the electrochemical performance of a single $LiNi_{1-x-y}Co_yMn_xO_2$ compositionally graded particle (hereafter referred to as a "gradient" material) is shown in Figure 1. The voltage versus capacity plot shows an increase in capacity for the first 13 cycles but a decrease for the 14th cycle. A scanning electron microscope (SEM) image of the microstructure of the particle after the 14th cycle (Figure 1 inset) reveals a moderate degree of cracking (grain-to-grain separations). This microstructure is generally similar to that observed in NCA, but with two notable differences. First, the gradient particle shows an increasing capacity for a much larger number of cycles that we have ever observed for NCA. Second, the particle cracking tends to be radial rather than isotropic.

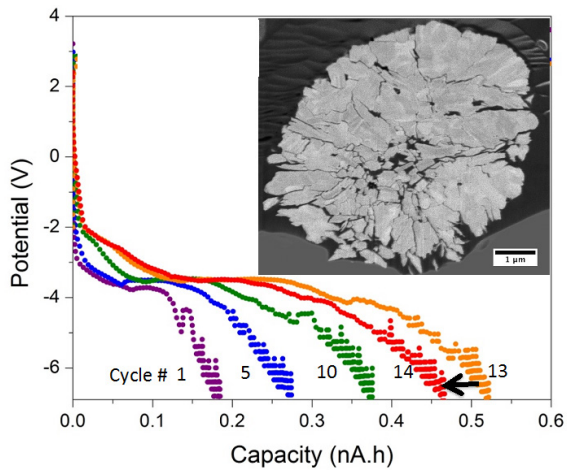

Figure 1. Voltage versus capacity plot measured for a single $LiNi_{1-x-y}Co_yMn_xO_2$ gradient particle, and SEM image of the particle structure after 14 cycles.

These differences are illustrated more definitively in Figure 2, which shows the microstructural evolution of a single NCA particle compared to that of a single gradient particle as a function of cycle. The NCA particle shows extensive cracking and fragmentation in just a few cycles, whereas the gradient particle shows very little cracking after five cycles, and the few small cracks that are

observed tend to be radial. Together, the data shown in Figures 1 and 2 confirm the aggressive, isotropic fracture mode in NCA and a much more fracture-resistant microstructure, with the anisotropic fracture being less deleterious to performance for the gradient material. Figure 3 compares the microstructure of these materials when subjected to *in situ* cycling with that observed in material harvested from a coin cell cycled 50 times. This comparison confirms that the behavior we observed in our single particle measurements is indeed representative of real battery systems.

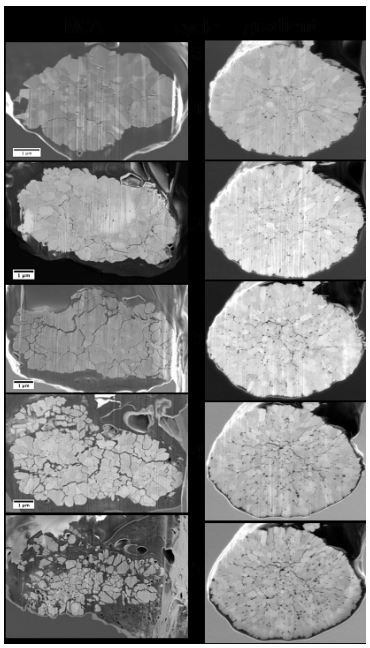

Figure 2. SEM images of an NCA particle and a gradient ($LiNi_{1-x-y}Co_yMn_xO_2$) particle as a function of cycle.

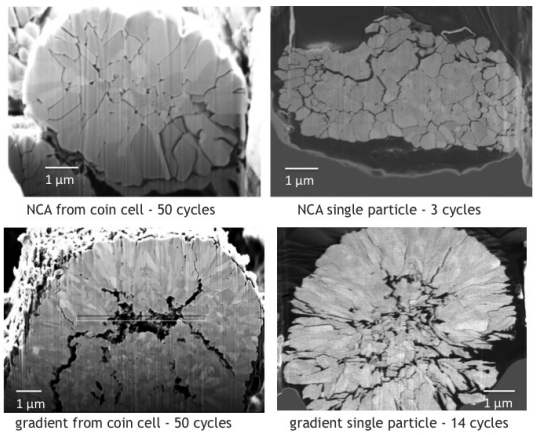

Figure 3. SEM images of NCA and gradient ($LiNi_{1-x-y}Co_yMn_xO_2$) material after cycling. Material cycled 50 times in a coin cell is compared with a corresponding single particle cycling measurement for the number of cycles indicated.

The microstructural basis for the radial fracture in gradient materials is illustrated in Figure 4. Transmission electron microscopy (TEM) revealed the radial grain structure that is prevalent in the gradient material. Figures 4b and 4c show the composition gradient for Mn and Ni, respectively, and also reveal the radial grain structure. The radial grain structure and refined grain size lead to particles that are more resistant to fracture; also, the fractures that do eventually appear are less detrimental to performance because they do not lead to isolated fragments that can lose electrical connectivity, as is the case for NCA.

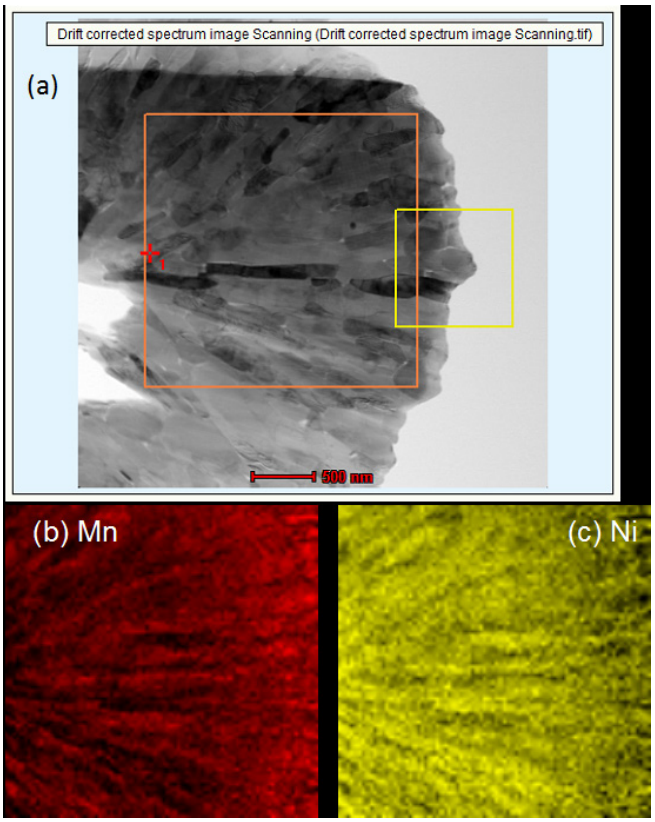

Figure 4. TEM data from gradient ($LiNi_{1-x-y}Co_yMn_xO_2$) material. (a) Bright-field TEM data reveal a radial-columnar grain structure associated with the gradient material. Composition maps (b) and (c) were obtained from energy dispersive x-ray spectrum imaging. They further reveal the columnar structure but also the compositional gradient for Mn and Ni, respectively.

Graphene-Enabled Superlubricity: Vanishing Friction and Wear in Static and Sliding Contacts

2012-072-R2

Anirudha V. Sumant and Ali Erdemir

Project Description

The main objective of this project is to understand the origin of the superlubric behavior of graphene, which our team recently discovered while conducting tribological studies on multilayer graphene films at the macro scale. This superlubricity, which we saw for the first time when

graphene slid against diamond-like carbon (DLC) surfaces at macro scale at room temperature, is important from both scientific and technological points of view. This project involves systematic tribological studies from macro to micro to nano scales in which various material pairs are compared in controlled atmospheric conditions. We used advanced surface characterization techniques to make detailed characterizations of the wear tracks in order to understand the surface chemistry of graphene in relation to its unusual tribological behavior.

Mission Relevance

This project is relevant to DOE's goal to find innovative ways to reduce energy consumption through fundamental research on materials. The total energy consumed in the United States and in Europe by industrial motor-driven systems (e.g., pumps, compressors, fans) is about 1.36 trillion kWh/year. It is estimated that these systems lose about 15%, or 204 billion kWh/year, as a result of motor inefficiency. About 20% of this loss, or ~41 billion kWh/year, is due to mechanical losses, and, of this, roughly 20% or 8.2 billion kWh/year can be attributed to bearings. Assuming a conservative approach, a minimum reduction in energy loss of 30% due to the low friction offered by new materials would yield a potential energy savings of 2.46 billion kWh/year; this is equivalent to 420,000 barrels of oil. These numbers make it obvious that research to discover new materials that could reduce wear and friction is important. If such research was fully developed and demonstrated, it could have huge positive impacts on many mechanical and tribological applications that could lead to tremendous savings on energy.

FY 2014 Results and Accomplishments

This project started in FY 2012. It was based on promising results in which we first showed that ultralow friction could be achieved when DLC-coated steel balls were slid against a few layers of graphene grown on a nickel (Ni) surface by using a thermal chemical vapor deposition (CVD) process. We studied macro-scale tribological properties of different carbon-based tribo-pairs under various ambient conditions to explore the nature of achieving ultra-low friction and wear, and we established conditions for achieving reproducible superlubricity. Then we demonstrated that multilayer graphene, either CVD-grown or deposited from graphene-containing ethanol solution on nickel substrate, can provide an extraordinarily low coefficient of friction (COF) (0.003–0.005) and negligible wear for a prolonged time (more than 5,000 cycles).

In FY 2013, we explored the successful role of graphene as a lubricant for steel tribopair. We showed that graphene layer, a few nanometers thick with less than 25% surface coverage, could drastically reduce the friction (by factor of four to five) and the wear (by four orders) of sliding steel surfaces, regardless of the operating environment. This was a major breakthrough, since no solid lubricant until then had demonstrated low friction and wear in a dry or humid environment.

In FY 2014, we concentrated on gaining a basic understanding of the graphene-enabled superlubricity mechanism. In experiments, we showed that stable macroscale superlubricity was facilitated by graphene nanoscroll formation, when graphene was used with crystalline nanoparticles. Figure 1 shows the successfully achievement of a nearly zero COF when graphene was used with diamond nanoparticles. Transmission electron microscopy (TEM) analysis of the wear track produced in a superlubricity sliding regime revealed that a large fraction of nanodiamond particles were wrapped by graphene nanoscrolls. Then molecular dynamics (MD) simulations were performed to explore the scroll formation mechanism and determine the mesoscopic link that bridges the nanoscale and macroscale tribological results. The simulations suggested that diamond nanoparticles can activate and guide the folding of initially planar graphene patches. During sliding in a dry environment, graphene tends to form scrolls, which reduce the contact area and translate into a low friction state. The diamond nanoparticles facilitate and lead the scroll formation by overcoming the potential barriers associated with graphene deformation. The scrolls are formed by two mechanisms. First, graphene platelets are highly reactive and easily attach to the dangling bonds present on the surface of diamond nanoparticles, initiating the scroll formation. Second, during the sliding process, the graphene patches encounter the three-dimensional structure of diamond nanoparticles, which act as an obstruction and make it preferable for graphene to wrap around.

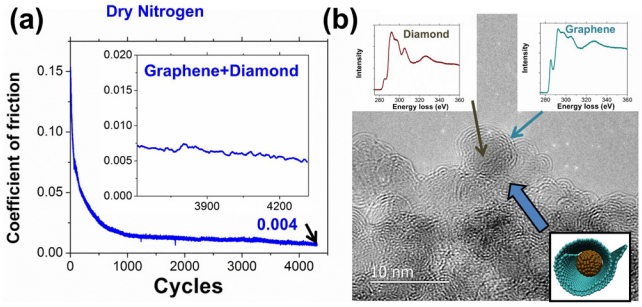

Figure 1. (a) The COF for DLC ball sliding against graphene coupled with diamond nanoparticles reaches its lowest value of ~0.004, which is assumed to be the superlubricity regime. (b) TEM images of the wear debris demonstrate scroll formation.

We also concentrated on understanding (a) the basic mechanism of graphene-enabled lubricity when a layer only one atom thick was applied to the steel surface and (b) ways to extend graphene's friction- and wear-reducing abilities (Figure 2). We showed that when tested in hydrogen, a single layer of graphene on steel could last for 6,400 sliding cycles, while a few (three to four) layers

could last for 47,000 cycles. Moreover, these graphene layers completely ceased to wear, despite the severe sliding conditions — including high contact pressures (~0.5 GPa) — typically observed in macroscale wear tests. The computational simulations showed that the extraordinary wear performance originated from hydrogen passivation of the dangling bonds in ruptured graphene, leading to significant stability and a longer lifetime of the graphene protection layer.

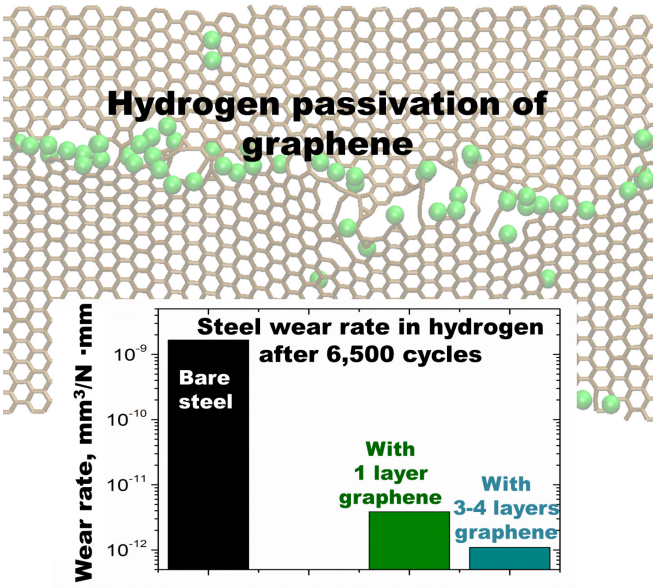

Figure 2. The mechanism of extraordinary wear resistance of a graphene layer on steel just one atom thick is revealed. A single layer of graphene can reduce steel wear by three to four orders of magnitude. The wear-life of graphene significantly increased when it was tested in a hydrogen environment. Hydrogen played a crucial role in preventing graphene from wear-induced damage by passivating carbon dangling bonds.

This work resulted in the following inventions/patents:

Sumant, A., A. Erdemir, J. Choi, and D. Berman, "Superlubricating Graphene Films." Patent Application No. 13/553,484 filed July 2012 and published January 2014. [ANL-IN-11-056].

Sumant, A., A. Erdemir, J. Choi, and D. Berman, "Superlubricating Graphene and Graphene Oxide Films." Patent Application No. PCT/US2013/051121 filed July 2013 and published January 2014. [ANL-IN-11-056].

Sumant, A.V., D. Berman, and A. Erdemir, "Reduced Wear and Friction on Sliding Steel Surfaces Using Solution Processed Graphene." Invention report disclosed July 2012. [ANL-IN-12-069].

Sumant, A.V., D. Berman, and A. Erdemir, "Nanoparticles-enabled Superlubricity in Graphene at Macroscale." Invention report disclosed February 2014. [ANL-IN-14-029].

Sumant, A.V., D. Berman, and A. Erdemir, "Effect of Hydrogen in Extending the Wear-life of Single and Few Layer Graphene Coated Steel Contacts." Invention report disclosed March 2014 and patent application filed June 2014. [ANL-IN-14-027].

Sumant, A.V., D. Berman, and A. Erdemir, "Graphene as a Protective Coating and Best Lubricant for Electrical Contacts." Invention report disclosed October 2014. [ANL-IN-14-105].

Rechargeable Nanofluids Technology for Electrical Energy Storage

2012-087-R2

Elena V. Timofeeva, Christopher Pelliccione, and Dileep Singh

Project Description

Flow batteries have multiple advantages over solid-state batteries, such as the separation of their power and energy components, ability to be rapidly replenished to a fully charged state, long cycle life, low maintenance requirements, and tolerance to overcharging/overdischarging. However, because of the low specific energy density of electrolytes (limited by the solubility of redox salts), flow batteries have not been seriously considered for transportation.

To solve that problem, we are developing novel rechargeable nanofluids (nanoscale electrode materials stably dispersed in electrolyte) that effectively charge and discharge as they are pumped through custom-designed flow cell(s). They represent a high-energy-density, rechargeable, renewable, and recyclable electrochemical fuel. Using nanoelectrofuels will increase the specific energy density of flow batteries to that (and higher than that) of solid-state lithium (Li)-ion batteries, making them a very attractive energy storage medium for electric vehicles (EVs).

We are working on this project with collaborators from the Illinois Institute of Technology (IIT).

Mission Relevance

This project expands the scientific foundations for new and improved energy storage technologies, addressing one of DOE's major mission areas: energy security. A flowable energy storage format for nanoelectrofuels addresses anxiety over the range of EVs in two ways. First, it improves energy density at the system level by 50%, with the same chemistries as those in solid state batteries, by reducing the amount of packing. Second it allows an EV's charge to be quickly replenished by

replacing the discharged fluid for the charged fluid. The energy density in the proposed nanofluids exceeds the U.S. Advanced Battery Consortium's long-term EV battery goal of 300 Wh/L, and the projected costs meet the transportation goal of less than $125/kWh.

FY 2014 Results and Accomplishments

In FY 2012, by using *in situ* x-ray adsorption spectroscopy (XAS), the research team demonstrated charging of electroactive nanofluids prepared by dispersing battery anode nanoparticles in Li-ion electrolytes. XAS results, combined with electrochemical characterization of the anode material, indicated partial charging/lithiation of unsupported nanoparticles in suspension, similar to the lithiation of the electrode nanoparticles in a solid-state battery assembly. However, as a result of limitations of the cell design and nanofluid formulations, only partial charging of nanoparticles was demonstrated, with no observation of significant discharge capacity.

In FY 2013, work focused on optimizing individual rechargeable nanofluids and their electrochemical performance versus the same nanomaterials in coin cell configuration. Unique hybrid nanomaterials for the battery anode were developed. High-energy-density tin (Sn) and Sn oxide nanoparticles were formed directly on nanographite sheets (GnP) through a wet chemistry route. By using the modified particle morphology, we achieved good electrical conductivity to an ensemble of individual anode nanoparticles and kept the size of individual particles under the self-healing threshold to address degradation of Sn nanoparticles due to the well-known volume expansion mechanism. An *ex situ* XAS study of cycled electrodes indicated the presence of amorphous Sn oxides in Sn samples. We found $Sn_3O_2(OH)_2$/GnP to be the most stable of a variety of our hybrid nanoparticle products, so we decided to use it as the model compound for our rechargeable nanofluid study.

In FY 2014, we synthesized sufficient amounts of $Sn_3O_2(OH)_2$/GnP anode material to conduct extensive electrochemical studies of it in solid-casted form (Figure 1a, and b). Despite the premise of having nanoparticles under the healing threshold and having graphite support for them to improve electrical contact to each particle, the charge/discharge capacity of the material was still observed to degrade fairly rapidly. An *in situ* XAS study (Figure 1c) of this electrode revealed a new mechanism for the degradation of this material that was not based on volume expansion but instead related to the nanoscale arrangement of Sn clusters within nanoparticle crystals. Charge/discharge cycling caused atomic shifts within those structures, resulting in the segregation of metallic Sn clusters, inside lithium oxide (Li_2O) cells, as depicted in Figure 1d. The resulting arrangement insulated atomic Sn clusters from the rest of the anode and prevented their participation in electrochemical processes.

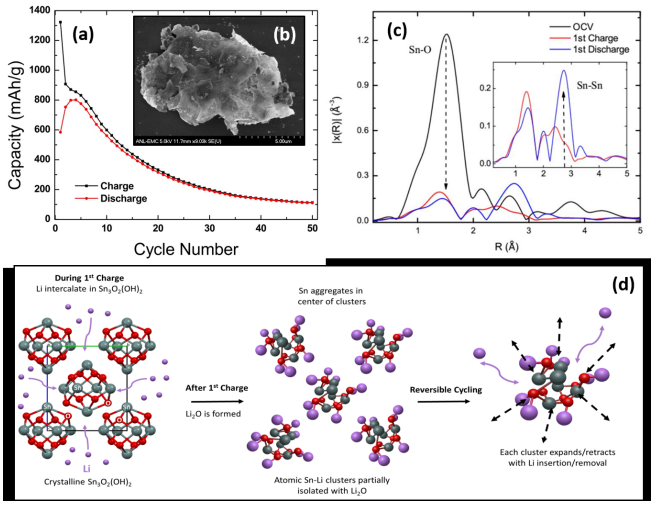

Figure 1. Investigation of solid casted $Sn_3O_2(OH)_2$/GnP nanoparticle anode. (a) Charge/discharge capacity as a function of cycle number, showing an initial discharge capacity of ~800 mAh/g that rapidly fades, losing more than 75% of its storage capacity in less than 50 cycles. (b) SEM of starting nanocomposite material. (c) Fourier transformed in situ *XAS spectra from solid casted electrode in consequent charged and discharged states. Subsequent modelling of those spectra revealed the mechanism for such rapidly fading capacity in this material, highlighting the importance of atomic arrangement and nanoscale architecture for long-term performance of high-capacity Li-ion battery materials.*

These hybrid nanomaterials were dispersed in a Li-ion electrolyte and tested in a custom nanoelectrofuel test cell simulating flow with a magnetic stirrer. The cell had two compartments (nanofluid and counter-electrode compartment) separated by a typical membrane used in Li-ion batteries. Copper mesh was used as the current collector in the nanofluid compartment, and Li metal was used as the counter-electrode immersed in the base 1 M $LiPF_6$ electrolyte.

Figure 2 summarizes experimental results from a 5 wt% $Sn_3O_2(OH)_2$/GnP suspension. Initial charging at rates typical for solid casted electrodes resulted in large overpotentials, and no nanoelectrofuel charging or discharging was observed. We gradually reduced the charge rates to see which current density was comparable with nanofluid charging kinetics. As Figure 2a shows, a charge rate of C/160 (based on the theoretical capacity of this material) was the first current density at which significant charge and discharge capacity was achieved. Scanning electron microscopy (SEM) of the current collector and nanoparticles separated from electrolyte after electrochemical tests showed significant formation of a solid electrolyte interphase (SEI) on the current collector.

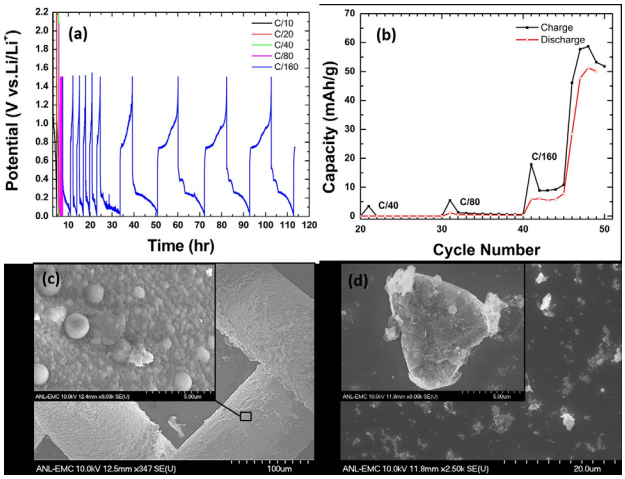

Figure 2. Investigation of $Sn_3O_2(OH)_2$/GnP nanoelectrofuel anode. (a) Charge/discharge curves of 5 wt% suspension of nanoparticles in 1 M $LiPF_6$ electrolyte (LIPASTE A49) at different chagrining rates (C-rates). (b) Summary of charge and discharge capacities as a function of cycle number for different C-rates, showing that nanoelectrofuel performance improves as the charge rate goes down. For the given charge rate, the discharge capacity improves with the number of cycles. Irreversible charge capacity spikes on the first cycle with each change in the c-rate, which is most likely due to the formation of SEI. SEM examination of the current collector (c) and nanomaterials (d) separated from the electrolyte after electrochemical tests, showing the formation of amorphous SEI, mostly on the current collector, and some signs of SEI formation on the unsupported nanoparticle surface. A small fraction of nanoparticles was incorporated into the SEI at the current collector.

Our experiments showed that nanoparticles in suspension can be used as energy storage media with multiple charge and discharge cycles of the fluids. However, the complexity of the nanofluid electrode was also revealed. More studies are needed to investigate the kinetics of suspension electrodes as a function of particle material, size, and morphology, since such an understanding is critical to effectively engineer flow systems for nanoelectrofuels.

This research resulted in the following inventions/patents:

E. Timofeeva, D. Singh, J. Katsoudas, and C. Serge. "Rechargable Nanoelectrofuel Electrodes and Electrochemical Devices for High Energy Density Flow Batteries." Invention report disclosed January 2013 and patent application filed May 2013. [ANL-IN-12-122].

E. Timofeeva, J. Katsoudas, C. Segre, D. Singh, J. Kropf, and J. Terry. "Radiolysis Mediated Charging of Nanoelectrofuels from Different Sources of Radiation." Invention report disclosed March 2014. [ANL-IN-14-036].

Aspects of this research will continue with resources provided by the Advanced Research Projects Agency-Energy (ARPA-E) Robust Affordable Next-Generation Energy Storage System Program (RANGE).

Novel Non-Carbon Catalyst Support for Polymer Electrolyte Fuel Cells

2012-180-R2

Xiaoping Wang, Nancy Kariuki, Debbie Myers, and Tammi Nowicki

Project Description

The objective of the project is to develop a new class of durable, non-carbon supports for state-of-the-art platinum (Pt) and Pt-alloy cathode electrocatalysts for polymer electrolyte fuel cells (PEFCs) that will significantly improve their durability and performance. These new support materials, based on transition metal silicides (TMSs), will be much more stable than the carbon blacks used in current PEFCs. The scope of the research includes identifying the most stable silicide support candidates, investigating the interaction between the support and catalyst, synthesizing the silicide-supported Pt electrocatalysts with the desired characteristics, and characterizing the activity and stability of these materials in simulated fuel cell environments.

Mission Relevance

This project is relevant to DOE's missions in basic science and energy. Improving the durability of PEFC technology by developing durable catalyst support for PEFCs is one of the missions of DOE's Fuel Cell Technologies Office. Successful development of silicides as catalyst supports will help to meet the target set by DOE of reaching a PEFC performance degradation level of less than 40% over 5,000 hours of operation by 2017, for automotive application.

FY 2014 Results and Accomplishments

In the first two years of this project, the chemical and electrochemical stability and the oxygen reduction reaction (ORR) activity for seven TMSs were investigated to identify the best support candidates. Three TMS candidates were chosen as support materials for making Pt electrocatalysts. Various synthetic approaches — colloidal synthesis with different capping agents, strong electrostatic adsorption (SEA), and wet impregnation — for making the silicide-supported Pt catalysts with the desired phase, composition, and microstructure were then explored. The prepared Pt/silicide catalysts were characterized by using transmission electron microscopy (TEM), x-ray diffraction (XRD), temperature-programmed oxidation/ reduction (TPO/TPR), and rotating disk electrode (RDE) techniques. Even though the best Pt/silicide catalyst exhibited significantly improved ORR activity over the silicide support alone, its activity was still far below that of a commer-

cial Pt/C catalyst. The poor ORR activity of the Pt/silicide catalysts could be attributed to the poor dispersion of Pt nanoparticles on the low surface area support and/or the possible chemical interaction between Pt and the support.

In FY 2014, we continued exploring and optimizing the synthetic procedures to improve the dispersion of Pt nanoparticles on the silicide support, and to minimize the interaction between the Pt and the support. The properties of the synthesized Pt/silicide catalysts were greatly improved by adopting a procedure to oxidize the surface of the silicide support before anchoring Pt nanoparticles and by eliminating a post-synthesis heat treatment. Our results and accomplishments are provided here in detail.

Synthesis of Pt/Silicide Catalyst using Oxidized Silicide Support

The silicide-supported Pt catalysts prepared earlier by using the as-received commercial silicides always exhibited much lower ORR activity than the commercial Pt/C catalysts, which was found to be mainly due to agglomeration and poor distribution of the Pt nanoparticles on the support. Considering the refractory nature of the silicide support and its low surface area, it was imperative that a surface treatment be done to improve the number of support surface active sites for anchoring Pt nanoparticles. A solution mixture of sulfuric acid and hydrogen peroxide was thus used to oxidize the support surface. The duration of this chemical treatment was optimized and 5 hours was found to yield the best ORR activity for the catalyst. Electrochemical characterization of the oxidized support showed that the chemical treatment did not significantly alter the electrochemical property of the support, which is consistent with the observation that the XRD pattern of the support was virtually the same with and without the treatment.

Both a citrate-based aqueous colloidal method and SEA were used to synthesize Pt nanoparticle catalysts with the oxidized support. In the colloidal method, hexachloroplatinic acid was reduced in the presence of tri-sodium citrate at pH 7 below 5°C, forming a colloid of Pt nanoparticles capped with citrate ions. After adding a desired amount of the treated silicide suspension to give a Pt loading of 20 weight-percent on the support, the pH of the mixture was lowered to release Pt nanoparticles from the citrate ions as a result of the protonation of the citrate ions, leading to precipitation of the Pt nanoparticles onto the support. The final Pt catalyst was obtained by centrifugation followed by vacuum drying. Before further characterization, the catalyst was lightly ground to break up large aggregates formed during drying.

In the SEA procedure, the Pt/silicide catalyst was prepared by impregnating a small volume of hexachloroplatinic acid solution onto the desired amount of the treated support, followed by a heat treatment in a reducing atmosphere at 200°C. During the impregnation step, the solution pH was controlled so that the adsorption of the Pt precursor onto the support was facilitated through the attraction of the opposite charges on the support surface.

Characterization of Pt/Silicide Catalysts on the Chemically Treated Support

The ORR activity of the synthesized Pt/silicide catalysts with the oxidized support was characterized by cyclic voltammetry combined with the thin-film RDE (TF-RDE) technique. Figures 1A and 1B show, respectively, the typical ORR cyclic voltammograms (CVs) obtained in O_2-saturated 0.1 M H_2SO_4 and the background CVs obtained in deaerated 0.1 M H_2SO_4 for the Pt/silicide catalysts with the oxidized silicide support, compared with those using the as-received support. Regardless of the synthesis approach used to fabricate the Pt/silicide catalyst (i.e., colloidal or SEA), the oxidized support exhibited significantly better electrochemical properties than the as-received support. The Pt/silicide catalyst with the oxidized support exhibited distinct Pt redox features in background CVs (orange and magenta curves in Figure 1A) and the well-defined sigmoidal shape of the ORR CVs with a limiting current plateau (orange and magenta curves in Figure 1B), resembling those observed for commercial Pt/C catalysts. The Pt/silicide catalysts with the as-received silicide support exhibited no noticeable Pt redox features in the background CVs (blue and black curves in Figure 1A), and their ill-defined ORR CVs showed a much lower ORR current, with no limiting current plateau (blue and black curves in Figure 1B).

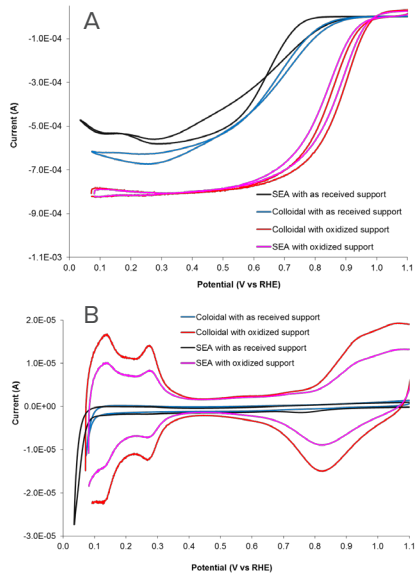

Figure 1. Cyclic voltammograms of various Pt/silicide catalysts prepared by using as-received silicide or chemically treated silicide as the support and by using either colloidal synthesis or the SEA method obtained respectively, the O_2-saturated electrolyte (A) and the deaerated 0.1 M H_2SO_4 (B) electrolyte. Scan rate was 10 mV/s; rotation rate was 1,600 revolutions per minute (rpm).

All these results indicate that using the oxidized silicide support yielded more active Pt/silicide catalysts. For the Pt/silicide catalysts that were prepared by using the oxidized support, their well-defined CVs allowed quantification of their ORR activity. The ORR specific activity of the Pt supported on the oxidized silicide was determined to be 340 $\mu A/cm^2$ by the colloidal method and 302 $\mu A/cm^2$ by SEA. While these numbers are higher than those determined for commercial Pt/C catalysts under the same condition, their ORR mass activity was significantly lower than that of the commercial Pt/C catalysts, which could be partially attributed to the poor dispersion of the Pt nanoparticles on the silicide, as indicated by the TEM/energy-dispersive x-ray spectroscopy (EDS) characterization that the destitution of the Pt nanoparticles was still not uniform and agglomeration still occurred. Another possible reason could be the formation of platinum silicide, which could have suppressed the catalyst activity.

Since the main purpose of the work was to develop more stable support materials for PEFC cathodes, the stability of the oxidized silicide support was investigated by running a DOE support testing protocol. The Pt supported on oxidized silicide was incorporated into a TF-RDE and cycled in perchloric acid electrolyte between 1.0 and 1.6 V at 100 mV/s for 24 hours. The electrochemically active surface area (ECSA) of the electrode before and after the cycling was compared. For comparison, the identical experiment was performed for the commercial Pt/C catalysts. The results showed that the Pt supported on the oxidized silicide lost 3% of its ECSA, while the Pt/C lost 16% of its ECSA. This reveals that the silicide support was indeed more stable than the standard carbon support. However, further work is needed to improve the dispersion of Pt on the silicide support to make Pt/silicide a viable catalyst material for practical PEFCs.

Curing Cancer with the Power of Fireflies

2012-181-R2

Tijana Rajh, Harry Fry, and Tamara Koritarov

Project Description

Photodynamic therapy (PDT) is an emergent technology used for the treatment of cancers, psoriasis, and other autoimmune diseases. In this method, light energy is converted to chemical energy, creating highly reactive oxygen species (ROS), which, under appropriate conditions, are highly disruptive to cell metabolism and lead to cell death. However, current PDT technology is limited by low penetration of light. To overcome this limitation, we linked a light source to a therapeutic nanoparticle for light to travel alongside the therapy to the intended treatment location. Our approach involves functionalizing semiconducting titanium dioxide (TiO_2) nanoparticles with the light-producing protein luciferase found in fireflies. Luciferase yields bioluminescence in the presence of its substrate, luciferin, and the highly energetic molecule adenosine triphosphate (ATP), which has recently been found to be present in a 100-fold excess at tumor sites. The light from the luciferase then activates attached semiconductor nanoparticles which results in efficient ROS production, inducing programmed cell death. The TiO_2-luciferase conjugates are also functionalized with antibodies to specifically target cancerous cells by binding the biomarkers expressed on their surface.

Mission Relevance

This project is relevant to key DOE missions in basic science. We believe that this approach represents a breakthrough in PDT technology because it eliminates PDT's major limitation. The approach's advantage is that it can be used not only for early detection but also for early treatment of cancers and autoimmune diseases. Moreover, light that is created *in situ* can also be used to power a variety of light-driven devices *in vivo,* deep in the tissue.

FY 2014 Results and Accomplishments

We developed an improved method of PDT to overcome the previous depth limitation by creating the light at the location of the tumor *in situ*. During FY 2012, TiO_2-luciferase conjugates (TiDoL) were developed, and it was confirmed that the photon-emitting oxidation of luciferin by the enzyme luciferase is, indeed, able to transfer energy to the TiO_2 nanoparticle when luciferase is conjugated to the particle surface. This energy transfer was confirmed by multiple photochemical and electrochemical methods. In FY 2013, we began to test the ability of TiDoL nanoparticles to generate reactive oxygen species and induce cell death in an A172 glioblastoma cell culture model.

During FY 2014, we determined the optimal conditions for making TiDoL and TiDoL-C225 suitable for use in *in vitro* and *in vivo* PDT treatments. We conjugated a bioluminescent protein, luciferase, to a semiconductor nanoparticle, TiO_2, and simultaneously to a cell specific antibody, anti-EGFR monoclonal antibody C225, in order to target colon cancer cells HCT116. We established the nanoconjugate synthesis protocols for TiO_2 and luciferase (TiDoL) and C225 (TiDoL-C225) by using DOPAC linkers. The nanoconjugate TiDoL-C225 was then activated by ATP and luciferin in a reaction that creates ROS and induces apoptosis in the tumor cells. The TiDoL-C225 nanoconjugate is able to bind specifically to colon cancer cells as the C225 antibody recognizes EGFR expressed at the surface of the cells. Furthermore, when it is activated, it will react only with the tumor cells.

The optimal cell staining protocols were developed in order to visualize the treatment process and analyze it with the laser confocal microscope (Figure 1a). The TiDoL nanoconjugate was found to be operational and effective at killing tumor cells only after being activated by luciferin and ATP, which then enhances the control we have over the therapy. The TiDoL-C225 nanoconjugate increases the efficacy of binding to tumor cells and the speed of the initiation of apoptosis, even in concentrations lower than those of the free TiDoL nanoconjugate. It was found that the TiO_2-modified C225 antibody undergoes receptor-mediated endocytosis, thus making the complex extremely responsive to light.

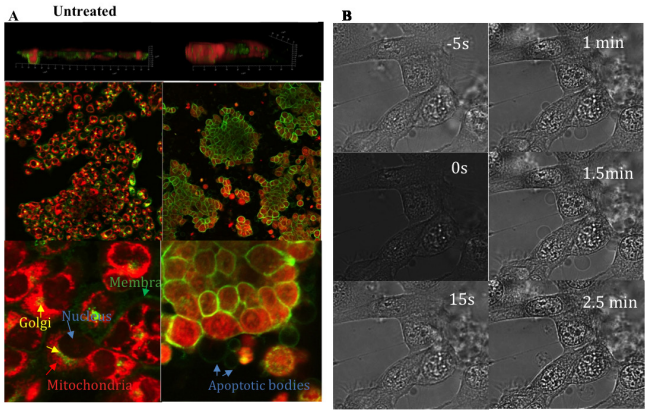

Figure 1. Treatment of HCT116 cells with TiDoL-C225 with luciferin. (a) Ex situ *imaging: The cells were stained 24 hours after treatment (60-minute incubation with luciferin) by using wheat germ agglutinin (green), which interacts with glycoproteins in membranes and Golgi apparatus, while MitoTracker (red) was used for staining mitochondria. After treatment with luciferin, the cells lost their morphological features, the Golgi apparatus disappeared, and proteins from mitochondria were present throughout the cell, suggesting increased permeability of the nuclear membrane. The outer membranes, however, preserved their integrity, with the apparent formation of apoptotic bodies that contained some of the mitochondrial proteins stained by mitotracker. Top: This shows a side view of the cells. Untreated cells are very thin and spread on the support, while treated cells are detached from the support and appear to be smaller and thicker. Middle: This shows a large imaged area of cells and reveals that 100% of them were affected by the injection of luciferin. Bottom: This zoomed-in region shows details of the morphological changes that occurred upon cell treatment. (b)* In situ *imaging: This shows the dynamics of the interaction of TiDoL-C225 with cells and the effects from the addition of luciferin. Luciferin was added in the sixth frame of the imaging. As the luciferin was added the image became dark as a result of enhanced absorption of light by luciferin. The first changes were observed 30 seconds after the addition of luciferin, when cells started to form apoptotic bodies that grew until 1.5 minutes passed, with concomitant reorganization of the nucleus. A minute after that, the cells injected their cytoplasmic material into the apoptotic bodies in preparation for cell digestion with microphage.*

Finally, our approach allowed us to monitor the tumor cells as they began to undergo apoptosis in less than 5 minutes after the luciferin and ATP were added to activate the reaction (Figure 1b). We observed all the morphological changes that are associated with apoptotic cell death, including detachment from the support, cell shrinking, rearrangement of nuclear chromatin, cell blabbing, cell budding, and the formation of picnoctic nuclei. The formation of the membrane-enclosed apoptotic bodies, which can be phagocyted and digested by nearby resident cells and therefore do not involve changes associated with inflammation, was directly observed. The advantage of this method of PDT with the TiDoL-C225 nanoconjugate is that it can be used for early detection and can also be developed into an effective treatment for cancers found in all tissue depths.

We also initiated *in vivo* studies of colon cancer treatment by using the nude mouse model xenografts. To date, results of these studies show that the largest tumor volumes were observed in tumors that were untreated, or treated with only C225. We found that either TiDoL or TiDoL-C225, after activation with luciferin, inhibited tumor growth, limiting the size of tumors to 30% of the size of untreated tumors or those treated with particles (only without luciferin activation). Exponential (rapid) growth continued in xenografts that received TiDoL or TiDoLC225 without luciferin activation, whereas linear (slow) growth was observed in tumors treated with TiDoL or TiDoLC225 with luciferin activation.

Improving the Stability of Rubisco Activase, the Weak-Link, in the Biological CO_2 Fixation Machinery

2013-013-R1

P. Raj Pokkuluri, Marianne Schiffer, and Rosemarie Wilton

Project Description

Rubisco activase is a chaperone that activates Rubisco (i.e., RuBisCO, which stands for ribulose-1,5-biphosphate carboxylase/oxygenase), which is the major plant enzyme that catalyzes the first step in photosynthetic carbon fixation by using atmospheric CO_2. The thermal instability of Rubisco activase is the major cause of temperature-dependent inhibition of CO_2 assimilation and net photosynthesis (affecting plant growth). In the context of global warming, it is an essential problem to solve. Our proposed solution is to develop heat-stable Rubisco activases by designing variants based on protein engineering principles. Stabilized variants of Rubisco activase (when incorporated into plants in collaboration with researchers at the University of Illinois) will improve the photosynthetic yields.

Mission Relevance

Our research aims to find solutions to two major problems: excess atmospheric CO_2 and risks to crop security. Engineering plants to assimilate higher CO_2 levels can mitigate both problems in one step. Removing excess CO_2 from the atmosphere is relevant to DOE's environ-

mental quality mission, and increasing plant biomass (for food and as feedstock for fuel and commodity chemicals) is relevant to its energy security mission.

FY 2014 Results and Accomplishments

Cloning and Expression of Rubisco Activase: In FY 2013, we cloned, expressed, and purified full-length long and short forms of Rubisco activase from soybeans (*Glycine max*) and *Arabidopsis thaliana*. We also prepared the AAA^+ domain fragments of each activase.

In FY 2014, our research included the following topics:

Crystallization Trials: Purified native and AAA^+ domains were used to survey crystallization conditions in which commercial reagent screens had been used without success. The refractory nature of these samples for crystallization can be understood by their high polydispersity. Rubisco activase is known to self-associate into various higher-order complexes.

Stability Mutants: On the basis of protein yields and the quality of the thermal stability data on purified protein samples that we obtained, we focused our stabilization strategy on the AAA^+ domain of the soybean short form. A panel of 48-point mutations was designed. Standard procedures were used to introduce all the designed mutants into the AAA^+ domain and confirm them by DNA sequencing. All mutants were prepared in small-scale (30-mL) cultures and partially purified by Ni^{2+} affinity beads. The thermal stability of the partially purified mutant samples was assayed by differential scanning fluorometry (DSF). Of the 48 point mutations, 16 were found to be stabilizing, with their T_m value (temperature midpoint of folded-unfolded transition) being at least 1 to 5°C higher than the native temperature.

Adenosine Triphosphate (ATP) Hydrolysis Activity: The stabilizing point mutations are useful only if they do not interfere with the activity of the protein. This attribute was assessed by using the ATP hydrolysis activity of each variant AAA^+ domain. Activity was not affected for five of the top six stabilizing variants.

Large-scale Protein Preparations: We prepared proteins from 1-L *E. coli* cultures of the native Rubisco activase soybean short AAA^+ domain and prepared the variants with stabilizing single mutations; we purified them first by Ni^{2+} affinity chromatography and then by size exclusion chromatography (SEC). These proteins elute as four major fractions, the species of which differ in their molecular weight. Circular dichroism spectroscopy revealed that the difference between the fractions was due mainly to the different multimers (i.e., number of protein subunits associated to form one entity) present in solution.

Proposed Work for FY 2015

Combining Stabilizing Mutations: We will complete the mutagenesis to combine the stabilizing mutations into one construct and confirm this effort by DNA sequencing. The stabilizing mutations that do not affect the activity will be combined, one at a time, to assess their additive effect. We will isolate the mutant proteins that are carrying multiple mutations. All of the stabilizing point mutations that have an additive effect on the overall thermal stability will be combined into one construct to obtain a "super-stable" Rubisco activase.

Obtaining Rubisco Activase from Miscanthus giganteus: We recently obtained the gene sequences for the short and long forms of Rubisco activase from *Miscanthus giganteus*, an important bioenergy crop. We will clone the two genes and express the proteins. The short and long forms of Rubisco activase and their respective AAA^+ domains from *Miscanthus* will be prepared, and their stabilities will be measured. Of the amino acids in the AAA^+ domain of *Miscanthus* Rubisco activases, 88% are identical to the soybean short AAA^+ domain for which we already found stabilizing mutations. In principle, the stabilizing mutations found for the soybean protein should be stabilizing for the *Miscanthus* protein, too.

Crystallization: Crystallization trials will be carried out with the stabilized versions of Rubisco activases (AAA^+ domains and the respective full-length short and long forms). The protein samples purified by SEC will be used. Initial crystal hits will be optimized, and then we will proceed with structure determination studies.

Spin-Based Thermal Power Generation

2013-016-R1

Axel Hoffmann

Project Description

Thermoelectric devices rely on the Seebeck effect to generate electric voltages from temperature gradients. This effect has been employed not only in temperature sensors but also for power generation, especially as energy scavengers that convert waste heat into useful electric power. To make thermoelectric generators efficient, it is desirable to decrease thermal conductivity while concurrently improving electrical conductivity. In conducting materials, the ratio of thermal conductivity (κ) to electric conductivity due to electron transport (σ) is universally given by the Wiedemann Franz law, $\kappa/\sigma = LT$, where T is temperature and the Lorenz number L is a constant of about 2×10^{-8} $W\Omega K^{-2}$. For this reason, despite decades of research, the efficiencies of thermoelectric power genera-

tion at room temperature are still rather low, and the figure of merit, $ZT = (\sigma/\kappa)S^2T$, has increased by a factor of only 3 to 4 (with S being the Seebeck coefficient).

A possible solution to this dilemma is spin-dependent charge and thermal transport. Spin-based effects allow charge conductivity to be decoupled from thermal conductivity; that is, a heat gradient over a ferromagnetic insulator can generate a spin current that is transferred into a metallic conductor, where the spin current is converted into a charge current. Recently, it was shown that heat currents result in concomitant spin currents in both ferromagnetic metals and ferromagnetic insulators. This is now known as the spin Seebeck effect. It is possible, too, to concurrently convert spin currents into charge currents through the so-called spin Hall effect. It has also been demonstrated that spin currents from ferromagnetic insulators can generate spin currents in adjacent metals through spin pumping. This approach allows thermal conductivity to be reduced and electrical conductivity to be increased independently from each other.

The goal of this project is to investigate the conversion of heat current to charge current in various combinations of materials and geometries. Besides providing a better fundamental understanding of the underlying physics of spin-caloric effects, this work will also allow for the development of thermoelectric devices superior to the ones that currently exist.

Mission Relevance

This project is relevant to DOE's energy and science missions, and it will have both fundamental and applied impacts. In terms of basic science, this work will lead to an improved understanding of the coupling between heat, spin, and charge currents. With respect to applications, it will explore the feasibility of the spin-mediated conversion of heat current to charge current for efficient thermoelectric power generation. Spin-based mechanisms for converting heat current to charge current provide a new paradigm and produce effects that are very different than traditional thermoelectric effects. Toward this end, for thermally driven spin currents, even a proper definition of the figure of merit is not clear at this time, since the resultant charge current is generated transversely with respect to the heat current and the scaling thus works very differently than it does in traditional thermoelectric devices. The project will directly address, at a fundamental level, energy conversion — an issue that directly relates to today's grand challenge of achieving sustainable energy.

FY 2014 Results and Accomplishments

In FY 2013, we focused on the growth and characterization of thin films of yttrium iron garnet (YIG). Our preferred growth technique was radiofrequency (rf) sputtering, since this allowed us to integrate the YIG films easily with other materials, such as platinum, which are known to have very large spin Hall effects. YIG is well-suited for thermally excited spin waves, since the anisotropy is very low, which reduces the amount of damping of magnetic excitations to the lattice. Moreover, the damping directly determines the line width of ferromagnetic resonance. Therefore, the quality of the YIG films can be best assessed through the ferromagnetic resonance measurements, since the line width of the resonance peak is very sensitive both to the exact stoichiometry of the films and to possible defects. We systematically showed how the ferromagnetic resonance properties change with the thin film's structural quality and added overlayers.

Furthermore, we designed a sample holder for longitudinal spin Seebeck measurements, in which the sample was clamped between two copper blocks, the temperature of which was individually controlled with Peltier elements (Tellurex) and PT100 resistance thermometers. This design had the advantage of being able to control the top and bottom temperature individually over a wide dynamic range (80 K) with sufficient stability (0.1 K). At the same time, the design allowed the temperature gradient to be reversed without having to remount the sample, which enabled the elimination of systematic errors due to stray thermoelectric voltages during the measurements.

In FY 2014, we made significant progress in fabricating high-quality YIG thin film; we can now achieve low magnetic damping in nanometer-thick films that is comparable to the intrinsic damping observed in bulk single crystals. The key to obtaining such low magnetic damping in YIG was careful control of the microstructure, which depended critically on the process parameters, such as growth temperature, sputter gas pressure, and the post-annealing procedure.

At the same time, we observed that very thin palladium (Pd) and platinum (Pt) layers give rise to a reduction of spin Hall effects at low temperatures. In contrast, no such reduction was observed by introducing a separating layer of copper (Cu) between Pt or Pd and the ferromagnetic layer. Thus, magnetic proximity effects in Pd and Pt may decrease spin Hall conductivities, which we also confirmed by *ab initio* calculations. Unfortunately, the addition of Cu shunts and therefore reduces spin Seebeck voltages, which means that additional pathways that move toward suppressing proximity effects are required. Toward this end, we investigated the spin Hall effect in metallic antiferromagnets and discovered that manganese platinum (MnPt) has a spin Hall angle almost comparable to that of Pt.

The last task was to finalize implementing our spin Seebeck measurement setup, which we tested with an international round-robin sample exchange as part of the European Metrology Research Programme's (EMRP's) spintronics and spin-caloritronics in magnetic nanosystem

(SpinCal) project. As part of this project, the same sample was repeatedly measured by several world-leading groups (from Europe, Japan, and the United States). The results measured by different research groups indicated a variation of the measured spin Seebeck coefficients by a factor of 3, with our results being fairly representative of the average. Nevertheless, the results indicate that there are additional concerns associated with calibrating the temperature gradients in these measurements, and we are working closely with the EMRP SpinCal project to develop a standard metrology methodology.

Proposed Work for FY 2015

In FY 2015, our research will include the following:

- Measure thermal conductivities and simulate heat current distributions
- Conduct detailed characterization of heat-to-spin current and spin-to-charge current conversion
- Investigate the influence of microstructure
- Test Onsager reciprocity

Seminars

Hoffmann, A. (2014). "Connecting Spin Waves to Charge Currents." Ohio State University, Columbus, OH, November 21, 2013.

Superlubricious Carbon Films Derived from Natural Gas for Home-Refueling Applications

2013-022-R1

Ali Erdemir, Osman Eryilmaz, and Giovanni Ramirez

Project Description

The main objective of this project is to develop novel catalytically active nanocomposite coatings that can extract highly durable and lubricious carbon films directly from natural gas and be deposited on sealing and sliding surfaces of advanced compressor systems. The project also aims to impart a fundamental understanding of the science behind lubricious film formation and its lubrication mechanisms. If the bench studies look very promising, we plan to work with industrial companies in the field and test optimized coatings in real compressor environments.

Mission Relevance

This project is relevant to DOE's missions on energy independence and protecting the environment. Lately, DOE has been soliciting ideas for breakthrough technologies that will enable home refueling of natural gas for vehicular uses. Compressing natural gas from home outlets to as much as 5,000 psi is a challenge but essential for achieving a reasonable driving range out of a vehicle powered by natural gas. Sealing and sliding surfaces of compressors are subject to high friction and wear losses. This project focuses on the design and development of catalytically active nanocomposite coatings that can extract superlubricious carbon films from natural gas and deposit them on sealing and sliding surfaces of compressor systems. If proven effective, these coatings can eliminate one of the major roadblocks toward the development of next-generation compressor systems in which natural gas can act as a lubricating agent.

FY 2014 Results and Accomplishments

During FY 2013, we synthesized a series of catalytically active MoN-Cu, VN-Cu, NbN-Ni, VN-Ni, and TaN-Ni coatings and tested them by using methane gas. When uncoated 440 steel (440C) pairs were tested in methane, the specific wear volumes were as much as 2×10^{-11} m^3. When the same tests were repeated by using VN-Cu-coated 440C, the wear volumes were reduced to 5×10^{-15} m^3 and, hence, the catalytically active nanocomposite coating resulted in a reduction in wear of more than three orders of magnitude. These findings are consistent with our original concept.

In FY 2014, we optimized these nanocomposite coatings to achieve greatly improved friction and performance. Among the many coating combinations we tried, 9.55 at.% Ni-containing VN coating on steel substrates provided excellent performance (Figure 1a). This coating is labeled VN-Ni 4000-180 in the bar graph; note that without any Ni or with more or less than 9.55 at.% Ni concentrations, the VN coating would not function as well (note that VN-Ni 4000-270 and 4000-500 coatings contained 14 and 26 at.% Ni). In a series of more realistic/relevant tests, we used cylindrical pins made out of PEEK (polyetheretherketone), which is the most desired seal material for compressor applications. In the test system, we pressed the cylindrical face of these pins against the highly optimized VN-Ni test samples (at 9.55 at.% Ni) under 50 MPa contact pressure, 1.2 m/s speed, 10 km sliding distance, and 180°C at the atmospheric pressure of methane.

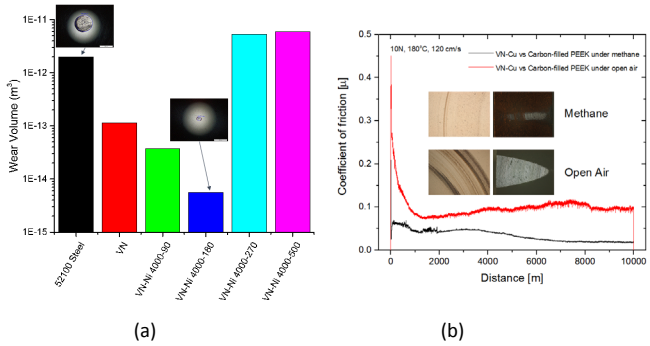

Figure 1. (a) Wear and (b) friction performance of VN-based nanocomposite coatings in methane. Note that VN-Ni composite coating with 4000-180 designation in (a) reduced wear by than 2 orders of magnitude below what was feasible with 52100 steel, while the friction coefficient of a VN-Cu coating in (b) was as low as 0.03 in methane.

The same test was also run in open air without the methane to see if there was a different result. As shown in Figure 1b, the friction coefficient of PEEK against the optimized Ni-containing VN in methane was remarkably low: toward the end of test, it was less than 0.03. Most importantly, the wear damage on both the cylindrical face and on the flat disk side was hard to discern. When the same test pair was evaluated in open air, the wear damage was rather significant and the friction coefficient was more than 0.1. Upon close examination, we confirmed the formation of a highly protective and slick carbon-rich tribofilm on the VN-Ni coated surface — we strongly believe that this was the reason for the extraordinary performance of PEEK versus VN-Ni in methane. In contrast, we observed no such film on sliding VN-Ni surfaces after testing in open air (only deep grooves were found on the VN-Ni coated surface, which was also slightly oxidized, perhaps because of the high temperature and an oxidizing environment). On the PEEK cylinder side, the wear damage was rather extensive and slanted toward the left side.

Proposed Work for 2015

In FY 2015, we will concentrate on testing optimized coatings against different seal materials under increased load, speed, and sliding distance to develop a wear performance map (with respect to various test parameters) that can be used as a guide in actual applications. We will also perform more in-depth surface and structural studies to understand underlying lubrication mechanisms. Ultimately, we will apply these coatings to a series of actual components for performance tests in natural gas.

Extreme Optomechanics

2013-035-R1

Jeffrey R. Guest, Xiao-Min Lin, and Matthew Pelton

Project Description

This project involves the development of a new method for the real-time measurement of mechanical vibrations in nanometer-scale oscillators at frequencies above 10 GHz. The ability to precisely measure the frequency at which mechanical oscillators vibrate underlies a wide range of technologies. Present methods for rapidly and accurately measuring mechanical vibrations cover a vast range of length and frequency scales. On length scales from the macroscopic down to the microscopic, mechanical motion can be read out electrically, by directly connecting the oscillator to electrical leads, or by coupling it capacitatively or magnetically to a readout circuit. On atomic and molecular length scales, optical spectroscopies, particularly Raman and Brillouin scattering, can be used to measure vibration frequencies. In between these two limits — for dimensions on the nanometer scale and frequencies in the 10s of GHz range — none of these methods are applicable. The scientific opportunity addressed in this proposal is to fill this technological gap by developing a new method to measure vibrations in this mesoscopic regime.

Our new method will have important technological implications, particularly for mass sensing. Since the frequency of a mechanical oscillator is directly related to its mass, measuring this frequency can provide an accurate means of weighing material that is adsorbed onto the oscillator. The smaller the oscillator, the larger the fractional change in oscillation frequency a given mass will produce, and thus the more sensitive the measurement. The demonstration of a method to monitor GHz vibration frequencies in nanostructures would thus open up a new frontier in ultrasensitive mass measurement. We will be able to measure vibrations in nanoparticles that were synthesized by using bottom-up chemical synthesis techniques, rather than the costly and complex top-down nanofabrication techniques that have been used so far. This, in turn, will facilitate the ability to functionalize the nanoparticles for binding to target molecules and will allow the sensors to operate in a liquid environment.

Mission Relevance

This project supports the DOE mission in use-inspired fundamental science. The investigations will yield new scientific insights into mechanical vibrations at the nanometer scale and will set the stage for future applications in ultrasensitive mass detection, enabling new nanoscale platforms for *in-situ* detection of targeted molecular species in fluids.

FY 2014 Results and Accomplishments

The ultimate success of this project hinges on being able to develop the ability to monitor the vibrations of individual nanoparticles in *real time* and in solution at ultrahigh frequencies (~20 GHz). In FY 2013, we designed the experimental setup, procured the necessary equipment, and began assembling it. In FY 2014, we focused on optimizing the experimental setup, including the laser, optics, and radio-frequency (RF) electronics to achieve the ability to monitor vibrations. The ultimate sensitivity of our approach will depend on how well we minimize noise in the detection of extremely small changes in transmission at ultrahigh frequencies; we successfully developed this monitoring capability and tested its efficacy, demonstrating a sensitivity to changes in transmission approaching $\Delta T/T \sim 4 \times 10^{-7}$, allowing us to detect changes in transmission at ultrahigh frequency to better than one part per million.

We also made progress in the synthesis and functionalization of tailored bipyramidal gold nanoparticles for these measurements, realizing different sizes of gold bipyramids with tunable plasmon wavelengths from the visible to the near-infrared, while improving their homogeneity. These different sizes of bipyramids will be ideal candidates for testing our optical setup, since different sizes of particles will have a different mechanical frequency response. To perform mass detection, chemical functionalization of nanoparticles with specific binding groups is being developed.

Understanding and quantifying the frequency shifts due to molecular binding will first require that they can be disentangled from effects due to the solvent environment of the vibrating nanoparticles. We therefore used transient absorption (TA) measurements to study the fluid-structure interaction for vibrating nanoparticles in viscous liquids. In the high-viscosity regime, the vibrational period is comparable to the intrinsic molecular relaxation time of the fluid. Rather than exhibiting the Newtonian fluid properties expected for conventional fluids, even simple fluids showed non-Newtonian, viscoelastic effects. In other words, rather than behaving like a simple, viscous liquid, the surrounding fluid began to behave like an elastic solid, as shown in Figure 1. These experiments represented the first direct mechanical measurement of the intrinsic viscoelastic response of simple bulk liquids, showing that a fundamental assumption of fluid mechanics does not apply on the short time scales and small lengths scales of nanoparticle vibration.

Proposed Work for FY 2015

We have been searching directly for nanoparticle oscillations by using the newly constructed frequency-domain apparatus on ensembles of our newly developed bipyramidal samples. We plan to continue to focus on realizing this new, real-time sensing platform in FY 2015. We also plan to develop the microscopy apparatus that will allow us to investigate nanoparticles one at a time by using our approach. We will continue to develop the functionalization of these nanoparticles to extend frequency-sensing to mass- and molecular-sensing. We are also currently extending the TA measurements to study viscoelastic effects in a range of solvents as a function of temperature, as well as exploring more complex nanoparticle structures. Once real-time sensing is demonstrated, we will begin to test the ability of our approach to perform mass-sensing and to measure local environmental changes in solution.

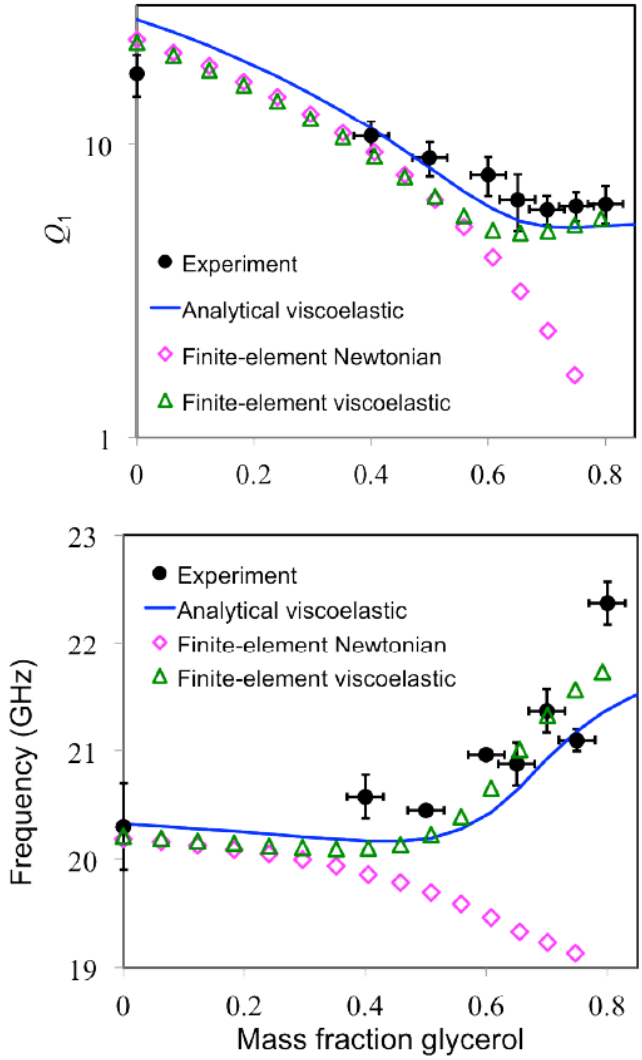

Figure 1. Quality factor (top) and frequency (bottom) of mechanical vibrations of bipyramidal gold nanoparticles in glycerol-water mixtures. Circles are determined by fitting experimental data, the dashed line is the result of an analytical model that treats the glycerol-water mixtures as viscoelastic fluids, triangles are the result of finite-element calculations that treat the mixtures as viscoelastic fluids, and diamonds are the result of finite-element calculations that treat the mixtures as Newtonian fluids. The strong agreement of the data with the viscoelastic calculations shows that even these simple fluids behave in a non-Newtonian fashion in this ultrahigh frequency nanoscale regime.

Development of Near-Field-Enhanced Terahertz Pump X-ray Probe Techniques for Ultrafast Control of Strongly Correlated Materials

2013-036-R1

Haidan Wen, Zhonghou Cai, Matthew J. Highland, and Il Woong Jung

Project Description

Strongly correlated materials exhibit complex coupling in multiple degrees of freedom, such as spin, charge, lattice, and orbital orders. The complexity not only offers rich physics, but also diverse functionalities. However, grand challenges remain: how can researchers characterize and control remarkable properties of matter that emerge from complex correlations far away from equilibrium? The recent development of intense terahertz (THz) sources provides the means to alleviate the complications arising from optical pumps and enables investigation of a wider range of condensed matter phenomena due to its unique properties. For example, the THz pulse can resonantly excite meV low-energy modes in strongly correlated materials or provide ultrafast electric fields to manipulate ferroelectric polarization.

In this project, we are developing terahertz pump hard x-ray probe techniques for the control of strongly correlated materials in their electronic ground states. In particular, we will design and implement a near-field approach based on nanoplasmonic enhancement to create a controllable 300-fs THz pulse with a peak field of 10 MV/cm that is confined in several hundred nanometers, providing an unprecedented high field condition extremely localized in space and time for the control of previously inaccessible phases of matter at ultrafast time scales.

Mission Relevance

This project is closely related to DOE's science and innovation mission. The project opens new scientific opportunities for *in situ* studies of nonequilibrium dynamics of materials in real time under extreme field conditions. Without the complication of optical excitation, these studies will allow novel, selective, ultrafast control of strongly correlated materials close to their electronic ground states. The technical breakthroughs enabled by a time-resolved hard x-ray nanoprobe create a unique tool to explore the nonequilibrium states of matter by using THz excitation, which is relevant to the development of next generation energy materials, sensors, and devices.

FY 2014 Results and Accomplishments

In FY 2013, we developed the laser-pump, hard x-ray nanodiffraction probe technique with 300 nm and 100 ps spatiotemporal resolution. We applied this technique to study the lateral strain map of photoexcited bismuth ferrite ($BiFeO_3$ [BFO]) thin films and revealed the dynamics of grain boundaries.

In FY 2014, we initiated the study of structural phase transition in vanadium oxide (VO_2) upon optical excitation. We were able to examine the photo-induced, localized structural phase transition around the pinning sites with 300-nm spatial resolution. We showed that the structural phase transition of a VO_2 thin film (Figure 1a), upon homogenous optical excitation, occurs inhomogeneously. Upon 800-nm, 100-fs pulse excitation, the monoclinic and rutile Bragg intensity were simultaneously monitored by either an unfocused or focused hard x-ray probe (Figure 1b). Scanning with a 300 nm x-ray beam revealed two-dimensional (2D) intensity maps of the corresponding structural phases at each time delay (Figure 1c). As marked by the red arrows in Figure 1c, the region showing a prominent increase of the rutile intensity was accompanied by a decrease of monoclinic intensity. Since each point in the 2D maps was obtained by averaging 10,000 pump-probe events, if the phase transition occurs at random nucleation sites for each pump-probe event, these inhomogeneous features would be washed out. The observation of this inhomogeneous increase of Bragg intensity supports the rutile phase developed at pinning sites during photo induced phase transition. Ongoing analysis will reveal the spatiotemporally resolved dynamics of the structural phase transition.

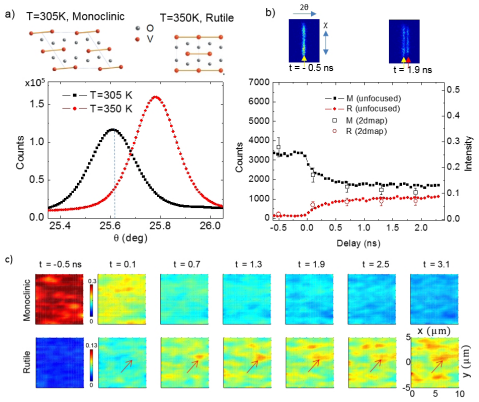

Figure 1. (a) The lattice structure of monoclinic and rutile phase of VO_2. The bottom plot shows the (002) Bragg peak of VO_2 below and above the transition temperature of T_c=340 K measured by x-ray diffraction probe of 10 keV at the APS; (b) The Bragg intensity as a function of delay using unfocused (solid) and focused (open) x-ray probe at θ=25.61 degree. The top images shows the diffraction peak on an area detector where the monoclinic and rutile peaks are well separated along 2θ direction. The yellow and red arrows point the monoclinic and rutile Bragg diffraction patterns respectively. The intensity spread along χ-direction is due to the mosaicity of the film. (c) The 2D Bragg intensity map as a function of delay. The arrows point to one of the pinning sites.

We designed and implemented the near-field THz pump, hard x-ray nanodiffraction probe capability on the 7ID-C beamline at the APS. Intense THz pulses were generated by nonlinear conversion of ultrafast laser pulses to the THz frequency in a lithium niobate ($LiNbO_3$) crystal based on the pulse-front-tilt technique. We developed *in situ* characterization of the THz field pulse, which is a key component for modeling the excitation in any THz-pump x-ray probe experiments. The measured THz waveform was a 300-fs single-cycle electric field pulse with a peak field of 200 kV/cm. This incident field can be further enhanced by using a split ring resonator. The simulation showed that the peak field in a 2-μm-wide gap can be enhanced to several tens of MV/cm, sufficient to drive the proposed structural changes in ferroelectrics. With a smaller gap, higher field enhancement is expected. The combination of near-field enhanced THz excitation and sub-micrometer x-ray probe enables low-energy excitation with 300 nm and 100 ps spatiotemporal resolutions, an instrument achievement not previously accomplished at any other synchrotron source in the world.

We also made significant progress in generalizing the application of the developed instrument. We combined a novel optical transient-grating excitation scheme with time-resolved hard x-ray nanodiffraction probe (Figure 2a). Optical transient grating is a spatially modulated optical intensity profile with a controllable period of several micrometers resulting from coherent optical interference. Using a time-resolved synchrotron-based hard x-ray probe smaller than the modulation period, we directly investigated the structural evolution within the optically induced spatial profile (Figure 2), providing insight into the time-dependent, in-plane transport dynamics. Initial studies on BFO and iron-rhodium (FeRh) thin films yielded a new understanding of energy transport in these systems. In particular, the structural profile of FeRh (Figure 2d) deviated from the sinusoidal excitation profile in comparison to the results for BFO (Figure 2c), highlighting the complexity of the photo induced phase transition process in FeRh.

Proposed Work for FY 2015

The technical development of the near-field THz excitation hard x-ray nanodiffraction probe has been achieved and opens up grand opportunities to control strongly correlated materials. In FY 2015, the initial study will focus on a study of THz excitation of a prototypical ferroelectric, barium titanate ($BaTiO_3$) film because it is susceptible to external electric fields at room temperature. The second material we will study is a lead titanate ($PbTiO_3$) film grown on dysprosium scandium oxide ($DyScO_3$) substrate, which is composed of ferroelectric polarization aligned along both the out-of-plane and in-plane axes. The THz field is expected to couple to them differently, depending on the alignment of the THz field polarization in these domains. The simultaneous measurement of diffraction Bragg peaks from these domains will shed light on ultrafast field manipulation of ferroelectrics. The success of the proposed work will open opportunities to study localized, ultrafast, nonlinear THz-matter interaction with unprecedented spatial resolution.

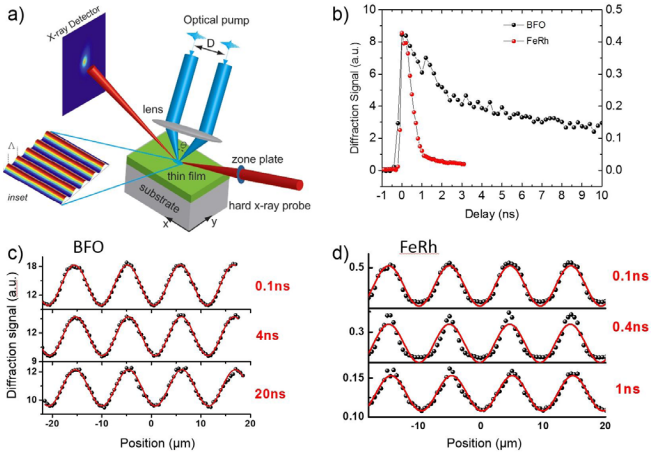

Figure 2. (a) The schematic of transient grating pump, hard x-ray nanodiffraction probe technique. The inset on the left shows the sinusoidal optical intensity profile with adjustable period Λ in micrometers on the sample as a result of coherent interference of two optical beams. The inset on the right shows the geometry of the two crossing beams and the interference of the wave fronts. (b) The diffraction signal at left side of the Bragg peak as a function of time; (c) Transient-grating-induced strain profile in BFO and (d) FeRh thin films as a function of time. Spheres are data points measured by the time-resolved x-ray nanodiffraction while the solid curves are sinusoidal fits.

Seminars

Wen, H. (2015). "Spatiotemporally Resolved X-ray Imaging." DOE-BES 'X-ray Scattering' PI Meeting, Washington, D.C., November 5–7, 2014.

Visualization of Stress-Induced Polarization Switching in Electromechanically Coupled Ferroelectric Polymers

2013-063-R1

Seungbum Hong and Charudatta Phatak

Project Description

The goal of this project is to study the strain-induced phase transition and polarization switching in a polyvinylidene fluoride (PVDF) -based polymer ferroelectric materials system by using both piezoresponse force microscopy (PFM) and *in situ* transmission electron microscopy (TEM). We will apply local stress by using nanoscale tips and gain a fundamental understanding of the phenomena, which will enable us to better control their behaviors and responses. The outcome of this research will lead

to design guidelines for high-performance piezoelectric energy harvesting devices.

Mission Relevance

This project is directly relevant to DOE's mission in energy. The outcome of this project will help us understand the science of new materials for clean and renewable energy harvesting so we can achieve the technological goals of developing high-efficiency vibration energy conversion devices.

FY 2014 Results and Accomplishments

In the project's first year, we confirmed that the polarization vector rotates toward the out-of-plane axis as a function of mechanical force applied to the poly[(vinylidenefluoride-co-trifluoroethylene (P[VDF-TrFE]) thin films.

In FY 2014, to further investigate the relationship between mechanical force and the material properties of P[VDF-TrFE] thin films, we applied mechanical force to these films at room temperature during atomic force microscopy (AFM) scanning (Figure 1a). As shown in Figure 1b, the surface morphology was irreversibly deformed under mechanical annealing forces of 1.0 μN (350 MPa), and the randomly oriented crystals in the pristine region became well aligned with the fast scanning direction after the mechanical annealing process. Furthermore, the average remanent vertical piezoresponse amplitude increased from 21.9 ± 3.3 pm/V to 28 ± 6.9 pm/V in the mechanically annealed region (see Figure 1, c and d). The average remanent lateral piezoresponse amplitude also increased significantly from 0.8 ± 0.2 (a.u.) to 1.7 ± 0.5 (a.u.) as estimated from the lateral piezoresponse amplitude-voltage butterfly loops in the mechanically annealed region.

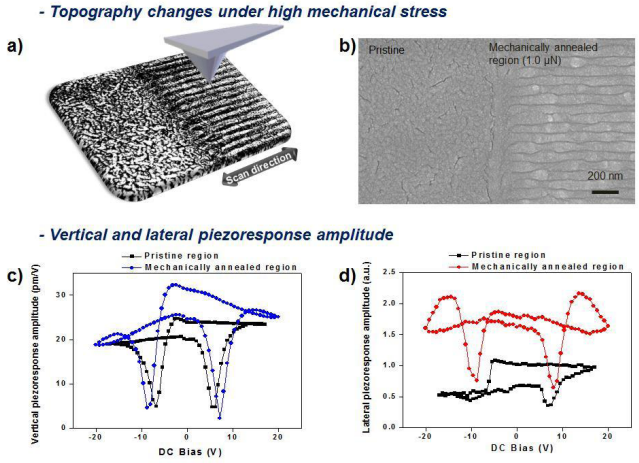

Figure 1. (a) Schematic illustration of mechanical annealing process on P(VDF-TrFE) thin film using AFM tip. (b) SEM image of the P(VDF-TrFE) thin film in pristine and mechanically annealed regions. (c) Vertical and (d) lateral amplitude-voltage butterfly loops obtained from pristine (black squares) and mechanically annealed regions (blue circles for vertical and red circles for lateral amplitude-voltage butterfly loops).

To explore the polarization switching behavior change induced by the mechanical annealing process, we obtained piezoresponse force microscopy (PFM) images. In Figure 2, a and b, we observed that the randomly oriented domains changed to stripe domains and the out-of-plane (OP) polarizations in the pristine region rotated in a downward direction. The in-plane (IP) phase images in mechanically annealed regions become more homogeneously uniform than the IP phase images in pristine regions. We believe that the mechanical annealing process leads to more uniform alignment of OP and IP polarization vectors. In addition, the alignment of OP and IP polarization might result in molecular chain alignment of the long trans sequence in the ferroelectric β-phase.

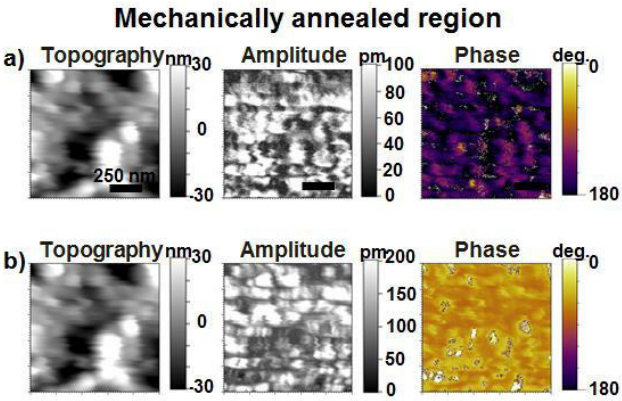

Figure 2. Topographical, (a) OP and (b) IP piezoresponse amplitude and phase images at mechanically annealed region with a mechanical force of 1.0 μN.

Figure 3 shows the change in the carbon K-edge obtained by using electron energy loss spectroscopy (EELS). The two peaks labeled π* and σ* represent the hybridization states of carbon in the film, such as sp^2, sp^3 or mixed. Preliminary study showed a change in the structure of the σ* peak under deformation. However, variations in sample thickness and electron beam instabilities also affect the EELS edge.

Proposed Work for FY 2015

We will use micro-focused grazing-incidence small-angle x-ray scattering (GISAXS) and grazing-incidence wide-angle x-ray scattering (GIWAXS) to investigate the structural ordering and crystallinity change of mechanically annealed regions versus pristine regions of a polymer film.

In addition, we will carry out *in situ* TEM deformation of the P(VDF-TrFE) film and observe the change in the carbon K-edge using EELS from the same region.

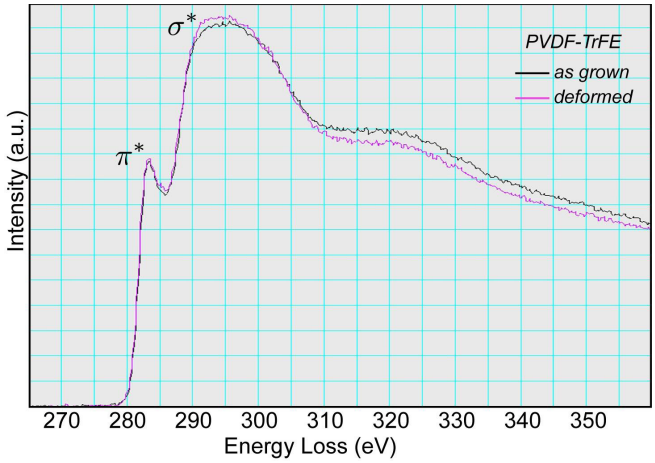

Figure 3. Carbon K-edge energy loss spectrum obtained from the as grown P(VDF-TrFE) and the mechanically deformed film.

Seminars

Heinonen, O., D. Karpeyev, S. Gu, S.M. Nakhmanson, B. Lee and S. Hong (2013). "Real Space Formulation for Coupled Elastic Problems." Purdue University, West Lafayette, IN, April 15–16, 2013.

Hong, S. (2015). "Functional Materials Design Based on Nanoscale Visualization and Manipulation." University of Texas, Dallas, TX, November 21, 2014.

Hong, S. (2014). "Visualization and Manipulation of Polarization and Screen Charges Using Atomic Force Microscopy." Ecole Polytechnique Federale de Lausanne, Lausanne, Switzerland, June 6, 2014.

Imaging Ecological Engineers: A Novel Quantum Dots Approach to Map Microbes in Complex Soil Structures with X-rays

2013-070-R1

Sarah O'Brien, Dionysios A. Antonopoulos, Maxim Boyanov, Kenneth M. Kemner, and Edward J. O'Loughlin

Project Description

This project aims to understand how soil microbes engineer their environments into dynamic three-dimensional complexes that promote microbial diversity, influence the terrestrial carbon cycle, support soil fertility, and impact the fate and transport of contaminants. The metabolic activities of soil microbes are the primary drivers of biogeochemical processes controlling the terrestrial carbon cycle, nutrient availability to plants, contaminant remediation, and other ecosystem services. However, we have a limited understanding of how microbes and microbial metabolism are distributed throughout the three-dimensional complex of the soil or how this phenomenon impacts emergent properties, such as microbial diversity or biogeochemical fluxes.

In this project, we are developing a novel application of quantum dots (or QDs, engineered semiconductor nanoparticles that produce size-dependent fluorescence) that uses their relatively high electron density (rather than their optical fluorescence characteristics) to track the microbially facilitated incorporation of organic substrates into soil aggregates by using x-ray transmission and fluorescence microtomography. Combined with their distinctive ability to tag metabolically active molecules and thus gain entry into cells, the relatively high x-ray absorption of cadmium (Cd) in QDs will allow us to uniquely image the role of bacteria in building soil aggregates and pore spaces and provide new insight into the living conditions of microbial cells.

Mission Relevance

This project is relevant to DOE's environmental quality mission. The ability to track particular metabolic functions in a variable, opaque environment could be invaluable to any research program that investigates microbial processes in opaque materials, from soils to subsurface sediments, to arctic permafrost to microbe-enabled industrial applications. It also meshes well with current DOE-supported work to characterize microbial metabolic functions using metagenomic sequence data.

FY 2014 Results and Accomplishments

Our initial experiments in FY 2013 determined that bacterial uptake of QDs is active and depends on the conjugated substrate and environmental conditions, which are prerequisites for our planned soil experiments. We grew two different non-pathogenic bacterial species commonly found in soil in one of four ecologically relevant experimental conditions: nitrogen limitation, phosphorus limitation, nitrogen and phosphorus limitation, or no-nutrient limitation. A slurry of conjugated QDs (representing each of five colors conjugated to five different organic substrates) was added to the cultures, and optical and confocal microscopies were used to evaluate bacterial preference for the various substrates under each of the four conditions.

We found that growth conditions affected uptake, with significantly more uptake when either N (glycine, adenine, glucosamine) or both N and P (glycerol phosphate) were limiting. In addition, phosphoserine appeared to be the preferred substrate, with greater uptake than any of the substrates that provided only N or only P. Uptake was similar for the two species, and we found no evidence for cytotoxicity issues at the QD concentrations we used.

Cellular uptake of unconjugated QDs was negligible, indicating that bacteria actively consume the QD-labeled nutrient rather than passively entering the cells. These findings are the first direct empirical evidence showing bacterial substrate preference that varies in response to environmental conditions.

X-ray fluorescence (XRF) imaging experiments performed in FY 2014 at the 2ID-D beamline at the Advanced Photon Source suggest that the x-ray mapping approach can, indeed, detect bacterial uptake of CdSe-core QDs (Figure 1). In addition, we hypothesize that the combined confocal microscopy and XRF approach we developed is capable of detecting biofilms based on images we collected of bacterial cells growing on a solid surface, where XRF-based elemental maps for P, which is associated with organic substances, and Se, which is associated with QDs, were concentrated in similar patterns as in an optical image where cells were embedded in extracellular polysaccharides of a biofilm. We demonstrated that this XRF imaging approach enables the identification of cells (and cell products, such as extracellular polysaccharides), and we are confident that this level of bioconcentration of QDs will allow us to detect the location of cells in the three-dimensional pore structure of a soil aggregate whether in a planktonic or surface-adhered state, such as a biofilm.

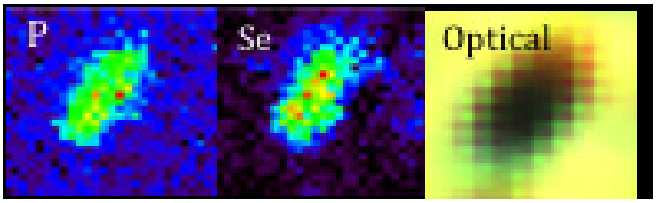

Figure 1. X-ray fluorescence-based elemental maps of phosphorus, which comes from cellular material, and selenium, which comes from quantum dots, and an optical image of a Pseudomonas.fluorescens cell. The similarity among these images shows that quantum dots can be used to label bacteria for detection by using hard x-ray techniques. Field of view ~3 × 3 μm.

Proposed Work for FY 2015

Continued work will involve further development of lab controls related to QD conjugation and XRF visualization of uptake kinetics. In addition, now that we demonstrated that the x-ray fluorescence approach works to image individual cells labeled with QDs in two dimensions, we will move on to image organisms in a three-dimensional, opaque soil medium.

Seminars

O'Brien, S.L. (2015). "The Microbial Habitat in Soil." University of Chicago, Chicago, IL, October 7, 2014.

O'Brien, S. (2013). "Connecting Microbial Ecology with Soil Biogeochemistry." University of British Columbia, Okanagan, Canada, September 11, 2013.

Ultra-Low Loss Superconducting Microstrip for Multi-Chroic Cosmic Microwave Background Detectors

2013-080-R1

Gensheng Wang, John Carlstrom, Clarence Chang, Valentyn Novosad, Thomas Proslier, and Volodymyr Yefremenko

Project Description

This project aims to develop ultra-low loss superconducting microstrip transmission lines, which are an essential technology for next-generation cosmic microwave background (CMB) experiments. A superconducting microstrip consists of a superconducting ground plane, a dielectric spacer, and a patterned superconducting transmission line. Loss in superconducting microstrips results from two known mechanisms. The first is two-level system (TLS) loss, which arises from the amorphous nature of the dielectric used in the microstrip. The second mechanism is quasi-particle loss associated with the breaking of Cooper pairs in superconductors with a gap that is comparable to the photon energies of interest.

For this project, we will implement two complementary methods for studying and mitigating these losses. First, we will fabricate half wavelength resonators for characterization at radio frequencies (RF) (1–10 GHz). Techniques for microstrip characterization at these frequencies are well established. The measurements will directly give the loss tangent of the superconducting microstrip and the transition temperature of the superconductor. Second, we will fabricate microstrip-coupled transition edge sensor (TES) bolometers for measurements at mm-wavelengths (100–300 GHz). These measurements will help us understand and control loss at mm wavelengths in superconducting microstrip transmission lines.

Mission Relevance

This project is relevant to DOE's mission in basic science. Ultra-low loss superconducting microstrip transmission lines are a critical technology for future measurements of the CMB. The CMB explores fundamental physics. Its polarization at angular degree scales is a unique probe of the energy scale of inflation, expected to be near energies favored by Grand Unified Theories. Its polarization at tens of arcminute angular scales is sensitive to the sum of the neutrino masses at a level relevant for resolving the neutrino mass hierarchy. CMB physics is an important dimension of the U.S. High Energy Physics program and was recommended by the Particle Physics Prioritization Panel.

FY 2014 Results and Accomplishments

In FY 2013, we successfully developed a low-loss dielectric recipe by sputtering silicon in oxygen plasma. We also developed techniques to control our fabrication at the nanoscale. These techniques eliminate nanometer-thick etching residuals and nano-cracks, which cause microwave loss.

In FY 2014, we successfully fabricated a low-loss superconducting microstrip transmission line with performance comparable to the best devices in the field. We used half-wavelength resonators to study the microstrip loss at radio frequencies and expanded these measurements in a new direction, enabling characterization of both dielectric and superconductor properties. Figure 1 shows the measured resonant frequency shift as a function of temperature, along with the best-fit loss model. The data at lower temperatures measures TLS loss and corresponds to a measured loss tangent of 0.0016. This loss tangent is sufficient for CMB experiments, which typically require loss tangents less than 0.005. The data at higher temperatures is our extension of the typical measurements and characterizes properties of the superconducting Nb (niobium) film. Our data show that the quality of our superconducting films is excellent.

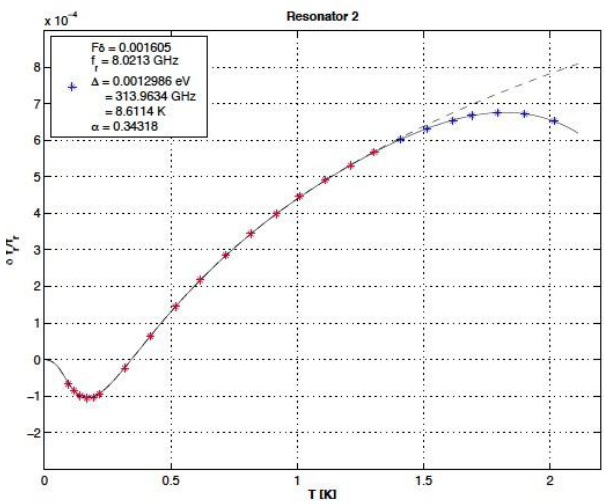

Figure 1. The resonant frequency shift (δfr/fr) of a half-wavelength resonator as a function of temperature. The stars indicate measured data. The dashed line is a Two-Level System (TLS) model. The solid line is a fit to the TLS model, including a Nb superconducting energy gap Δ. α is the fraction of kinetic inductance of the resonator. F is the filling factor, which is close to 1. Fδ characterizes the loss.

In addition to the half-wavelength resonators, we also fabricated a microstrip loss test device (Figure 2) consisting of a coupling antenna, microstrip transmission line, bandpass filters, and a pair of TES bolometers. This device was used to study the microstrip loss at mm wavelengths. The loss is estimated by comparing the readout power difference between the two TESs, each being fed by different microstrip lengths. Several batches of the loss test device have been fabricated. The testing results indicate that our microstrip has a loss tangent less than 0.002 at 215 GHz, sufficient for future CMB experiments.

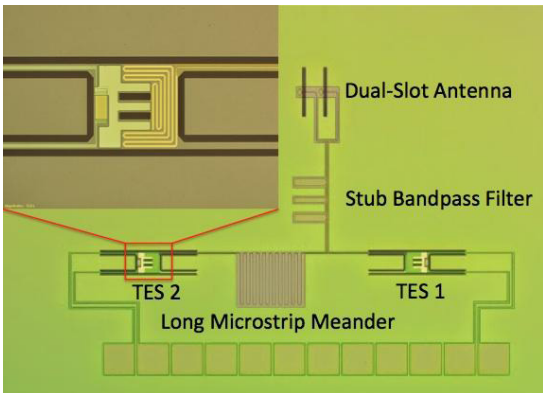

Figure 2. A microstrip loss test device. The dual-slot antenna couples the device to millimeter wavelength radiation. The signal propagates along the microstrip, passes through the stub bandpass filter, and is split equally between two TES detectors. For each TES, the microstrip is terminated with a lossy metal meander on the thermally isolated island with the TES. On the right, TES 1 measures the radiation power propagating along a short microstrip. On the left, TES 2 measures the radiation power propagating along a long microstrip meander. The loss at mm wavelengths is estimated by comparing the difference power measured by TES 1 and TES 2. The inset shows a TES bolometer that has an island supported by four silicon-nitride (SiN) legs. On the island, there are a TES on the left, a gold (Au) film in the middle as an add-on heat capacity, and a long Au meander as the lossy microwave terminator.

Proposed Work for FY 2015

Our initial mm wavelength loss measurement was at 215 GHz. In FY 2015, we will investigate the frequency dependence of our superconducting microstrip through additional loss measurements at lower frequencies (90 GHz and 150 GHz). The loss at these three frequencies is not only important for CMB measurements, but would help connect our data at millimeter wavelengths to our data at RF. Our goal is to parameterize and eventually model the frequency dependence of our microstrip loss. We will also investigate alternate methods of microstrip fabrication. One technique we will study is fabricating the superconducting microstrip transmission line by using lift-off instead of the typical etch-based micromachining. We have already fabricated an initial set of resonators, and data to date indicate that the loss tangent of microstrip made with lift-off might be smaller than that of resonators made with the traditional etching method. Another fabrication technique we plan to study is an alternate dielectric growth recipe. Specifically, we plan to investigate the loss in dielectric grown by using plasma-enhanced chemical vapor deposition (PECVD) as opposed to our current films, which are grown by direct current (DC) magnetron sputtering. The growth rate for PECVD dielectric is substantially faster compared to magnetron sputtering.

Graphene Windows for Advancing Electron RF Guns

2013-096-R1

Katherine Harkay, Richard Gulotty, Nicholas Sereno, Anirudha V. Sumant, and Chun-xi Wang

Project Description

This project explores the possibility of developing large (on the order of millimeter) suspended graphene membranes and investigating their use for overcoming some long-standing challenges in high-brightness radio frequency (RF) photoinjectors, which are electron sources for some electron accelerators. Since its discovery in 2004, graphene's extraordinary properties have been demonstrated, stimulating a wide range of applications.

In this project, we will investigate whether graphene membranes can act as protective windows for electron sources. We will fabricate millimeter-scale, high-quality suspended graphene at the Center for Nanoscale Materials at Argonne. We will study the strength and diffusivity of the membranes at the Advanced Photon Source by using experimental data combined with finite element simulations. In addition, we will investigate the ability of the membranes to survive in a typical accelerator environment — in particular, the exposure to the driving laser — through Raman laser ablation experiments.

Mission Relevance

This project is relevant to DOE's mission in science. High-brightness electron sources are fundamental to frontier scientific facilities, such as x-ray free electron lasers and energy-recovery-LINAC-based x-ray light sources. Electron guns are the electron sources/injectors for these billion-dollar machines. Since electron beam quality will deteriorate as it approaches the target, the requirement for initial beam quality is extremely demanding. Furthermore, better quality beams can have a big impact on the cost of such facilities. With their extraordinary properties, graphene windows can potentially prevent degradation of cathode material in the electron source and thus significantly advance electron sources to meet demanding beam quality.

FY 2014 Results and Accomplishments

In FY 2013, we developed a process for growing large-area, high-quality graphene on copper film; the graphene layer number was controlled by using different gases during cooling stage. As a result, we were able to reliably grow large-area single- and bi-layer graphene. The next step we developed was to transfer single- and bi-layer graphene onto another silicon substrate with prefabricated holes by using a polymethyl methacrylate (PMMA) transfer handle with minimum residual contamination as a result of leftover PMMA. We further developed a new process to grow large-area reduced oxide graphene-like carbon (R-GOC) on copper film, and we were able to transfer R-GOC without the use of PMMA, thereby eliminating the contamination introduced during PMMA removal. By controlling the deposition time, we were also able to control the thickness of the R-GOC film. Most importantly, we discovered that the R-GOC-graphene film can be converted to graphene by using laser ablation on an area of 100 μm^2 — a discovery that enabled us to fabricate large area free-standing R-GOC films on holes for vacuum leak measurements.

In FY 2014, the major accomplishments in this project were the development and testing of reduced graphene oxide like carbon (R-GOC) -supported graphene membranes (Figure 1), as well as testing of the polymethyl methacrylate (PMMA) -supported and freestanding millimeter-scale graphene membranes (Figure 2). Fabrication of the R-GOC-supported graphene samples was accomplished through the synthesis of R-GOC graphene on copper by chemical vapor deposition (CVD), followed by transfer of the R-GOC graphene to the aperture substrates. The R-GOC-graphene film can be deposited as thin as 4 nm thick. Laser ablation experiments were carried out on transferred R-GOC-graphene films by using monochromatic laser light and Raman spectroscopy, which showed that the R-GOC-graphene film could be converted to a continuous single layer graphene with no significant signal of contaminates. R-GOC also did not suffer from the pitting/hole problem of graphene. We showed an alternative method for suspended graphene fabrication that completely avoids polymer residues and the use of solvents.

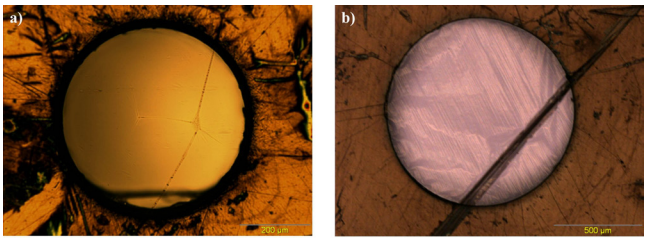

Figure 1. Optical images 10-nm-thick R-GOC-supported graphene membranes on stainless steel, 0.5 mm (a) and 1 mm (b) diameter.

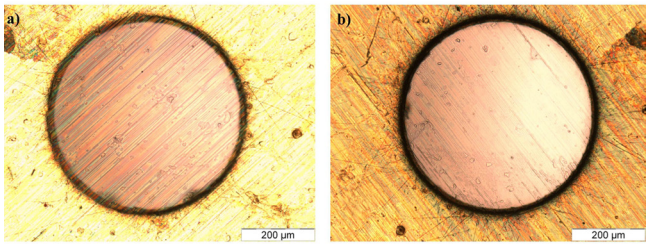

Figure 2. Optical images of 0.5-mm-diameter PMMA-supported graphene membrane (a) and freestanding graphene membrane after acetone and IPA cleaning (b).

The next stage was to scale up the fabrication area. Up to one millimeter-sized graphene membranes were achieved on metallic substrates with the R-GOC support. Breaking strength and helium diffusivity experiments were carried out on the R-GOC supported samples, as well as on the PMMA transferred/supported films.

We designed and fabricated a two-chamber vacuum system and data acquisition system for testing the graphene membrane's breaking strength and helium diffusivity (see Figure 3). This setup was used to measure the differential pressure at membrane rupture, ΔP, the light intensity change at membrane rupture, ΔI_0, as well as the helium leak rate across the membranes. Finite element simulations were carried out to extract the breaking strength and helium permeability of the R-GOC and PMMA supported membranes. The membranes were found to be impermeable to helium and transparent to light.

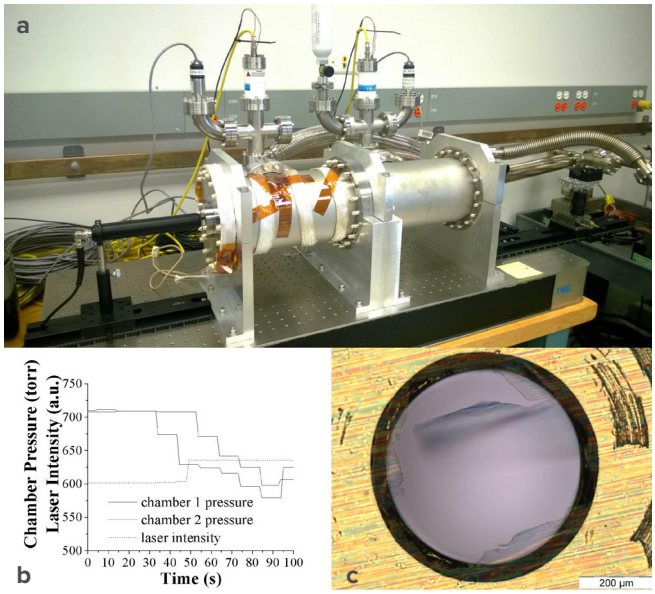

Figure 3. Optical image of two-chamber vacuum system for testing membrane breaking strength and helium diffusivity (a). Plot of pressure gauge readings of each chamber with light transmission intensity of the laser during differential pressure test of bilayer graphene (b). Optical image of ruptured graphene membrane (c).

Regarding the ability of graphene to withstand the drive laser for the RF gun, in the ablation experiments, a Raman laser with power density of 1.5 GW/m^2 was used at atmosphere in the presence of oxygen. However, we calculated that a typical drive laser for the RF gun delivers 0.6k W/m^2, peaking at 20.8 TW/m^2 in a vacuum. Further experiments with a typical driving laser in vacuum are required to determine the survivability of graphene or supported graphene in the driving laser environment.

Our project findings lead us to conclude that graphene may be an acceptable window material for maintaining the high vacuum accelerator environment, especially for high-brightness electron RF guns, but more experimental work is needed to develop more effective fabrication methods if a large graphene membrane completely free of polymer residue and pits is desired. Further experimental work is also needed to determine the survivability of graphene in the driving laser environment.

3-D Compositional Control of Intermediate-Band Solar Cells

2013-100-R1

Alex B.F. Martinson and Michael J. Pellin

Project Description

Intermediate band (IB) solar cells are designed to retain the high output voltages of large bandgap semiconductors while harvesting significantly more of the solar spectrum, thereby exceeding the Shockley-Queisser (S-Q) limit of solar conversion efficiency. By using the intermediate band as a stepping stone, electron-hole pairs may be generated from photons with insufficient energy to pump electrons directly from the valence band (VB) to conduction band (CB). However, it appears likely a new level of compositional control over these active layers will be required to precisely tune mid-gap states while minimizing recombination. Advances in atomic layer deposition (ALD) and sulfide-based photovoltaics (PV) in our lab, combined with recently identified IB materials, reveal a new opportunity to rapidly advance this emerging field.

In this work, we will fabricate thin films of the most promising bulk IB materials identified to date and leverage the three-dimensional (3-D) compositional precision of ALD. We will probe the extent to which, as has been postulated, $V_{0.25}In_{1.75}S_3$ satisfies the demands of an IB solar absorber in polycrystalline thin film form. We seek to investigate the complex photophysics expected from a multilevel system by using time-resolved optical spectroscopies. We will thereby probe the kinetics of excited state populations and quantify the dynamics of charge recombination as a function of material composition. Finally, the first $V_{0.25}In_{1.75}S_3$ IB PV device stacks will be fabricated and tested.

Mission Relevance

This project is relevant to DOE's missions in basic science and energy. Our basic science understanding of IB materials is incomplete, especially in the area of thin film synthesis/deposition. More generally, our control over the precise 3-D location of atoms in alloys and doped materials used in PV and other optoelectronic materials is lacking. If promising IB materials can be fabricated into efficient PV device stacks, there is an opportunity to considerably exceed the theoretical limit of present PV technologies. Higher PV efficiencies have a compounding economic

effect due to reductions in the *overall* $/watt of PV that includes land use, hardware, installation, and maintenance.

FY 2014 Results and Accomplishments

In FY 2013, we fabricated alloy indium-vanadium sulfide thin films by using atomic layer deposition. A comprehensive screening of commercially available volatile indium precursors revealed a lack of adequate routes to In_2S_3 that meet the materials and process requirements of IB PV. We developed and tested a novel In precursor and ALD process, which enables low-temperature growth without risk of oxygen contamination. Through optical, electrical, and structural characterization, we explored the resulting material space and verified conditions under which a polycrystalline, lightly n-doped base is routinely produced.

In FY 2014, we investigated the optoelectronic properties and photophysical dynamics of semiconducting base (indium (III) sulfide [In_2S_3]) and intermediate band (V:In_2S_3 [V-substituted In_2S_3]) thin films. In addition, the thin-film synthesis has been further refined to correlate composition with distinct IB properties. An additional absorption feature is clearly seen upon V substitution. With increasing V content, an ever larger fraction of the solar spectrum is harvested (Figure 1). Furthermore, the energy of this new transition (centered at 1.8 eV) is in reasonable agreement with that computationally predicted previously. In addition to the creation of a discrete density of states within the semiconductor gap, the operation of an intermediate band device is expected to depend most crucially on the photoexcited charge lifetime. As such, ultra-fast transient absorption (TA) and photoluminescence experiments were performed. At least two spectral signatures were observed, each of which decays at a characteristic time constant, revealing the excited state dynamics of In_2S (Figure 2). The ~100 ns lifetime is further corroborated by photoconductivity measurements, from which a similar excited state time constant is deduced. Preliminary measurements of V:In_2S_3 reveal a far more complex story, as expected.

This work resulted in the following invention/patent:

Martinson, A., A. Hock, R. McCarthy, and M. Weimer. "Oxygen-free Atomic Layer Deposition of Indium Sulfide." Invention report disclosed March 2014. Patent Application No. 14/335,745 filed July 2014. [ANL-IN-14-022].

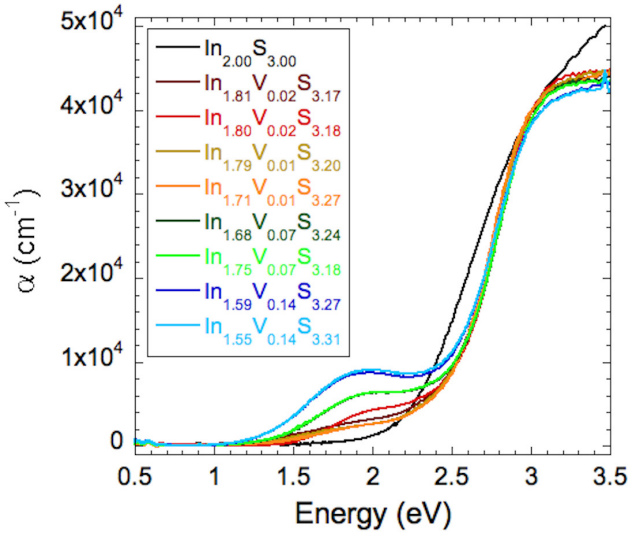

Figure 1. Increasing vanadium concentration leads to increased sub-band gap absorption in $V_xIn_yS_z/In_2S_3$ films grown at 200°C.

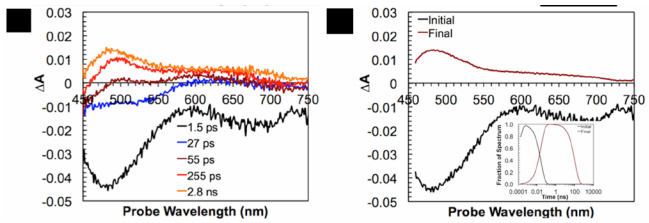

Figure 2. Transient absorption measurements and the best-fit, time-dependent model spectrums of the data for indium sulfide thin films grown at 225°C. The inset shows the contribution of each spectral component used to fit in time.

Proposed Work for FY 2015

In FY 2015, we will continue to refine our understanding of and control over the intermediate density of states. A tight feedback loop between thin-film fabrication and optoelectronic properties — especially those that probe the new IB — will provide new insight into this exciting class of materials. Low energy photoluminescence, transient absorption, and photoconductivity will identify the most likely candidates for trial in the first intermediate band photovoltaic devices. Schottky junctions and p-i-n diodes with V:In2S3 will be fabricated and tested for IB response.

Nanolaminate Coatings for Improved Nuclear Fuel Cladding Performance

2013-116-R1

Michael J. Pellin and Abdellatif Yacout

Project Description

As exemplified by the Fukishima reactor accident, nuclear materials — particularly in the claddings used to protect

nuclear reactor fuel — are critical to a reactor's severe accident tolerance. More capable materials offer the ability to extend fuel burn-up and reduce operation costs. Zircaloy, the material of choice for claddings in nearly all operating nuclear reactors because of its many outstanding properties in a nuclear environment, fails when driven beyond design limits, such as in a loss of coolant accident (LOCA), as a result of degradation of its passivating oxide layer. While excellent in many regards, Zircaloy (in its many alloy forms) can either burn exothermically or produce explosive hydrogen (H_2) gas mixtures when driven beyond normal operating temperature limits in a water environment. In addition, a fraction of the generated hydrogen embrittles the cladding alloy, ultimately leading to mechanical failure.

Our project will enhance the passivation properties of the Zircaloy passivation layer with the addition of a nanolaminate (NL) layer followed by annealing to produce phase-pure intermetallic layers, the stability of which resists oxidation at much higher temperatures than standard Zircaloy. Subsequent nanolaminate layers of t-ZrO_2 can then be applied to slow the oxidation rate, allowing the material to survive at temperatures above 900°C.

Mission Relevance

This work supports several DOE's mission in energy. Nuclear fuel cladding is the first and most important of the three barriers between highly radioactive materials in a nuclear reactor core and the environment. Overall, enhanced cladding would help catalyze the timely, material, and efficient transformation of the nation's energy system, while improving U.S. leadership in clean energy technologies. More specifically, if successful, advanced cladding would improve the materials degradation issues in our light water plants, bring potentially disruptive technology to the nuclear industry and bridge basic discoveries with energy relevant outcomes. This approach has the advantage of maintaining the use of traditional cladding materials instead of resorting to new cladding materials, such as silicon carbide (SiC), that might have the potential for improved performance, but at much higher cost. Our approach also has the flexibility to address, with stepwise addition of different layers, the many material issues that limit the lifetime and operating conditions of current claddings, including pellet-clad interactions (e.g., using nitride barrier layers), fretting (e.g., using super hard nitride layer stacks), and delayed hydride cracking.

FY 2014 Results and Accomplishments

In FY 2013, we developed atomic layer deposition (ALD) methods to deposit a variety of protective, adherent films on the surface of several Zircaloy clad alloys. The deposition was demonstrated to be uniform on both the outside and inside of the clad tubes. These depositions delayed the onset of oxidation to temperatures near 600°C — a significant improvement over uncoated Zircaloy. The thermal expansion differences between film and cladding often led to failure when the underlying Zircaloy phase transition was reached.

In FY 2014, we discovered that phase-pure intermetallic films can be grown on all types of Zircaloy cladding materials. These intermetallic films dramatically improve the corrosion resistance of the Zircaloy cladding. Despite their stability, they can be grown at temperatures below 650°C — crucial to maintaining the carefully designed underlying Zircaloy mechanical strength. Our process involves growing an alumina layer on the Zircaloy clad material by using ALD. This layer is then transformed into a phase-pure Zr_2Al_3 intermetallic layer with a low-temperature anneal at any temperature between 500 and 650°C. Our findings showed that (1) alumina could be reduced to a metallic alloy simply by heating in a vacuum environment, (2) very high temperatures were not required to make the conversion, and (3) the formation of a strain-relaxed system is unique, allowing the addition of oxide layers (such as zirconium dioxide [ZrO_2], in its tetragonal form) for water dissolution resistance or SiC for improved scratch (fretting) resistance (Figure 1).

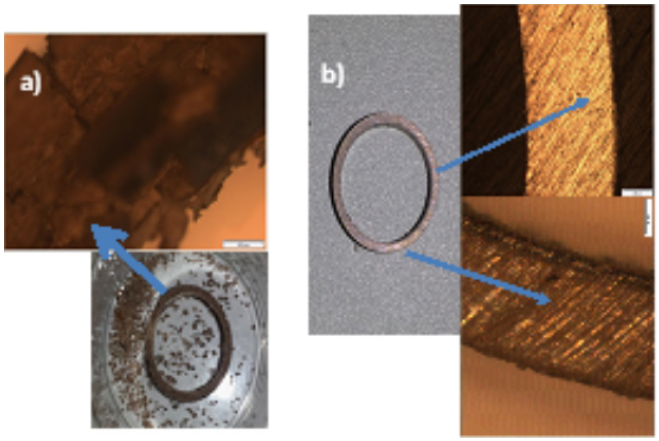

Figure 1. Peformance of Zircaloy two-ring cladding section after 30 days of heating at 550°C in air: (a) oxidation of an uncoated cladding section at high and low magnifications; (b) performance of a coated Zircaloy-2 section under the same conditions.

Proposed Work for FY 2015

We will focus on ATLAS (Argonne Tandem Linear Accelerator, a heavy ion accelerator capable of generating fission fragment energies) studies to demonstrate the radiation hardness of our nanolaminate films. Initial studies have been promising. Showing that nanolaminate films are stable at high radiation doses would make the technology far more attractive to potential technology adopters. In-pile experiments are expensive and are usually reserved for materials with a high expectation of success. Because we have built an accident tolerance scheme based on tried clad materials, this condition is relaxed somewhat. However, demonstrating that our materials are stable in ion

experiments at ATLAS will demonstrate that the technology is worthy of in-pile testing.

We will also test these films on a Westinghouse water test loop to demonstrate their ability to withstand both boiling water reactor and pressurized water reactor high-temperature/pressure water environments. In these cases, the addition of t-ZrO_2 films should improve cladding life in the reactor environment.

Magnetic Separation of Rare Earth Elements

2014-004-N0

Ross J. Ellis and Thomas Demars

Project Description

The separation of rare earth elements (REEs) by using current technology is costly and environmentally damaging. A new approach to separating REEs is to exploit the magnetic properties of REEs, which change considerably across the series and therefore could lead to more efficient processes. Such an approach is timely because new magnetic hybrid materials have been recently reported, namely magnetic surfactants and ionic liquids, that incorporate REEs. This project targets these new materials as potential media in which to achieve magnetically assisted REE separation. The objectives of our work in FY 2014 were to synthesize new magnetic hybrid liquids containing paramagnetic lanthanides that are amenable to separation and to investigate their magnetic responses.

Mission Relevance

Our project is relevant to DOE's missions in energy and science. The importance of REEs, which consist mainly of the lanthanides, has increased in clean energy applications because of their unique magnetic, optical, and chemical properties. As the demand for these technologies continues to rise and supply from the Chinese monopoly becomes more controlled, REE prices have become volatile. For example, prices of many REEs increased by 300–700% in 2010. Volatile REE prices have already caused the costs for some energy technologies to escalate and they may jeopardize the widespread adoption of many critical energy solutions by U.S. manufacturers (e.g., wind turbines and energy efficient lighting, to name just two). This has led to urgent DOE initiatives aimed at improving domestic technology for REE production.

FY 2014 Results and Accomplishments

Initially, we synthesized magnetic ionic liquids and surfactants and investigated their properties in terms of their suitability as potential media for the separation of REEs]. These materials were found to be either of extremely high viscosity or to decompose upon mixing with water, rendering them unsuitable for separation applications. Instead, new materials were sought in systems that were more robust and liquid.

Through our research, we discovered a new kind of magnetic hybrid microemulsion material. This material was synthesized easily and spontaneously in the solvent extraction of REEs by using a malonamide amphiphile N,N'-dimethyl-N,N'-dioctylhexylethoxymalonamide (DMDOHEMA) in n-heptane. The responsive phase forms as a layer between the heptane oil and aqueous phase, as shown in Figure 1. Here, the response of paramagnetic Gd(III) and Ho(III) phases (top and bottom row of Figure 1) is compared to diamagnetic Eu(III) (middle row). The paramagnetic phases are clearly attracted by the magnet, overcoming both gravity and surface tension.

Figure 1. Effect of magnetic field on third phases formed with Gd(III) (top row), Eu(III) (middle row), and Ho(III) (bottom row). The magnet was smoothly moved up and down through the oil phase to a distance of 5 mm from the third phase interface.

The responsive phases were investigated by using superconducting quantum interference device (SQUID) magnetometry, and their structure was characterized by using small-angle x-ray scattering (SAXS) and extended x-ray absorption fine structure (EXAFS) to understand the origins of the responses. We found that the phases were not superparamagnetic, as was the case for the analogous magnetic ionic liquids. Instead, the metal ions were isolated, completely hydrated in water channels that made up a bicontinuous mesoscopic structure of the responsive middle-phase microemulsion.

Proposed Work for FY 2015

The new responsive microemulsions discovered in FY 2014 present a two-pronged opportunity to (1) investigate the fundamental origins of magnetic response in paramagnetic hybrid liquids and (2) investigate the properties of the new systems to develop concepts that could exploit the magnetic moments of the REEs to assist in their separation. A specific hypothesis in this work is that the structure of the magnetic phases influences the response. Therefore, conditions will be varied to manipulate the microemulsion structure and the magnetic response will be compared. By understanding the correlation between the structure and magnetic properties, we will reach a fundamental understanding of this new class of magnetic material. This will assist us in developing these systems for their applications in a separations process.

Dynamics of Spin Ice

2014-018-N0

Axel Hoffmann and Olle Heinonen

Project Description

The dynamics of magnetic systems is full of complexities, making it an intriguing research topic from a fundamental point of view, but also attractive for applications, such as information processing. Toward this end, the nascent research field of magnonics aims at processing information with spin waves, the behavior of which can be controlled by the magnetic state of the underlying magnetic elements. In that respect, we have shown very recently, theoretically, that so-called artificial spin-ice systems exhibit specific oscillations tied to peculiar magnetic defects.

Frustrated magnets, such as spin ice, have been of scientific interest for a long time because of their highly degenerate ground states, which result in complex magnetic ordering and collective behavior. These frustrated magnets can be realized in crystalline materials, but analogous physics can also be observed in artificial spin ice, which consists of patterned magnetic nanoscale elements with dipolar interactions. Compared to crystalline systems, the artificial spin-ice systems have the advantage that the magnetization state of each individual "spin" (i.e., single domain magnetic particle) is directly accessible through magnetic microscopy.

Artificial spin ices exhibit large versions of elusive magnetic monopoles, which were originally predicted by Nobel Prize (physics, 1933) winning researcher Paul Dirac, and are connected by a chain of magnetic defects called Dirac string. Up to now, experimental investigations of these systems have exclusively focused on the statistics of the defects and their quasi-static evolution after field and thermal cycling. But the new theoretical predictions open up new opportunities for characterizing topological defects in crystalline and artificially frustrated magnetic systems, as well as for using these defect strings and monopoles in information storage and computing devices based on magnetic oscillations.

The goals of our project are to experimentally investigate the localized dynamics due to topological defects in spin-ice systems and to ultimately develop new approaches for their controlled manipulation. Toward this end, Brillouin light scattering microscopy is an ideal tool, since it enables spatial imaging of the magnetization dynamics with high frequency and spatial resolution. Using this tool, we will test theoretical predictions at a microscopic level, which will be used to explore novel ways to control and manipulate the evolution of the topological defects.

Mission Relevance

This project is relevant to DOE's energy and science missions, and it will have both fundamental and applied impacts. The prospect that certain dynamic modes will only propagate along defect Dirac strings opens up exciting possibilities for guided energy and information flow in magnonic systems. This means that a controlled manipulation of the topological defects in spin-ice systems may enable fundamentally new ways of information processing with magnetization dynamics. The most direct impact of this work will be in terms of a better fundamental understanding on how topological defects impact the dynamic behavior of frustrated magnetic systems. Artificial spin-ice systems are ideal model systems for this, since they allow correlating statistical information from the whole ensemble, which is typically the only information available in crystalline frustrated systems, with a detailed microscopic arrangement of the individual spins comprising the frustrated system.

FY 2014 Results and Accomplishments

We started the fabrication of artificial spin-ice structures integrated with co-planar waveguides and are currently optimizing the corresponding processing. Initially, we pursued transparent substrates for optical access from the backside. However, electron beam lithography on insulating MgO substrates has been challenging because of distortions by charge accumulations, which now leads us to consider an alternative pathway toward fabrication with the patterned magnetic structures on top of a coplanar waveguide.

In addition, we prepared spin-ice structures without integration into coplanar waveguides and measured thermally activated magnetization dynamics with Brillouin light scat-

tering. We observed an excitation, which is reasonably consistent with what is expected for the largest amplitude resonance from micromagnetic simulations. However, at this point, it is unclear whether this is an artifact from the laser. Furthermore, we observed that the patterned structure was physically damaged by the highly focused laser intensity used for detecting low-intensity thermally activated modes. Thus, it will be necessary to reduce the incident laser light intensity, which should be no problem for resonantly driven dynamics for the samples integrated with coplanar waveguides.

Parallel to refining the experimental investigation, we also pursued additional theoretical studies of the dynamics in artificial spin-ice structures with micromagnetic simulations. One important insight from these simulations is that the interactions depend sensitively on the separation between the individual elements. Even only a small variation in the lattice constant from 415 to 405 nm gives rise to a significant change of the internal magnetization structure. Importantly, as the separation becomes closer, this may introduce additional symmetry breaking magnetization structures. This asymmetry is also reflected in different frequency dependencies of the magnetization dynamics as a function of the radio frequency (rf) field direction.

Proposed Work for FY 2015

Our proposed work for FY 2015 includes the following:

- Adapting our existing Brillouin light scattering microscope to imaging by using a longitudinal magneto-optical Kerr effect.
- Characterizing dynamics globally (impedance spectroscopy) and locally (Brillouin light scattering microscopy).
- Extending investigations beyond square lattices to honeycomb and Kagome lattices.
- Fabricating samples with integrated microwave antennas for single element excitation.
- Imaging of spatial distribution of defect dynamic modes upon local excitation.

Seminars

Hoffmann, A. (2014). "Connecting Spin Waves to Charge Currents." Ohio State University, Columbus, OH, November 21, 2013.

Exploring the Universe with Full-Sky Simulations of the Cosmic Microwave Background

2014-019-N0

Katrin Heitmann

Project Description

The cosmic microwave background (CMB) is witnessing a paradigm shift through measurements of arc-minute scale anisotropies by a new generation of telescopes, such as the South Pole Telescope (SPT), and the Planck Satellite. By combining these CMB observations with large-scale structure surveys, it is possible to address and connect some of the most fundamental questions in physics about the nature of dark energy, dark matter, the sum of the neutrino masses, and the number of relativistic species. To realize the potential of these measurements, next-generation studies in theory, modeling, and simulation are needed. Accurately capturing the physics of the real universe will be crucial for interpreting CMB experiments to answer fundamental science questions.

Our leadership computing capabilities at Argonne position us far ahead of the field to build an advanced program in simulating the CMB sky. This project is based on a set of state-of-the-art simulations carried out on Mira, the 10-petaflops IBM Blue Gene/Q system. The major aims of our proposal are to extract exciting science from the simulations and to establish Argonne's theoretical CMB effort. We will generate a set of CMB maps spanning different cosmological models and astrophysical effects.

Mission Relevance

Our project is relevant to DOE's mission in science and technology. The project addresses key areas in the High Energy Physics (HEP) DOE Office of Science Cosmic Frontier focus area and touches upon related questions in the Intensity Frontier (the mass of the neutrino). This project seeds a new CMB theory, simulation, and analysis effort at Argonne, complementing the already existing, successful experimental effort. Argonne is the first of the DOE HEP Laboratories at which CMB-related research and development (R&D) is supported. Broader impacts of this science are in the areas of nanofabrication and new sensor technologies, both of which are very important components of DOE's R&D portfolio. The connection of this project to the experimental activity is the innovative use of high-performance computing, which is one of the drivers for DOE's exascale computing initiative.

FY 2014 Results and Accomplishments

We built a first set of CMB maps including astrophysical effects and scaled up our analysis pipeline to enable efficient processing of our very large simulations. The first CMB map includes foreground sources using a semi-analytic approach. Dark matter halos were identified and the Sunyaev-Zel'dovich (SZ) effect was added by using a semi-analytic model for gas physics. Infrared sources were also added to the halos by using a semi-analytic approach calibrated to observations. The resulting synthetic maps in different wavebands were used to investigate the effects of different biases on the CMB lensing power spectrum.

We finished work on the efficient construction of light-cone outputs. First, we enhanced the Hardware/Hybrid Accelerated Cosmology Code (HACC) to produce particle light cones *in situ*. Second, a new, parallel stand-alone tool was written that can extract light cones from output files efficiently. Figure 1 shows a halo light cone constructed from one of our simulations. We integrated this light-cone capability with our SZ modeling pipeline, optimized to work within the HACC framework. Figure 2 shows an example of a kinetic (k) SZ map created from one of our light-cone halo catalogs. The pipeline is currently applied to a large simulation for which we have synthetic sky maps showing the galaxy distribution. The kSZ map from this simulation and the galaxies will be cross-correlated to understand how the two are connected.

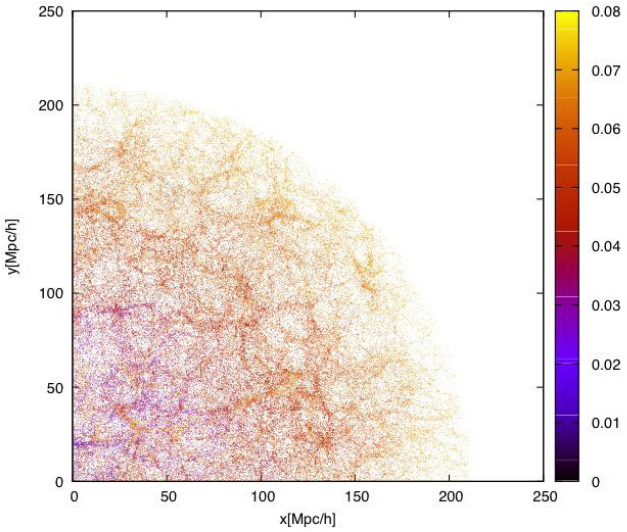

Figure 1. Halo light-cone output; colors indicate the redshifts of the halos.

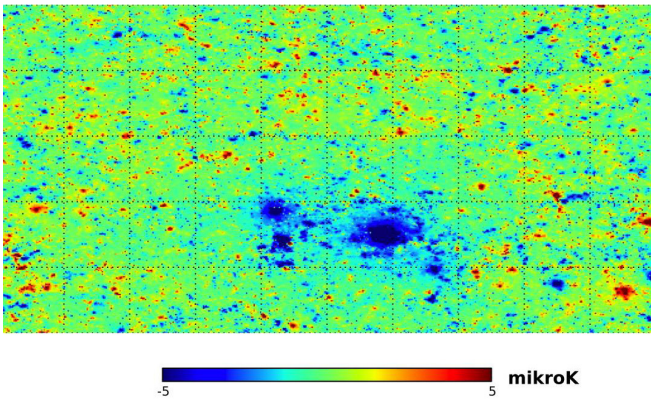

Figure 2. Simulated map showing the kinetic SZ effect.

Finally, using a large INCITE (Innovative and Novel Computational Impact on Theory and Experiment) allocation, we have increased our set of cosmological simulations that will be used for this project. The INCITE program is a competitive award of large allocations of supercomputing time at DOE's leadership computing facilities.

Proposed Work for FY 2015

In FY 2015, we will continue to apply our new pipelines to the large new simulations, spanning several cosmological models. We will analyze the new maps and investigate how the different probes are sensitive to cosmology. We will also work on the cross-correlation of our SZ maps with optical synthetic maps. The results from this work will lay the foundation for new observational work. We will closely collaborate with the SPT team to make our effort most valuable for the survey.

Development of Large-Area Vacuum Ultraviolet Microchannel Plate Photodetectors for Use in Large Liquid Argon and Xenon Time Projection Chambers

2014-023-N0

Jonathan M. Paley and Zelimir Djurcic

Project Description

The goal of this project is to reconfigure and optimize the large area photodetectors developed at Argonne for operation in a liquid argon (Ar) time projection chamber (LArTPC). Noble liquid time projection chambers (TPCs) are used in many neutrino, dark matter, and neutrinoless double beta decay experiments, and the vacuum ultraviolet (VUV) scintillation light produced in these particle detectors is used for both determining the absolute timing

of the interactions inside the liquid, as well as for calorimetry. This information greatly enhances the detector's particle identification capabilities, and it improves the level of signal-to-background events.

Traditional glass-based photomultipliers (PMTs), silicon photomultipliers (SiPMs), and avalanche photodiodes (APDs) are all detector technologies that have been successfully used in LAr and liquid xenon time projection chambers (LXeTPCs) for scintillation light measurements. These technologies have served adequately, but they are very expensive per unit area. The microchannel plates (MCPs) that we plan to develop in this project will have similar or better performance and potentially cost significantly less per unit area.

The core components of the large area photodetectors are a pair of MCPs that are coated with a resistive layer via atomic layer deposition (ALD) and photocathode. The behavior of these components is fundamentally different at cryogenic temperatures than at room temperature, and so significant effort on this project will be dedicated to measuring the performance of these components at different temperatures and optimizing the design of a device for operation in a cryogenic environment.

Mission Relevance

The project is relevant to DOE's mission in science by potentially reducing the cost while simultaneously increasing the scientific output of high energy particle physics experiments. LArTPC detector technology is a central component of the next 10–20 years of experimental neutrino physics, a key driver of the DOE's Office of High Energy Physics investment in facilities and research. The main neutrino detector in the future Long Baseline Neutrino Facility, recently strongly endorsed by the Particle Physics Project Prioritization Panel (P5), will be a 10–40 kiloton LArTPC, and many smaller neutrino experiments planned over the next two decades also plan to use this detector technology. This project has the potential of putting Argonne in a leadership role in the development and implementation of large area cryogenic photodetectors that are needed to perform some of the desired measurements in these experiments. This technology could also be easily commercialized if the global market for such detectors is large enough.

FY 2014 Results and Accomplishments

In FY 2014, we tested several components of a 6-cm Large Area Picosecond Photodetector (LAPPD) in liquid nitrogen and observed no degradation of the parts after several minutes at cryogenic temperatures. We also measured the resistivity across a functionalized microchannel plate (MCP) at cryogenic temperatures and observed an increase in resistivity of two orders of magnitude at liquid nitrogen (LN_2) temperatures. This requires a modification to the ALD "recipe" to obtain a reasonable resistivity at cryogenic temperatures. We also demonstrated that a sealed mechanical test device holds the vacuum when submerged in LN_2. The device was left in a dewar of LN_2 for ~15 minutes, and no degradation of the vacuum was observed.

Proposed Work for FY 2015

Preliminary tests show that the MCP resistance goes up at a low temperature, it behaves like a semi-conductor. We will work with the Energy Systems Division to begin measurements of the resistance of MCPs with different ALD recipes at room and cryogenic temperatures.

We will work with the LAPPD group at Argonne National Laboratory to design and build a test setup to study the performance of a bialkali photocathode when it is exposed to low temperatures and when it is exposed to VUV light.

VUV light will not penetrate the glass window of the LAPPD. The traditional approach is to coat the surface of the glass that is exposed to the VUV scintillation light with a wavelength shifter chemical. These wavelength shifting chemicals have been demonstrated to work; however, they tend to be very reactive and cannot be exposed to large amounts of UV light. We will therefore also investigate the possibility of using magnesium fluoride (MgF_2) windows in LAPPDs that are VUV transparent.

Furthermore, we plan to investigate the possibility of using the ALD-functionalized MCP as the photocathode itself, where the device is in a pure gas Ar, but close to cryogenic temperatures, environment.

New Paradigms for High T_c Superconductivity in Acene-Based Materials

2014-025-N0

Wai-Kwong Kwok

Project Description

The discovery of a new class of high-temperature superconductors (HTS) is a marked rare event. Recently, superconductivity has been observed in a new family of compounds, reductively doped acenes, which represent the first class of organic HTS in over a decade. As this field is in its infancy, there is significant potential for discovering higher high- temperature (T_c) superconductors. The growth of this field is currently limited by a synthetic bottleneck that can be addressed through chemical methods. The project's central hypothesis is that solution-based synthetic techniques represent an elegant and rapid method

for uniformly doping acenes to a precise dopant level, thus enabling the discovery of new HTS with high shielding fractions. The technique is amenable to single crystal growth that will provide specimens for detailed property measurements. This project will develop solution-based chemical doping methods and complement them with the use of a versatile and elegant electrochemical procedure in which the doping potential is set and the stoichiometry is determined by electron counting.

Mission Relevance

The project is relevant to DOE's mission in science. The search for new materials is at the very heart of scientific research and was clearly accentuated in the DOE's report on "Basic Research needs for Superconductivity." Furthermore, several key reports have recognized the importance of crystal growth capabilities as a key requirement for the continued development of basic energy sciences, and this project contributes to this important national goal. Although the payback is enormous, the search for HTS is a highly risky endeavor, as history shows that many of the major HTS discoveries were serendipitous. However, history also shows us that when a new superconductor is discovered, it initiates a frenzy of synthesis and/or doping activities that inevitably result in even higher transition temperature superconductors. This project represents a timely endeavor to target the crystallization of *molecular-based superconductors*, an area that has very recently proven to be a ripe fertile ground for new discoveries for superconductors with $T_c > 30$ K.

FY 2014 Results and Accomplishments

Commercial samples of picene, dibenzopentacene, coronene, and phenanthrene were obtained. It was found that, as received, picene and dibenzopentacene contained significant impurities on the level of 10%. As this is unacceptable for precise measurements, purification strategies for these materials were developed. Solution-based recrystallizations proved difficult for the larger acenes and efforts therefore turned to sublimation techniques. Initial attempts to use a simple vacuum sublimation apparatus yielded high-purity *polycrystalline* powders rather than the desired single crystals. A more elaborate three-zone sublimation procedure was developed that has yielded promising results, suggesting that it is possible to grow the first single crystals of picene and dibenzopentacene. Solid-state potassium doping of phenanthrene in sealed quartz tubes was initiated where white phenanthrene powder turns black upon doping for the transformation from an insulating to a metallic state (Figure 1).

a. Before b. After

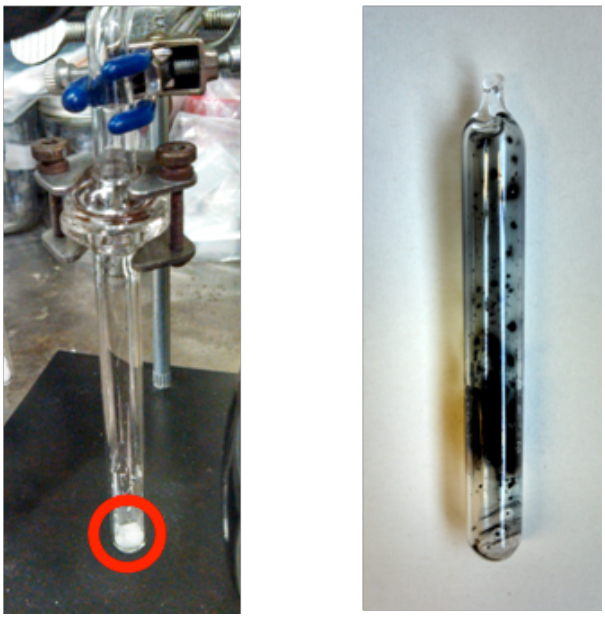

Figure 1. (a) Before: Air-sensitive doping of phenanthrene with potassium. White phenanthrene with potassium metal in sealed glass tube. (b) After: The black K3 (phenanthrene) after vacuum sealing and heat treatment at 200°C.

A potentiostat with controlled potential Coulometry (CPC) capabilities was obtained, assembled, and tested. The planned CPC doping of acene materials must be performed in a dry box to prevent oxidation of the air-sensitive products. A dry box was assembled and an electrochemical cell suitable for these experiments was designed and constructed.

In collaboration with researchers at Scuola Internazionale Superiore di Studi Avanzati, we carried out *ab-initio* density functional calculations for La-phenanthrene, as a generic case of [three electron doping, to investigate the structure and properties of a conceptually simple case. Surprisingly, it was found that the lowest energy state is not metallic, but band insulating, with a disproportionation of two inequivalent polycyclic aromatic (PA) molecular ions, thus challenging the common assumption that three electrons will automatically metalize a polycyclic aromatic hydrocarbon (PAH). However, metastable metallic states are indeed predicted to be accessible.

Proposed Work for FY 2015

Research in FY 2015 will focus on solution-based doping of acenes. The infrastructure is now in place to perform these experiments and produce tangible materials for physical property measurements. Chemical doping with alkali metals will be achieved through Schlenk techniques. We will electrochemically dope materials through the CPC technique that will allow the incorporation of a wide range of cations to stabilize predetermined dopant levels of selected acenes. Regarding single crystal speci-

mens, potassium doped coronene will be targeted with the goal of extracting its electronic and magnetic properties. Theory will be used to both understand experimental results and guide synthesis. This will be especially useful for the design of phenanthrene-based molecules for targeted synthesis.

Exploring the Direct Observation of the ^{229m}Th Isomeric Decay

2014-034-N0

Wei Jiang, Peter Mueller, and Jake Zappala

Project Description

^{229}Th has drawn considerable attention recently because of the potential of building an optical clock with extremely high accuracy and stability and the opportunity to test the temporal variations of the fine structure constant. All of these interesting ideas are based on a ^{229}Th nuclear transition with very low energy that can be accessed by lasers (~159 nm). The isomer decays via a highly suppressed M1 transition with a lifetime estimated to be a few hours, corresponding to a transition linewidth of a few μHz.

Despite the great opportunities of the ^{229}Th isomeric nuclear transition, decay of the ^{229m}Th has so far not been observed unambiguously. It is important to perform an experiment that can observe this transition directly, determine the lifetime of the ^{229}Th isomer, and measure the transition energy more precisely. In this project, we are studying a novel approach for observing the ^{229}Th isomer decay by implanting it onto a substrate and detecting the VUV photons directly. After ion implantation, there will be induced luminescence background from the substrate. It is desirable to find a proper material whose luminescence decays very fast and fluoresces at a wavelength far from 159 nm.

To find a material suitable to make a substrate, we will build an ion implantation station. We will use a $^{232}Th^+$ ion to simulate the effect of the $^{229}Th^+$ and $^{229m}Th^+$ ions. This setup will help us to understand the luminescence background induced by the ions and to find a suitable substrate material.

Mission Relevance

Our project is relevant to DOE's mission in science. Our project will investigate the feasibility of direct measurement of the ^{229m}Th isomer lifetime and transition energy. If the project is successful, it will result in an experimental campaign to measure the ^{229m}Th isomer lifetime and transition energy precisely, which will benefit many applications, including building optical clocks with extremely high accuracy and stability and the opportunity to measure the temporal variations of the fine structure constant.

FY 2014 Results and Accomplishments

We fabricated a setup to test various substrate candidates (e.g., MgF_2, Sapphire) in FY 2014. The ions are guided by various ion optics and then focused onto an MgF_2 substrate. We finished debugging the system with a test potassium ion source. The ion flux at the substrate can be varied from 10^5 s^{-1} to 10^8 s^{-1}. We did systematic studies of the luminescence from an MgF_2 substrate under the bombardment of K^+ ions.

Energy Dependence of the Luminescence on the Incident Ion Beam Energy. Figure 1 shows the energy dependence of the luminescence on the incident ion energy (up to 12 keV). The induced luminescence is measured by a photomultiplier tube (PMT, 140–300 nm). We found that the luminescence intensity has a quadratic dependence on the energy of incident ion beam.

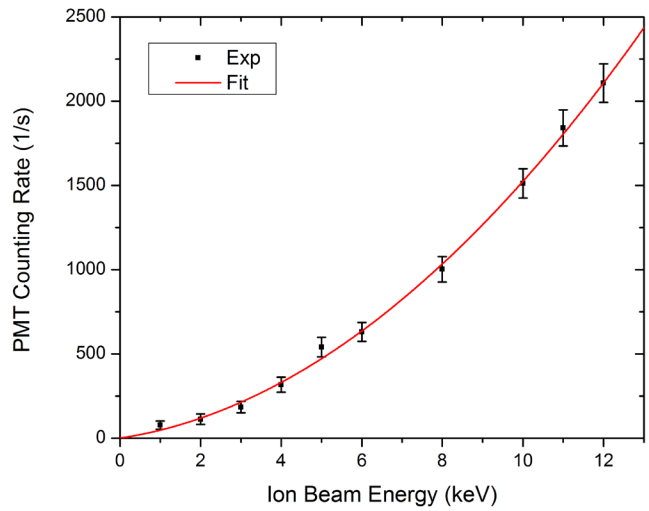

Figure 1. Energy dependence of the luminescence on the incident ion energy.

The integrated luminescence intensity (140–300 nm) induced by the ions is quite low. For a 5-keV K^+ ion beam with a beam intensity of 10^8 ions/s, we get a counting rate about 700 counts/s from our PMT (photomultiplier tube) with a light collection efficiency of 1%.

Spectrum of the Induced Luminescence. The spectrum of the induced luminescence is shown in Figure 2. We scanned from 140 to 300 nm. The peak of the luminescence is longer than 300 nm (Figure 2 b), and the intensity decays sharply toward the short wavelength side and vanishes around 200 nm. Below 200 nm, the induced luminescence is below our detection limit. This is very encouraging since at the interested wavelength for Th^{229} (159 nm), there is negligible luminescence background.

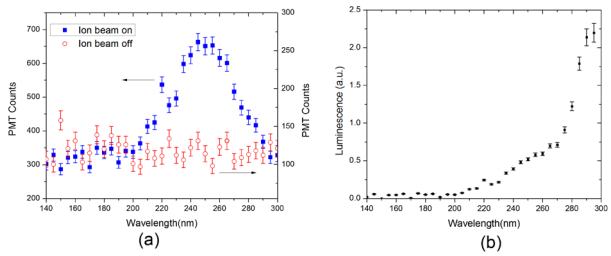

Figure 2. Spectrum of the induced luminescence, (a) measured directly from the PMT. (b) after the quantum efficiency of the PMT at different wavelengths is taken into account.

Temporal Behavior of the Luminescence. Figure 3 shows the measured luminescence after the ion beam is shut off. The intensity of the luminescence will drop two orders of magnitude immediately (within 200 ms) after the ion beam is removed. The remaining luminescence then decays slowly. By fitting the decay curve of the remaining luminescence, we found there are two components: one with a decay constant about 5 seconds, and the other slower component has a decay constant of about 90 seconds. This decay constant is still relatively fast compared to the estimated ^{229}Th isomer lifetime (a few hours).

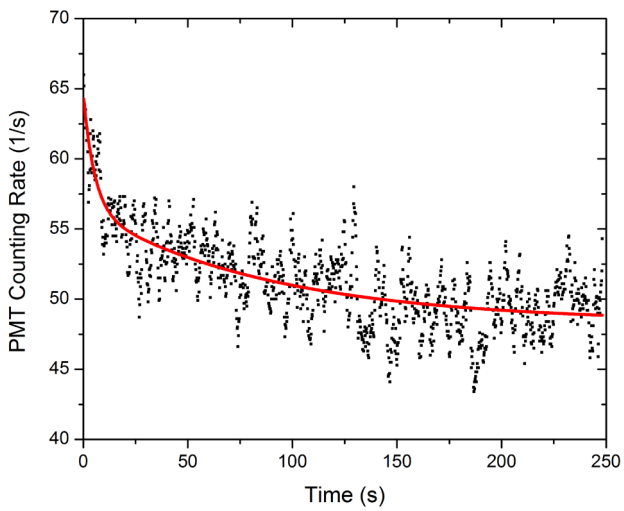

Figure 3. Temporal behavior of the luminescence.

To summarize, we successfully fabricated a setup to measure the induced luminescence of different materials under the bombardment of low energy ions. We carried out systematic studies of the luminescence from an MgF_2 substrate under the bombardment of K^+ ions. The results are very promising. It shows that the MgF_2 substrate produces very low luminescence background at the wavelength relevant to the direct observation of the ^{229}Th isomeric decay. We are planning to do the same measurements with a $^{232}Th^+$ ion beam to see if the property of the induced luminescence has any dependence on the species of the incident ions.

Proposed Work for FY 2015

In FY 2015, we will install a $^{232}Th^+$ laser ion source. We will perform systematic studies of the luminescence from various substrates under the bombardment of low energy $^{232}Th^+$ ions and find a material that produces minimal background at the wavelength relevant to the direct observation of the ^{229}Th isomeric decay.

Plastic Artificial Leaves for Water Splitting

2014-046-N0

Lin X. Chen

Project Description

The main challenge of using sunlight as an energy source is coupling single photon events with the multiple electron/hole redox reactions for water splitting, $2H_2O \rightarrow 2H_2 + O_2$ in which two half reactions are catalyzed separately. On the basis of our knowledge of organic photovoltaics (OPV) with conjugated polymers and artificial photosynthesis, we integrate a single, organic, photovoltaic p-n junction and water-splitting catalytic transition metal center into a bilayer organic "artificial leaves" (Figure 1). This idea is based the exciton splitting into holes and electrons at the interface of a single p-n junction composed of p- and n- type conjugated polymers layers. These charged carriers will be respectively collected by the catalytic metal sites, ligated with functional bipyridyl (bpy) sites incorporated in the polymer backbones (bottom of Figure 1). An artificial leaf can be formed when the oxidation and reduction catalytic reactions proceed as it absorbs sunlight to allow water oxidation/reduction take place simultaneously without external wiring (Figure 1).

Mission Relevance

This project is relevant to DOE's missions in energy and the environment. The goal is to discover and develop catalyst materials for renewable energy utilization and especially for solar fuel generation. The research will provide a deep understanding of how new materials can better use renewable energies. Its novel design, consisting of versatile devices, could be developed for multiple applications related to energy sustainability, in alignment with the DOE mission. If the results are promising, we expect to see interest from the energy industries, which could lead to lower-cost, lighter, more flexible, and/or more environmentally friendly devices.

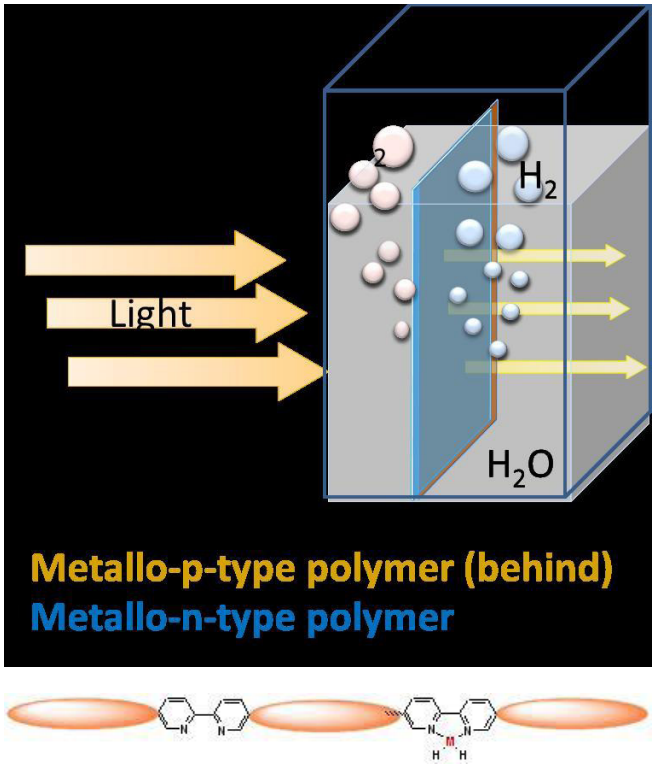

Figure 1. (Top) Illustrates the concept of bilayer, single-junction, polymer artificial leaves. (Bottom) Shows a general motif of the proposed metallo-polymers connecting metal-binding bpy sites and oligomer sections (orange ovals).

FY 2014 Results and Accomplishments

Polymer Screening to Identify Proper n-type Polymers as Platforms for Catalytic Reduction Metal Centers. One challenge in forming plastic artificial leaves is selecting the n-type polymers that would be suitable for accumulating electrons for hydrogen generation reactions. We measured the redox potentials of 12 n-type polymers used in previous work through collaboration with the University of Chicago to evaluate their potentials in the targeted application. These n-type polymers will be coupled with an efficient p-type polymer, PTB7 modified for binding metal centers for the water oxidation catalyst. Of the 12 n-type polymers, about half had enough force for the electron transfer reactions as planned. The next steps were to dope metal center catalysts into these polymers and to verify the redox potentials of the metallopolymer films.

Synthesis of New Metallopolymers. A few polymer were synthesized with metalloporphyrins inserted into a polythiophene network (Figure 2). The oligothiophene fragments harvest the light and to donate electrons to the metalloporphyrin moieties for catalytic reactions. The absorption spectra of poly-iron(II) and cobalt(III) tetra thiopheneporphyrins (pFeTTP and pCoTTP) show very broad absorption for effective light harvesting.

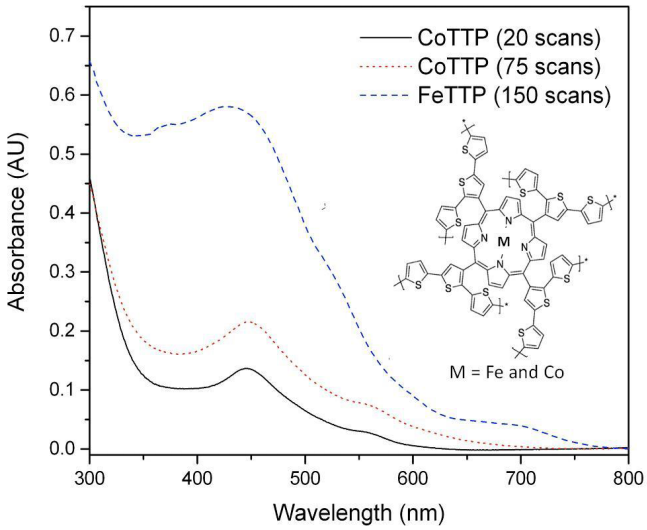

Figure 2. Structure of newly synthesized polythiophene network with cross-linked metalloporphyrins (Fe and Co).

Characterization of the Photophysics of Metallopolymers by Means of Ultrafast Transient Absorption Spectroscopy. Exciton dynamics of the pFeTPP and pCoTPP were characterized by ultrafast transient absorption spectroscopy detecting the exciton lifetime and find evidence of redox reactions at the metal centers. The transient absorption spectral signals shows that both polymers had a very short-lived exciton state due to the excited state being quenched by the metalloporphyrin with open-shell metal centers. The excited state absorption feature showed a very short decay time of a few picoseconds due to the electron transfer quenching, suggesting that the polymer and metalloporphyrin blocks are successfully coupled to achieve rapid charge separation. The results also indicated that the open-shell metal centers promoted rapid intersystem crossing which could hinder or promote the electron transfer, which is a key point to be investigated further.

Proposed Work for FY 2015

In FY 2015, we will do the following:

- Complete spectroelectrochemistry on the polymers to obtain the redox potentials of metal centers.
- Take parallel transient absorption and spectroelectrochemistry measurements of reference compounds to confirm the spectral assignments.
- Changing the relative ratio of the oligothiophene -to-metalloporphyrin moieties in the materials to search for the optimal redox reaction efficiency.
- Continuously investigate the synthesis of donor/acceptor polymers with metal centers.
- Apply beam time at Argonne's Advanced Photon Source (APS) to investigate the local structures of the metal centers in these polymers.

Carbon Nano-Network as Next Generation Support for Catalysis and Electrocatalysis

2014-051-N0

Di-Jia Liu and Jeffery Miller

Project Description

This project will focus on developing a new type of catalyst substrate — a carbon nano-network — for catalytic and electrocatalytic applications. It will contain macropores and micropores almost exclusively and thus be fundamentally different from conventional supports. It will overcome the shortcomings of traditional carbon supports by providing the following morphological advantages: (a) a highly micropore-dominant surface area and a pore volume crucial for enhancing the activities of heterogeneous and electrocatalytic reactions, (b) direct macropore-to-micropore connections as a result of "short-cutting" the mesopores and thus lowering the reactant's mass-transport resistance and improving the overall reaction rate, and (c) catalysts that are interconnected through a protective fibrous network and have better charge/thermal conductivities and chemical stability. The carbon nano-network substrate will be prepared through the electro-spin method, which produces a finely dispersed metal-organic-framework (MOF) encapsulated inside nanofibers. Upon thermolysis, a new structure will form that will feature active-site decorated, catalyst "pods" connected by a network of carbon fibers. The goal of the project is to design and fabricate several nano-network catalysts with different morphological properties and demonstrate their improved performance in fuel cells and in biofuel catalysis.

Mission Relevance

The research being done for this project focuses on improving energy efficiency and renewable energy production. The project is therefore relevant to DOE's missions in energy security and environmental quality. A pore-size-controlled carbon nano-network would not only have a strong impact on fundamental catalysis science but also have practical applications in next-generation catalysts and electrocatalysts. The new materials developed from this work could be applied directly to solve some of the most pressing problems related to energy conversion and environmental protection.

FY 2014 Results and Accomplishments

The objective of the first phase of the project was to develop new synthesis chemistry and material for an MOF-based, nano-network, non-precious-metal electrocatalyst (NPMC). The main accomplishments included the following:

Development of a One-Pot Process for MOF-Based Catalyst. MOF synthesis has been perceived as an expensive process, with multiple steps involving wet-chemistry-based crystallization and separation. We developed and improved a robust, one-step synthesis approach that significantly simplified the preparation of the MOF-based catalyst precursor at much lower cost. The new process dealt with the solid-state synthesis of a zeolitic imidazolate framework (ZIF, a subclass of MOF), in which metal oxide was physically mixed with organic ligands and transition metal compounds. The ZIF was formed through a simple heat treatment of the solid mixture (Figure 1). The one-pot synthesized precursor was further pyrolyzed at an elevated temperature to form the final catalyst. We tested the catalyst under the fuel cell operating conditions by applying it to the membrane electrode assembly (MEA). The current-voltage polarization study showed that the fuel cell prepared with the new Argonne MOF-based NPMC achieved high current density at different voltages and the peak power density of 620 mW/cm^{-2}.

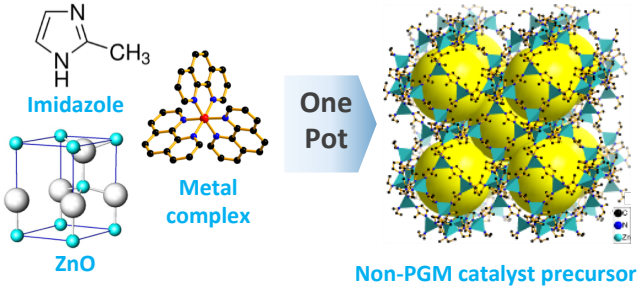

Figure 1. One-pot synthesis of the NPMC catalyst precursor through ZIF approach.

Investigation of MOF-Based Electro-Catalyst in Alkaline Media. A second research focus of this phase was to investigate the oxygen reduction reaction (ORR) activity of Argonne's MOF-based catalyst for application in alkaline membrane fuel cells (AFCs). Compared to a proton-conducting membrane fuel cell, an AFC has the potential to achieve higher ORR reactivity and durability when NPMC is used as the cathode catalyst. To this end, we tested our MOF-based catalyst in the alkaline medium by using the rotating disk electrode (RDE) method. For comparison, a carbon supported platinum catalyst (Pt/C) was also tested under the same conditions. We found that the NPMC material not only outperformed Pt/C, with a higher onset potential and mass current density, but it also demonstrated significantly better stability against oxidative corrosion. We are now improving the Argonne catalyst as a potential substitute for the costly platinum used in alkaline fuel cell applications.

This work resulted in the following invention:

Liu, D.-J. "Alkaline Fuel Cell Non-Platinum Group Metal Electrocatalysts Using Metal Organic Framework Materials and Method of Preparation." Invention report disclosed July 2014. [ANL-IN-14-079].

Proposed Work for FY 2015

A major task will be to explore a variety of new MOFs to further improve electrocatalyst activity. We will also develop and improve the electro-spin method to better incorporate newly optimized MOFs into the nano-fibrous network. Electrocatalytic activity and durability will be tested at both RDE and fuel cell levels. We will simultaneously start investigating MOF-based and nanofibrous-based catalysts in biofuel upgrade reactions. Transition-metal-based MOFs will be used to prepare bi-metallic and multi-metallic catalysts for selected catalytic hydro-deoxygenation reactions. Various characterization tools will be applied to study the catalyst's physical and chemical properties during synthesis and under reaction conditions.

Seminars

Liu, D.-J. (2014). "Oxygen Reduction Reactions in Fuel Cell & Li-Air Battery: Insights of New Catalyst Design & Catalytic Mechanism." Peking University, Beijing, China, September 23, 2014.

Thin Film Skyrmion Spin Textures

2014-054-N0

Suzanne G.E. te Velthuis and Axel Hoffmann

Project Description

A few years ago, it was discovered that certain magnetic materials lacking inversion symmetry could form complex magnetization patterns with magnetic spins, forming vortex-like structures. More surprisingly, this "skyrmion" structure of the magnetization could be manipulated with electric currents up to five orders of magnitude smaller than the currents required for current-driven magnetization dynamics in ordinary ferromagnetic systems. This feature makes magnetic skyrmions promising candidates as information carriers in low-power, ultradense memory and logic devices. The goals of this project are to explore the possibility of creating and stabilizing room-temperature skyrmions in a variety of thin films and to then develop new approaches for skyrmion manipulation. We will characterize the magnetic texture associated with skyrmions by means of optical imaging, neutron scattering, and electric transport measurements. New strategies for forming and manipulating individual skyrmions in patterned structures will be investigated, and the results may directly affect applications in information storage and computation.

Mission Relevance

This project is relevant to DOE's mission in science. The main impacts from this work will be on low-power information storage and logic device concepts. Individual magnetic skyrmions are extremely stable and exhibit particle-like behavior. These features, combined with the skyrmions' demonstrated ability to be manipulated with low electric currents, open new opportunities to overcome the challenges of recent information processing concepts based on magnetic domain wall motion. The focus on the underlying fundamental science is of interest to DOE's Office of Basic Energy Sciences. The demonstration of the controlled manipulation of skyrmions in magnetic thin films should generate opportunities for technology transfer.

FY 2014 Results and Accomplishments

We studied skyrmions in samples consisting of the magnetic insulator YIG (yttrium iron garnet or $Y_3Fe_5O_{12}$) films (around a micrometer thick) coupled to a thin layer (4 nm) of nonmagnetic heavy metal platinum (Pt). The long-range dipole interaction helped to stabilize, in the YIG, a lattice of magnetic bubbles with a hexagonal symmetry, for certain values and orientations of the applied magnetic field. These bubbles, which can form at room temperature, can be topologically equivalent to skyrmions. Because the period and size of the skyrmions in this system were on the order of micrometers, we were able to use magneto-optical Kerr effect (MOKE) microscopy to image them and study their behavior while driving an electric current though the Pt layer. The longitudinal flow of the charge current in heavy metals such as Pt, which have strong spin-orbital interactions, results in the generation of a transverse spin current. Such a spin current flow subsequently generates a spin accumulation at the Pt/YIG interface, which, in turn, exerts an interfacial spin transfer torque on the localized magnetization in YIG. We observed the motion of individual skyrmions, and we saw changes in the density of the skyrmions that depended on the current density. These results indicated it is indeed possible to manipulate magnetic skyrmions with pure spin currents generated in an adjacent layer. In addition, Hall resistivity measurements exhibit a signal imposed on the ordinary Hall resistivity, which is thought to be related to the magnetic skyrmions in YIG.

A second heterostructured system that we fabricated and started to study consisted of a thin layer of ferromagnetic metal $Co_{20}Fe_{60}B_{20}$ with perpendicular magnetic anisotropy, sandwiched between nonmagnetic heavy metal tantalum (Ta) and insulating TaO_x deposited on Si/SiO_x. We conducted studies on this system that already suggest there is great potential for room-temperature skyrmions to have practical applications. The structural asymmetry in the present system is important with regard to stabilizing chiral domain walls and providing the efficient inter-

facial spin-orbit torques that might contain contributions from Rashba and spin Hall effects. With regard to the YIG system, depending on the applied magnetic field, a range of magnetic spin textures (including stripe domains and micrometer-sized skyrmions) could be stabilized. To explore the role of lateral geometric confinement, a sample was laterally patterned into a wire with a narrow constriction (or neck) in the middle. We found that when a pulsed current was applied through the wire from left to right, stripe domains, initially present on both sides of the constriction, could be transformed into a dilute gas of skyrmions on the right-hand side. More important, these skyrmions could be easily de-pinned from local structural defects with a de-pinning current as low as 4×10^6 A/cm^2. These skyrmions moved at a relatively high speed after de-pinning.

Proposed Work for FY 2015

Further work will include the following:

- Conducting a detailed characterization of skyrmion lattices with neutron scattering;
- Exploring, in detail, the influence of the constriction geometry in the wires on skyrmion formation and stability and understanding the origin of the observed skyrmion formation; and
- Investigating current-induced magnetization dynamics.

Directly Probing Nanoscale Dynamics in Shear Thickening Complex Fluids

2014-077-N0

Suresh Narayanan, Jonghun Lee, Xiao-Min Lin, and Alec Sandy

Project Description

The viscosity of concentrated colloidal suspensions varies depending on the shear rate. With an increasing shear rate, the viscosity initially decreases (shear thinning). Then it abruptly increases beyond a critical shear rate, which is known as shear thickening. Even though we have known about this non-Newtonian fluid behavior for a long time, the dynamics of shear-thickened fluids have remained unclear. The goal of this project is to link macroscopic rheology and microscopic particle dynamics. We will study the dynamics of a silica nanoparticle suspension under large-amplitude oscillatory shear by using small angle x-ray scattering (SAXS) and x-ray photon correlation spectroscopy (XPCS). SAXS is a powerful method for studying the microscopic perspective of rheology, having very high spatial and temporal resolution in a regime where the rheological properties are governed. We will examine the dynamics of silica nanoparticles by measuring the intensity-intensity autocorrelation function. The combined x-ray spectroscopic and rheometric results will provide a deeper understanding of shear thickening.

Mission Relevance

The project is relevant to DOE's mission in science. It is a scientific challenge to connect nanoscale motion in shear-thickening, complex fluids under shear flow to their macroscopic rheological properties. At the nanoscale, nonequilibrium behavior can be observed directly, and the averaging over many subsystems that is done for macroscale measurements is not required. The nature of such fluctuations is one metric associated with the existence of nonequilibrium in a system. Understanding how the fluctuations occur, measuring the evolution and fluctuations of the systems, and characterizing the approach to equilibrium constitute a significant aspect of the five "grand challenges" identified by DOE.

FY 2014 Results and Accomplishments

We prepared silica nanoparticles by using the Stober method, and we modified the surfaces of these nanoparticles with 3-(trimethoxysilyl) propyl methacrylate for a neutral surface charge. Surface charge neutralization excludes repulsive forces between particles, and silica particles behave as ideal hard spheres. Finally, the nanoparticles were dispersed in ethylene glycol with a 60% volume fraction.

Oscillatory shear at a frequency of 5 Hz was applied to this highly concentrated silica suspension. The suspension showed shear-thickening behavior at high strains (Figure 1). To understand the dynamics of the particles under different shear regimes, SAXS and XPCS measurements were taken at different strains. At low strains (about 1% strain), SAXS showed an isotropic scattering pattern, which implies that the particles were randomly distributed (Figure 2a). XPCS showed beating patterns that came from the Doppler shift of x-rays scattered by the particles being sheared (Figure 2b). In the shear-thinning regime (about 100% strain), the particles were hexagonally packed due to the shear flow (Figure 2c). The corresponding XPCS pattern is shown in Figure 2d. In the shear-thickening regime (about 1,000% strain), particles showed an anisotropic scattering pattern (Figure 2e), and the correlation of XPCS patterns increased at every half period, which would be shown by a solid-like material (Figure 2f).

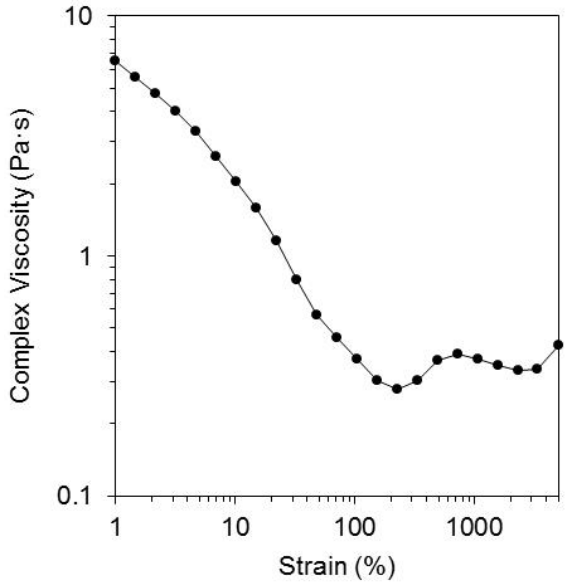

Figure 1. Complex viscosity of silica suspension in ethylene glycol with varying strain.

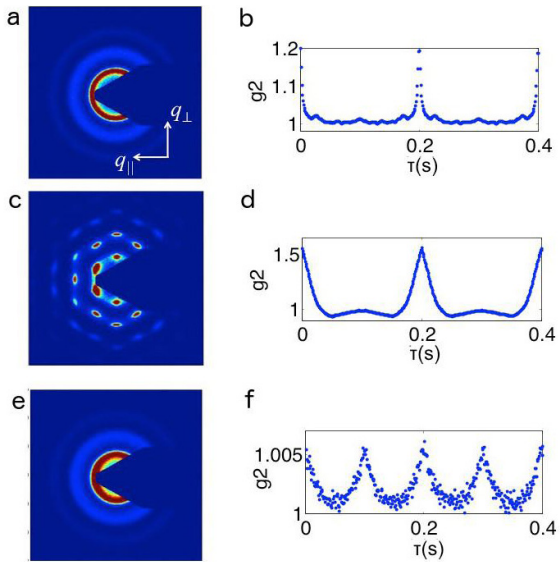

Figure 2. SAXS and XPCS (first two cycles) of silica suspension measured at 1% strain (a and b), 100% strain (c and d), and 1,000% strain (e and f). $q_{||}$ denotes the scattering direction parallel to the shear flow direction, and $q_\perp$ denotes the scattering direction perpendicular to the shear flow direction.

Proposed Work for FY 2015

A quantitative analysis of the SAXS and XPCS results will be done to reveal the dynamic process during shear thickening. In addition, we plan to study anisotropic particles in suspension to understand the general perspective of microscopic dynamics under shear.

Pb-Assisted Corrosion/Cracking Mechanisms at the Interface between Pb-Containing Solution and Nickel Oxide

2014-081-N0

Seungbum Hong and Hawoong Hong

Project Description

The goal of this project is to study the fundamental mechanisms of lead (Pb) -assisted corrosion/cracking by using both *in situ* x-ray reflectivity and advanced *in situ/ex situ* atomic force microscopy (AFM) imaging techniques. We will perform *in situ* x-ray reflectivity imaging on pre-oxidized nickel [Ni(110)]–liquid interface or at a molecular beam epitaxy (MBE) -grown NiO-liquid interface while we vary the Pb concentration and the pH. The surfaces of the interfaces will be characterized by AFM in air and Pb-contained solution.

Mission Relevance

This project is related to DOE's energy security initiative. The major benefits of the proposed work would be to provide guidance for identifying the fundamental mechanisms of Pb-assisted stress corrosion cracking on nickel base alloys (e.g., A600 or A690) in the short term, and developing mitigation methods for this problem in the long term. Eventually, our work will enhance the reliability and safety of nuclear power plants and help extend plant life (or license renewal). The major beneficiaries/customers of the proposed work are the nuclear power industry and DOE.

FY 2014 Results and Accomplishments

For our specimen, we chose a nickel [Ni(110)] single crystal (99.99%, fabricated by Princeton Scientific Corporation). It was mechanically polished and then electro-polished in a solution of 30% nitric acid. After the specimen was polished, to improve its surface crystallinity, we moved it into the ultra-high vacuum chamber at the 33 ID-E beamline at Argonne's Advanced Photon Source (APS). There it was sputtered with argon (Ar+) ions and annealed at 700°C. We exposed the clean Ni surface to ultra-high-purity oxygen to grow a coalesced NiO layer. We characterized the processed surface by using reflection high-energy electron diffraction (RHEED) before and after each sputtering/annealing cycle. Figure 1a shows RHEED patterns after the electro-polishing and sputtering/annealing cycles. Before the sputtering/annealing cycles, the RHEED pattern showed no evidence of crystallinity on the surface. Figure 1b shows that after the fourth cycles, the RHEED image had multiple parallel streaks, which are typically observed for atomically flat metal surfaces.

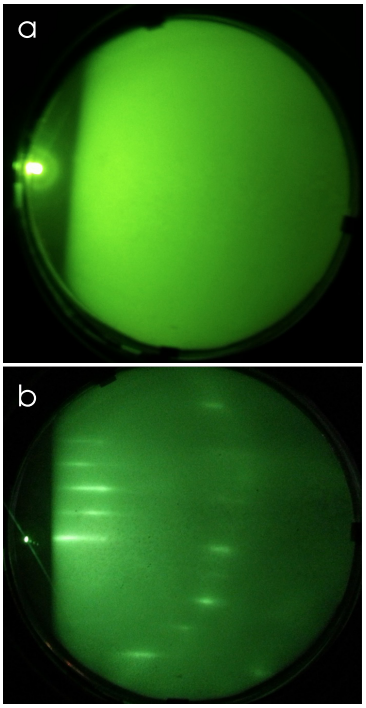

Figure 1. RHEED images (a) after electropolishing and (b) after the fourth sputtering/annealing cycles.

With the surface prepared as described above, the high-resolution x-ray reflectivity from the surface — under water and without water — was measured. The experiment was conducted at the APS 5 ID-C beamline. In Figure 2, the open red circles show the measured crystal truncation rod (CTR) data and the best-fit curve for Ni(110)/NiO in a helium environment [Figure 2a] and for the Ni(110)/NiO/water structure [Figure 2b]. The CTR data could be obtained with only small statistical errors even at the low-intensity regions. These CTR data confirm that the surface pretreatment procedure developed for Ni(110) was suitable for the x-ray reflectivity study. The observed oscillatory features resulted from the interference between the interfacial layers. As measured up to 6Å^{-1} in Q, perpendicular momentum transfer (Q = 2πL/d, where, L: Lattice vector in reciprocal space, d: spacing of substrate layers), the layered structure could be resolved in atomic scale. We observed a distinct beating pattern for the Ni(110)/NiO in the helium environment, indicating that multiple film layers made up the interfacial structure. However, the pattern changed drastically after exposure to water, as indicated by the Ni(110)/NiO/water data. In general, we expected the water to interact only with the top surface layer of the oxide thin film, but the x-ray reflectivity we observed indicated a strong influence of the water interaction on the oxide film surface.

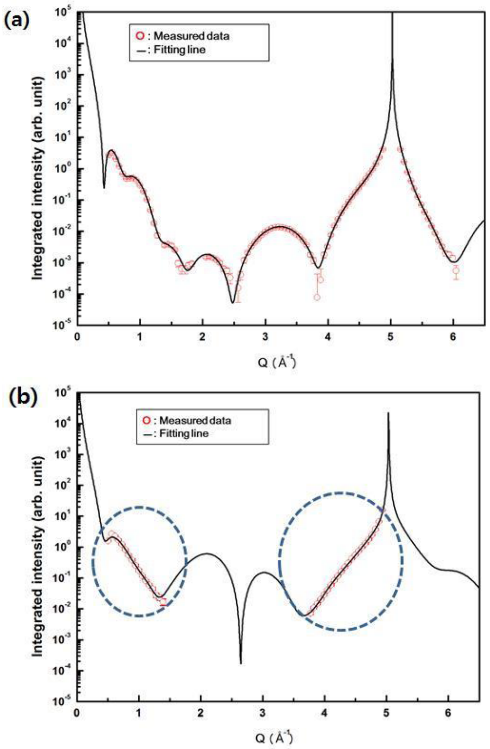

Figure 2. In situ *x-ray reflectivity data as a function of Q for the Ni(110)/NiO (a) helium interface and (b) water interface. The solid lines indicate the best fit for the measured integrated reflectivity. The open red circles represent integrated data. The blue circles indicate regions at interface b where the oscillatory features changed from those at interface a.*

Proposed Work for FY 2015

We will measure the *in situ* x-ray reflectivity to observe the effect of the solution's pH and Pb concentration on the oxide surface interaction. We plan to measure the *in situ* AFM image on the surface in a solution at various pH levels and various Pb concentrations. We will develop a room-temperature, aqueous cell equipped with control devices with electrochemical potential.

Seminars

Hong, S., Y.-Y. Choi and J.J. Kim (2015). "Design of Model Experiments for Stress-induced Nanoscale Phenomena." Pusan National University, Busan, Korea, November 11, 2014.

Probing the Chemistry of Atmospheric Dust Particles Using X-ray Spectromicroscopy: Implications for Climate Science

2014-084-N0

Yan Feng, Rao Kotamarthi, Barry Lai, and Stefan Vogt

Project Description

Iron (Fe) is a key micronutrient that is vital for all organisms. In many ocean regions, its availability controls primary productivity, affecting marine biogenic emissions and carbon dioxide fluxes between the ocean and atmosphere. About 95% of the global Fe supply to the open ocean is from atmospheric dust particles (aerosols), and most photosynthetic aquatic organisms can take up Fe only in the dissolved form. It is thus critical to understand the solubility and, in turn, the bioavailability of Fe in atmospheric dust aerosols. Two key parameters determine Fe dissolution in dust: (1) the dust's Fe content and (2) the chemical mechanisms that lead to dissolvable Fe. Because of a lack of fundamental understanding about dust chemistry, it is conventionally assumed in current earth system models (ESMs) that the soluble Fe fraction is constant; the details on chemistry are eliminated and thus decoupled from the atmospheric influences (J.L. Dufresne et al., "Climate Change Projections Using the IPSL-CM5 Earth Model from CMIP3 to CMIP5," *Climate Dynamics,* **40** (9–10), 2123–2165, 2013). This simplification has been subject to an increasing amount of scrutiny, since for ESMs to be integrated and effective tools, they must resolve the role of chemistry within the dust particle. This is essential in order to understand the biogeochemical feedbacks in the changing climate.

This project strives to address the composition of Fe in dust and the fundamental lack of understanding about the mechanisms involved in atmospheric transport, by using experimental studies to evaluate and improve the models' representation of dust Fe chemistry. The development and improvement of modern microscopy and microanalytical techniques (such as x-ray fluorescence [XRF] microspectroscopy at Argonne's Advanced Photo Source [APS]) offer researchers the ability to probe the chemistry of individual dust particles. Elemental compounds in mineral dust can be measured by using hard x-ray microscopy for quantities down to the trace level. In addition, the microspectroscopic beamlines can be used to determine the oxidization states of Fe(II) or Fe(III), which are linked to the solubility of Fe.

In this project, the capabilities at the APS are being used to (a) map the chemical composition of dust particles collected from multiple locations (from the remote Southern Ocean to polluted urban regions and dust-source regions) with respect to dust mineralogy and Fe speciation and (b) derive statistical relationships with other chemical components, depending on the atmospheric conditions. We will use the derived datasets representative of different regions to evaluate and improve the existing process model for Fe dissolution and speciation. Then we will incorporate the process model into the Community Atmospheric Model (CAM), which is part of the ESM, and perform climate simulations of the bioavailability of Fe. Analyses will be performed at different temporal scales (seasonal, interannual, decadal) to study variations in atmospheric Fe deposition, perturbed by changes in aerosol emissions projected for future climate scenarios.

Mission Relevance

The project is tied to DOE's mission in climate science. The success of this initiative will establish Argonne as a significant player in developing DOE's next-generation ESMs focused on the feedback between ocean biogeochemical cycles and atmospheric aerosols. Although biogeochemical coupling between the ocean and atmospheric processes could be substantial, it has not been adequately included in climate assessments to date. This topic has been projected as a major and transformational research area of climate science in the next decade by DOE, the National Science Foundation (NSF), and U.S. Department of Agriculture (USDA). The outcome of this research will provide interdisciplinary engineers and scientists with the sophisticated tools needed to make more reliable and more certain decadal and regional climate projections for policy and decision making.

FY 2014 Results and Accomplishments

Throughout FY 2014, we focused on developing a library of samples and a collection of data.

Sample Collection. To date, we have gathered aerosol samples from six sites representative of areas influenced by desert dust, anthropogenic sources, or both. The samples collected from outside collaborators include these:

1. Bermuda: 54 samples representing North American, mixed, and Saharan air masses.
2. Atlantic Ocean (geotraces): 9 samples collected on a transect across the Atlantic from New England to Cape Verde Islands representing marine, North American, and Saharan air masses.
3. Mediterranean: 14 samples collected on Crete representing European and Saharan air masses.
4. Southern Ocean: 6 samples collected on a north-south transect from Australia to the eastern Antarctic representing pristine ocean air.
5. Pacific Ocean: 3 samples collected at the Mauna Loa Climate Observatory in Hawaii representing

free-troposphere and long-range transport aerosol. Potentially, more than 200 samples are available from this site.

6. South America: 6 samples representing the Patagonian desert air masses.

Sample Analysis. We completed the synchrotron beamline runs (numbers approximate) on most of the samples listed. Small areas of the collected samples (about 40-μm square) were scanned by the x-ray beam (energy = 7,200 eV) in microscopic XRF mode. These XRF maps provided spatially resolved elemental data. An energy scan of the Fe x-ray absorption near-edge structure (XANES) region (e.g., 7,090–7,180 eV in 0.5-eV steps, 0.4-μm x-ray spot size, 0.5–3-s dwell time) was then collected for Fe-containing spots identified from XRF maps as well on large filter regions. In this way, both the bulk and particle Fe could be characterized.

Linear combination fitting was then completed for sample Fe XANES spectra from a database of known Fe mineral standards (e.g., Fe oxides, organics, silicates, sulfides, sulfates) to determine the composition of the unknown aerosol Fe XANES spectra. The oxidation state was also determined by using the Fe XANES spectra using the pre-edge region of the scan. Figure 1 illustrates an example analysis for a sample collected in Bermuda.

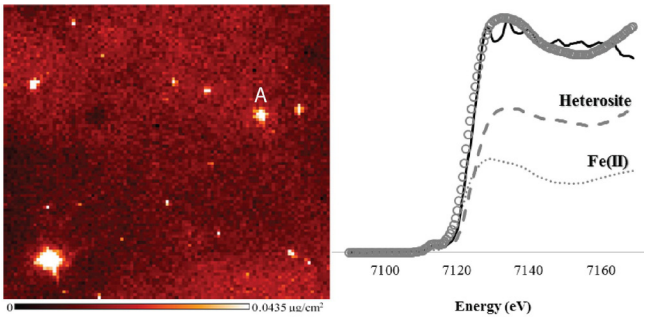

Figure 1. XRF map (left) for an aerosol sample collected in Bermuda. This sample was influenced by North African air masses and has individual particles containing Fe (bright white areas). The composition of an individual particle (Particle A in left panel) was determined through the XANES spectroscopy and linear combination fitting (right).

Because the Mediterranean dataset was the most developed, it was the focus of our initial data analysis. Bulk Fe XANES showed that regardless of the source region (i.e., Europe or North Africa), the composition of Fe in aerosols was uniform. Linear combination fitting showed some dust Fe particles were about 60% goethite [an Fe(III) oxyhydroxide] and 40% heterosite [an Fe(III) phosphate]. The finding of heterosite could be significant. Heterosite could only have been formed as a result of transformation in the atmosphere, and it would strongly support the acid processing hypothesis. In addition, individual particles that were interrogated often contained heterosite.

Proposed Work for FY 2015

We will add dust samples collected in South Asia (in progress for sample transferring) and complete beamline tests for the samples that were collected in FY 2014. With a group at Georgia Institute of Technology, we will also conduct data analyses for all the samples and analyze aerosol particles for bulk Fe concentrations and speciation and other mineral species. For the Southern Ocean samples, we will also work with a group at Rutgers University for the independent characterization of soluble and total Fe in the collected dust aerosol samples and compare results with those from our microscopic analysis of the XRF imaging. We will use these data products to characterize the statistical relationships between acidic species, mineral composition, Fe oxidation state, and solubility. We will work to implement multiple mineral dust tracers in the global climate model (CAM). Developing this new modeling capability will give us the dust mineralogy framework that will allow us to incorporate a process-scale heterogeneous chemistry model for dust Fe dissolution in CAM. The process-scale model of dust Fe dissolution will at first be based on our previous work and updated with recent developments. The simulated Fe concentrations and chemical transformation of Fe in the atmosphere will be evaluated with the derived statistical characteristics from the x-ray microscopic and microspectroscopic analysis and other observations.

Tuning the Transport Properties of Coupled Majorana

2014-095-N0

Wade DeGottardi, Lei Fang, Wai-Kwong Kwok, and Konstantin Matveev

Project Description

Hailed as one of the top scientific discoveries of 2012 by *Science* (see http://www.sciencemag.org/site/special/btoy2012/), an experiment offering evidence for Majorana fermions in a superconducting wire by the Kouwenhoven group at Delft (F.H.L. Koppens et al., Nature **442**:766 [2012]) has set off a firestorm of interest in further exploring Majorana physics. This excitement is driven by the promise that these particles hold for applications to quantum computing. Like any computer, the operation of a quantum computer is based on the ability to store and manipulate information. In a quantum computer, the units of storage are microscopic degrees of freedom subject to the laws of quantum mechanics. Remarkably, quantum computers can perform operations "exponentially" faster than ordinary computers, and this feature has led to a great deal of excitement and research activity (D.P. DiVincenzo, "Quantum Computation," *Science* **270** (5234): 255–261 [1995]). One of the biggest challenges in quantum computing is

minimizing the loss of information due to environmental noise. Majorana fermions are very promising because the information they store is expected to be immune to many of the forms of noise that plague other implementations (C. Nayak et al., Rev. Mod. Phys, **80**:1083 [2008]).

In this project, we are constructing a device which can probe thermal and electrical transport through a system of coupled Majoranas (Figure 1). The architecture consists of a topological insulator (bismuth selenide [BiSe]) on a substrate that has a thin superconducting strip. The role of the insulator is to render the electronic degrees of freedom spinless — a crucial ingredient for isolating Majorana fermions (V. Shivamoggi, G. Refael, and J.E. Moore, Phys. Rev. B **82**:041405(R) [2010]). We are also constructing devices with copper (Cu)-doped BiSe in which we have detected signatures of superconducting order. These two ingredients — spinless electrons and superconductivity — are sufficient to generate Majorana fermions in the cores of vortices (L. Fu and C.L. Kane, Phys. Rev. Lett. **100**:096407 [2008]).

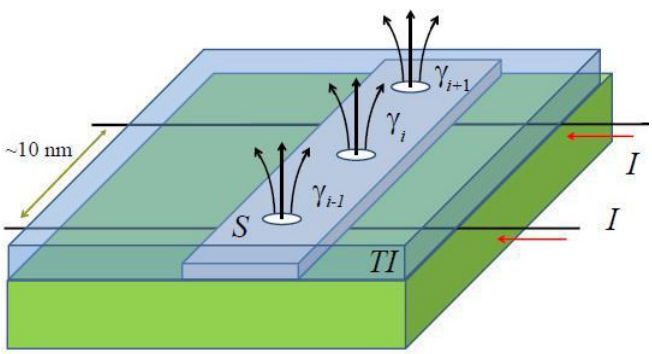

Figure 1. Diagram of the proposed experimental setup. A topological insulator is deposited on a substrate with a thin strip of superconductor, which contains a line of vortices, a vortex lattice. Vortices are shown as circles threaded by magnetic flux. Control currents (red) would allow the tuning of the spacing between vortices.

Mission Relevance

This project supports DOE's science mission. Superconductivity is a cornerstone of material science research. Majorana fermions represent an exciting new aspect of superconducting order. The quantum information encoded by these exotic quasiparticles is expected to enjoy unprecedented decoherence times. Applications to quantum computing arising from this project would strongly support the DOE mission of leading innovation in computer technology.

FY 2014 Results and Accomplishments

We synthesized centimeter-sized single crystals of $Bi_2Te_2Se_x$ (x = 0.95~1.05). A single crystal sample is shown in Figure 2(c). In Figure 3(a), the temperature-dependent resistivity of single Bi_2Te_2Se and bismuth selenide (Bi_2Se_3) crystals is plotted. In contrast to the metallic behavior of Bi_2Se_3, Bi_2Te_2Se demonstrates pronounced insulating behavior. The respective resistivities differ by three orders of magnitude, suggesting that the Fermi energy of Bi_2Te_2Se lies below or at the bottom of the conduction band. The synthesis of a topological insulator (TI) sample that limits the effects of the bulk represents a significant milestone in our progress. In particular, our proposed scheme of probing subgap states by using a scanning tunneling microscope (STM) requires that surface states can be differentiated from bulk conducting states.

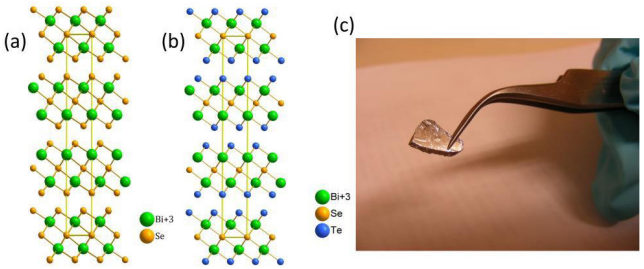

Figure 2. Crystallographic structures of (a) Bi_2Se_3, (b) Bi_2Te_2Se, and (c) a crystal of Bi_2Te_2Se (about 1 cm in size).

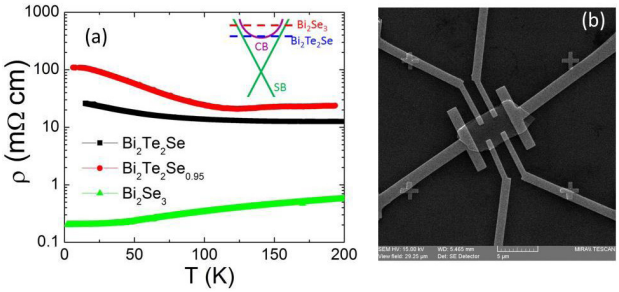

Figure 3. (a) Temperature-dependent resistivity measurements of single crystals of Bi_2Se_3 and Bi_2Te_2Se. (b) SEM picture of a nanocrystal of Bi_2Te2Se deposited on contacts of a Hall bar geometry.

Our project requires an understanding of the collective properties of coupled Majorana fermions. Our theoretical work has involved studying the low-energy properties of a system of coupled Majoranas. This work has shown that a chain of Majorana fermions exhibits topological insulating phases hosting end modes that enable low-energy tunneling into the system.

Proposed Work for FY 2015

We will fabricate the topological insulator (BiSe)-superconducting device shown in Figure 2. Once complete, initial tests of the device will characterize the induced superconductivity in the topological insulator through transport and STM measurements. This data will be analyzed for signatures of Majorana fermions.

Single Cell Structural Genomics of Uncultured Sediment Archaea: On the Trail for Novel Proteases

2014-108-N0

Karolina Michalska, Gyorgy Babnigg, Robert Jedrzejczak, Andrzej Joachimiak, and Joseph Mootz

Project Description

Marine sediments are the ultimate sink of organic carbon on Earth. At the same time, this cold ecosystem represents one of the richest microbial niches, predominantly inhabited by archaea and estimated to constitute about one-tenth of the total planet biomass. These organisms actively participate in sulfur, nitrogen, and carbon cycling. The latter process occurs mainly through methanogenesis (a process that converts simple organic molecules and carbon dioxide [CO_2] into methane [CH_4]) and reverse methanogenesis (anaerobic methane oxidation). A recent study identifying novel archaea through single-cell genomic sequencing reports that these organisms encode putative extra- and intracellular protein-degrading enzymes (proteases) to utilize detrital proteins as a source of basic nutrients. Thus, these newly discovered microorganisms might be key players in deep-sea biogeochemistry. However, their physiology and molecular adaptations to this unique environment are poorly understood. In particular, the predicted proteases have not been studied. Therefore, the purpose of this project is to investigate properties of these uncharacterized enzymes, which may reveal some unknown functions.

Mission Relevance

The project is relevant to DOE's mission in environment. DOE is committed to characterizing the ecosystems that are pertinent in carbon sequestration. Moreover, DOE funds several large-scale projects that characterize highly specific classes of proteins. However, no such work has been done to study proteases, which are indispensable for turning over biomass-derived proteinaceous material in various environments. The characterization of archaeal enzymes will help us understand how these microorganisms contribute to global carbon cycling via protein remineralization in marine sediments.

FY 2014 Results and Accomplishments

We analyzed genomes of four novel archaea (*Thermoplasmatales archaeon* SCGC AB-539-C06, *T. archaeon* SCGC AB-540-F20, *Thaumarchaeota archaeon* SCGC AB-539-E09, and *T. archaeon* SCGC AB-539-N05) derived from marine sediment. Fifty-five genes encoding putative proteolytic enzymes were cloned for recombinant expression. Eleven proteins were successfully purified in a large scale. For 10 of them, crystallization screens were set up, and two proteins were crystallized thus far. Six were analyzed for proteolytic activity.

Bathyaminopeptidase (BAP) from *T. archaeon* E09 was characterized in detail. BAP is a true example of an enzyme identified exclusively in the uncultured organisms; highly similar sequences were found only in estuarine sediment in North Carolina. The closest bacterial homolog from the cultured microorganisms is α-amino acid ester hydrolase (AEH) — an enzyme involved in synthesis of β-lactam antibiotics.

We discovered that BAP is an intracellular aminopeptidase with a preference for dipeptides with L-Cys ($K_m^{L\text{-}Cys\text{-}AMC}$ = 80 ± 17 μM), or a hydrophobic/aromatic residue at the N-terminus. In contrast to the known bacterial enzymes, BAP does not bind D-phenylglycine–based compounds, which are the most preferred substrates of AEH. Therefore, BAP may indeed perform roles that are distinct from those of its bacterial relatives. Even though BAP functions in a cold ecosystem (2°C), its optimal temperature is ~30°C, suggesting that its activity may increase with the rising temperature of the sediment.

The enzyme is a hollow sphere tetramer with four active sites localized inside the assembly (Figure 1). This arrangement poses significant restrictions on the size of substrates, which could reach the catalytic pockets only through two narrow openings. Small differences observed in the active site explain why BAP activity differs from that of its bacterial cousins.

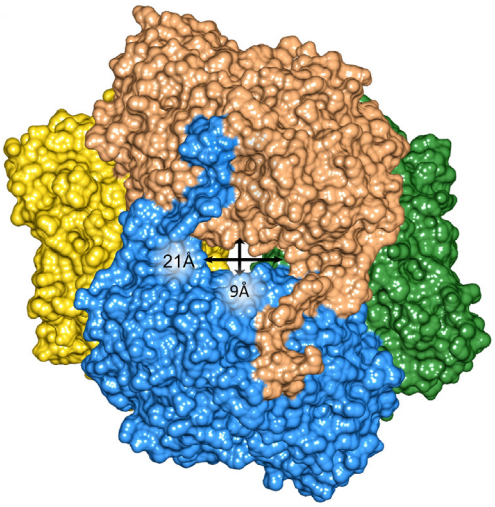

Figure 1. Crystal structure of BAP. Each monomer is shown in a different color.

In addition to BAP, we characterized two intracellular metallo-peptidases belonging to the M42 and M20 families. The M42 class enzyme is an aminopeptidase with

activity toward peptides containing N-terminal aromatic and aliphatic amino acids, with N-terminal tyrosine being the preferred substrate. The M20 class enzyme is an Xaa-His dipeptidase with broad substrate specificity. Both enzymes require divalent cations for activity, with M42 having a preference for Co^{2+} or Zn^{2+}, depending on pH (Figure 2), and M20 requiring Co^{2+} or Mn^{2+}. The optimum temperature for M42 activity is ~45°C, which is significantly higher than the temperature of the environmental niche occupied by *T. archaeon*. Similar to BAP, M20's optimum activity occurs at ~30°C.

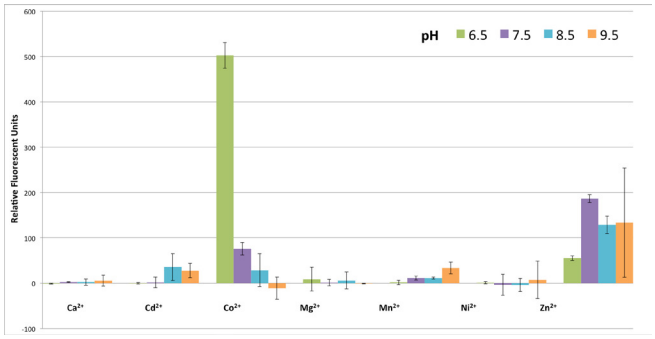

Figure 2. M42 metal dependence. Relative fluorescent units are a direct measure of activity.

Proposed Work for FY 2015

In FY 2015, we will continue the functional characterization of the remaining nine proteins. We will also work on optimizing expression constructs and crystallizing other targets. In addition, we will design two active site mutants of BAP to co-crystallize it with substrates in order to obtain more detailed insights into specificity determinants. Likewise, we will investigate the structural aspects of M42 to obtain a better understanding of its mode of action.

LDRD

Advanced Computing

ANNUAL REPORT

2014

Towards the Exascale Sky

2011-213-R3

Salman Habib and Katrin Heitmann

Project Description

The unveiling of the large-scale universe by sky surveys has transformed cosmology, fundamental physics, and astrophysics. An intense global effort is under way to fathom the deep mysteries posed by the existence of dark energy and dark matter. Next-generation surveys (e.g., the Dark Energy Survey [DES]), the Dark Energy Spectroscopic Instrument (DESI), and the Large Synoptic Survey Telescope (LSST) promise new discoveries and an unprecedented increase in our knowledge of the universe. To extract this scientific knowledge from observations requires simulations of structure formation in the universe at unprecedented computational scales. This project was aimed at developing a leading-edge computational capability for large-scale cosmological simulations and their analysis. We developed a petascale cosmology code suite: the Hardware/Hybrid-Accelerated Cosmology Code (HACC) framework. It is designed to exploit the full set of current and future high-performance computing (HPC) architectures. In addition, we are conducting an associated science program on innovative and improved cosmological probes and analysis methods.

Combined with the arrival of the Mira supercomputer here at Argonne National Laboratory, our theoretical and modeling capabilities have put us in a unique position, enabling us to make breakthroughs in fundamental aspects of cosmology and make the most accurate predictions from structure formation probes of the "dark universe." The design of HACC (the first exascale computational cosmology capability for next-generation sky surveys targeted to future supercomputer architectures) encompasses all HPC architectures, including many core and hardware-accelerated systems. HACC's development is proceeding in conjunction with hardware and software advances and with input from Argonne computer scientists and performance engineering experts. In addition, we are co-developing the Cosmic Calibration Framework (CCF) with a number of collaborators at universities and other Labs. The CCF is an advanced statistical framework that melds HPC simulations with observational data to provide rigorous, error-controlled estimates of parameters for cosmological and particle physics models.

Mission Relevance

This project is relevant to DOE's basic science mission. The HPC advances that underlie this project will have broad impacts in several fields, including accelerator and plasma physics, computational co-design, particle transport simulations, and the management and analysis of very large datasets. The advent of large-scale sky surveys presents a significant and timely opportunity for Argonne to play a crucial role in DOE missions, covering both the discovery sphere (cosmology and particle physics) and the capability sphere (HPC and large datasets).

FY 2014 Results and Accomplishments

In FY 2011, the project work focused on porting the key codes to Argonne systems, including a new tree algorithm, and developing a new Fast Fourier Transform (FFT) method. In FY 2012, HACC was fully implemented on Mira, and broke the 10 petaflop performance barrier for the first time (on the Sequoia system at Lawrence Livermore National Laboratory). An initial HACC implementation was tested on the prototype Titan system at Oak Ridge National Laboratory. An *in situ* analysis framework for HACC was developed. This allows the code to run analysis tasks at the same time as the main simulation is running.

In FY 2013, we implemented HACC on Titan, the heterogeneous supercomputer at Oak Ridge National Laboratory, with the code kernel performance exceeding 20 petaflops. We further improved the performance of the code on Mira by adding hyper-local trees implemented with chaining meshes, replacing the original rank-local tree data structure. We made the time-stepping in HACC locally adaptive, by using density estimation based on the tree particle data structure with recursive coordinate bisection, which is native to the force evaluation scheme. Work with computer scientists at the ALCF and Argonne's Mathematics and Computer Science (MCS) Division included adding a data compression scheme that improves data transfer rates and reduces the amount of data that has to be stored (overall improvement equaled a factor of about two). We also made excellent progress working on the analysis framework associated with HACC. A new parallel halo merger tree code was developed and linked to a semi-analytic structure formation code called Galacticus. This aspect of our work on large data analytics was continued with support from the National Energy Research Scientific Computing Center, where we have access to large storage and analysis capabilities for post-simulation data processing.

In FY 2014, a new task-based load balancer was developed for the heterogeneous computing version of HACC. This scheme was used very successfully at the Oak Ridge Leadership Computing Facility (OLCF) and resulted in producing the world's largest high-resolution cosmological N-body simulation. Work on particle-based hydrodynamic simulations began by following an earlier implementation of grid-based methods.

New results on the effects of neutrino mass on cluster abundance were obtained following on our work on implementation of neutrinos in HACC. It was shown that the cluster abundance depends on the neutrino mass following a universal form of the mass distribution function (Figure 1). This result makes inferences from cluster observations (especially observations of high redshift clusters with the South Pole Telescope) much more straightforward. A technique for handling this inference problem followed from our earlier work in this project on the halo concentration-mass relation.

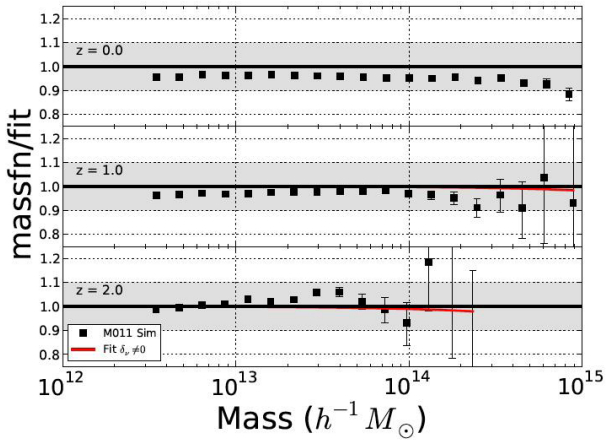

Figure 1. Universality of the halo mass function in cosmologies with massive neutrinos. The plot shows the ratio of the mass function evaluated from the simulations to the mass function predicted by universal fitting forms (i.e., a shape independent of the underlying cosmology). The results are consistent with the assumption of universality in both shape and amplitude at the ~5% level.

A number of improvements were made to the HACC analysis framework, including new work on a gravitational lensing pipeline. The main aim of the pipeline is further analysis of weak gravitational lensing on the scale of individual galaxies (galaxy-galaxy lensing) by using DES results.

Mobile Device Vulnerability Research

2011-214-R3

Charlie Catlett and Rajesh Sankaran

Project Description

The underlying goal of this project has been to investigate cybersecurity and privacy vulnerabilities associated with mobile devices, along with the mechanisms for detecting and preventing attacks. The work has involved the evaluation of existing location service architectures and the development of an experimental, privacy-preserving architecture. In FY 2014, the focus was on devices embedded in urban environments and potential interactions with mobile devices. Work included designing and prototyping an embedded systems architecture for remote/embedded sensing and computing.

Mission Relevance

This project is relevant to DOE's national security mission. Argonne and its sister laboratories, as well as DOE and other federal agencies, are increasingly reliant on mobile devices for mission-critical applications and services, and they also host visitors who typically carry at least one such device. An understanding of the related risks and potential protective measures is essential to their cybersecurity. In FY 2014, the relevance of this mission increased, with a focus on interactions with embedded urban devices.

FY 2014 Results and Accomplishments

In FY 2012, we explored vulnerabilities associated with the use of mobile devices and particularly related to sensors, in the context of both commercial devices (smartphones, tablets) and increasingly common urban sensors that interact with people and mobile devices, such as air quality sensors or accelerometers. Accelerometers, in particular, relate to an emerging genre of mobile devices for health monitoring.

In FY 2013, we developed a wearable sensor device for use in evaluating the interaction of such devices, with similar sensing systems embedded in the environment, such as in buildings. This work led to a proposed architecture for privacy-preserving, in-building navigation, which was proposed for implementation through a National Science Foundation call for cyber-physical systems research.

In FY 2014, we created an architecture for remote sensing and embedded computation and communication. The target environment was urban; devices were placed on city street signal light poles. The devices were to collect information using sensors and wireless antennas (Wi-Fi and bluetooth). The goal was to explore mobile device privacy and security vulnerabilities inherent to interactions between mobile and embedded devices.

We developed prototype software for (a) the collection of sensor data via embedded microprocessors; (b) making microprocessors resilient to common in-field failure modes; (c) reporting of robust sensor data to a centralized database; and (d) management, provenance, and data aggregation from networks of devices. Concurrently, collaborating students and faculty members at the School of the Art Institute of Chicago prototyped external enclosures and sensor shielding approaches designed to protect electronics from weather and external influences while ensuring that the sensors (e.g., temperature, sound, light) could still detect ambient conditions accurately.

We also built a set of working prototypes of the embedded urban sensing platform, several of which were deployed on rooftop locations with weather and air quality sensors. A set of 12 prototypes were built in late FY 2014 and are expected to be deployed on the University of Chicago campus in early 2015.

Seminars

Catlett, C. (2014). "Toward an 'Urban Science'." Argonne Training Program on Extreme Scale Computing (ATPESC), St. Charles, IL, August 5, 2014. (also see 2013-206-R1).

Catlett, C. (2014). "Urban Resilience." Virginia Tech, Arlington, VA, May 15, 2014.

Catlett, C. (2013). "Urban Center for Computation and Data: Opportunities for Computational Urban Sciences." Extreme Scale Computing School, Chicago, IL, August 8, 2013.

Catlett, C. (2013). "Urban Sciences and Computer Science." University of Chicago, Chicago, IL, January 15, 2013.

Catlett, C. (2013). "Emerging Opportunities in Urban Sciences." University of Illinois at Urbana-Champaign, Urbana, IL, December 10, 2012.

Catlett, C. (2012). "CLS Research Roadmap Overview." Oak Ridge National Laboratory, Oak Ridge, TN, March 28, 2012.

Catlett, C. (2012). "Ubiquitous Computing in Chicago "Pervasive Computing and Privacy Research at Argonne National Laboratory." Illinois Institute of Technology, Chicago, IL, November 14, 2011.

Catlett, C. (2011). "Pervasive Computing and Privacy Research at Argonne National Laboratory." Illinois Institute of Technology, Chicago, IL, September 30, 2011.

Extreme-Scale Electromagnetic Modeling with Nanoscience Applications

2012-114-R2

Misun Min, Paul Fischer, and Stephen K. Gray

Project Description

The goal of this project is to provide an enhanced high-fidelity code that will enable future-generation electromagnetic device simulations for the predictive modeling of biological sensing, plasmonic, photovoltaic, and photosynthetic devices. The simulations will help researchers discover and explore innovative solutions for current energy shortages and medical diagnosis and national security problems. To achieve this goal, we propose to dramatically increase the capabilities of the Argonne-developed electromagnetic code NekCEM by producing a single, comprehensive electromagnetic software package that will run in parallel at an extreme scale.

Mission Relevance

Our computational efforts will include leading-edge simulations in nanotechnology-based science applications that are clearly related to the DOE future science mission and that will take full advantage of extreme-scale computer architectures in the upcoming years. This project will help scientists advance new scientific discoveries that will deliver real benefits to society, industry, and science by means of highly efficient and accurate predictive modeling, while significantly reducing both the costs and the risks associated with the design process. The first customers will be materials scientists and engineers, with possible extensions to the material synthesis and photovoltaic solar cell industries in the future.

FY 2014 Results and Accomplishments

In prior years, we improved NekCEM's peak performance on the Blue Gene/P (BG/P) supercomputer from 10 to 40 teraflops; added threaded input/output (I/O), reducing the total simulation time by completely hiding the I/O latency with the perceived write performance of 70 gigabytes on BG/P and 50 gigabytes on the Cray XK6; added restart I/O swap routines by using a crystal-router communication kernel; and added hybrid MPI (message passing interface)/OpenMP algorithms, achieving performance speed upwards of 30% on the Blue Gene/Q and 50% on Cray XK6 for 4 million data point simulations on 128 MPI ranks with 8 threads, compared to 1024 MPI ranks. We also developed a non-reflecting boundary treatment in a frequency-domain acoustic solver for solving scattering phenomena in multi-layered media with complex structure and initiated developing a drift-diffusion solver based on spectral element discontinuous Galerkin methods.

In FY 2014, we significantly expanded the simulation capabilities of the NekCEM code by adding new algorithm features for solving Helmholtz and drift-diffusion equations. Three key NekCEM accomplishments are summarized here, with detailed results enumerated below them.

Development of a Drift-diffusion Solver (Two-dimensional [2D]/Three-Dimensional [3D]/Parallel).

1. Developed explicit, implicit, and semi-implicit backward differentiation formula (BDF)1/BDF2 time-stepping schemes.
2. Developed boundary conditions for homogeneous, inhomogeneous, Dirichlet, and Neumann boundaries

and a multiple set of boundaries for multiple (electron/hole/potential) fields.
3. Developed five different preconditioners: Jacobi method, finite difference method (FDM), generalized FDM (GFDM), spectral element (SE) method, multi-grid method, and projection method. Significantly reduced iteration numbers per time step from 5,000 to 10 for problems having 150,000 grid points.
4. Validated the algorithms with convergence studies in nondimensional units.
5. Validated the algorithms in physical units for 2D/3D ion channel simulations.
6. With resources provided through a DOE grant, working on positive-negative (p-n) junction nanowire solar cells.

Development of a Quantum Mechanical Solver (Serial/Parallel).

1. Developed time-stepping schemes (exponential/Runge-Kutta 4 [RK4]) for density matrix calculations.
2. Performed absorption/concurrence studies for nanoparticle and quantum dot interactions.
3. Performed parameter sweep studies for cavity quantum electrodynamic models.
4. Developed communication kernel, imported it into Cetus/Vesta, and tested it on 512 cores.
5. With resources provided under a DOE Advanced Scientific Computing Research (ASCR) grant, working on spintronic systems.

Development of a Hybrid (MPI)/OpenACC Version (Multiple Graphics Processing Unit [Multi-GPU] Runs on Titan).

1. Developed MPI/OpenACC version for the full simulation routines in the Maxwell solver.
2. Developed OpenACC communication kernels for intra node.
3. Performed weak scaling up to 4,096 GPUs (1 GPU per node, 512,000 grid points per node) on OLCF XK7, Titan. Hybrid MPI/OpenACC runs were more than two times faster than MPI-only runs on 4,096 nodes (using 16 cores per node). MPI/OpenACC was selected for the Oak Ridge Leadership Computing Facility (OLCF) OpenACC Hackathon project at Oak Ridge National Laboratory, October 27–31, 2014.
4. With resources provided by a DOE CESAR grant, extending OpenACC into drift-diffusion and quantum mechanical solvers.

Seminars

Min, M. (2014). "Scalable High-order Algorithms and Simulations for Electromagnetics and Fluids." Iowa State University, Ames, IA, November 19, 2013.

Min, M. (2014). "High-Order Algorithms and Performance for PDEs in Electromagnetics and Fluids." Brown University, Providence, RI, October 25, 2013.

Min, M. (2013). "Scalable High-order Algorithms for Energy Applications." DOE Applied Math PI Meeting, Albuquerque, NM, August 6–8, 2013.

Min, M. (2013). "Scalable Algorithms toward Exascale Computing for Energy Applications." Purdue University, Lafayette, IN, February 22, 2013.

Min, M. and P. Fischer (2012). "Scaling of PDE Solvers at Exascale." DOE PI Meeting, Washington, D.C., October 17–19, 2012.

A Future for Energy-Efficient General-Purpose Computing Based on Heterogeneity

2012-202-R2

Andrew A. Chien

Project Description

Most research on academic and industrial architectural computing focuses on a mainstream, multicore approach. This is because heterogeneity is inherently difficult to assess in the context of general-purpose computing, which has long been the defining framework of the computer architecture community. Now heterogeneous architecture is being explored, particularly in the embedded systems ("system on chip" [SoC] integration) community and application-specific integrated circuit (ASIC) community (focused on design). Neither approach directly addresses mainstream computer architecture — the persistent software-hardware compact.

Within the computational science, high performance computing (HPC), and DOE communities, interest has begun to grow in "hybrid computing" [central processing unit-graphics processing unit (CPU-GPU) computing], which is a bimodal variant of the broader heterogeneity challenge. This is a reactive effort, in which the complexities of GPU hardware — driven by graphics computation — are being inflicted on scientific computing, and the software and applications that need to "cope" with them. There is significant programming difficulty with regard to exploiting GPUs. A further problem is that the parallel code structures for GPUs are often different and incompatible with the code structures needed for multicore CPUs, creating major software architecture and portability difficulties. Nevertheless, there is a growing effort to build a new parallel software ecosystem/infrastructure that effectively

exploits GPUs in research and commercial communities (from libraries to applications). These efforts are largely a software response to hardware-imposed heterogeneity, since the major features of GPUs have been defined by embedded graphics applications.

The advent of change in semiconductor technology scaling has created an inflection point (all integrated circuits are now increasingly energy- and heat-limited) for computer architecture and, as a consequence, for programming tools. Multicore and graphic processing units (GPUs) are the first examples of this, but the changes in architecture will be profoundly greater. We are exploring new programming technologies that can be co-designed with the underlying architectures to exploit 10-fold or more heterogeneity while delivering 10-fold or greater energy efficiency and thereby providing much higher performance. The key is to balance the exploitation of architectural customization with the provision of coverage for general purposes. Integral to this approach is the programming and compilation challenge of flexibly exploiting heterogeneity with modest programming/porting effort.

Mission Relevance

The project is relevant to DOE's mission in science. The potential implications of this project are broad, extending across the full range of DOE users of exascale (and petascale) high-performance computer (HPC) systems, and the project is likely to affect emerging data-intensive computing (or "big data") systems. The project is expected to inform the DOE Advanced Scientific Computing Research (ASCR) roadmap for high-performance and data-intensive computing, including hardware architectures (in partnership with vendors) and software tools.

FY 2014 Results and Accomplishments

In FY 2012, using the 10×10 approach, we have staked out a pioneering view of heterogeneity (systems with 10 or more programmable accelerators) that should be conveniently programmable. This perspective is unique in both its breadth (it studies broad workloads) and its systematic approach (it balances general-purpose utility and heterogeneity to achieve high levels of energy efficiency). The 10×10 approach creates a new paradigm for thinking about application workloads, programmability, and exploiting customization; it unlocks radical new opportunities. Beyond its fostering of tangible architecture inventions, the 10×10 perspective is important for enabling a systematic view of heterogeneity, enabling DOE to chart a strategic, high-payoff, managed risk research strategy across a range of its computational research portfolio in a period when hardware architecture is changing dramatically.

In FY 2013, we studied processors under memory architecture and their potential benefit for exascale applications (mini-apps), exploring both memory-capacity limited and compute-limited applications. Our studies showed that only a few of these mini-apps (and presumably their corresponding full-scale applications) will benefit from stacked dynamic random access memory (DRAM) chip modules. However, those applications will derive a 3- to 5-fold benefit in performance per compute node. With regard to portable heterogeneous programming in Open Computing Language (OpenCL), we identified key factors for performance portability and proposed new directions for OpenCL. Finally, we identified several specific memory hierarchy customization opportunities.

In FY 2014, we made substantial progress in characterizing workloads and understanding the potential benefits of heterogeneous architecture and radical new memory approaches. In this stage of the project, we focused on designing and evaluating exemplar 10×10 designs that incorporate up to six different heterogeneous microengines. These designs included acceleration support for sort, fast Fourier transform (FFT), bit-nibble-byte, generalized pattern matching, and data layout transformation. In achieving challenging signal and image processing benchmarks, these systems — by using two memory systems (DDR3 and HMC) and extrapolating process technology to a 7-nm complementary metal-oxide semiconductor (CMOS) — improved by a factor of more than 1,000 over simple, in-order reduced instruction set computer (RISC) cores, and they achieved extraordinary power efficiencies (from 10 to 75 gigaflops per watt).

Seminars

Chien, A. (2013). "Technology Scaling and the Future of Microprocessors: The 10×10 Approach." Purdue University, West Lafayette, IN, October 9, 2012.

Chien, A. (2012). "Technology Scaling and the Future of Microprocessors: The 10×10 Approach." University of Illinois at Urbana-Champaign, Urbana, IL, February 9, 2012.

Guha, A., P. Cicotti, A. Snavely and A. Chien (2012). "An Empirical Foundation for Heterogeneity: Clustering Applications by Computation and Memory Behavior." University of Chicago, Chicago, IL, February 16, 2012.

Guha, A. and A. Chien (2012). "Systematic Evaluation of Workload Clustering for Designing Heterogeneous, General Purpose Architectures." University of Chicago, Chicago, IL, June 19, 2012.

MADNESS for Materials

2013-199-R1

Nichols A. Romero, Laura E. Ratcliff, and Alvaro A. Vázquez-Mayagoitia

Project Description

Although there are many feature-rich density functional theory (DFT) codes available, only a small subset of them are designed to run efficiently on petascale supercomputers. Even fewer of these codes are able to treat systems with greater than 10,000 electrons, because of the inherent cubic scaling of DFT. The next generation of leadership-class computers will pose a number of new challenges to these codes in terms of weak and strong scaling, single-core performance, time to solution, and even precision. Further along the exascale roadmap, computational issues like managing ever greater amounts of node concurrency will require exploratory research.

We propose a massively parallel reduced-scaling DFT code for materials based on the well-established MADNESS framework, which uses a multi-resolution multi-wavelet basis in conjunction with parallel task-based runtime. The successful outcome of this project will produce a reduced-scaling DFT code capable of running on up to millions of threads on Mira (Argonne's 10-petaflop Blue Gene/Q) and permitting robust DFT calculations on materials containing in excess of 10,000 electrons.

Mission Relevance

Our work is relevant to DOE's missions in energy storage and basic science. In particular, our work is of interest to the ASCR (DOE Office of Advanced Scientific Computing Research) and BES (Basic Energy Sciences) programs in DOE's Office of Science. A massively parallel reduced-scaling DFT code designed for the Blue Gene series architecture that meets the needs of the DOE materials research community is not available. Such a code will be a strategic capability that will enhance Argonne's ability to deliver petascale science and beyond in key areas, such as energy storage and catalysis. Additionally, we anticipate that Argonne industry partners who are performing exploratory materials research will benefit from the success of this project.

FY 2014 Results and Accomplishments

Work in prior years has focused primarily on performance issues concerning Blue Gene/Q. The thread scaling was improved by leveraging the Blue Gene/Q port of the Intel Thread Building Block (TBB) library. Some of this work is ongoing: we saw improvements in performance thanks to the use of TBB as well as Google Perftools Thread-Caching Malloc (TCMalloc). However, the majority of our efforts in FY 2014 were focused on expanding the scientific capabilities of our MADNESS applications.

A linear response code was implemented by a research aide (Yukina Yokoi) to calculate polarizabilities of small molecules. It is still in beta-stage implementation and we are continuing to validate its correctness and robustness.

In collaboration with scientists at Stony Brook University, we implemented pseudopotential functionality in the molecular DFT code (called moldft). This functionality will make the simulation of materials containing transition metals feasible. This feasibility was validated against the BigDFT wavelet code, with which we found good agreement for several systems, but which has revealed some correctness issues for some small molecules. We are actively working to improve the performance of the pseudopotential code.

One of the goals of the MADNESS framework is to guarantee precision in a robust manner. We previously had encountered difficulties in controlling the precision of generalized gradient approximation (GGA) calculations. After significant investigation, we established the origin of this issue and implemented an interim solution. We may explore more robust solutions in the future.

Progress was made in improving certain algorithmic kernels exhibiting quadratic or higher computational complexity. Figure 1 demonstrates scaling that is close to linear, with only a small quadratic component. We will need to confirm this weak scaling behavior for larger systems.

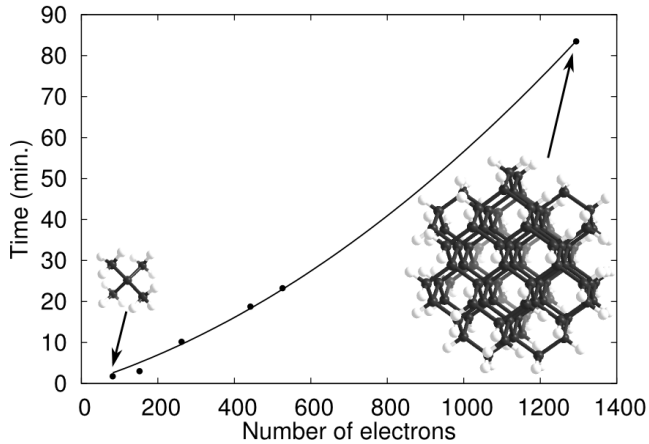

Figure 1. Time taken to simulate hydrogen-terminated silicon clusters of various sizes using moldft. The calculations were performed using 1024 nodes on Mira.

Proposed Work for FY 2015

In the third year of our project, we will continue to work on the computational aspects, including thread and message passing interface (MPI) scaling, as well as improving the remaining kernels with quadratic scaling. With respect

to scientific functionality, we will focus on hardening the periodic DFT.

We have recently migrated the MADNESS project from GoogleCode to GitHub. Our new URL is https://github.com/m-a-d-n-e-s-s/madness. There are plans to release a developer's version of MADNESS in the first quarter of 2015. This version will be followed by another release that is ready for production science.

Mathematical Techniques to Model Urban Data

2013-206-R1

Charlie Catlett and Sven Leyffer

Project Description

Urbanization in developing economies such as China and India over the next three decades will drive the design and construction of about 60 billion square meters of floor space. Current practices and tools used for city designs and operations do not scale up to accommodate the magnitude and pace of such growth, portending megacities that, because of inefficiency, will have direct and indirect impacts on the natural environment, climate, and global energy supplies. Popular ideas about "smart cities" and investments in "smart projects" are often driven by technology companies seeking new markets, while the actual design and operation of today's growing cities suffer from a paucity of scientific data analysis and modeling methods and tools.

Transparency and open data initiatives in many cities are exposing unprecedented detail about the urban environment and its systems: engineered (e.g., transportation, utilities), natural (e.g., air, water), and human (e.g., social, economic, health). The data comes from many independent sources with diverse properties including resolution, content, and degrees of complexity, however they share two key attributes — time and location. Increasingly, urban data is analyzed with machine learning techniques and, in some cases, via social network analysis, but these approaches are often limited in terms of scale. The limits are due partly to the lack of high-performance software and hardware tools but more to the fact that the data is typically organized and represented using traditional database methods designed to graph or map a particular variable or compare a small number of datasets.

The project's goal is to develop and prototype strategies to represent urban social/economic data so that a variety of mathematical methods and tools can be used for data analysis and visualization. The focus is on analyzing interactions and patterns among multiple independent datasets. To support such work, we will account for complexity in terms of variations in ontologies as well as temporal and spatial resolutions. There are hundreds of relevant datasets for Chicago, from high-volume streams (e.g., videos) to traditional administrative databases (e.g., inspections, expenditures, contracts, service or emergency calls, crimes, or building code violations) to low-volume streams (e.g., global positioning system [GPS] tracks). Irrespective of volume, the complexity and diversity of the data present challenges to scientific inquiry.

Our original approach was to exploit the fact that all of the urban data is unified by the common attribute of geographical location. In most cases, the location is represented as latitude and longitude; in other cases, it is represented by a location proxy (e.g., street address, business name, utility account number) that can be transformed into latitude and longitude. The urban environment was seen as a two-dimensional surface, with each dataset represented by values indexed to this surface. The data available varied in terms of time resolution, from a specific time of day (e.g., crimes, 311 or 911 calls, location of city vehicle) to daily (e.g., building code violations), monthly (building occupancy), or longer times (e.g., geography, infrastructure, public transport routes).

Based on our interactions with urban scientists (e.g., sociology, economics, public safety) in the first year of the project, we decided to exploit the urban date/time data. Adding this second common attribute enables us to represent a location or area (e.g., street segment, block, polygon) as a time series of vectors that can be analyzed using a variety of existing mathematical and machine learning tools.

A key challenge remains that the resulting datasets and graphs are likely to be massive and well beyond current analytical capabilities. Thus, there is an opportunity to develop new multiscale analysis and machine-learning tools for sequential and time-dependent data, which can be based on organizational connections within the data, on geography, or on other relationships (e.g., commute times by public transport, distance from particular services).

Mission Relevance

The project is relevant to DOE's missions in environment and energy. A primary customer of the results from this work would be the U.S. Government, particularly the U.S. Department of Energy (DOE), whose research portfolio does not presently include investigations necessary to fully understand global urbanization and its impact on the planet's climate and energy supplies. Given the magnitude of the energy- and climate-related impacts caused by cities and their growth, there is opportunity and need for DOE to explore research questions that move beyond

the individual components of cities (e.g., buildings, vehicles, utility grids) and develop the capability to examine cities as multiscale complex systems. Similarly, city, state, and other federal governments in the United States and abroad require tools and methodology to transform their growing, diverse, data sources into understanding for both the operation of their cities and to plan for growth and renovation.

FY 2014 Results and Accomplishments

In FY 2013, we analyzed available urban data in the context of extensive discussions with sociologists, energy scientists, economists, and urban designers, to select an initial set of data for the research. On the basis of this initial work, we elected to refine our strategy from "mashups of two dimensional (2-D) surfaces" to time series vectors, which hold much greater analytic promise with respect to using machine learning and similar techniques.

In addition, working with collaborators at The University of Chicago Becker-Friedman Institute, we helped to create software to begin to construct multi-data set vectors, summing values over a single period rather than building sub-sampled time series data.

Building off of the previous year's work, in FY 2014 we created a test system that allows a scientist to specify a set of data sources, a sampling period (e.g., daily, weekly, monthly, annual), a start and end date, and a location (e.g., address, latitude/longitude, street segment, block, polygon). As a result of the successful completion of this test system, through a National Science Foundation (NSF) grant, we will continue to work on the back-end, underlying database infrastructure. This database infrastructure is useful for implementing the mathematical approaches that this project is exploring.

Also, in FY 2014, we worked with scientists at the University of Chicago and with the summer student fellowship program "Data Science for Social Good" (http://dssg.uchicago.edu) to identify a set of roughly 40 datasets related to a variety of urban science questions of interest to sociologists, economists, and others. Our analysis of the types of research questions to be asked further guided our decision to implement our approach (integrate all data using time and location as the organizing principles) in a geospatial database (PostGIS). Using a prototype developed by the NSF-funded project, we were able to validate our designs using the initial 40 datasets.

Proposed Work for FY 2015

During FY 2015, we want to extend the principles we developed and implemented in several ways. First, to answer many urban research questions (e.g., in an econometrics analysis or an evaluation of impacts from a particular intervention like a new transport system), (1) a particular area for study must be bounded, and (2) similar areas in the city that might act as controls need to be identified. After meeting with geographic information system (GIS) groups from multiple labs (including Argonne) and universities, we identified some uniquely well-suited work done by urban GIS experts at Arizona State University. We intend to leverage their work in spatial analytics and econometrics. Second, we will extend the focus, which has been on place-based questions and data, to incorporate (a) entity data (e.g., census or labor datasets) and (b) new, much more frequent types of events (e.g., those from sensor networks).

Seminars

Catlett, C. (2014). "Toward an "Urban Science." Argonne Training Program on Extreme-Scale Computing, St. Charles, IL, August 3–15, 2014. (also see 2011-2014-R3).

Catlett, C. (2014). "The City of Chicago Technology Plan." Chicago Architecture Foundation, Chicago, IL, June 4, 2014.

Catlett, C. (2014). "Creating Integrated Computational and Mathematical Capabilities to Transform the Design, Planning, and Operation of Cities to Achieve Sustainability and Resilience," University of Illinois at Urbana-Champaign, Champaign, IL, November 4, 2013.

Catlett, C. (2014). "Computation and Data-Enabled Urban Design and Operation." Illinois Institute of Technology, Chicago, IL, October 23, 2014.

Catlett, C. (2013). "Emerging Opportunities in Urban Sciences." University of Illinois at Urbana-Champaign, Champaign, IL, December 10, 2012.

Catlett, C. (2013). "Urban Sciences and Computer Science." The University of Chicago, Chicago, IL, January 15, 2013.

Catlett, C. (2013). "Urban Center for Computation and Data: Opportunities for Computational Urban Sciences." Extreme Scale Computing School, Chicago, IL, August 8, 2013.

Catlett, C. (2013). "Urban Social Sciences and Mathematics." Argonne Fermilab Annual Collaboration Workshop, Chicago, IL, October 7, 2012.

General-Purpose Technical Cloud Platforms

2013-208-R1

Daniel Murphy-Olson and Narayan Desai

Project Description

Our project aims to broaden the applicability of the Magellan system, an experimental cloud computing system from its current bio-informatics domain to a larger set, including cosmology and materials. To do this, we need to improve the system in several ways. First, we need to improve the overall system performance. Clouds have a thicker software stack compared with traditional high performance computing (HPC) systems, which incurs some additional overhead. In this project, we are reducing the overheads to make a wider range of applications effective to run on this platform. Second, we are building a system where continuous availability is a key goal. This property is needed to support aggregated scientific services with distributed user communities. Finally, we are developing methods to effectively harness the extreme flexibility afforded by the cloud architecture to user communities ranging from computer scientists to domain scientists.

Mission Relevance

Our project is tied to DOE's mission in science. Cloud systems support a range of computing applications poorly served by traditional large-scale DOE computational platforms. These applications are primarily services, where the scientific community at large can use a project's software platform to answer scientific questions. These projects have historically been implemented on small-scale computing infrastructure, limiting the scope and breadth of their activities. Cloud computing infrastructure has enabled large-scale comparative analysis and data integration activities that were difficult to accomplish on traditional platforms. The expansion of this approach will enable new computational approaches across a range of disciplines.

FY 2014 Results and Accomplishments

In FY 2013, we performed the first production release of the Magellan system based on the Openstack Essex release. We developed a novel user coordination system called "poncho" that enables streamlined rolling maintenance and the development of high-availability (HA) user applications. This system provides an application programming interface (API) for communication between users and the Magellan operations team that describes the impact of service operations and enables many operations to be conducted automatically, without manually coordinating with users. This non-invasive management technique has minimized the need for a preventative maintenance schedule that other large systems require.

We made excellent strides in improving the performance of virtual resources. We deployed experimental Ethernet emulation software that uses the system's quad data rate (QDR) infiniband to provide high-performance networking to virtual machines (VMs). This software is alpha quality and was released in a preliminary form. With this software, we see nearly 15 gigabits of network bandwidth and 25 microseconds of latency between nodes. While the latency is at the level we expect, the bandwidth is only half of what we expect to see. We are working with the vendor to improve this performance to increase the level of other infiniband protocols (nearly 30 gigabits), and we expect it can be improved substantially.

Similarly, we greatly improved the performance of persistent block storage ("volumes") in the system. This storage presents a block device directly to a VM. We built several high-density, high-performance, storage targets that present aggregated virtual disks via the Internet Small Computer System Interface (iSCSI). We modified Openstack to make use of iSER, which is a set of remote direct memory access (RDMA) extensions to the iSCSI protocol. With iSER, RDMA is used for the data path, so little tuning is required. With this change, volume performance increased to 1,800 MB/s, with considerable latency improvements. We expect that this single node performance is the best that we are likely to get out of our current storage servers, although we might further improve aggregate throughput.

We also began to test model distributed, fault-tolerant storage. This new upgraded storage would enable the use of commodity components to build system-level aggregated storage resources.

We began working with new application groups at Argonne to test model data-intensive applications on Magellan. The first group we began working with was the cosmology group. The group wants to do high-speed, interactive analytics on its simulation timestep files, which are currently about 40 TB each. We engaged in basic requirements discussions with the group. A collaboration was initiated with members in the group who will be exercising our new test model system with a real application.

Finally, we developed a set of practices for building resilient applications on Magellan.

In FY 2014, we developed a new release of the Magellan system control plane based on Openstack Havana. This release has brought with it several improvements, most notably migration of instances, improved network performance, and the ability of an end user to download images from the system. This release is currently being beta tested by several users.

We developed and placed into production a system that can request replacement parts automatically from our hardware vendor. This system has reduced the human effort required to request a replacement part from an hour or more to almost zero. This result will increase the number of machines that can be supported per allocated FTE (full-time equivalent) and will allow us the flexibility to scale the system without also needing to scale personnel.

We completed evaluations of Ceph, GlusterFS, and Sheepdog (distributed storage software to improve storage performance and availability. We ultimately selected Sheepdog to host the ephemeral storage layer for the Openstack Havana deployment. This enhancement will improve availability by allowing us to migrate instances from hypervisors with hardware issues and performance by allowing ephemeral disk performance to scale beyond the bandwidth of a single disk.

One of the lessons learned from managing the KBase development environment on Magellan is that it was difficult for users and project administrators to determine what instances might be idle through the traditional Openstack user interfaces. We developed a periodic utilization report for projects using the system, which helps give users the visibility into the system necessary to optimally use their allocation.

We developed a security group reporting utility that helps project owners view all of the network access control lists and how they map to nodes. This utility enables project owners to meet lab cybersecurity requirements, while still allowing a great deal of freedom for project owners to define network controls that meet the needs of their applications.

Finally, we developed a prototype building block approach for scaling the system up and enabling buy-in. We selected several building blocks for high memory, compute, and storage. We procured several of the storage building blocks for the Cosmology group at Argonne and are beginning to test and tune these for throughput and manageability.

Proposed Work for FY 2015

The FY 2015 work will focus on streamlining operations and refining a model for continuous acquisition that supports easy buy-in to the Magellan system by new projects. This work will have several components. The first component is continued collaboration with applications groups, which will drive the architecture of the system and help them to prepare for KBASE-style proposals. The second component is improving the system operations processes. The third component is developing a model for easy buy-in to the system.

Multiscale Materials Modeling Using Accurate *ab initio* Approaches (M^3A^3)

2013-212-R1

Álvaro A. Vázquez-Mayagoitia, Yuri Alexeev, and Anatole von Lilienfeld

Project Description

In this project, we will advance the state of the art of materials modeling by developing force fields (FFs) for complex materials by using machine learning (ML) — a systematic method for transforming large data sets of accurate materials properties, obtained from experiment or from *ab initio* quantum chemistry simulations — into accurate FFs for a broad class of systems. The creation of ML models requires training data, and the process is obviously susceptible to the garbage-in-garbage-out problem.

Hence, to enable the generation of high-quality training data sets, we will employ petascale supercomputers running massively parallel quantum chemistry codes. We will develop a data set of high-accuracy energies and properties (e.g., electrostatic moments, polarizabilities and hyperpolarizabilities, and torsional potentials) to cover a broad spectrum of chemical space by using high-performance computing (HPC) resources and benchmark-quality methods, such as quantum Monte Carlo, many-body perturbation theory, coupled-cluster theory, and density-functional theory (DFT).

Mission Relevance

The project is relevant to DOE's mission in science. Atomic simulation of materials is one of the dominant uses of HPC resources within DOE and around the world. Materials science and chemistry simulations use approximately one-third of the central processing unit (CPU) time of DOE's computing facilities. Increasing the ratio of accuracy to computational cost in atomistic simulation methods has an immediate practical payoff. For example, using few processors, our machine learning and force field methods could compute in milliseconds the total internal energy of molecules with hundreds of atoms.

FY 2014 Results and Accomplishments

In FY 2013, we developed and validated the performance of our ML models, predicting several physical chemical properties. We could predict DFT energies and polarizabilities within a data set of 7,000 different molecules. Also, we created multiple datasets of energies and forces to train our ML models, exploring the evolution of the structure of ions and small molecules in aqueous solutions.

In FY 2014, we calculated quantum chemistry data for the equilibrium geometries of over 134,000 molecules (Figure 1). We also spent considerable effort to further improve the predictive accuracy of the ML models. To this end, we developed ML models of the deviation of computationally inexpensive yet more approximate baseline quantum chemistry methods from more accurate but computationally more expensive quantum chemistry methods. These results suggest that we can easily reach chemical accuracy for thermochemical properties as well as electron correlation.

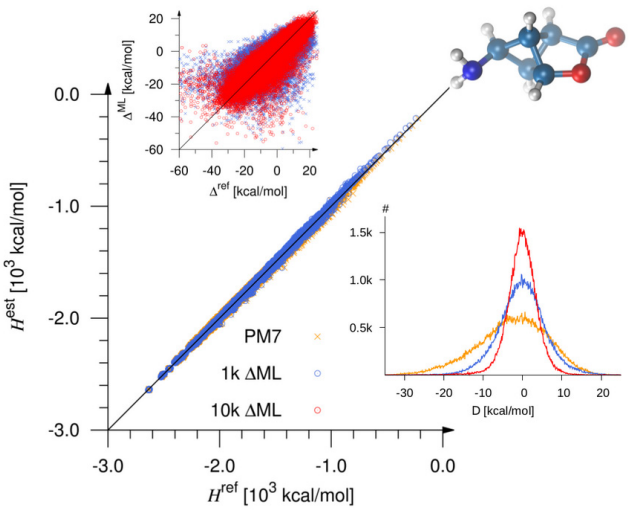

Figure 1. Enthalpies of atomization for 134,000 molecules: ML-model-corrected prediction (vertical) versus reference level of theory (horizontal). The upper inset shows the correlation of the ML model of the correction versus the actual correction. The lower inset compares the error distributions for the baseline method (PM7), ML model trained on 1,000 molecules, and ML model trained on 10,000 molecules

Furthermore, we developed ML models for the learning total energies and atomic forces. Results for forces on cis/trans-butadiene derivatives look very promising. In Figure 2, the correlation of ML- versus DFT-based predictions is shown. Furthermore, we proposed a new model to correct, with explicitly correlated wave function methods, the forces and binding energies of aqueous solutions of small molecules and ions computed with periodic DFT in the context of *ab initio* molecular dynamics.

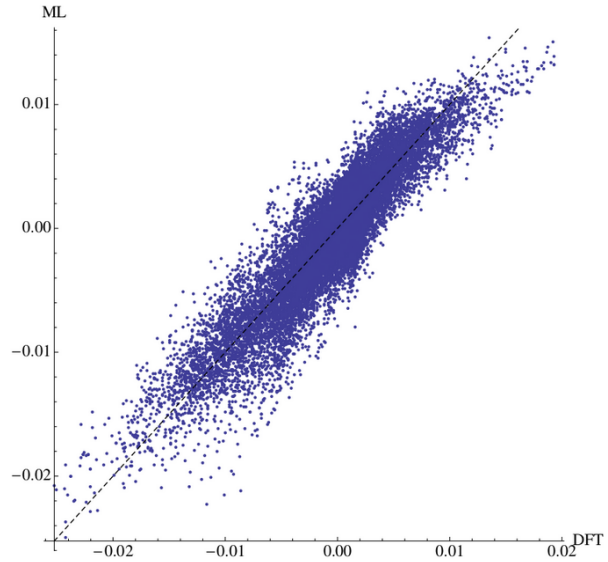

Figure 2. Scatter plot showing correlation between largest components of ML-predicted and DFT reference atomic forces, with ML trained on 1,000 molecules drawn from over 2,000 cis/trans-butadiene derivatives. Forces shown are given in atomic units, Ha/Bohr.

Proposed Work for FY 2015

In FY 2015, we will continue exploring a wide variety of ML methods that have been designed for different domains to see how they work in the framework of atomistic simulation. For example, we will continue validating our models for learning from molecular properties, toward the goal to create ML parametrized force fields informed by first-principles quantum chemistry calculation. As a result, we will considerably reduce the time to solution for hybrid molecular dynamics using *ab initio* and classical models, thereby enabling the simulation of unprecedented time-lengths.

The other major thrust of our investigation will be the evaluation of the accuracy of an ML workflow for condensed-phase systems, which necessarily have many more interactions between molecules. What trade-offs exist between the accuracy of the ML procedure itself and the assumptions used to define the many-body truncation scheme? The first task will be to compare the error associated with truncating at pair-wise interactions versus the systematic error of the training data set and the ML fitting process. The results will ensure that the ML schemes developed are balanced in terms of their error properties and thus of practical value.

X-PECT: Performance Framework to Characterize and Transform Applications and Architectures at Extreme Scales

2013-213-R1

Kalyan Kumaran, Vitali Morozov,
Venkatram Vishwanath, and Yao Zhang

Project Description

In this work, we are developing an integrated performance modeling and projection framework to study and analyze the performance of future scientific applications, HPC (high-performance computing) architectures, and the interactions among them. In particular, we are contributing to the following technically challenging areas:

1. Abstracting workloads' code structure to understand the code's potential behaviors;
2. Modeling the performance for different hardware components, so that they can be combined to form complex systems;
3. Developing mechanisms to explore workload transformations and hardware design options to better match workloads to machine characteristics; and
4. Tuning and searching for the optimized software-hardware configurations.

The delivered framework will project the performance and power for future workloads on future systems. It will also guide application developers to tune their code and help hardware designers to evaluate the impact of hardware features on application performance, at an early stage. The techniques developed herein have the potential to be incorporated into compilers and runtimes on production systems to optimize application performance.

Mission Relevance

Leadership computing facilities, a strategic area for the DOE, accelerate scientific discoveries and technological innovations by enabling large-scale, computationally intensive projects that address "grand challenges" in science and engineering. A key challenge is to understand how to better design facilities to meet the needs of scientific applications, as well as how to effectively scale applications to fully exploit the features of future systems. The framework that we are developing addresses these challenges by using performance models to provide insights for scalable science on leadership systems, and therefore is critical to the DOE's basic science mission.

FY 2014 Results and Accomplishments

In FY 2013, we built our first prototype hardware performance model for Argonne Leadership Computing Facility's (ALCF) Mira's node architecture to estimate the latency in memory, computation, and communication. We also extended our framework to automatically extract static code structure in applications, model complex loop structures in workloads, and capture runtime behavior.

In FY 2014, our research included the following:

1. We developed SKOPE, a framework for modeling and exploring workload behavior. SKOPE includes algorithm structure representations, a formalized code skeleton language, hardware performance models, and a mechanism to explore code transformations and architecture features.
2. We formalized the syntax of the code skeleton language and explored semi-automatic ways to extract code skeletons.
3. We used SKOPE for performance analysis, tuning, and projection for several use cases: (1) project the multi-node scaling trends of scientific workloads; (2) explore code transformations including kernel fusion, loop partition, and cache optimization; and (3) detect hotspots of applications and use this information for hardware-software co-design.
4. We developed Raexplore (Rapid Architecture Exploration), a software component of SKOPE for hardware modeling and exploration. It is currently implemented on the Mira supercomputer and Intel Xeon Phi processors and is easily extensible to other architectures.
5. We built detailed hardware performance models to capture the performance impact of major architectural components, including instruction pipeline, cache, and memory. Our models are validated for a variety of experiments, including threads scaling, cache contention, surface-mount technology (SMT) performance, and cross-architecture prediction, for a number of scientific applications.
6. We used Raexplore to analyze the performance of the CORAL benchmarks, which are being developed according to the DOE's mission needs. We explored the node-level design options for next-generation processors in terms of their major architecture features, such as the number of cores, cache size, and memory bandwidth. We also explored the optimal processor resource allocation between the number of cores and the last-level cache (LLC) size under the chip area constraint.
7. We developed a web application, SuperInsight (superinsight.alcf.anl.gov), that integrates the SKOPE technologies to provide performance analysis and prediction for supercomputing applications and systems. The web application also supports

data management and sharing features to facilitate collaborations among computer architects, application scientists, and performance engineers.

Proposed Work for FY 2015

In the next year, we will continue to build upon our framework and extend its capabilities to the following areas:

1. Build system-level performance models for torus and dragonfly networks.
2. Extend the SKOPE language to describe network activities.
3. Model concurrency and load balance at the system level.
4. Integrate node-level and system-level models to explore hardware design options for full systems.

Urban Systems Integration Modeling and Analysis

2013-218-R1

Leah Guzowski and Charlie Catlett

Project Description

We are creating a general-purpose framework for exchanging data between city design and/or configuration tools and computational modeling tools, based on an industry-standard data representation scheme. In contrast to one-time, customized integration of specific tools, such an open framework will enable the incorporation of an array of tools over time. In this project, we will define a framework to support the integration of data from (1) design tools, (2) computational simulations, and (3) engineering studies to use in making key decisions that must be informed by these various sources. Implementing the framework will require that each "module," whether a computer application or an engineering study, be adapted to import data from and export data to the framework.

To ensure that the framework is feasible and to understand its requirements, we will implement a proof-of-concept by using an existing model, such as hydrology, transportation, and/or energy. This task will require selecting an appropriate, industry-standard data representation format (or language), modifying the system object model design tool (used to configure the location, orientation, use, and other factors of a set of buildings) to export data in this format, and modifying the existing model to import such data.

Mission Relevance

The project is relevant to DOE's missions in energy and the environment. Scientific simulations that are used to model energy demand and supply, the environment and climate, or infrastructure are typically developed and tuned for regional or continental scales rather than for city or area-within-city scales. Adapting these scientific models to a scale of hundreds of acres and providing a framework for the exchange of information between city design tools and the various computational models would significantly improve the ability of researchers, scientists, and industry to explore the impacts of design and engineering options to optimally "ground" critical decisions related to energy and infrastructure development.

FY 2014 Results and Accomplishments

In FY 2014, we successfully developed a general-purpose framework, "LakeSim," for exchanging data between city design and/or configuration tools and computational modeling tools, based on an industry-standard data representation scheme.

The LakeSim framework enables urban designs on scales of hundreds to thousands of buildings to be imported from traditional computer-aided design (CAD) and from zoning and projected construction schedule data to emerging industry tools (Figure 1). This project utilized ESRI's *CityEngine*. CityEngine was chosen to facilitate integration into existing industry processes (such as at Skidmore, Owings & Merrill) in order to ensure that the LakeSim project could benefit from interaction "in the field." More recently, open source tools with similar capabilities, such as "UrbanCanvas" developed by a team at UC-Berkeley (UrbanSim team), have become available. LakeSim was modularly prototyped to allow replacement of components like this to be straightforward. To prototype this integration, the LakeSim project began with a focus on using open source computational modeling tools from DOE to forecast energy demand on a per-building resolution for a given configuration of buildings with respect to building construction type and size, zoning (e.g., residential, commercial, retail), and construction schedules as the site is constructed and occupied over multiple decades. Using CityEngine as an interface, LakeSim enables designers and policymakers to modify zoning and projected construction dates for individual buildings or for groups of buildings (e.g., blocks or districts).

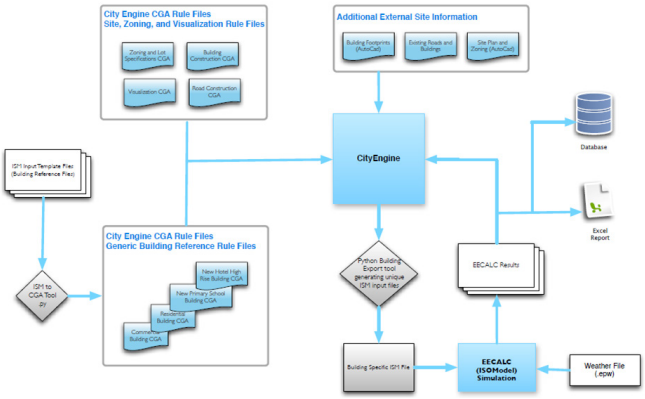

Figure 1. Schematic showing "LakeSim" framework with input from weather and building configuration data, ESRI CityEngine as the user interface, and EECalc to perform per-building energy demand forecast.

To evaluate energy demand and potential energy savings, LakeSim deploys normative energy calculations derived from the European Committee for Standardization (CEN) and the International Organization for Standardization (ISO) and translated into an Energy Performance Standard Calculation Toolkit (EECalc), developed by Argonne and the Georgia Institute of Technology. The EECalc toolkit calculates thermal energy demands for heating and cooling by using a monthly, quasi-steady-state method. Thermal energy demand accounts for heat losses by transmission and ventilation, heat gains from solar and internal sources, and the effect of thermal inertia driven by building mass.

Developing an Integrated Sensor Network for Science

2014-160-N0

Peter Beckman, Nicola Ferrier, Yuki Hamada, Katarzyna Keahey, and Rajesh Sankaran

Project Description

The availability of small, inexpensive sensors linked together with wired and wireless networks is dramatically changing many data-driven science domains. Research projects on urban environments, terrestrial ecosystems, and soil biology are just a few of the areas hoping to answer science questions by deploying sensors. However, several computer science challenges must be overcome before effective sensor networks can be deployed. In this project, we are (1) designing a secure and extensible sensor computing platform capable of *in situ* data processing; (2) developing an architecture for data movement, caching, and verification from the sensor to the cloud computing platform; and (3) enabling the support of local autonomous actuation of motors and control of algorithmic feature analysis.

Mission Relevance

Advanced sensors, computational science simulation and modeling, and climate science are all key parts of DOE's mission. Effectively leveraging these to provide near real-time data to predictive simulations will enable DOE-funded researchers to better understand energy usage, infrastructure threats, and our environment.

FY 2014 Results and Accomplishments

In FY 2014, we focused on designing a robust, reusable architecture that can be the basis for atmospheric base station sensors and urban sensors that can be deployed along the streets in downtown Chicago. We have named this architecture "Waggle."

The Waggle system consists of two components: the Waggle Field Node (Figure 1) and Waggle Cloud Infrastructure (Figure 2). The Waggle Field Node constitutes a modular, scalable, fault-tolerant, secure, and extensible platform for hosting sensors and actuators in the field, supports *in situ* computation, and works in concert with the Waggle Cloud Infrastructure. We designed and fabricated two printed circuit boards. One of the boards provides a number of sensors, including temperature, humidity, vibration, barometric pressure, ambient light, and magnetic field. The other circuit board we designed provides power management and monitors current draw (milliamps), internal temperature, and a heartbeat mechanism to the compute board. We also built a sensor data cache for the Linux compute board, so *in situ* computation can analyze aggregate sensor data and create new data products. The Cloud Infrastructure is designed with the goal of scaling to several hundreds of thousands of Waggle Field Nodes, supporting real-time scientific simulation and analysis based on data sensed by Waggle Field Nodes, extending methods for inter-node communication and data exchange, and serving raw and processed data to end users and applications running on other high-performance computing resources.

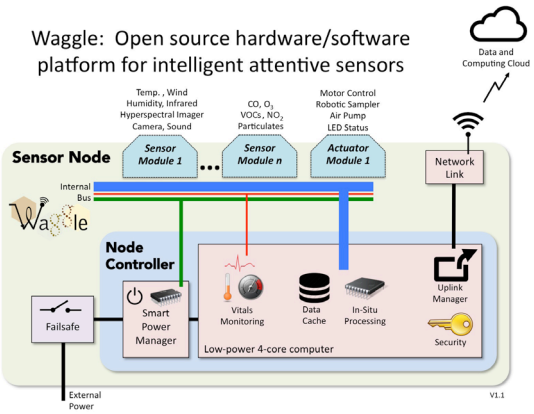

Figure 1. The Waggle Sensor Node Architecture (VOC = volatile organic compounds).

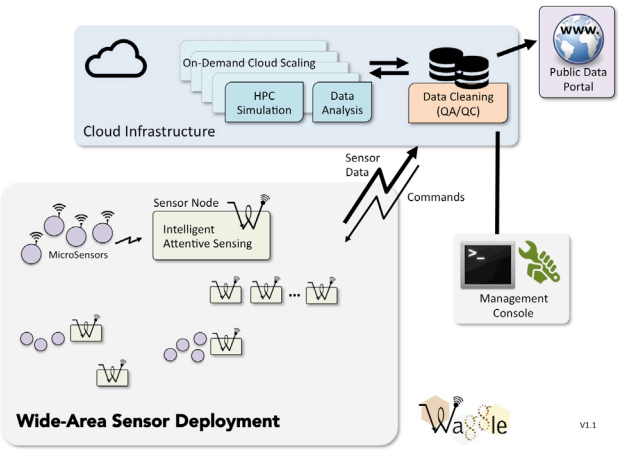

Figure 2. Waggle Cloud Computing Architecture (QA/QC = quality assurance/quality control).

Proposed Work for FY 2015

The team will focus on the *in situ* computational modules to be added to the base system and the deployment of the system in the city of Chicago. We will explore using Docker and OpenCV to provide simplified deployment of *in situ* computer vision. Similarly, we will explore *in situ* audio processing modules to detect and classify important audio signatures, such as car horns, bird calls, or idle trucks.

Emerging Compute and Data Infrastructure

2014-163-N0

Craig Stacey and William Allcock

Project Description

The relative maturity of computing has resulted in a variety of different markets driving the design of computational components. Mobile computing (ARM) (Advanced RISC [reduced instruction set computer] Machines), the convergence of the gaming industry with supercomputing, and the rapid commoditization of storage and network spaces have all contributed components with vastly different performance, power footprint, and cost scaling. It is clear that some of these components will provide capabilities for future computing systems, but it is unclear at this point how best to make use of them.

We will procure hardware components that are likely to be useful in future systems and assess them by using application kernels or embed them into larger systems for testing. We will make use of existing test-bed infrastructure at Argonne as appropriate.

An ongoing component of this project will be the collection of vendor roadmap information (under non-disclosure agreements [NDAs]) to understand new hardware that is under development. Similarly, engagements with vendors on prototype hardware will enable us to drive the design of products toward our requirements.

Mission Relevance

This work addresses the DOE mission of innovation in extreme-scale computing for scientific workloads. This work will benefit users of future large-scale systems designed and built at Argonne, as well as the community designing large-scale systems. This work is of interest to DOE, the National Science Foundation (NSF), and the National Institutes of Health (NIH), as well as the defense community.

Access to this hardware will enable prototyping of new approaches to address both traditional high performance computing (HPC) problems and data-intensive computing applications and service-oriented ensembles. These efforts will enable us to develop a solid understanding of the properties of these components. We will thus be able to prune the system hardware design space down to a much smaller, more manageable size.

FY 2014 Results and Accomplishments

We evaluated the ARM Cortex-A15 processor architecture and defined a set of benchmarks for input/output and central processing unit intensive applications. These benchmarks will be reused with ARM Cortex-A57 processor systems with additional benchmarks for floating point performance. In addition, we examined the use of containers and virtualization with the Kernel-based Virtual Machine (KVM) software on the A15 test system. We began engagements with HPC-oriented vendors of ARM systems to examine the requirements for test deployment.

We procured a number of enterprise solid-state disks (SSDs) and benchmarked the use of them in two storage systems, ZFS and Ceph. With ZFS we used the SSDs as a Layer 2 Adaptive Replacement Cache (L2ARC). The L2ARC operates as a least recent used (LRU) read cache with memory above it in the cache hierarchy. We benchmarked this setup with our existing virtual-block-device workload. The first configuration used them as L2ARC cache, whereas in the second they were configured as a ZFS intent log (ZIL) device. In both configurations, we found that ZFS was not able to take advantage of SSD capacities beyond 20–30 gigabytes, thereby rendering larger SSDs useless in terms of performance gains.

As an L2ARC cache we primarily saw input/output operations per second (IOPS) increase for short/bursty traffic; however, under synthetic benchmarks simulating random read traffic the performance gain was negligible,

and in some use cases actually degraded the performance slightly. Configuring the SSDs as a ZIL, we again saw similar behavior in that if the storage disks were servicing requests, the ZIL would give us a buffer of about 10–20 gigabytes of high IOPS before falling back to the magnetic only IOPS rate. Across both configurations, we saw about a tenfold performance boost in both read IOPS and write IOPS while the reads/writes were going to the SSD devices.

We found there may be some value in configuring two storage systems provisioned with SSD only and hybrid/SSD configurations. Modern SSDs are becoming more usable as their endurance and capacity are reaching a more desirable price/performance value that makes deployment in smaller storage arrays such as the ones used on Magellan a more viable option.

On the software-defined networking side, we procured of a proof of concept system with BigSwitch Networks and devised a collaboration plan with that company to develop and extend the control software. If this proof of concept is shown to be viable, we will be able to enable increased bandwidth and throughput to the APS, HEP, and other high-output sources at a much lower financial cost than existing solutions require.

Proposed Work for FY 2015

We plan to survey smart memory space and build a roadmap based on product availability. We will procure and evaluate NVDIMMS (non-volatile dual in-line memory modules or comparable components. We will continue our work in evaluating software-defined networking technologies, deploying the test system. It will contain approximately 500 compute cores and be connected to the laboratory and wide-area network at a speed of 100 gigabytes per second. One of our goals it to be able to dynamically provision high-performance links between the Advanced Photon Source and this system by using the OpenFlow protocol. We expect this first system to be generally available for several research projects in cosmology, biology, and high-energy physics in early FY 2015.

Scalable Stochastic Algorithms for Exascale Computational Mesoscience

2014-166-N0

Dmitry Karpeyev, Juan J. de Pablo, and Olle Heinonen

Project Description

Responding to the needs of materials science, the field of computational mesoscience has become an active area of computational mathematics. This project aims to devise and implement scalable computational materials science methods that take *full* advantage of the modern hardware.

We focus on the scalable algorithms for simulating the dynamics of charged particles in electrolytes. Specifically, we want to devise and write fast computer codes that simulate the translocation — slow, thermally driven transport — of DNA molecules (or similar polymers) through narrow channels. The polymer is modeled as a collection of point "beads" connected by springs and suspended in an electrolyte (fluid with dissolved ions). Simulations of translocations are generally extremely time-consuming, in large part because the motion of polymers is dominated by thermal fluctuations, which take "one step back for every two steps forward." These simulations are also difficult to parallelize, which is representative of the types of problems facing computational soft-matter science. We are pursuing this project with researchers at the Argonne/University of Chicago joint Institute for Molecular Engineering (IME).

Mission Relevance

This project intends to bring exascale-capable numerical algorithms to DOE's supporting sciences mission. This will help advance the energy sciences by enabling and expanding the use of modern and future leadership-class hardware in materials and chemistry. Examples of such beneficial efforts include the recently inaugurated Chicago Hierarchical Materials Design center (CHiMaD), as well as the Argonne-led Joint Center for Energy Storage Research (JCESR, aka the Battery Hub). In the long term, we expect broader benefits to accrue to DOE's energy sciences research, reaching beyond computational materials science. This could include the modeling of nuclear fuels performance, global climate, and power grid optimization. The main benefit will be better utilization of modern and emerging hardware in computational sciences.

FY 2014 Results and Accomplishments

We developed two complementary prototype codes for modeling the motion of charged particles — modeling the DNA beads — as they interact with both the fluid in which they are suspended and an external electrostatic field.

The fluid flow and the electrostatic field are governed by the Stokes equation (fluid) and Poisson's equation (electrostatics). Together, they dominate the computational time of the DNA simulation and account for the bulk of the computer memory usage — from hundreds of MB to tens of GB — which is determined by the need to resolve the so-called Debye length in the electrolyte (the size of the ion shells around the DNA beads) and the electrostatic field over very large surrounding material domains. We developed a fully parallel code that simultaneously solves the Stokes and Poisson's equations in the presence of

point forces and charges. This code is fast and very accurate away from the particles, and it parallelizes very well.

To improve the accuracy of the flow and electrostatic field calculation near the particles, we developed a benchmark version of the General Geometry Ewald-like Method (GGEM) that takes an optimal time to compute the particle-particle-particle-fluid interactions. This is a serial code that has been used extensively for bead suspensions in periodic and nonperiodic geometries. Our main near-term goal was to develop a parallel extension for GGEM suitable for massively parallel computers.

In FY 2014, we developed parallel algorithms that identify and rapidly exchange particles that interact with each other but are located on different processors — the "halo" particles. The halo exchange contains most of the communication required to calculate the force on the particles and the fluid. We implemented a fully parallel algorithm that identifies and moves all of the interaction partners and has the complexity of the full-force calculation algorithms. A substantial achievement was that regardless of the size of the interaction "halo," and regardless of the number of processors used (see Figure 1), the time spent in the setup phase of the algorithm is essentially constant, which implies that the algorithm is scalable.

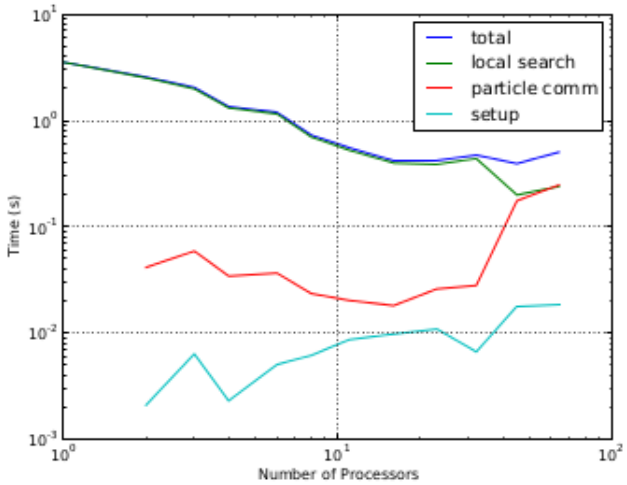

Figure 1. Particle computation runtime for different processor numbers.

Proposed Work for FY 2015

In FY 2015, we plan to develop a fully parallel simulation of clouds of charged point particles swimming in nanochannels. These particle "swarms" will test the capabilities of our software to rapidly move particles between the processors of massively parallel compute clusters, as well as between the memories of the different sockets on a multicore chip. We will start by studying the scalability of the communication algorithms developed in FY 2014 out to tens of thousands of processors. Building on this software infrastructure, we will demonstrate that a O(N log N) computation is possible for N self-propelled particles in arbitrarily shaped channels. This will be a substantial step forward. Such algorithms have existed for single-processor computers for some time. On parallel machines, fast particle methods have been known for free-space particles. The novelty is in the coupling of interacting particles and fields in complex geometries, which is our goal.

Improving and Validating Models of the Urban-Climate Connection with Dense Sensor Networks

2014-167-N0

Robert Jacob, Edwin Campos, Charlie Catlett, Beth Drewniak, Rao Kotamarthi, Rajesh Sankaran, and Man Wu

Project Description

Urban areas change their own climates, most famously by creating an urban heat island (UHI) and by introducing mechanical drag on air flow and moisture transport within cities. They also emit pollutants that have strong negative local effects. To better understand how climate change will affect cities, it will be necessary to better understand and model the interactions between cities and the regions surrounding them. Models of urban areas suffer from a common problem: lack of validation data from within the city. To better sample larger regions, most climatological and meteorological sensor networks are located outside urban areas. They also have not taken advantage of new low-cost computation and sensing devices available through the commercial cell phone industry. This project will design and deploy a dense sensor network that can measure urban weather and climate in detail and provide validation data for urban weather and climate simulations.

Our major task is to identify and develop a low-cost, low-power sensor node for measuring basic meteorological quantities. The device making these measurements will also need software/hardware for managing power and communicating data. We will identify locations in the City of Chicago for deploying about a dozen prototype nodes to test the hardware and software and assess the quality of the data. We will also augment Argonne's existing weather station to provide measurements for comparison. Assuming the initial deployment is successful, we will then expand the network to cover more of the City of Chicago. The data we collect will be combined and compared with data from citizen observer networks to make diurnal, monthly maps of UHIs. This data will also be compared with simulations of the UHI from urban weather models.

Mission Relevance

This project is primarily relevant to DOE's missions in science and environment. The urban boundary layer is one of the most poorly measured and understood layers in the urban atmosphere. Our sensor network will have the capability to dramatically improve our understanding of this area of the Earth's climate system. We will combine this data with modeling of the urban atmosphere to help inform both where the models need to improve and where more measurements are needed.

FY 2014 Results and Accomplishments

After extensive research, we found most of the current commercially available weather sensor systems have some flaw that prevents them from being used in our research. Typically, they do not take advantage of rapid advancements in sensor technology, power production and storage, embedded computing, and communications. Furthermore, the methods by which data can be obtained from them are often restrictive because of proprietary software and hardware components.

We were able to develop a weather system with limited number of sensors at a price point below $300, with plenty of local computation power for parsing and data manipulation. With another LDRD research team (see project 2014-160-N0), we developed the software infrastructure to support the strong link between sensors and computing. We integrated several sensors that measure the same quantity into the system in the first phase to evaluate the sensors and understand their performance limitations. These sensors are mounted on a printed circuit board designed by us and housed in a radiation shield.

To test the sensor network, we have a rooftop-mountable platform designed to be a self-contained unit, powered by a solar panel that can be detached for easy placement. The unit can also be powered by regular alternating current electricity, or power-over-Ethernet. The construction of the rooftop units is simple: a bucket with a rod held in place by concrete cured *in-situ*. The bottom-heavy pole mount is easily deployed. We deployed two such "Weather Pots" at Argonne by using Ethernet to power and collect their data. Figure 1 shows data from the temperature sensors from one day of operation. We also identified a region in Chicago, where we would like to deploy the next dozen units.

Proposed Work for FY 2015

In FY 2015, we will make our first large-scale deployment of our newly developed sensor platform. We will also begin modeling the urban weather of Chicago and compare predictions from the model with our observations.

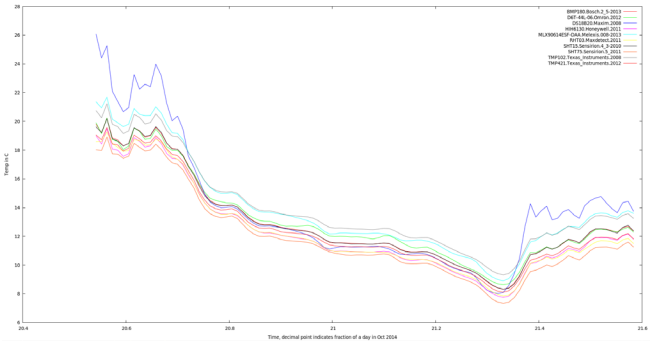

Figure 1. Temperature over 1 day from several temperature sensors includes the temperature recorded by a sensor network node deployed at Argonne on the roof of Building 240.

Advanced Pipeline for High-Throughput Digitization of Large-Scale Collections

2014-174-N0

Mark Hereld and Nicola Ferrier

Project Description

The technologies required to merge high-performance computing with real-world systems for high-throughput data collection and automated manufacturing are fast becoming usable. Integrating these technologies presents new challenges that must be met in order for us to routinely apply the technologies to new kinds of science and engineering problems. In this project, we are designing and building components for scalable automated workflows in the context of a particularly challenging domain for which we have a ready supply of world-class exemplar objects: digitization of the Field Museum of Natural History (FMNH) collection of pinned insects.

Mission Relevance

High-throughput science is increasingly important in many areas of basic science, and will have impacts in environmental and other areas of critical interest to DOE. The problems we are working on — high-speed digitization of streaming objects, physical object processing pipelines, and image and data analysis pipelines — are seen in high-throughput genomics, experiment and analysis handling at large facilities (including the Advanced Photon Source), and automated collection and analysis in the environmental sciences, and they can be anticipated in materials and nanoscience. As with the explosion of activity in metagenomics, such large-scale automated digitization will enable important new advances in science at the level of ecosystems and collections. The analysis methods and data handling to be developed will feed into Advanced Scientific Computing Research (ASCR) goals. Other agencies have significant interest in the analy-

sis, data handling, and automation aspects of the work: notably National Science Foundation CISE (Computer & Information Science & Engineering), National Institutes of Health, and National Science Foundation, where these methods might be applied to data pipelines relevant to the BRAIN (Brain Research through Advancing Innovative Neurotechnologies) initiative.

FY 2014 Results and Accomplishments

In our initial year, we made progress toward a design specification for our high-throughput collection system: developing specific criteria in terms of object flow rates, data acquisition rates, imaging resolution, and computational demands.

Our advances include tests performed and development of software. We designed a database and developed software to perform statistical analysis on the data. We performed experimental evaluation of cameras and optical configurations including light field cameras, mirror configurations of plenoptic cameras, and structured light. Computer vision tools to identify the drawers and individual unit trays were developed. These will be used to (1) automatically populate the database and assist us in analyzing collection statistics and (2) for future specimen handling and tracking in the pipeline (Figure 1). Software was implemented to identify specimen labels, and structured light was used to identify the plane for individual labels (Figure 2). This geometric information was used with images collected from multiple viewpoints to align, rectify, and combine the images to create a high-quality composite image that could be used in standard optical character recognition (OCR) packages to obtain the label text information.

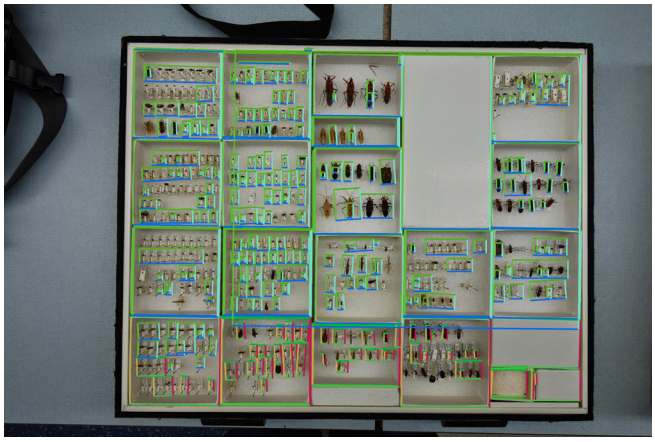

Figure 1. Example output from our automated identification of drawer and unit trays from images.

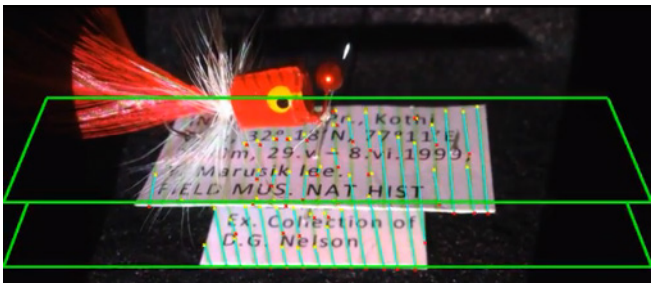

Figure 2. Example of identifying specimen labels and the three-dimensional plane for each label using structured light (array of projected lines shown in blue).

Proposed Work for FY 2015

Our goal for FY 2015 is to build a functioning test model of an advanced multi-sensor head for high-throughput object inspection and capture. Along with the test model, we will begin development of a workflow for automated generation of image object database by using data collected by the multi-sensor head. Experimental evaluation of methods for obtaining three-dimensional data will be performed. This will enable the system to collect more sophisticated specimen data but will introduce challenges for data management and throughput. In the longer term, we plan to develop a fully integrated pipeline with methods for object handling and fault detection that can handle millions of objects.

PARIS: Data Knowledge-Based Extreme-Scale Resilience

2014-181-N0

Franck Cappello

Project Description

As the number of components and the projected use of aggressive power-saving technologies increase, future extreme-scale computational systems will be less reliable than existing systems because of faults from internal or external causes. The high-performance computing community has recognized this “exascale resilience challenge” and is exploring solutions to make numerical science applications provide correct results.

This project, referred to as PARIS, explores fundamental properties of numerical science applications to improve the resilience of extreme-scale executions and to provide efficient solutions to system failures and silent data corruptions (SDCs).

Objects and phenomena studied by using time-dependent numerical simulations and data analytics have important characteristics that are reflected in the data dynamics and data semantics and that could be leveraged to discover

new resilience techniques. Data dynamics refers to the steps of the data transformation applied during execution by the computational/analytical patterns of the application. Successive transformations of data could be represented by a trajectory that could be modeled, analyzed, and monitored. Data semantics considers the meaning of the data, as well as the correlation between data. Numerical science applications data are linked and should stay consistent during execution with the analyzed object or phenomena. We seek to leverage the data dynamics and data semantics to devise new SDC detection, data compression, and self-healing techniques.

Mission Relevance

Extracting knowledge from large-scale numerical simulations and data analytics is key to the DOE mission. System failures, especially SDCs, are severe threats to producing timely and accurate DOE mission-critical results. PARIS will provide a way to detect SDCs, reducing the risk of corrupted results. Use of self-healing algorithms will also help avoid costly rollback recoveries. Application programmers will be able to leverage PARIS mechanisms to reduce development effort for dealing with SDCs. We will provide mechanisms for cosmology (HACC [Hardware/Hybrid Accelerated Cosmology Code]), climate (Accelerated Climate Model for Energy [ACME]), and reactor (Nek5000) simulation codes.

FY 2014 Results and Accomplishments

We formulated SDC detection as a time-series prediction problem. At each time-step, our detector dynamically predicts the possible range for each next-step data value of the application, based on recent time-series data. The detector considers a value an outlier if it falls outside this range. We compared popular trajectory modeling and prediction methods and proposed a new method that requires less memory and has better detection performance: it can detect 75% of injected SDCs in HACC with a very small false-alarm rate. From application datasets, we extracted spatial properties, such as bounded range of values, low-proximity variations, and partial low entropy. Detection based only on spatial properties can detect over 50% of SDCs with negligible overhead. We also explored the use of data semantics, such as variable correlation, to improve detection and reduce memory consumption and detection complexity. We observed that, in HACC, SDCs in velocity can be detected using position. Thus, by using the correlation between variables, we can reduce the number of variables to track and hence reduce the memory footprint of the detection method.

We also proposed a masking technique that partially decreases the entropy of scientific datasets. Our approach shows up to 15% improvement in compression ratio while reducing compression time by 50%.

Proposed Work for FY 2015

We will integrate spatial and temporal data analytics and combine them with data semantics analytics to improve SDC detection. Our objective is to reach a detection capability close to classic detection methods with a much lower resource overhead. We will also collaborate with NCAR (National Center for Atmospheric Research) researchers to evaluate the benefits of our new compression algorithm for climate data.

Dynamic Data Mirroring for Data-Intensive Science

2014-182-N0

Ian T. Foster and Steven Tuecke

Project Description

In this project, we are conducting research and development (R&D) aimed at enabling flexible, high-speed use of diverse computing and storage resources within a laboratory or multi-laboratory system generating and evaluating science data. A key aim is to address the need for multiple views of the same data via what we call *dynamic data mirroring*. In brief, the idea is that if multiple incompatible views of the same data are required at the same time (e.g., cloud storage for long-term storage and web-based sharing of the complete data set, laptop access for ad-hoc interactions with portions of the data, supercomputer file systems for high-performance analysis), then multiple copies of (portions of) that data are created and kept synchronized so that, in our example, one user browses shared dataset via a browser, another views and edits portions from their laptop, while another applies high-performance analysis procedures, and the like. The need for mirroring is determined via either explicit user requests (e.g., "make this directory available for supercomputer access") or by automated policies driven, for example, by user access patterns. In either case, automation of the mirroring process allows it to be performed behind the scenes, without user involvement; thus, we expect to reduce user effort, facilitate the use of high-performance platforms, and avoid the confusion and errors that inevitably result when data mirroring is managed manually.

Our project involves the design and evaluation of a set of novel data mirroring approaches. Using existing Globus services, General Parallel File System (GPFS), and Hadoop Distributed File System (HDFS) software, we will assemble a highly instrumented, end-to-end software system that supports mirroring among Globus-managed storage services, GPFS-based supercomputers (for high-performance analysis), and HDFS clusters (for MapReduce computations). We will then work with big data projects at

Argonne to evaluate and demonstrate the effectiveness of the proposed approach.

Mission Relevance

The project is relevant to DOE's mission in science. Large-scale data management is increasingly important to DOE mission goals, particularly in the Office of Science and across the DOE complex of supercomputing resources and other facilities, because of rapidly growing data volumes generated both by instruments and via simulations.

FY 2014 Results and Accomplishments

We established the Petrel high-performance research data storage system, working in concert with colleagues at Argonne's Advanced Leadership Computing Facility (ALCF). This system integrates >1-PB storage based on repurposed disks from the Intrepid supercomputer, high-speed network connections to other Argonne facilities, the GPFS file system, Globus data transfer and sharing services, and account and allocation management capabilities. We worked with diverse groups across Argonne, in particular from the Advanced Photon Source, to integrate Petrel into their workflows. We also worked to optimize data movement between Petrel and other Argonne storage systems as a first step toward high-speed data mirroring. Figure 1 shows elements of the resulting system.

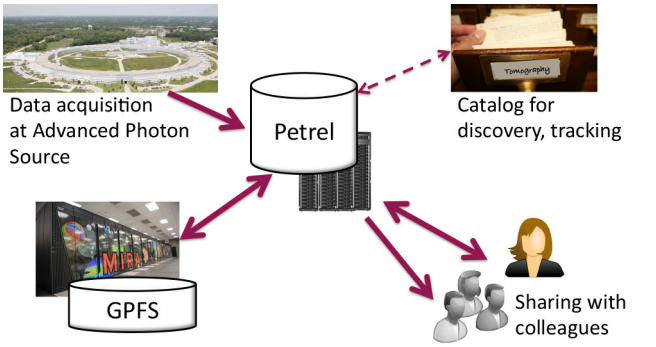

Figure 1. Elements of the dynamic data mirroring test system showing the Petrel data service and associated data flows, including upload of data collected at Advanced Photon Source beamlines; recording of associated file names and metadata in a Catalog; mirroring of data to the ALCF's IBM Blue Gene/Q Mira supercomputer for analysis; and sharing of results with colleagues.

We also worked with colleagues at the National Center for Supercomputing Applications (NCSA) to establish a test of a materials data facility that uses Petrel storage to support the storage and publication of large materials data sets. Through this effort, we demonstrated the ability to publish data and associated metadata.

In another project initiative, we experimented with the use of the Data Management Application Programming Interface (DMAPI) that is implemented within GPFS and other file systems to enable automated data mirroring based on update detection. We use DMAPI to detect changes and then use notifications of changes to drive data mirroring operations.

Finally, we incorporated Petrel and related technologies into several of the "BES Data Pilots" presented by a multi-laboratory team of researchers in November at SC14, the supercomputing meeting sponsored annually by The International Conference for High Performance Computing, Networking, Storage, and Analysis. These Pilots, each of which demonstrated how advanced computing can benefit Basic Energy Sciences research in some way, used the Petrel system to store and mirror data from a range of DOE experimental facilities.

Proposed Work for FY 2015

We will implement dynamic data mirroring for GPFS and HDFS and evaluate its use with real science applications. We then plan to build on these developments to explore on-demand computing using both GPFS and HDFS clusters.

LDRD

Applied Energy and Sustainable Transportation

ANNUAL REPORT

2014

20-kV/10-A 4H-SiC Vertical Trench Field-Controlled Thyristor (VTFCT)

2012-208-R2

Krishna Shenai

Project Description

This project focuses on the development of a 20-kV/10-A silicon carbide (SiC) vertical trench field-controlled thyristor (VTFCT) using a junction gate field-effect transistor. This device would have applications in electric vehicles and utility grids. The trench-based design has a small pitch (~2 µm) and allows control of the potential barrier in the channel, which enables a high blocking gain (>500) and device operation at very high temperatures (>200°C) with low leakage currents. The SiC field-controlled thyristor (FCT) was chosen over a metal-oxide-semiconductor based device to mitigate concerns about gate oxide reliability and threshold voltage instabilities. Additionally, the FCT is not a regenerative device; thus, ratings for large changes in current (di/dt) and voltage (dv/dt) are not required for transportation and utility-scale grid applications. This VTFCT represents a 5 to 10 times performance improvement over current Si technology. Performance and reliability of operation will be quantified. Specifically, techniques were developed to quantify performance, and tests at the Advanced Photon Source (APS) were used to evaluate the device under stress.

Mission Relevance

This project is related to DOE's mission in energy security. The proposed 20-kV/10-A gate-controlled SiC thyristor would have a transformational impact on next-generation power semiconductor materials and devices, as well as on power electronics. The device could be used for applications in next-generation hybrid and all-electric transportation systems and stand-alone electrical power sources. Furthermore, it could be integrated into a conventional alternating current electrical grid as well as in direct current micro grids. This new technology would benefit advanced power semiconductor devices and power electronic converters, and it would be used in integrating sensor networks and wireless technology. DOE considers wide-bandgap semiconductor materials to be a "keystone" technology in the following areas: switches, non-laser diodes, laser diodes, solar cells, converters, communications, and light-emitting diodes.

FY 2014 Results and Accomplishments

Commercial 600 V, 650 V, 1200 V and 1700 V 4H-SiC Junction Barrier Schottky (JBS) power diodes rated up to 30 A, and commercial 1200 V 4H-SiC power MOSFETs rated up to 200 A were successfully tested from room temperatures up to 250°C using Agilent B1505A test equipment to determine their detailed current (I-V) and capacitance (C-V) characteristics. Key static device parameters were extracted from the measurements and measured data was compared with detailed two-dimensional (2-D) device simulations. Large variations in static device parameters were observed when more than 100 packaged commercial devices of each rating were tested. A simple and accurate reverse engineering methodology was developed to extract the drift-region parameters. It was conclusively shown that all commercial 4H-SiC power devices are rated for punch-through leakage current and not for avalanche breakdown. The measured diode specific on-resistance plotted in Figure 1 clearly shows that there is significant opportunity for further on-resistance reduction provided that crystal defect density in the semiconductor is significantly reduced from its current value in the state-of-the-art material. Devices with voltage ratings that are higher than 1.7 kV were not commercially available, and hence, were not characterized.

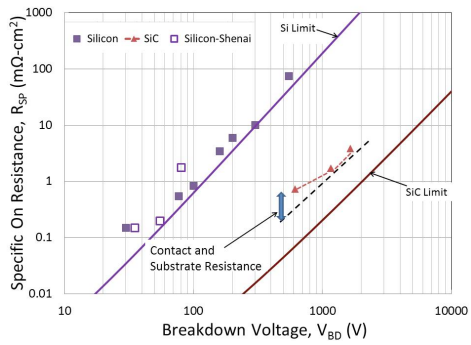

Figure 1. Specific on-resistance vs. breakdown voltage for silicon and 4H-SiC majority carrier devices. The measured on-resistance is significantly higher than the theoretical minimum.

Because of discrepancies found between the product data sheet values and the measured data of static parameters for commercial devices, the switching performance of 4H-SiC power devices under resistive switching were evaluated. The measured and simulated power losses matched reasonably well (Figure 2). The agreement with the product data sheet values was also reasonable.

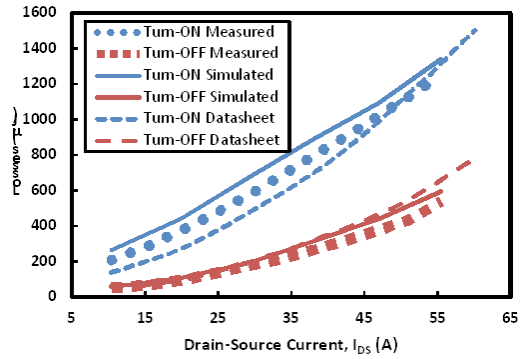

Figure 2. Comparison of simulated and measured switching losses for commercial 1200 V/50 A 4H-SiC power MOSFET.

Electrical and thermal material parameters were incorporated into two-dimensional (2-D) electro-thermal mixed device-circuit simulation tools from Silvaco and validated simulations with measurements performed on high-voltage 4H-SiC power diodes and transistors. Silvaco's 2-D device simulation tool, ATLAS, was updated to include the most accurate material parameters for both SiC and gallium nitride (GaN) semiconductors. Extensive simulations of power diodes and power MOSFETs were performed. Figure 3 illustrates electric field and potential distributions obtained from 2-D simulations of optimized 2.5 kV GaN merged-pin Schottky (MPS) diode structures, where the anode metal is extended beyond the active junction and used as a field plate to reduce electric field crowding. The field-plate length, junction termination extension length, p^+ region thickness, and mesa depth were adjusted to optimize the on-state and reverse blocking characteristics for a specified diode breakdown voltage along with drift- and buffer-region parameters. The results indicate that the breakdown occurs at the trench bottom corner of the mesa oxide interface. Further design optimization is feasible to cause the avalanche breakdown voltage to occur in the diode bulk.

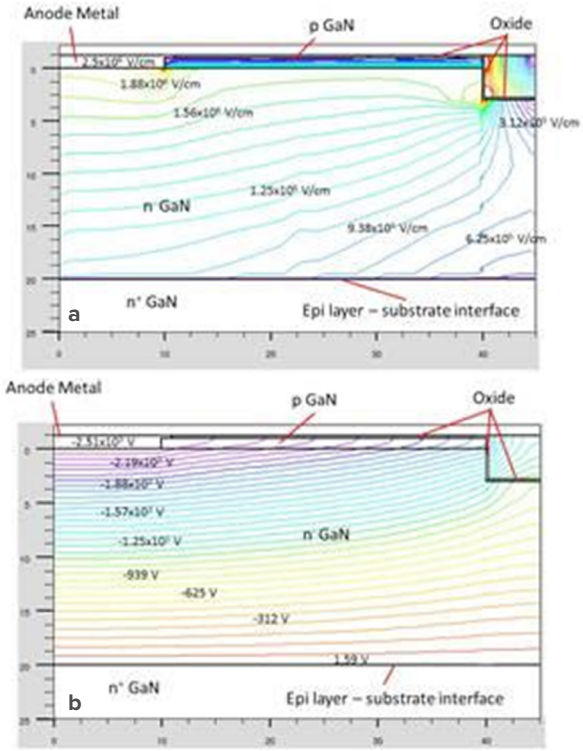

Figure 3. (a) Electric field and (b) potential distributions at avalanche breakdown for 2.5 kV GaN power diode designs optimized using 2-D simulations.

An experiment was designed to image the 4H-SiC power diode using synchrotron white beam x-ray tomography (SWBXT) while it is reverse-biased in the single event burnout (SEB) stress test circuit shown in Figure 4. By monitoring the diode under the electrical stress *in situ* by SWBXT, micro-plasma generation and local "hot spot" formation in the vicinity of defect sites can be investigated in real-time. The SWBXT in the back reflection geometry is particularly suitable for imaging threading screw dislocations (TSDs) and micropipes in SiC which are primarily responsible for device performance degradation and failure. In the experiment, the slit-limited synchrotron white beam x-ray radiation at 1-BM-B white beam station at the APS was used. This beam is incident directly on the diode material installed in the SEB test circuit and the back reflected beam from the (0001) basal planes is recorded on a high resolution x-ray film placed on the same side as the incident beam. Device leakage current I_L is sampled and monitored as the diode is stressed while it is simultaneously imaged in the synchrotron beam. The diode was subjected to increasing reverse voltage stress starting at the rated 600 V and SWBXT images were recorded at 100 V intervals until the diode exhibited breakdown. Under normal diode operation, the back reflection topograph (Figure 5) shows contrast from TSDs in addition to phase contrast effects from contact leads. Immediately prior to increased leakage current at 900 V as measured by the sensing and signal processing circuitry, an excited TSD below the contact lead exhibited higher strains than normal. This phenomenon suggests that increased leakage current was caused by charge generation in the vicinity of excited TSD in a region which is favorable to current filamentation. A higher local electric field in the vicinity of the semiconductor-metal contact interface and the proximity of the TSD to the contact lead makes it more vulnerable to excitation, and thus, to contributing to higher leakage current at a lower voltage than if the defect were not present. TSDs away from this region did not exhibit any change in strain levels. The diode breakdown was not initiated in the edge termination region suggesting good integrity of the diode edge termination design. On the other hand, when the de-capped silicon power diode with the identical voltage and current rating was subjected to the same experiment, the silicon diode also exhibited breakdown at 700 V, but the crystal simply suffers inhomogeneous deformation due to stressing limits of the material being reached. As there were no detectable defects present in the material being stressed, the merged P-i-N Schottky (MPS) silicon diode breakdown corresponded to the designed avalanche breakdown of 700 V.

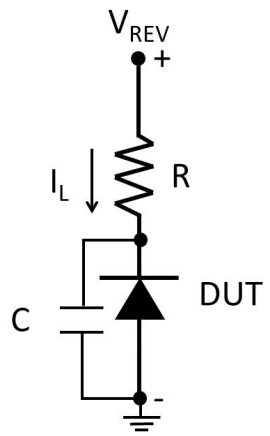

Figure 4. A schematic of the test circuit used for SEB stress evaluation where the DUT represents the 4H-SiC JBS power diode studied. The diode leakage current, I_L is monitored as the reverse bias voltage, V_{REV} is increased using advanced signal processing and data acquisition circuitry.

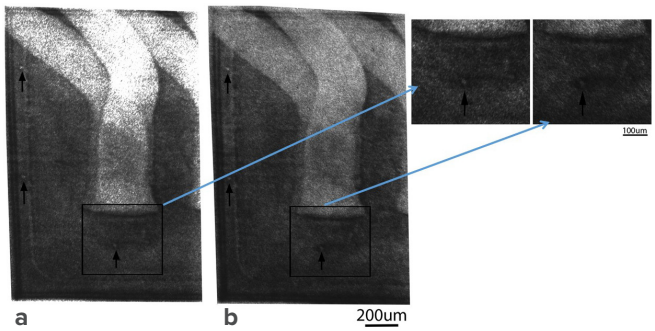

Figure 5. Back reflection topographs (g = 000 16) recorded from de-capped 4H-SiC JBS power diode at (a) 700 V showing contrast from TSDs as indicated by arrows; (b) 900 V showing enhanced contrast due to strains at 1 threading screw dislocation shown in enlarged inset. The white contrast features are due to the metal leads absorbing the x-ray beam.

Development of Predictive Multi-Dimensional Combustion Modeling Capability with Detailed Chemistry

2013-148-R1

Sibendu Som, Michael J. Davis, Marta Garcia Martinez, Douglas E. Longman, and Raghu Sivaramakrishnan

Project Description

Computational modeling of internal combustion engines (ICEs) is an arduous task, primarily because the length and time scales of the problem pose a variety of challenges. The predictive capability of modeling ICEs is significantly hampered by the inability of current spray and combustion models to capture the in-cylinder stochastics arising and evolving from the fuel spray injection and the interactions between fluid dynamics (turbulence) and the chemistry of fuel combustion. The main objective of our research is to address this issue by developing predictive multi-dimensional combustion modeling capability for engine applications. Achieving this objective involves developing high-fidelity large eddy simulation (LES) turbulence and turbulence-chemistry interaction (TCI) models, developing detailed chemistry of combustion for various engine fuels and additives with different reactivities together with global sensitivity analysis (GSA), and improving the scalability of sub-models and the CONVERGE tool together with performance optimization on Argonne's IBM Blue Gene/P and Q supercomputers (IBM BG/Q). The predictive ability of these robustly validated models will enable combustion engineers and scientists to better predict the combustion and emission characteristics of fuels with different reactivities.

Mission Relevance

This project is directly relevant to DOE's mission in energy; specifically, its vehicle technology mission of developing high-efficiency, low-emission vehicles. Our project supports this mission by developing predictive simulation capabilities for different processes occurring in an internal combustion engine. These simulation capabilities are then incorporated into software tools such as CONVERGE and extensively used by original equipment manufacturers (OEMs). The use of the CONVERGE tool in the current project facilitates the transfer of our model enhancements and development approach to OEMs, such as Cummins, Inc.; Caterpillar, Inc.; Chrysler, Inc.; General Motors; Ford Motor Company, and others. This work envisages developing a pathway for intelligent engine design with different fuels based primarily on computational tools aided by high-performance computing (HPC).

FY 2014 Results and Accomplishments

After the successful implementation of a first GSA study on an engine simulation in FY 2013, GSA was further extended to a constant-volume spray combustion chamber with well-characterized initial and boundary conditions documented on the Engine Combustion Network (ECN) website (http://www.sandia.gov/ecn/) in FY 2014. A list of 17 experimental initial and boundary conditions with uncertainty ranges were identified across five constant volume vessels around the world. In total, 120 three-dimensional (3D) simulations were performed for targets involving spray, combustion, and emission parameters. The sensitivity of different variables to liquid length, vapor penetration length, ignition delay, lift-off length, and soot emission targets of interest were identified. It can now be used to better standardize ECN test conditions, which further demonstrates the usefulness of the GSA technique developed by our group.

We implemented a flamelet-based approach called the multi-flamelet Representative Interactive Flamelet (mRIF) model to ECN Spray A (a single component fuel, n-dodec-

ane) in FY 2013. The results of the mRIF model were encouraging, compared to those of so-called well-mixed models, which do not account for the effect of turbulence chemistry interactions. We then extended the implementation of the mRIF model to multi-component fuels, n-dodecane and m-xylene, which contain an alkyl-benzene that represents an important chemical class present in diesel fuels. This study was conducted in FY 2014.

In FY 2014, we continued the development of the GSA for the engine simulations by testing it systematically with homogeneous auto-ignition. The GSA for the ongoing engine simulations was compared to the homogeneous ignition cases with a simple matching procedure developed previously. This allowed us to probe the chemistry directly in the engine by pointing to those conditions that led to the observed sensitivities in the engine simulations. We also collaborated with researchers at the Combustion Research Facility. Sandia National Laboratory to extend our quantum tunneling work to another chemical reaction: the abstraction of hydrogen by HO_2.

In FY 2014, tests were conducted in a twin-piston rapid compression machine (tpRCM) to acquire data for a variety of three- to five-component blends, where n-heptane, iso-octane, methyl cyclohexane, toluene, and 2-hexene were used to cover the normal-, iso- and cyclic-alkanes, aromatics, and olefins, respectively, found in commercial fuels. Comparisons were made to measurements by using a well-characterized gasoline (RON=94.4, MON=88.8), as well as to simulations by using a detailed gasoline surrogate chemical kinetic model.

In FY 2013, efforts were made to improve the performance of the CONVERGE solver on Argonne's supercomputer, Mira, an IBM BG/Q. First, input/output (I/O) performance on the BG/Q was optimized by having only a single message passing interface (MPI) rank-read restart data and broadcast it to all other ranks. This resulted in the simulations running over 20 times faster when restarting a typical case on 2048 cores. In FY 2014, MPI I/O was implemented to speed-up writing of restart files, and files for post processing, which resulted in an over 600 times speed-up improvement in these write operations on 2048 cores, bringing write times down from minutes to seconds. Another major achievement was the implementation of an improved algorithm for load balancing chemical kinetics calculations. In the original version of CONVERGE, the chemistry work was distributed on the basis of an attempt to equalize the number of computational fluid dynamics (CFD) cells being solved for chemistry by every MPI rank, which resulted in significant load imbalances, since the CFD cells in the domain have vastly differing computational penalties associated with chemical kinetics calculations, particularly during ignition. A novel scheme was proposed, wherein CFD cells were weighted by the computational effort associated with chemical kinetics. This scheme was incorporated by Convergent Science, Inc. (CSI), into the CONVERGE code and resulted in an over eight times improvement in load balance and a 3.4 times faster time to solution near ignition for a test case run on 2048 cores. With this improvement to load balancing, the CONVERGE code now scales with over 90% efficiency on 2048 processors, and with 80% efficiency on 4096 processors when the mesh size is around nine million cells.

Proposed Work for FY 2015

To effectively capture TCI effects, another advanced flamelet based model will be implemented, tested, and validated against experimental data available in literature. The TCI model results will also be compared against the results of a well-mixed combustion model that does not account for turbulence chemistry interactions per se.

GSA will be further applied to the chemical kinetics used for engine simulations for a speed-load condition simulated previously. The effect of different uncertainties on the chemical kinetics for an n-heptane mechanism on engine performance and emission characteristics of interest will be assessed.

We will begin implementing a new algorithm for reaction pathway analysis (RPA) that can interface with GSA and be applied to engine simulations. Our earlier attempts to compare GSA with RPA was not complete, as we showed that some reactions that lie along a pathway to a given species had large sensitivity coefficients and some did not, so we will adopt a more complete approach to RPA.

As the calculations grow in size and complexity, the use of leadership computing resources can play a vital role in the engine design process by significantly reducing the time scales to obtain and analyze scientific results. Nevertheless, in order to take advantage of the hundreds of thousands of cores available at the Argonne Leadership Computing Facility (ALCF), Mira (786,432 cores and ranked fifth in the world's top supercomputers), and their highly scalable torus network, ALCF expertise and support will be essential for detecting bottlenecks and improving the parallel performance of the CONVERGE tool. Efforts will be focused on improving load balance for the transport of species, as well as better memory management when using large meshes on the order of 200 million cells.

Seminars

Som, S. (2013). "Towards Predictive Simulations of the Internal Combustion Engine." University of Connecticut, Storr, CT, July 11, 2013.

Atomic Layer Deposition System for Continuous, High-Speed Thin-Film Processing

2013-154-R1

Joseph Libera, Jeffrey W. Elam, Anil Mane, and Angel Yanguas-Gil,

Project Description

Atomic layer deposition (ALD) is a thin-film coating technology that provides atomic-level control over thickness and composition and superb conformality over complex surfaces. Based on these attributes, ALD has been successfully integrated into the high-volume manufacturing of microelectronics. Furthermore, research at Argonne and elsewhere has demonstrated that ALD holds tremendous promise in applications far removed from microelectronics and could revolutionize nanomanufacturing in a broad range of energy technologies, including photovoltaics, solid-state lighting, lithium batteries, and catalyst manufacturing. However, a major barrier to the use of ALD technology in these applications is the need to speed up the throughput by 10–100 times and to transition from batch to continuous processing. To overcome this barrier, we developed a design that enables continuous, high-speed ALD; is compatible with roll-to-roll manufacturing; and runs at speeds of up to 100 times, in comparison to existing processes.

In this project, we will design and fabricate a bench-scale ALD tool to demonstrate this novel ALD technology. We will use computational fluid dynamics simulations to guide our design and base it on modifications of our existing equipment to conserve laboratory resources and expedite development. We will validate our design by depositing high-performance moisture barrier coatings and transparent conducting coatings on continuous rolls. Our work will focus on establishing the necessary results to support industrial and government investment that will carry this technology through pilot and production scales.

Successful deployment of our continuous ALD technology would revolutionize low-cost manufacturing in a wide range of energy technologies. A great deal of fundamental and applied research over the past two decades has demonstrated the superiority of ALD films for such applications as moisture barriers and transparent conductors. The major obstacle to industrial use of these films is the lack of scalable processes and equipment. The situation is analogous to the birth of the microelectronics industry, when the excellent semiconducting properties of silicon were understood but the manufacturing (lithography, polishing, deposition) had not yet been developed. Similarly, there is currently a deficit of useful tools and manufacturing processes for ALD films that are broadly accepted as having great technological promise.

Mission Relevance

The proposed project is tied to DOE's mission in energy security and environmental responsibility. Many clean energy industries are facing a common technological hurdle: the need for a continuous process to deposit precise, thin-film coatings at high rates that can be integrated into their existing manufacturing practice. For instance, high-performance moisture permeation barriers and robust transparent conducting (TC) layers could radically transform the manufacturing of photovoltaics, solid-state lighting, and electrochromic windows. In this project, we will develop a new ALD tool that will allow this ideal solution to be realized. Our continuous ALD approach will coat polymer films wound on rolls, as well as large area float-line glass suitable for immediate implementation in the energy industries. In addition, this continuous ALD technology will be suitable for moving powder beds to enable the deposition of protective coatings on lithium battery electrode materials and facilitate high-volume catalyst synthesis. Potential industries that will benefit from our technology include technical glass, solar glass, photovoltaics, transparent conducting oxides for flat panel displays, solid-state lighting, smart windows, lithium battery manufacturing, catalyst manufacturing.

FY 2014 Results and Accomplishments

Accomplishments made in FY 2013 include the following:

- Modifications to our research ALD reactor to enable high speed operation.
- First demonstration of our high speed technology.
- First trials of high speed deposition.
- Modeling of our high speed ALD using computational fluid dynamics.

Major accomplishments made in FY 2014 include the following:

- A high-speed virtual valve design was developed to overcome the limitation of reducing the purge times to very small values (which was causing nozzle tip CVD). The high-speed virtual valve design was implemented and tested by using commercial valves.
- Reactant cross-talk was eliminated by the high-speed virtual valve arrangement. This was first tried by using a single injector and then scaled up to a dual injector configuration. Successful depositions yielding an 8-in. wide deposition zone at 2 Hz were demonstrated. This process is suitable for roll-to-roll production.
- We discovered that local heating during static substrate tests results in non-uniform ALD growth when attempting high cycle rates above 2 Hz. Better

performance is expected when substrate translation is implemented such that the build-up of heat is avoided.
- The computational fluid dynamics (CFD) modelling was advanced to account for physical phenomena, including mass transfer, reactive sticking coefficients, and the temporal-spatial tracking of reactant and product concentrations.

Proposed Work for FY 2015

Major planned activities for FY 2015 include the following:

- The high-speed deposition design will be tried on several other ALD systems.
- Final design of production deposition systems will be completed by using both the advanced CFD capability, as well as empirical results.
- Deploy the optimized design in an existing roll-to-roll vacuum web coating machine.

Fast High-Efficiency Process to Fabricate Aligned Nanotubes in Nano-Composite Membranes for High-Performance Filtration Applications

2013-156-R1

Patricia Ignacio-de Leon, Xing Chen, and Meltem Urgun-Demirtas

Project Description

This project aims to develop and demonstrate a new and fast high-efficiency process for producing high-performance molecular transport layers on microporous supports to fabricate membrane nanofilters that will yield significant energy savings and have wide applicability to separation processes. Our goal is to eliminate the substantial performance gap between laboratory-scale and commercial membranes by developing processes that employ controllable force (e.g., magnetic fields) to manipulate responsive material phases or components to affect/direct nanostructure assembly. This technology would become the basis of a novel, high-throughput manufacturing process for producing nanostructured composite membranes useful for applications, such as water purification and desalination, nanofiltration, gas separation, and combined catalytic transformation of and separation of products from reactants.

In FY 2014, this project demonstrated (a) a scalable electrospinning production process to synthesize multimetallic nanotubes of controllable diameter and surface chemistry and (b) a dynamic process to embed perpendicularly oriented nanotubes into the permselective layer of a narrow-web nanofilter via magnetic alignment.

Mission Relevance

This project is related to two DOE mission areas: energy security and environmental quality. The benefits of the project include better membrane performance (greater permeation rate; equivalent or better rejection performance toward salts, pathogens, and pharmaceuticals); lower operating pressures; and reduced energy consumption, operation cost, and waste. Current reverse osmosis (RO) technology provides potable water by desalinating three main sources of input water: brackish inland waters, municipal wastewater and seawater. Combined worldwide desalination provides 13 billion gallons daily of potable water, yet meets less than 1% of the world's demand for water. The global market for RO membrane elements is forecast at $1.4B by 2015. However, given the improved economics offered by the proposed nanofiltration technology (30–50% less energy use, up to 10× higher flow, 90% less membrane area needed, one-third cost reduction), the water purification market is expected to expand beyond projections.

Commercial membrane filtration original equipment manufacturers (OEMs) that license the technology would realize near-term benefits. In the medium term, engineering, procurement, and construction companies and engineering consulting service providers that deploy this technology in their systems would benefit from this technology advance. In the long term, two-thirds of the world's population would have greater access to water for drinking, industry, and agriculture.

FY 2014 Results and Accomplishments

In FY 2013, a scalable, robust process to produce aligned Fe_2Co nanofibers was identified by performing a series of two-level Plackett-Burman design experiments to evaluate the significant nanotube processing parameters. The process employs vertically configured electrospinning electrodes under field-mediated deposition conditions. The fibers are then thermally treated to initiate nitrate salt oxidation and remove the polymer component in the as-spun fibers (~20 nm in diameter). A second thermal treatment under reducing conditions converts the metal oxide (hydrophilic) to a Fe_2Co (hydrophobic) magnetic nanotube (Figure 1). Fe_2Co has a high saturation magnetization and is relatively inert to oxidation and will be explored throughout the rest of the project. Magnetic alignment of Fe_2Co nanorods has also been demonstrated.

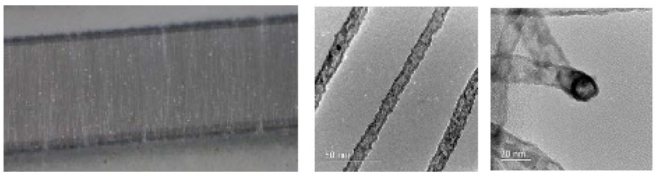

Figure 1. As-spun nanofibers containing polymer and inorganic salts (left) undergo thermal conversion into Fe_2Co nanotubes (middle and right).

Scalable Process to Fabricate Nanotubes of Controllable Diameter and Surface Chemistry. In FY 2014, the electrospinning electrodes were scaled from the vertical to the tubular configuration (both shown in Figure 2), thus increasing the production rate from 0.01 mg/day to 250 mg/day (a 25,000-fold increase). This new system is an automated, continuous process that integrates nanofiber production and the first thermal treatment. A prototype reactor was also built in a glove box to explore rapid thermal processing of the nanotubes in a well-controlled environment. Initial samples from the new configuration evidently formed nanotubes after the first heat treatment. Nanotubes of different diameters were also produced by changing the variables associated with the electrospinning process, such as the composition of the precursor solution containing the iron (Fe) and cobalt (Co) salts. We can create nanotubes of various lengths (<1 to ca. 7 μm) via sonication in a quick-drying solvent (such as ethanol) and by adjusting the power level (20–100 W at 30 kHz) and duration (10 s to 30 min) of sonication.

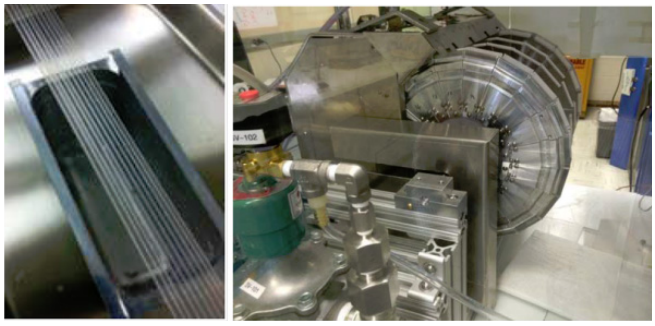

Figure 2. (Left) Vertical electrode configuration with field-mediated fiber deposition; (right) prototype system for integrated electrospinning and infrared (IR) heating with pneumatic fiber collection.

Dynamic Process to Magnetically Align Nanotubes Perpendicular to Permselective Layer of a Narrow-Web Nanofilter. Nanofibers were incorporated into a permselective layer of a composite membrane via encapsulation in a thin polymer onto a microporous support such as polyethersulfone (PES) or regenerated cellulose. The permselective layer consists of nanotubes that function as pores/nanochannels, embedded in a nonporous polyamide resulting from interfacial polymerization between a nonpolar phase (trimesoyl chloride dissolved in hexane) and a polar aqueous phase containing *m*-phenyldiamine. Magnetic nanotube orientation occurs during the interfacial polymerization upon application of an external magnetic field with lines perpendicular to the support. By optimizing the monomer concentrations, we achieved a continuous, uniform thin coverage of the polymer over the entire support (Figure 3).

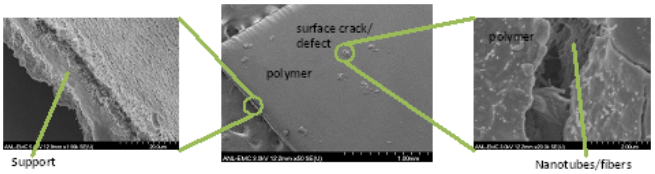

Figure 3. SEM images of a composite membrane comprised of nanofibers embedded in polyamide atop a PES support.

A dynamic web-coating system, consisting of a moving conveyor equipped with a drawdown bar (Figure 4), is also under construction. This system will allow us to scale composite membrane production from ca. 15 cm^2 at a time to >1200 cm^2 (a 100-fold increase) per batch using an automated system. A filtration test system was also fabricated to test the performance of the composite membranes in terms of flux and rejection of a target component in the feed stream.

Figure 4. Conveyor with a drawdown wire-wound bar for a web-coating system.

Proposed Work for FY 2015

In FY 2015, our research will focus on:

- Wide-web dynamic magnetic orientation of nanotubes in a permselective layer of a composite membrane to demonstrate process scalability, and
- Quantification and optimization of scaled membrane properties.

Through this research we will:

- Demonstrate scalable magnetic alignment of nanotubes in a permselective layer in a wide-web format, and
- Optimize process and membrane properties consistent with intended application.

Grid Level Energy Storage for Integration of Renewable Energy

2014-120-N0

Audun Botterud, Emil M. Constantinescu, Kevin Gallagher, Prakash Thimmapuram, and Canan Uckun

Project Description

We are developing advanced optimization and simulation methods to analyze the value of energy storage and improve our understanding of the role it can play in a future power grid with large shares of variable renewable resources. Energy storage is widely considered to be key for the large-scale expansion of renewable energy. However, most energy storage technologies are expensive and do not scale up to the magnitudes required for grid-level storage. To better understand the role of energy storage in the power grid, we are conducting a detailed analysis of the possible applications of such technologies in a power system dominated by variable renewable resources.

Toward this end, we are developing advanced methods for storage and grid operations based on stochastic programming, considering the uncertainty and variability in renewable resources, such as wind and solar power. We are also developing a detailed energy storage representation within an agent-based model of the electricity market. This comprehensive modeling framework enables us to analyze what type of and how much energy storage is needed and where it should be placed in the grid to enable high levels of renewable resources to be available. We are also investigating the profitability of different storage technologies and to what extent the investor's incentives are aligned with the benefits provided to the power system. The Argonne project team is collaborating with faculty from the University of Chicago.

Mission Relevance

The project is relevant to DOE's mission in energy. The project is leading to a set of novel algorithms for the advanced analysis of grid-level energy storage in the power system and improved technology assessments and cost-benefit analyses for energy storage. Grid-level energy storage is of key interest to DOE, which recently developed a department wide Grid Energy Storage Plan. The project clearly supports this plan as well as DOE's mission to ensure America's security and prosperity by addressing its energy, environmental, and nuclear challenges through transformative science and technology solutions. DOE's Offices of Electricity Delivery and Energy Reliability (OE) and Energy Efficiency and Renewable Energy (EERE) are both very interested in energy storage for the power grid and have relevant programs in this research area. Moreover, energy storage is receiving increasing levels of attention from the electric power industry, and our work is very relevant to developers of batteries and other energy storage technologies.

FY 2014 Results and Accomplishments

We established a comprehensive, multidisciplinary, analytical framework for analyzing energy storage with regard to the grid integration of renewable energy. It involves the characterization of renewable energy resources, representations of energy storage, and different approaches for modeling the planning and operation of the power grid (Figure 1). So far, we developed an initial approach based on numerical weather prediction (NWP) and Gaussian processes to characterize the renewable resource base. Scenarios for wind and solar generation were generated for selected locations in the Western United States. We also built a framework for characterizing various battery technologies, covering parameters such as investment and operating costs, lifetimes, roundtrip efficiencies, and response rates. In terms of power grid modeling, we developed a model that maximizes profit from energy arbitrage when there is uncertainty in electricity market prices for an independent storage owner. We also built a stochastic unit commitment model that minimizes the cost of operating the power grid; it accounts for the variabilities and uncertainties in wind and solar power and for contributions from energy storage toward balancing supply and demand in the grid. Initial testing on small-scale systems indicated cost savings from energy storage could be significant (Figure 2).

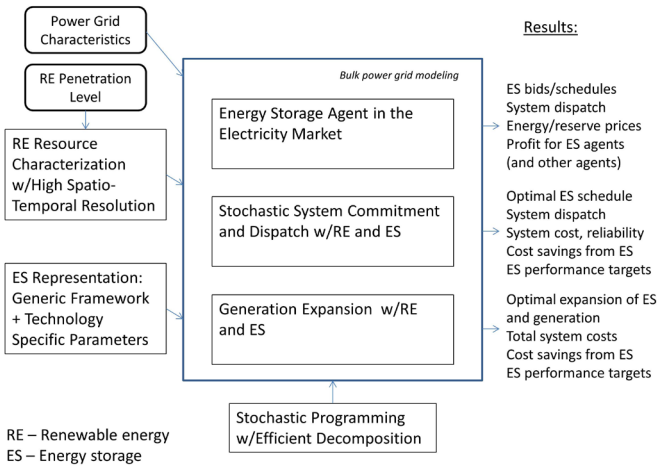

Figure 1. Analytical framework.

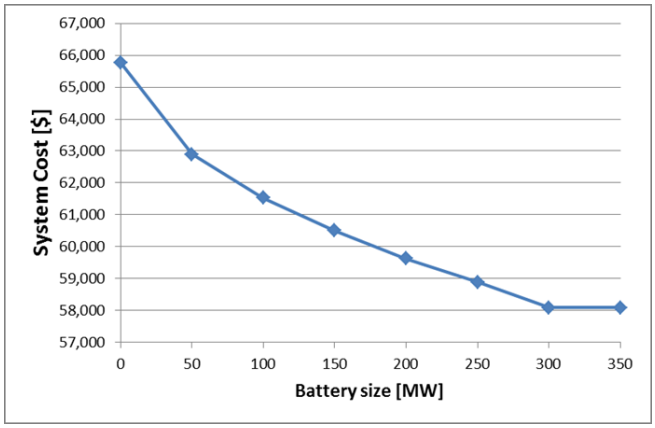

Figure 2. Operating cost with increasing energy storage capacity in six-bus power system.

Proposed Work for FY 2015

We plan to refine the different algorithms and scale up the power grid analysis to larger and more realistic power systems. We will also continue to integrate the different parts of the analytical framework, connecting the energy storage technology and renewable resource characterizations more closely to the power grid modeling. Moreover, we will calculate the maximum potential revenue for energy storage from historical prices in selected U.S. electricity markets, thereby estimating an upper bound on storage costs for the technology to break even under today's conditions. We also plan to develop a system expansion model to investigate the longer-term implications of energy storage on the optimal portfolio of power generation technologies.

Magneto-Dielectric Composite Substrates Comprised of High Aspect-Ratio Magnetic Nanofibers for Smart Antennas Operating at Microwave Frequency

2014-169-N0

Xing Chen

Project Description

We aim to develop and demonstrate a novel magneto-dielectric composite substrate based on high-aspect-ratio magnetic nanofibers for microwave frequency antennas. Materials with high μ (magnetic permeability) and matched ε (diaelectric permitivity), which may be tuned for specific antennas, are highly desirable in microwave communications and wireless/microwave power transmission because they may allow for antennas with smaller size, larger bandwidth, better impedance match, and higher efficiency. To obtain currently unavailable substrate materials with usable magnetic permeability and low loss at 1–10 GHz frequency, we use nanostructured composites that consist of high-aspect-ratio magnetic nanowires that are embedded in a dielectric matrix comprised of high dielectric constant nanoparticles dispersed in a flexible polymer; the high aspect ratio of the nanowires leads to high permeability because of the magnetic shape anisotropy, and the density of dielectric nanoparticles controls the effective dielectric permittivity of the composite.

Mission Relevance

This work is aligned with DOE's mission in advanced manufacturing of applied energy materials. New antenna technology will enable cutting-edge devices for cellular communication and wireless power transmission. Smart antenna had a global market of $13.5 billion in 2012 and is expected to grow significantly (+50%) by 2018. Successful development of this program will deliver substrate material that benefits smart antenna properties, cost, and functionality and will attract great interest in this field.

The Department of Defense (DoD), Advanced Research Project Agency-Energy (ARPA-E), and Defense Advanced Research Projects Agency (DARPA) are federal agencies interested in these targeted applications. The U.S. military is experimenting with smart antenna technology to reduce power consumption on high-speed multimedia battlefield networks. ARPA-E had a program designed to put together a "battlefield situation awareness" network by combining smart antennas with existing commercial technology.

FY 2014 Results and Accomplishments

In FY 2014, we prepared magnetic ferrite nanowires of various sizes and compositions. We are establishing an automated, scalable, and robust process of fabricating magnetic nanowires, which covers the three main stages of nanofiber production. As shown in Figures 1a and 1b, cobalt-ferrite ($CoFe_2O_4$) nanowires with a diameter of approximately 30 nm were obtained in our initial integrated fabrication system; nickel-ferrite ($NiFe_2O_4$) nanowires with a diameter of approximately 20 nm were obtained in a conventional electrospinning system. Magnetic nanofibers with appropriate diameter (approximately 20–30 nm), small grain size, and low roughness are ideal for the project. Direct current magnetic properties were measured by using PPMS (Physical Property Measurement System). The ferrite nanowires demonstrate good direct current magnetic properties for soft magnetic material, providing a solid material foundation for antenna projects.

In FY 2014, nanowires were integrated into thin films by using a drawdown process. Nanowires, dielectric $BaSrTiO_3$ nanoparticles, and polymer are mixed into water-based solvent. A well-established magnetic/dielectric film with clean interface was obtained and examined by using scanning electron microscopy. Figure 1c shows the surface and cross-section view of nanowires composite film; nanowires are imbedded in a polymer matrix, and the thickness of film is ~20 um. The radiofrequency and microwave properties of $CoFe_2O_4$ nanowires were measured by a vector network analyzer using a resonance cavity; they showed good permeability values and a low loss at frequencies up to 5.5 GHz. The saturation magnetization is expected to be much stronger for metal nanowires, compared with ferrite nanowires, which would result in a much larger permeability proportional to saturation magnetization. Magnetic permeability helps reduce device size while maintaining the microwave bandwidth of the device. It also helps to match the impedance of the device to air. Magnetic permeability is the central focus of this project — no useable magnetic permeability was available in this frequency range in prior work at device level.

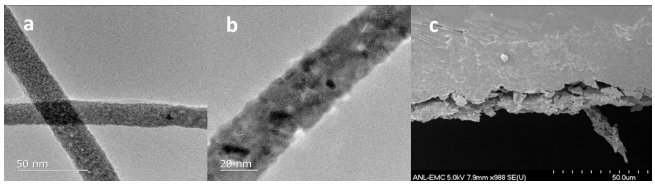

Figure 1. (a) Co-ferrite (~30 nm) nanofibers prepared by new integrated electrospinning system; (b) $NiFe_2O_4$ (~20 nm) nanofibers prepared by legacy electrospinning system; (c) SEM images of magnetic nanowire/dielectric thin film by drawdown process.

This work resulted in the following inventions:

Chen, X. and Z. Zhou. "Tunable Broadband Microwave Absorber." Invention report disclosed October 2014. [ANL-IN-14-097].

Chen, X. and Z. Zhou. "RF Energy Harvesting with Magnetodielectric Composite Substrate." Invention report disclosed October 2014. [ANL-IN-14-098].

Chen, X., Z. Zhou, G. Grocke, and V. Vajda. "Integrated System for High Aspect Ratio Nanofiber Production." Invention report disclosed November 2014. [ANL-IN-14-109].

Proposed Work for FY 2015

In FY 2015, we will optimize the soft magnetic properties to reduce the coercivity field further and decrease the hysteresis loss. Metallic nanofibers with higher saturation magnetization will also be explored. Materials loss, including dielectric, eddy current and magnetic losses, will be measured and analyzed. In particular, eddy current loss will be monitored closely; this will determine whether an insulating coating of the metallic fibers is needed. If so, the atomic layer deposition method will be used to apply a uniform coating to these metallic fibers. Materials integration will also be explored using the draw-down method. The integrated nanofiber-containing composite material will be tested for microwave properties.

LDRD

Biological and Environmental Systems

ANNUAL REPORT

2014

Knowledge Discovery in Microbial Community Composition and Metabolite Turnover Using Satellite Remote Sensing Data

2012-016-R2

Jack A. Gilbert and Peter Larsen

Project Description

The molecular characterization of a microbial community's structure is essential for exploring the life-support system of planet Earth. In the past 5 years, the application of direct sequencing of genetic information from environmental samples has revolutionized our understanding of microbial dynamics and, more importantly, of the functional metabolic pathways that mediate the recycling and transformation of all inorganic and organic compounds in every ecosystem.

In the field of metagenomics (i.e., the sequencing of DNA extracted from every organism in a community at once), we are developing several products that will revolutionize the exploration of the microbial function and that are directly relevant to understanding microbially mediated remediation, carbon turnover, and the potential for microbial biofuel production. We have used metagenomic data collected from the surface waters of oceanic provinces and terrestrial soil sites across Europe and America to develop two techniques: predictive relative metabolic turnover (PRMT) and microbial assemblage prediction (MAP). The techniques use environmental information to predict the consortia of microbial species present and the functional capacity of turnover metabolites (e.g., lipids, carbon dioxide, pollutants). The environmental parameters can be obtained from satellite remote sensing data. By defining the relationships between the parameters and the microbial dynamics, researchers can extrapolate a community's composition and metabolite turnover through space and time.

Although the tools and prediction methods are currently the most sophisticated in the field, they require further development to reach their full potential. The prediction process could be taken to a new level of scientific discovery by leveraging the high-performance computing resources at Argonne, designing and implementing advanced mathematical inference and knowledge discovery tools, and applying the tools to experimental data. The goal of this project is to develop global microbial weather maps that can forecast and hindcast microbial activity, which will serve to focus our search for relevant microbial biochemistry. Our techniques now enable the prediction of thousands of metabolites in a single system; we want to increase that capability to predicting tens of thousands of metabolites in thousands to millions of systems over hundreds of time points. The calculations required to do this require the use of high-performance computing.

The questions we want to answer are an integral part of the microbiology challenge for current specialists, and addressing these problems at different scales of resolution requires exascale computation.

Mission Relevance

The project is relevant to DOE missions in science and the environment. DOE scientists can use the predictions of surface-level communities to identify areas where microbial consortia capable of specific activities (e.g., those associated with remediation) exist. Another DOE area of interest is exploring microbial dynamics in tundra ecosystems and refining the regional- and local-scale predictions of carbon turnover associated with surface microbial communities. The use of the tools has been recognized by the DOE Office of Biological and Environmental Research (BER) as having the potential to help focus research efforts by highlighting areas with a high probability of error in these models. These areas could be subject to further research or site-directed research (e.g., DOE's Next Generation Ecosystem Experiment or NGEE).

FY 2014 Results and Accomplishments

In FY 2012, we researched a number of options for representation of biological data in mathematical models, and developed and partially tested mathematical tools for improved prediction on microbial abundances datasets of large magnitude and dimension. We also developed tools and practices that are sufficient to achieve proof of concept for problems with hundreds of variables.

In FY 2013, we explored the implementation of MAP/PRMT for an increasingly high-throughput framework and were working to improve the accuracy of predictions and the ability of the tools to handle larger datasets. However, we were unable to significantly improve on the existing characterization. While we did explore the potential to extrapolate these observations to global scale systems, we reduced our ambitions and focused on continental scale extrapolations.

In FY 2014, we completed the program of software development. Due to budget restrictions, we could not progress the development of the software any further. The tool was therefore made available through publication. The MAP/PRMT protocol was applied to a large-scale marine dataset to create a prediction matrix from satellite data to microbial community structure and final metabolite turnover potential. We also applied the neural network Bayesian tools developed here to a number of other datasets.

Tool development will continue with resources from Exxon and the Alfred P. Sloan Foundation.

Carbon Flux from Thawing Permafrost: Development of a Predictive Model Linking Microbial Activity and Biogeochemistry with Carbon Metabolism

2012-074-R2

Julie Jastrow, Dionysios A. Antonopoulos, Jack A. Gilbert, Kenneth M. Kemner, Roser Matamala, R. Michael Miller, and Edward J. O'Loughlin

Project Description

The potential impact of warming in permafrost regions is a source of uncertainty in climate model predictions. Current global models predict the terrestrial source/sink dynamics of greenhouse gases on the basis of vegetative growth responses to environmental forcing factors, assuming that changes in the amount of organic carbon stored in soils can be predicted by these responses. This approach works reasonably well for temperate and tropical ecosystems but not for permafrost regions. This project seeks to link biogeochemical constraints on microbially mediated carbon metabolism as a means for predicting decomposition processes in permafrost regions. The objectives are to (1) develop and test a laboratory microcosm system for evaluating the impact of key environmental drivers on microbially mediated carbon decomposition rates in permafrost-affected soils and (2) generate multidisciplinary data needed to assess the potential for developing biogeochemical system-level models capable of predicting carbon fluxes caused by changing environmental drivers in permafrost regions.

Mission Relevance

This project is relevant to DOE's missions in basic science and the environment. A primary goal of DOE's environmental mission, and the basic science that supports it, is to develop a predictive understanding of the Earth's climate and environmental systems, which is needed to make informed decisions on energy use and production. Soils of the northern circumpolar region store one of the planet's largest reserves of carbon. Warming is expected to increase microbial activity, decompose perennially frozen organic deposits into carbon dioxide (CO_2) and methane (CH_4), and return carbon sequestered for tens of thousands of years to the global carbon cycle. The amount and rate of release of these greenhouse gases from thawing permafrost and the extent to which their release will accelerate climatic change are largely unknown.

FY 2014 Results and Accomplishments

In FY 2012, we assembled the infrastructure required for working with frozen soils and built a system for incubating soil microcosms at precise low temperatures. We characterized bulk samples of the seasonally thawed active-layer organic and mineral horizons and upper permafrost of soils from four sites representing different arctic tundra ecoregions. In FY 2013, we developed a method for manipulating drainage conditions to enable comparisons of soils with widely differing moisture and ice contents. From FY 2013 through FY 2014, five drained replicates of each soil type (4 sites × 3 soil layers) were incubated at -1, 1, 4, 8, and 16°C (300 total incubations).

On average across all sites, the cumulative CO_2 release increased as temperature increased, and this response was remarkably greater for surface organic horizons than for the mineral portion of the active layer (Figure 1a). The upper permafrost layer, which includes highly organic material mixed by frost churning (cryoturbation) into mineral soil, exhibited an intermediate response. Crossing the freezing threshold increased the amount of CO_2 released, after which the cumulative CO_2 flux remained constant until a second response threshold was crossed between 4°C and 8°C. Overall, the cumulative CO_2 release was strongly influenced by the amount of organic carbon in each soil type, particularly the amounts of carbon in the water-extractable and lightly-decomposed particulate organic matter fractions.

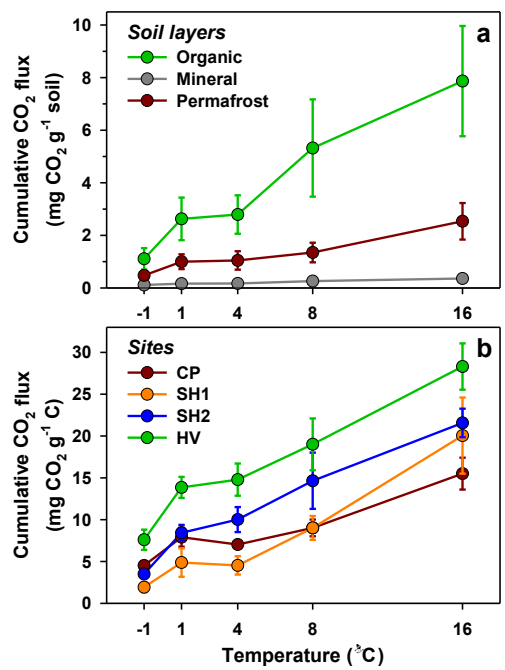

Figure 1. Effect of temperature on the cumulative release of CO_2 during 60-day incubations of soils from four sites in a latitudinal gradient across the North Slope of Alaska. (a) Amount of CO_2 released on a soil mass basis (averaged across sites) from the (1) surface organic horizon of the seasonally thawed active layer, (2) mineral horizon of the active layer, and (3) mixed (cryoturbated) organic and mineral horizons of the upper permafrost. (b) Amount of CO_2 released from the upper permafrost layer of each site normalized on the basis of soil organic carbon concentration. Site key: CP = Coastal Plain Low-Centered Polygon; SH1 = Sagwon Hills Frost Boil; SH2 = Sagwon Hills High-Centered Polygon; HV = Happy Valley Frost Boil.

The three soil layers also differed in the chemical composition (i.e., quality) of their constituent organic matter and in the conditions influencing microbial access to organic substrates, thus making it more informative to independently examine the responses of each layer. We focused on the permafrost layer, because the impact of global warming on the release of carbon that has been stabilized for hundreds to thousands of years by perennially frozen conditions is of greatest concern. To investigate how organic matter quality affects decomposition rates, we compared CO_2 releases among permafrost soils from the four sites after normalizing for variations in permafrost organic carbon content (Figure 1b). The cumulative CO_2 release at all incubation temperatures was directly related to the relative amount of water-extractable carbon, with the strongest correlations ($r > 0.92$) occurring below 4°C. Above 4°C, the CO_2 release was more strongly related ($r > 0.95$) to soil organic matter quality, as assessed by infrared spectroscopy. Specifically, the CO_2 release was greater for sites where the relative intensity of key spectral indicators suggested soil organic matter was fresher and less decomposed before its incorporation into permafrost.

The effect of incubation temperature on the structure of the permafrost microbial community followed two distinct patterns (Figure 2) that were related to the availability of labile substrates. Proteobacteria (which typically respond rapidly when labile substrates become available) proliferated and displaced other phyla at incubation temperatures above freezing for permafrost soils from the two sites (Happy Valley Frost Boil and Sagwon Hills High-Centered Polygon) with overall greater CO_2 release (Figure 1b). In contrast, in the incubations of permafrost soils from the two sites (Coastal Plain Low-Centered Polygon and Sagwon Hills Frost Boil) with lower-quality soil organic matter and less water-extractable carbon, warming had little effect on the structure of the microbial community, and decomposition generally proceeded at a slower rate. These findings suggest that substrate quality and availability are likely to be major drivers of initial responses by the microbial community to permafrost thawing.

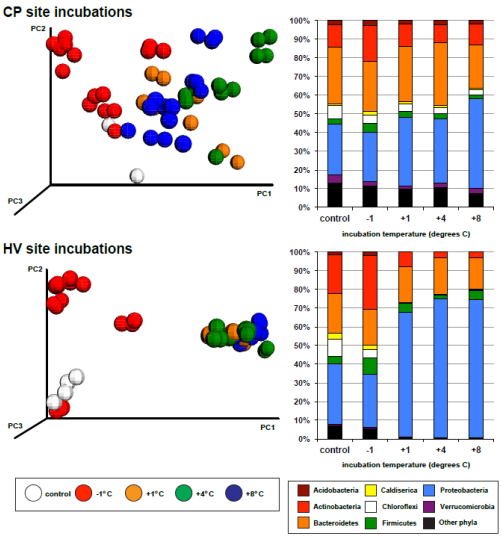

Figure 2. Effect of warming on the structure of microbial communities after 60-day laboratory incubations of upper permafrost soils. The ordination for the Happy Valley Frost Boil (HV) site shows distinctly different community structures for temperatures above and below freezing (controls indicate microbial community structure before incubation); a similar response was seen for the Sagwon Hills High-Centered Polygon site (data not shown). In contrast, the microbial community structure of upper permafrost soil from the Coastal Plain Low-Centered Polygon (CP) site (and also the Sagwon Hills Frost Boil site; data not shown) was not greatly altered by warming. The microbial community was evaluated by sequencing inventories of the organisms present after incubation by using a broadly occurring gene marker (encoding 16S rRNA) and the Illumina MiSeq at Argonne's Next Generation Sequencing Core.

Modeling the Interactions of Biophysical, Biogeochemical, and Microbial Dynamics in Permafrost-Affected Soils: From Pore Scale to Regional Scale

2012-205-R2

Zhaosheng Fan

Project Description

High-latitude regions contain approximately 30–60% of the world's terrestrial soil organic carbon. Over the past decades, the mean annual air temperature in high-latitude permafrost regions has increased by 0.2–0.3°C per decade and is projected to further increase by 4–7°C by the end of this century. Because of their huge carbon stocks and great warming potential, high-latitude ecosystems have the potential to drive important interactions with and receive feedback from Earth's climate.

The objective of this work is to improve our quantitative and predictive understanding of high-latitude soil carbon cycling and its potential role in altering greenhouse gas concentrations in the atmosphere, thus changing

the global climate. To achieve this goal, we are developing mechanism-based models to represent and simulate fundamental and important interactions of the soil's physical, hydrological, geochemical, biogeochemical, and microbial community dynamics. The resulting models will then be used to investigate the mechanisms controlling high-latitude soil carbon dynamics and better evaluate the interaction between high-latitude regions and the global carbon cycle.

Mission Relevance

This project is relevant to DOE's mission in basic science and the environment. One of DOE's primary missions is to provide quantitative and predictive understanding of the terrestrial ecosystems that can affect atmospheric greenhouse gas concentration changes due to the large carbon stocks in these ecosystems. There is a need to understand the impacts of and feedbacks from a changing climate on terrestrial ecosystems. The outcome of this work will help to improve projections of the role of high-latitude ecosystems in the context of climate change.

FY 2014 Results and Accomplishments

Roots and litterfall can release readily decomposable carbon sources into soil. This newly added carbon may increase or suppress the decomposition of older soil organic matter — phenomena known as "positive or negative priming effects." In temperate regions, recent research suggests priming effects can be a critical mechanism controlling soil carbon dynamics, yet virtually nothing is known about priming effects in boreal ecosystems. To investigate the importance of priming effects in boreal forest soils, we developed a mechanistic model in FY 2012 and FY 2013 that can simulate the simultaneously occurring processes in soil and their interactions: physical, chemical, biological, and hydrological. We then performed model sensitivity analyses for two black spruce forest sites, with and without underlying permafrost. Modeling results suggest that priming effects might be accelerated for sites where permafrost degradation leads to drier soil conditions and favorable water transport into deeper layers.

The two most important determinants of life in soil are water and oxygen. Soil-water dynamics have been relatively well represented in ecosystem and Earth system models (E&ESMs); however, oxygen is still either missing or very poorly represented in existing E&ESMs. Traditionally, the models that attempt to account for oxygen availability have simply divided the soil domain into an aerobic zone located above the water table and an anaerobic zone below it. To address problems with this approach, we developed a mechanistic model in FY 2014, based on soil pore characteristics (e.g., pore-size distribution and pore connectivity) to estimate the movement and concentration of oxygen within individual soil pores and the soil profile (Figure 1). The oxygen-based modeling approach was used to simulate emissions of the greenhouse gases CO_2 and CH_4 from an Alaskan fen peat land (Figure 2). The results were then compared with those produced by using the water table-based modeling approach. The physically realistic oxygen-based approach was found to reduce biases in the simulated fluxes of CO_2 and CH_4. The model comparisons also revealed that the existence of anaerobic microsites in unsaturated soil might cause models using the traditional water table-based approach to substantially underestimate CH_4 emissions and overestimate CO_2 emissions. This new oxygen-based approach can be used to improve other modeling applications — for example, simulations of the soil habitat and its corresponding effects on microbial population dynamics, microbial physiology, and microbial processes in both saturated and unsaturated soil zones.

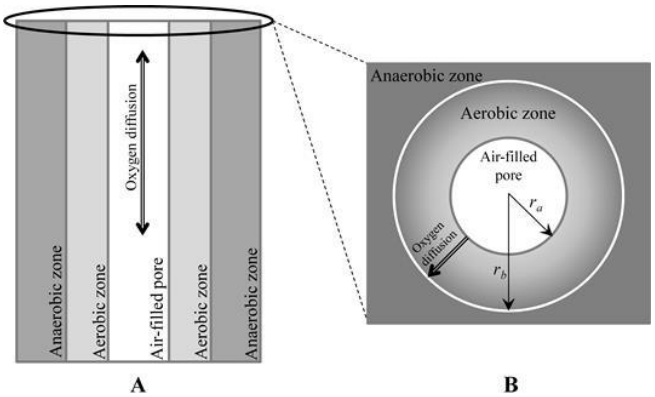

Figure 1. Model schematic used to simulate (A) vertical and (B) radial movement of O_2 in soil-water systems.

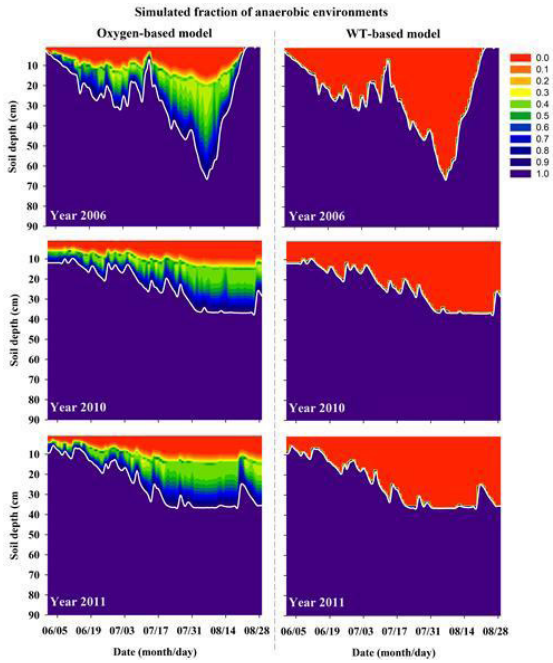

Figure 2. Simulated fraction (proportion) of anaerobic zones in an Alaskan fen peat land. White lines denote the observed water table position.

Proposed Work for FY 2015

Soil organic carbon (SOC) plays an important role in the global carbon cycle. However, largely unknown is how plant litter inputs impact magnitude, composition, and source configuration of the SOC stocks through microbial catabolism and anabolism over the long term, mostly as a result of uncoupled research on litter decomposition and SOC formation. In FY 2015, we plan to expand our developed soil models to include more fundamental processes that are currently poorly represented in the earth system models. Specifically, we will develop a mechanisms-based model to examine how microbes act as a valve controlling soil carbon sequestration. We also plan to integrate the mechanism-based soil biogeochemical model and the statistics-based Predicted Relative Metabolomic Turnover into a single model. We will test the integrated model when metagenomic data, along with the biogeochemical information, become available from laboratory incubation studies on permafrost soil.

Seminars

Fan, Z. (2013). "Priming Effects in Northern Boreal Forest Soils: A Quantitative Evaluation." 4th NACP All-Investigators Meeting, Albuquerque, NM, February 4–7, 2013.

Fan, Z. (2013). "Response of High-Latitude Peatlands to Climate Change — Improving Model Predictive Capabilities." University of Chicago, Chicago, IL, February 14, 2013.

Developing, Improving, and Testing Methods for Predicting Spatial and Vertical Distributions of Soil Organic Carbon at Regional Scales

2012-206-R2

Umakant Mishra and John Krummel

Project Description

Perennially frozen soils of the northern circumpolar region (land area above 60°N) (19 million km^2 or 16% of the global soil area) store the largest quantity of soil organic carbon (SOC) in the terrestrial biosphere. Soils of this area are expected to experience much higher increases in temperature over the next century (3.2–3.5°C by 2100) than soils in temperate or tropical regions. Therefore, high-latitude SOC stocks (which are preserved, in large part, because of low temperatures) are a potentially vulnerable component of the global carbon cycle.

Current global estimates of SOC stocks substantially underestimate permafrost-affected SOC, mainly because of the paucity of observations at high latitudes. Moreover, current estimates of SOC stocks in permafrost-affected soils have been made by stratifying the study area, averaging point observations of SOC stocks within each stratum, and multiplying by the areal extent of that stratum. In addition, most observations rarely extend below the upper meter of the soil profile, even though high-latitude soils often contain considerably deeper SOC because of cryoturbation. As a result, estimates of total SOC stocks in high-latitude regions remain highly uncertain, with current assessments suggesting that the total amount of frozen carbon in permafrost soils could be equal to or even double the amount of carbon presently in the atmosphere. Recent studies have also recognized the need for more accurate assessments of the spatial heterogeneity of SOC stocks in permafrost-affected soils.

The objectives of this project are to (1) estimate spatially resolved SOC stocks in bedrock, distinguishing active-layer and permafrost-layer stocks, on the basis of geospatial analysis of soil profile observations and spatially referenced environmental variables for permafrost affected soils; (2) quantify the prediction errors and uncertainties associated with the estimates; and (3) investigate the environmental controls that determine regional-scale SOC stocks.

Mission Relevance

The objectives of this study are relevant to DOE's missions in science and the environment. DOE, as well as other agencies, is now demanding tighter coupling and iteration between empirical studies and model development, in which the uncertainties in model predictions will help in identifying priorities for new observations and experiments, which, in turn, will be used to improve and test new models. The results of this study will produce spatially distributed estimates of permafrost SOC stocks, which are important for developing and testing Earth system models (ESMs).

Outside of DOE's Office of Biological and Environmental Research, agencies such as the National Science Foundation, National Aeronautics and Space Administration, and U.S. Department of Agriculture, as well as private foundations, are giving increasing priority to research related to climate change, coupled natural and human systems, ecosystem services, and land-use/land-cover change impacts on SOC stocks.

FY 2014 Results and Accomplishments

In FY 2013, we completed a study of the state of current knowledge about the characterization of soil carbon in permafrost-affected soils and their potential vulnerability to changing climatic conditions. We determined existing differences between empirical and earth system model estimates of the size and distribution of permafrost region

SOC stocks, and research efforts that will reduce this discrepancy were identified. Five research challenges for improving empirical assessments of the distribution and potential mineralization of SOC stocks in the northern permafrost region were highlighted. These challenges include (1) improving the number and robustness of observations, (2) predicting the spatial and vertical distributions of SOC stocks, (3) characterizing existing carbon forms to better predict their fate, (4) using improved observation-based SOC estimates to inform model development, and (5) quantifying uncertainties in observations and predictions. These challenges are interlinked and suggest opportunities to organize, prioritize, and coordinate future permafrost soil carbon research efforts.

In FY 2014, We completed a study where we used geospatially referenced soil-profile description data coupled with environmental data — such as topography, climate, and land-cover types — to predict the variability of active layer thickness at fine-scale resolution across Alaska. The predicted active layer thickness ranged from 0.14 to 0.93 meters, with a spatial average of 0.46 meters and a 30% coefficient of variation. Surface air temperature, land cover type, and slope angle were the primary controllers of the spatial variability. While comparing our results with projections of active-layer thickness produced by the Coupled Model Intercomparison Project Phase 5 (CMIP5) Earth system models for Alaska, we found CMIP5 projections had lower coefficients of variation but substantially larger prediction errors than the observation-based estimates (Figure 1). In addition, CMIP5 projections showed large inter-quartile ranges in predicted active layer thickness (0.35 to 4.4 meters), with some models substantially overestimating the predictions derived from geospatial estimates. These comparisons call attention to the need for better process and spatial heterogeneity representations in Earth system models to enable more realistic estimates of regional-scale active layer thickness and improved predictions of permafrost carbon feedback to climate under future warming scenarios.

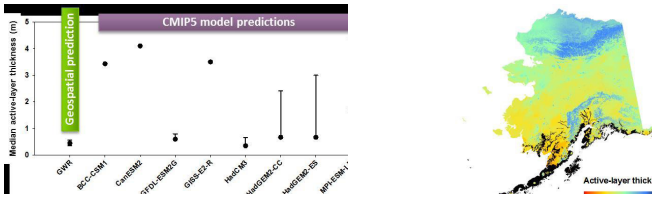

Figure 1. Predicted active-layer thickness (right) and comparison of observation based predictions with earth system model predictions (left).

In an ongoing scaling study, our initial results showed that as the spatial resolution of environmental data increased, the strengths of environmental controls on SOC stocks and predicted spatial heterogeneity of SOC stocks decreases. Similarly, we found that the mean value of SOC stocks can be used to predict its higher-order moments. This study is in progress and we hope to complete it in FY 2015.

Proposed Work for FY 2015

We will complete a study on investigating environmental controls and spatial variability of organic layer thickness across Alaska.

The surface organic layer of soils, located at the interface between atmosphere and pedosphere, impacts ecosystem functioning of Arctic/boreal environments by regulating permafrost dynamics and stability, water and nutrient availability, soil respiration, thermal conductivity, and the magnitude of carbon loss due to combustibility. For the first time, this study will show the fine-scale spatial heterogeneity of organic layer thickness across Alaska, its environmental controls, and the amount of SOC stocks stored within this layer.

Seminars

Mishra, U., J.D. Jastrow, R.M. Matamala, K.E. LaGory and J.R. Krummel (2014). "Environmental Controls and Spatial Representation of Soil Properties Across Alaska: Comparison Between Geospatial and CMIP5 Earth System Models." Korea Polar Research Institute, Seoul, South Korea, June 16, 2014.

Mishra, U., K.E. LaGory, J. Krummel, J.D. Jastrow and R. Matamala Paradeda (2014). "Benchmarking Earth System Models: A New Domain for Soil Scientists." USDA-Natural Resource Conservation Services, Lincoln, NE, March 18, 2014.

Identifying Novel Pathways for Anaerobic Microbial Oxidation of Methane

2013-177-R1

Edward J. O'Loughlin, Dionysios A. Antonopoulos, and Kenneth M. Kemner

Project Description

Although not as prevalent in the atmosphere as carbon dioxide (CO_2), methane (CH_4) is an important greenhouse gas (GHG) that accounts for approximately 20% of human-induced radiative forcing. Atmospheric methane concentrations have increased by nearly 160% since 1850, largely because of human activities relating to large-scale land management and agricultural practices (e.g., wetland rice production, the raising of ruminant livestock, and mining operations). Moreover, increased methane emissions due to the warming of Arctic permafrost have been identified as a potentially significant factor resulting from (and contributing to) global climate change.

Extensive biogeochemical research has been conducted that focuses on the causes and effects of variation in global fluxes of methane throughout the Earth's history. However, although it is known that methane formation (methanogenesis) and consumption (methane oxidation) in soils are the result of highly specialized microorganisms, the underlying microbial processes and key microbial players are poorly understood. Methane formed during methanogenesis can be oxidized to carbon dioxide via *aerobic* methane oxidation by methanotrophic bacteria — obligate aerobes that use methane as a sole carbon and energy source. While the aerobic oxidation of methane by microorganisms has been known since the early 1900s, anaerobic microbial methane oxidation has only recently been identified. In environments devoid of sufficient oxygen to support aerobic methane oxidation (suboxic to anoxic conditions), other oxidants commonly found in aquatic and terrestrial systems (e.g., sulfate, nitrate) are thermodynamically capable of serving as terminal electron acceptors for anaerobic methane oxidation.

This project focuses on the identification of anaerobic methane-oxidizing microbes from a diverse range of aquatic and terrestrial environments, characterization of the relevant metabolic pathways of anaerobic methane oxidation in these organisms, and assessment of the effects of key environmental parameters on the contribution of anaerobic methane oxidation to overall methane and carbon dioxide flux from surface and near-subsurface environments.

Mission Relevance

This project is relevant to DOE's missions in science and the environment. An improved understanding of the global terrestrial carbon cycle has become a policy imperative, both domestically and internationally. It is crucial in efforts to model, predict, and potentially mitigate the effects of increasing concentrations of GHGs, such as carbon dioxide and methane, on global climate. Identification of the microorganisms and the relevant metabolic pathways controlling anaerobic methane oxidation will provide fundamental insight into a key component of net methane flux to the atmosphere and will refine our understanding of the linkages between the biogeochemical cycling of carbon and key major/minor elements.

FY 2014 Results and Accomplishments

In FY 2013, we collected soils/sediments from 25 separate locations in 12 different states from habitats representing a diverse range of terrestrial and aquatic (freshwater, estuarine, and marine) environments throughout the continental Unites States and one site in Costa Rica. We used six of these samples to create microcosms designed to promote the growth of microorganisms that can use nitrate/nitrite, sulfate, sulfur, iron(III) oxide, manganese(IV) oxide, or humic substances as terminal electron acceptors for anaerobic methane oxidation. In the nitrate-amended incubations, we observed depletion of methane and increased carbon dioxide, coupled with the reduction of nitrate to nitrogen gas, which is consistent with nitrate-dependent anaerobic methane oxidation.

Expanding on FY 2013 sampling efforts, in FY 2014 we collected additional soils/sediments, expanding our sample library to include soils/sediments from 36 separate locations in 13 different states and Costa Rica. These samples were collected from habitats representing a diverse range of terrestrial and aquatic (freshwater, estuarine, and marine) environments. In FY 2014 we used 11 of these samples to create microcosms designed to promote the growth of microorganisms that can use nitrate/nitrite, sulfate, sulfur, iron(III) oxide, or manganese(IV) oxide, as terminal electron acceptors for anaerobic methane oxidation. These new microcosms combined with those initiated in 2013 comprise 17 ongoing enrichment experiments. In several of the longest running incubations (primarily those established in FY 2013), we observed oxidation of methane to carbon dioxide, coupled with the reduction of nitrate to nitrogen gas. We generated inventories of the microbes in these enrichments by targeting the 16S rRNA gene, a broadly occurring gene found in all microorganisms. Results from the Argonne wetland enrichments are provided as an example. Principal coordinates analysis (PCoA) indicates the development of distinct microbial populations in the nitrate-amended enrichments (Figure 1). The secondary nitrate enrichment was dominated by *Methylophilaceae*, *Rhodocyclaceae*, and *Methylococcaceae*. Organisms within these taxa have not previously been characterized as having the capacity for anaerobic methane oxidation, suggesting that the enriched populations are novel members of these families. Extracted DNA from the nitrate secondary enrichment sample was also used to construct a paired-end library that will be used for genome reconstruction efforts of predominant organisms from the enrichment.

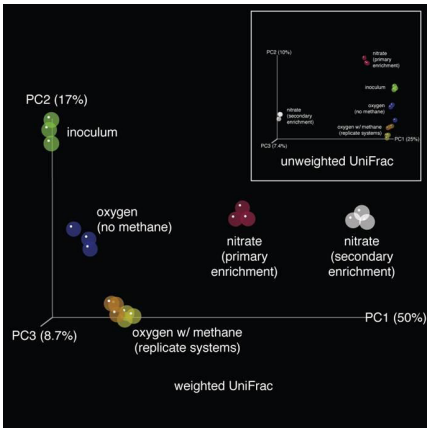

Figure 1. Principal coordinates analysis (PCoA) of weighted and unweighted (inset) UniFrac distances representing differences between the inoculum and enrichments. The secondary nitrate enrichment is the most distinct relative to the inoculum.

Proposed Work for FY 2015

In FY 2014, our focus will be on completion of assembly and annotation of genomes of anaerobic methanotrophs in the Argonne wetland nitrate secondary enrichment. We will continue to monitor the enrichment microcosms established in FY 2013–14 to identify additional microcosms showing evidence of anaerobic methane oxidation, and identification of candidate microbes for in-depth taxonomic and metabolic characterization. In addition, we will use multi'omic approaches on select isolates for identification of novel methane-oxidation pathways.

Annotating, Modeling, and Exploring Enzyme Promiscuity

2013-194-R1

Christopher Henry, Andrzej Joachimiak,
Ross Overbeek, Samuel Seaver, and Fangfang Xia

Project Description

Recent structural and mechanistic studies have demonstrated that enzymes often mediate many side reactions. Documented side reactions can get sidelined, however, because enzymes are seen as highly specific agents. Despite increasing evidence for the catalysis of side reactions by metabolic enzymes, the side reactions have failed to appear in genome annotations or metabolic models, where they might be considered by researchers seeking to correct mis-annotations, design metabolic engineering strategies, identify new pathways to engineer, or select enzymes to form components of a new pathway.

Enzyme promiscuity is one reason why it is so challenging to knock out undesirable by-products in industrial strains: even though the primary genes associated with undesirable activities are identified and knocked out, enzymes with secondary activities associated with the undesirable pathway may remain. However, the promiscuous activities of enzymes also hold great potential, since they can represent new pathways that make the production of known products more efficient or lead to novel products. Better knowledge of the secondary functions of enzymes will unveil all the potential these enzymes have if properly engineered.

There has not yet been any systematic study of alternative possible functions for enzymes involved in central metabolism. "Phylogenetic gene trees" assembled from well-annotated reference genomes provide a mechanism to study all of the possible functions that may be catalyzed by enzymes with similar amino acid sequences. Cheminformatic techniques make it possible to identify all reactions that involve a similar class of biochemical transformation and to automatically generate novel reactions. Structural proteomics makes it possible to explore how protein structure governs enzyme specificity. In experiments, high-throughput pipelines for protein expression, purification, and functional assay enable the rapid validation of proposed secondary functions for enzymes, and metabolomics provides a means for observing the substrates and products of proposed secondary functions.

The objective of this project is to identify and predict alternative functions of promiscuous enzymes by:

1. Fabricating phylogenetic trees of enzyme function, in which the distances between "leaves" indicate the probability that an enzyme whose primary function lies at one leaf will perform the functions found at the other leaves;
2. Proposing novel enzymatic reactions based on patterns of enzyme activity, rules of biochemistry, and substrate similarity and adding these reactions to the phylogenetic trees of enzyme functions;
3. Characterizing the conformational diversity of selected enzyme functions through molecular dynamics simulations and using this biophysical feature for annotating enzyme promiscuity;
4. Applying promiscuous trees of enzyme functions to propose new annotations for poorly annotated gene clusters found in genomes and metagenomes;
5. Obtaining and analyzing protein structures for a variety of enzymes contained within a few protein families; and
6. Designing and synthesizing one or two ancestral enzymes and testing for increased promiscuity, then validating developed models of enzyme promiscuity/sequence relationships by designing, synthesizing, and characterizing one to five enzymes with increased/decreased promiscuity.

Mission Relevance

This project is relevant to DOE's mission in science. An improved understanding of enzyme promiscuity will have an impact on many objectives of the DOE Office of Biological and Environmental Research, as follows:

1. Proposing alternative annotations for enzymatic genes for which current functions appear to be mis-annotated, improving annotations, and integrating new pathway models;
2. Improving the accuracy and reliability of flux predictions made by metabolic models, by accounting for pathway activity that arises as a result of promiscuous enzyme activity;
3. Guiding metabolic engineers trying to knock out undesirable cellular activities (because all the enzymes that might have the undesired activity can now be identified);

4. Exploring the fundamental contribution of enzyme promiscuity to organismal fitness; and
5. Identifying secondary activities in new enzyme functions being engineered into cells and investigating the link between promiscuity and protein structure to support the engineering of substrate specificity.

The database of promiscuous functions and improved annotations is relevant to the DOE-funded KBase project. The improved capacity for supporting metabolic engineering and studying the link between promiscuity and protein structure also directly applies to the burgeoning DOE area of synthetic biology.

FY 2014 Results and Accomplishments

In this project, we are taking a combined bioinformatic, cheminformatic, molecular dynamic, and molecular biology approach to understanding enzyme promiscuity. We are combining many orthogonal data sources to attack a single problem and obtain a more complete picture of enzyme promiscuity. So far, work on all approaches has proceeded in parallel.

In FY 2013, our bioinformatics team assembled phylogenetic gene trees for more than 100,000 enzyme families. We applied these trees to curate annotations and improved the consistency of their functional annotation. We also developed methods to predict potential novel promiscuous functions for genes on the basis of other functions present in our phylogenetic gene trees. Our cheminformatics team applied the BNICE algorithm to propose novel compounds and reactions based on the trypC enzyme. We also applied BNICE to one step for every native metabolite in the known biochemistry databases. From this, we constructed a large database of all potential novel biochemistry that could arise given our enzyme reaction rules and the known substrates. Finally, our structural proteomics team identified 48 distinct trypC enzymes, with widely varying promiscuity, from various organisms. Sequences and data were sent to the laboratory, where genes were cloned, synthesized, purified, and crystallized. This effort produced a library of purified proteins of varying promiscuity that we tested to predict promiscuous functions proposed by our bioinformatic and cheminformatic approaches.

In FY 2014, our bioinformatics team began work to use conserved domains in CDD, or the "Conserved Domain Database," as a new means to predict alternative functions for genes. Specifically, we developed machine-learning-based approaches to associate potential biological functions with proteins on the basis of the conserved domains they contain. We used our current annotations in the SEED database to train our classifiers, and we applied these classifiers to predict a set of alternative potential functions for genes on the basis of their domains. This method was applied to predict potential genes for each step of a completely novel pathway to produce coenzyme Q, which is proposed to exist in a strain of Klebsiella. This work demonstrates how the bioinformatics portion of this research links specific gene sequences to predict novel biochemical functions. Our cheminformatics team continued work on our new database of novel potential biochemistry, which we now call the MINE, for Metabolic Integrated Network Explorer. We constructed a new website for our MINE database, located at http://minedatabase.mcs.anl.gov/. This website permits analysis of metabolics data, exploration of potential novel chemistry, and rapid structure-based searching for compounds. The MINE database has already been applied, with collaborators at Lawrence Berkeley National Laboratory, to propose potential novel pathways and produce derivatives for lignin. This example demonstrates the widespread potential applications of these tools and research. Finally, our structural proteomics team completed work on seven new protein structures. We are now conducting a molecular-dynamics-based analysis of these protein structures, predicting their promiscuity and exploring the potential for these proteins to bond with a wide range of substrate compounds. This analysis will add a whole new dimension to our promiscuity analysis (i.e., the prediction of potential substrate promiscuity for enzymes based on docking of alternative substrate structures to the enzyme surface).

Proposed Work for FY 2015

We will continue to use our predicted novel biochemistry database (the MINE) in combination with our database of genome-scale metabolic models to predict the potential impacts of promiscuous biochemistry of organism phenotypes. When differences in phenotype occur with the inclusion of potential promiscuous biochemistry in models, we will compare these predictions with experimentally observed phenotypes to find experimental evidence for our promiscuity-based mechanisms.

We also plan to apply a combination of TNseq and gene knockout analysis to experimentally validate (i) the novel coenzyme Q biosynthesis pathway predicted by our cheminformatics tools and (ii) the genes mapped to our predicted pathway steps by our CDD-based promiscuous function prediction algorithm. We are conducting TNseq on the wild-type strain with the known pathway to coenzyme Q intact, and we will compare TNseq results with data from a strain where the known coenzyme Q pathway has been knocked out. This study, once complete, will demonstrate how our entire enzyme promiscuity analysis pipeline can be applied to the discovery of a completely novel biochemical pathway from beginning to end.

Additionally, we will apply our protein expression, purification, and functional assay pipeline to one final family

of proteins involved in an important oxidation/reduction pathway step in metabolism, as this chemistry is demonstrated to have different promiscuity characteristics compared with our previously studied enzyme families. We will continue validating our cheminformatic predictions by conducting binding assays and functional assays with metabolites predicted to be alternative substrates of our expressed and purified proteins. We will apply molecular dynamic approaches to our new protein structures obtained in previous years to search for enzymes with more flexible conformers or more open binding sites. From these simulations, we will assign enzymes a predicted promiscuity index, which may be experimentally tested later. Results of this study will be confirmed against the known promiscuity levels of all analyzed proteins. We will complete work in applying our enzyme promiscuity analysis pipeline to the discovery and validation of a completely novel metabolic pathway for coenzyme Q production. Finally, we will expand our MINE website to link with metabolic models and pathway search tools to facilitate the search of our database of potential promiscuous biochemical reactions, to identify novel pathways with potential industrial or medical applications.

Identifying Patterns and Association among Hyperspectral Data and Meteorological and Biological Measurements for Investigating Near-Surface Atmosphere-Biosphere Interactions

2014-132-N0

Yuki Hamada, David Cook, Nicola Ferrier, and Roser Matamala

Project Description

Atmosphere, plants, and soils control terrestrial carbon and water cycles. To enable more accurate climate forecasting, researchers need to gain a better understanding of ecosystem dynamics at the biosphere-atmosphere interface. The goal of this project is to better understand the indicative power of hyperspectral data in carbon and water exchange between the near-surface atmosphere and the biosphere by exploring analytics for investigating temporal patterns and associations between hyper-volume, high-temporal-frequency hyperspectral data and meteorological and biological measurements.

The objectives are to (1) construct an environmentally resistant optical tower system that is equipped with a spectrometer (or hyperspectral sensor) and other optical sensors/instruments; (2) design an autonomous data collection workflow for high-temporal-frequency, multi-sensor optical data in a synchronized manner with a near-real-time data transmission strategy; (3) develop a methodology for quality assurance (QA)/quality control (QC), preprocessing, and organization of the hyperspectral data and explore a methodology for investigating temporal patterns and associations between the hyperspectral data and meteorological and biological measurements collected by using a flux tower; and (4) identify whether the high-temporal-frequency hyperspectral data provide meaningful information about ecosystem carbon and water fluxes.

Mission Relevance

This project is relevant to DOE's initiative in biology and the environment because it brings together a multidisciplinary group of scientists capable of resolving current roadblocks in developing a method for high-temporal-frequency hyperspectral data collection and analysis for application to ecosystem research. Outcomes of this project will benefit DOE Biological and Environmental Research (BER) Terrestrial Ecosystem Science (TES) by contributing new technologies to the AmeriFlux network; it will also benefit DOE-BER Systems Biology KBase by integrating hyperspectral data into cloud computing to study plant/ecosystem activities. This project will demonstrate the effectiveness of high-temporal-frequency hyperspectral data in studying ecosystem functions and surface biosphere-atmosphere interactions. Obtaining advanced knowledge about these relationships can make hyperspectral measurements essential to environmental studies for rapidly identifying ecosystem responses to environmental changes and translating the resulting information into predictive models.

FY 2014 Results and Accomplishments

In FY 2014, we procured sensors and associated components for an optical tower system and built the following subsystems for software development and initial indoor testing: (1) hyperspectral sensor and a red-green-blue (RGB) camera connected to a single-board computer and (2) shadowband radiometer and albedometer connected to a datalogger. We deployed the solar panel system to the study site independently of the optical tower system to ensure the solar system generates and supplies sufficient power for the optical system. We designed and procured the elements needed to construct the data network. We also developed Linux-compatible software to autonomously operate our systems by writing new codes and rewriting Windows-based proprietary software. In addition to completing the initial indoor testing for the subsystems, we fabricated an optical tower at Argonne's 484 Area for preliminary outdoor testing. The system consists of sensors and associated components, including a spectrom-

eter, an actuator with a reference panel, a thermal infrared sensor, a RGB camera, a pan-tilt unit (PTU), a shadowband radiometer, and an albedometer (Figure 1).

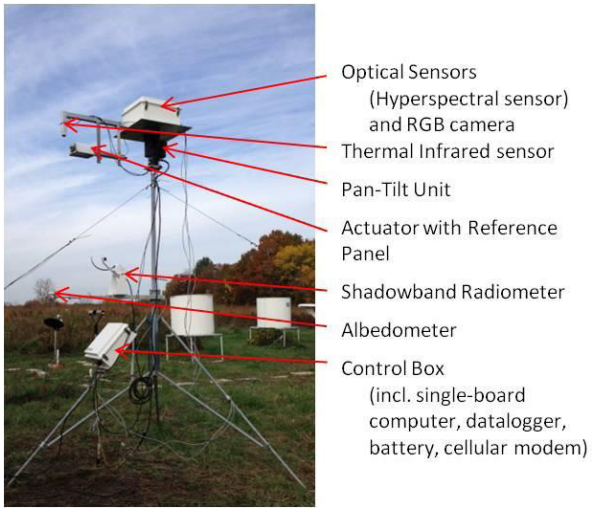

Figure 1. EcoSpec optical tower system (prototype).

The PTU and the enclosure housing the spectrometer and RGB camera rotate 340° (-170° = east, 0 = south, and 170° = west) and collect data from 12 locations (or ground sampling areas) around the tower for each rotation (Figure 2). The software we developed moves all the components in a synchronized manner; first positioning sensors at a given location and extending a reference panel, optimizing settings and collecting a series of hyperspectral data, and then capturing a footprint photograph and recording ancillary data as outlined in Figure 3. This sequence was designed to collect optical data at a high temporal frequency yet minimize power consumption from dawn to dusk throughout the growing season.

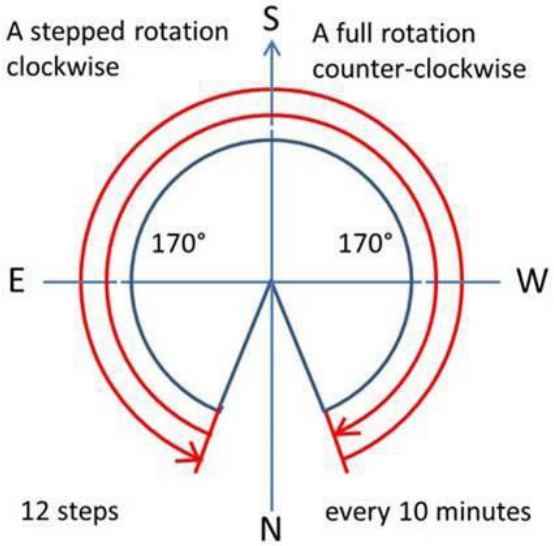

Figure 2. Pan-tilt unit rotation scheme.

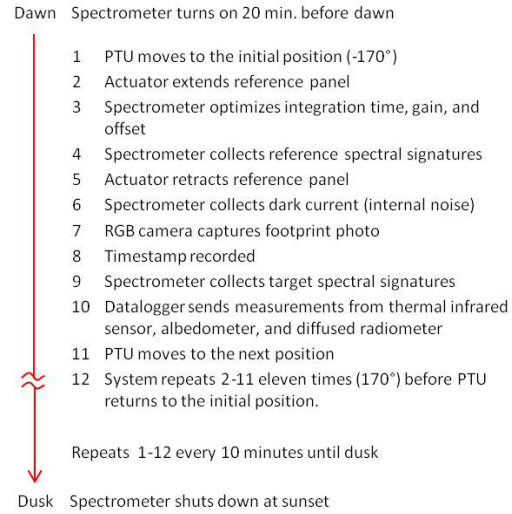

Figure 3. Synchronized data collection timeline for optical tower system.

Proposed Work for FY 2015

In FY 2015, we will (1) initiate outdoor testing, (2) update the prototype program, (3) initiate development of protocols, and (4) deploy the optical tower system and initiate data collection. In early fall, we will conduct outdoor testing to examine accuracy and robustness of instrumentation as much as possible. During the winter, we will conduct the indoor testing (Phase II) and update current software for further improvement. We will also perform indoor experiments to understand the effects associated with the amount and angle of incoming light on spectral reflectance from targets and explore solutions to these issues. Furthermore, we will develop a set of protocols for data collection, QA/QC, compilation, and data processing associated with the optical tower system. In the spring, we plan to deploy the optical tower system to the Fermilab Agricultural AmeriFlux site and collect data for analysis with flux tower measurements.

Minimizing Environmental Microbial Community Complexity at the Bench: Isolating and Characterizing Minimal Stable Communities (MSCs) over Time

2014-141-N0

Dionysios A. Antonopoulos and Folker Meyer

Project Description

Many natural environments (e.g., soil) exhibit ultra-high levels of microbial community diversity, inhibiting study of the specific interactions between organisms and determination of how these interactions contribute to a com-

munity's stability. This project is focused on uncovering components of microbial community stability by isolating and studying what we term "minimal stable communities" (MSCs) via a high-throughput screening, cultivation, and monitoring platform. The work proposed here addresses three key challenges to address stability: (1) dissecting ultra-complex communities for study in the laboratory, (2) monitoring community responses over time to defined disturbances (abiotic/biotic) at the population and gene level, and (3) integrating the different data types produced. For a given complex microbial community, we want to determine the microbial *interactions* that are the basis for stability; in other words, what are the "building blocks" for stability?

Mission Relevance

This project has direct relevance to development of the DOE Systems Biology Knowledgebase platform, as well as other components within the DOE Genomic Science program. Notably, the research described here would contribute to the development of "omics" experimental capabilities and enabling technologies needed to achieve dynamic, systems-level understanding of organism and/or community function.

FY 2014 Results and Accomplishments

Microbial communities in complex, heterogeneous environments such as soil consist of hundreds if not thousands of different taxa. Present approaches for characterizing the diversity in these communities based on phylogeny (e.g., approaches based on 16S ribosomal RNA) provide a coarse profile of the microbes present, but they are not able to accurately characterize the functional capabilities of the constituent microorganisms. Methods such as community-level physiological profiling (CLPP) provide a different, functional view of microbial communities by focusing on the ability of a mixed inoculum to respire using a particular substrate. One such example is the Biolog EcoPlate™, which utilizes a 96-well microtiter plate containing a variety of carbon substrates and a redox indicator dye (tetrazolium violet) that turns a vivid purple in the presence of actively respiring microbial cells. We used this approach to enrich for "minimal communities" in each well of the microtiter plate according to substrate and then coupled it with massively parallelized DNA sequencing to compare the profiles of the enrichments *en masse* between samples from different environments.

The CLPP experiments used soil suspensions or natural waters from five disparate environments: soil from a restored prairie and an adjacent forest on site at the Fermi National Accelerator Laboratory, tropical soil from a Caribbean lowland rainforest within the EARTH University Forest Reserve in Costa Rica, and surface water and sediment from a palustrine emergent wetland on site at Argonne National Laboratory. Our approach for uncovering hypothetical minimal communities from environmental materials required an initial "washing" and dilution of material, which separated microorganisms from the environmental particulate matrix, and a subsequent dilution of recovered microbes, which segregated potential minimal communities volumetrically. As a result of this dilution by several orders of magnitude, the actual biomass (cell number) was minimal, and we monitored the length of incubation time required for respiration and/or growth to enable color development of the indicator dye. Using the earliest maximal color development across wells (72 hours), we obtained samples from individual wells in each EcoPlate™ (and the environmental material used as inoculum) and extracted DNA from each. Sequencing libraries were generated to inventory the organisms present in each well by targeting a broadly occurring gene found in all microorganisms (encoding ribosomal RNA, a gene important in the production of proteins). These were then sequenced by using an Illumina MiSeq instrument at Argonne's Next Generation Sequencing Core to produce over 16.6 million paired sequences (30,773 ± 18,819 per amplicon library) and the data were analyzed by a standard analysis pipeline (QIIME).

Ordination by using principal coordinates analysis (PCoA) was used to compare the composition of microbial communities from the EcoPlate™ enrichments and environmental samples. The PCA results for these 480 samples are shown in Figure 1. The taxonomic composition of the enriched communities in individual EcoPlate™ wells was also determined. The results indicate that the most "active" populations in the EcoPlate™ enrichments is determined by the enrichment source, although these organisms are not necessarily the most dominant taxa in the original environment. More surprisingly, we found that a single type of organism would occur frequently across the wells, and that this organism was distinct for the enrichments from the tropical soils when compared to those from the temperate and wetland environments (hence driving the separation of samples along the first [horizontal] principal axis in Figure 1). However, each individual well consisted of multiple organisms supporting the concept of enriching minimal communities using this approach. These additional organisms are what created an additional separation of the prairie, forest, and wetland samples along the second (vertical) principal axis in Figure 1.

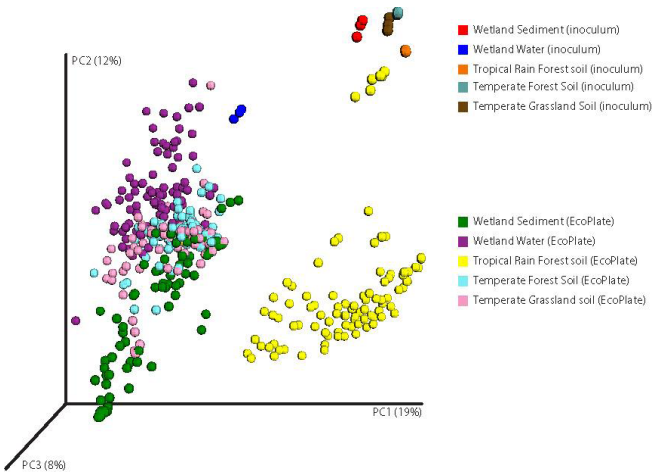

Figure 1. Principal coordinates analysis comparing the composition of microbial communities from the EcoPlate™ enrichments and environmental samples (upper right-hand corner).

In summary, we now have a novel dissection approach to studying natural complex communities by uncovering natural sub-communities (candidate MSCs) based on substrate utilization. We will use this approach to monitor their stability and expression dynamics over time in response to abiotic/biotic perturbations. Further analyses of such minimal communities will enable detailed functional characterization of metagenomes, metatranscriptomes, and other "omics"-enabled research to better understand the coupling between microbial community structure and biogeochemical processes like carbon cycling.

Proposed Work for FY 2015

We will verify our results with replicate enrichments and will then commence continuous cultivation of candidate MSCs in a parallelized small-volume system ("ministat") to test their stability. Continuous culture systems, unlike static (batch) systems, provide a constant influx of feed and efflux of biomass in such a way that the flow rate of the system is commensurate with the growth rate of the organisms in the culture vessel. By controlling the flow rate, the actively (continuously) growing minimal communities in the main cultivation vessel maintain a constant cell density, and the cellular processes likewise occur at a constant rate. In this context, the response of the minimal communities to a disturbance can be monitored over time via the efflux biomass as it is collected. Each subsequent collection represents a different state of the minimal community.

Developing Remote Automated Sensors to Direct Sampling of Aerobic-Anaerobic Switching in Floodplain Ecosystems to Characterize the Response of Microbial Carbon Metabolism at High Temporal Resolution

2014-145-N0

Jack A. Gilbert, Christopher Henry, Kenneth M. Kemner, Sarah O'Brien, and Edward J. O'Loughlin

Project Description

Variation in the localized concentration and availability of terminal electron acceptors (such as iron and nitrate) are likely to influence the abundance of anaerobic respiratory microorganisms that utilize the reduction of these compounds for energy. Thus, changes in the concentration and availability of terminal electron acceptors will alter the onset of methanogenesis and flux of methane as a result of the competition between methanogenic archaea and anaerobic respiratory bacteria for the same electron donors (e.g., hydrogen and acetate). Additionally, terminal electron acceptors (e.g., iron and nitrate) are required for anaerobic methanotrophy that will also modulate methane flux to the atmosphere. However, the genomic and regulatory response to differences in starting concentrations of electron acceptors is poorly characterized, especially regarding their influence on time-to-onset and duration of methanogenesis, and the resultant flux of methane to the atmosphere. The impact of anaerobic respiration and methanotrophy on methanogenesis should be directly linked to the concentration of terminal electron acceptors and to the production of electron donors by microbial fermentation of organic matter; however, the genotypes and functional markers responsible for these processes are poorly characterized. In this project, our objective is to capture the genomes of the key organisms involved in this process and determine how they will respond to changing concentrations of terminal electron acceptors with regard to the development of methane.

Mission Relevance

The project is tied to DOE's mission in environment. The DOE's Biological and Environmental Research Program is developing new initiatives aimed at advancing understanding of Earth's integrated biogeochemical processes to identify key factors controlling the storage, release, or transport of carbon, nutrients, or contaminants in the environment. The Genomic Science program specifically has highlighted the value of genome sequencing of microbes

and complex environmental assemblages of organisms, which has provided the vital blueprint necessary to understand the functional potential of organisms and interactive communities. Microbial communities are essential components of all ecosystems, but particularly at the interface between terrestrial ecosystems and aquatic ecosystems. An example of this interface that is of particular interest to Argonne is floodplains. These are periodically flooded terrestrial environments that develop temporary anoxia. Elucidating the metabolic capabilities and interactions that enable bacterial, archaeal, and viral assemblages to adapt to the dynamic change in redox potential in these environments is essential to our understanding of ecosystem stability and the key factors controlling the storage, release, or transport of carbon, nutrients, or contaminants in the environment. The Genomic Sciences program is investing in research aimed at developing a knowledgebase comprised of bacterial genomes and functional models to capture their metabolic potential.

FY 2014 Results and Accomplishments

In FY 2014, we embarked on a new strategic development of this research area. Through collaboration with researchers from Hope College, in Holland MI, we had access to their local series of floodplains, representing a gradient since restoration that enables us to test our hypotheses about the influence of the microbial biogeographic distribution (and the biogeochemistry that mediate their metabolisms) on methane turnover and flux in these environments. Subsequently, fellow researchers at Argonne, provided us with extensive geographical information assessment (GIS) of these locations. We implemented a field site sampling in July 2014; where we collected samples from 4 floodplain sites, collecting >60 soil samples. We extracted DNA and created 16S rRNA libraries from these studies and they are in the process of being sequenced. We intend to target a series of these samples for shotgun metagenomics and genome-assembly to explore strain level variation in methanogens and methanotrophs through this system. We started biogeochemical analysis of these soils, and are gathering these data to create a physicochemical analysis of these sites.

Proposed Work for FY 2015

In FY 2015, we aim to conclude data acquisition from the field sites and start lab-based microcosm studies with material collected in the field to explore the time to onset of methane production as a function of different concentrations of terminal electron acceptors. We expect to continue the analysis and interpretation of these data through early FY 2015.

We will also start a new experimental phase, the design of which is still being implemented but which will aim to explore seasonal dynamics and the influence of changing genotype abundance and electron acceptor concentration across seasons on methane dynamics. The work will include:

- Initiation of historic remotely sensed data collection, processing, and analysis for extracting environmental/contextual information such as land-cover-land-use (including plant community composition and structure) and flood patterns.
- Data generation and analysis, with a focus on outlining the relationship between seasonal activity and methane turnover in these ecosystems.

In addition, we expect to:

- Integrate the environmental/contextual information extracted from historic remotely sensed data into existing geospatial environmental data (e.g., climate/weather) at EVS and
- Identify environmental/contextual information necessary to collect using UAV and determine appropriate specifications for near-surface remotely sensed data collection.

Biology@speed: D-Factory, a Novel Experimental Framework

2014-157-N0

Gyorgy Babnigg, Andrew Binkowski,
Robert Jedrzejczak, Andrzej Joachimiak,
Karolina Michalska, and Boguslaw Nocek

Project Description

Current capabilities at Argonne in next-generation sequencing and bioinformatics are unmatched with respect to experimental throughput. Nevertheless, future biological studies will require more automation, significantly higher throughput, and direct translation of *in silico* ideas to executable workflows on a highly modular experimental platform. The aim of this project is to develop a technology platform enabling high throughput (HTP) biology or "biology at speed." This platform consists of a hardware layer, including modular microfluidics core engines coupled with detectors, and an abstraction layer describing workflows coupled with an application programming interface (API). Scale-up experiments are performed to benchmark the system. The platform development uses off-the-shelf products, incorporates in-house developed technologies designed specifically for a given task, and/or relies on collaboration with the Center for Nanoscale Materials (CNM) or outside vendors. The development of this experimental framework is tightly linked with other Argonne projects focusing on the investigation of minimal microbial communities (see 2014-141-N0) and automated remote sensors (see 2014-145-N0). The microfluid-

ics-based HTP assay platform will be continuously tested and benchmarked against these experimental efforts.

Mission Relevance

The project is relevant to DOE's mission in science. Biology@speed will reduce current bottlenecks in experimental biology. The modular and reconfigurable design makes it compatible with current and future science needs. The project is, therefore, relevant to the DOE Systems Biology Knowledgebase (KBase) and other biology projects funded by DOE and the National Institutes of Health (NIH).

FY 2014 Results and Accomplishments

The focus of the project is to establish a microfluidics framework at the laboratory scale and test its capabilities using other experimental efforts. Consequently, during FY 2014, special emphasis was given to the building of the microfluidics infrastructure. Several avenues were pursued: (a) collaboration with the CNM, (b) the use of fabrication resources offered by universities and industry, and (c) the testing of off-the-shelf microfluidics products. The work began with the design of a microchemostat (Figure 1a). Several microchemostats and single-cell manipulation chips (not shown) were acquired from the Stanford Microfluidics Foundry. Devices were designed to support the HTP assay platform development. These designs integrate droplet generation, assay, and potential sorting capabilities (Figures 1b and c). Several microfluidics devices were acquired from commercial vendors: droplet generators, droplet mergers (Figure 1d), and double-emulsion generators. To support the HTP assay development, we have partially installed a dedicated confocal microscope for detection of fluorescent signals from microfluidics assays and developed several ancillary controlling devices.

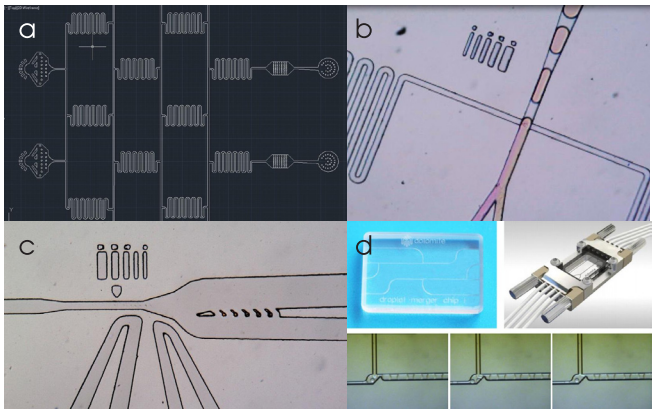

Figure 1. Microfluidic chips to the Biology@speed project. A microchemostat designed to support the minimal stable community work (a); PDMS chips from a commercial vendor: a droplet generator (b); and a droplet sorter (c); and off-the-shelf product, droplet mergers (d).

We also established and tested several techniques for the cultivation of target microbes, whole-genome amplification, messenger RNA isolation, and complementary DNA library generation. We successfully cultivated more than a dozen anaerobic microbes (e.g., *Anaerostipes caccae*, *Clostridium bartlettii,* and *Bacteroides intestinalis*) and a few aerobes (e.g., *Kytococcus sedentarius*), with special emphasis on those with abundant carbohydrate-active enzymes (e.g., *Bacteroides*) or those that can be co-cultivated. Initial tests revealed that the whole-genome amplification worked at 95% efficiency when tested with a sample of 67 gene candidates from three representative microbes. However, the efficiency of the complementary DNA library construction was poor and highly dependent on the target organism. Several expression vectors were developed for this project utilizing variants of green fluorescent protein for the detection of positive expression clones using fluorescence-activated cell sorting. Initial assays were tested for the feasibility of miniaturization. These included assays for glycoside hydrolases, which are important in DOE missions, and beta-lactamases, which are relevant to NIH initiatives. Finally, several three-dimensional printed designs and electronic controllers were created to support this project.

Proposed Work for FY 2015

The microfluidics framework will be expanded to include two-layer designs for single-cell manipulation and implementation of automated multi-step laboratory protocols. Special chips will be designed and tested for HTP assays. The imaging capabilities of the newly installed confocal microscope will be tested. The imaging station will be integrated with fluidics control, valve control, and sorting devices using a web-based framework. The microchemostats and single-cell manipulation chips will be tested with samples provided by other experimental efforts at Argonne. The development of the computational abstraction layer and fluidics API will begin.

Soft X-ray Scanning Transmission X-ray Microscopy: Giving Argonne a Nanoscale Picture of Carbon in Soils and in Energy Materials

2014-162-N0

Kenneth M. Kemner, Maxim Boyanov, Chris Jacobsen, Julie Jastrow, Sarah O'Brien, Edward J. O'Loughlin, and Ruben Reininger

Project Description

The number of scanning transmission x-ray microscopes (STXMs) available at synchrotron sources in the United States for carbon micro(spectro)scopy has decreased in recent years; now, only two STXMs are available at the Advanced Light Source (ALS) at Lawrence Berkeley National Laboratory. As a result of (1) an increase in the

requests for access to these STXMs by scientists who previously used the decommissioned STXM at the National Synchrotron Light Source (NSLS) and (2) a growing biogeochemistry research community investigating carbon cycling, the oversubscription rate (i.e., the ratio of beam time requested by researchers to the amount of beam time available) for the STXM beam lines at the ALS is more than 3. Therefore, we are exploring the feasibility and determining the cost to develop a soft x-ray STXM at a bending magnet beam line at the Advanced Photon Source by making use of previously used beam line components. These components come from a previously operated STXM at X1A at the NSLS-I and beam lines at the decommissioned synchrotron at the University of Wisconsin, Madison.

Mission Relevance

The project is relevant to DOE's missions in science and energy. We anticipate future calls for proposals from the DOE's Biological and Environmental Research Division and other agencies to improve our understanding of the global carbon cycle. Therefore, we anticipate researchers at Argonne and other institutions will experience increased difficulty in gaining access to the amount of beam time required to address the key scientific questions related to the biogeochemical cycling of carbon. Similarly, STXM capabilities will be needed to measure the unique types of samples resulting from studies in Argonne scientists' labs related to novel energy materials.

FY 2014 Results and Accomplishments

In FY 2014, we developed a design concept for an STXM that would be able to make use of existing pieces of a previous microscope that used to be assembled at the National Synchrotron Light Source at Brookhaven National Laboratory. Next, we investigated what locations (i.e., beamlines) at the Advanced Photon Source would be conducive for the future assembly of said microscope. We found three potential locations (the bending magnet beam lines at sectors 10, 14, and 20). After analysis of (1) the existing equipment that was in place at those beam lines, (2) the "open space" that had no infrastructure available to support an x-ray microscope but also no physical structures that would obstruct the future assembly of the microscope, (3) the future plans of the existing activities already at the beam line, (4) the time required to assemble the STXM to the point that it was operable, and (5) the cost to assemble the STXM at each potential beam line, we identified beam line 20BM as the best location for parasitic operation of the STXM.

After identifing beam line 20BM as the best location for parasitic operation of the STXM, we determined a layout of the STXM beam line at 20BM. Used beam line components (microscope, monochromator, additional stands) were identified and shipped from NSLS-I X1A. Three used mirror chambers (including pumps, vacuum valves, and motors) were identified and shipped from the synchrotron in Wisconsin. A quote for the new mirrors for these chambers was obtained. We identified additional parts needed for the beam line (collimator, fast valve, beam shutter, beam pipe, pumps, and computers). We also identified additional action items required for assembly of STXM beam line (move PSS panel, cut a hole in 20BM FOE, develop a new data-acquisition control system, survey and align, plumb beam line for water, and electrical services to run and cool vacuum pumps and operate motors.

Impact of Radiation and Surface Turbulent Fluxes on the Transition from Stratocumulus to Cumulus Cloud Regime

2014-183-N0

Virendra P. Ghate

Project Description

Marine stratocumulus clouds cover vast areas of Eastern subtropical oceans. These clouds reflect greater amounts of solar (shortwave) radiation back to space compared to the ocean surface, while emitting similar amounts of terrestrial (longwave) radiation as the surface because of the lower heights of their cloud tops. Hence, they are a significant component of the Earth's radiation budget and need to be accurately represented in the global climate models (GCMs) used to predict the future climate and future energy needs.

The overall goal of this project is to improve the representation of marine stratocumulus clouds in GCMs and specifically understand the transition of the stratocumulus clouds to the cumulus cloud field in the context of changes in the boundary layer radiation and surface energy fluxes.

Mission Relevance

This project falls under DOE's energy, environment, and basic research missions. The research uses data collected at the Atmospheric Radiation Measurement's (ARM's) Climate Research Facility to quantify the interactions among aerosols, clouds, precipitation, radiation, dynamics, and thermodynamics to improve our fundamental, process-level understanding, with the ultimate goal of reducing uncertainty in global and regional climate simulations and projections.

FY 2014 Results and Accomplishments

The first step in the transition from a stratocumulus to a cumulus cloud field is for the stratocumulus cloud to become thermodynamically decoupled from the underly-

ing sea or land surface. We focused our efforts on characterizing the thermodynamic and radiative structure of stratocumulus-topped boundary layers (STBLs). To this end, we analyzed data collected at the ARM's observation facilities in the Southern Great Plains (SGP) and the Azores, as well as data collected in the South-East Pacific (SEP) region by the National Oceanic and Atmospheric Administration (NOAA) during stratocumulus cloud conditions. Significant differences in the strength, depth, and location of the boundary layer inversion were found among the three locations. Shown in Figure 1 are the mean profiles of equivalent potential temperature and saturation equivalent potential temperature at the three locations, along with the locations of the cloud layer, the surface lifting condensation level (LCL), and cloud base LCL. Statistically significant differences were found between cloud thickness and inversion structure at the three locations. In addition, the amount of radiative cooling near STBL tops and the surface energy fluxes also differed among the three locations.

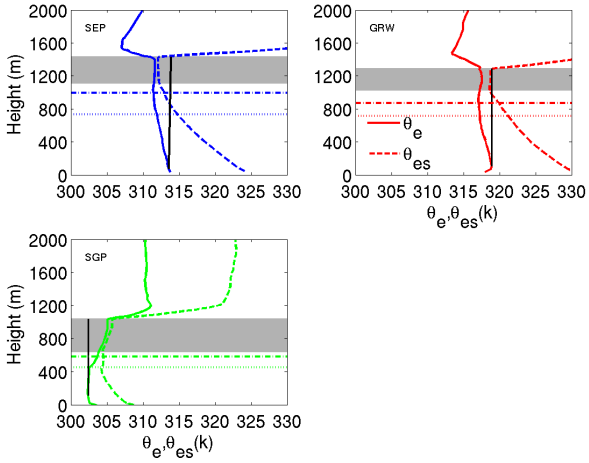

Figure 1. Profiles of equivalent potential temperature (solid-color lines) and saturation equivalent potential temperature (dashed lines) in the South-East Pacific (SEP) and at ARM facilities in Graciosa (GRW) in the Azores and in the Southern Great Plains (SGP) along the location of the cloud layer (grey shades), surface lifting condensation level (dotted lines), and cloud base lifting condensation level (dash-dot lines). The vertical black line denotes the equivalent potential temperature at 100 m often used to diagnose convective available potential energy (CAPE).

After characterizing the mean thermodynamic and radiative structure of the STBL, we classified the STBL as coupled or decoupled on the basis of the difference between the cloud base height and the height of the LCL calculated from surface observations. The observations broadly suggest that decoupled STBL is deeper and associated with lower radiative cooling near cloud top as compared to the coupled STBL. In contrast with previous modeling and observational studies, our results suggest that the surface energy fluxes play a lesser role in causing STBL decoupling.

Proposed Work for FY 2015

During ARM's MAGIC field campaign, observations of the transition of a stratocumulus to a cumulus cloud field were made by instrumenting a container ship transiting routinely from California to Hawaii. In FY 2015, we will apply the algorithms and techniques we developed to the data collected during a few transects of the MAGIC field campaign to assess the role of radiative cooling and surface fluxes in determining the transition from a stratocumulus to a cumulus cloud field.

Self-Assembled Functional Membranes for Filtration and Photocatalytic Water Treatment

2014-187-N0

Seth B. Darling and Jeffrey W. Elam

Project Description

As society enters a period of water crisis, new filtration technologies will be a central piece of the solution to addressing the grand challenge of identifying sustainable water supplies. Through this project, we are using a low-cost combination of block copolymer self-assembly and a novel technique called sequential infiltration synthesis (SIS) to prepare nanoporous membranes with unique and tunable mechanical, filtration, and catalytic properties.

Our novel approach involves the synthesis of photocatalytic low-fouling membranes, wherein the top layer is a nanoporous titania membrane. These photocatalytic membranes have nanopores whose size and shape can be controlled; as such, they possess the potential to overcome the limitations of current filtration systems.

We will prepare nanoporous titania membranes by using cylinder-forming block copolymer thin films on a solid substrate as templates. Several polymeric material systems will be explored, with the first being poly(styrene-*block*-methyl methacrylate) (PS-*b*-PMMA). PS cylindrical domain size and spacing will be varied from ~15 to 50 nm with the molecular weight of the starting polymer material. Orientation of the self-assembled microdomains will be manipulated by using surface chemistry, such as through the application of brush layers of random copolymers to obtain a neutral interfacial interaction and therefore vertical orientation of the cylindrical domains. These oriented block copolymer films will serve as a template for the growth of nanoporous photocatalytic material. Titanium dioxide (TiO_2) will be selectively and controllably grown within the PMMA domains by using SIS, the self-limited, gas-phase technique developed at Argonne.

SIS entails alternating exposure of a polymeric film to gas-phase precursors by using an atomic layer deposition (ALD) reactor operating in semi-static mode; the precursors penetrate into the film and chemically react with moieties on the polymer chains. In the case of titanium dioxide, typical precursors are titanium tetrachloride and water. Under these conditions with a PS-*b*-PMMA film as the substrate, TiO_2 grows selectively in the PMMA domains because of chemical interactions between the titanium tetrachloride ($TiCl_4$) molecules and the carbonyl moieties along the PMMA chains. Subsequent reaction with water completes one SIS cycle and leaves hydroxyl groups available, which in turn seed the TiO_2 growth in subsequent SIS cycles. An important advantage of SIS is that the reaction is self-limited, meaning a well-defined amount of material will be grown with each cycle, so by selecting the number of cycles, the amount of material grown — and hence the nanostructure dimensions — can be tuned precisely. The residual polymer will then be removed by thermal treatment, which will also serve to crystallize the titania into the anatase phase and thereby render it photocatalytically active.

Mission Relevance

This project is relevant to DOE's missions in science and the environment, with particular synergy with the Materials Chemistry program within the Materials Sciences and Engineering (MSE) Division. Our society is entering a period of water crisis. New filtration technologies will be a central piece of the solution to this grand challenge. Here we are using a low-cost combination of block copolymer self-assembly and a novel technique called sequential infiltration synthesis to prepare nanoporous membranes with unique and tunable mechanical, filtration, and catalytic properties. The Department of Homeland Security (DHS), Department of Defense (DOD), and Environmental Protection Agency (EPA) also have strong interest in water-treatment technologies.

FY 2014 Results and Accomplishments

During FY 2014, having surveyed current knowledge and practice, we carried out initial calculations to determine the optimal dimensions for ultrafiltration membranes and developed two methods to fabricate a multifunctional TiO_2 membrane. Following method I, we established the optimal experimental parameters to form vertically oriented PS cylinders in a PMMA matrix, which serves as a template for selective TiO_2 deposition. We then successfully established SIS conditions for TiO_2 deposition. Figure 1A shows a representative scanning electron microscopy (SEM) image of such a TiO_2 membrane (pore diameter: 41.9 ± 6.3 nm) grown by using method I. Through method II, we successfully developed a fabrication method for N-doped and undoped TiO_2 membranes via ALD using aluminum oxide (Al_2O_3) filters as a template. Figure 1B shows absorption spectra of doped and un-doped TiO_2 membranes. A clear distinction of the absorption edge spanning toward visible transitions was observed for the novel N-doped TiO_2 membrane, and this observation is in good agreement with the calculated imaginary part of the permittivity of N-doped TiO_2.

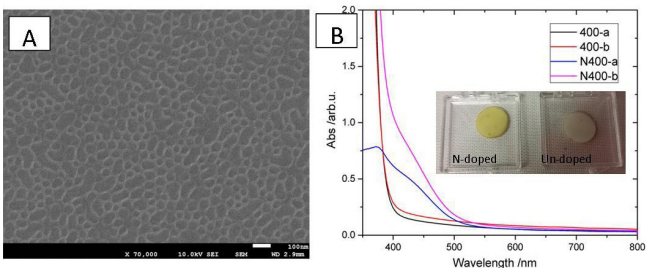

Figure 1. (A) Results from method I showing an SEM image of TiO_2 membrane via SIS process on PS-b-PMMA and (B) method II results showing absorption spectra of N-doped and un-doped TiO_2 obtained via an ALD process on Al_2O_3 membranes at 400°C. The letters a and b refer to two different samples. The inset shows a photograph of doped and un-doped TiO_2 membranes.

In addition, we designed and fabricated a dead-end filtration test set-up and began filtration tests for commercially available membranes in order to establish our figure-of-merit quantity.

Proposed Work for FY 2015

After manufacturing the membranes, their efficacy will be tested. The first step will determine the mechanical stability and processing speed capabilities of the membranes by monitoring the flux and permeability of deionized water traversing the membranes as a function of filtering pressure.

The selectivity of the membranes will be assessed by passing solutions containing particles of various types (e.g., ions, organic molecules) through the membranes and analyzing the material that traverses the membrane for particle content. The next phase will involve transitioning from model particles to biomaterials, as well as exploring the membrane photocatalytic activity. Removal of viruses and the antibacterial properties of the membranes will be tested against *Escherichia coli* bacteria. As the project evolves, separation of other biomaterial classes such as proteins will be explored.

Timescale of Groundwater Transport: A Prerequisite for Developing and Maintaining Groundwater Reservoirs

2014-188-N0

Zheng-Tian Lu and Wei Jiang

Project Description

Assessing groundwater behavior in aquifer systems is an indispensable part of developing and maintaining groundwater reservoirs. With the recent development of the Atom Trap Trace Analysis (ATTA) method at Argonne National Laboratory, measurements have been enabled of rare noble gas isotopes that possess nearly ideal chemical and physical properties for determining the timescale of groundwater transport. Our project will apply these tracers to investigate two aquifer systems that are important sources of groundwater exploitation in Israel. This project will be conducted with researchers from the University of Chicago and Ben Gurion University. Our research involves pursuing technical developments to enhance the sample throughput capacity and promote accurate data interpretation. Once successfully implemented in Israel, this new methodology can also be used to quantify potential groundwater production from many hydrogeologically complex basins around the world.

Mission Relevance

This project supports missions in DOE's Office of Nuclear Physics, which has long supported the development of the novel isotope trace analysis method as an application within the field. By using the laser spectroscopy and atom-trapping tools of nuclear physics, we have developed a sensitive instrument with a wide range of applications in the earth and environmental.

FY 2014 Results and Accomplishments

For the first time, the ages of samples of very old groundwater in Israel have been revealed. We sampled 32 wells across Israel; samples from 10 of these wells were analyzed (Figure 1), among which 5 samples were found to be older than 30 ka, beyond the reach of ^{14}C dating (ka stands for a thousand years). The oldest water found so far, at an age of 236 +/− 28 ka, is located near the Dead Sea.

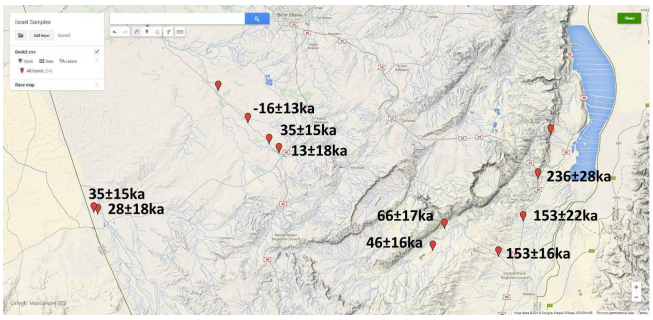

Figure 1. ^{81}Kr ages of groundwater in Israel, where "ka" denotes "one thousand years."

Regarding development of instrumentation for ^{81}Kr dating, we demonstrated that the ion current resulting from collisions between metastable krypton (Kr) atoms in a trap can be used to measure the trap loading rate precisely. We measured both the ion current of the abundant isotope ^{83}Kr (isotopic abundance = 11%) and the single-atom-counting rate of the rare isotope ^{85}Kr (isotopic abundance ~ 1×10^{-11}) and found the two quantities to be proportional at a precision level of 0.9%. This work resulted in a significant improvement in ATTA as an analytical tool for isotope ratio measurements.

A simple yet highly efficient method was developed to generate optical sidebands on the output of a high-power tapered amplifier at the GHz frequency range. This method is now applied to the ATTA laser system and improves both the efficiency and reliability of atom trapping.

We also analyzed groundwater samples extracted near the Waste Isolation Pilot Plant (WIPP), New Mexico. The ^{81}Kr ages are found to be ~130,000 and ~330,000 yr for high-transmissivity and low-transmissivity portions of the aquifer, respectively, implying substantial physical attenuation of conservative solutes in the Culebra Dolomite aquifer and providing limits on the effective diffusivity of contaminants into adjacent formations. A second field campaign to extract more samples from this region is being planned with hydrologists from Sandia National Laboratory. We believe that ^{81}Kr will become a standard tracer for mapping and characterizing isolated aquifers of particular interest worldwide (e.g., those near nuclear waste repositories), as well as storage sites of captured CO_2.

Proposed Work for FY 2015

The remaining 22 samples extracted during the field campaign of FY 2014 will be fully analyzed, followed by a second field campaign. Both an upgrade to the gas recirculation system and the development of a vacuum ultraviolet (VUV) lamp are under way. The lamp is to be used to realize optical excitation of Kr atoms into the metastable level. If successful, it would replace the discharge source, resulting in possibly dramatic improvements in atom-counting efficiency and reduction in the memory effect.

Membrane-Biofilm Nexus: Advanced Membrane Autopsy as a Tool for Revealing Membrane Biofouling and Development of New Membrane Materials and Structures

2014-189-N0

Meltem Urgun-Demirtas, Seth Snyder, and Jack A. Gilbert

Project Description

The interdependency of water and energy requires development of cost-effective water treatment technologies. Technological advances in membrane separations have been used extensively in water and wastewater treatment applications. However, membrane biofouling is a major obstacle in the application of membrane filtration processes to water purification and reclamation. Obtaining a fundamental understanding of the nature of biofouling is crucial for sustainable operation of membranes to meet desired water quality and performance criteria. With researchers at Ben Gurion University (BGU) and the University of Chicago (UofC) we are developing a tool to diagnose, predict, and provide guidance for the prevention and control of membrane biofouling. We have outlined three tasks, including: (1) metagenomics of fouled membranes, (2) modeling of biofouling mechanisms, and (3) development of new anti-fouling membrane surfaces.

Mission Relevance

The project is tied to DOE's mission in energy security and environmental quality. This project offers energy savings in water treatment, a critical focus of the energy-water nexus (EWN). Increasing our core understanding of biofouling will be of significant interest to water/wastewater utilities and the membrane industry, as this tool is expected to help resolve current operational issues relating to membrane biofouling. It also seeks to provide sustainable membrane operation through effective cleaning and mitigation strategies and to reduce power, cleaning, and membrane replacements costs. This project seeks to provide essential industrial knowledge to further development of more robust "smart" membranes and more efficient water treatment processes.

FY 2014 Results and Accomplishments

We conducted an extensive review of utilization of membrane types and materials, both at wastewater treatment plants and in published research. We found that polyethersulfone ultrafiltration (PES UF) membranes are in wide use and chose them as the initial ultrafiltration membranes to be used in this project. Initial experiments in the designed membrane unit were conducted by using PES UF filters (150 kDa MWCO [molecular weight cut-off]) (Figure 1). These membrane filters were initially tested with tap water to (1) determine the initial colonizers on the membrane surface, determine the method detection limits of the metagenomics tool, and develop methods for membrane handling for metagenomics sampling and (2) evaluate performance and compare our findings with manufacturer's data.

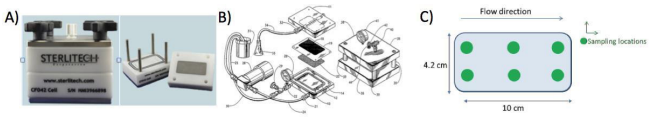

Figure 1. (A) Membrane unit used for this project (adapted from Sterlitech), (B) system setup (Osmonics), and (C) sampling locations on the membrane for metagenomic testing.

Three membrane filters were tested using tap water (potable, 25 L) with trials lasting ca. 8 hours. We developed a protocol to preserve attached bacteria and prevent contamination. Metagenomic analysis yielded a bacterial concentration of about 10 ng RNA/liter — less than the amount needed for metagenomic analysis. Therefore, we decided to use reclaimed water from the Stickney Water reclamation plant (WRP) in Illinois to increase the probability of detection.

We developed a "toolbox" of methods for membrane modification. A series of polysulfone membranes were modified by using ultraviolet (UV) -initiated graft polymerization via a traditional approach (UVA Cube) and a specially developed approach (3-D printed membranes). Using patterned UV light, we obtained patterned surface modifications on the membrane (Figure 2). In addition, printing methods were developed that showed precise control of the surface chemistry and hydrophobicity. These methods were extended to nanoparticle deposition on membranes and provide the capability for iterative testing and feedback/guidance for developing biofouling models.

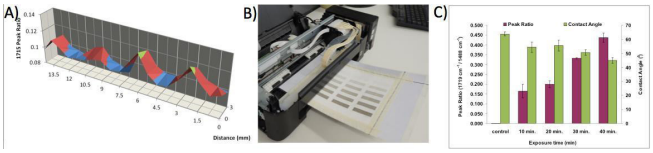

Figure 2. The growing toolbox of membrane fabrication techniques: (A) patterned modified membranes made via 3D printing methods, (B) functional nanoparticles printed on membranes, and (C) printed membranes series with decreasing hydrophobicity.

Initial experiments with patterned membranes were conducted by using final effluent from the Stickney WRP. The performance of each membrane was determined by flux measurements and collection of water samples. The decline in the flux measurements (or the flow rate of fil-

trate i.e., the water passing through the membrane, per unit area of membrane) is an important factor in modeling the fouling mechanism. We analyzed the feed water, permeate, and retentate samples to characterize the performance of membrane. We also analyzed surface properties and the morphology of membranes (virgin and fouled membranes) by using the contact angle (hydrophilicity) and scanning electron microscopy (SEM). These experiments are ongoing and in progress; however, data gathered to date show significant differences between functionalized and control membranes. Modified membranes yielded a lower net loss in flux and may indicate a slower kinetics of fouling. In progress are the metagenomic analyses, and we expect that this method will generate quantitative data that reveal the structure and function of the microbial community on the membrane surface and on the initial colonizing bacteria, as well as provide the information for the biofouling modeling.

Proposed Work for FY 2015

In FY 2015, we plan to:

- Reveal the community structure and function in biofilms,
- Identify the mechanism for initial colony attachment and the rate of cells' adhesion,
- Deliver the biofouling model, and
- Fabricate "smart" membranes.

Turbulent Transports in Cumulus Topped Boundary Layers

2014-193-N0

Virendra P. Ghate

Project Description

Boundary-layer cumulus clouds are intimately tied to the turbulence in the boundary layer and form when enthalpy, moisture, and momentum are transported upward from the Earth's surface. These clouds are a crucial component of the Earth's radiation budget and need to be represented accurately in global climate models (GCMs) used to predict the future climate, extreme weather events, and energy demands. As these clouds occur at spatial and temporal scales much smaller than can be modeled in the GCM grid box and temporal resolution, their effects and the associated processes need to be parameterized in the GCM.

The overall goal of this project is to improve the representation of cumulus clouds in GCM. The specific objectives of the project are to (1) characterize the vertical velocity structure of the entire cumulus-topped boundary layer, (2) explore the similarities and differences between subtropical and tropical shallow cumuli, and (3) characterize the turbulent transport of water vapor within the cumulus-topped boundary layer.

Mission Relevance

This project falls under DOE's energy, environment, and basic research missions. The research to be conducted uses data collected at the Atmospheric Radiation Measurement's (ARM's) climate research facilities to quantify the interactions among aerosols, clouds, precipitation, radiation, dynamics, and thermodynamics and thus to improve our fundamental, process-level understanding, with the ultimate goal of reducing the uncertainty in global and regional climate simulations and projections.

FY 2014 Results and Accomplishments

In the project's first year, we identified 14 cases of shallow cumulus cloud occurrences at ARM's observation site in the Azores and 19 cases of shallow cumulus cloud occurrences at its site on Manus Island. A total of 200 hours' worth of data collected at the Azores site and 306 hours' worth of data collected at the Manus site by multiple instruments were analyzed to generate ensemble statistics of thermodynamic and dynamic parameters. In addition, a one-dimensional radiative transfer model was used to simulate the profiles of shortwave and longwave radiative fluxes.

The updrafts within the cumuli over Manus were stronger, with a mean velocity of 0.77 m s^{-1} as compared to the updrafts within the cumuli over the Azores, which had a mean velocity of 0.58 m s^{-1}. The mean radar reflectivity within the cloudy updrafts was −25.22 dBZ at Manus, whereas it was −29.96 dBZ at the Azores. The results of our analyses collectively suggest that the shallow cumuli over Manus were thicker and are associated with deeper mixed layers that had a greater amount of longwave radiative cooling near cloud top as compared to the cumuli over the Azores. The updrafts within the cumuli were stronger and contained relatively bigger drops over Manus as compared to the cumuli over the Azores. Figure 1 shows the thermodynamic and wind structure of the cumulus-topped boundary layers at the two locations, along with the cloud locations. Apart from the differences in the potential temperature and water vapor mixing ratio, the boundary layer wind structure also differed greatly between the two locations.

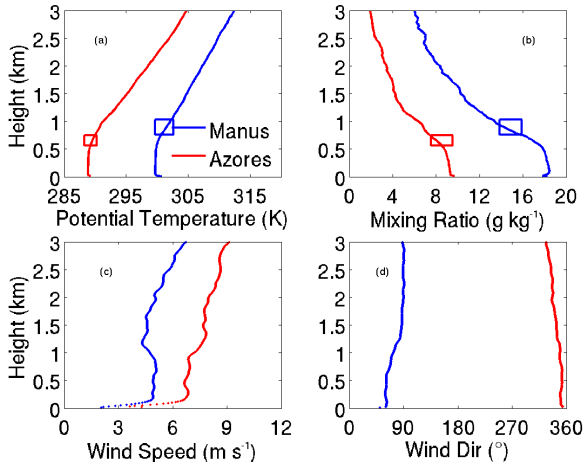

Figure 1. Averaged profiles of potential temperature (a), water vapor mixing ratio (b), wind speed (c), and wind direction (d) associated with cumulus-topped boundary layers observed at the ARM observing facilities at Azores (red) and Manus (blue). The boxes in the upper panels correspond to the average cumulus cloud locations and thicknesses at the two sites.

Proposed Work for FY 2015

In FY 2015, we will pursue completing the following tasks:

1. Combine the data collected by the vertically pointing Doppler cloud radar and Doppler LIDAR to characterize the turbulence structure of the entire cumulus-topped boundary layer and
2. Use the high temporal and range resolution observations of the water vapor mixing ratio made by a Raman LIDAR to characterize the transport of water vapor within a cumulus-topped boundary layer.

LDRD

Director's Grand Challenge

ANNUAL REPORT

2014

Integrating Simulation and Observation: Discovery Engines for Big Data

2013-165-R1

Ian T. Foster, Salman Habib, and Ray Osborn

Project Description

This project leverages new data sources, innovative data-intensive computing technologies, and high-performance computational simulation to advance cosmology and materials science. We aim not only to develop transformative new capabilities in those disciplines, but also to advance the technologies of acquiring, managing, integrating, analyzing, and sharing large quantities of experimental, observational, and simulation data.

In both cosmology and materials science, rapid evolution in sensor technology is producing a tsunami of data that are transforming the nature of inquiry in what historically have been data-poor disciplines. For example, in cosmology, digital sky surveys can now capture detailed information on the location and brightness of billions of celestial objects, with detailed spectra for millions of them. In materials science, advances in instrumentation and experiment design have accelerated the rate at which data can be collected at Argonne's Advanced Photon Source (APS) and other major DOE facilities, with rapidly increasing use of state-of-the-art multidetectors capable of data rates of 1 GB/s or more. At the same time, advances in high-performance computing enable new computational simulations capturing unprecedented detail.

This data explosion introduces the exciting opportunity of rigorously testing explanatory models of phenomena, such as cosmic acceleration — models that could previously not be formulated and/or tested because of inadequate data. By using supercomputers, it is now becoming feasible to bring together results from theoretical modeling and data in new ways, testing existing approaches with unprecedented rigor, and/or inferring entirely new models from first principles.

To seize this opportunity, we are developing new methods for (1) creating and analyzing virtual skies from large-scale simulations, carried out on supercomputers such as Mira, with unprecedented detail and (2) enabling new research modalities based on the integration of advanced data analysis and simulation methods and high-performance computing with data collected from APS beamlines (Figure 1). We also work on (3) data and workflow management technologies, with the goal of automating time-consuming tasks associated with data ingestion, data storage management, definition and application of computationally intensive analysis processes, indexing and discovery of data products, and other data pipeline activities.

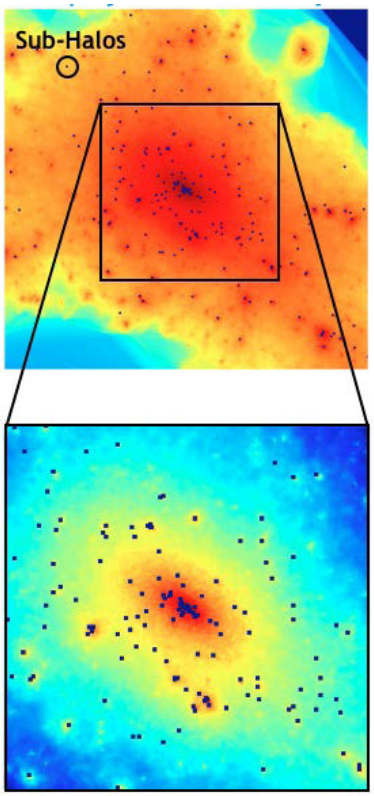

Figure 1. Subhalo tracking in a large halo from a supercomputer simulation. Colors depict halo density from our new density algorithm. The detailed subhalo tracking is accomplished by using the history of individual particles as they traverse a merger tree to their final end locations.

Mission Relevance

Our project is tied to DOE's mission in science. Large-scale data management is increasingly important to DOE mission goals, particularly in the Office of Science, because of rapidly growing data volumes from both instruments and simulations. Our work is addressing major challenges in Basic Energy Sciences and in High Energy Physics, developing technologies important for the APS upgrade, and producing results that will enable creation of an effective Science Data Facility for DOE.

FY 2014 Results and Accomplishments

Our work in FY 2013 was concerned with refining the design of various project components, building initial prototypes, and producing our first scientifically useful outputs. We performed our first large-scale cosmological simulations; developed our first high-performance data analysis codes; and deployed our first methods and tools for data collection, management, and cataloging.

Our work in FY 2014 included the following:

Cosmology

In cosmology, we:

- Ran some of the world's largest cosmological simulations and created a multi-Petabyte dataset as an input for our large data analysis tasks — a dataset that is bigger than any contemporary observational dataset in terms of raw size;
- Designed and prototyped a SaaS portal for cosmological data analysis;
- Designed and implemented new approximate algorithms for large data problems in cosmology, including density estimation, merger tree, and sub-halo tracking; and
- Designed and investigated database solutions for Level 3 simulation data.

Materials Science

In materials science, we:

- Developed innovative new end-to-end high-performance APS data processing pipelines for three different experimental modalities (diffuse scattering, near- and far-field HEDM) — including real-time data reduction workflows — for diffuse scattering experiments on bilayer manganites, other transition metal oxides, and iron-based superconductors (Figure2);

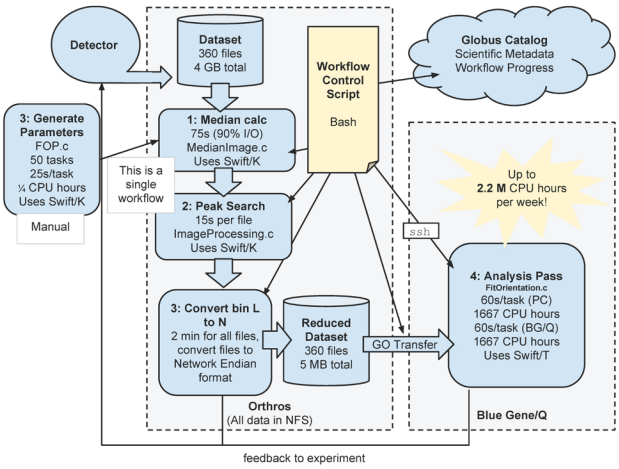

Figure 2. Our Near-Field High Energy Diffraction Microscopy (NF-HEDM) data reconstruction and analysis pipeline, showing the preparatory phase that is performed on an APS cluster and the analysis phase that is performed on the Argonne Leadership Computing Facilities IBM BG/Q supercomputer.

- Engaged with 10 APS sectors in various ways;
- Designed methods for simultaneous visualization of experimental data and defect model simulations;
- Completed molecular dynamics simulations for modeling diffuse scattering, thus integrating theory with experiment; and
- Created data analysis pipelines to accelerate high-energy diffraction microscopy experiments.

Data and Workflow Management

In data and workflow management, we:

- Created file system and management methods for interactive parallel analysis;
- Created new catalog methods supporting free text and metadata export;
- Created a pluggable dataset ingestion and publication architecture;
- Created a catalog used for multi-experiment data collection; and
- Completed integration of Swift, Galaxy, MPI, and OpenMP for parallel computation — enabling large-scale parallel execution on up to 100K cores

Proposed Work for FY 2015

We plan to achieve large-scale integration of experiment and simulation in both cosmology and materials science, expand use of high-performance computing, and extend our methods to additional APS beamlines.

In cosmology, we aim to complete/optimize our scalable algorithms suite; release the first production version of the SaaS cosmology portal for analyzing simulation data; complete our database implementations; and carry out science analyses exercising the full system including observational data.

In materials science, we aim to apply our end-to-end APS data processing pipelines to challenging experimental studies, evaluate their performance in realistic settings, and collect data for publication. We will also extend our techniques to handle other x-ray techniques within the APS.

In data and workflow management, we will demonstrate large-scale end-to-end applications with multiple science groups; develop methods for high-speed data acquisition and analysis, with on-demand computing, automated data ingest, and cataloging for notebook and search; and demonstrate our ability to create large catalogs of experimental, simulation, and derived data.

Seminars

Almer, J., S. Stock and R. Suter (2014). "Studies of Complex Materials using High-Energy X-rays." Diamond Light Source, Oxfordshire, England, May 29, 2014.

Foster, I. (2014). "Publication Services for Materials." 2014 Seminar at the PRISMS Center, University of Michigan, Ann Arbor, MI, June 24, 2014.

Habib, S. (2014). "Computing the Universe: How to Stuff a Supercomputer Inside a Laptop." Carnegie Mellon University, Pittsburgh, PA, April 2014.

LDRD

Hard X-ray Sciences

ANNUAL REPORT

2014

Feasibility Study of Applying Thin-Film High-Temperature Superconducting Films on Copper or Niobium-Sputtered-on-Copper for the Purpose of Achieving Helium-Free Operation with Cryocoolers

2013-111-R1

Alireza Nassiri, Robert Kustom, and Thomas Proslier

Project Description

This project focuses on feasibility studies of the application of magnesium diboride (MgB_2) thin films with high superconducting critical temperature (T_c) to radio frequency (RF) cavities. Studies are directed toward applying the films to niobium cavities, with the goal of increasing the accelerating gradients to greater than 50 MV/m. Our research has been directed toward depositing MgB_2 films onto copper (Cu) or other high-thermal conductivity metal substrates, which would allow future cavities to be fabricated as film-coated copper structures.

Mission Relevance

This project supports DOE's mission in science. By achieving the successful thin-film coating of MgB_2 or other possible high-T_c material films, it would be possible to design and build helium-free superconducting RF (SRF) systems for synchrotron light source storage ring cavities, future x-ray free electron lasers (XFELs), and energy recovery linacs (ERLs). These future projects would benefit from lower design, equipment, and fabrication costs that easily could be 10–20% of current construction costs for a liquid helium system. A cryocooler system also promises greatly reduced operational complications and maintenance. RF cavities using thin-film technology and cryocooler systems have the potential to attract researchers and practitioners in the industrial and medical fields for whom performance of linear accelerators at the highest accelerator field levels would be less important than simplicity of installation, operation, and maintenance. In addition to RF applications, the ability to coat superconducting MgB_2 films onto objects with arbitrarily complex shapes could be very beneficial for a superconducting magnet operating at 10 K, thereby supporting DOE missions by eliminating the use of liquid helium at either 4.5 K or 2 K and, thus, reducing the cryogenic footprint and increasing cost-effectiveness.

FY 2014 Results and Accomplishments

In FY2013, the following tasks were accomplished:

- By using hybrid physical-chemical vapor deposition (HPCVD), successfully coated MgB_2 on 2-in.-diameter sapphire substrate at Temple University (see Figure 1). The film thickness variation across the film is about 10%, as shown in Figure 2. The zero-resistance T_c of the film is almost independent of the location at 39.5 K, whereas the residual resistivity changes between 0.5 μΩ•cm and 1.3 μΩ•cm.

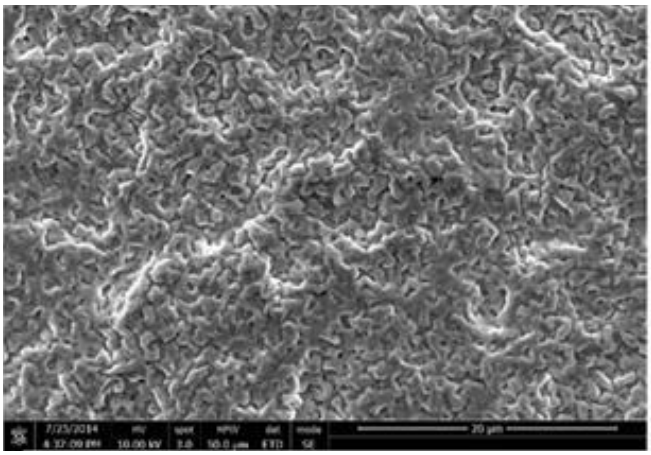

Figure 1. MgB_2 film deposited on 2-in. Nb-buffered Cu disk.

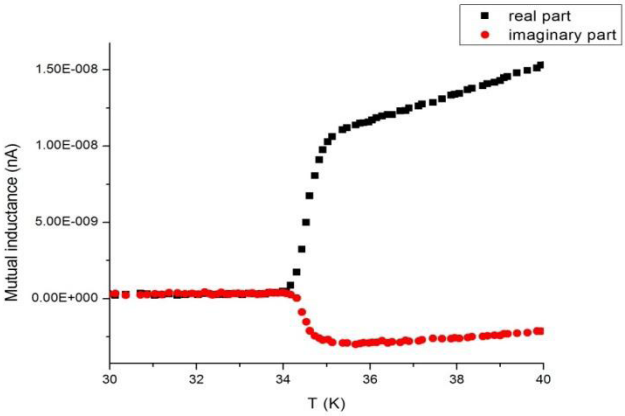

Figure 2. Mutual inductance measurement of MgB_2 film on 22-in.-diameter Nb-buffered Cu disk.

- Produced a design of a 5-cell 500-MHz RF cavity. This cavity operates with cryocoolers in the temperature range of 8–12 K. The second stage is connected to the cavities through commercially available thermal links that are fabricated with many thin high-conductivity Cu foils capable of flexing and absorbing motion and differences in thermal contraction. The first stages are connected to heat shields and other heat intercept points from the room temperature flanges.
- Conducted atomic layer deposition (ALD) experiments in a homemade ALD system, with *in situ* monitoring

(RGA and QCM). After modifying the ALD system to be able to handle safely Diborane gas (B_2H_6), we attempted to use $Mg(Cp)_2$ and B_2H_6 below the decomposition point of Diborane (<250°C) without success. Our chemist collaborators at Illinois Institute of Technology suggested using TriEthylBorane [$(B[Et])_3$ or $(B[C_5H_5])_3$] as a more reactive source of Boron and stable to higher temperature (350°C), relying on the combination of both precursor's organic ligands at high temperature to form volatile compounds, as seen in the literature with other precursors. However, this attempt did not succeed with $Mg(Cp)_2$.

- In parallel to the synthesis effort, investigated the growth of epitaxial magnesium oxide (MgO) as a potential tunnel barrier or nucleation layer for the growth of epitaxial MgB_2 (001). We found that at a moderate temperature of 300°C, as compared to the usual deposition techniques (sputtering) that require temperature >600°C, we can grow epitaxial MgO (111) on C axis-sapphire.

In 2014, we continued our investigation on using ALD technique to grow MgB_2 on Cu. We made significant progress with very encouraging results pursuing HPCVD techniques to coat MgB_2 thin film on both sapphire and Cu coupons. Our pursuit of achieving demonstrating successful deposition of MgB_2 on a large Cu sample (2-in. coupon) began with MgB_2 films deposited on commercial thin Cu foils, cut into 5 mm × 5 mm size. Films were deposited at 620°C on Cu covered by an approximately 80-nm-thick MgO buffer layer deposited by sputtering. We found that the surface morphology changed significantly with temperature. Films were less uniform at higher temperature. Substrates used in depositions at temperatures above 650°C readily showed cracks in the buffer layer, while depositions at lower temperatures allowed for a more uniform coverage of the substrate.

Next, sputtered films of niobium (Nb) were investigated as a buffer layer. This process was adapted to 2-in. Cu disks. The MgB_2 depositions were performed in a larger HPCVD chamber. Films deposited on these 2-in. disks showed a very uniform coverage with no visible crack formation (Figure 1). However, the T_c of these films was lower, close to 34 K (Figure 2), which is attributed to non-optimum temperature distribution across the Cu disk and a slightly different gas flow pattern due to its size. Further optimization is under way to achieve better film characteristics.

Proposed Work for 2015

Our research in FY 2015 will include the following tasks:

- Measure MgB_2-coated copper coupons
- Prepare HPCVD-coated Nb cavities
- Measure superconducting properties of MgB_2-coated niobium cavities at cryogenic temperatures
- Fabricate a single-cell 3-GHz copper cavity
- Prepare a HPCVD-coated copper cavity
- Measure superconducting properties of MgB_2-coated copper cavity at cryogenic temperature
- Prepare and measure surface resistivity of as a function of temperature 2-in. copper disks coated with MgB_2 by using plasma-enhanced atomic layer deposition (PE-ALD)

The Tao of Fusion: Pathways for Big-Data Analysis of Energy Materials at Work

2013-168-R1

Chris Jacobsen, Francesco De Carlo, Ian T. Foster, Sven Leyffer, Todd Munson, Suresh Narayanan, Thomas Peterka, Nicholas Schwarz, Stefan Vogt, and Stefan Wild

Project Description

The Advanced Photon Source (APS) at Argonne is the largest single scientific user facility in the United States, and it generates 100–300 Terabytes of data per month across 60 different experimental endstations serving about 5000 researchers per year. We are developing data workflow management tools to allow for automated transfer of data from a computer tied in with an x-ray detector to a central storage system with cataloged metadata and experiment-based access control. We are developing optimization methods for combining images taken at different length scales and from different instruments. These activities are aimed at the imaging of energy materials via tomography and fluorescence microprobe analysis and are geared toward real-time analysis of the per-pixel time correlations at the heart of x-ray photon correlation spectroscopy. Our goal is to pioneer capabilities that might then serve as a model for facility-wide implementation and for follow-on computational research.

Mission Relevance

This project is relevant to the Department of Energy's mission in Basic Energy Sciences (BES) and in Advanced Scientific Computing Research (ASCR). It aims to test a possible approach for facility data management and access, in which beamline data are automatically transferred to a central storage system (and, upon confirmation, deleted from the beamline computer to free up its storage space). Access permission is to be automatically configured to include users listed on the Experiment Safety Approval Form (ESAF) and provided through APS User Accounts, as well as Globus Online. This approach will allow for far more efficient management of data, freeing up BES facility staff to concentrate on user support and analysis, and will

lead to better utilization of the data through easy dissemination. Multiscale and multimode x-ray imaging leverages expertise from ASCR-supported research at Argonne and serves as an example of the "big data" analysis capabilities needed for more effective utilization of the data taken at BES light source facilities.

FY 2014 Results and Accomplishments

In FY 2013, we acquired a data storage system with about one-tenth the cost and rack space per terabyte as previous systems used at the APS.

We began testing the Spade (nest.lbl.gov/projects/spade/html/) data transfer system from Lawrence Berkeley National Laboratory as a possible code base that we may want to contribute to in the future. This system is being tested as an approach for automatic data transfer from a beamline data acquisition computer to a central data store. We also identified a method for organizing data access, and initiated the software development effort required to test it and put it into production. We worked with the Globus Catalog team to provide specifications first, and early testing later, of the capabilities it can provide for metadata catalogs to enable searches through datasets.

Project work in FY 2013 also resulted in the development of a multiprocessor framework and the acquisition of parallel computing hardware for real-time photon correlation spectroscopy analysis. We demonstrated multiscale and multimode image fusion on example fluorescence data sets, and we delivered (via a contract to 2ndlook.co) an open-source software package, MANTiS. This was written in Python/Qt, which provides a story-board-guided approach to spectromicroscopy analysis.

In FY 2014, we have achieved results as follows:

- Demonstrated an approach for automatic data transfer from a beamline data acquisition computer to a central data store.
  - We completed a daily database update system to create user accounts on our storage system from the APS User database. (*As a result, our storage server now has 16,000 user accounts, which is significant.*) We also established a daily database update from the APS ESAF database, which is separate from the user database. With these two connections, we can have Unix accounts for each user and Unix groups for the data from each experiment (as defined by an ESAF). Access to data will initially be limited to those users who are listed on an ESAF. A web interface will then be provided to let the experiment's principal investigator, as well as the responsible APS beamline scientist, add or remove users from the Unix group to add or revoke data access privileges.
  - We have tested the software package Spade from Lawrence Berkeley National Laboratory to automatically transfer data from a beamline computer to the project's 0.24-petabyte data storage system. After some testing, we will have Spade verify the integrity of data on the central storage system and then automatically delete it at the beamline computer so as to free up its more limited data space. This storage server has Globus Online access to enable users to transfer their data to their home institutions in a rapid, robust fashion.
- Developed and published a software package, TomoPy, that provides a streamlined workflow for tomographic data reconstruction and analysis. This program is proving popular and is being adopted by Berkeley Lab and Brookhaven National Laboratory.
- Explored a supercomputer implementation of TomoPy, enabling a 700-fold speedup of reconstructions.
- Began developing a program, "Maps2Py," to incorporate fluorescence tomography data into the TomoPy framework.
- Developed a flexible HDF5 file schema for the storage of multimodal imaging data.
- Developed a model-based reconstruction scheme for x-ray fluorescence tomography, which is also able to incorporate other data modalities, such as differential phase contrast imaging.
- Delivered (via a contract with 2ndlook.co) an open-source software package, MANTiS, written in Python/Qt, which provides a storyboard-guided approach to spectromicroscopy analysis. This package has since been enhanced by the addition of non-negative matrix analysis capabilities.

This work resulted in the following software copyright:

Gursoy, D., F. De Carlo, W. Di, and D. Vine. "TomoPy: A Python Toolbox to Perform X-ray Data Processing and Image Reconstruction." Software copyrighted February 2014. [ANL-SF-13-123].

Proposed Work for FY 2015

By the end of FY 2015, we propose to complete our project activities as follows:

- Begin operations of our data management system, as described above, for one or more beamlines within our project. We will transfer data from our central storage system to the Petrel system, which has been set up as a data storage prototype system with about 1.7 petabytes of capacity. Work is under way to make this storage system automatically mounted by the Argonne Leadership Computing Facility General Parallel File System (GPS) file system, providing for rapid access to APS data for large-scale analyses involving supercomputer resources.

- Continue to enhance TomoPy and Maps2Py as described above. In particular, we will work toward moving the parallelized version of TomoPy from the status of test tool to a routinely deployed tool and will begin to test Maps2Py with users of the 2-ID beamline's family of x-ray microprobes.
- Test automated tomography reconstruction and automated fluorescence spectra fitting, as part of the automated data workflow system.
- Test model-based fluorescence reconstructions (incorporating other data modalities) on experimental data sets of known samples.

Seminars

Jacobsen, C. (2014). "Cryo Microscopy: Advantages, Challenges and Opportunities." Canadian Light Source, Saskatchewan, Canada, January 14, 2014.

Jacobsen, C. J. (2014). "The Cold, Hard Truth About Cells: Cryo X-ray Microscopy at the Advanced Photon Source." MAX-IV Laboratory, Lund University, Sweden, September 26, 2014.

Jacobsen, C. (2014). "X-ray Microscopy." X-ray and Neutron School, Argonne/Oak Ridge, June 16, 2014.

Jacobsen, C.J. (2014). "Oscillators, X-rays and Global Carbon: Adventures in X-ray Nanofocusing." University of Illinois Chicago, Chicago, IL, April 2, 2014.

Jacobsen, C.J. (2014). "Data and Network Needs at the Advanced Photon Source." DOE ESNet Networking Requirements Review, Washington, D.C., September 10, 2014.

Jacobsen, C.J. (2013). "Oscillators, X-rays and Global Carbon: Adventures in X-ray Nanofocusing." Kansas State University, Manhattan, KS, October 22, 2012.

Jacobsen, C.J. (2013). "Vignettes on the History of X-rays and X-ray Microscopy." Xradia, Inc., Concord, CA, February 2, 2013.

Jacobsen, C.J. (2013). "X-ray Imaging." 15th National School on Neutron and X-ray Scattering, Argonne/Oak Ridge School on X-ray and Neutron Science, Argonne, IL, August 10–24, 2013.

Jacobsen, C.J. (2013). "X-ray Radiation Damage: Limitations and Solutions." Xradia, Inc., Concord, CA, February 22, 2013.

Superconducting Radio Frequency Cavities for Hard X-ray Science

2014-122-N0

Peter Ostroumov, Zachary Conway, Alireza Nassiri, and Alexander Zholents

Project Description

It is possible to produce intense, tunable, high-repetition-rate, hard x-ray pulses with sub-picosecond (sub-ps) durations by adding superconducting deflecting cavities to existing storage rings. Based on this concept, transverse deflecting radiofrequency (RF) cavities are used to impose a correlation between the longitudinal position of an electron within a bunch and its vertical momentum. As the bunch traverses an undulator magnet, the x-ray radiation that is emitted preserves the correlation, and a short x-ray pulse can be chosen by using a pair of slits to select a small, angular range of the pulse after a drift space of about 20 meters (A. Zholents et al., "Generation of Subpicosecond X-ray Pulses Using RF Orbit Deflection" 1999, *Nucl. Instrum. Methods Phys. Res. A* 425, p. 385). The goal of this project is to develop, construct, and test a prototype RF deflecting cavity that exhibits superb electromagnetic properties for operation in Argonne's Advanced Photon Source (APS) storage ring.

Mission Relevance

This project is relevant to DOE's basic science mission. The APS currently operates with electron bunch lengths of 20 ps, and this new RF deflecting cavity would be even more critical in the APS-upgrade lattice, for which a 49-ps bunch length is proposed as the beam is spread out longitudinally, with the objectives being to reduce intra-beam scattering and degradation of the beam lifetime.

Using a superconducting RF (SRF) deflecting cavity is the most cost-effective and technically feasible scheme for producing sub-ps x-ray pulses in electron storage rings. Because of the cavity, there are more customers in all third-generation light sources where storage rings are the operational backbone.

FY 2014 Results and Accomplishments

The primary goal of the work was to demonstrate a high-performance, SRF deflecting cavity, referred to as a quasi-waveguide multi-cell resonator (QMiR). The cavity, as built, is shown in Figure 1. It is composed of a rectangular waveguide that is perturbed from the top and the bottom by three cells that make it strongly coupled to a deflecting RF eigenmode. This eigenmode resonates at 2.815 GHz and is the highest-frequency mode in the lowest-frequency pass-band (2.4 to 2.815 GHz) of the cavity.

The QMiR's uncomplicated geometry makes it well suited for fabrication. Note two things:

Figure 1. The QMiR at 21.75 feet long (top). Niobium parts just before final welding (bottom).

The cavity body was machined from two high-purity (residual resistivity ratio [RRR] of >280), solid blocks of niobium for making an upper and a lower half (Figure 1). The halves were welded together to make the cavity body. The half of the cavity with the waveguide welded into it was conventionally machined so that the side walls were 0.375 inch higher than the height required to achieve the desired resonant frequency. This extra material facilitated the tuning of the resonator during fabrication. Removal, via wire electrical discharge machining (EDM), was done in several steps to achieve the target frequency. The measured frequency dependence for the wire-EDM tuning cuts was +32 MHz/mm, and we achieved a machining tolerance of ±0.04 mm. This was verified by coordinate measuring machine (CMM) measurements made after each wire-EDM step. After the tuning cuts were finished, the cavity halves were welded together.

The Argonne low-beta cavity electropolishing (EP) tool was modified to enable horizontal EP of the QMiR. Functionally, this system is identical to the one used to horizontally polish elliptical cell cavities, except that the aluminum cathode for the QMiR is a flat plate of high-purity aluminum with a 0.063 × 1-inch cross section. During EP, the cavity rotates at about 1/5 revolution per minute (rpm), and the anode-to-cathode voltage is fixed at 18 V. The aluminum cathode was masked to achieve an anode-to-cathode surface area ratio of about 6:1 and to maintain a minimum distance of about 0.5 inch between the anode and cathode along the entire length of the cavity. Because of its unique geometry, the cavity was processed in several steps to ensure that enough niobium material was removed during polishing.

Cold testing of the cavity at 2 K was finished in June 2014. The cavity was fully submerged in a superfluid helium bath and surrounded with two layers of magnetic shielding, which, at room temperature, reduced the ambient field around the cavity to <0.02 mG. The magnetic field at 2 K was not measured but is expected to be less than 0.1 mG, which corresponds to an additional residual resistance of 0.05 nΩ, which is negligible. Work on the QMiR is still ongoing, but results to date from the 2 K RF test (see Figure 2) showed already that the QMiR can achieve deflecting voltages more than 33% greater than the design requirements, and no field emission was observed. The 2 K performance was measured with a fixed coupler; it extends to the limit of the RF power source available for testing. The cavity never quenched during the first set of tests. Brief periods of conditioning were observed, but none lasted longer than about 2 seconds, and the cavity was easily excited to higher stored energies at each step. The total conditioning time was less than 1 hour to reach the field levels reported in Figure 2.

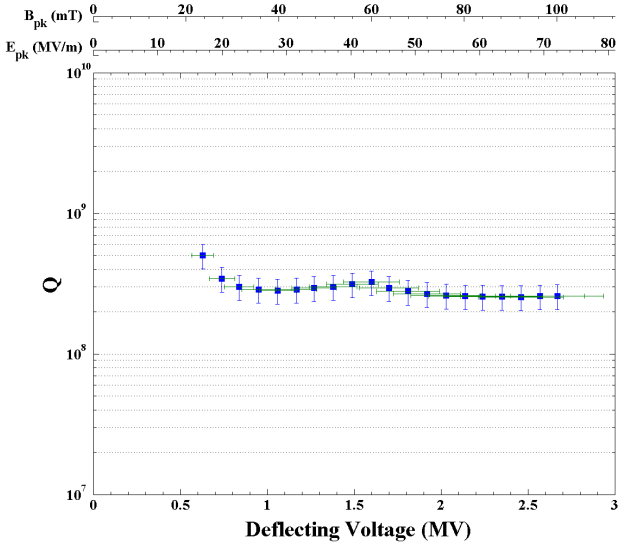

Figure 2. 2 K Q-curve measured for the QMiR. Decay curves were measured at deflecting voltages of 0.7 and 2.6 MV, and all had the same calibration.

Conclusion: In the 2 K cold tests of the QMiR, the measured deflecting voltage (2.7 MV) exceeded the design goal of 2.0 MV. This result demonstrates the excellent electromagnetic and mechanical properties of the QMiR and the viability of the design and fabrication techniques. Electron storage rings may use this cavity for producing ps x-ray pulses with high repetition rates. Given its high field performance, we believe a cavity like this could also be used at the end of a linac in a beam switchyard for distributing high bunch repetition-rate beams to multiple applications.

Development of a Novel Analyzer System for Resonant Inelastic X-ray Scattering with Better Than 10-meV Resolution

2014-127-N0

Jung Ho Kim, Thomas Gog, and Xianrong Huang

Project Description

State-of-the-art resonant inelastic x-ray scattering (RIXS) developments pioneered at Argonne's Advanced Photon Source are now propagating to light sources worldwide. Maintaining scientific leadership in this field will require timely development of the next-generation analyzer system: a system that will pave the way in overcoming the intrinsic energy resolution limit of conventional spherical analyzers. This project focuses on developing an energy resolution that is better than 10 meV — that is, an energy resolution that would be more than three times better than the best one now. The incident photons are being highly monochromatized by a four-bounce silicon (Si) crystal monochromator, producing a 7-meV photon beam. A two-dimensional (2D), multilayer Montel mirror, which collects scattered x-rays with a sufficiently large solid angle of 10 × 10 mrad, is being placed between the sample and the proposed analyzer.

The new analyzer is exploiting three bounces of Si crystals rather than the single bounce of spherical analyzers. The first crystal collimates the scattered beam emerging from the sample. The second crystal disperses the beam, producing a rainbow of energies reminiscent of a prism. The last crystal selects a specific energy and transfers it to the detector. The improved energy resolution of 10 meV that is expected will enable studies of a class of emerging materials that have remained inaccessible, either due to the inherent small energy scales, irresolvable within the current energy resolution of RIXS, or due to the unavailability of samples having a large enough volume in single-crystalline form, as demanded by inelastic neutron scattering.

Mission Relevance

The project is tied to DOE's mission in science. The last few decades have seen a revolution in novel, complex materials that offer a large variety of electronic phenomena important for fundamental science and immediately useful in the technological development of devices. Prominent examples are high-Tc superconductivity, which promises the loss-free transmission of electric power, and colossal magneto-resistance, which enables the highest-density magnetic storage media. The RIXS technique is uniquely suited for studying the electron dynamics in these exciting materials, leading to a more microscopic-level understanding of them and contributing to the ultimate goal of harnessing them in practical devices.

These advances have come in lockstep with improvements in the energy resolution of RIXS, necessary to discern the subtle new electronic features. The significant improvement in the energy resolution of RIXS that should result from this project has broad scientific implications in materials science and is well aligned with one of the Grand Challenges highlighted in the DOE Basic Energy Sciences (BES) program and its Materials Sciences and Engineering Division (MSE).

FY 2014 Results and Accomplishments

All essential optics and Si crystals were designed and manufactured in FY 2014. A Montel mirror for use at 11.215 keV was designed by using three independent calculations. The first was made by the mirror manufacturer, Incoatec; the other two were made by fellow researchers from the Universidade Federal da Integração (UNILA) and Argonne's X-ray Science Division, Optics Group. The mirror was manufactured and delivered in FY 2014. All three Si crystals of the new analyzer system were designed and manufactured. The 7-meV monochromator was designed and implemented, and its working principles and performance were thoroughly tested and characterized. A comparison of the measured angular scans and calculations using dynamical diffraction theory confirmed that the energy resolution is close to theoretical expectations (Figure 1).

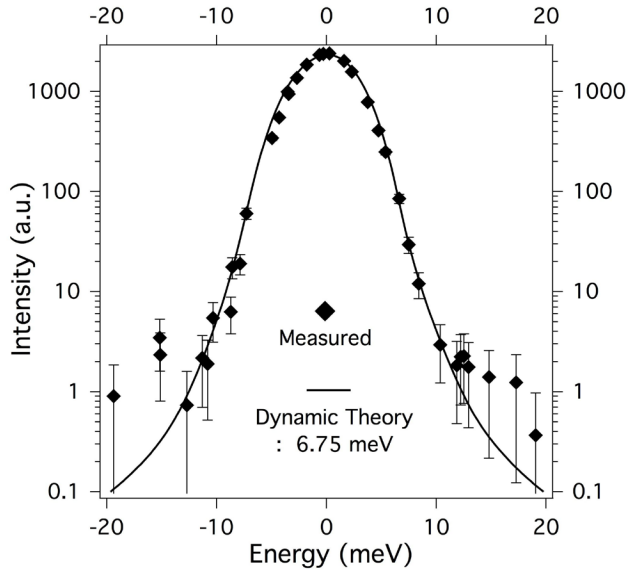

Figure 1. Comparison of the measured energy resolution of the high-resolution monochromator implemented for this project with the resolution calculated using dynamical diffraction theory.

Proposed Work for FY 2015

In FY 2015, the Montel mirror, which collects scattered x-rays from the sample with a sufficiently large solid angle of 10 × 10 mrad, will be commissioned. Then the major focus will be on commissioning the assembled analyzer system, verifying its working principle and performance characteristics. At the same time, preliminary studies of available iridium compounds (such as $Na_4Ir_3O_8$, Na_2IrO_3, and $R_2Ir_2O_7$ [R = rare earth]) will be conducted. These materials exhibit exotic ground states and novel electronic phenomena, such as quantum spin liquids, and they have great potential for contributing to scientific and technological advances.

Three-Dimensional Coherent Diffraction Imaging Using Polychromatic Hard X-rays

2014-134-N0

Stephan O. Hruszkewycz, Paul H. Fuoss, Ross J. Harder, Matthew J. Highland, Wenjun Liu, and Jörg Maser

Project Description

In this project, we are developing a three-dimensional coherent x-ray diffraction imaging (3D-CDI) technique that uses the energy spectrum and integrated flux delivered by an Advanced Photon Source (APS) undulator to rapidly measure volumetric coherent diffraction and that provides ~100-fold reduction in data acquisition time. The central concept of the technique is to scatter a range of x-ray energies from a sample and use a series of very thin analyzer crystals to extract simultaneous slices of coherent scattering from the scattered x-ray beam. The demonstration of this imaging technique has implications beyond the coherent diffraction imaging and materials communities. The ability to measure instantaneous volumetric reciprocal space maps can greatly benefit incoherent ultrafast time-resolved measurements at dedicated timing instruments. This reciprocal space mapping approach can be adapted to improve certain ultrafast pump-probe experiments and can be especially useful in "one-shot" pump-probe studies.

Mission Relevance

This project is relevant to DOE's mission in science and innovation. Development of polychromatic coherent diffraction methods will provide a fundamentally new capacity for the study of novel nanoscale materials and will address outstanding challenges in the field of 3D-CDI, making advances towards *in situ* real-time materials studies. Demonstrating and developing polychromatic 3D-CDI will be useful at DOE light sources that emphasize both coherent imaging and time-resolved physics, including the new National Synchrotron Light Source (NSLS II) and potential diffraction-limited synchrotron facilities.

FY 2014 Results and Accomplishments

We designed and built a post-sample analyzer that resolves the spectrum of a diffracted polychromatic x-ray beam and tested it at the APS. This instrument, shown in Figure 1a, positions the sample and analyzer to diffract in the horizontal plane in a dispersive geometry, such that each pixel in the area detector maps a unique wavelength and exit angle from the diffracting sample. We used this instrument to measure scattering from tilted ferroelectric domains in a lead titanate ($PbTiO_3$ [PTO]) thin film (100-nm thick) grown on a single-crystal dysprosium scandium oxide ($DyScO_3$ [DSO]) substrate. In this ferroelectric, domains with polarization oriented out of the plane of the film adopt a well-defined tilt (~0.3°) away from the surface normal with four-fold in-plane symmetry. We illuminated this film with an unfocused pink beam containing photons with energies ranging from 8 to 9.5 keV by introducing a 3-mm taper in the undulator (Figure 1b). We positioned a single-crystal membrane of 2-µm-thick (001) silicon (Si) in the diffracted beam, such that the 004 Si Bragg reflection dispersed the diffracted pink beam onto a charge-coupled device (CCD) area detector. By scanning the Si membrane, we obtained a series of CCD images that resolved the DSO 003 Bragg peak and two of the four c-domain satellite peaks from the PTO film (Figures 1c-e).

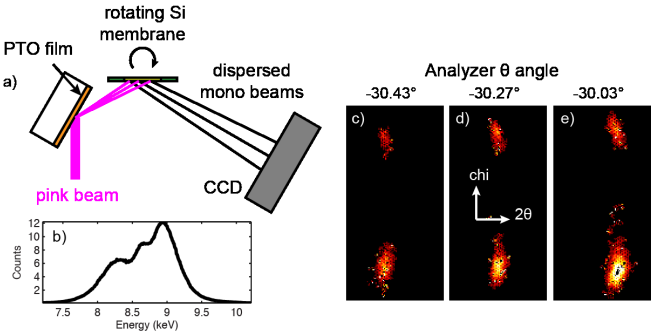

Figure 1. First-generation polychromatic diffraction analyzer system. Schematic of experimental arrangement is shown in (a). The sample and CCD detector were fixed, while the rotating analyzer dispersed the energies in the diffracted pink beam. The tapered undulator provided a broad energy spectrum (b) so that the PTO c-domain twin peaks (c-e) could be recorded.

Interpreting these data requires mapping each detector pixel at every analyzer angle to a unique photon wavelength and exit beam vector. After these quantities are determined, the intensity information in the detector can be rendered in regular three-dimensional (3D) reciprocal space coordinates – a crucial step for 3D coherent diffraction imaging. We developed a numerical ray-tracing code to perform this transformation and have applied it to experimental PTO/DSO diffraction data. The transformed data (Figure 2) are shown in reciprocal space coordinates

alongside their theoretically expected positions. We will (1) extend this initial ray-tracing software by improving the algorithm speed and flexibility and (2) incorporate it into a unified polychromatic coherent Bragg peak phasing program.

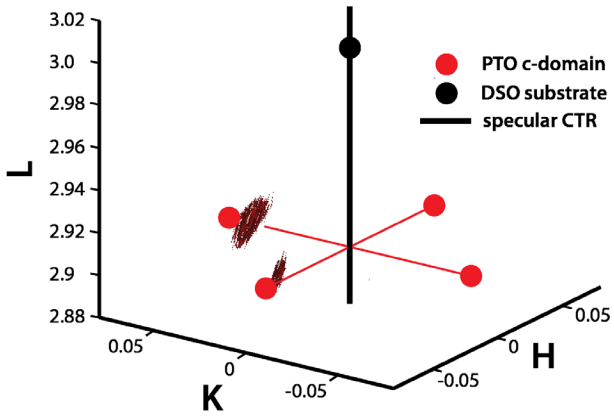

Figure 2. Plot of transformed data from the PTO domain scattering peaks measured with our analyzer system. The resulting 3D c-domain peaks appear in reciprocal space near the positions predicted by theory. In the figure, CTR indicates the crystal truncation rod. The round dots are the predicted theoretical positions of the Bragg peaks, and are shown alongside the measured Bragg intensity data.

Proposed Work for FY 2015

The horizontal scattering design we used in the first measurement demonstrated the feasibility of using a thin single-crystal silicon membrane as a diffracted pink-beam analyzer. This initial apparatus using a horizontal scattering design will be improved with a new configuration that makes better use of the incident beam. We have completed the preliminary design and are in the process of constructing a 3D-CDI instrument that will scatter in the vertical plane, thereby minimizing losses in diffracted intensity due to the horizontal polarization of the synchrotron beam. The new design allows for flexible expansion of the polychromatic diffraction analyzer system to meet the goals of this project over the next two years. In particular, we will measure 3D coherent diffraction patterns by using multiple Si membranes to disperse the pink beam into different angular and energy components. The new design incorporates a high-efficiency Pixirad-1 detector with a tunable energy discrimination window that we plan to utilize to separate the intensity contributions from two different analyzer membranes diffracting simultaneously into the detector.

$YBa_2Cu_3O_7$ High-Temperature Superconducting Prototype Undulator

2014-137-N0

Ulrich Welp and Yury Ivanyushenkov

Project Description

The goal of this project is to develop a short-length superconducting undulator prototype that uses yttrium barium copper oxide ($YBa_2Cu_3O_7$ [YBCO])-coated conductors for the magnet coils. Undulators, as the sources of x-rays, are at the very heart of synchrotron storage rings, as well as free electron laser-based light sources. Advances in brilliance and range of beam energy tunability in the upgrade of the Advanced Photon Source and other next-generation light sources are, therefore, intimately tied to progress in undulator technology. Present superconducting undulators are fabricated with NbTi superconducting wires, a well-established technology. However, niobium-titanium (NbTi) has nearly reached the limits of its performance. At the same time, tremendous progress has been made in high-temperature superconductors (HTS), in particular, YBCO-coated conductors. The YBCO tapes currently under development meet or exceed the performance of NbTi under operating conditions typical for undulators, which would enable a higher on-axis field and, therefore, a higher value for the undulator strength parameter than can be achieved with NbTi. Furthermore, NbTi undulators operate at liquid helium temperature, which requires complicated and expensive cryogenic installations. In contrast, HTS undulators could meet the performance of NbTi while running at a higher temperature, ~10 K, thereby enabling simpler and cheaper cooling systems.

Mission Relevance

This project addresses the area of novel insertion devices within advanced light sources and is related to DOE's mission in science and innovation. In this mission, user facilities such as the Advanced Photon Source play a central role, since they enable us to gain new knowledge about structure and function of new materials that could form the basis for innovative devices. Our project aims at establishing the technology for a new generation of high-temperature superconductor (HTS) undulators that will result in enhanced brilliance and tunability of x-ray beams, thereby directly supporting the DOE's mission.

FY 2014 Results and Accomplishments

Recently, it was shown that barium zirconium oxide ($BaZrO_3$ [BZO]) and barium tin oxide ($BaSnO_3$ [BSO]) inclusions form nano-sized columns, about 5 nm in diameter, by a self-assembly process during superconductor film

growth and significantly improve the critical current. Conductors incorporating BZO currently under development contain 15% Zr and show an engineering critical current density of ~1700 A/mm^2 at 4.2 K in a 5 T perpendicular field. This performance is almost sufficient for our undulator application.

We chose a layout for the coil and winding assembly that uses a unique U-shaped conductor geometry, as shown in Figure 1. The HTS tape, shown in red, is wound into grooves. Subsequent windings have opposite current flow directions, as marked by the arrows. Our design uses 4-mm-wide HTS tapes with a 4-mm gap in between, resulting in a 16-mm magnetic period. To minimize dissipation in the undulator and to avoid overloading the cooling capacity of the cryogenics, we utilize a U-shaped conductor geometry. The header forms the beginning of the windings in two adjacent grooves, as indicated for the first two grooves shown in Figure 1, and the windings in these two grooves are wound simultaneously. Similarly, subsequent pairs are wound by each having a superconducting joint established through the U-shaped conductor at the center. The connection between these pairs is established through resistive joints in the outer-most winding layer, as shown in Figure 1 in orange. In collaboration with SuperPower, a commercial manufacturer of HTS conductors, we have demonstrated that such U-shaped tapes can be produced. Our test results on four 1-meter-length samples that have a 40-μm-thick Cu stabilizer show that the reduction of critical current density (at 77 K, self-field) due to slitting is small, indicating that we will be able to produce conductors in this geometry that carry sufficient current.

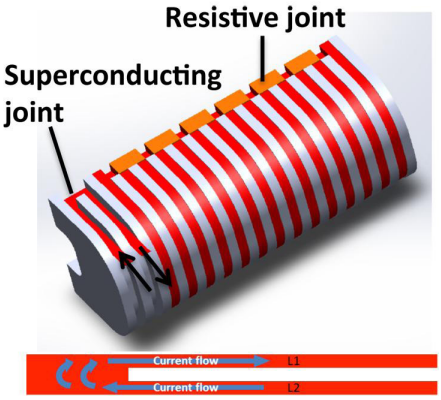

Figure 1. Layout of the undulator magnet. The HTS conductor (shown in red) is wound into the grooves of the magnet core. The connection between the windings in the first two grooves is superconducting and formed by the U-section (see schematic at bottom). The connection between successive such pairs is established through resistive joints (indicated in orange).

There is no prior experience in winding U-shaped HTS tapes. For this reason we performed initial test windings using U-shaped "dummy" tapes, that is, 100-μm thick Hastelloy steel substrate tapes cut into a U-shape at SuperPower. Figure 2 shows our winding setup. The first coil consists of two pairs of wound U-shaped tapes. We plan on winding the magnets without inter-layer insulation, but the windings will be potted in diamond-powder filled epoxy. The high resistance of the steel substrate minimizes potential issues due to current sharing. Furthermore, the relatively small size of the windings and the large degree of flux cancellation result in a low self-inductance and, therefore, in short time constants for settling the current after ramping the field. The possibility of avoiding inter-layer insulation greatly facilitates cooling the magnet and, at the same time, increases the engineering critical current density.

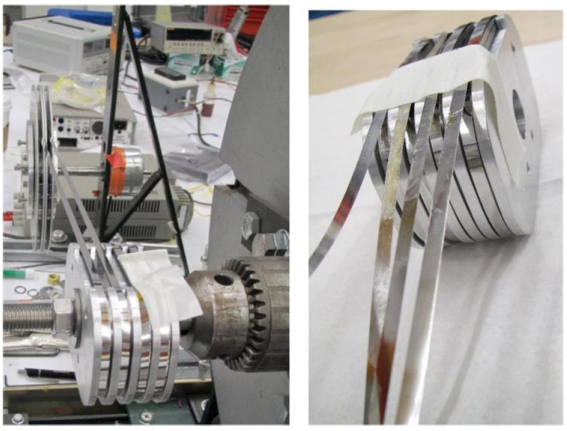

Figure 2. Setup for winding U-shaped conductors (right) and the first magnet windings obtained with U-shaped conductors (left).

Proposed Work for FY 2015

In FY 2015, we will wind initial undulator coils with currently available conductors in order to explore their magnetic performance in relation to our models, test for degradation of the critical current density due to the winding process, and evaluate the thermal stability and quench behavior of the coils. We will fine-tune our design based on the outcomes of these tests. At the same time, our partners at the University of Houston will finalize the synthesis procedures for the high-performance YBCO-coated conductor needed to achieve the anticipated performance of the HTS undulator.

Automation of *in situ* Crystallization Plate Screening and Data Collection at Room Temperature

2014-175-N0

Craig M. Ogata

Project Description

The field of protein crystallography continues to evolve by incorporating an increasing amount of automation from sample crystallization to structure solution. The macromolecular samples being targeted for structural investigation continue to grow in size and complexity. These targets for structure determination are often produced or purified in limited quantities and are difficult to crystallize. The search for x-ray diffracting samples has resulted in an increasing amount of synchrotron beam time devoted to screening small, 5–10-micrometer- size crystals at liquid nitrogen temperatures. The goal of this project is to provide the capability to screen crystals in their original, *in situ*, growth environment at room temperature. This would eliminate damage to the sample as a result of mechanical manipulation and the introduction of chemical cryo-protectants. A secondary goal is to optimize room temperature diffraction data collection procedures and analysis methods for multiple, randomly oriented crystals.

In situ screening will provide early feedback that can be used to direct future crystallization attempts. In addition to feedback for crystallization, there is the opportunity for room temperature data collection on high-symmetry space group crystals (e.g., virus crystals) or from multiple crystals or multiple positions on large crystals. The room temperature data collection will take advantage of micro-beam collimators, with 5-, 10-, 20-, and 300-micrometer-diameter apertures. The automation, support, and motion control for these plates are required to accelerate and move the sample precisely along defined trajectories for data collection in two dimensions (grid) or three dimensions (vector).

Mission Relevance

The project is relevant to DOE's mission in science. The ability to easily obtain fast x-ray diffraction feedback on important biological samples in their crystallization environment is important. There is renewed interest in room temperature data collection as a result of experiments by the group at the Diamond Synchrotron Light Source in England and at the free electron laser (FEL) at the Linac Coherent Light Source (LCLS), Stanford Linear Accelerator Laboratory (SLAC), California. At this time, only a few undulator source beam lines at third-generation sources, such as the Advanced Photon Source (APS), are capable of exploiting the use of a variety of mini-beam data-collection tools that can circumvent radiation damage on a single crystal by automatically moving to fresh, un-exposed, regions of the crystal.

At the LCLS, one of the high-profile successes is serial femtosecond crystallography (SFX). The "diffract before destroy" data collection method has been the primary method for data collection at the Coherent X-ray Imaging (CXI) end station at the LCLS. The samples are delivered at room temperature in a stream of nanocrystal solution, produced by a gas dynamic virtual nozzle (GDVN), in a vacuum chamber environment. Diffraction images are recorded when the x-ray laser pulse and a crystal sample in the stream intersect. Only a single image is recorded per "hit." Over 100,000 images are needed to complete a dataset, so large sample quantities are necessary. The setup in this project will be used to explore a compromise between current synchrotron data-collection methods and the SFX methods at the LCLS. Room temperature data collection will accelerate radiation damage, requiring an increasing number of samples. This project will perform this investigation in preparation for the expected APS Upgrade to a multi-bend achromat (MBA) lattice. The Upgrade is predicted to increase source brightness by a factor of ~90–336 in the range of 8–20 keV and flux density by 4.6–10.4 times over the same range.

FY 2014 Results and Accomplishments

Two main concepts were explored during FY 2014. The first was the identification and characterization of a variety of crystallization formats. These consisted of a crystallization microfluidic array chip, capable of holding 96 different crystallization conditions, developed by collaborators at the University of Illinois at Urbana-Champaign. *In situ* data collection from test protein crystals of lysozyme, thaumatin, and RNAse was completed. The vector data collection was successfully applied to the crystals (Figure 1). We also tested a second type of chip that is used for membrane protein crystallization, the *in-meso* chip. We began collaborative work on a preliminary model silicon nitride–based crystal sample holder developed by researchers at Johns Hopkins University. Data were collected from lysozyme crystals, approximately 10 micrometers in size, which were loaded onto their chip. Virus samples mounted in commercial room temperature loops and large protein complexes mounted in test model grids were also tested on the GM/CA (National Institute of General Medical Sciences [GM] and the National CAncer Institute [CA]) undulator beam line.

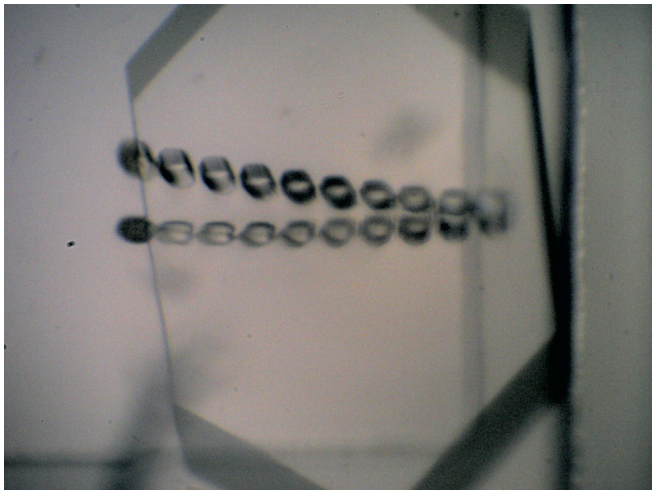

Figure 1. Vector data collection at the GM/CA 23-IDB beam line. The image shows a trail of discrete data collection sites left as footprints, marking the spots at which data were collected on a well-diffracting RNAse crystal grown in a microfluidic chip.

The second aspect of the project refers to hardware development. Design for a large-format crystallization plate holder and an improved microfluidic chip holder are complete. The prototype chip and grid manufacturers are developing fiducial marks on their devices, in order to locate crystals from offline optical or UV methods; the X- and Y-coordinates for crystals will be transferred to the data-collection program. Finally, one of the key developments relevant to the project was the installation of a Pilatus3 6M detector on the GM/CA undulator beam line. This state-of-the-art detector is capable of collecting diffraction images at the rate of a 100 Hz with no electronic noise. It has enabled fast data collection by using shutterless techniques in all data collection modes. The availability of a fast, large format detector is crucial for exploring the possibility of room temperature data collection at high dose and high frame rates. It distinguishes the capabilities of the work on this beamline.

Proposed Work for FY 2015

Our goals for FY 2015 include manufacturing the large and small crystallization chip holders. We will continue crystallographic characterization of a variety of samples in an assortment of crystallization plates/chips. Work will progress toward a fully automated plate delivery system and its integration into the beam line controls.

Long SCU Magnet

2014-184-N0

Yury Ivanyushenkov and Matthew Kasa

Project Description

The first superconducting undulator (SCU) model design has been in operation in Sector 6 of the Advanced Photos Source (APS) storage ring since January 2013. It has been experimentally confirmed that this device, with magnetic length of only 0.33 m, generates higher photon flux at the photon energies above 80 keV than the conventional 2.4-m-long Undulator A, an undulator at the APS. This finding proves that SCUs, even when short, outperform conventional undulators at the high-energy x-ray range. Calculations predict that SCUs with magnetic lengths above 1 m will outperform conventional undulators over the entire x-ray spectrum. Therefore, it is important first to confirm that prediction and then to extend the length of SCU magnets even further.

In this project, we will design and fabricate several 1.1-m-long SCU magnets that will subsequently be used to build longer magnetic assemblies. The magnetic performance of the magnets will be measured in a horizontal cryostat (some parts of which already exist), after the cryostat itself is completed. An existing horizontal magnetic measurement system will be used for the magnetic measurements, and we will also perform magnetic modeling of the long magnetic structures. As part of the project, a two-magnet assembly will be fabricated and tested in a horizontal cryostat, as will fabrication of a test model of a superconducting helical undulator.

Mission Relevance

This project supports development of novel insertion devices that will enable brighter synchrotron x-ray radiation sources — an important part of DOE's mission in delivering major scientific tools to transform our understanding of nature and to advance the energy, economic, and national security of the United States.

FY 2014 Results and Accomplishments

FY 2014 was devoted to fabricating the magnet cores, as well as completing the horizontal cryostat. A new design (compared to the SCU0 magnet), including a novel winding scheme was tested on short cores. Three 1.1-m-long cores were fabricated. The length of the cores was reduced from 1.2 m to 1.1 m to enable use of the SCU0-type cryostat. (This small length reduction does not affect project goals.)

The core fabrication included machining the cores (performed by an outside company), followed by precise coil winding and vacuum resin impregnation, which was completed at the APS SCU facility. It should be noted that an SCU magnet must deliver a high-quality magnetic field. Non-superconducting undulators are usually magnetically tuned to achieve such a precise field. Tuning an SCU in a similar way is challenging because a superconducting magnet is contained inside a cryostat. Argonne researchers at the APS are pursuing an approach that relies on the very precise and controlled fabrication and winding processes, which could potentially lead to a shimming-free

magnet. The measured deviation of the magnet core dimensions from nominal values is within 30 μm rms for a 1.1-m-long magnet. The precise winding of SCU magnets was also achieved, as evident in Figure 1, which shows a cross section of a typical winding pack.

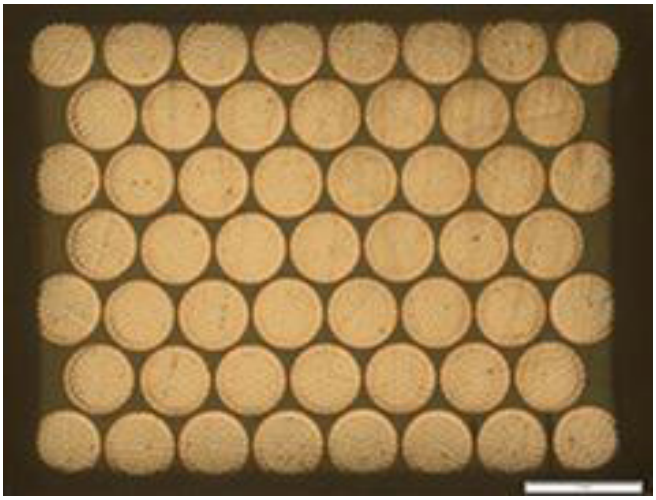

Figure 1. Section through a typical superconducting coil winding pack.

The two-core assembly shown in Figure 2 was tested in a vertical liquid helium cryostat. The magnetic performance of the magnet was measured with a movable Hall probe mounted on a vertical mechanical stage. Figure 3 shows that the design magnetic field of 0.95 T has been achieved. The measured undulator phase errors are remarkably small — within 4.5-degree rms, as shown in Figure 4.

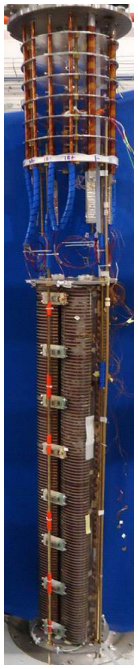

Figure 2. Two-core magnet assembly.

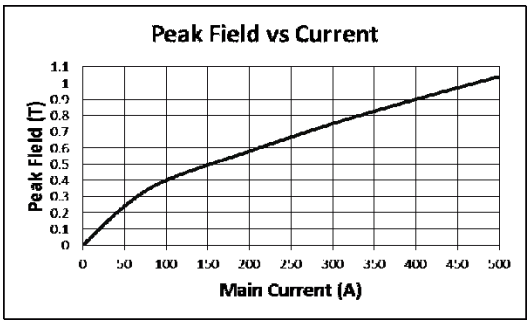

Figure 3. Measured undulator field.

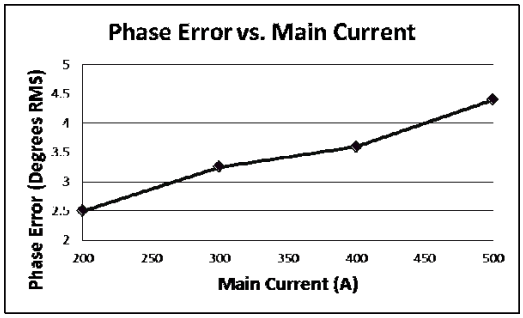

Figure 4. Measured undulator phase errors.

In addition, assembly began on the horizontal, 2-m-long cryostat, which includes a vacuum vessel containing two radiation shields, current lead assemblies, and a cold mass. The cold mass includes the two-core magnet assembly shown in Figure 2. The cold mass assembly uses four cryocoolers to cool the cryostat. Figure 5 shows the cryostat assembly at the APS SCU facility.

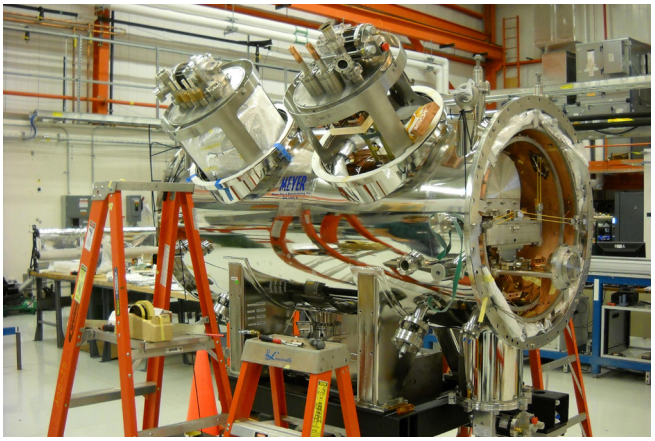

Figure 5. Assembly of 2-m-long horizontal cryostat at the APS SCU facility.

Proposed Work for FY 2015

The assembly of the 2-m-long horizontal cryostat will be completed in FY 2015, and the SCU magnet will be tested in this cryostat with an existing horizontal measurement system. The measured undulator field profile will then be used for magnetic modeling of a 2.2-m-long, two-magnet system. The simulation will also include a phasing scheme. As a result, the proposed long SCU magnet made of 1.1-m-long sections will be pursued.

LDRD

Materials for Energy

ANNUAL REPORT

2014

Polyelectrolyte Brushes in Multi-Valent Ionic Media

2011-217-R3

Matthew Tirrell

Project Description

The overall objective of this project is to understand and exploit the new phenomena and properties that arise when a highly charged polyelectrolyte is placed in a medium in which there are ions, small or large, that are both multi-valent and oppositely charged. We have characterized both the change in size and the intermolecular interactions in such systems. These changes lead to numerous possibilities for creating new self-assembled materials that we are developing in the course of this project.

Mission Relevance

The project is tied to DOE's mission in science. This work specifically addresses Grand Challenge Number 4 of the DOE's Basic Energy Sciences Advisory Committee (BESAC) report, *Directing Matter and Energy: Five Challenges for Science and the Imagination:* "How can we master energy and information on the nanoscale to create new technologies with capabilities rivaling those of living things?" Polyelectrolyte applications are continuing to emerge and expand in novel materials, driven in part by a growing demand for polymeric materials that respond to environmental changes. Current efforts in multilayer formation and behavior, chemical gating, and drug delivery all exploit polyelectrolytes that respond to external stimuli, ranging from electrical and mechanical stimulation to environmental changes in pH and salt concentration. This increased interest necessitates a deeper fundamental understanding of the structure and properties of these complex materials. Although polyelectrolytes have been well studied in environments consisting exclusively of mono-valent ions, much less attention has been given to their behavior in the presence of multi-valent ions — despite the importance of multi-valent ions in many potential products and processes, such as energy storage, environmental technologies, and hybrid systems in synthetic biology. This work will provide one pillar of a new foundation for soft materials science that will contribute to future efforts in developing materials for energy and synthesis science. We are leading the way in introducing attractive forces between polyelectrolytes as a new tool for creating self-assembled materials that have biomimetic character.

FY 2014 Results and Accomplishments

Prior to the most recent fiscal year, we reported on data related to both the interfacial tension and the thermodynamics of polyelectrolyte complexes and their formation. Interfacial tension with water was found to be very low and tunable even lower with added salt, at the expense of forming less of the complex phase. Calorimetric measurements demonstrated the entropic driving force for complex formation, owing to the release of counterions from the complex. Our work in FY 2014 involved work focusing on the subtle effects of the nature of the salt environment on polyelectrolyte complexation and further efforts to understand self-assembly processes in charged block copolymers.

As one interesting result, we found that the nature of the added salt has specific effects that go beyond the charge of the ion. Figure 1 compares two monovalent ions and two divalent ions in the polyacrylic acid–polyallylamine hydrochloride (pAA-pAH) system. Evidently, the overall charge of the ion dominates its interaction with the complex. However, an examination of the turbidity data, when scaled by ionic strength to cancel the effects of charge alone, clearly demonstrates a difference in the interaction of the various cations with the pAA/pAH system. The observed trends in critical salt concentration (or critical ionic strength) correlate directly with the expected Hofmeister ordering (i.e., K+ > Na+ > Mg^{2+} > Ca^{2+}), where K+ shows the highest salt stability and Ca^{2+} shows the lowest. Given the proven utility of polyelectrolyte complexes as encapsulants and as surface active agents, this work has important implications for understanding whether they will be effective in media of differing ionic natures.

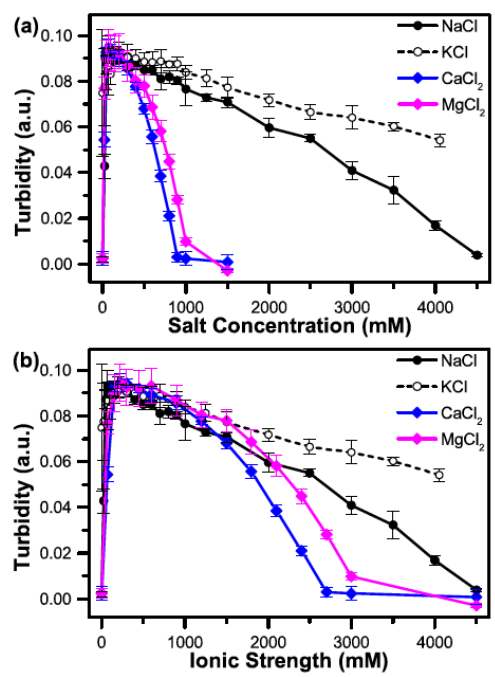

Figure 1. Plots of turbidity as a function of (a) salt concentration and (b) ionic strength for a series of chloride salts, investigating the effects of various cations. (All samples were prepared at 1 mM total monomer concentration, 50/50 mol% pAA/pAH ratio at pH 6.5. Complexes were prepared by adding pAA to a solution containing a mixture of pAH and the desired quantity of salt.)

In our work on self-assembly of block copolymers, we investigated the nature of the coacervate core structure of hydrogels and micelles formed from complexation between pairs of diblock or triblock copolymers containing oppositely charged end-blocks as a function of polymer and salt concentration. Our objectives were to determine the size and water content of the polyelectrolyte complex domains in these novel self-assembled materials.

We studied both ABA triblock copolymers of poly[(allyl glycidyl ether)-*b*-(ethylene oxide)-*b*-(allyl glycidyl ether)] and analogous poly[(allyl glycidyl ether)-*b*-(ethylene oxide)] di-block copolymers that were synthesized to be nearly exactly one half of the symmetrical tri-block copolymers. The poly(allyl glycidyl ether) blocks were functionalized with either guanidinium or sulfonate groups via post-polymerization modification. Mixing of oppositely charged block copolymers resulted in the formation of nanometer-scale coacervate domains. Small angle neutron scattering (SANS) experiments were used to investigate the size and spacing of the coacervate domains. The SANS patterns were fit by using a previously vetted, detailed model consisting of polydisperse core-shell micelles with a randomly distributed sphere or body-centered cubic (BCC) structure factor. For increasing polymer concentration, the size of the coacervate domains remained constant while the spatial extent of the poly(ethylene oxide) (PEO) corona decreased. However, increasing salt concentration resulted in a decrease in both the coacervate domain size and the corona size as a result of a combination of the electrostatic interactions being screened and the shrinkage of the neutral PEO blocks. Additionally, for the triblock copolymers that formed BCC ordered domains, the water content in the coacervate domains was calculated to increase from approximately 16.8% to 27.5% as the polymer concentration decreased from 20 to 15 wt%.

The kinetics of formation and structural evolution of these novel polyelectrolyte complex materials was also examined. The mechanism and speed of the assembly process, as well as the organization of these domains, were probed by using dynamic mechanical spectroscopy and small angle x-ray scattering (SAXS). SAXS revealed that the equilibrium morphologies of both the di-block copolymer and the tri-block copolymer materials were generally qualitatively the same, with some apparent quantitative differences in phase boundaries, possibly attributable to lack of full equilibration. Slow kinetics and difficulties in reaching equilibrium phase structures, especially in tri-block materials, is a principal message of this work. Figure 2 shows how much more slowly tri-block materials develop their equilibrium moduli than do di-blocks. Detailed analysis of the SAXS data revealed that the tri-block copolymer materials formed ordered phases via a nucleation and growth pathway and that the addition of small amounts (~20%) of corresponding di-block copolymers increased the rate of structure formation and enhanced several key physical properties.

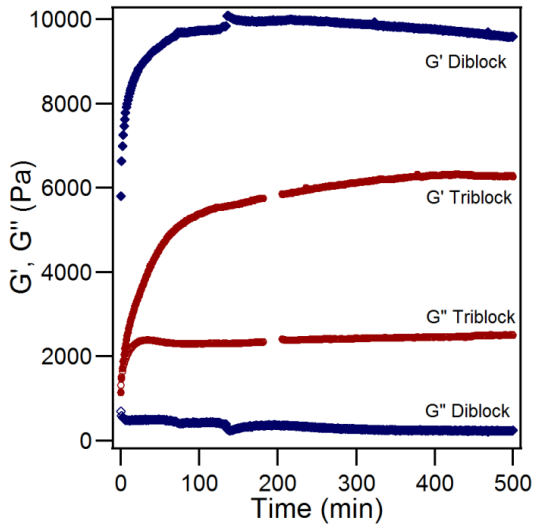

Figure 2. Dynamic mechanical spectroscopy data showing the evolution of G' and G" with time for both the di-block and the tri-block copolymer materials. (The di-block copolymers not only equilibrate faster, but G' for the di-block copolymer was significantly larger over the entire time sweep. Both systems were tested at 20 wt% and 0 M NaCl, which corresponds to the BCC phase.)

Work started in this project will continue under the DOE Field Work Proposal (FWP) 16341.1, *Solvent-assisted, Non-equilibrium, Directed, Self-assembly of Complex Polymeric Materials*.

Mesoscale Elastic Problems

2012-015-R2

Olle Heinonen, Dmitry Karpeyev, and Michael Welland

Project Description

The length and time scales of mesoscale systems are much larger than those of atomic systems but smaller than those of macroscopic systems. A goal of this project is to develop scalable codes for inhomogeneous mesoscale systems in which the elastic strain fields are coupled to bound and free charges. To achieve this goal, we are using a cross-disciplinary approach that integrates materials science, condensed matter physics, applied math, and computational science. Part of the work is being conducted with Professor Serge Nakhmanson at the University of Connecticut and Professor Byounghak Lee at Texas State University.

Mission Relevance

The project supports the DOE Basic Energy Sciences (BES) mission to support research in areas relevant to energy efficiency through use-inspired research and development on new materials for energy storage and the efficient

use of energy. The project also addresses challenges articulated in the September 2012 BES Advisory Committee report, "From Quanta to the Continuum: Opportunities for Mesoscale Science," by studying how nanoscale building blocks can be combined into larger (macroscale) systems with new properties inherently derived from the interactions between the building blocks.

FY 2014 Results and Accomplishments

In FY 2014, we studied the ferroelectric behavior of patterned disks of a specific ferroelectric material, $PbSr_2Ti_2O_7$. This layered material has been predicted to develop an in-plane ferroelectric polarization that is free to rotate in the plane when unstrained or under slight compressive strain. We developed a mesoscale model for the polarization in patterned disks with sizes ranging from a few tens of nanometers to micrometers. Our modeling shows that the polarization in disks that are a few hundred nanometers in diameter can be made to switch between a vortex-like polarization, in which the polarization is in the plane of the disks and curls around the circumferential direction, and a uniformly polarized state by applying a bi-axial tensile strain. This opens the possibility of creating structures with a dielectric response that can, by the application of external stress, be dynamically tuned between a large dielectric response in the vortex-like state to a small longitudinal response in the uniform state. Such structures may have interesting applications in energy storage and harvesting and in information technologies.

In another investigation, we studied how lithium (Li) intercalates into $LiFePO_4$ nanoparticle electrodes used in Li-ion batteries. Previous work by Cogswell and Bazant (M.Z. Bazant, 2012, "Theory of Chemical Kinetics and Charge Transfer based on Nonequilibrium Thermodynamics," *Accounts of Chem. Research* 46, 1144) considered a two-dimensional (2D) model that included spinodal decomposition with elastic strain energy and a concentration-dependent surface free energy, with a steady influx of Li. We extended this model to three-dimensional (3D) particles with anisotropic mobility and concentration-dependent bulk and surface elastic energy. The results showed that the microstructure was dominated by surface effects, with the 3D model showing significantly different intercalation and phase separation behavior that depended on the particle size and geometry, with stripes of the lithiated phase appearing as slow (but not asymptotic, time-independent) intermediates; this result was in agreement with previously unexplained experimental micrographs.

We also studied how elastic strain affects the electronic band gap distribution in core-shell nanoparticles, such as Zn-ZnO or ZnO-TiO_2. These have properties that are attractive for application in such areas as catalysis and photovoltaics — the latter since the photon energy that can be absorbed is determined by the band gap. If the particles are not too small (i.e., have a diameter larger than about 5 nm), the strain can be described by classical elasticity, and a local band gap can be related to the local strain (Figure 1). This could lead to tailoring of the strain distribution so that the band gap would be better tuned to the solar spectrum. Zn-ZnO particles were particularly interesting because the metallic Zn core can be faceted and irregular, giving rise to a very inhomogeneous strain and a broader band gap distribution (Figure 2).

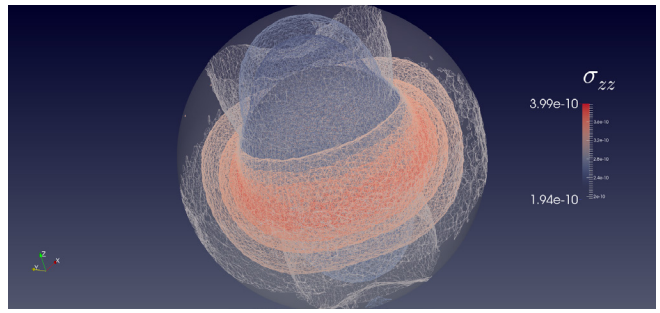

Figure 1. zz-component of the stress in a Zn-ZnO core-shell nanoparticle with a 25-nm outer diameter and a 15-nm-diameter Zn core

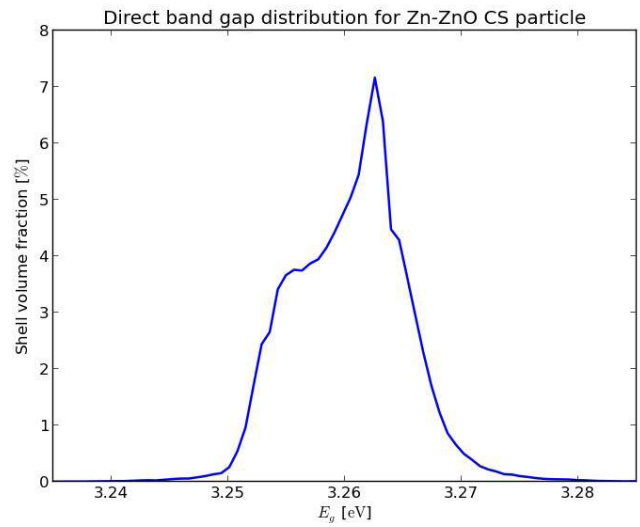

Figure 2. Band gap distribution in the Zn-ZnO core-shell nanoparticle shown in Figure 1. The bulk band gap for ZnO is 3.20 eV; the stress distribution in the particle leads to a broader distribution of band gap.

Seminars

Heinonen, O. (2014). "Mesoscale Computational Materials Science – What Is It, How Do I Do It, and Why Should I Care?" University of Illinois, Urbana-Champaign, Urbana, IL, July 23–25, 2014.

Membrane-Bound, Broad-Spectrum, Photo-Driven Protein Devices

2012-204-R2

Suzanne G.E. te Velthuis

Project Description

The goal of this project is to create biomolecular materials that exploit the full potential associated with designing and synthesizing energy and molecular-transducing, pore-forming protein mimics, all of which are bound to an organizing lipid membrane so they can be used for biosensing device applications. The membrane is composed of lipids that naturally organize into regions with distinct lipid compositions. Controlling these regions so they form into well-defined structures will enable us to obtain new, multifunctional materials that include bio-inspired, synthetic, pore-forming peptides. We will optimize the properties of the lipid-peptide compositions and search for modifications we can make to the surface chemistry on which they will be used.

Peptides for this research are being synthesized at Argonne's Center for Nanoscale Materials. We are doing research on the membranes and substrates with collaborators at the University of Illinois-Chicago (Ursula Perez-Salas group). Several techniques must be used to characterize the combined peptides/membrane system, including neutron and x-ray scattering and optical fluorescence microscopy.

Mission Relevance

Research on biomolecular materials lies within the science mission of DOE, being a core activity in the Division of Materials Sciences and Engineering in DOE's Office of Basic Energy Sciences. In this project, we will explore the use of bio-inspired molecules, methods, and concepts to create novel materials and processes that can be used in energy-related applications.

FY 2014 Results and Accomplishments

In FY 2012, we were able to jump-start the first spin echo resolved grazing incidence scattering (SERGIS) measurements on lipid monolayers exhibiting micrometer-sized lateral lipid domains, as well as on lipid stacks from mixtures that also exhibit domain formation. Using small angle neutron scattering (SANS), we also characterized the formation of nanopatterns on surfaces using block-copolymer films. During FY 2013, we were able to control nanopatterns on surfaces by using thin block-copolymer films and self-assemble domain-forming lipid mixtures on these surfaces. The conformation of lipid domains on the surface pattern was investigated by fluorescence microscopy and spin-echo resolved neutron scattering.

In FY 2014 we synthesized two *de novo* peptides: TH1 and PRIME. These peptides are building blocks for forming bundles and creating pores through membranes having various sizes and functions. The milestones of this work are described here.

- *Synthesis of TH1-TAMRA.* TH1 is a small, helical peptide consisting of a hydrophilic interior core and a membrane-facing hydrophobic exterior. The peptide consists of 29 amino-acid residues capable of spanning the membrane's bilayer. Small modifications to the leucine-rich peptide sequence increased helix-helix interactions; these led to the formation of dimer or tetramer peptide bundles. Helix-helix interactions and pore-facing residues determined the size and type of selective molecule allowed through the pore. TH1 was synthesized by using a protein synthesizer. To trace the behavior of TH1 in a mixed lipid membrane, it was labeled with the fluorescent dye TAMRA. Circular dicroism (CD) showed that the structure of TH1 was indeed a-helical.
- *Synthesis of PRIME.* A protein synthesizer was used to produce these metalloporphyrin-binding, membrane-spanning, transmembrane helices. Characterization of PRIME showed that it also conformed to the a-helical structure and that the synthesis product achieved the molecular weight of individual helices.
- *Characterization of TH1-TAMRA in Giant, Unilamellar Vesicles (GUVs) of Mixed Lipids by Using Fluorescence Microscopy.* We co-dissolved 0.05 mol% of TH1-TAMRA in chloroform with a lipid mixture consisting of dioleoylphosphocholine (DOPC), dipalmitoylphosphocholine (DPPC), and cholesterol at a 1:1:1 ratio. After chloroform was removed, we used the electro-formation technique to form GUVs. These vesicles are typically between 10 and 30 μm in diameter. Without TH1, the GUVs exhibited two lipid environments: One was rich in DPPC and cholesterol, and the other was rich in DOPC. Rhodamine, labeled dipalmitoylphosphoethanolamine (DPPE), was used to visualize the single DOPC-rich region (Figure 1A). When a-helical TH1 peptide was added to this lipid mixture, the peptide caused the domains to break up into many smaller domains (Figure 1B). This behavior showed that TH1 preferred only one of the two available membrane environments. We also found that the miscibility temperature got a few degrees higher in the presence of TH1; this result means that it promotes lipid phase separation.

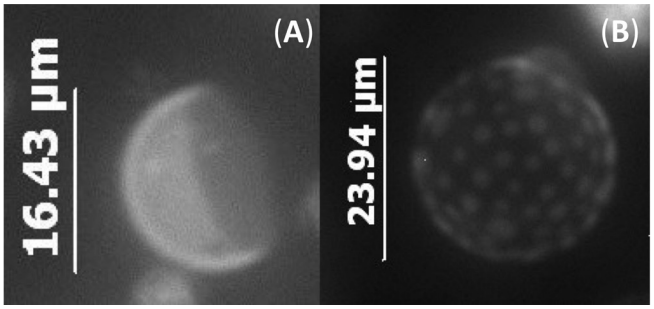

Figure 1. Fluorescence microscopy images of mixed lipid GUVs without the helical peptide TH1 (A) and with it (B). The membrane consists of a 1:1:1 molar mixture of DPPC, DOPC, and cholesterol. The bright region in Figure 1(A) corresponds to the DOPC-rich region of the membrane, visualized with the lipid marker DPPE with a rhodamine fluorescent dye. When TH1-TAMRA was added, many small domains formed, which indicates that TH1 has a preference for one of the two membrane lipid environments found in the GUVs. In this case, there was no lipid marker, and only the TH1 location was imaged.

Atomistically Informed Mesoscale Modeling for Advanced Electrical Energy Storage Systems

2012-209-R2

Larry A. Curtiss, Mihai Anitescu, Olle Heinonen, Dmitry Karpeyev, Marius Stan, and Dieter Wolf

Project Description

The goal of this project is to develop a mesoscale modeling capability and a code suitable for leadership-class computational platforms that capture the most important microstructural processes that take place during electrochemical crystal growth and dissolution during discharging and charging at the cathode of, for example, a lithium (Li) -air battery. Such a mesoscale model requires, as input, lower-scale information on the fundamental reaction, diffusion, and interfacial processes that control these microstructural processes. Because very little is known about these processes, the project consists of two complementary thrusts. The first thrust focuses on developing *atomic-level* (molecular dynamics, MD) simulations to determine the formation of lithium oxide (Li_2O_2) nanostructures at the carbon cathode and growth into the electrolyte. The interatomic interaction potentials needed for these simulations incorporate the local charge states associated with the electrochemical reaction at the electrode-electrolyte interface during the battery charge/discharge cycle. The second thrust focuses on using the atomic-level insights into the underlying mechanisms that were obtained to develop a *mesoscale* modeling approach that is based on phase-field theory and that incorporates the applied-math algorithms and computer-science tools needed for leadership-class computational platforms.

Mission Relevance

The project is relevant to DOE's missions in energy and science. This theoretical and computational project addresses key challenges associated with bridging the mesoscale by using approaches that employ lower length scales in hierarchically structured systems. The insights gained from the simulations will also allow for the interpretation and understanding of microstructure-level experimental observations of advanced electrical energy systems. It is expected, too, that they will lead to predictions of novel (i.e., as-of-now unobserved) phenomena, based on the identification of the underlying mechanisms seen in the simulations. The scale-bridging methodologies developed in this project will be applicable not only to Li-air batteries but also to Li-ion batteries. This work will help in developing new energy storage materials that are critical to DOE's energy mission.

FY 2014 Results and Accomplishments

In FY 2013, we developed a comprehensive fitting database for developing Li_2O_2 interatomic potentials from density functional calculations by determining cohesive energies, bond lengths, and bond stiffnesses for high-symmetry structures of crystalline and molecular Li and oxygen (O), as well as Li_2O_2 compounds.

In FY 2014, we used this first-principles database to develop Buckingham-type charge-transfer potential for Li_2O_2 that uses the concept of split-charge equilibration in combination with the bond-order approach. This potential incorporates the complementary concepts of covalency and ionicity that depend on the local chemical environment in order to model short-range bonding and long-range electrostatics across a wide range of stoichiometry. This is achieved by determining all charges self-consistently, "on the fly," on the basis of the local environment. This potential is now available for systematic MD simulations of the structure and properties of surfaces, individual nanoparticles, and fully dense Li_2O_2 nanocrystalline microstructures.

In parallel to these atomic-level developments, we began to develop a phase-field code for the model case of electrochemical crystal growth at the carbon electrode in the Li-air system. Our formulation of the partial differential equations (PDEs) governing the reversible growth and dissolution of Li_2O_2 during discharging and charging of a Li-air battery was inspired by extensive electronic structure calculations by the principal investigatorsand numerous experimental investigations of the discharge process in Li-O_2 systems. We initially considered the following specific mechanism involving five chemical reactions for forming crystalline $Li_2O_{2(crys)}$ at the carbon cathode by the reaction of Li^+ and O_2^- in solution (sketched schematically in Figure 1).

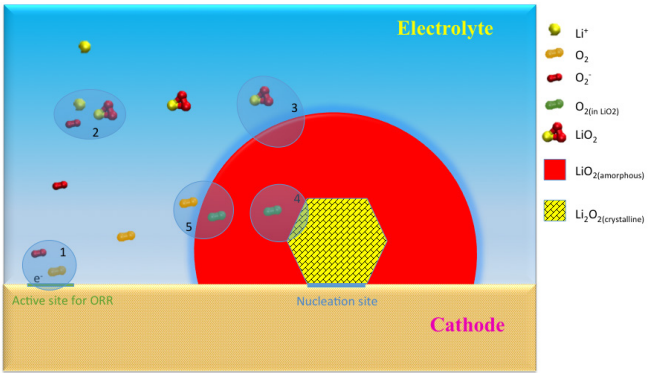

Figure 1. Schematic of the assumed mechanism for the formation of LiO_2 in solution and subsequent deposition on the carbon cathode as an amorphous solid. Numbers correspond to the five reactions described in the text.

Molecular O_2 enters the system through the porous cathode in what is assumed to be an externally maintained partial pressure. While molecular O_2 is assumed to be present everywhere in the system, it is also assumed that it is reduced to O_2^- only at the cathode surface (Reaction 1, bottom left of Figure 1). In contrast, Li^+ ions enter the system from the anode. (This has not yet been explicitly included in the model, which simplified the initial formulation of the mesoscale model. However, the effect of the Li anode will be fully incorporated later; this will include the Poisson equation that ensures self-consistency in the charge distribution across the entire system.) Reaction 2 captures the reaction of the Li^+ ions in the electrolyte with the dissolved O_2^-; the ions are deposited as amorphous LiO_2 — $LiO_{2(amorph)}$ — on the substrate (Reaction 3). Reaction 4 describes the solid-state transformation of amorphous LiO_2 into crystalline LiO_2 and subsequently (according to experimental evidence) into crystalline $Li_2O_{2(crys)}$ (Reaction 4), thereby releasing molecular O_2 that can diffuse back into the electrolyte (Reaction 5).

Our phase-field model for the formation of crystalline $Li_2O_{2(crys)}$ by these five chemical reactions is naturally divided into the following two successive stages involving five distinct species (see Figure 1): three species in solution (O_2^-, Li^+, and LiO_2) and two as solid phases ($LiO_{2(s)}$ and $Li_2O_{2(s)}$). Stage 1 captures the *reaction-diffusion* process in the electrolyte (Reactions 1 through 3) by which, upon saturation, LiO_2 is deposited on the cathode as an amorphous solid. Stage 2 then describes the solid-state *phase transformation* of the continually growing amorphous LiO_2 phase into the crystalline Li_2O_2 phase (Reactions 4 and 5).

The mathematical formulation of all this phase field model involves the usual expression for the free-energy functional of the system in terms of the bulk chemical free-energy density plus gradient terms for the phase compositions due to the presence of the interfaces. The five coupled governing PDEs thus obtained can be solved numerically by using the semi-implicit spectral method to solve the governing equations. For a first test, we used estimates for the required input parameters. Soon some of these parameters will come from the atomistic simulations (notably those associated with surface and interface energies, diffusivities, and mobilities), while others will be derived from density functional theory (DFT) calculations or extracted from experimental estimates.

Proposed Work for FY 2015

In FY 2015, we will do the following:

- Perform MD simulations of nanocrystalline Li_2O_2, including the grain surfaces and the grain boundaries in them. The predicted Li_2O_2 surface structures and nanoparticle shapes will be validated against those obtained from first-principle calculations and the sparse amount of experimental data that is available. Such validation is important since it will lend credence to the potentials we developed for these simulations.
- Continue to develop and apply our phase-field code for electrochemical crystal growth that incorporates standardized numerical routines and algorithms.
- Expect that our investigation of the simple model system just described will provide some initial insights into some of the irreversible microstructural processes during discharging and charging at the cathode that limit the performance and lifetime of the Li-air battery system.
- Continue developing leadership-class solvers for sparse-matrix problems. The code development will be done within the PETSc libraries (e.g., with preconditioners made readily available within PETSc).

Key results obtained from the combined atomistic and mesoscale simulations will be validated. For example, we might compare the predicted oxide-electrolyte interface and evolved structure obtained from our mesoscale model with experimental data (e.g., transmission electron microscopy [TEM] or x-ray imaging). In addition, we have close connections with experimental groups in Argonne's Chemical Sciences and Engineering Division and Materials Science Division for experimental validation on both model and real systems.

Hierarchical Modeling of Self-Assembly in Nanostructured Soft Materials at Equilibrium and Far from Equilibrium

2013-184-R1

Juan J. de Pablo and Raymond Bair

Project Description

The overall aim of this project is to develop new computational methods that will enable design of materials and processes capable of leading to predictable self-assembly of macromolecular systems for engineering applications. As such, the proposed work involves significant elements of model and algorithm development, but it also relies extensively on prediction and validation by state-of-the-art experimentation. This project has been extremely successful and is having an impact on technologies that are now starting to be considered for large-scale applications, including the fabrication of self-assembled membranes for separations and water purification or the assembly of novel photonic band-gap materials.

Mission Relevance

This project is relevant to DOE's missions in science and energy. Advanced materials are at the heart of multiple technologies that are essential for the harvesting, storage, and manipulation of energy. Next-generation supercapacitors, batteries, and membranes for advanced separations all rely on structured materials with characteristic lengths in the range of 5 to 100 nm. By achieving control over the self-assembly of macromolecular systems into ordered structures, it will be possible to arrive at technologies of relevance to DOE's mission faster, more reliably, and over a wider range of application domains. The work pursued in this project is essential to that goal in that it will enable computational design of such materials and of processes for their integration, and will accelerate interpretation of demanding characterization experiments on the basis of physical models.

FY 2014 Results and Accomplishments

During FY 2013, our team was focused on development and implementation of physics-based models and fast algorithms for prediction of self-assembly in mesostructured materials. In FY 2014, our research group continued to make significant advances in the general area of theory and simulation of macromolecular self-assembly, while demonstrating their general applicability in the context of several concrete examples. Our efforts in the area of protein misfolding and aggregation focused on two aspects of the modeling of large, unstructured polypeptides. Such molecules are poorly understood and are of considerable scientific and medical interest. We focused on simulations of islet amyloid polypeptide (amylin), a molecule that is implicated in the onset of Type II diabetes. Using a variety of novel, enhanced sampling and free-energy calculation techniques, we completed a comparative study of the predictions of seven different force fields. We are now pursuing simulations of misfolding and aggregation in the vicinity of bilayer membranes and have engaged in productive discussions with APS scientists who are considering experiments to validate such predictions.

In related work, we sought to examine protein aggregation with model materials. More specifically, we considered polyelectrolyte solutions that, under suitable conditions, phase-separate into a liquid-like coacervate phase and a coexisting supernatant phase that exhibit an extremely low interfacial tension. Such interfacial tension provides the basis for most coacervate-based applications, but little is known about it, including its dependence on molecular weight, charge density, and salt concentration. By combining a Debye-Huckel treatment for electrostatic interactions with the Cahn-Hilliard theory, we derived explicit expressions for this interfacial tension. Our predictions were shown to be in quantitative agreement with experiments and to provide a means to design new materials based on polyelectrolyte complexation.

We continue to make advances in the development and application of coarse-grained models of DNA. The interaction of DNA with proteins occurs over a wide range of length scales and depends critically on its local structure. In particular, recent experimental work suggests that the intrinsic curvature of DNA plays a significant role in its protein-binding properties. We completed the 3SPN.2.C, a new version of our widely used 3-Site-Per-Nucleotide coarse-grained model that includes a description of curvature, which successfully predicts the structural, mechanical, thermodynamic, and kinetic properties of DNA. This model was applied to study four phenomena: (1) DNA oligomer hybridization, (2) DNA-mediated aggregation of nanoparticle arrays, (3) DNA-nucleosome complexation, and (4) sub-elastic flexibility of DNA.

Liquid crystals (LCs) are being explored as novel detectors for toxic biomolecules. The basic principle of detection relies on morphological changes in the LC in response to adsorption of biomolecules at the LC interface. These morphology changes rely strongly on material properties of the LCs, quantified through the Frank elastic constants, and on molecular interactions between surface-active particles and the LC droplets. To more fully understand these cases, we developed new methods for the *in silico* study of elastic constants, permitting these properties to be isolated and determined from simulation when they cannot be obtained from experiments.

Most importantly, in the area of directed assembly of block polymers, we developed a new computational approach to investigate the free energy barriers that arise during annealing of block copolymers in thin films. The overall aim of this work will be to identify pathways that enable elimination of all defects in thin films over macroscopic areas. We will investigate two approaches, namely, thermal annealing and solvent annealing. We also performed a systematic study of the use of top-coat strategies in block copolymer lithography. This approach is important because the morphology of a block copolymer thin film is particularly sensitive to its boundary conditions. Lithographic applications of block polymers in the microelectronics and memory device industries require formation of morphologies with perpendicularly oriented domains. Current fabrication targets envisage the creation of dense arrays of structures with domain sizes in the sub-10-nm regime. Such length scales can be reached by resorting to block polymers with highly incompatible blocks (and a large Flory-Huggins parameter, χ). High χ values, however, generally lead to large differences in the surface energies of the corresponding blocks, thereby interfering with formation of the sought-after perpendicularly oriented domains.

In our work, a coarse-grain model was used to develop a top-coat strategy that enables control of the orientation of block copolymer domains in highly incompatible block polymer materials. A systematic study of a wide range of polymeric material combinations was performed, and the conditions leading to optimal assembly of perpendicular morphologies were clearly identified. We considered the effect of molecular weight, block polymer film thickness and architecture, and degree of incompatibility. Our results were summarized in the form of generic phase diagrams that will serve as a guide for experimental deployment of the top-coat strategy put forth in our work.

Proposed Work for FY 2015

In FY 2015, we aim to make progress on the following fronts:

- We plan to complete a model for association of block polyelectrolytes that will include ionic correlation effects. That model will be used to describe ordered charged copolymers, such as those envisaged for use in batteries.
- We plan to complete calculations of the interaction of charged DNA with charged particles. The results will provide insights into design rules for creation of hierarchical materials for applications in sensing or energy harvesting.
- We plan to complete calculations of the free energy barriers that arise during annealing of copolymers assembled on chemically patterned substrates. Understanding such barriers will lead to strategies for defect-free assembly of mesostructured materials for nanomanufacturing applications.

Computational Molecular Science

2013-202-R1

Gregory A. Voth and Christopher J. Knight

Project Description

The main objectives of this project are to develop methodologies to accurately parameterize molecular simulation models, efficiently compute reactive simulations, and enhance configurational sampling. The accurate description of multiscale phenomena requires both models and software that are uniquely designed for the task of accounting for the long-time evolution of (relatively) high-frequency motion within inhomogenous systems. It is the inhomogeneity of biological and material systems and their respective interfaces that necessitates accurate interactions and large system sizes to properly account for environmental effects on chemical dynamics.

Mission Relevance

In support of DOE's missions in energy and science, we are developing simulation tools that can be used at both the smallest molecular scales and the largest mesoscopic scales. Directly incorporating information from calculations that retain electronic degrees of freedom in models provides a framework to significantly extend the molecular understanding of complex phenomena. Such simulation advancements will greatly facilitate innovation and discovery within the general scientific community and advance solutions to challenging scientific problems. The improved computational performance of reactive simulations on DOE leadership computing resources resulting from this project has already extended the readily accessible time scales of polymer electrolyte membrane simulations (Figure 1) by an order of magnitude. Understanding charge transport mechanisms in inhomogeneous systems like these is critical to optimizing electrochemical conversion and storage device performance, which is directly relevant to DOE's mission of energy security. Detailed microscopic information on material properties, such as the modulation of charge transport dynamics near complex interfaces, will facilitate a greater understanding of molecular mechanisms in energy production and storage processes.

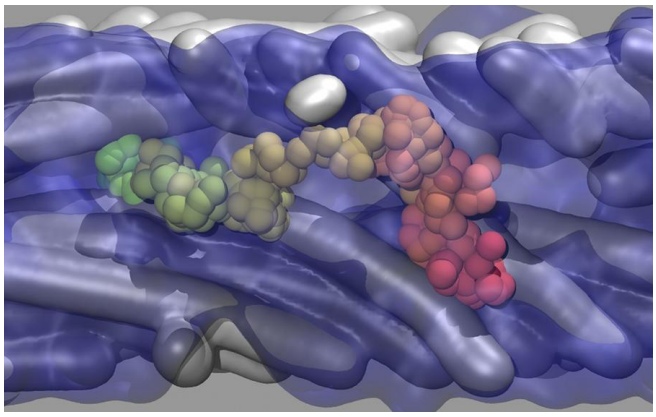

Figure 1. Partial view of a polyelectrolyte membrane simulation, accessible with the latest RAPTOR code, containing 12,429 particles with 120 reactive protons. The membrane polymer chains (solid white), water (translucent blue), and the complex pathway traversed by one of the excess protons (overlapping spheres) are shown. All other protons are hidden for clarity.

FY 2014 Results and Accomplishments

Milestones completed during FY 2013 were critical to the success of the second year of this project. The parameterization of nonreactive electrolyte/electrode models for molecular simulations in the previous year facilitated the development of a reactive methodology. The design of new parallelization strategies in FY 2013 for reactive simulations and cellular-scale, coarse-grained simulations paved the way for development of newly implemented methods and algorithms in FY 2014.

In FY 2014, the parallel performance of reactive simulations with the RAPTOR code was further improved with optimizations to the recently implemented multiple-copy parallelization framework (Figure 2). In addition to parallelization of key compute kernels, support was added to model polarization of electrodes by reactive ions and the application of a constant bias voltage across simulation cells. Furthermore, the overall improved computational efficiency enabled implementation of the exact Hellmann-Feynman forces for long-range electrostatic interactions with a modest overhead compared to a previously implemented approximation. The improved RAPTOR code was an essential factor in the receipt of a 2014–2015 DOE ALCC (ASCR [Advanced Scientific Computing Research] Leadership Computing Challenge) award of computing time.

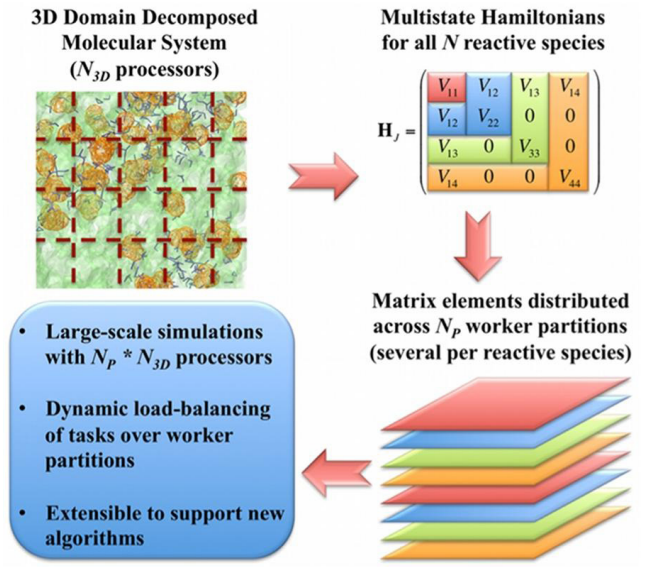

Figure 2. Scheme illustrating the two-level parallelism presently in use in large-scale reactive simulations with the RAPTOR code, where multiple copies of the original domain decomposed system are used to simultaneously compute Hamiltonian matrix elements.

There was favorable progress in two separate but related sub-projects to develop enhanced sampling algorithms. The first sub-project sought to accelerate sampling in reactive simulations without imposing reaction coordinates that could potentially hinder sampling of the relevant regions in phase space. By coupling continuous coordinates that track the location of reactive species in the system to external degrees of freedom, temperature-accelerated simulation methods can be used to enhance configurational sampling of the reactive degrees of freedom and accelerate computation of multidimensional free energy surfaces (FESs). Studies on glutamic acid deprotonation in water successfully reproduced the FESs at significantly reduced computational expense compared to umbrella sampling. The second sub-project focused on development of a multi-configurational coarse-grained (MC-CG) method that couples separate CG models that, for example, represent different protein conformations. Application to the un/folding process of the endophilin A1 N-terminal helix in solution using a two-state CG Hamiltonian successfully reproduced the underlying FESs obtained from all-atom simulations.

Also completed this year was a study on the proton transport mechanisms of [FeFe]-hydrogenase, which belongs to a class of enzymes that reversibly catalyze the reduction of protons and oxidation of molecular hydrogen. In this study, water pathways and corresponding FESs for proton transfer between different sites were examined for three important oxidation states to identify conditions resulting in increased enzymatic activity. Understanding key details of this enzymatic process will contribute to the improved design of environmentally friendly energy sources.

Proposed Work for FY 2015

In FY 2015, work will continue on improving the computational performance of reactive simulations with the RAPTOR code and related simulation methods (e.g., MC-CG). In particular, on-the-fly load-balancing in simulations with many reactive species will be improved to reduce the idle time of computer resources.

Additional interaction potentials for reactive forcefield development in the parallel FitEVB code, which is interfaced to the RAPTOR and LAMMPS codes, will be incorporated to support modeling the solvation and dynamics of ions and solvent decomposition reactions at electrochemical interfaces.

Enhanced sampling algorithms developed during FY 2014 will be further investigated. The computational efficiency of temperature-accelerated reactive molecular dynamics is currently being investigated in studies of proton transport pathways in cytochrome c oxidase, which is a transmembrane protein that plays a key role in the synthesis of adenosine triphosphate in bacteria.

Seminars

Knight, C. J. (2014). "Computationally Efficient Reactive Models Derived from Condensed Phase ab Initio Simulations." University of Kansas, Lawrence, KS, December 12, 2013.

Knight, C. (2014). "Computationally Efficient Reactive Models Derived from Condensed Phase ab Initio Simulations." Louisiana State University, Baton Rouge, LA, July 17, 2014.

Mesoscale Materials by Design from Assemblies of Ionic Polymers and Nanoparticles

2013-215-R1

Derrick C. Mancini

Project Description

At present, there is considerable interest in the design and synthesis of mesoscale materials, including those that incorporate hydrogel and other ionic polymers with inorganic nanoparticles, to achieve complex multifunctionality with many applications, such as energy storage and drug delivery. In this project, we integrated theory and experiment to understand the parameters that drive the solution of self-assembly of nanoparticle-polymer composites into complex mesoscale materials with multiple functionality. We discovered and verified the underlying relationships among hierarchical structure, composition, and the functional properties associated with these mesoscale materials when enabled through in-solution templating approaches. Structure-directing molecular templates and precursors (such as solution makeup including ions and surfactants; polymer brush morphology, chemistry, and functionality; or assisting biomolecules) can, therefore, be utilized to organize hierarchical building blocks that self-assemble into more complex structured materials over greater distances. The modeling studies can be used to predict self-assembled structures on the basis of the templates and the precursors in solution. Functionality can be further extended by incorporating biomolecules and their analogs into the mesoscale assemblies.

We synthesized nanoparticle-brush structures by using ionic polymers, particularly the hydrogel poly(N-isopropylacrylamide) (PNIPAm). We modeled these materials to begin to understand how they will interact with templates or how they will undergo self-assembly in solution. We began to characterize the self-assembly process by using x-ray and neutron scattering techniques. No other work of a comparable scale is under way in the United States, although there is continued growing interest by many. Nevertheless, no attempts have been undertaken to create such materials and model them atomistically by using molecular dynamics (MD) and then extend the model to coarse-graining (CG) techniques.

Mission Relevance

The development of mesoscale-structured polymer and nanoparticle composites will contribute to DOE's science, environment, and energy missions. These materials are of widespread interest because they have applications in energy storage and conversion, environmental mitigation systems, sensor technology, and drug delivery.

FY 2014 Results and Accomplishments

In FY 2013, we characterized our first assemblies from nanoparticle-brush structures by using small-angle x-ray scattering (SAXS), as well as infrared (IR) and ultraviolet-visible (UV-Vis) light spectroscopy. For our first synthesis of functional composite materials by the self-assembly of nanoparticle-brush structures, we synthesized hydrogel-nanoparticle composites; we analyzed the precursor brush structures for both nanoparticle substrates by dynamic light scattering (DLS), SAXS, IR and UV-Vis spectroscopy, and electron microscopy; we synthesized the bulk hydrogel-nanoparticle composites from the precursor brush structures using appropriate cross-linkers and copolymer media; and we characterized the composite gels by x-ray scattering.

In FY 2014, we extended the MD modeling to a multi-scale approach by using results from the atomistic MD to implement a CG modeling by using the MARTINI force fields. This approach allows the number of subunits (such as brush structures) that can be followed in a full self-assem-

bly to be scaled up and followed for enough time steps to simulate a full self-assembly path. This is one of the first such calculations done from scale-up of first principles as opposed to top-down modeling for such structures.

We will extend this approach to other materials and more complex structures. Specifically, we extended this to gold (Au) nanoparticles that have been functionalized with brush structures.

Directed Self-Assembly and Three-Dimensional Characterization of Block Copolymers in Semi-Thick Films

2013-216-R1

Paul F. Nealey

Project Description

The central aim of this work is to develop a fundamental understanding of directed copolymer assembly in semi-thick copolymer films. The project will form the basis for design rules for creation of equilibrium and non-equilibrium nanostructured materials with precisely controlled architectures at the scale of 10 nm in three-dimensions. Intrinsically coupled with the goal of the project is the advancement of tools that are capable of characterizing the structure with equal precision. Characterization of the three-dimensional structure of the films and how they evolve will require using and advancing the capabilities of small-angle x-ray scattering (SAXS), grazing-incidence small-angle x-ray scattering (GISAXS), and resonant soft x-ray scattering (RSoXS), as well as additional complimentary techniques, such as scanning transmission electron microscopy (STEM) tomography. A unique aspect of the research relates to the direct comparison of dynamic experimental scattering data to simulated scattering profiles that are generated from dynamic structures that are predicted by molecular simulation.

Mission Relevance

The project is relevant to DOE's missions in science and energy. Beyond contributing new knowledge to the scientific community, directed copolymer assembly finds a wide variety of potential practical applications relevant to DOE's missions. We also anticipate that the project will be the impetus to develop a suite of state-of-the-art, three-dimensional nanoscale characterization tools for soft materials at Argonne National Laboratory. The block copolymer systems we are developing, with their well-defined architectures, are ideal for the development of such tools. Thus, the materials and tool development included in this project are broadly applicable in science-based research on structure-property relationships in nanoscale material architectures for energy transfer, chemical sensing, and information technology.

FY 2014 Results and Accomplishments

In FY 2013, progress was made towards designing new components (sample chambers) for the instruments at beamline 8-ID-E of the Advanced Photon Source to leverage our investigation of the three dimensional structure of block copolymer (BCP) films. The capability of x-rays to probe sample characteristics with the desired resolution throughout the polymer films was also established with GISAXS experiments.

The Liu-Nealey (LiNe) flow implemented at IMEC, Leuven, Belgium (formerly the Interuniversity Microelectronics Centre), uses chemical patterns for the directed self-assembly (DSA) of block copolymer (BCP) films, enabling the fabrication of 28-nm pitch line/space patterns on 300-mm wafers. To characterize in unprecedented detail the three-dimensional structure of constituent polystyrene guiding stripes, GISAXS experiments with the shortest sample-to-detector-distance (SDD) at beamline 8-ID-E at the Advanced Photon Source (APS) were performed in FY 2014. We invested significant effort into expanding current modeling methods to quantitatively capture the observed scattering intensity. On the basis of scanning electron microscope (SEM) images, we observed that within a few nanometers of resolution, roughness and shape polydispersity are present and contribute to diffuse background scattering. We developed software that accounts for such features in modeling x-ray scattering, and current predictions approximate the experimental image (Figure 1).

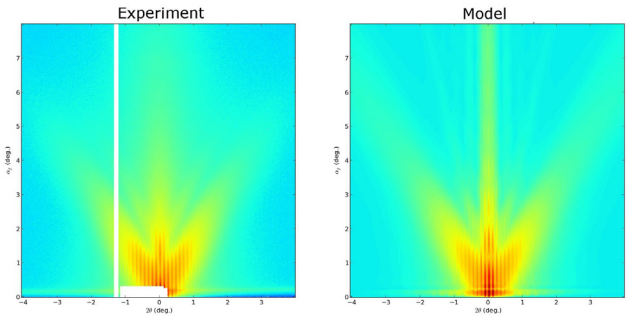

Figure 1. Grazing incidence x-ray scattering image (left) as recorded from experiments on polystyrene stripes that guide copolymer assembly. The image on the right is produced by developed software that predicts the scattered intensity on the basis of the three-dimensional structure of the sample.

To enhance the contrast in x-ray scattering experiments with block copolymer films, we applied the recently developed sequential infiltration synthesis (SIS) to our

polystyrene (PS) and poly(methyl methacrylate) (PMMA) samples, staining PMMA domains with Al_2O_3. These samples are also ideal candidates for STEM tomography, which complements x-ray scattering methods in providing three-dimensional structure at local lengthscales. We finished our first detailed investigation of self-assembled BCP structures by using STEM tomography, which uncovered details of defects present in such samples (Figure 2). Molecular simulations suggest that the source of such defects is the kinetics of assembly, further emphasizing the need for accurate determination of the temporal evolution of our structures.

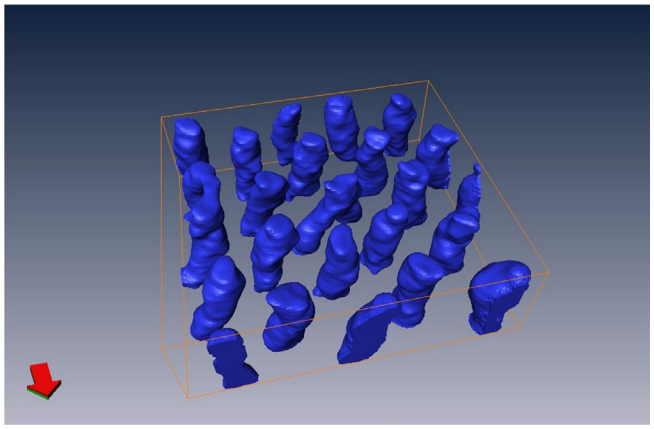

Figure 2. STEM tomography of cylinder-forming PS-PMMA film treated with Al_2O_3 SIS. Blue domains in the reconstructed volume correspond to high PMMA density.

In pursuing the goal of high-throughput analysis of samples, we further developed the infrastructure at the 8-ID-E APS beamline with two new chambers for experiments that will focus on the evolution and dynamics of structure during assembly.

Proposed Work for FY 2015

Following the original aims of the project, we will test the developed tools for three-dimensional characterization by using GISAXS with samples that contain programmed defects provided by our partner, IMEC. Furthermore, STEM experiments on directed self-assembled copolymer structures will be applied to evaluate the applicability of the method in extracting three-dimensional information. We anticipate that the new chambers will be commissioned, providing us with new capabilities to prove the dynamic evolution of our samples by using x-ray scattering techniques. Finally, within the next year, we will also explore the new RSoXs instrument that is being developed at APS.

Transition Edge Sensors for Fundamental Physics

2013-219-R1

Clarence Chang, Valentyn Novosad, Gensheng Wang, and Volodymyr Yefremenko

Project Description

The goal of our project is to develop large arrays of superconducting transition edge sensors (TES) for applications in fundamental physics. The TES is an ultra-sensitive thermal detector that exploits the sharp superconducting-to-normal transition of a superconducting film. The fabrication of large TES detector arrays requires engineering of material transport properties; tuning of superconducting properties; and nano-machining of superconducting circuitry, mechanical, and thermal structures. Our project involves studies of precision fabrication techniques and novel production processes, all with the goal of mass-producing large arrays of TES detectors. Our detector development project will enable the fabrication of a 16,000-element TES detector array for the South Pole Telescope (SPT). Such an array will not only revolutionize our understanding of the cosmic microwave background (CMB), but it will also support DOE missions by positioning Argonne to address the technical challenges confronting future experiments requiring large arrays of TES detectors. For example, large TES arrays are relevant for the detection of long-wavelength photons, x-ray spectroscopy, gamma-ray spectroscopy, and heavy particles.

Mission Relevance

This project is directly relevant to DOE's High Energy Physics Program. In particular, Argonne staff will develop new technology required for building large TES detector arrays, including the largest CMB focal plane in the world. This detector array will push the boundaries of CMB science, which explores the physics of our universe, the nature of cosmic inflation, and the neutrino sector. CMB measurement is a cornerstone of modern cosmology and a critical element of high energy physics in the United States. Developing the capability to mass-produce large TES detector arrays will not only sustain leadership in CMB science, but it will also lay the foundation for exploring new opportunities across a broad spectrum of applications. Potential future directions range from particle physics to national security.

FY 2014 Results and Accomplishments

Our team achieved several accomplishments in FYs 2013 and 2014. Our first accomplishment was the acquisition and commissioning of new equipment for TES detector array development. Five new tools, including four micro-fabrication tools (stepper, inductively coupled

plasma [ICP] etcher, and two AJA International, Inc. sputtering systems) and one adiabatic demagnetization refrigerator (ADR) for detector testing, were installed and successfully commissioned. We integrated these new tools into our detector fabrication process. Figure 1 shows an image of a multi-chroic CMB pixel fabricated by using our new tooling. Our second accomplishment was the successful investigation of new superconducting materials for our TES detectors. Specifically, we developed a TES fabrication recipe by using titanium (Ti) where we used a nanolayer of gold (Au) to passivate the film surface without compromising the superconducting transition temperature. Results to date from measurements of our films strongly suggest that our TES recipe is yielding repeatable superconducting properties with good uniformity over 150-mm wafers. We also combined this new TES material with our previously developed technique of transition engineering to fabricate new TES detectors. Characterization of these TES detectors demonstrated excellent operational performance.

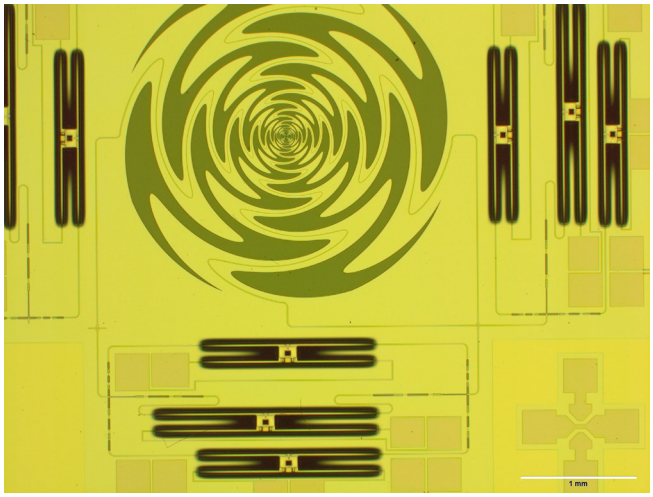

Figure 1. A sinuous antenna coupled TES detector. The central feature is a broadband sinuous antenna that couples to millimeter wavelength radiation. The vertical polarization of the signal propagates along the horizontal microstrips to the right and the horizontal polarization propagates toward the bottom. For each polarization, two lumped element triplexers split the signal into three channels centered at 90 GHz, 150 GHz, and 220 GHz, respectively. For each channel, the signals are symmetrically fed to a dissipative resistor from both sides on a TES bolometer. The signal in each channel is measured by the TES bolometer. The TES bolometers on the left are not connected to the antenna and are used for non-optical studies.

Proposed Work for FY 2015

Our work in FY 2015 will focus on scaling up our detector fabrication recipes and processes to consistently fabricate complex detector architectures having uniform and predictable performance across large (150 mm) substrates. As previously discussed, we have already fabricated a number of individual multi-chroic pixels. In FY 2015, we will perform extensive cryogenic characterizations of these devices and, on the basis of the results of these measurements, we will adjust our fabrication techniques to optimize our device performance. In parallel, we will migrate our processing from fabricating individual detectors on 100-mm wafers to fabricating detector arrays on 150-mm wafers. All of our new tools are compatible with and optimized for processing these large substrates. We will use feedback from subsequent testing of our arrays to optimize our recipes to realize uniform and consistent fabrication.

Integration of Scalable Microwave Reactor with High-Energy X-ray Beamline for High-Throughput Screening Energetic Nanomaterial Synthesis

2014-121-N0

Yugang Sun, Jonathan D. Almer, Zonghai Chen, Joseph Gregar, John Okasinski, and Yang Ren

Project Description

This project focuses on integrating microwave reactors and high-energy x-rays from Argonne's Advanced Photon Source (APS) in order to directly probe the complex chemical and physical processes involved in synthesizing colloidal energetic nanoparticles. The ultimate goal is to provide a generic platform for studying the reaction kinetics, intermediate species, structural transitions, and defect evolution of nanoparticles in real time and under reaction conditions. Using this platform, we will be able to create predictive and rational designs for functional nanoparticles with controlled architectures that range from the atomic and molecular to the continuum scale.

Microwave-assisted synthesis has recently been demonstrated to be a greener strategy than conventional heating methods with regard to its potential scalability because of its higher level of thermal management and its dramatically reduced reaction time. Such advantages motivated us to systematically screen the reaction conditions required for the scalable synthesis of functional colloidal nanoparticles by using *in situ* high-energy x-ray techniques. These are crucial for large-volume reaction systems because of the strong penetration of high-energy x-rays in solutions. The rapid reaction kinetics in large, statistically relevant sample volumes can be captured by seamlessly integrating (a) microwave nanoparticle synthesis; (b) high-energy, small- and wide-angle x-ray scattering (SAXS/WAXS) at APS beamlines; and (c) glassware fabrication, then applying the results to energy storage and catalysis at Argonne, a site where such expertise resides. Specifically, integrating an *in situ* microwave reactor on a high-energy x-ray beamline will establish the capability

to carry out high-throughput screening of the synthesis of functional nanomaterials at a large scale, and this will likely have a significant impact on our understanding and optimization of functional nanomaterials for energy applications.

Mission Relevance

This research represents a key component needed for discovering and designing a wide variety of energy-relevant materials. It aligns well with the mission of one of the three core research areas (materials discovery, design, and synthesis) in the Materials Sciences and Engineering Division of DOE's Office of Basic Energy Science (BES), tying in closely with research in synthesis and processing science. Because of the importance of the synthesized nanomaterials for energy applications, this project is also relevant to programs in DOE's Office of Energy Efficiency and Renewable Energy (EERE) and Energy Frontier Research Centers (EFRCs), which focus on energy research using, for example, high-quality nanoparticles for catalysis, energy conversion, and energy storage. Success in developing such key instruments will also benefit the Materials Genome Initiative.

FY 2014 Results and Accomplishments

In FY 2014, we started work by selecting a microwave reactor, modifying critical components (e.g., cavity, enclosure), assembling the modified pieces, integrating the modified microwave reactor with the high-energy synchrotron x-ray beamline, and conducting a preliminary *in situ* evaluation. The major achievements are summarized as follows.

- *Fabrication of a Microwave Cavity Compatible with Synchrotron X-ray Beamlines*. On the basis of the engineering details and critical parameters of a commercial microwave reactor, we fabricated a microwave cavity with a geometry and apertures that were compatible with *in situ* x-ray measurements. The as-fabricated cavity was also exchangeable with the original cavity in the microwave reactor. The necessary inserts, made of special Teflon blocks, were also fabricated for such compatibility. The as-fabricated cavity and corresponding inserts were able to allow x-ray beams to pass through in order to probe colloidal nanomaterials in a glass tube reaction vessel. The cavity and reaction vessel were evaluated at APS beamlines 11-ID-C, 1-ID-D, and 1-BM-B, demonstrating the promise for *in situ* probing of colloidal nanomaterials in the glass tube reaction vessels.
- *Assembly of the Modified Microwave Reactor*. The as-fabricated microwave cavity and corresponding inserts were integrated with other components of the reactor. The assembled system was proved to be capable of synthesizing nanomaterials, as proven by the synthesis of MnO_2 nanostructures. The reassembled microwave reactor was also evaluated for its compatibility with synchrotron x-ray scattering techniques at the APS beamlines (Figure 1).

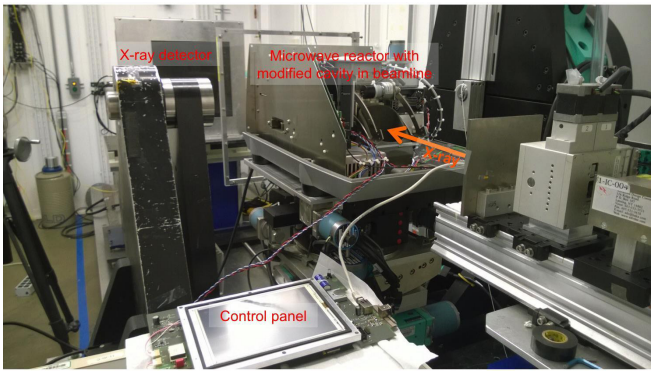

Figure 1. Assembled microwave reactor with specially fabricated microwave cavity. The microwave reactor was placed and aligned in the x-ray beam at APS's beamline 11-ID-C.

- *Real-time Probing of the Synthesis of $CuInS_2$ Nanocrystals*. We also used the integrated system shown in Figure 1 to monitor the synthesis of colloidal $CuInS_2$ nanocrystals in real time. In a typical synthesis, we used bismuth (Bi) nanoparticles as catalysts to facilitate the growth of $CuInS_2$ nanocrystals by heating a reaction solution with the microwave reactor. Figure 2 presents the time-resolved WAXS patterns recorded when a reaction solution was heated to and maintained at 270°C. Apparently, two crystalline phases of $CuInS_2$ were formed. The tetragonal chalcopyrite $CuInS_2$ nanocrystals started to appear when the temperature reached ~230°C; hexagonal wurtzite $CuInS_2$ nanocrystals formed only after the temperature reached 270°C. The amount of both types of $CuInS_2$ nanocrystals continuously increased with time. We also studied and compared *in situ* reactions at other temperatures. The results provided feedback that helped us understand the growth mechanism of $CuInS_2$ nanocrystals and design the synthesis to achieve nanocrystals with tailored properties (e.g., crystalline phase purity) and better performance.

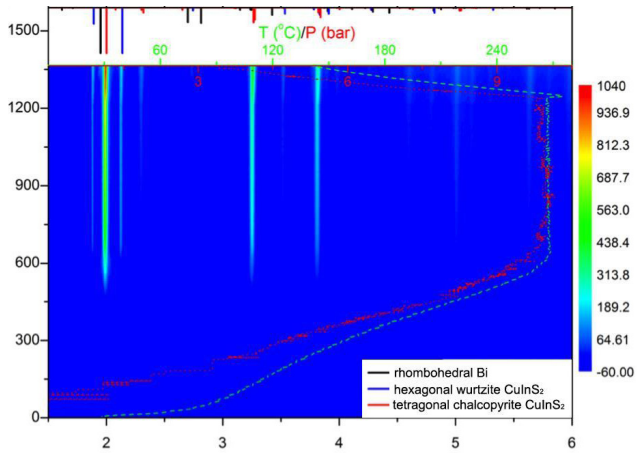

Figure 2. The evolution of WAXS patterns of the crystalline $CuInS_2$ nanocrystals formed at different reaction times. The sticks associated with the top axis represent the standard powder diffraction patterns of crystalline Bi (black), tetragonal chalcopyrite $CuInS_2$ (red), and hexagonal wurtzite $CuInS_2$ (blue). The dependencies on time of the solution's temperature (green dashed curve) and pressure above the reaction solution (red dotted curve) are also plotted.

Proposed Work for FY 2015

In FY 2015, we will work to improve the compatibility and efficiency of the microwave reactor with regard to the high-throughput screening associated with nanomaterial synthesis. Specifically, we will:

- Design the microwave reactor's enclosure and integrate an automated sample handling system with the reactor;
- Implant a remote control system (hardware and software) to synchronize communication between the microwave reactor and synchrotron x-ray beam;
- Establish the data collection and analysis protocol for studying nucleation and growth of nanoparticles; and
- Apply the integrated system to synthesize interesting energy-related nanomaterials.

Length-Scale Bridging Computational Scheme for Structure and Transport

2014-128-N0

Olle Heinonen, Dmitry Karpeyev, Nichols A. Romero, Peter Zapol, and Xiaoliang Zhong

Project Description

This project addresses the many-fold computational challenges encountered in systems in which a local domain has to be treated quantum mechanically (including electronic correlations) but is interacting with and influenced by larger regions that cannot, because of their sizes, be treated quantum mechanically. Examples are metal/insulating oxide/metal (MIM) heterostructures, where electrostatics and strain from the larger structure, composed of electrodes and surrounding encapsulation, significantly influence both the atomic structure and the transport of charged species. On the other hand, the atomic structure and transport phenomena are inherently quantum mechanical, and they are frequently strongly affected by electronic correlations. Such structures are ubiquitous in resistive random access memories, battery electrodes, and catalytic systems — all of which are important strategic research areas.

The goal of this research is to develop a scalable computational framework and codes that will concurrently combine and merge state-of-the-art, first-principle, quantum mechanical calculations for structure and transport with mesocale calculations for strain and electrostatic fields on large irregular domains. The research will use, as a prototypical system, MIM heterostructures in which the insulating oxide is a transition metal oxide; that is, in which strain and electrostatic fields can be used to manipulate oxygen defects and the conductance of the heterostructure, with important applications in low-power, nonvolatile memories. Part of the work will be conducted in collaboration with researchers at Trinity College, Dublin.

Mission Relevance

The project supports the mission of DOE's Office of Basic Energy Sciences (BES) to foster work in areas relevant to energy efficiency, through use-inspired research in and development of new materials for information storage and the efficient use of energy. The general scientific community will also benefit, since the codes that are developed will be made available to the public.

FY 2014 Results and Accomplishments

We investigated titanium (Ti) oxides (TiO_2, Ti_2O_3, and Ti_4O_7) that are frequently used in experiments on resistive-switching structures. Applying bias voltages to such structures leads to the creation of oxygen vacancies, which change the local stoichiometry and electronic structure. Then stoichiometric TiO_2 can initially give rise to regions with Ti in different oxidation states. A more important consideration is that TiO_2 and Ti_2O_3 are insulators, while Ti_4O_7 is insulating in its low-temperature (LT) phase and metallic in its high-temperature (HT) phase. Therefore, the creation of oxygen vacancies and their subsequent migration can lead to regions of high-conducting, metallic Ti_4O_7.

We used a development version of the electronic structure and transport code *smeagol* to calculate the electronic structure of the different Ti-oxides. Since transition metal oxides typically have strong electronic interactions (so-called correlation effects), standard applications of electronic structure codes using the so-called local den-

sity approximation (LDA) can fail miserably because they do not adequately treat electronic correlations. We used a version of *smeagol* that includes electronic interactions beyond LDA by correcting for electronic self-interactions (SICs). Previous research by others had reached different conclusions regarding the electronic structure of the LT and HT phases of Ti_4O_7. By using *smeagol* code with SICs, we found that we could reproduce the insulating behavior and electronic band gaps of TiO_2 and Ti_2O_3 as well as the metallic behavior of the HT phase of Ti_4O_7. In addition, we found that the LT phase of Ti_4O_7 is a novel antiferromagnet insulator. We also predicted that the LT phase of Ti_4O_7 could have a strain-induced phase transition from an insulating antiferromagnet to a metallic ferromagnet at about 4% applied compressive strain.

Proposed Work for FY 2015

With collaborators at the National Institute of Advanced Industrial Science and Technology (AIST) in Japan, we will start studying MIM structures with hafnium dioxide (HfO_2) as the metal oxide. These structures are of intense interest to the information technology and semiconductor technology industries because they could be the basic structures in future random access memories. We will calculate the electronic conductivity of HfO_2 MIM structures with titanium nitride (TiN) electrodes, since this is the metal of choice for the semiconductor industry. We will also use the so-called nudged elastic band method to calculate diffusion energy barriers of oxygen vacancies, which we will then use as input to more coarse-grained models of charge transport in these structures.

The electronic transport depends on (i.e., is sensitive to) the atomic structure near interfaces between the oxide, such as HfO_2, and the metal electrodes. We will work with Argonne's Nanoscience and Technology Division to use advanced molecular dynamic simulations to generate quenched disorder at interfaces, which will yield more realistic interface structures. Together with Argonne's Mathematics and Computer Sciences Division, we will also build software tools that will generate a workflow that runs molecular dynamic simulations, feeds the output to electronic structure calculations, runs them, and collects and does post-processing of the data. We will also start using meso-scale finite element simulations to calculate electrostatic fields and strain in larger structures encompassing the MIM structure, then feed the calculated inhomogeneous electrostatic and strain fields to the quantum mechanical transport calculations.

The Design and Synthesis of Novel Oxides: Coupling Materials Informatics with a Next-Generation Deposition System Employing *in situ* X-ray Scattering and Photoemission Spectroscopy

2014-129-N0

Dillon D. Fong, Richard Rosenberg, and Jonathan Z. Tischler

Project Description

The primary goal of this project is to upgrade an existing diffractometer-mounted chamber in order to build the world's first *in situ* synchrotron pulsed laser deposition (PLD) system with both surface x-ray diffraction (SXRD) and hard-angle x-ray photoemission spectroscopy (HAXPES) capabilities. Working with collaborators at Northwestern University and Oak Ridge National Laboratory, the new experimental capabilities will be combined with computational materials design that will focus on developing novel $A_2B_2O_5$ materials that display metal-insulator transition behavior.

We will design new oxide materials ($A_2B_2O_5$ compounds), starting from polyhedral building units (Figure 1), in order to create a novel class of functional materials that undergo metal–insulator transitions (MITs). Our strategy is to understand the chemistries that give rise to particular polyhedral geometries through the confluence of a next-generation *in situ* deposition system with computational tools that quantify the likelihood of a metal oxide being stabilized in a targeted configuration. The PLD system will be the first to exploit both *in situ* atomic and electronic structure probes (i.e., SXRD and HAXPES), making it a revolutionary tool for understanding electronic-atomic structure relationships as the MIT material grows and evolves.

Mission Relevance

The project is relevant to DOE's missions in science and energy. This project focuses on complex oxide materials, an area that is rich in scientific research possibilities and has an outstanding potential for providing solutions that would meet many of our technological needs. Our aim is to discover and design new oxide materials that can exhibit tunable catalytic activities and electronic properties, which are of direct interest to the Office of Basic Energy Sciences.

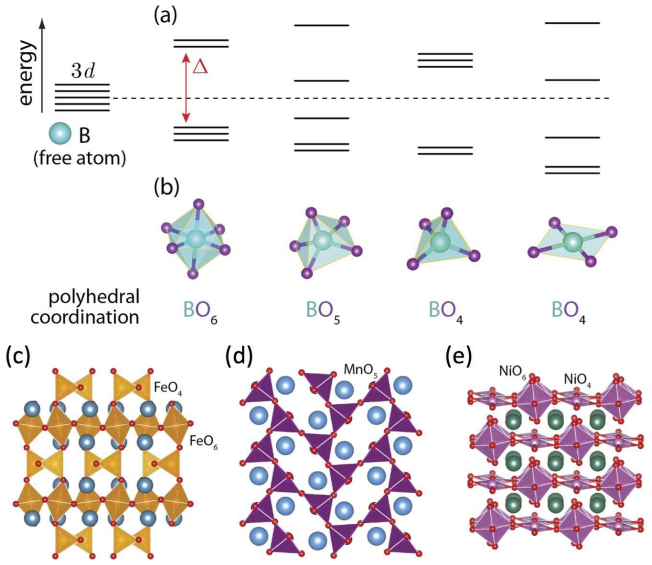

Figure 1. Top shows schematic transition metal d-orbital energy-level diagrams: (a) The crystal field split (Δ) orbital levels that were induced by (b) polyhedra with different B cation coordination geometries. Bottom shows illustrations of the diverse polyhedra found in A2B2O5 compounds: (c) FeO_4 tetrahedra and FeO_6 octahedra found in $Ca_2Fe_2O_5$, (d) pyramidal MnO_5 found in $Sr_2Mn_2O_5$, and (e) square planar NiO_4 and octahedral NiO_6 found in $La_2Ni_2O_5$.

FY 2014 Results and Accomplishments

In FY 2014, we redesigned the *in situ* PLD system at Sector 33 of Argonne's Advanced Photon Source (APS), and we received the mechanical components of the hemispherical electron analyzer (VG Scienta EW4000). The electron analyzer fits on the current diffractometer table and points down along the sample's normal direction. This geometry permits easy control over the attenuation length and thus allows variable information depth profiles for HAXPES; it enables the protection of the HAXPES lens system from the deposition flux, and it does not interfere with the current scattering geometry.

Even before the *in situ* PLD-HAXPES system was available, we had been performing real-time growth studies of $A_2B_2O_5$ materials; in this case, the material was $Sr_2Co_2O_5$ with *in situ* PLD-SXRD. We found that the successful growth of this system was extremely sensitive to the strain state, temperature, and oxygen partial pressure. For example, the 225 phase was favored when it was grown on $SrTiO_3$(001), while the 113 perovskite phase was favored when it was grown on $(La_{0.18}Sr_{0.82})(Al_{0.59}Ta_{0.41})O_3$ (LSAT)(001) substrates (see H. Jeen et al., 2013, "Reversible redox reactions in an epitaxially stabilized $SrCoO_x$ oxygen sponge," *Nature Materials* 12, 1056). Figure 2 shows the intensity from the 00½ position in reciprocal space for $Sr_2Co_2O_5$/$SrTiO_3$(001) deposition (along with the diffuse scatter on the right), which reflects the layer-by-layer growth oscillations from heteroepitaxy as well as the appearance of the brownmillerite phase. With our *in situ* capability, we were able to map the stability of the brownmillerite phase as a function of both growth temperature and oxygen/ozone pressure. With the future HAXPES capability, we will be able to quickly determine the cobalt (Co) valence state and retrieve information on the oxygen stoichiometry in combination with the scattering data, and we will be able to monitor the evolving electronic structure as oxygen is inserted/removed from the lattice.

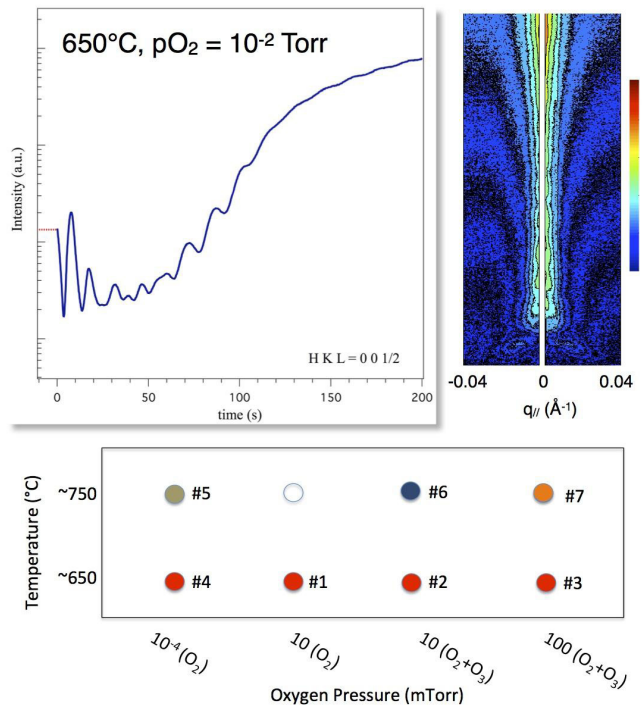

Figure 2. Top shows the intensity from the 00½ position as a function of time during growth of $Sr_2Co_2O_5$ on $SrTiO_3$(001). The diffuse intensity is shown on the right. Bottom shows phase map with the brownmillerite phase (red) at 650°C and other unidentified phases or phase mixtures at 750°C.

Proposed Work for FY 2015

During FY 2015 and 2016, we will install the HAXPES capability with the upgraded growth chamber and conduct the first growth studies. Also, we will begin constructing a digital materials library for $A_2B_2O_5$ structures, including elemental descriptors, stability parameters, and materials properties. As shown in Figure 1, interesting coupling between the polyhedral tiling and electronic behavior exists, and the researcher will mine the digital materials library for the design rules that will lead to coupled theory-*in situ* synchrotron synthesis studies of novel phases.

New Materials for Natural Gas Storage and Conversion Technologies

2014-130-N0

Theodore Krause, Di-Jia Liu, Jeffery Miller, and Randall Winans

Project Description

This project will develop new catalyst technology for the selective oxidation of methane — the primary component of natural gas — directly to methanol. Methanol can then be converted to transportation fuels (e.g., gasoline, diesel, or aviation fuel) by a number of existing process technologies. In current industrial practice, producing methanol first involves the steam reforming of methane to generate synthesis gas, which is a mixture of carbon monoxide and hydrogen. The synthesis gas is subsequently converted to methanol via a catalytic process. The production of synthesis gas is a costly, energy-intensive process that makes the conversion of methane to transportation fuels uneconomical in today's market. The technical challenge for the direct conversion of methane to methanol is to develop a catalyst that activates and oxidizes methane while preventing the methanol, once formed, from being subsequently oxidized to carbon dioxide, which is the more-favored thermodynamic product. A successful selective oxidation catalyst would allow for the development of new process technologies for recovering stranded natural gas that currently is either flared or reinjected into the well during oil recovery.

Our approach to catalyst development is based on "single-site" catalysts consisting of a catalytically active metal atom isolated in the framework of a porous organic polymer (POP), a metal oxide such as SiO_2, or a zeolite. Our hypothesis is that by having only one catalytically active site present, secondary reactions, such as the oxidation of methanol to carbon dioxide, will be prevented from occurring at the catalytic site where the initial reaction step to convert methane to methanol occurs. The POP, metal oxide, or zeolite provides a framework for stabilizing the isolated single metal atom, thus inhibiting the metal atoms from agglomerating to form large metal particles under reaction conditions. Once metal particles form, a large number of catalytically-active metal sites are within atomic distance of each other; that can lead to multiple reaction steps occurring in concert and result in the overoxidation of methane to carbon dioxide.

For this project, new single-site catalysts supported by a POP, metal oxide, or zeolite are synthesized by using organometallic complexes consisting of first-row transition metals or selective platinum group metal complexes as precursors based on synthetic techniques that we developed previously. The catalysts are screened by using high-throughput experimental techniques to identify the catalysts that exhibit two features: high convertibility and high selectivity. Because methane is the least reactive of the small hydrocarbon molecules (i.e., it has the highest carbon-hydrogen bond strength) and because oxygen is a highly-reactive oxidant, screening tests are initially conducted by using the more reactive small hydrocarbon molecules, such as hexane, cyclohexane, and cyclohexenes, and "soft" oxidants, including organic peroxides and nitrous oxide (N_2O). Once candidate catalysts that meet both criteria have been identified, they undergo further development so the reaction mechanism can be understood. Then this information is used to optimize their performance targeting, using methane and oxygen (air) as the reactants.

Mission Relevance

The project is relevant to DOE's missions in energy and environment. The development of catalysts that can lead to cost-competitive technologies for converting domestic reserves of natural gas to gasoline and diesel will reduce our dependency on foreign oil imports and reduce greenhouse gas emissions.

FY 2014 Results and Accomplishments

A wide range of catalysts supported by POP, metal oxide, or zeolite containing scandium, titanium, vanadium, chromium, manganese, iron, cobalt, nickel, copper, zinc, and gallium were prepared and tested in a high-throughput screening pressure reactor and a plug-flow microreactor system. The catalysts were characterized by using a number of analytical techniques (including x-ray absorption spectroscopy) at Argonne's Advanced Photon Source to confirm the single-site nature of the catalysts. Screening results, obtained when mild oxidants (e.g., tertiary-butyl peroxide and N_2O) were used, showed that all catalysts displayed some degree of oxidation activity. The best-performing catalysts were those containing vanadium, chromium, copper, and nickel. Reaction studies showed that oxidative dehydrogenation was completed, with oxidation of alkanes to the corresponding alcohol. We found that for copper catalysts, oscillatory behavior occurred, depending on the reaction conditions using N_2O; the catalyst promoted either oxidative dehydrogenation or thermal cracking of cyclohexene, depending on the concentration of N_2O in the feed stream.

In-situ X-ray Characterization of Doped Materials by Atomic Layer Deposition for Energy Applications

2014-133-N0

Thomas Proslier, Jeffrey W. Elam, Steve Heald, Jeffrey Klug, Michael J. Pellin, Christian Schlepuetz, and Angel Yanguas-Gil

Project Description

Doping is the key materials synthesis technology that has enabled revolutionary advances in semiconductor manufacturing over the last 40 years. Full realization of the potential of doped materials would require precise, atomic-scale control over the concentration, position, coordination, and spacing of dopants in the host lattice. However, conventional doping methods, such as ion implantation and diffusion, randomly introduce the dopant atoms into the host lattice, and the material properties are averaged over this statistical concentration and distribution. It is clear that this random distribution limits the range of material properties that one could achieve and hinders performance and applications.

In contrast, atomic layer deposition (ALD) offers the unique ability to control, at the atomic level, the three-dimensional (3-D) distribution of dopants while also controlling their chemical and structural (i.e., crystallographic) environment. With atomically precise and local doping control, ALD enables more efficient use of dopants and achieves superior performance. It also enables new pathways to transformational breakthroughs. To achieve this goal, we need to better understand the science of ALD synthesis, and the best way to accomplish this is through *in situ* studies.

In this project, we have developed a unique instrument for performing *in situ* studies of dopant concentration, local chemical environment, and structure (including short- and long-range order) during ALD using synchrotron x-ray measurements, such as x-ray diffraction (XRD), extended x-ray absorption fine structure (EXAFS), and x-ray absorption near edge structure (XANES). Ultimately, after these fundamental analyses are conducted, the optimal doped materials can then be straightforwardly scaled up to ALD for production-scale applications.

Mission Relevance

This project is tied to DOE's mission in basic energy sciences. It will provide a powerful research tool that can be applied to a large pallet of materials and energy-related research areas for which uniform doping is the main technical challenge. These research areas include thermoelectrics, solar cells, lasers, catalysis, and batteries, which are at the heart of DOE clean energy strategic research priorities. The results of this project may also be of interest to the Department of Defense, particularly the Defense Advanced Research Projects Agency.

FY 2014 Results and Accomplishments

Chamber Design and Construction. The design of two portable ALD chambers (one for XRD and the other for EXAFS studies), based on the flow simulations in the ALD regime, is done and the construction underway. For *in situ* XRD analysis, we chose a compact (60-mm diameter) graphite dome chamber from Anton-Paar (Figure 1) that will be mounted onto a custom base with gas and heating feedthroughs.

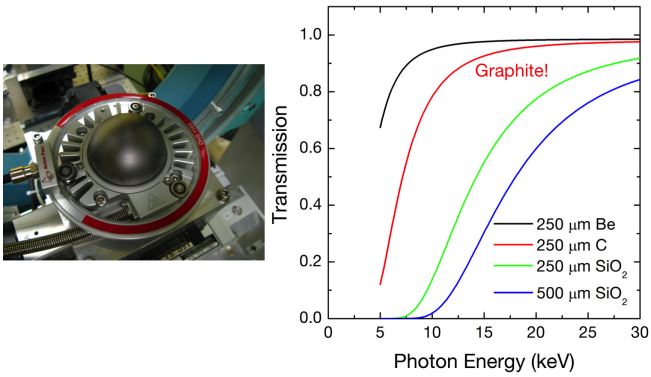

Figure 1. (Left) Graphite dome used for in situ *x-ray diffraction studies. (Right) The transmission of graphite versus photon energy compared with that of SiO_2, Be, and C.*

Graphite offers the best compromise between transmission capability and versatility. A boron nitride substrate heater from Shin-Etsu will enable a large range of *in situ* chemistry studies up to 600°C; it will also enable rapid *in situ* annealing and its effect on nucleation/crystalline growth.

Preliminary Results. We ran two self-contained doping projects by *ex situ* EXAFS at the Advanced Photon Source (APS). The first project was aimed at demonstrating the possibility of controlled doping in three dimensions. Due to the nature of the emissive properties of rare earth doped materials, the presence of clustered dopant ions is readily evidenced and detrimental. To this end, a series of experiments was devised to prove that ALD-deposited Er^{3+}:Y_2O_3 has 3-D dopant placement, and that once deposited these dopants remain fixed during post-processing. In particular, we were able to demonstrate that the exclusion volume around each dopant can be tuned by the size of the precursor molecules used to synthesize the dopant Er_2O_3. This molecule size, in turn, influences the emissive properties of the dopants.

The results and fitting obtained from this EXAFS run are shown in Figure 2. Over 16 samples were analyzed by

EXAFS using a four-element vortex at both the yttrium (Y) and Er edges on flat samples and nanopowders. The following conclusions were drawn:

1. No change in the number of Er atoms in the second shell after a post-deposition anneal in a model nanolaminate sample indicated that the 3-D doping structure is not modified by post-annealing up to 700°C for 5 h, and Er diffusion was negligible.
2. The disorder parameter increased as the thickness of the Y_2O_3 layer decreased. An amorphous-to-crystalline transition of the host Y_2O_3 occured as the film thickness increased from 2 to 10 nm. This result gives a possible explanation why the lifetime of doped films grown on a 10-nm-thick base layer is ~30% higher than that for the ones grown without base layers.
3. The number of Er atoms present in the second shell increased as the distance between the doping layers decreased and as the doping increased. This trend stopped for cycle ratios lower than 1:16, which imposed a limit on the minimal possible distance between doping layers (and, therefore, the maximal concentration achievable), which here was 2 nm.

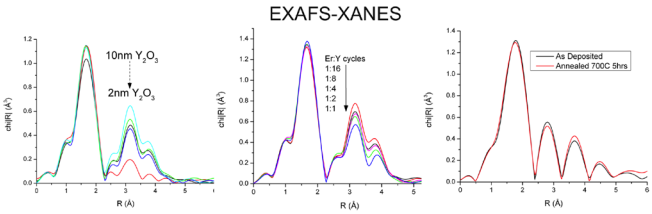

Figure 2. EXAFS measurements of crystallinity of as-deposited films as a function of the host thickness (left), the proximity of dopants as a function of doping level (middle), and crystallinity of as-deposited versus annealed films (right).

The second project aimed at understanding the impact of synthesis and doping on the microstructure of high dielectric constant (k) materials. Our approach was based on the use of XAFS to understand the impact of synthesis and doping on the coordination environment of hafnium (Hf) in pure and doped hafnium oxide (HfO_2) films synthesized by ALD. We characterized as-deposited and annealed samples of undoped HfO_2, aluminum (Al)-doped HfO_2, and magnesium (Mg)-doped HfO_2. A key result was that Al and Mg dopants both stabilized the cubic phase of HfO_2, a structural analog of yttria-stabilized zirconia, whereas the undoped films were monoclinic. This resulted in distinct EXAFS spectra, as shown in Figure 3, of annealed films that were consistent with the corresponding crystalline structures. The as-deposited films were all amorphous, but differences in the EXAFS spectra were observed between the undoped and doped materials. These differences are much larger than those expected from pure substitutional doping, indicating a change in the underlying Hf coordination environment. These results were also supported by our analysis of the XANES part of the absorption spectrum.

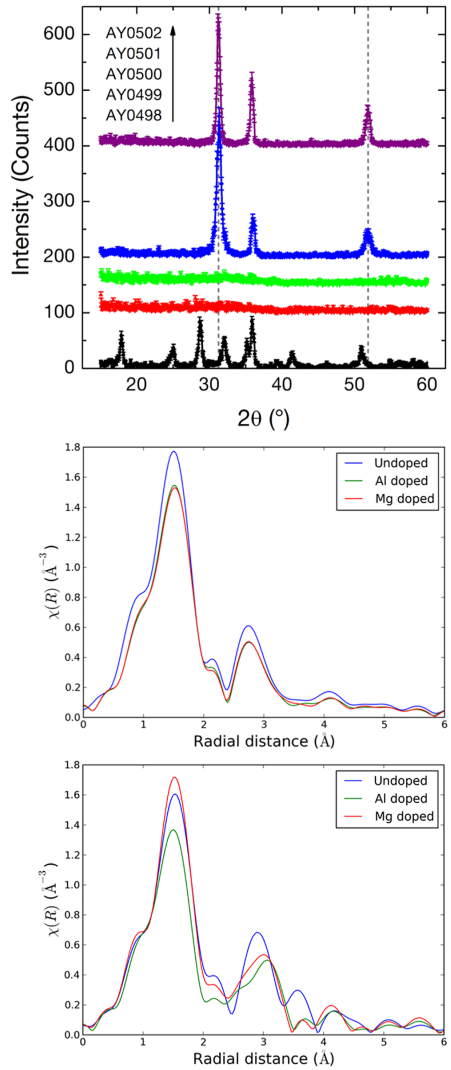

Figure 3. (Left) Grazing incidence XRD measurements of annealed HfO_2 (black curve), 3:3 and 1:1 nanolaminates (red and green), and Al- and Mg-doped HfO_2 (blue and purple) films, showing a transition from monoclinic to cubic as a consequence of doping. EXAFS measurements at Hf L3 edge of as-deposited (center) and annealed (right) HfO_2 samples that are undoped, doped with Al, and doped with Mg.

Proposed Work for FY 2015

Proposed work for FY 2015 includes the following tasks:

- Test/optimize the new portable ALD system on an APS beamline for surface diffraction with high temperature growth alloys.
- Investigate an expanded group of doped materials, including multicomponent, complex layered oxides: strontium (Sr)-doped $LaMnO_3$ and Sr-doped $LaCoO_3$ for fuel cells. By the end of the second year, we will open up the project to the broader material synthesis community interested in high doping homogeneity.
- Develop precursors for multicomponent and complex alloys.

- Study multicomponent, layered, and complex alloys for thermoelectrics [bismuth (Bi)-doped lead telluride (PbTe)] and for photovoltaics [cadmium (Cd)-doped zinc sulfide (ZnS)].

Seminars

Klug, J. (2015). "Atomic Layer Deposition of Nanoscale Superconductors." Illinois Institute of Technology, Chicago, IL, November 20, 2014.

Fast Electronic Structure Methods for Rapid Reaction Screening for Inorganic Materials Synthesis and Particle Formation

2014-139-N0

Albert Wagner, David Dixon, Murat Keceli, Álvaro A. Vázquez-Mayagoitia, and Peter Zapol

Project Description

If calculations and simulations are to assist experimental programs directed at the synthesis of new materials and chemicals, new codes must be developed capable of studying experimental systems with very large numbers of atoms. We are developing highly parallelized codes to enable the discovery of new synthesis pathways via simulations involving up to tens of thousands of atoms for molecules and solids. One code involves semi-empirical molecular orbital (SEMO) theory, and the other involves semi-empirical density functional theory based on tight binding (TB-DFT). Two computational needs must be addressed:

- An efficient method to calculate the energy of molecular systems by the parallelization of available eigensolver methods for massively parallel computers.
- An improved training set for optimizing the "empirical" SEMO/TB-DFT parameters by supplementing scattering measurements of molecular energies with systematic and accurate *ab initio* electronic structure calculations on small molecular systems.

Mission Relevance

The project is relevant to DOE's missions in energy and science. Reliable computational methods that predict reaction mechanisms are needed for use in condensed-media synthesis planning and the management of particle growth in a broad variety of environments. The need for making and breaking chemical bonds means that electronic structure must be explicitly included in the simulation. At present, SEMO/TB-DFT electronic structure methods are the fastest available. Success in developing efficient semi-empirical code will enable basic energy science studies in areas relevant to DOE's mission, such as combustion (soot formation), heterogeneous catalysis, nuclear chemistry (aggregation phenomena), materials phase changes, and multilayered materials.

FY 2014 Results and Accomplishments

Parallelized Eigensolver: For the TB-DFT method, conventional eigensolvers scale cubically in problem size for the computational time and quadratically for the memory requirement. Using the shift-and-invert parallel spectral transformations (SIPs) method and parallel libraries that take full advantage of the largely zero matrix elements in the TB-DFT Hamiltonian matrix whose eigenvalues we seek, we demonstrated effective parallelization for three example systems: metallic single-wall carbon nanotubes, diamond nanowires, and crystal diamonds of varying sizes. Figures 1 and 2 show representative results for examples with matrix sizes as large as 512,000 × 512,000 (128,000 carbon atoms) run on up to 266,144 cores on Argonne's Blue Gene/Q supercomputers. The results in Figures 1 and 2 show that the eigensolution can be obtained in tens of seconds for any size of our problems given enough computer cores. Conventional eigensolvers cannot handle the largest problems in the figures and become competitive with SIPs only for the smallest problems.

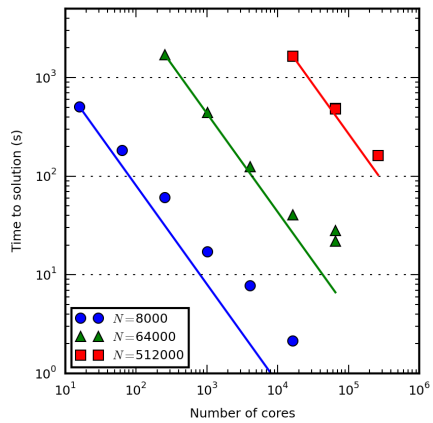

Figure 1. Time to solution vs. number of cores for different sizes of nanotube as measured by the matrix size.

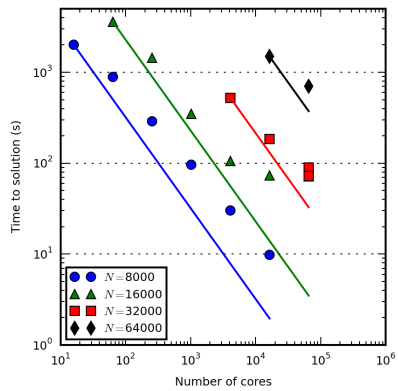

Figure 2. Same as in Figure 1, only for different sizes of diamond.

Training Set Improvements: We use *ab initio* electronic structure methods, namely, coupled cluster with a full treatment of single and double excitations [CCSD(T)], to predict the nucleation energies leading to the formation of transition metal oxide clusters, which are widely used as catalysts and catalytic supports in industrial practices and which also exhibit many different types of bonding motifs. The resulting systematic set of structures and energies improves the training set for transition metal SEMO parameters. We examined $(M'_2O_5)_n$ and $(M_2O_7)_n$, where $n \leq 5$; M' = V (vanadium), Nb (niobium), and Ta (tantalum); and M = Mn (manganese), Tc (technetium), and Re (rhenium). We determined that $(Mn_2O_7)_n$ exhibits interesting bonding behavior with the presence of O_2^{2-} groups either bonded to a single Mn or bridging Mn groups, while $(Tc_2O_7)_n$ and $(Re_2O_7)_n$ do not bond this way. The cluster structures can have a coordination number quite far from the bulk coordination number, consistent with the slow convergence of the nucleation energy to its bulk value.

Proposed Work for FY 2015

Proposed tasks are as follows:

- Development of a formal connection with TB-DFT developers.
- Generation of a parallel Hamiltonian build. The SIPs work currently uses a modestly parallel SEMO or TB-DFT generation of the Hamiltonian matrix in a separate job from the parallel eigensolve. We will develop a fully parallel united code.
- Further optimization of SIPs with each iteration of the self-consistency process.
- Formulation and solution of an illustrative science problem that requires our software.

Developing Predictive Models of Wide Bandgap Semiconductor Synthesis and Processing

2014-151-N0

Paul H. Fuoss, Jeffrey A. Eastman, Jeffrey W. Elam, Ross J. Harder, Matthew J. Highland, Martin V. Holt, Stephan O. Hruszkewycz, Angel Yanguas-Gil, and Peter Zapol

Project Description

In this project, we seek to develop a nanoscale understanding of the physical and chemical processes associated with the growth of wide bandgap (WBG) semiconductors, such as gallium nitride (GaN) and aluminum nitride (AlN), and to follow the structural evolution of a semiconductor as it is processed into a device. In this work, we examine the synthesis of AlN by using three growth techniques: sputtering of AlN in a reactive environment of nitrogen, atomic layer deposition (ALD), and metal organic chemical vapor deposition (MOCVD). State-of-the-art synchrotron techniques are being used to discover common growth mechanisms and highlight differences between the growth techniques. Through the use of advanced x-ray imaging techniques, we are able to follow the evolution of strain and the behavior of defects during the growth process, device processing, and cycling of prototype devices. From that data, we are able to isolate critical attributes of the AlN layer. At the same time, complementary multiscale computational studies, from macroscopic chamber flows to atomistic modeling of surface reactions, are used to develop models that predict strain evolution and defect generation during semiconductor growth and device processing.

Mission Relevance

This project's development of a nanoscale understanding of the synthesis and processing of WBG materials is relevant to the DOE mission in energy technology because it could enable higher performance devices, which have enormous potential for revolutionizing the control and transmission of electrical power. This potential has led to a significant interest in improving WBG technologies with GaN and AlN templates, which are considerably less developed than those for silicon and optoelectronic materials. This development will require a much deeper understanding of the physics and chemistry of the WBG materials. The needed understanding starts at the beginning of the growth process, where the detailed mechanisms of the creation of the AlN nucleation and diffusion barrier layer, as well as the role of interfacial defects, are poorly understood and extends through device processing and, ultimately, performance.

FY 2014 Results and Accomplishments

We explored the synthesis of AlN using *in situ* diffraction analysis of sputter deposition and optical spectroscopy of ALD deposition. Our sputter deposition measurements explored the initial nucleation and growth of AlN films on sapphire and revealed a three-step relaxation process proceeding from coherent epitaxy to relaxed epitaxy and, ultimately, a mosaic film. The ALD studies focused on developing fundamental information regarding chemical processes occurring in both ALD and MOCVD. Because of its pulsed nature, ALD separates the growth into two isolated steps: the interaction of trimethylaluminum with a nitride surface and the displacement of a methyl-containing species by NH_x species. Our mechanistic studies of AlN synthesis employing the *in situ* generation of NH_x species by Ar/H2/N2 plasmas indicate that reaction pathways involving atomic hydrogen are not reaction limiting for the surface species.

Our initial imaging experiments used the Hard X-ray Nanoprobe at the Center for Nanoscale Materials in the Advanced Photon Source (APS/CNM) to investigate an indium gallium nitride (InGaN)/GaN multi-quantum well (MQW) device grown on GaN template substrates. This technology, critical to solid-state lighting applications, shares processing challenges and defect characteristics with other WBG nitride materials, and we therefore chose it to provide baseline data for work with AlN systems. We examined pit formation in InGaN MQWs by using both fluorescence and diffraction from the individual layers of the device structure (see Figure 1). We found that the displacements of the Bragg peaks for the GaN and InGaN buffer layer are not strongly correlated with the presence of pits. This finding indicates that pit nucleation does not occur at the GaN/buffer layer interface, but arises from crystalline defects occurring during InGaN or MQW growth.

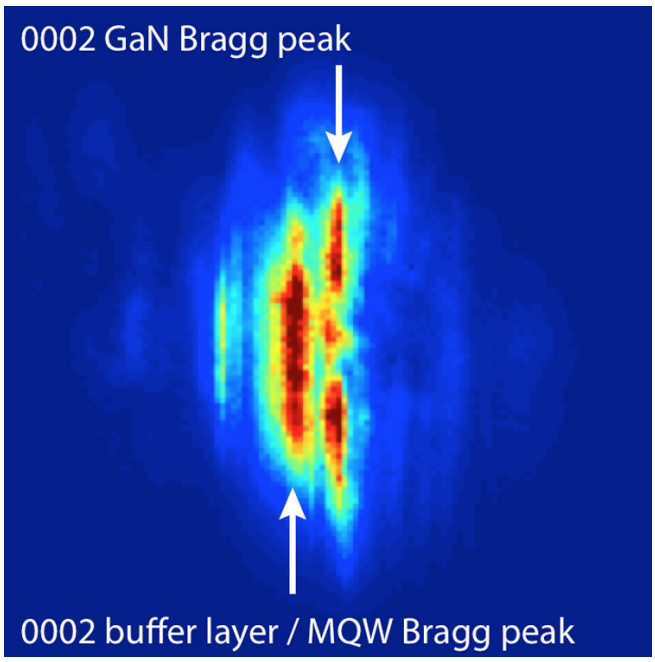

Figure 1. Convergent beam nanodiffraction pattern taken with a 60-nm beam at APS/CNM. The 0002 GaN, 0002 InGaN buffer layer, and 0th order MQW Bragg peak are all visible. Using different regions of interest, the motion of the different peaks could be independently extracted.

A primary goal of the project is to establish multi-scale connections between reactor-scale and atomistic simulations. Focusing on the important but poorly understood interaction of ammonia with WBG surfaces, we used first principles calculations to determine binding energies and reaction barriers of NH_x species (x = 0–3) on the AlN (0001) surface. We also created surface kinetic models based on the different NH_x surface species that take the computational results of our first principle calculations as input parameters. The surface kinetic models were integrated on larger simulations that also incorporate homogeneous processes, as well as the characteristic residence time of gas-phase species as obtained from computational fluid dynamics simulations. These larger simulations capture the main aspects of surface- and gas-phase kinetics during materials synthesis, and they will be applied to understand the role of ammonia pyrolysis during the MOCVD of AlN and GaN.

Proposed Work for FY 2015

Single-crystal AlN is an indispensable component in many WBG semiconductor applications and will be the focus of our research activities in FY 2015. We will develop nanoscale understanding of AlN processing with three interacting thrusts: synthesis, imaging, and computation.

In the synthesis thrust, *in situ* x-ray studies of the three primary methods of producing AlN will provide insight into the environmental factors critical to the control of nucleation and initial growth of AlN and, ultimately, on the quality of the film. Specifically, we will study AlN growth by reactive magnetron sputtering, pulsed atomic layer epitaxy, and MOCVD by using synchrotron techniques to monitor nucleation and growth as a function of substrate surface treatment and gas- and plasma-phase nitrogen chemistry in the growth environment.

The performance of AlN-based WBG devices depends not only on the average defect concentration, but also on the local nanoscale distributions of strain and mesoscale interactions of individual dislocations and other defects. In the imaging thrust, we will use state-of-the-art hard x-ray based techniques, including Bragg projection ptychography, to image the evolution of the nanoscale distributions of strain and defects in AlN. We will focus on non-destructively mapping of strain and defect concentrations in functional AlN devices grown by epitaxial lateral overgrowth at the APS/CNM Nanoprobe.

The goal of the computational thrust is to develop approaches for multiscale modeling of AlN growth processes that will be coupled to our experimental efforts and will provide deep insights into AlN materials synthesis and properties. We will develop a combined computational approach for modeling gas-phase reactive transport, surface reactions and diffusion, and defect formation in which data obtained at one scale will be passed to another. Kinetic calculations and measurements will enable surface reactivity studies that predict the species that arrive at the surface and will, in turn, be affected by the outflow of species from the surface determined by surface reactivity models. Quantum calculations will benefit chemical kinetics studies, as well as mesoscale-phase field models, by providing chemical activation energies.

Bridging the Electronic and Atomistic Scales: Force Field Development for Reactive Interfaces from First Principles

2014-161-N0

Subramanian Sankaranarayanan, Maria Chan, Michael Davis, Stephen K. Gray, and Benoit Roux

Project Description

Atomistic interactions at reactive interfaces and low dimensional systems (molecules and clusters) underlie energy capture, conversion, and storage by materials. Such dynamic processes combine the remarkable complexity of interfacial reactions, transport phenomena, and microstructural evolution with the formidable intricacies of material defect chemistry and solvation dynamics at the interface. Breakthroughs in fundamental understanding of the atomistic-scale dynamical processes at reactive interfaces and low dimensional systems are urgently needed for the design and development of novel functional materials for energy applications. This emphasizes the need for attaining an atomistic-level description of the key dynamical processes across reactive interfaces where there are rapid changes in the character of both strong (ionic and covalent) and weak (e.g., dipole–dipole type interactions, dispersion force, hydrogen bonding) bonding. These atomic-scale phenomena can be captured via classical molecular dynamics (MD) simulations; however, the accuracy of these simulations hinges on the accuracy of their potential function, and on the efficiency of the dynamic propagation algorithm for adequate sampling of the relevant dynamical motions.

In this project, we are (1) developing a new *ab-initio* based highly accurate and robust, yet computationally efficient, force-field to address the broad ranges of time and spatial scales relevant to reactive interfaces and processes and (2) re-parameterizing existing force fields in order to accurately describe arbitrary compounds and small clusters through automatic global optimization of an objective function based on quantum mechanical (QM) calculations and thermodynamic experimental data.

Mission Relevance

The project is relevant to DOE's mission in energy. The project will lead to the development of a novel force-field fitting methodology and a fundamental understanding of the dynamics across reactive interfaces and low dimensional systems on the target systems relevant to several energy applications (e.g., energy conversion, storage, and fuel production). Success in this project could change the landscape for the role and impact of theory/modeling/simulation on the design and synthesis of new materials, including those for energy applications and new chemistries. The work intersects with several other cross-cutting DOE themes, including data-driven science, mesoscale modeling, and materials by design. This project will also lead to the development of a well-documented, free, and user-friendly open-source code for modeling dynamics at chemically reactive functional interfaces.

FY 2014 Results and Accomplishments

During FY 2014, we established a force-field fitting methodology that allows development of new *ab initio*-based force fields for classical simulations of materials and interfaces. In particular, we developed several new reactive *ab initio*-based force fields for target systems; these encompass a broad range of materials: (1) metal clusters, (2) oxides, and (3) soft-matter organic systems. We introduced a new hybrid force field to capture dimensionality effects and global minimum structures in metal clusters. Using gold as a representative target system, we established a multistep force-field fitting procedure that includes (1) generating and manipulating extensive fitting datasets through electronic structure calculations and genetic algorithms, (2) defining proper functional forms, (3) formulating novel highly optimized fitting procedures, and (4) coding and implementing these algorithms on high-performance computers (HPCs). Our new hybrid empirical potential can describe structure and thermodynamics over all length scales, from nanoscale up to bulk (Figure 1). We used high-throughput density functional theory calculations (DFTs), coupled with a global structural optimization scheme using a genetic algorithm (GA), to identify the ground state structures of Au nano-clusters near their critical cluster size. We discovered a new global minimum structure of a 13-atom planar cluster.

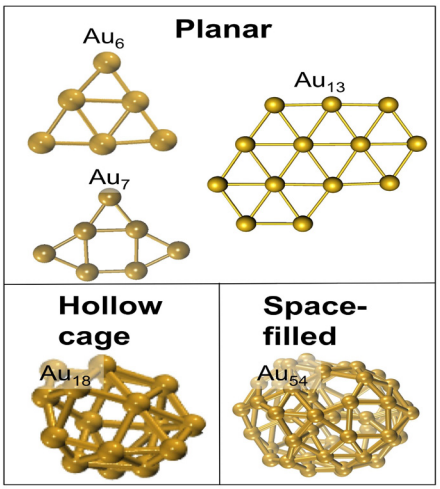

Figure 1. Diversity of configurations predicted by our new hybrid potential: either global minimum structures obtained by genetic algorithm optimization (planar Au_6, Au_7, Au_{13}) or via a long-time molecular dynamics simulation of agglomeration of Au (gold) atoms from random positions in vacuum (hollow Au_{18}, space-filled Au_{55}).

In addition, we derived a new variable charge potential (Morse+QEq) that can successfully predict the relative stabilities of technologically important iridium oxide (IrO_2) bulk phases and surfaces. We also laid the groundwork for a new agnostic approach to force-field fitting by developing a new class of flexible potentials that overcome the limitations imposed by the predefined functional forms traditionally used in all classical MD simulations. We also began development of a more robust Drude polarizable model for organic molecules in solvents.

Proposed Work for FY 2015

In FY 2015, we will continue to develop the flexible model based on *ab initio* data and to target a range of different inorganic and organic systems. The primary focus of this new class of potentials is to enable accurate prediction of inter-atomic forces, thereby allowing high-fidelity dynamic and statistical simulations of reactive interfaces, properties, and functionalities of new materials, as well as pathways and mechanisms of their synthesis and assembly. We will explore a range of target systems and gain crucial insights into the atomic-scale processes at reactive interfaces relevant to energy applications. We plan to reparameterize the hybrid potential model developed for freestanding gold clusters to develop a force field for supported gold clusters (gold on alumina and gold on graphite/graphene). Toward this end, we initiated collaboration with other Argonne scientists, who use alumina or graphene layers to support the growth of sub-nanometer clusters for catalysis applications. The experimental data will be used to evaluate the predictive power (structure and transport properties) of the hybrid potential model for supported clusters. We will perform a more elaborate test of the predictive power of our flexible force field; we are in the process of using it to identify global minima of gold nano-clusters at various cluster sizes (n = 3–55 atoms). We are currently looking at sparse regression techniques to aid in fitting and understanding the parameter sensitivity of force fields.

After establishing the predictive power of our agnostic data-based approach by using the gold test system, we will extend our approach to reformulate several other potential functions (with two, three, and many-body interactions). Preliminary test systems will include Li-Si, for which we already have generated extensive DFT dataset, and other ionic oxide systems that are currently modeled by using Buckingham-type models. These test systems will allow us to test the coupling of the variable charge framework with our linearly independent basis expansion treatment of non-electrostatic interactions.

In FY 2015, we also plan to improve the electrostatic description using the existing Drude model by explicitly accounting for induced polarization over traditional non-polarizable models with fixed partial charges. We will also begin development of a computational tool that allows systematic optimization of van der Waals (VDW) parameters in non-polarizable force fields (such as GAFF [general AMBER force field] and CGenFF [CHARMM General Force Field]) targeting a large collection of experimental data like density, vaporization enthalpy, and solvation free energy (SFE). Finally, we plan to extend our basis functions approach to model the soft-matter systems, such as the ethane-water system. We have obtained a test dataset (from Benoit's group) comprising QM vdW binding energies for several organic systems.

Defect-Localized Spins in Semiconductors for Quantum Optoelectronics

2014-191-N0

David D. Awschalom

Project Description

The purpose of this project is to create robust electronic spins that can be used as quantum bits (qubits) in gallium nitride (GaN). These spins will be bound to crystalline point defects that are generated in GaN through damage or ion implantation. Therefore, they will be only a few atoms large in scale, making them suitable for use in a number of emerging applications in quantum information processing, quantum communication, and quantum sensing.

GaN has already proven to be an extremely versatile semiconductor in the microelectronics industry: it possesses many unique electronic, optical, and materials growth properties not easily obtained in other semiconductor materials, such as silicon, diamond, or gallium arsenide. GaN forms the basis of many high-power and high-frequency electronic devices, as well as a number of optoelectronic, micro-electromechanical, and low-dimensional quantum systems.

We are seeking to leverage the unique capabilities of GaN materials growth and device design to develop a new generation of quantum-enabled electronics. To meet this objective, we must discover and/or create robust quantum states suitable for integration into GaN-based device structures. Defect-bound spin qubits may be ideal for this purpose, as they have been shown to exhibit exceptionally robust quantum properties in other wide-bandgap systems such as diamond and silicon carbide. However, no examples of defect spin qubits are known to date.

Mission Relevance

This project is relevant to DOE's basic science mission. Electronic access to the quantum-mechanical phase space of a spin qubit would enable a new class of quantum-coherent optoelectronic devices in which traditional microelectronic interfaces are used to control extended quantum modes throughout a given structure. These fundamental material studies may establish a powerful device paradigm in which the quantum state of a material can be seamlessly interconverted between electronic, magnetic, optical, and vibrational degrees of freedom via the quantized spin of a single point defect. Such capabilities could have profound implications for energy-efficient electronics, high-speed computing (quantum information processing), secure encrypted communication, and basic sensor technologies.

FY 2014 Results and Accomplishments

We were able to generate optically active point defects in GaN that have an associated electronic spin state. These defects were generated by using high-energy electron irradiation performed at Argonne. A commercially purchased sample of bulk, undoped GaN (unintentionally n-type) was bombarded with 3-MeV electrons to a dose of 2e18 cm^{-2}. The resulting damage to the crystal lattice includes a species of defect that emits infrared light in the 1,400–1,600-nm range when the sample is excited with either ultraviolet (240–400-nm) or infrared (~1,140-nm) light. This defect is identified in the literature as the E=0.88eV feature because its luminescence profile exhibits a sharp zero-phonon line at ~0.88eV, as well as a highly structured phonon sideband at low temperature. These properties are in marked contrast to many of the other luminescent point defects in GaN, which typically have very broad, featureless luminescence profiles. The zero-phonon line persists to ~125 K, while the phonon sideband can be observed from low temperatures up to room temperature. This behavior is similar to what is observed for the nitrogen-vacancy center in diamond and the divacancy in silicon carbide, two defect spin qubits capable of room temperature operation. It is notable that this defect luminescence overlaps directly with several of the optical windows commonly used in fiber-based telecommunications, including the E, S, C, and L bands.

The 0.88eV defect luminescence is associated with a spin-1, optically detected magnetic resonance (ODMR) feature. Specifically, manipulation of a spin-1 state can be detected optically by monitoring the photoluminescence intensity of these defects as microwave radiation is applied to the sample. However, many details of the defect, such as its exact electronic structure and atomic configuration, remain unknown.

We were able to observe two ODMR resonances in the 0.88eV luminescence when microwave radiation is applied to the sample. We excited the sample simultaneously with both ultraviolet and infrared light and then monitored the luminescence as a function of applied microwave frequency. Only the 0.88eV luminescence band was collected, as a 1,400-nm long pass filter and an indium gallium arsenide (InGaAs) detector with a 1,700-nm cutoff were used to eliminate other potential sources of light. The two ODMR features are sensitive to magnetic fields and move to higher microwave frequencies as a static magnetic field is applied along the *c* axis of the sample.

We also observed a dip in scans of the photoluminescence intensity as a function of external magnetic field (no microwaves were applied) (Figure 1). This dip may be representative of a spin-level anti-crossing, similar to what is observed in magneto-photoluminescence measurements of the diamond nitrogen-vacancy and silicon carbide divacancy. However, more detailed measurements are needed to determine whether this is the case. While preliminary, these data offer exciting potential.

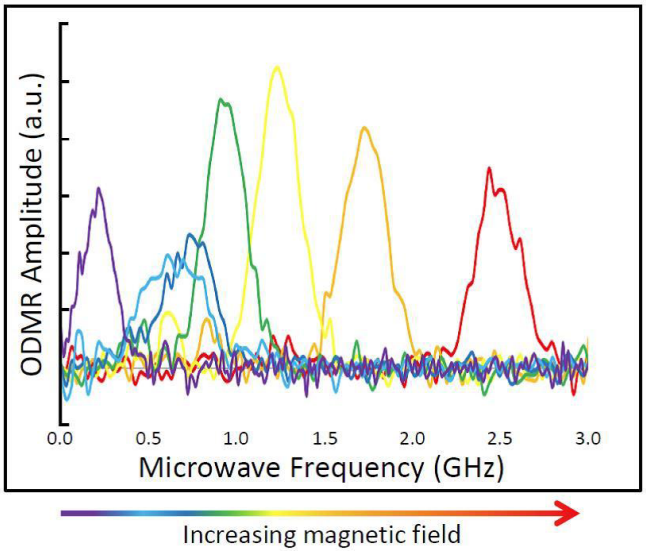

Figure 1. Optically detected magnetic resonance (ODMR) of defect spins in gallium nitride (GaN). In the figure, several distinct ODMR measurements are overlaid — each as a different color. Each color corresponds to a measurement taken at a different external magnetic field strength. At zero magnetic field, an ODMR peak is seen at ~200 MHz (purple trace). The resonance shifts to higher frequencies with increasing magnetic field (indigo through red traces) as the field couples to the defect spins and alters the energies of their quantum states.

Proposed Work for FY 2015

Future experiments include making precisely calibrated measurements of defect photoluminescence as a function of applied microwave or magnetic fields. In addition, we will determine whether the quantum state of these defects can be coherently controlled by using time-resolved optical and microwave pulse sequences applied to the sample. Appropriate pulse sequences will be used to measure the coherence time of these defects at various temperatures in order to determine how strongly the quantum states

interact with their environment in the GaN crystal lattice. Finally, additional electron irradiation and ion implantation experiments will need to be performed to optimize the defect generation process and help determine the microscopic atomic structure of these defects.

Computational Spectroscopy of Heterogeneous Interfaces

2014-192-N0

Giulia Galli

Project Description

This project's aim is the development and application of large-scale quantum simulation methods to model, at the microscopic scale, the physical and chemical processes involved in photo-electrochemical (PEC) energy conversion. The main focus is on processes occurring at the interface between solid photo-electrodes and simple electrolytes (e.g., water with dissolved salts). Although primarily applied to PEC, the results of this project are also relevant to other problems of interest in renewable energy applications, including electrical energy storage and solar-to-thermal energy conversion.

This project encompasses *ab initio* molecular dynamics (MD) simulations to obtain atomic trajectories and compute ensemble averages of thermodynamic properties, as well as the development and use of first principles methods to obtain vibrational and electronic spectra of heterogeneous interfaces. These methods are applied to oxides and semiconducting electrodes interfaced with simple aqueous solutions, with two main goals: (1) to provide knowledge and computational tools to interpret a large body of ongoing experiments on fuel production from water and (2) to establish design rules to predict Earth-abundant, non-toxic oxides and semiconductors with interfacial properties optimally suited to oxidizing and reducing water.

Mission Relevance

The project aligns well with DOE missions concerning the development of renewable energy sources. One of DOE missions is to develop renewable energy resources for which the developments of new materials is key. In this project we are optimizing the interfacial properties of materials to be used as photoelectrodes for water photocatalysis. At the level of both fundamental research and applications, the proposed research will be of interest to several federal agencies in addition to DOE, including the National Science Foundation (NSF) and Department of Defense (DoD), as well as to industrial partners interested in catalysis.

FY 2014 Results and Accomplishments

By combining *ab initio* molecular dynamics simulations and many-body perturbation theory calculations of electronic energy levels, we determined the band edge positions of functionalized Si(111) surfaces in the presence of liquid water, with respect to vacuum and to water redox potentials. We considered surface terminations commonly used for Si (silicon) photoelectrodes in water splitting experiments, encompassing hydrophobic [CH_3-Si(111), H-Si(111), and F-Si(111)] and hydrophilic [COOH-Si(111)] surfaces. A snapshot representative of one of our simulations is presented in Figure 1. We found that when exposed to water, the semiconductor band edges were shifted by approximately 0.5 eV in the case of hydrophobic surfaces, irrespective of the termination. The effect of the liquid on band edge positions of hydrophilic surfaces was much more significant and was determined by a complex combination of structural and electronic effects. These include structural rearrangements of the semiconductor surfaces in the presence of water, changes in the orientation of interfacial water molecules with respect to the bulk liquid, and charge transfer at the interfaces between the solid and the liquid.

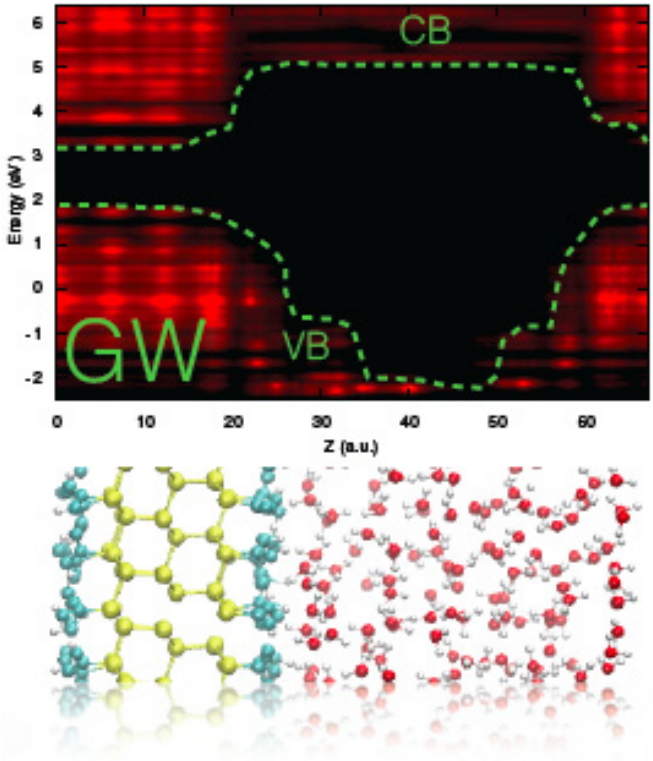

Figure 1. Snapshots representative of ab initio simulations of water (right hand side) on functionalized Si surfaces (left hand side).

Our results showed that the use of many-body perturbation theory is critical to obtaining results in agreement with experiments; they also showed that the use of simple computational schemes that neglect the detailed micro-

scopic structure of the solid-liquid interface may lead to substantial errors in predicting the alignment between the solid band edges and water redox potentials.

Proposed Work for FY 2015

All results obtained so far for water in contact with semiconductor surfaces correspond to electrochemical measurements at the point of zero charge; work is in progress to compute band edge alignments of photoelectrodes in contact with water under different pH conditions and with water with dissolved ions. In addition to completing these simulations, we will also investigate catalysts on oxide surfaces representative of materials used as anodes (e.g., WO_3) and water directly in contact with oxides.

LDRD

National Security

ANNUAL REPORT

2014

Unconventional Signatures for Characterizing Culture Conditions

2013-171-R1

Daniel Schabacker, Lucy Stols, and Rose Wilton

Project Description

Microbial forensics is the scientific discipline dedicated to analyzing evidence from a bioterrorist attack, biocrime, or inadvertent release of a microorganism or toxin for the purpose of identifying the perpetrator (attribution). An important facet of microbial forensics is the analysis of variations (whether cellular or molecular) among strains and among preparation methods, with the goal of inferring the origin of a particular isolate or forensic sample. At present, microbial forensics is dominated by analysis of DNA. While DNA analysis provides a wealth of information, identifying the methods used to culture and prepare the biological threat agent (BTA) — information that can be critical for forensic analysis — requires a different data set. That information is often resident in the matrix associated with the BTA and in the molecular composition (in particular, the proteome) of the BTA itself. Therefore, while DNA analysis is a critical tool, it is not adequate as the sole forensic methodology.

Delivering an agent requires preparing it to remain effective when outside of its optimal growing conditions. Exposure to environmental stresses, such as temperature, ultraviolet radiation, and drying, can reduce the agent's activity. Some pathogens, like the anthrax bacterium, can encapsulate themselves into a hardy, long-lasting spore not easily susceptible to those conditions. Other agents require further processing that minimizes damage and allows the BTA to retain its activity when dispersed.

The inherent need to stabilize and protect BTAs from inactivation during storage, transport, and dissemination results in a state of suspended animation or metabolic inactivity. While in this state, the molecular signatures indicative of growth conditions and preparation methods are preserved, thus providing an ideal opportunity for forensic analysis.

In this project, we are developing a novel forensic methodology that is especially suited to BTA attribution. Our approach quantitatively analyzes the molecular composition (mainly the proteome) of BTAs, which varies with culture conditions and preparation methods. As a result, our methodology can provide detailed information regarding the methods used to culture, purify, and store the BTA. Our approach consists of four stages:

1. Lysis of the BTA;
2. Automated, high-resolution fractionation of the extract by chromatofocusing and reversed-phase high-performance liquid chromatography;
3. Adsorption of the protein(s) in each fraction to a spot on a protein "chip" by using a conventional robotic system; and
4. Interrogation of the types and levels of proteins on the chip by applying nonspecific protein dyes, specific antibodies, and lectins (to detect glycoproteins), followed by quantitation of binding using a commercially available chip-reader. The resulting information-rich data set can be rapidly and quantitatively analyzed by using existing software.

Our method requires a minimum amount of sample, can be implemented by using off-the-shelf technology, and is relatively insensitive to environmental contamination.

Mission Relevance

This project supports the national security mission of DOE to reduce the global danger from weapons of mass destruction by enhancing the capability to attribute a BTA to individuals or organizations. This approach goes beyond current microbial forensics methods that identify the BTA strain; it provides information on how a BTA was cultured and prepared for dissemination providing insight into the operator's expertise and resources and enhancing attribution. The Interagency Microbial Forensics Advisory Board, led by the Federal Bureau of Investigation (FBI) and White House Office of Science and Technology Policy, has identified our technical approach as a viable solution for identifying culture conditions and preparation methods used in BTA production. Our approach is specific, relatively insensitive to interferents, high-throughput, and inexpensive, and it provides a depth of characterization unavailable with any other known method.

In addition, high-resolution characterization of protein expression resulting from varying culture conditions and sample preparation methods would be valuable in cancer research, where identifying these changes would facilitate more precise biomarker discovery by removing uninformative changes due to variations in laboratory technique. Stakeholders who may be sponsors and customers include the FBI Laboratory; Defense Intelligence Agency, Chemical, Biological, Radiological, Nuclear Explosives Technical Collection Office; National Bioforensic Analysis Center; U.S. Department of Homeland Security Science and Technology Directorate; and the Defense Threat Reduction Agency.

FY 2014 Results and Accomplishments

In FY 2013, we confirmed that spent media from *E. coli* had adequate protein complexity in both autoclaved and untreated forms for use as a discriminator. Results were analyzed by using the newly developed ProFAST (*PROtein Fraction Array Statistics Tool)* software (software copyright number ANL-SF-13-015).

In FY 2014, we focused on expanding growth conditions to obtain the data sets required to confirm the ability to discern growth conditions. Broadening the number of media types, particularly by matrixing media selection such that a media component (e.g., agar) or condition (e.g., growth at 27°C) was shared by at least two media types, provided more resolution power with more conditions for the same number of experimental samples than a series of binary comparisons would provide.

ProFAST was significantly expanded and optimized to include Quantile Normalization, Cluster, Heatmap, Principle Component Analysis, M2 Statistics, and Prediction Analysis for Microarrays in R analysis. Additional statistical tools such as ANOVA, Artificial Neural Networks, Bayesian Networks and Support Vector Machine (SVM) were evaluated. These statistical tools were used to classify data, by using whole-proteome signatures (all fractions) or a subset of fractions.

Four growth conditions were analyzed by using ANOVA (Adjusted Bonferroni correction, 10,000 permutations, pVal < 0.05) to identify fractions significant by media type. We identified 79 fractions out of 960 fractions as significant by media type. These 79 fractions are displayed on the x-axis in Figure 1. The various growth media are seen on the y-axis near the right side of the figure. Looking closely, one can see that all four growth media were successfully clustered using the 79 prioritized fractions.

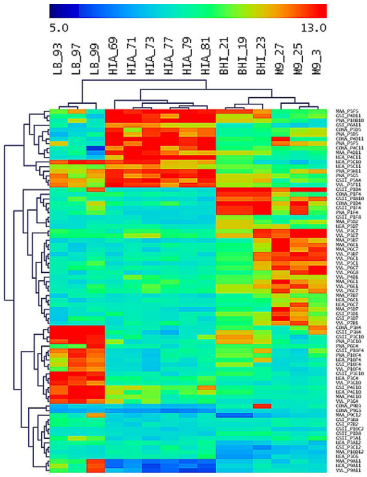

Figure 1. Hierarchical Cluster: Cluster (average linkage, Euclidian distance) for 79 fractions. Data were normalized and log2-transformed. Signal is identified as significant by media according to ANOVA. Media composition (3-LB, 6-HIA, 3-BHI, 3-M9) are on the y-axis; ANOVA prioritized fractions are on the x-axis.

An SVM model was built and successfully classified unknown growth media by using the 79 data points chosen by ANOVA as significant. The SVM model was validated by introducing random noise to the data and re-checking SVM prediction accuracy. The model was determined to be highly resistant to the addition of noise and able to assign a confidence to an unknown classification.

Proposed Work for FY 2015

Project work in FY 2015 will involve the development of a JAVA version of ProFAST, expansion of media compositions, validation of the classification methodology, and validation of fraction prioritization.

Technical milestones will include the following:

- *ProFAST.* Additional statistical tools including ANOVA and SVM will be incorporated. ProFAST will be moved to JAVA.
- *Additional Signatures*. Additional growth conditions for analysis will be provided by the National Biodefense Analysis and Countermeasures Center and Northwestern University.
- *Validation of Classification and Fraction Prioritization Methodology*. Additional statistical tools will be evaluated with the expanded signature database.

Ratiometric Semiconductor Nanocrystal-Based Sensors for Threat Reduction Applications

2013-173-R1

Richard D. Schaller, Elena A. Rozhkova, Daniel Schabacker, Elena V. Shevchenko, and Rosemarie Wilton

Project Description

This project focuses on the development of low-cost, easy-to-use ratiometric fluorescence resonance energy transfer (FRET) -based sensors with applications in chem-bio-rad-nuclear threat reduction scenarios. Our objective is to produce a sensor capable of rapidly and sensitively detecting the presence of such species as botulism toxin or uranium ions with high specificity. Our approach entails causing association or dissociation of a FRET donor (D) and acceptor (A), both of which are highly fluorescent but not significantly overlapping spectrally at their emission wavelengths, upon exposure to analyte. Because FRET efficiency is highly sensitive to D-to-A distance, the ratio of D and A spectrally resolved emissions will change sensitively with small amounts of analyte binding. Relative D and A emission maxima intensities then can be correlated with lab-based assays to directly read

out analyte absence/presence and a calibrated analyte concentration. Semiconductor quantum dot FRET donors are targeted because of their optical tunability and high optical stability.

Mission Relevance

Accurate, reliable sensors are crucial to a wide array of national security efforts. Ideally, one would like a non-expert to be capable of sensitively, reliably, and persistently detecting a wide assortment of threat agents ranging from biological to nuclear in the field. Such capability would bolster anti-terrorism efforts and aid the warfighter, in addition to facility inspectors. While lab-based methods can sensitively detect numerous threat agents, most require specialist operators or otherwise lack fieldability. Our efforts target a sensor platform that is field compatible, simple to operate and interpret, compatible with sensitivity to multiple threat agents, and robust against minor system degradation. The technology being pursued has the potential to yield compact, hand-held sensors that rapidly facilitate the identification and quantification of threat agents.

FY 2014 Results and Accomplishments

In FY 2013, we developed a strategy to detect botulism neurotoxin (BoNT) and began development of two phage display single-chain fragment variables (scFv) as well as conjugation chemistry to place energy transfer-capable chromophores on these antibody fragments. We developed highly fluorescent semiconductor nanocrystals of the appropriate size and emission energy and then modified their surface functionalization in order to place these normally hydrophobic particles in solution together with scFvs. We developed a means to isolate and work with the BoNT binding domain receptor, which is a safer variant of the toxin to experiment with than the active form. Modifications of scFvs were investigated for successful chemical conjugation and binding affinity to BoNT. With the development of DNAzymes that can lyse in response to the presence of certain ions with high specificity, we initiated efforts to conjugate chromophores to prepared DNAzymes.

During FY 2014, we successfully demonstrated ratiometric photoluminescence sensing BoNT by using a semiconductor nanocrystal FRET donor and bright organic dye acceptor, with each conjugated to a thermally stabilized antibody fragment (or scFv) that adheres with high affinity to BoNT. Thermal stabilization of the scFvs was achieved via random mutation and selection for continued binding affinity for BoNT. Using this approach, we were able to increase the protein unfolding temperature by ~12°C, to 60°C. This increase in stability bolsters use of the materials in fieldable scenarios. Further, directed site mutations were utilized to remove chemical moieties that would foul attempts to controllably conjugate chromophores to the scFvs. A key challenge has been to arrive at antibody fragments that adhere to independent, proximal regions on the toxin and can therefore be used in a sandwich-type assay format. Specifically, the quantum dot donor and dye acceptor need to be proximal for efficient FRET.

Figure 1 shows results of a successful ratiometric FRET sandwich assay with low nanomolar sensitivity and very rapid readout. We successfully sensed fissionable material through the initial demonstration of lead detection, and so we are now in a position to attempt uranyl ion sensing in FY 2015. We also replaced laser excitation of the donor material with a light-emitting diode approach in order to lower complexity for sensing in a rad environment that is not set up for laser work. Here, functionalized DNA (a DNAzyme) was conjugated to chromophores in a similar approach to the BoNT sensing approach, and selectivity for lead was demonstrated. The uranyl DNAzyme has been appropriately conjugated, and experiments on uranyl will commence shortly.

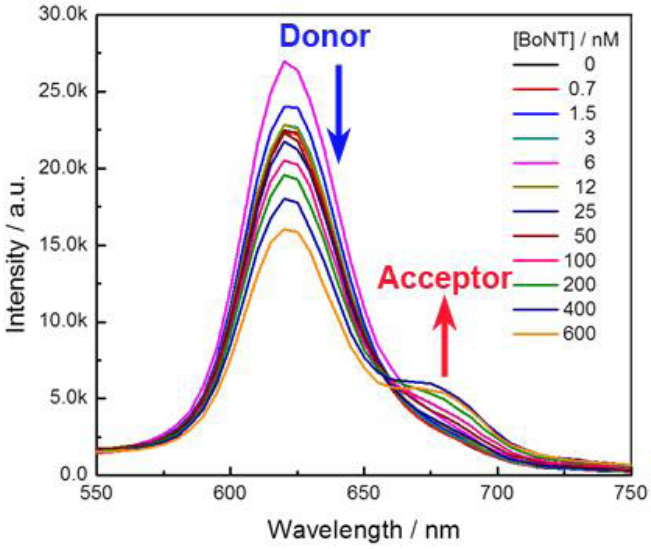

Figure 1. Ratiometric BoNT sensing, with nanocrystal donor emission at 625 nm decreasing and dye emission at 675 nm increasing upon addition of the toxin at indicated concentrations.

Proposed Work for FY 2015

In FY 2015 key efforts will include improving sensitivity limits for the homogeneous BoNT-sensitive assay and the means to persistently sense this toxin. We will also work to demonstrate performance of this sensor in the presence of common interfering compounds. Efforts using the DNAzyme-based sensor for fissionable materials will continue with the aim of demonstrating first-ever ratiometric sensing with this platform and determining elemental selectivity, as well as the range of conditions under which this platform can operate. For persistent sensing, we have begun work to bind sensor elements to solid substrates in gel drop formats, but we aim to improve upon this approach through tethering of species to high-sur-

face-area substrates. Furthermore, we are in discussions with a potential sponsor of this work to identify the specific utility of the approach described with respect to the sponsor's needs.

Uranium and Plutonium Detection by Plasmonic Graphene-Based Nanosensors

2013-178-R1

Michael Kaminski, Carol Mertz, Leonidas Ocala, and Anirudha V. Sumant

Project Description

One of the most important pieces of information after a release of nuclear material is detecting the presence of uranium (U) and/or plutonium (Pu). Their presence, especially following a supercritical nuclear event, would severely limit the list of potential actors and provide the White House with critical information to guide a proper and timely response. Unfortunately, identification of uranium and plutonium in the field represents an acute gap in field detection capabilities. Clean samples containing little background radiation (e.g., interdicted uranium or plutonium sources) can be assayed by using low-energy gamma-ray spectroscopy, but the presence of a significant x-ray and gamma-ray background (viz., that emitted by fission products and activation products from a nuclear detonation) renders such techniques useless. Instead, samples must be sent to specialized fixed laboratories for selective extraction of the target elements and radiometric analysis (i.e., alpha spectrometry counting) or isotopic analysis (i.e., mass spectrometry), adding days to the response time.

The goal of this project is to develop a new hand-held analytical instrument that identifies U and Pu and their isotopes in a liquid and possibly a solid sample. Samples containing Becquerels of Pu and U can be as small as tens of nanoliters and the analytical identification can be obtained in near-real-time (<1 min), according to calculations. The basis for the device is the graphene nanosensor, which is able to detect elemental U and Pu by characteristic changes in the plasmonic properties of graphene sheets. Since graphene is a conducting system, a current will encounter different impedance depending on whether a U or a Pu atom has been absorbed. Other molecules present in solution create distinguishable signals, as each molecule has a distinctly different effect on the plasmonic properties of graphene, yielding different vibrational and excitation spectra and different current-voltage characteristics. The analytical sensitivity of the proposed device is unparalleled by any current instrument and is expected to be in the range of tens of atoms or less. In fact, the response of the graphene plasmon is so sensitive that we expect to be able to measure the energy of the nuclear decay particle emitted by Pu and U atoms and thereby demonstrate a miniature device capable of producing important isotopic ratio information.

The information gathered in this project will provide a strong foundation for continued exploration of this area of detection. Sheets of the graphene sensor are in the micrometer domain (~1 × 1 μm) and will yield a sensor device that is entirely hand-held, compatible with minimal sample size, and minimal in its battery power requirements. With this technology, the potential exists to perform fully portable isotopic forensics in the field or develop "pixie dust" sensors that can be dropped onto a suspect location and interrogated at very long distances (the graphene ribbon can have light emitting tags for positive samples). A library can be developed to recognize lanthanide, actinide, and fission product atoms or chemicals related to nuclear reprocessing or undeclared activities.

Mission Relevance

Our project is tied to DOE's mission in national security. The work applies both to the National Nuclear Security Administration (NNSA) and its mission of verifying nuclear activities with International Atomic Energy Agency (IAEA) member nations and to DOE's mission as a partner in homeland security. In both these areas, there is an urgent need for field-deployable analytical instruments for the rapid and sensitive determination of weapons materials and weapons-related materials.

In addition, outside of DOE there is a similar need. The need for hand-held devices for the identification of U and Pu was identified by the Program Needs Joint Working Group of the American Association for the Advancement of Science (AAAS), with internationally recognized co-authors at Lawrence Livermore and Los Alamos National Laboratories. Specifically, they described a priority need for a portable system to provide rapid indication of the presence of U and Pu in post-detonation debris and an accurate and precise measurement of isotopic ratios. The International Atomic Energy Agency (IAEA) has expressed similar interest in developing a portable system to screen samples as part of its non-proliferation and verification activities. Intelligence agencies have expressed an interest in obtaining small, field-robust units for remote or stand-off detection of undeclared materials. The U.S. Environmental Protection Agency (EPA) has expressed similar interest in meeting its needs for analysis of radionuclides in waters. Our sensor may be able to meet these needs.

FY 2014 Results and Accomplishments

In FY 2013, we pursued both experimental testing and theoretical calculations. First, *ab initio* density functional theory of U and Pu complexes with graphene and graphene oxide was established, and the effects of actinide speciation and solvation on bonding to the graphene surface was investigated. Concurrently, we began synthesis experiments to produce graphene nanoribbons and testable devices. Using chemical vapor deposition, we produced graphene and transferred it to silicon wafers and micro-fabricated various two-electrode configurations on top of graphene.

In FY 2014 our research included the following:

Sensor Research. We observed the effect of a large bias gate voltage on the electrical conductivity of graphene ribbon devices when exposed to a very low concentration of europium (Eu) in a microfluidic device (Figure 1a). We find a direct correlation between the level of concentration of Eu ions in the solvent and the change in electrical conductivity of graphene (Figure 1b), observing a change of up to three orders of magnitude at the lowest concentration tested (0.1 mM). Our results suggest that the microfluidic reservoir based on graphene ribbon sensors is a promising procedure for detecting very low levels of Eu in liquid solutions.

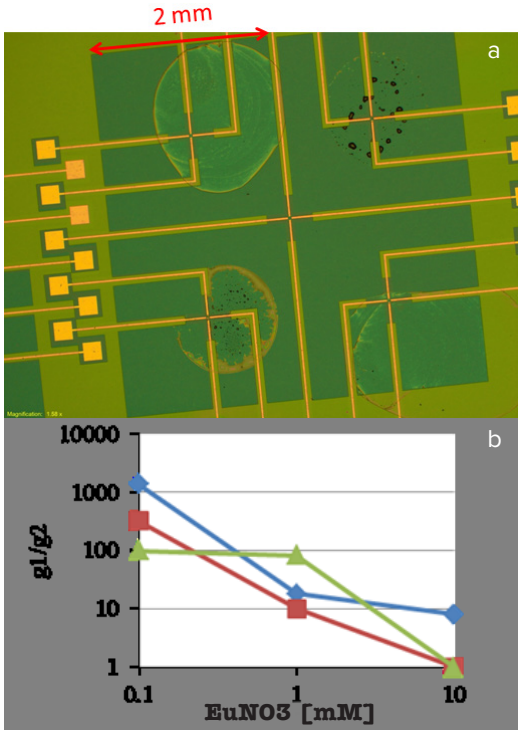

Figure 1. Response of graphene sensor device to europium. (a) Light microscope image of fluidic device showing a set of five graphene ribbon devices. (b) g1 and g2 represent the electrical conductivity of graphene before and after exposure to europium solution under a bias voltage. Four tests were performed with DI water (not shown in the plot), of which three resulted in electrical breakdown ($g_1/g_2 = \infty$) and one resulted in $g_1/g_2 = 1$.

We are exploring the effects of geometry, mainly a nanoscale ribbon width, as well as functionalization through incorporation of carbon and oxygen functional groups, on the electrochemical response of graphene to aqueous samples (Figure 2).

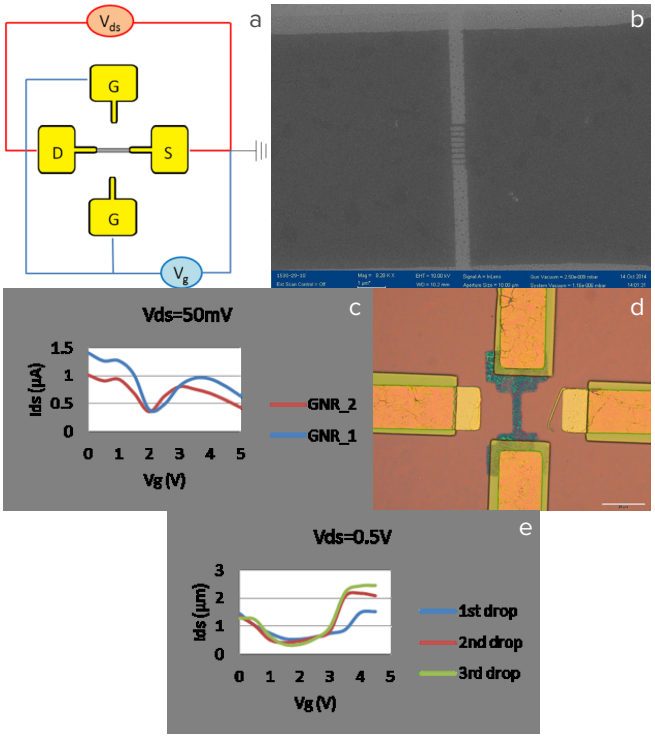

Figure 2. (a) Diagram showing circuit schematic with gate (G), drain (D) and source (S) wiring for the graphene nanoribbon (GNR) and measured voltage (V_{ds}, drain-source; V_g, gate) and current (I_{ds}, drain source) responses. (b,c) Graphene nanoribbons (50-nm width): (b) Electron microscope image and (c) electrochemical response to distilled water. (d,e) Carbonyl-functionalized reduced graphene oxide: (d) Light microscope image of graphene across the D-S and (e) electrochemical response to distilled water.

Solvation of Actinide Salts in Water Using a Polarizable Continuum Model. Density functional theory was applied to study the structure and solvation of U(VI), Pu(IV), and Pu(VI) by using relativistic small core effective core potential. We found that zero-point vibrational energy corrections to the binding energies cancel nicely with the corresponding empirical dispersion corrections in vacuum, even though these corrections individually contribute by up to 3%. In solution, dispersion corrections can exceed zero-point energy correction by up to 13%, depending upon the size of the molecule; this observation may be because these corrections are more suited to gas phase calculations. We also found that solvent effects are critical in examining the structure of these solvated ions. In vacuum, we observe hydrolysis of Pu(IV) ions for nine-coordination, which was suppressed on introduction of solvent effects by using a polarizable continuum model. The eight-coordination was found to be most stable for both Th(IV) and Pu(IV) ions, with the nine-coordinated complex 1.7 kcal/mol and 2.3 kcal/mol higher in energy for Th(IV)

and Pu(IV), respectively. In the case of U(VI) nitrate complexes, the $UO_2(NO_3)_2$ complex with nitrates in monodentate mode is more stable in both vacuum and solution phase than the hydrated mononitrate complex, as well as completely solvated $UO_2(H_2O)_5^{2+}$ ions with counter-ions far from the central ion. For the uranyl mononitrate complex, monodentate mode is preferred to bidentate mode in solution phase. In the case of PuO_2^{2+}, both monodentate and bidentate are equally favored for the mononitrate complex in solution phase. We observed that nitrates are very strongly bonded to Pu(IV) ions and they do not dissociate easily, but they preferentially stay in the first-coordination shell.

Unlike nitrates, chlorides are weakly bonded to Pu(IV) ions. Pu(IV) ions, however, have a greater affinity for chlorides than Th(IV) ions in solution. The coordination number for aquo-chloro complexes of Pu(IV) is found to be eight, with three chlorides present in the first shell. In the case of Pu(VI) chlorides, PuO_2^{2+} retains a five-fold coordination number, with two chlorides replacing two water molecules bonded to each Pu(VI) ion. The coordination number for chloro-aquo complexes of Th(IV) ($N_w + N_{Cl}$) is found to be 9–10, and one chloride enters the first coordination shell at 2.8 Å, forming an inner sphere complex. The natural bond orbital (NBO) analysis performed on actinide complexes reveals formation of covalent bonds between the actinide ion and both water and counter-anions present.

Proposed Work for FY 2015

We propose to continue to develop the sensor and begin testing of radioactive solutions. Multiple sensor chips will be fabricated and tested with graphenes of different functionalities. We will also increase the complexity of the theoretical model to accommodate graphenes of different functionalities and solutions containing multiple salts.

Seminars

Bobadilla, A., L. Ocola, A. Sumant, J.M. Seminario and M. Kaminski (2014). "Electrochemical Response of Graphene Ribbon to Eu (III)." Texas A&M, College Station, TX, June 5, 2014.

Crime on the Urban Edge: Simulating the Interface between Transitional and Local Crime

2014-194-N0

Pamela Sydelko, Ignacio Martinez-Moyano, and Michael North

Project Description

The goal of this project is to create a computational system model of the converging relationships between transnational crime groups and urban street gangs to help policy makers discover ways to disrupt crime systems and anticipate how crime organizations will react to those disruptions.

The main objectives of the proposed work are to:

1. Engage an advisory board made up of key stakeholders to build a systems mapping of the transnational organized crime and domestic urban crime gangs,
2. Utilize anticipatory systems and systemic intervention methodologies to establish a high-level genetic algorithm (GA) framework, and
3. Develop an anticipatory systems dynamics model by using the systems map and GA framework.

Ultimately, this research will provide a model that promotes better understanding systems complexity and supports multi-agency intervention planning that takes into account that for every intervention action there are adaptive behavior changes in the system that emerge from new intervention pathways.

Mission Relevance

This project is relevant to DOE's research in energy planning, policy, and the economy. The anticipatory systemic interventions methodology developed in this project can be applied to any class of complex problems where initial interventions (a purposeful action to create change) create potential needs for subsequent interventions. Many energy planning problems are of this class because consumer behavior, economic behavior, and technological changes can all be highly complex and adaptive.

FY 2014 Results and Accomplishments

Work began on this project in June 2014. The FY 2014 effort focused on:

- Formally surveying and developing knowledge in systems thinking, theory, and methods development.

- Reviewing information on transnational organized crime (TOC), domestic gang organizations, and illicit trafficking in terms of sociocultural behaviors, economic behaviors, network formation, and interdiction procedures and policies.
- Conducting interviews with practitioners and policy makers involved in these areas.
- Assembling a subject matter expert (SME)/stakeholder group that will provide guidance and advice as the project develops. Each member of this board brings their own "mental model" of the TOC and gang systems. Because the members are part of agencies that are charged with addressing some portion of the problem, they reflect the perceptions of the agencies they represent. At present, interventions to the problem are carried out primarily through the perceptions of each agency, with very loose ad hoc collaboration. In addition, the members have their own assumptions on how these systems may evolve and adapt. We gathered knowledge/data to construct system maps for the SMEs and their assumptions about the future of these systems for each of "their perceived view of the problem." The LDRD team will then be synthesizing the data to construct several scenarios that reflect the differing SME system maps and assumptions (and combinations of those perceptions) (for details, see (1) Jackson, M.C., 2001, "Critical Systems Thinking and Practice," *European Journal of Operational Research* **128**:233–244 and (2) Midgley, G., Cavana, R.Y., Brocklesby, J., Foote, J.L., Wood, D.R.R., and Ahuriri-Driscoll, A., 2013, "Towards a New Framework for Evaluating Systemic Problem Structuring Methods," *European Journal of Operational Research* **229**:143–154.). This task will employ a combination of two methods (systems thinking and foresight (for details, see (1) Miller, R., Poli, R., and Rossel, P., 2010, "Making Anticipatory Systems More Robust, foresight **12**:72–85; (2) Poli, R., and Hodgson, A., 2013, "Towards an Ontology of the Present Moment," *On the Horizon* **21**:24–38; and (3) Rosen, R., 2012, *Anticipatory Systems*, Springer. These scenarios will be used later as we bring the whole group together in a combined systems and foresight exercise that facilitates a holistic view of the system and the ability to use anticipation. All of this knowledge and data are needed to build a robust anticipatory system dynamics model that can be used on the whole of the system to explore combined interventions on the system and expected adaptations of those systems.
- Participating in systems thinking methods and helping build an initial systems map of the converged TOC and local gang networks (which will be used as a start to the systems model). During this task, the SMEs outlined the structure of the research and how each of them will be asked to participate. Background was given on systems science, examples of how it has been used, and a quick exercise on how to create a rich picture of their systems (which is a precursor to a system map).

Proposed Work for FY 2015

Our work in FY 2015 will entail the following:

1. Further research and stakeholder engagement to develop a set of possible counter-crime interventions;
2. Development of a new methodology (based on combining anticipatory methodologies with soft systems methodologies);
3. Development of a high-level systems dynamics model that will include system components, inter-dependencies, and feedback loops among the components; and
4. Development of a high-level GA framework.

LDRD

Nuclear Energy

ANNUAL REPORT

2014

Nanolaminate Materials for Extreme Environments: A Demonstration of Argonne Capabilities for Design, Synthesis, and Accelerated Testing of Radiation-Tolerant NE Materials

2013-152-R1

Abdellatif Yacout, Jonathan D. Almer, Meimei Li, Michael J. Pellin, Marius Stan, and Di Yun,

Project Description

Argonne has a long history of proposing, developing, and testing important new materials for nuclear reactors. By combining the capabilities of high-energy heavy-ion irradiation at the Argonne Tandem Linear Accelerator System (ATLAS), high-energy x-ray analysis at the Advanced Photon Source (APS), and multiscale modeling and simulations through the Argonne Leadership Computing Facility (ALCF), this work will make available a new nuclear materials research capability. This capability can accelerate materials development for the extreme nuclear reactor environment, thereby allowing for testing materials at radiation doses of hundreds of displacements per atom and reducing the required testing time from years (in the reactor) to days (in this study). While this approach is not expected to be a replacement for in-reactor neutron irradiations done in support of reactor licensing activities, it can shorten the development cycle of new or improved nuclear materials by limiting in-reactor testing to those candidates that show most promise.

This project will make a "first" demonstration of the power of this concept by examining the stability of nuclear materials, including a class of nanomaterials (nanolaminates) under simulated extreme conditions, to provide insight into damage mechanisms of neutrons and elucidate the role of fission fragments at high doses.

Mission Relevance

This project is relevant to DOE's missions in science and energy. Within the scope of this work is the development of an understanding of the characteristics of nanolaminates that promote material stability in extreme environments, such as those found in a nuclear reactor. This understanding will be achieved through the synergistic use of Argonne's user facilities demonstrating their ability to rapidly accelerate materials screening for extreme environments. The demonstration will begin to develop a case for an *in situ* irradiation effects capability using similar tools (the proposed extreme materials [XMAT] beamline at the APS). It will also dramatically strengthen the case for the DOE's Office of Nuclear Energy's investment in the proposed XMAT beamline, demonstrating its technical viability.

FY 2014 Results and Accomplishments

In FY 2013, significant progress was achieved in relation to starting the utilization of Argonne facilities to demonstrate the objectives of this project. In addition, innovations were achieved in relation to materials testing and characterizations in a high-temperature steam environment, thermal analysis modeling, nanolaminate synthesis and characterizations, and lower-scale modeling and simulations. Activities at Argonne facilities included energetic (MeV/nucleon) heavy ion irradiations (at ATLAS) of nuclear cladding materials (including nanolaminate-coated materials) and nuclear fuel materials, as well as characterizations of those materials at the APS and the Intermediate Voltage Electron Microcope (IVEM). Sample characterizations were performed at APS beamlines 1, 10, and 34 by utilizing different characterization techniques (extended x-ray absorption fine structure (EXAFS), x-ray diffraction (XRD), small-angle x-ray scattering (SAXS), and diffraction tomography). *Modeling and simulation* activities included density functional theory (DFT) simulation of CeO_2, which is a promising material and an important non-radioactive surrogate for studying nuclear fuel containing PuO_2.

In FY 2014, further progress was achieved in relation to the utilization of Argonne facilities to demonstrate the objectives of this project, including the following activities and accomplishments:

- *High-Energy Ion-Irradiations at the ATLAS and Intermediate Voltage Electron Microscope (IVEM).* A special irradiation stage was designed and used to irradiate 19 fuel samples with a high-energy 80MeV xenon (Xe) ion beam. Four different nuclear fuel types were included: monolithic uranium-molybdenum (U-Mo), dispersion U-Mo, dispersion coated U-Mo, and uranium-zirconium. In addition, two different advanced steels, including HT9 and MA957, were irradiated with high-energy iron ions. The U-Mo dispersion fuel irradiations were successful in producing radiation damage effects in fuel similar to those encountered during neutron irradiations (Figure 1). The IVEM was utilized to investigate the response of nano-crystalline copper (Cu) to ion irradiation at conditions similar to in-core neutron irradiation experiments. Results to date confirmed the occurrence of grain growth in this material similar to neutron-irradiated samples, while differences were found in grain size distributions.

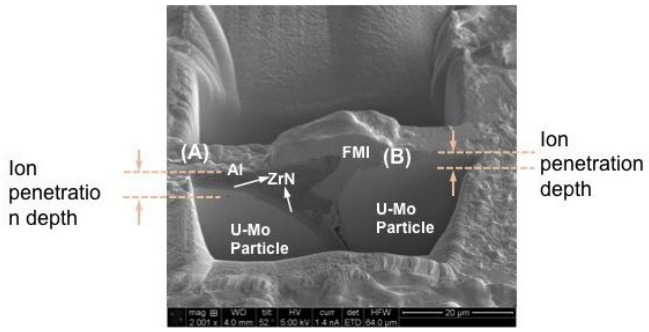

Figure 1. Scanning electron microscopy (SEM) of ion-irradiated cross sections of two U-Mo particles after sections removed using focused ion beam (FIB) technique: one with intact coating region (A) and other with missing coating region (B). FMI is fuel matrix interaction (appears only in region B).

- *X-ray Analysis at the APS of Ion-Irradiated Fuel and Cladding.* At the APS, three U-Mo/aluminum dispersion fuel samples irradiated with 84 MeV Xe at ATLAS were characterized by using high-energy x-ray diffraction, where a detailed description of microstructure evolution in the samples was acquired as a function of irradiation damage level (irradiation depth profile), including phase composition and gas bubble morphology. For the first time, micro-diffraction was used to analyze the lattice strain induced by high-energy Xe ion irradiations in steels (HT9 and MA957). High-energy x-ray diffraction was used to analyze lattice strains, dislocation structures, textures, and other microstructural developments during *in situ* mechanical loadings in those materials. X-ray tomography was used to study the *in situ* zirconium oxide (ZrO_2) development during high-temperature air exposure of Zr-based cladding materials. The experiments aimed to study the performance of advanced coatings for Zr claddings at temperatures beyond the design limit. Microbeam diffraction was used to study the depth-resolved distribution of lattice strain and dislocation density in both single crystal Mo and polycrystalline U-Mo fuels irradiated with high-energy heavy ions.
- *X-ray Analysis at the APS of Neutron-Irradiated Cladding Materials.* Research was conducted to characterize irradiation-induced defects and phase changes in neutron-irradiated ferritic-martensitic steels and austenitic stainless steels by using combined high-energy synchrotron x-ray techniques of small angle/wide angle x-ray scattering, far field high energy diffraction microscopy (FF-HEDM), and tomography. It was demonstrated that high-energy x-rays can be used to non-destructively study irradiation-induced microstructural changes on a wide-range of length scales, from millimeters down to micrometers in real space and down to the atomic level in reciprocal space. In particular, the grain-scale HEDM data provides an opportunity to reveal irradiation-induced defects in new ways.
- *Modeling and Simulations.* Using Argonne's ALCF, we studied the microstructural evolution of Mo and U-Mo system due to ion irradiations by using atomistic methods, including DFT and molecular dynamics (MD). Single defect formation energy and bonding energy of interstitials or vacancies in Mo and U-Mo alloy were studied by using DFT calculations. The results will be used as input for future kinetic Monte Carlo simulation of voids and gas bubble nucleation in Mo and U-Mo. We used displacement cascade simulations in U-Mo by using MD simulations to simulate the formation of defect clusters in U-Mo alloys due to ion irradiation. The defect cluster size distribution was obtained as a function of primary knock-on atomic energy and Mo composition. We used DFT and MD to simulate the microstructure of irradiated Mo by introducing SIA (self-interstitial atom) defects or dislocation loops for comparison with synchrotron-EXAFS spectroscopy measurements in Xe ion beam-irradiated Mo single crystals.

Proposed Work for FY 2015

A major activity in FY 2015 will involve ion irradiation and characterization of neutron-irradiated materials including irradiated fuel samples. In addition, *in situ* thermal annealing studies with different fuel materials at the APS will demonstrate the ability to study *in situ* fuel microstructural changes (e.g., recrystallization and grain growth). Activities related to neutron-ion irradiation equivalency will continue, where comparisons will be made between ion and neutron irradiated materials, such as single and polycrystalline Cu, silicon carbide (SiC), steel cladding materials, and light water reactor (LWR) pressure vessel steel materials. Fundamental studies of radiation-induced damage in ion-irradiated materials in fuel and structural materials will continue, and comparisons to neutron-irradiated materials will be made.

Development of a Computational Fluid Dynamics Multiphase Boiling Capability to Predict the Critical Heat Flux in Nuclear Reactor Fuel Assemblies

2014-177-N0

Adrian Tentner, Paul Fischer, Oana Marin, Elia Merzari, Aleksandr Obabko, Prasad Vegendla, and Kent Wardle

Project Description

This project will further develop and expand the extended boiling framework (EBF) modeling concept previously developed by Argonne and implement it into Nek5000, a high-performance, highly scalable, open-source computational fluid dynamics (CFD) code developed at Argonne. The activities associated with the proposed project are particularly synergistic with Argonne's expertise and interest in high-performance computing, since multi-phase flow simulations are typically very expensive computationally and scalability is essential. The goal of the project is to develop a new two-phase version of the Nek5000 code, named NEK-2P, to simulate the two-phase flow and heat transfer phenomena that occur in a light water reactor (LWR) fuel bundle under various operating conditions, with special emphasis on the prediction of critical heat flux (CHF).

Boiling flows are subject to the phenomenon known as boiling crisis where, for high-cladding surface heat fluxes (exceeding the critical heat flux or CHF), the heat transfer between the cladding and coolant deteriorates, leading to sharply higher cladding surface temperatures. Such temperatures lead to a deterioration of cladding structural integrity and ultimately to fuel pin failure and radionuclide release. The avoidance of CHF conditions is essential for the safe functioning of LWRs. The proposed computational tool will provide an accurate modeling capability for the study of two-phase flow phenomena in LWRs, which will help reduce uncertainty in the prediction of performance and safety characteristics.

Mission Relevance

The project is relevant to DOE's mission in energy. Multiphase flow and boiling are of fundamental importance in the design of nuclear reactors used for energy generation, the vast majority of which are cooled by water. The LWRs can be divided into two major types: boiling water reactors (BWRs), which are designed to operate under saturated boiling conditions, and pressurized water reactors (PWRs), which are designed to operate at higher pressure than the BWRs and under subcooled boiling conditions. The assessment of fuel assembly behavior under two-phase flow conditions is particularly important, because many design and safety criteria depend on it.

The Nuclear Regulatory Commission requires vendors to accurately evaluate the CHF phenomenon in their nuclear reactor designs and to demonstrate that the boiling crisis can be avoided in their reactors even under unlikely, hypothetical accident scenarios. New fuel assembly designs need therefore to be tested in very expensive high-power, full-scale water loops, very few of which exist. The two-phase CFD code developed by this project will help reduce the number of experiments required to develop new reactor designs, thus streamlining the design and facilitating prototyping of reactor components.

FY 2014 Results and Accomplishments

During FY 2014, the research and development effort was focused on (A) the evaluation and extension of the EBF models in the context of the existing CFD code STAR-CD, with the goal of exploring and improving the capability of the EBF models to predict the occurrence of CHF under boiling flow conditions similar to those encountered in BWR fuel bundles, and (B) the development of a two-phase variable density solver for the Nek5000 code, which can be used for the simulation of two-phase boiling flows in heated channels and provide the framework for the implementation of the EBF models in Nek5000.

The Extension of the EBF for Improved Prediction of Critical Heat Flux (CHF). This work reviewed the key EBF two-phase flow phenomenological models and focused on the extension and validation of models that describe the cladding-to-coolant heat transfer and the onset of CHF. The EBF wall heat transfer models were extended, and the extended models were used in the context of STAR-CD to perform analyses of CHF experiments that measured the axial distribution of wall temperature in two-phase upward flow in a vertical channel with a heated wall. The void fraction distributions calculated with the enhanced model are shown for three of the six experiments analyzed in Figures 1a through 1c and the corresponding wall temperature distributions are shown in Figures 1d through 1f. The good agreement between the simulated axial distribution of wall temperatures and experimental data illustrates the ability of the extended EBF model to capture the onset of CHF for a wide range of thermal-hydraulic conditions relevant for BWRs.

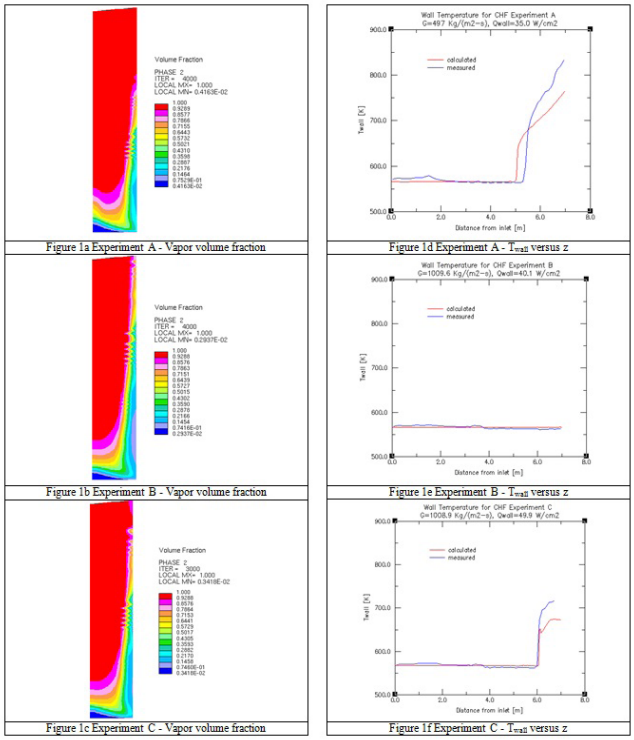

Figure 1. Calculated void fraction distributions (1a–1c) and wall temperatures (1d–1f) for three analyzed Becker CHF experiments.

The Development of a Two-phase Variable Density Solver for the NEK5000 Code. Nek5000 is a highly scalable open-source transient CFD code developed at Argonne. The code is based on the spectral element method and it is written in FORTRAN and C languages. The original Nek5000 was built for the simulation of single-phase constant-density flows. A later version of the code, referred to as the low-Mach version, was modified to allow the simulation of single-phase variable-density perfect-gas flows. The project team decided to use the low-Mach version as the platform for the implementation of the two-phase modeling capabilities in Nek5000. Because only one velocity field is available in the low-Mach version, we decided to begin with the implementation of a homogeneous two-phase model. Two main changes were implemented in the Nek5000 low-Mach solver in order to implement the two-phase homogeneous boiling model:

1. The original solver, which was designed to solve for the temperature as one of the independent variables, was modified to solve for the fluid enthalpy instead of temperature (this change is necessary because the enthalpy of the fluid remains monotonic through the transition from liquid to vapor, while the temperature is monotonic only in subcooled-liquid and superheated-vapor regions, but remains constant in the two-phase region), and
2. The original low-Mach formulation, which was designed for the treatment of variable-density fluids that obey the perfect gas law, was modified to allow the treatment of the density changes that occur in the two-phase mixture during the transition from liquid to vapor.

The two-phase homogeneous model implemented in Nek5000 was tested through the simulation of the Becker CHF experiment C, which was also analyzed in Task A with STAR-CD and EBF. The 7-m-long tube with heated walls was simulated with the two-phase version of Nek5000, named Nek-2P, on the Argonne high-performance computing center BLUES cluster using 256 processors. A total of 6.8 million points are considered to describe the entire geometry. As shown in Figure 2, the initial two-phase Nek5000 results capture some important features of the boiling flow in the heated pipe; however, as expected, these results are also missing some features that will only be captured after the implementation of the EBF models. The temperature shown in Figure 2a remains equal to the saturation temperature over most of the domain and some superheated temperatures are observed only near the outlet of the pipe, where the vapor volume fraction becomes 1.0 and the vapor becomes superheated. Significant vapor volume fraction changes and associated density changes occur in a region near the pipe inlet as a result of vapor phase formation (Figure 2b), which lead to higher velocities of the two-phase mixture as shown in Figure 2c. The void fraction distribution calculated with the new Nek5000 homogeneous two-phase solver does not capture yet the formation of the liquid films on the heated pipe walls (see Figure 1c, which shows the corresponding results obtained with STAR-CD and EBF), which play a central role in the prediction of CHF. The simulation of the liquid films will require (a) the extension of the two-phase solver to include a drift-flux model, allowing different velocities for the liquid and vapor phases, and (b) the implementation of the EBF methodology in the Nek5000 solver.

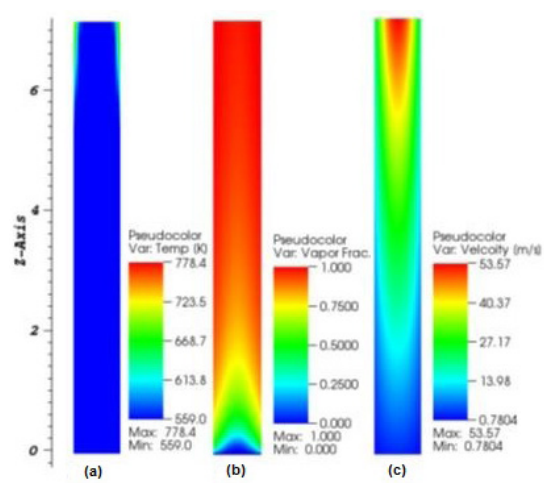

Figure 2. Two-phase NekK5000 simulation of Becker CHF experiment C: 2d contour plot of (a) temperature, (b) vapor volume fraction, and (c) velocity magnitude.

Proposed Work for FY 2015

In FY 2015, we plan to continue a parallel approach in which code development, model development, and validation proceed simultaneously. While the necessary Nek5000 two-phase modeling capabilities are implemented, the EBF model development and validation for CHF prediction will continue in the framework of the existing STAR-CD code. As the Nek5000 code two-phase capabilities advance, we will gradually implement the EBF models in Nek5000 and compare the results of Nek5000 two-phase flow simulations with those of STAR-CD calculations and with experimental data. The focus of our research will be the following three tasks:

Numerical Two-Phase Modeling. Two separate efforts are planned: (1) continue the development of the spectral element (SE) multiphase (MP) Navier-Stokes solver, with a focus on the implementation of a drift-flux model (MP-DF), and (2) continue the development of the two-velocity spectral element multiphase Navier-Stokes solver (MP-2V) in Nek5000.

Physical Two-Phase Modeling. This task will cover the multiphase EBF model implementation in Nek5000 and further development. We will initially implement the EBF models in the available spectral element two-phase drift flux (MP-DF) Nek5000 solver and evaluate the models for their ability to capture boiling flow and critical heat flux phenomena. As the two-velocities solver (MP-2V), we will implement the EBF models in the MP-2V Nek5000 solver and compare the two-phase CHF results obtained with the MP-2V formulation with those obtained with the MP-DF formulation and with the experimental data. The strategy for the implementation of the EBF models in Nek5000 will be closely coordinated with the first task above.

Exploratory Mesoscale Simulation of Boiling Phenomena. This task will explore the simulation of boiling phenomena by using the mesoscale lattice Boltzmann method (LBM), with the goal of obtaining detailed information that can be used to refine the boiling models used in the CFD simulation. The LBM simulations will focus on the modeling of vapor bubble formation and growth on a vertical heated wall in contact with a subcooled flowing liquid, bubble departure, and subsequent coalescence in the subcooled liquid flow.

Feasibility Study of a Fast Reactor for Isotope Production

2014-190-N0

Yoon Il Chang

Project Description

Special nuclear-security-relevant isotope production has traditionally been done using heavy water and light water reactors. However, a fast (higher neutron energy) spectrum reactor could provide a unique advantage because of its superior neutron economy. It is not well recognized whether fast spectrum reactors are capable of accomplishing such a mission. This project aims at establishing feasibility and quantifying the advantages of a fast spectrum reactor relative to thermal spectrum reactors. We will complete a feasibility study of a sodium-cooled fast reactor (SFR) applied to tritium production (TP), with emphasis on optimizing the core design parameters, such as the lower operating coolant temperature to fit a lithium target used in a current production reactor, and by constructing the reactor with low capital cost investment and currently available fissile materials. To accomplish this, we will collaborate with experts at the Savannah River National Laboratory (SRNL).

Mission Relevance

The project is relevant to national security. If successful, this study will identify cost effective and safe approach based on a SFR technology to satisfy an important element of the national security mission, a stable TP for a longer term. It will also support the long-term mission of DOE's Nuclear Energy Office by demonstrating a Generation-IV reactor technology.

FY 2014 Results and Accomplishments

Through the feasibility study, we were able to conclude that the SFR offers several advantages for use in tritium production, summarized as follows:

- Use of an SFR offers an intrinsic advantage for tritium production because of its superior neutron economy. The SFR-TP, when optimized for tritium production, can produce about 2 kg of tritium per year at a modest reactor power level of 400 megawatt thermal (MWth).
- The SFR-TP was further optimized for tritium production by operating at low coolant temperatures — that is, at 200°C at the inlet and 300°C at the core outlet. The lower operating temperatures allow for development of a much simpler lithium-based target assembly based on a lithium-aluminum alloy with aluminum cladding, which has been utilized in the Savannah River production reactors. The lithium target assemblies operate in the 200–250°C temperature

range. These reduced operating temperatures also support greatly enhanced safety margins and structural design margins.

- Another major advantage of the SFR-TP is that it can be fueled solely by DOE's existing inventory of excess fissile materials, without generating a new need across the DOE complex to obtain (and thus transport) unobligated enriched uranium.
- All of the above advantages contribute to the finding that a very low capital cost investment, below $1 billion, would be needed to acquire and begin producing a secure, stable source of tritium supply for the longer term.

LDRD

Sustainable Energy Production and Use

ANNUAL REPORT

2014

Improved Catalytic Performance by Applying Electrochemical Control

2011-210-R3

Stefan Vajda

Project Description

The aim of this project is to conduct interdisciplinary studies on the effect of the electrochemical potential on the activity of small cluster-based catalysts supported on novel carbon-based materials. The emphasis is on the controlled synthesis of atomically precise metal, metal alloy, and metal composite clusters by using synthesis techniques developed at Argonne National Laboratory based on gas-phase physical cluster fabrication. The work also includes state-of-the-art characterization, with results applied to help understand and design the new materials.

Mission Relevance

The project is relevant to DOE's missions in energy and science. The design of new catalytic materials (including optimizing their size and composition at the subnanometer scale and fine-tuning their properties via applied external electrochemical potential) represents a fundamental, new approach to solving energy-related problems. The project does this by identifying environmentally friendly and efficient catalysts for producing fuels and improving energy storage.

FY 2014 Results and Accomplishments

The first two years of the project were devoted primarily to the design, development, and testing of the experimental setup, including *in situ* experiments at the synchrotron, in which we demonstrated the feasibility of monitoring and controlling the evolution of the oxidation state of silver clusters.

In FY 2014, we continued studying the effect of an external electric field on the performance of a catalyst based on size-selected silver clusters made of up to 15 atoms. The results showed that it is feasible to control the oxidation state, thermal stability, and catalytic performance of clusters by varying the applied external field; the oxidation state of the clusters and their aggregates were found to depend on the (1) particle size, (2) support material used, and (3) electrical field applied.

We finished our studies of the activity of cobalt (Co) clusters supported on iron oxide (FeOx) film during electrochemical water splitting under oxygen evolution reaction (OER) conditions. Figure 1 shows the activity of oxidized 27-atom cobalt (Co27Ox) clusters. To the best of our knowledge, these results indicate, for the first time, that subnanometer-size cobalt clusters are active and — very importantly — stable under the harsh reaction conditions of electrochemical water splitting.

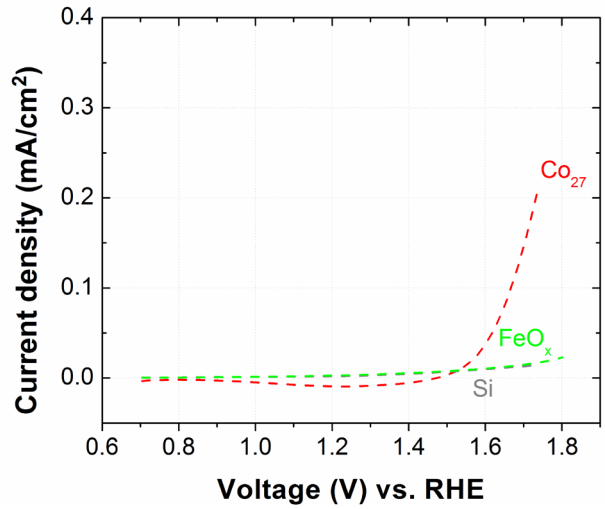

Figure 1. Current density on Co27Ox clusters deposited on a thin (about 3-nm) Fe_2O_3 film (red). Also shown are the current densities of the FeOx film without the Co clusters (green) and of the base silicon (Si) support without clusters and the FeOx film.

LDRD

Other Novel R&D

ANNUAL REPORT

2014

Enabling Sodium-Ion Batteries for Grid Storage

2014-185-N0

Christopher Johnson

Project Description

The introduction of new high-performance, low-cost batteries and their technological development is a key driver for the deployment of advanced large-scale electrical energy storage systems for maintaining and delivery of electricity on the grid. Sodium-ion batteries (SIBs) that operate at ambient temperature constitute a serious contender for this application if the energy density can be improved. The search for electrode materials that possess desirable properties (such as low cost and low toxicity, long cycle life, high rate capability, and high energy density) and that are easily synthesized will foster the rollout of an environmentally sustainable battery technology by using earth-abundant and recyclable elements. In this project, we synthesize new materials for both electrodes, characterize the chemistry and structures, and operate them in battery SIB. From this information, we optimize and continue research and development into identifying new systems and applying emerging technologies, such as the use of nanoscience into SIBs, to make improvements in high power.

According to our calculations, to achieve the targeted grid storage requirements, the anodes and cathodes must meet specific capacity values of 600 mAh/g and 200 mAh/g, respectively, at ~3.5 V in order to generate an energy density of at least 350 Wh/kg, which would match our grid storage target. The performance metrics from full cell optimization and fabrication will yield (1) an SIB-specific energy (350 Wh/Kg) and energy density (750 Wh/L); (2) a compact, lightweight SIB; (3) economical and scalable precursors and products; (4) exceptional cycle life (~1,000 cycles) and calendar life (~15 years); and (5) fast recharge in SIB full pouch-type cells. In addition, the total cost must achieve $100/kWh to meet the DOE grid storage objective.

Mission Relevance

This project supports DOE's energy and science missions. Specificlly, grid storage topics fall into the domain of DOE's Office of Electricity (OE). SIBs are drawing large interest as an energy storage option to satisfy backup power needs for stationary grid power networks. The energy security and reliability of the grid is paramount in the United States. The needs for new materials-based technologies for this area are outlined in the DOE Report "Energy Storage Program Planning Document (Feb. 2011). Our strategy lies in a potential for our technology to achieve an optimal balance between battery performance and cost. A grid storage system will require large capacity batteries wherein material production cost and raw material expense must be minimally apportioned. SIB may offer a good low cost option if one can identify and employ the correct electrode and electrolyte chemistry for this application.

Highly synergistic benefits could be expected between this project and other electrochemical energy storage programs in DOE's Energy Efficiency and Renewable Energy (EERE) and Batteries for Advanced Transportation Technologies, given that the core technologies comprising the SIB system complement the battery system (non-SIB research) activities in the Joint Center for Energy Storage Research (JCESR) and at other national laboratories pursuing SIB technologies.

FY 2014 Results and Accomplishments

Here we summarize our findings, along with some preliminary work on sodium iron oxide, the research direction that we will be pursuing in the future.

The implementation of layered electrode materials based on an understanding the structure-property relationship is imperative for the development of SIBs. Novel layered intergrowth $Na_{1-x}Li_xNi_{0.5}Mn_{0.5}O_2$ cathodes have shown high-rate performance. The field emission scanning electron microscopy (FESEM) image is shown in Figure 1. The good electrochemical properties are attributed to the synergistic effect of an intergrowth structure that results from the direct incorporation of lithium (Li) in the matrix. This finding highlights the importance of multiphase intergrowths with an orientation relationship that can attain the stability and performance for future optimized SIBs. This new development — discovered only this past year by Argonne researchers — provides some design rules for layered oxides.

The layered sodium-ion cathode material P2-$Na_{0.85}Li_{0.17}Ni_{0.21}Mn_{0.64}O_2$ (studied previously) was investigated by using *operando* x-ray absorption microscopy (XAS) to characterize structural changes occurring in the material during electrochemical sodiation/desodiation. On the basis of x-ray absorption near edge structure (XANES) data, the primary mode of charge compensation in this material is attributable to $Ni^{2-3/4+}$ redox activity, whereas the manganese (Mn) remains in the +4 oxidation state, thereby providing stability to this material during extended cycling. Investigation of the initial state of the compound by high-resolution, synchrotron x-ray diffraction (XRD) and ^6Li magic-angle spinning (MAS) nuclear magnetic resonance (NMR) revealed a significant amount of structural disorder that resulted from integration of a

small amount of a monoclinic layered Li phase within the overall hexagonal layered sodium (Na)-structure, which manifests as Li-induced stacking faults. We were able to obtain high-quality, extended x-ray absorption fine structure (EXAFS) data by using our cell construction; the data revealed the local structural evolution around the redox's active nickel (Ni) centers. This knowledge will help guide our designs for new cathode materials based on layered structures.

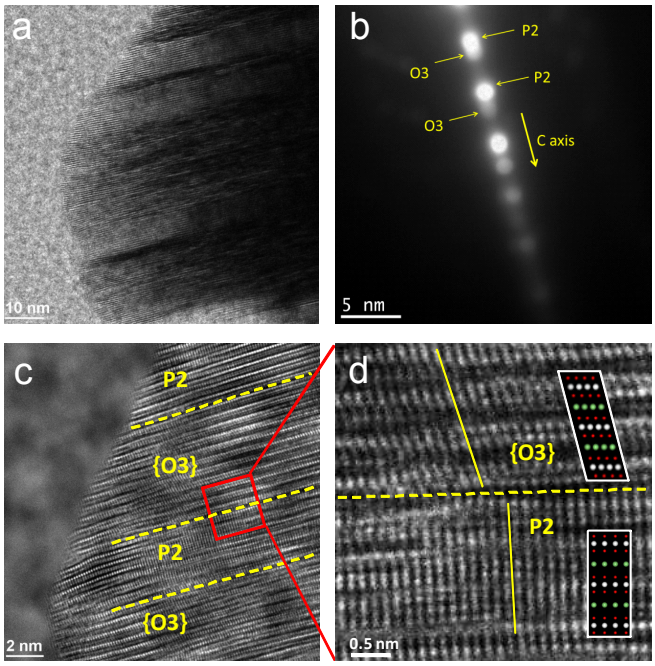

Figure 1. Transmission electron microscopy analysis of $Na_{0.7}Li_{0.3}Ni_{0.5}Mn_{0.5}O_{2+d}$: a) Low magnification TEM image shows intensity streaking along c-axis indicating intergrowth structure of thin crystal domains. b) Convergent-beam electron diffraction (CBED) pattern shows distinguishable diffraction spots corresponding to P2 or O3 structure. The two parallel systematic rows of the reflection support the topotactic relationship between P2 and O3 structure. c) and d) High-resolution TEM images directly showing the intergrowth stacking of the P2 and O3 lattices.

The electrochemical sodium insertion/extraction of Na_xVS_2, and Na_xTiS_2 in the voltage range where either intercalation ($0.2 \leq x \leq 1$) or displacement-conversion reaction ($x > 1$) occurs. Both $Na_xVS_2$and Na_xTiS_2showed good reversible capacities, as high as ~160 mAh/g at an average voltage of ~1.9 V, as compared to Na in the region for the intercalation reaction ($0.2 \leq x \leq 1$). When Na insertion was forced further to the $x > 1$ composition, Na_xVS_2 exhibited the direct displacement-conversion reaction at 0.3 V versus Na without further Na intercalation, which contrasted with the wider Li intercalation range of $0 < x \leq 2$ for Li_xVS_2. The displacement-conversion reaction for Na_xVS_2 ($x > 1$) was reversible with a specific capacity of above 200 mAh/g up to 15 cycles; however, the displacement reaction for Na_xTiS_2 ($x > 1$) was not observed.

Tin (Sn) and antimony (Sb) metals were high-energy ball-milled with carbon in order to create a SnSb_C alloy carbon composite worthy of cycling as a high-capacity, 500-mAh/g anode in a full-cell Na-ion battery. In the cell, coupled with a cathode consisting of a layered transition metal oxide cathode, $NaNi_{1/3}Mn_{1/3}Fe_{1/3}O_2$, was cycled for more than 50 cycles with near 100% coulombic efficiency, yielding a resultant gravimetric energy density of 145 Wh/kg (based on electrode material only), and an even better volumetric energy density of 215 Wh/L as a result of the high density inherent in the SnSb_C anode. *In situ* synchrotron XRD measurements indicate a progressive amorphization of the SnSb during sodiation without any observable binary sodium-tin or sodium-antimony alloy phase formation. The electrochemically active amorphous phase remains present during desodiation.

We also evaluated iron-containing layered $NaFeO_2$ as we are interested in using iron in sodium-layered transition metal oxides because it is possible to access the Fe^{3+}/Fe^{4+} redox couple reversibly in Na systems. Figure 2 shows the voltage profile (initial cycle) of the $Na/NaFeO_2$ electrochemical cell in a Na battery. In Figure 3, we observed that indeed $NaFeO_2$ can be oxidized and reduced reversibly in a Na cell at 3.4 V. The collected Mössbauer data for charged $Na_{1-z}FeO_2$ proves the existence of tetravalent Fe(IV) in this case (Figure 3). The use of iron therefore represents a strategy to increase the energy density of the SIB, while at the same time dramatically lowering the cost of the cathode, given that iron is only about one-tenth the cost of Mn.

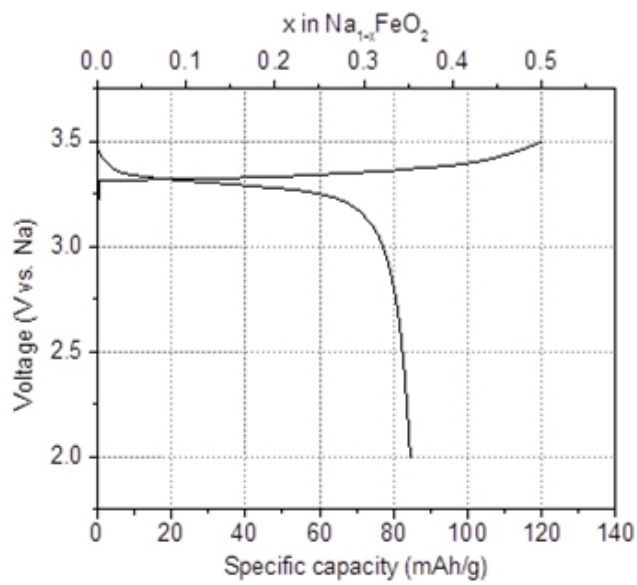

Figure 2. Electrochemical voltage profiles of $Na/NaFeO_2$ on the first initial cycle.

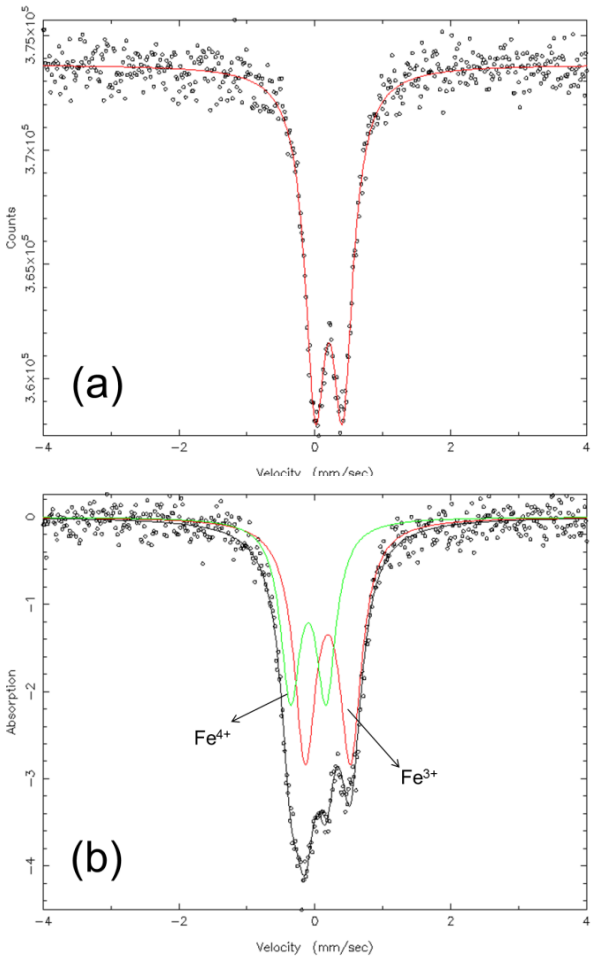

Figure 3. Mössbauer spectra of (a) $NaFeO_2$ and (b) $Na_{0.56}FeO_2$, indicating the presence of Fe^{4+} in the material on charge.

Proposed Work for FY 2015

The SIB is envisioned as a low-cost, safe, reliable, and long-lasting battery system for grid storage. We must use earth-abundant elements in order to achieve this objective. Therefore, we will focus on low-cost carbon materials for the anode and low-cost sodium-iron oxide materials for the duration of this project. Our preliminary $NaFeO_2$ study and assessment are encouraging (as shown above). However, more synthesis is needed in order to design a Mn-rich surface and a Fe-rich core ($NaMnO_2$@$NaFeO_2$), a material that is more robust to the electrolyte. We also need to scale up and optimize the synthesis and particle morphologies of the material. To do this, we will turn to co-precipitation reactions, wherein the $Mn(OH)_2$ precursor is formed in the core, and then FeO(OH) is coated on the surface of the particle. Subsequent Na reactions will form the $NaFeO_2$@$NaMnO_2$ epitaxially matched composite. In this way, we can also improve the stability and the cycle life.

The carbon work requires careful assessment of the properties needed to enable long life and high rate for the material. Our future work will set the design rules for various physical and chemical properties needed from the carbon for this application, such as pore volume, surface area, extent of graphene content, and surface moieties, among others.

LDRD

Appendix

ANNUAL REPORT

2014

LDRD

Intellectual Property Events Occurring in FY 2014

(As a Result of LDRD Projects and Subsequent Related Sponsored Research)

ANNUAL REPORT

2014

Invention Disclosures

2005-024

Elam, J., C. Marshall, J. Libera, and J. Dumesic. "Improved Hydrothermal Performance of Catalyst Supports." Invention report disclosed April 2014. [ANL-IN-09-085B].

2007-044

Liu, D.-J., S. Ma, and B. Goenaga. "Non-Platinum Metal Electrocatalysts Using Metal Organic Framework Materials and Method of Preparation." Invention report disclosed September 2014. [ANL-IN-09-069B]. (also see 2010-158).

2010-158

Liu, D.-J., S. Ma, and B. Goenaga. "Non-Platinum Metal Electrocatalysts Using Metal Organic Framework Materials and Method of Preparation." Invention report disclosed September 2014. [ANL-IN-09-069B]. (also see 2007-044).

2010-188

Xiong, H., T. Rajh, E. Shevchenko, S. Tepavcevic, and C. Johnson. "High Capacity Electrode Materials for Batteries and Process for their Manufacture." Invention report disclosed March 2014. [ANL-IN-11-004B].

2010-191

Krumdick, G., Y. Shin, and O. Kahvecioglu-Feridan. "Method for Continuous Production of Concentration-Gradient Size-Selected Particles." Invention report disclosed May 2014. [ANL-IN-14-045].

2010-194

Campos Ortega, E., and R. Ware. "An Early Warning System for Aircraft Icing." Invention report disclosed June 2014. [ANL-IN-14-051].

2010-202

Hock, A., and S. Kraft. "Direct Additive Manufacturing of Electronic Materials." Invention report disclosed December 2013. [ANL-IN-13-117].

2011-027

Heifetz, A., R. Klann, and M. Winstein. "Detection of Nuclear Sources in Search Applications Using Spectral Data Clustering." Invention report disclosed March 2014. [ANL-IN-14-033].

2011-116

Johnson, C., and S. Hokang. "Electrode Materials for Rechargeable Battery." Invention report disclosed October 2013. [ANL-IN-10-031B].

2011-153

De Lurgio, P., G. Drake, J. Anderson, and M. Oberling. "Modular Instrumentation System with Highly Redundant Communication Methods for Environmental Monitoring." Invention report disclosed November 2013. [ANL-IN-13-088].

2012-072

Sumant, A., D. Berman, and A. Erdemir. "Low Friction Wear Resistant Graphene Films." Invention report disclosed March 2014. [ANL-IN-14-027].

Sumant, A., D. Berman, and A. Erdemir. "Nanoparticles Enabled Superlubricity in Graphene at Macroscale." Invention report disclosed February 2014. [ANL-IN-14-029].

2012-087

Timofeeva, E., J. Kastoudas, D. Singh, C. Segre, and J. Terry. "Radiolysis Mediated Charging of Nanoelectrofuels from Different Sources of Radiation." Invention report disclosed April 2014. [ANL-IN-14-036]

2012-208

Shenai, K. "Robust Scalable High-Power Vertical GaN Devices and Method of Manufacturing." Invention report disclosed March 2014. [ANL-IN-13-061].

Shenai, K., A. Mane, and J. Elam. "Later AL 2D Channel SiC Power Moset and Method of Manufacturing." Invention report disclosed August 2014. [ANL-IN-14-063].

Shenai, K. "Novel High-Voltage Merged PiN-Schottky (MPS) Barrier Diode (MPS) and a Method to Produce the Structure." Invention report disclosed March 2014. [ANL-IN-13-065].

Shenai, K., and S. Gupta. "NG Powered Fast Charger." Invention report disclosed April 2014. [ANL-IN-14-025].

2013-100

Martinson, A., A. Hock, R. McCarthy, and M. Weimer. "Oxygen-Free Atomic Layer Deposition of Indium Sulfide." Invention report disclosed March 2014. [ANL-IN-14-022].

2014-051

Liu, D.-J. "Alkaline Fuel Cell Non-Platinum Group Metal Electrocatalysts Using Metal Organic Framework Materials and Method of Preparation." Invention report disclosed July 2014. [ANL-IN-14-079].

2014-185

Johnson, C., N. Sa, C. Liao, A. Lipson, D. Zhou, B. Ingram, D. Proffit, J. Vaughey, and A. Burrell. "Multivalent Ion Batteries." Invention report disclosed July 2014. [ANL-IN-14-064].

Patent Applications

2005-024

Elam, J., C. Marshall, J. Libera, and J. Dumesic. "Improved Hydrothermal Performance of Catalyst Supports." Patent No. 14/265,983 filed April 2014. [ANL-IN-09-085B].

2007-044

Liu, D.-J., S. Ma, and G. Goenaga. "Non-Platinum Metal Electrocatalysts Using Metal Organic Framework Materials and Method of Preparation." Patent application filed September 2014. [ANL-IN-09-069B]. (also see 2010-158).

2010-158

Liu, D.-J., S. Ma, and G. Goenaga. "Non-Platinum Metal Electrocatalysts Using Metal Organic Framework Materials and Method of Preparation." Patent application filed September 2014. [ANL-IN-09-069B]. (also see 2007-044).

2010-188

Xiong, H., T. Rajh, E. Shevchenko, S. Tepavcevic, and C. Johnson. "High Capacity Electrode Materials for Batteries and Process for Their Manufacture." Patent application filed March 2014. [ANL-IN-11-004B].

Shevchenko, E., T. Rajh, C. Johnson, and B. Koo. "Hollow Nanoparticle Cathode Materials for Sodium Electrochemical Cells and Batteries." Patent application filed December 2013. [ANL-IN-13-024]. (also see 2011-116).

2010-191

Shin, Y., and G. Krumdick. "Method and Apparatus for Preparing a Specific Sized Positive Electrode." Patent Application No. 14/265,638 filed April 2014. [ANL-IN-12-083].

Shin, Y., G. Krumdick, and K. Tayek. "Method for Producing Size Selected Particles." Patent Application No. 14/265,638 filed April 2014. [ANL-IN-12-115].

2010-203

Brushett, F., A. Jansen, and J. Vaughey. "Aqueous-Non-Aqueous Immiscible Liquid Flow Battery." Patent application filed February 2014. [ANL-IN-12-124].

Brushett, F., A. Jansen, and J. Vaughey. "Quinozaline and Its Derivatives as Redox Species for Aqueous Flow Batteries." Patent application filed February 2014. [ANL-IN-12-125].

2011-022

Erdemir, A., Q. Chang, K. Mistry, M. Thackeray, and V. Pol. "Novel Materials as Additives for Advanced Lubrication." Patent Application No. 14/109,557 filed December 2013. [ANL-IN-13-048].

2011-116

Johnson, C., and S. Hokang. "Electrode Materials for Rechargeable Battery." Patent Application No. 14/048,663 filed October 2013. [ANL-IN-10-031B].

Shevchenko, E., T. Rajh, C. Johnson, and B. Koo. "Hollow Nanoparticle Cathode Materials for Sodium Electrochemical Cells and Batteries." Patent application filed December 2013. [ANL-IN-13-024]. (also see 2010-188).

2012-072

Sumant, A., D. Berman, and A. Erdemir. "Low Friction Wear Resistant Graphene Films." Patent application filed June 2014. [ANL-IN-14-027].

2013-063

Roelofs, A., and S. Hong. "Charge Gradient Microscopy." Patent application filed April 2014. [ANL-IN-13-039].

2013-100

Martinson, A., A. Hock, R. McCarthy, and M. Weimer. "Oxygen-Free Atomic Layer Deposition of Indium Sulfide." Patent Application No. 14/335,745 filed. [ANL-IN-14-022].

Patents Granted

2004-103

Lin, Y., and E. St. Martin. "Bioprocess Utilizing Carbon Dioxide and Electrodeionization." Patent No. 8,580,096 granted November 2013. [ANL-IN-06-090].

2005-024

Elam, J., C. Marshall, J. Libera, and J. Dumesic. "Hydrothermal Performance Catalyst Supports." Patent No. 8,741,800 granted June 2014. [ANL-IN-09-085].

2006-118

Welp. U., V. Vlasko-Vlasov, A. Chen, and S. Gray. "Multiscale Light Amplification Structure for Surface Enhanced Raman Spectroscopy." Patent No. 8,837,039 granted September 2014. [ANL-IN-11-109].

2007-044

Liu, D.-J., S. Ma, and G. Goenaga. "Non-Platinum Metal Electrocatalysts Using Metal Organic Framework Materials and Method of Preparation." Patent No. 8,835,343 granted September 2014. [ANL-IN-09-069]. (also see 2010-158).

2007-113

Bakhtiari, S., N. Gopalsami, T. Elmer, and A. Raptis. "Millimeter Wave Sensor for Far-Field Standoff Vibrometry." Patent No. 8,686,362 granted April 2014. [ANL-IN-08-041].

2007-126

Pol, V., and P. Thiyagarajan. "Process for Remediation of Plastic Waste." Patent No. 8,580,222 granted November 2013. [ANL-IN-07-070].

2008-183

Chollet, M., and B. Adams. "Continuously Variable Focal Length Lens." Patent No. 8,611,502 granted December 2013. [ANL-IN-10-033].

2009-097

Lin, Y., S. Snyder, and M. Urgun Demirtas. "Methane Production Using Resin-Wafer Electrodeionization." Patent No. 8,679,314 granted March 2014. [ANL-IN-10-027].

2009-138

Bahns, J., L. Chen, S. Gray, and S. Sankaranarayanan. "Method for Patterning Nanoparticles." Patent No. 8,835,805 granted September 2014. [ANL-IN-11-009].

2009-212

Hu, S., P. Mueller, W. Jiang, and Z. Lu. "Isotopic Abundance in Atom Trap Trace Analysis." Patent No. 8,674,289 granted March 2014. [ANL-IN-11-098].

2010-050

Welp. U., V. Vlasko-Vlasov, A. Chen, and S. Gray. "Multiscale Light Amplification Structures for Surface Enhanced Raman Spectroscopy." Patent No. 8,837,039 granted September 2014. [ANL-IN-11-109].

2010-158

Liu, D.-J., S. Ma, and G. Goenaga. "Non-Platinum Metal Electrocatalysts Using Metal Organic Framework Materials and Method of Preparation." Patent No. 8,835,343 granted September 2014. [ANL-IN-09-069]. (also see 2007-044).

2011-116

Johnson, C., and S. Hokang. "Electrode Materials for Rechargeable Battery." Patent No. 8,577,438 granted October 2013. [ANL-IN-10-031].

Johnson, C. "Electrode Materials for Sodium Battery." Patent No. 8,835,041 granted September 2014. [ANL-IN-10-056].

Non-publication Copyrights

2010-194

Campos Ortega, E. "Beam Propagator for Weather Radars, Modules 1 and 2." Software copyrighted October 2013. [ANL-SF-13-101].

Campos Ortega, E. "Display_UHFwindprof_MomentsFiles." Software copyrighted November 2013. [ANL-SF-13-113].

2013-168

Gursoy, D., F. De Carlo, W. Di, and D. Vine. "A Python Toolbox to Perform X-ray Data Processing and Image Reconstruction." Software copyrighted February 2014. [ANL-SF-13-123].

LDRD

Publications and Presentations I

(Derived from LDRD Projects Active in Fiscal Year 2014)

ANNUAL REPORT

2014

Director's Competitive Grants

2012-012-R2

Abouimrane, A., Y. Cui and K. Amine (2014). "Mechanism Understanding of New Li-Se Rechargeable Battery System." International Battery Association Meeting, Brisbane, Australia, Mar. 3–7, 2014.

Abouimrane, A., Y. Cui and K. Amine (2014). "Se-based Positive Electrode Material for Rechargeable Battery Applications." TMS 2014 143rd Annual Meeting, San Diego, CA, Feb. 16–20, 2014.

Abouimrane, A., D. Dambournet, K. Chapman , P. Chupas, W. Weng, Y. Cui, H. El Tayeb and K. Amine (2013). "Selenium and Selenium Sulfide—A New Class of Positive Electrode Material for Room Temperature Lithium and Sodium Rechargeable Batteries." Proceedings of 222nd Meeting of The Electrochemical Society, Honolulu, Hawaii, Oct. 7–12, 2012, *ECS Meeting Abstracts* **335**.*

Abouimrane, A., D. Dambournet, K.W. Chapman, P.J. Chupas, W. Weng and K. Amine (2012). "A New Class of Lithium and Sodium Rechargeable Batteries Based on Selenium and Selenium-sulfur as a Positive Electrode." *Journal of the American Chemical Society* **134**(10): 4505-4508.*

Cui, Y., A. Abouimrane, J. Lu, T. Bolin, Y. Ren, W. Weng, C. Sun, V.A. Maroni, S.M. Heald and K. Amine (2014). "(De)Lithiation Mechanism of Li/SeS_x (x = 0-7) Batteries Determined by *in situ* Synchrotron X-ray Diffraction and X-ray Absorption Spectroscopy." 224th ECS Meeting, San Francisco, CA, Oct. 27–Nov. 1, 2013.

Cui, Y., A. Abouimrane, C.J. Sun, Y. Ren and K. Amine (2014). "Li-Se Battery: Absence of Lithium Polyselenides in Carbonate Based Electrolyte." *Chemical Communications* **50**(42): 5576-5579.*

Cui, Y.C., A.A. Abouimrane and K. Amine (2014). "Mechanism Study of Li/Se Rechargeable Batteries in Different Electrolytes." 225th ECS Meeting, Orlando, FL, May 11–16, 2014.

Cui, Y., A. Abouimrane, J. Lu, T. Bolin, Y. Ren, W. Weng, C. Sun, V.A. Maroni, S.M. Heald and K. Amine (2013). "(De)Lithiation Mechanism of Li/SeS_x (x = 0-7) Batteries Determined by *in situ* Synchrotron X-ray Diffraction and X-ray Absorption Spectroscopy." *J. Am. Chem. Soc.* **135**(21): 8047-8056.*

2012-061-R2

Miller, D.J., C. Proff, J.G. Wen and D.P. Abraham (2013). "Evolution of Cation Ordering in $Li_{1+x}(Mn,TM)O_2$ with Number of Cycles." 2012 Materials Research Society Fall Meeting, Boston, MA, Nov. 25–30, 2012.

Miller, D.J., C. Proff, J.G. Wen, D.P. Abraham and J. Bareno (2013). "Observation of Microstructural Evolution in Li Battery Cathode Oxide Particles by *in situ* Electron Microscopy." *Advanced Energy Materials* **3**(8): 1098-1103.*

Miller, D.J., C. Proff, J.G. Wen and D.P. Abraham (2013). "Revealing Positive Electrode Oxide Changes on Electrochemical Cycling by *in situ* Electron Microscopy." 222nd Meeting of the Electrochemical Society, Honolulu, HI, Oct. 7–12, 2012.

Miller, D.J., C. Proff and J.G. Wen (2013). "What Can We Learn from Measurements of Li-ion Battery Single Particles?" 2013 Materials Research Society Spring Meeting, San Francisco, CA, Apr. 1–5, 2013.

Miller, D., K. Cooley, J. Wen and D. Abraham (2012). "Microstructural Evolution of $Li(Ni,Co,Al)O_2$ and $Li(Ni,Co,Mn)O_2$ Battery Cathode Material as a Function of Cycling Revealed by Electron Microscopy." 2011 Materials Research Society Fall Meeting, Boston, MA, Nov. 28–Dec. 2, 2011.

Miller, D., C. Proff, K. Cooley, J. Wen and D. Abraham (2012). "Microstructural Evolution of $Li(Ni,Co,Al)O_2$ Battery Cathode Material Revealed by Operanda Electron Microscopy." Gordon Conference on Advanced Characterization, Theory and Mechanisms of Processes in Rechargeable Batteries Across Length Scales, Ventura, CA, Mar. 4–9, 2012.

Miller, D., C. Proff, J. Wen and D. Abraham (2012). "Direct Observation of Microstructural Evolution in Li Battery Cathode Oxide Particles During Electrochemical Cycling by *in situ* Electron Microscopy." Proceedings of Microscopy and Microanalysis 2012, Phoenix, AZ, July 28–Aug. 2, 2012. **18**(S2): 1108–1109.

Miller, D., C. Proff, J. Wen, D. Abraham and S. Wang (2012). "Probing Local Behavior and Microstructural Evolution of Li-ion Battery Cathode Materials." 2012 Materials Research Society Meeting, San Francisco, CA, Apr. 9–13, 2012.

Indicates refereed publication

Miller, D.J., K. Cooley, J.G. Wen and D.J. Abraham (2012). "Microstructural Evolution of Li(Ni,CoAl)O_2 Battery Cathode Particles." 2012 Microscopy & Microanalysis Meeting, Phoenix, AZ, July 29–Aug. 2, 2012.

Proff, C., D.J. Miller, J.G. Wen and D.P. Abraham (2013). "Correlating Behavior of Li-ion Batteries with Electrochemical Cycling of Single Cathode Oxide Particles." 2012 Materials Research Society Fall Meeting, Boston, MA, Nov. 25–30, 2012.

Yang, G.-M., C.-F. Cheng, W. Jiang, Z.-T. Lu, R. Purtschert, Y.-R. Sun, L.-Y. Tu and S.-M. Hu (2012). "Direct Observation of Microstructural Evolution in Li Battery Cathode Oxide Particles During Electrochemical Cycling by *in situ* Electron Microscopy." 2012 Microscopy & Microanalysis Meeting, Phoenix, AZ, July 29–Aug. 2, 2012.

2012-072-R2

Berman, D., A. Erdemir, A.V. Zinovev and A.V. Sumant. "Nanoscale Friction Properties of Graphene and Graphene Oxide." *Diamond and Related Materials*.* (to be published)

Berman, D., S.A. Deshmukh, S.K.R.S. Sankaranarayanan, A. Erdemir and A.V. Sumant. "Origin of Macroscale Superlubricity Enabled by Graphene Nanoscroll Formation." *Science*.* (to be published)

Berman, D., S.A. Deshmukh, S.K.R.S. Sankaranarayanan, A. Erdemir and A.V. Sumant (2015). "Extraordinary Macroscale Wear Resistance of One Atom Thick Graphene Layer." *Advanced Functional Materials* **24**(42): 6640-6646.*

Berman, D., A. Erdemir and A.V. Sumant (2015). "Graphene as a Protective Coating and Superior Lubricant for Electrical Contacts." *Applied Physics Letters* **105**(23).*

Berman, D., A. Erdemir and A.V. Sumant (2014). "Extraordinary Wear Resistance of Single and Few Layer Graphene." 2014 Gordon Research Conference on Tribology, Waltham, MA, July 20–25, 2014.

Berman, D., A. Erdemir and A.V. Sumant (2014). "A Few Layers of Graphene for Low Friction and Extreme Wear Resistance in Inert and Humid Environments." American Vacuum Society Symposium 2013, Long Beach, CA, Oct. 27–Nov. 1, 2013.

Berman, D., A. Erdemir and A.V. Sumant (2014). "Graphene: A New Emerging Lubricant." *Materials Today* **17**(1): 31–42.*

Berman, D., A. Erdemir and A.V. Sumant (2013). "Few Layer Graphene to Reduce Wear and Friction on Sliding Steel Surfaces." *Carbon* **54**: 454–459.*

Berman, D., A. Erdemir and A.V. Sumant (2013). "Reduced Wear and Friction Enabled by Grapheme Layers on Sliding Steel Surfaces in Dry Nitrogen." *Carbon* **59**: 167–175.*

Berman, D., A. Erdemir and A.V. Sumant (2013). "Few Layers Graphene to Reduce Wear and Friction on Sliding Steel Surfaces." CNM/APS User Meeting, Argonne, IL, May 8, 2013.

Erdemir, A. and A.V. Sumant (2014). "Graphene as a Solid Lubricant for Macroscale Friction and Wear Reduction." Annual Meeting for Society of Tribologists and Lubrication Engineers, Orlando, FL, May 18–22, 2014.

2012-087-R2

Katsoudas, J.P., E.V. Timofeeva, C.U. Segre and D. Singh (2014). "Integration of Flow Batteries into Electric Vehicles: Feasibility and the Future." TechConnect World: Innovation Conference and Expo 2014, Washington, D.C., June 15–18, 2014.

Katsoudas, J.P., E.V. Timofeeva, C.U. Segre and D. Singh (2014). "Integration of Flow Batteries into Electric Vehicles: Feasibility and the Future." Proceedings of the TechConnect NanoTech Conference and Expo, Washington, D.C., June 15–18, 2014, *NanoTech 2014* **3**(Chapter 6: Energy Storage): 435–438.*

Katsoudas, J.P., E.V. Timofeeva and C.U. Segre (2013). "Design of Electrochemical Cells for *in situ* XAS Experiments." TechConnect Nano Tech Conference and Expo, Washington, D.C., May 13, 2013.

Katsoudas, J.P., E.V. Timofeeva and C.U. Segre (2013). "Design of Electrochemical Cells for *in situ* XAS Experiments." *Technical Proceedings of the 2013 NSTI Nanotechnology Conference and Expo* **1**(13–15).

Pelliccione, C.J., E.V. Timofeeva and C.U. Segre (2015). "*In situ* XAS Study of the Aging Mechanism in Hybrid $Sn_3O_2(OH)_2$/Graphite Battery Anode Nanomaterials." *Chemistry of Materials* **27**(2): 574–580.*

Indicates refereed publication

Pelliccione, C.J., E.V. Timofeeva, J.P. Katsoudas and C.U. Segre (2015). "Sample Chamber for *in situ* X-ray Absorption Spectroscopy Studies of Battery Materials." *Review of Scientific Instruments* **85**(12).*

Pelliccione, C.J., E.V. Timofeeva and C.U. Segre (2014). "XAS Study of Passivation Mechanism of Hybrid $Sn_3O_2(OH)_2$/GnP Anodes for Li-ion Batteries." 63rd Annual Conference on Applications of X-ray Analysis/Denver X-ray Conference, Big Sky, MN, July 28–Aug. 1, 2014.

Timofeeva, E.V. (2014). "High Energy Density Nanoelectrofuel Flow Batteries." 7th Annual Spring Forum of Microgrid Interconnections and Grid Storage, Richard G. Lugar Center for Renewable Energy and Purdue School of Engineering and Technology at IUPUI, Indianapolis, IN, May 6, 2014.

Timofeeva, E.V., D. Singh, W. Yu, D.M. France, N.G. Demas, G.R. Fenske, C.U. Segre, J.P. Katsoudas and V.K. Ramani (2014). "Engineered Nanofluids for Cooling, Batteries and Other Cool Applications." 2014 September Colloquium, Department of Chemistry, Illinois Institute of Technology, Chicago, IL, Sept. 3, 2014.

Timofeeva, E.V., C.J. Pelliccione, T.J. Chrobak, D. Singh, J.P. Katsoudas and C.U. Segre (2014). "Hybrid $Sn_3O_2(OH)_2$/Graphite Nanomaterials as Anode for Lithium Ion Batteries." APS/CNM/EMC User Meeting, Argonne, IL, May 12–15, 2014.

Timofeeva, E.V., J.P. Katsoudas, C.U. Segre and D. Singh (2013). Fact Sheet: High Energy Density Rechargeable Nanoelectrofuels and Novel Cell Designs for Flow Batteries.

Timofeeva, E.V., J.P. Katsoudas, C.U. Segre and D. Singh (2013). "Rechargeable Nanofluids Electrodes for High Energy Density Flow Battery." TechConnect Nano Tech Conference and Expo, Washington, D.C., May 15, 2013.

Timofeeva, E.V., J.P. Katsoudas, C.U. Segre and D. Singh (2013). "Rechargeable Nanofluid Electrodes for High Energy Density Flow Battery." Proceedings of TechConnect NanoTech Conference and Expo, Cleantech 2013, Washington, D.C., May 12–16, 2013, *Energy Storage* 9: 263-366.

2012-180-R2

Wang, X., T.L. Nowicki, N.N. Kariuki, D. Myers, C.-K. Lin and Y. Ren (2014). "Non-Carbon Catalyst Supports for Polymer Electrolyte Fuel Cells." 227th Electrochemical Society Meeting, Chicago, IL, May 24–28, 2015.

2013-016-R1

Bai, L., P. Hyde, Y.S. Gui, C.-M. Hu, V. Vlaminck, J.E. Pearson, S.D. Bader and A. Hoffmann (2013). "Spin Pumping in the Nonlinear Dynamics Regime Analyzed Using a Symmetry-Based Method." *Physical Review Letters* **111**(217602).*

Hoffmann, A. (2014). "Connecting Spin Waves to Charge Currents." International Workshop on Nanoscale Spectroscopy and Nanotechnology 8, Chicago, IL, July 28–31, 2014. (also see 2014-018-N0).

Hoffmann, A., H. Schultheiss, S. Vogt, S. Jain, F.Y. Fradin, S. Bader, Z. Wang, Y. Sun, Y.-T. Song, M. Wu, T. Sebastian and B. Hillebrands (2014). "Electric Control and Detection of Spin Waves." Concepts in Spintronics, Santa Barbara, CA, Sept. 30–Oct. 4, 2013. (also see 2014-018-N0).

Hoffmann, A., W. Zhang, V. Vlaminck, J.E. Pearson, S.D. Bader, R. Divan, L. Bai, P. Hyde, Y. Gui and C.-M. Hu (2014). "Insight About Spin Hall Effects from Spin Pumping." SPIE NanoScience+Engineering, San Diego, CA, Aug. 17–24, 2014. (also see 2014-018-N0).

Hoffmann, A. (2014). "Magnetization Dynamics in Nanometer-thick Yttrium Iron Garnet Films." Workshop on Oxide Materials: Nanoscale Spectroscopy and Nanotechnology, Cali, Columbia, Sept. 15–19, 2014. (also see 2014-018-N0).

Hoffmann, A. (2014). "Reduction of Spin Hall Effects Due to Magnetic Proximity." Spin Caloritronics VI, Isree, Germany, July 14–18, 2014. (also see 2014-018-N0).

Hoffmann, A. (2013). "Spin Hall Effects in Metals." *IEEE Transactions on Magnetics* **49**(10): 5172–5193.*

Houchen, C., L. Peng, Z. Wei, L. Tao, A. Hoffmann, D. Longjiang and W. Mingzhong (2014). "Nanometer-Thick Yttrium Iron Garnet Films With Extremely Low Damping." *IEEE Magnetics Letters* **5**: 1–4.*

Liu, T., H.C. Chang, V. Vlaminck, Y.Y. Sun, M. Kabatek, A. Hoffmann, L.J. Deng and M.Z. Wu (2014). "Ferromagnetic Resonance of Sputtered Yttrium Iron Garnet Nanometer Films." *Journal of Applied Physics* **115**(17).*

**Indicates refereed publication*

Schultheiss, H., J.E. Pearson, S.D. Bader and A. Hoffmann (2013). "Thermoelectric Detection of Spin Waves." 12th Joint Magnetism and Magnetic Materials (MMM)/Intermag Conference, Chicago, IL, Jan. 14–18, 2013.

Schultheiss, H., J.E. Pearson, S.D. Bader and A. Hoffmann (2012). "Thermoelectric Detection of Spin Waves." *Physical Review Letters* **109**(23): 237204.*

Sola, A., M. Kuepferling, V. Basso, S. Zullino, E. Olivetti, M. Pasquale, T. Kikkawa, K. Uchida, E. Saitoh, D. Meier, T. Kuschel, G. Reiss, H. Jin, S. Boona, S. Watzman, J. Heremans, W. Zhang, M.B. Jungfleisch, J.E. Pearson, A. Hoffmann and H.W. Schumacher (2014). "Round Robin Comparison of the Spin-seebeck Coefficient: Results and Outlook." Spin Caloritronics VI, Isree, Germany, July 14–18, 2014. (also see 2014-018-N0).

Vlaminck, V., H. Schultheiss, J.E. Pearson, F.Y. Fradin, S.D. Bader and A. Hoffmann (2013). "Mapping Microwave Field Distributions via the Spin Hall Effect." *Applied Physics Letters* **102**(19): 252406.*

Zhang, W., M.B. Jungfleisch, W. Jiang, J.E. Pearson, A. Hoffmann, F. Freimuth and Y. Mokrousov (2015). "Spin Hall Effects in Metallic Antiferromagnets." *Physical Review Letters* **113**(19): 196602.*

Zhang, W., V. Vlaminck, J.E. Pearson, R. Divan, S.D. Bader and A. Hoffmann (2014). "Determination of Pt Spin Diffusion Length by Spin-Pumping and Spin Hall Effect." *Applied Physics Letters* **103**(24): 242414.*

Zhang, W., V. Vlaminck, J.E. Pearson, R. Divan, S.D. Bader and A. Hoffmann (2014). "Determination of the Spin Diffusion Length via Spin Pumping and Spin Hall Effects." American Physical Society March Meeting, Denver, CO, Mar. 3–7, 2014. (also see 2014-018-N0).

Zhang, W., V. Vlaminck, J.E. Pearson, R. Divan, S.D. Bader and A. Hoffmann (2014). "Quantifying Spin Diffusion Lengths from Spin Pumping and Spin Hall Effects." Intermag 2014, Dresden, Germany, May 4–8, 2014. (also see 2014-018-N0).

2013-022-R1

Burgo, T.A. and A. Erdemir (2014). "Bipolar Tribocharging Signal During Friction Force Fluctuations at Metal-insulator Interfaces." *Angewandte Chemie* **53**(45): 12101–12105.*

De Lima Burgo, T., A. Erdemir, O. Eryilmaz and J.G. Ramirez Gonzalez (2014). "Tribocurrent-like Friction Force at a Metal-Insulator Interfaces." The 2014 Annual Meeting of the Electrostatistics Society of America, South Bend, IN, June 17–19, 2014.

Eryilmaz, O., G. Ramirez and A. Erdemir (2015). "Tribological Performance of Diamond Like Carbon and Nitride Based Coatings Against PTFE Based Composite Seal Materials in Oil Free Methane Environment." 42nd International Conference on Metallurgical Coatings and Thin Films (ICMCTF-2015), San Diego, CA, Apr. 20–24, 2015.

2013-035-R1

Pelton, M., D. Chakraborty, E. Malachosky, P. Guyot-Sionnest and J.E. Sader (2014). "Viscoelastic Flows in Simple Liquids Generated by Vibrating Nanostructures." *Physical Review Letters* **111**: 244502.*

2013-036-R1

Zhu, Y., Q. Zhang, P. Chen, Z. Cai, D.A. Walko, E.M. Dufresne, M. Highland, I.W. Jung, J.-U. Thiele, E.E. Fullerton, C. Adamo, D.G. Schlom, J. Wang, J.W. Freeland, P.G. Evans and H. Wen (2014). "Transient Grating-induced Phase Inhomogeneity in FeRh Studied by Time-resolved Hard X-ray Nanodiffraction." American Physical Society (APS) March Meeting, Denver, CO, Mar. 3–7, 2014.

Wen, H. (2013). "Correlation of Structural and Electronic Dynamics in Complex Oxides." Symposium of Complex Metal Oxides and Unconventional Interfaces, CINT User Conference, Santa Fe, NM, Sept. 24–26, 2013.

2013-063-R1

Chang, S., S.K. Selvaraj, Y.-Y. Choi, S. Hong, S.M. Nakhmanson and C.G. Takoudis (2014). "Atomic Layer Deposition of Tin-titanate as a Potential Ferroelectric Material." 14th International Conference on Atomic Layer Deposition, Kyoto, Japan, June 15–18, 2014.

**Indicates refereed publication*

Choi, Y.-Y., P. Sharma, C. Phatak, D.J. Gosztola, Y. Liu, J. Lee, J. Li, A. Gruverman, S.P. Ducharme and S. Hong. "Enhancement of Local Piezoresponse in Polymer Ferroelectrics via Nanoscale Control of Microstructure." *ACS Nano*.* (to be published).

Choi, Y.-Y., T.G. Yun, Q. Nadeem, H. Paik, H.S. Roh, J. Hong, S. Hong, S.M. Han and K. No. "Vertically Aligned P(VDF-TrFE) Core-shell Structures on Flexible Pillar Arrays." *Scientific Reports*.* (to be published).

Choi, Y., P. Sharma, C. Phatak, D.J. Gosztola, Y. Liu, J. Lee, J. Li, A. Gruverman, S.P. Ducharme and S. Hong (2014). "Enhancement of Local Piezoresponse in Polymer Ferroelectrics via Nanoscale Control of Microstructure." International Workshop on Nanoscale Spectroscopy and Nanotechnology, Chicago, IL, July 28–31, 2014.

Heinonen, O., D. Karpeyev, S. Gu, S.M. Nakhmanson, B. Lee and S. Hong (2013). "Real Space Formulation for Coupled Elastic Problems." CMCSN, Purdue University, West Lafayette, IN, Apr. 15–16, 2013.

Hong, S. (2015). "Functional Hybrid Materials Design Based on Nanoscale Visualization and Manipulation." 3rd International Symposium on Hybrid Materials and Processing, Busan, South Korea, Nov. 10–13, 2014.

Hong, S., Y. Choi, S. Tong, C.M. Phatak and A.K. Roelofs (2014). "Functional Materials Design Based on Nanoscale Visualization Using Atomic Force Microscopy." 2014 Piezoresponse Force Microscopy and Nanoscale Phenomena in Polar Materials, Ekaterinburg, Russia, July 14–17, 2014.

Hong, S., D. Kim, Y.Y. Choi, H.S. Roh and K. No (2014). "Proof of Principle Experiments for Piezoelectric Energy Harvesters." International Conference on Small Science 2013, Las Vegas, NV, Dec. 15–18, 2013.

Hong, S. (2014). "Visualization and Manipulation of Electric Polarization and Charges using Atomic Force Microscopy." 2014 Joint IEEE International Symposium on the Applications of Ferroelectric, International Workshop on Acoustic Transduction Materials and Devices & Workshop on Piezoresponse Force Microscopy (ISAF/IWATMD/PFM), State College, PA, May 12–16, 2014.

Hong, S. (2013). "Visualization and Manipulation of Electric Polarization and Charges using Atomic Force Microscopy." IEEE-Ultrasonics, Ferroelectrics, Frequency Control Society (UFFCS), European Frequence and Time Forum (EFTF), and PFM Symposium, Prague, Czech Republic, July 21–26, 2013.

Kim, Y., S. Hong, S. Oh, Y.-Y. Choi, H. Choi and K. No. "Influence of Alkaline Treatment on the Ferroelectric Properties of Poly(Vinylidene Fluoride Trifluoroethylene) Films." *Journal of Nanomaterials*.* (to be published).

Kim, D., H.S. Roh, Y. Kim, K. No and S. Hong (2015). "Selective Current Collecting Design for Spring-type Energy Harvesters." *RSC Advances* **5**(14): 10662–10666.*

Kim, Y., S. Hong, Y. Choi, J. Ryu and K. No (2013). "Characterization of Poly(Vinylidene Fluoride-trifluoroethylene) Films Fabricated by Electrophoretic Deposition." The 7th World Congress on Biomimetics, Artificial Muscles and Nano-Bio (BAMN2013), Jeju Island, South Korea, Aug. 26–30, 2013.

Kim, D., S. Hong, J. Hong, Y. Choi, J. Kim, M. Park, T. Sung and K. No (2013). "Fabrication of Vertically Aligned Ferroelectric Polyvinylidene Fluoride Mesoscale Rod Arrays." *Journal of Applied Polymer Science* **130**(6): 3842–3848.*

Kim, D., S. Hong, D. Li, H. Roh and K. No (2013). "Spring-type Piezoelectric Energy Harvester." The 7th World Congress on Biomimetics, Artificial Muscles and Nano-Bio (BAMN2013), Jeju Island, South Korea, Aug. 26–30, 2013.

Kim, D., S. Hong, D. Li, H.S. Roh, G. Ahn, J. Kim, M. Park, J. Hong, T.H. Sung and K. No (2013). "A Spring-type Piezoelectric Energy Harvester." *RSC Advances* **3**(10): 3194–3198.*

Kim, S., S. Hong, Y.Y. Choi and K. No (2013). "Effect of Nucleation Time on Bending Response of Ionic Polymer Metal Composite Actuators." *Electrochimica Acta* **108**: 547–553.*

Li, D., S. Hong, S. Gu, Y. Choi, S. Nakhmanson, O. Heinonen, D. Karpeev and K. No (2014). "Polymer Piezoelectric Energy Harvesters for Low Wind Speed." *Applied Physics Letters* **104**(1): 012902–012904.*

2013-070-R1

O'Brien, S.L., M.D. Whiteside, D.J. Sholto-Douglas, D.A. Antonopoulos, M.I. Boyanov, D.M. Durall, M. Jones, B. Lai, E.J. O'Loughlin and K.M. Kemner (2014). "Imaging Nutrient Uptake in Bacterial Biofilms Using Quantum Dots." 99th Ecological Society of America Annual Meeting, Sacramento, CA, Aug. 10–15, 2014.

**Indicates refereed publication*

O'Brien, S.L., M.D. Whiteside, D.J. Sholto-Douglas, D.A. Antonopoulos, M.I. Boyanov, D.M. Durall, M. Jones, B. Lai, E.J. O'Loughlin and K.M. Kemner (2014). "A Novel Nanoparticle Approach for Imaging Soil Bacteria." Synchrotron Environmental Science VI, Argonne National Laboratory, Sept. 11–12, 2014.

O'Brien, S.L., M.D. Whiteside, D.J. Sholto-Douglas, D.A. Antonopoulos, M.I. Boyanov, D.M. Durall, M. Jones, B. Lai, E.J. O'Loughlin and K.M. Kemner (2014). "A Novel Nanoparticle Approach for Imaging Soil Bacteria." Midwest Geobiology Symposium, Chicago, IL, Sept. 27, 2014.

2013-080-R1

Benson, B.A., P.A.R. Ade, Z. Ahmed, S.W. Allen, K. Arnold, J.E. Austermann, A.N. Bender, L.E. Bleem, J.E. Carlstrom, C.L. Chang, H.M. Cho, S.T. Ciocys, J.F. Cliche, T.M. Crawford, A. Cukierman, T. de Haan, M.A. Dobbs, D. Dutcher, W. Everett, A. Gilbert, N.W. Halverson, D. Hanson, N.L. Harrington, K. Hattori, J.W. Henning, G.C. Hilton, G.P. Holder, W.L. Holzapfel, K.D. Irwin, R. Keisler, L. Knox, D. Kubik, C.L. Kuo, A.T. Lee, E.M. Leitch, D. Li, M. McDonald, S.S. Meyer, J. Montgomery, M. Myers, T. Natoli, H. Nguyen, V. Novosad, S. Padin, Z. Pan, J. Pearson, C.L. Reichardt, J.E. Ruhl, B.R. Saliwanchik, G. Simard, G. Smecher, J.T. Sayre, E. Shirokoff, A.A. Stark, K. Story, A. Suzuki, K.L. Thompson, C. Tucker, K. Vanderlinde, J.D. Vieira, A. Vikhlinin, G. Wang, V. Yefremenko and K.W. Yoon (2014). "SPT-3G: A Next-Generation Cosmic Microwave Background Polarization Experiment on the South Pole Telescope." Proceedings of the SPIE—The International Society for Optical Engineering, Montreal, Quebec, Canada, July 23, 2014, **9153** (Millimeter, Submillimeter, and Far-infrared Detectors and Instrumentation for Astronomy VII).*

Chang, C.L., P.A.R. Ade, Z. Ahmed, S.W. Allen, K. Arnold, J.E. Austermann, A.N. Bender, L.E. Bleem, J.E. Carlstrom, S.T. Ciocys, J. Ding, V. Novosad, J. Pearson, G. Wang and V. Yefremenko (2015). "Low Loss Superconducting Microstrip Development at Argonne National Lab." *IEEE Transactions on Applied Superconductivity—ASC Special Issue* **PP**(99): 1.*

2013-096-R1

Gulotty, R., K.J. Perez Quintero, G.R.S. Iyer, D. Berman, A.A. Balandin and A.V. Sumant. "Direct Wafer-scale Synthesis of R-GO-like Carbon Films on Dielectric Substrates with Excellent Thermal and Electrical Conductivities and Optical Transmittance." *Nanoscale*.* (to be published).

Gulotty, R., S. Das, Y. Liu and A.V. Sumant (2015). "Effect of Hydrogen Flow During Cooling Phase to Achieve Uniform and Repeatable Growth of Bilayer Graphene on Copper Foils Over Large Area." *Carbon* **77**: 341–350.*

Gulotty, R., S. Das, Y. Liu and A.V. Sumant (2014). "Controlled, Repeatable, Fast CVD Growth of Uniform Single and Bilayer Graphene on Copper Foils Over Large Area." Materials Research Society (MRS) Spring Meeting, San Francisco, CA, Apr. 21–25, 2014.

Gulotty, R., S. Das, Y. Liu and A.V. Sumant (2014). "Controlled, Repeatable, Fast CVD Growth of Uniform Single and Bilayer Graphene on Copper Foils Over Large Area." New Diamond and Nano Carbons Conference, Chicago, IL, May 25–29, 2014.

Gulotty, R., S. Das, Y. Liu and A.V. Sumant (2014). "Effect of Hydrogen During Cooling-Phase to Achieve Continuous Growth of Bilayer Graphene on Copper." APS/CNM/EMC Users Meeting, Argonne, IL, May 12–15, 2014.

Gulotty, R., A.V. Sumant and C.-X. Wang (2014). "Robustness and Efficacy of Graphene Membranes for Accelerator Applications." New Diamond and Nano Carbons Conference, Chicago, IL, May 25–29, 2014.

Gulotty, R., R. Divan and A.V. Sumant (2013). "Synthesis and Fabrication of Large Area Low-Defect Density Graphene Membranes for Accelerator Applications." APS User Meeting, Argonne, IL, May 7, 2013.

2013-100-R1

McCarthy, R.F., M.S. Weimer, A.S. Hock and A.B.F. Martinson (2015). "Spatial and Chemical Control of Substitutional Intermediate Band Materials: Toward the Atomic Layer Deposition of $V_{0.25}In_{1.75}S_3$." Argonne National Laboratory Postdoctoral Research and Career Symposium, Argonne, IL, Oct. 23, 2014.

Indicates refereed publication

McCarthy, R.F., M.S. Weimer, M.J. Pellin, A.S. Hock and A.B.F. Martinson (2014). "Atomic Layer Deposition of In_2S_3 Via a Novel Indium Amidinate Precursor." Argonne National Laboratory Postdoctoral Research and Career Symposium, Argonne, IL, Oct. 10, 2013.

McCarthy, R.F., M.S. Weimer, A.S. Hock and A.B.F. Martinson (2014). "Chemical and Spatial Control of Substitutional Intermediate Band Materials: Toward the Atomic Layer Deposition of $V_{0.25}In_{1.75}S_3$." Proceedings of the 40th IEEE Photovoltaic Specialists Conference, Denver, CO, June 8–13, 2014: 250–253.*

McCarthy, R.F., M.S. Weimer, A.S. Hock and A.B.F. Martinson (2014). "Chemical and Spatial Control of Substitutional Intermediate Band Materials: Toward the Atomic Layer Deposition of $V_{0.25}In_{1.75}S_3$." 40th IEEE Photovoltaic Specialists Conference (PVSC), Denver, CO, June 8–13, 2014.

McCarthy, R.F., M.S. Weimer, J.D. Emery, A.S. Hock and A.B.F. Martinson (2014). "Oxygen-free Atomic Layer Deposition of Indium Sulfide." *ACS Applied Materials & Interfaces* **6**(15): 12137–12145.*

2013-116-R1

Mo, K., D. Yun, W. Mohamed, M. Pellin, J. Almer and A.M. Yacout (2014). "Synchrotron Radiation Study on Steam Oxidation Behavior of Zircaloy-2 with Advanced Coatings." Proceedings of the Nuclear Fuels and Structural Materials for the Next Generation Nuclear Reactors (NFSM) 2014 American Nuclear Society Annual Meeting, Reno, NV, June 15–19, 2014.*

Mohamed, W., D. Yun, K. Mo, M.J. Pellin, M.C. Billone, J. Almer and A.M. Yacout (2015). "Depth Profile of Oxide Volume Fractions of Zircaloy-2 in High-temperature Steam: An *in situ* Synchrotron Radiation Study." *Journal of Nuclear Materials* **454**(1–3): 192–199.*

Yacout, A.M., M. Pellin and M.C. Billone (2013). "Development and Testing of Nanolaminate Coatings for Conventional LWR Cladding." Proceedings of the LWR Fuel Performance Meeting/Top Fuel 2013, Charlotte, NC, Sept. 15–19, 2013: 847.*

Ye, B., S. Bhattacharya, K. Mo, D. Yun, W. Mohamed, M. Pellin, J. Fortner, Y.S. Kim, G. Hofman and A. Yacout (2014). "80 MeV Xe Irradiation on U-Mo/Al Dispersion Fuel." 19th International Conference on Ion Beam Modification of Materials, Leuven, Belgium, Sept. 14–19, 2014.

Ye, B., Y.S. Kim, G. Hofman, A. Yacout, S. Bhattcharya, K. Mo, D. Yun, W. Mohamed, M. Pellin and J. Fortner (2015). "Xe Irradiation on ZrN-Coated U-Mo/Al Dispersion Fuel." RERTR 2014, Vienna, Austria, Oct. 12–15, 2014.

Yun, D., K. Mo, R. Xu, W. Mohamed, B. Ye, M.J. Pellin and A.M. Yacout (2014). "Characterization of High Energy Xe Ion Irradiation Effects in Single Crystal Molybdenum with Depth Resolved Synchrotron Microbeam Diffraction." Proceedings of the Nuclear Fuels and Structural Materials for the Next Generation Nuclear Reactors (NFSM) 2014 American Nuclear Society Annual Meeting, Reno, NV, June 15–19, 2014.*

Yun, D., K. Mo, R. Xu, W. Mohamed, B. Ye, M.J. Pellin and A.M. Yacout (2014). "Characterization of High Energy Xe Ion Damage in U-10Mo Metallic Alloy Fuel with Depth Resolved Synchrotron Microbeam Diffraction." Proceedings of the Nuclear Fuels and Structural Materials for the Next Generation Nuclear Reactors (NFSM) 2014 American Nuclear Society Annual Meeting, Reno, NV, June 15–19, 2014.*

Yun, D., W. Mohamed, B. Ye, M. Kirk, P. Baldo and A. Yacout. "*In situ* TEM and Synchrotron Characterization of U-10Mo Thin Specimen Annealed at the Fast Reactor Temperature Regime." *Metallurgical and Materials Transaction A*.* (to be published).

Yun, D., K. Mo, W. Mohamed, M.J. Pellin and A.M. Yacout (2015). "Irradiation Behavior Study of U-Mo/Al Dispersion Fuel with High Energy Xe." NuMat Conference 2014, Clearwater, FL, Oct. 27–30, 2014.

Yun, D., K. Mo, W. Mohamed, M.J. Pellin and A.M. Yacout (2015). "Modeling Beam Heating and Sample Temperature by High Energy Heavy Ion Irradiation, and Comparison with Experimental Measurements." NuMat Conference 2014, Clearwater, FL, Oct. 27–30, 2014.

Yun, D., W. Mohamed, B. Ye, M. Kirk, P. Baldo and A. Yacout (2013). "Preliminary Assessment of Microstructural Evolution of U-10Mo Thin Specimen Annealed at Typical Fast Reactor Temperature Regime." 2014 American Nuclear Society Annual Meeting, Atlanta, GA, June 16–20, 2013.

**Indicates refereed publication*

Yun, D., J. Wright, J. Terry, K. Mo, R. Xu, W. Mohamed, B. Yei, K. Logan, M. Pellin and A. Yacout (2015). "Study of Xe Ion Beam Irradiated Mo Single Crystal by Synchrotron Extended X-ray Absorption Fine Structure and Microdiffraction." NuMat Conference 2014, Clearwater, FL, Oct. 27–30, 2014.

2014-018-N0

Heinonen, O. (2014). "Resonant Dynamics of Topological Magnetic Structures." American Physical Society March Meeting, Denver, CO, Mar. 3–7, 2014.

Hoffmann, A. (2014). "Connecting Spin Waves to Charge Currents." International Workshop on Nanoscale Spectroscopy and Nanotechnology 8, Chicago, IL, July 28–31, 2014. (also see 2013-016-R1).

Hoffmann, A., H. Schultheiss, S. Vogt, S. Jain, F.Y. Fradin, S. Bader, Z. Wang, Y. Sun, Y.-T. Song, M. Wu, T. Sebastian and B. Hillebrands (2014). "Electric Control and Detection of Spin Waves." Concepts in Spintronics, Santa Barbara, CA, Sept. 30–Oct. 4, 2013. (also see 2013-016-R1).

Hoffmann, A., W. Zhang, V. Vlaminck, J.E. Pearson, S.D. Bader, R. Divan, L. Bai, P. Hyde, Y. Gui and C.-M. Hu (2014). "Insight About Spin Hall Effects from Spin Pumping." SPIE NanoScience+Engineering, San Diego, CA, Aug. 17–24, 2014. (also see 2013-016-R1).

Hoffmann, A. (2014). "Magnetization Dynamics in Nanometer-thick Yttrium Iron Garnet Films." Workshop on Oxide Materials: Nanoscale Spectroscopy and Nanotechnology, Cali, Columbia, Sept. 15–19, 2014. (also see 2013-016-R1).

Hoffmann, A. (2014). "Reduction of Spin Hall Effects due to Magnetic Proximity." Spin Caloritronics VI, Isree, Germany, July 14–18, 2014. (also see 2013-016-R1).

Jungfleisch, M.B., W. Zhang, W. Jiang, H. Chang, J. Sklenar, S.M. Wu, J.E. Pearson, A. Bhattacharya, J.B. Ketterson, M. Wu and A. Hoffmann. "Spin Waves in Micro-structured Yttrium Iron Garnet Nanometer-thick Films." *Journal of Applied Physics*.* (to be published).

Sola, A., M. Kueoferling, V. Basso, S. Zullino, E. Olivetti, M. Pasquale, T. Kikkawa, K. Uchida, E. Saitoh, D. Meier, T. Kuschel, G. Reiss, H. Jin, S. Boona, S. Watzman, J. Heremans, W. Zhang, M. B. Jungfleisch, J.E. Pearson, A. Hoffmann and H.W. Schumacher (2014). "Round Robin Comparison of the Spin-seebeck Coefficient: Results and Outlook." Spin Caloritronics VI, Isree, Germany, July 14–18, 2014. (also see 2013-016-R1).

Zhang, W., V. Vlaminck, J.E. Pearson, R. Divan, S.D. Bader and A. Hoffmann (2014). "Determination of the Spin Diffusion Length via Spin Pumping and Spin Hall Effects." American Physical Society March Meeting, Denver, CO, Mar. 3–7, 2014. (also see 2013-016-R1).

Zhang, W., V. Vlaminck, J.E. Pearson, R. Divan, S.D. Bader and A. Hoffmann (2014). "Quantifying Spin Diffusion Lengths from Spin Pumping and Spin Hall Effects." InterMag 2014, Dresden, Germany, May 4–8, 2014. (also see 2013-016-R1).

2014-019-N0

Van Engelen, A., S. Bhattacharya, N. Sehgal, G.P. Holder, O. Zahn and D. Nagai. "CMB Lensing Power Spectrum Biases from Galaxies and Clusters Using High-Angular Resolution Temperature Maps." *Astrophysical Journal* **786**(1): 13.* (to be published).

2014-023-N0

Dharmapalan, R. and J.M. Paley (2014). "LArLArPD: Large Area Picosecond Photodetector (LAPPD) in Liquid Argon (LAr)." Liquid Argon TPC R&D Workshop (LArTPC14), Fermi National Accelerator Laboratory, Batavia, IL, July 8–9, 2014.

2014-051-N0

Liu, D.-J. (2014). "Improving Non-PGM Catalyst Performance through Rationally Designed PEMFC Cathode Architectures." 2014 Gordon Research Conference for Fuel Cell, Bryant University, Smithfield, RI, Aug. 3–8, 2014.

**Indicates refereed publication*

Zhao, D., J.L. Shui, L.R. Grabstanowicz, C. Chen, S.M. Commet, T. Xu, J. Lu and D.J. Liu (2014). "Highly Efficient Non-precious Metal Electrocatalysts Prepared from One-pot Synthesized Zeolitic Imidazolate Frameworks (ZIFs)." *Advanced Materials* **26**(7): 1093–1097.*

Zhao, D., J.-L. Shui, L.R. Grabstanowicz and D.-J. Liu (2015). "A Versatile Preparation of Highly Active ZIF-based Non-PGM Catalysts through Solid State Synthesis." the 226th Meeting of the Electrochemical Society, Cancun, Mexico, Oct. 5–10, 2014.

2014-054-N0

Jiang, W., P. Upadhyaya, W. Zhang, G. Yu, M.B. Jungfleisch, F.Y. Fradin, J.E. Pearson, Y. Tserkovnyak, K.L. Wang, O. Heinonen, S.G.E. te Velthuis and A. Hoffmann. "Blowing Magnetic Skyrmion Bubbles." *Science*.* (to be published).

Hoffmann, A. (2014). "Magnetic Skyrmions in Metals and Insulators." Workshop on Oxide Materials: Nanoscale Spectroscopy and Nanotechnology, Cali, Colombia, Sept. 15–19, 2014.

2014-077-N0

Lee, J., S. Narayanan, X.-M. Lin and A.R. Sandy (2015). "Rheological Behavior of silica Nanoparticles Measured by Small Angle X-ray Scattering." 2014 Society of Rheology (SOR) Annual Meeting, Philadelphia, PA, Oct. 5–9, 2014.

2014-084-N0

Feng, Y., A. Ito, B. Lai, A. Lango and E. Ingall (2014). "Bio-availability of Iron Inputs to the Ocean Driven by Aerosol Chemistry in Dust." DOE 2014 Climate Modeling Principal Investigator (PI) Meeting 2014, Potomac, MD, May 12–15, 2014.

Feng, Y., A. Lango, B. Lai, E. Ingall and Y. Gao (2014). "Characterization of Dust Deposition and Mineralogy Export to the Southern Ocean." Workshop on Clouds, Aerosols, Radiation and Air-Sea Interface of the Southern Ocean: Establishing Directions for Future Research, University of Washington, Seattle, WA, Mar. 18–19, 2014.

2014-095-N0

DeGottardi, W. (2014). "Topological Insulating Phases of Non-Abelian Anyonic Chains." *Physical Review B* **90**(7): 075129.*

2014-108-N0

Michalska, K., A. Steen, G. Chhor, K.M. Fayman, M. Endres, G. Babnigg, K. Lloyd, R. Jedrzejczak and A. Joachimiak (2014). "Discovery of Proteins from 'Microbial Dark Matter'." NIH Structural Biology Horizons Workshop, Bethesda, MD, Dec. 9–10, 2013.

Michalska, K., A. Steen, G. Chhor, K.M. Fayman, M. Endres, G. Babnigg, K. Lloyd, R. Jedrzejczak and A. Joachimiak (2014). "Structural Genomics of Sedimentary Archaea in Postgenomic Era." DOE Joint Genome Institute 9th Annual Genomics of Energy & Environment Meeting, Walnut Creek, CA, Mar. 18–20, 2014.

Michalska, K., A. Steen, G. Chhor, K. Fayman, M. Endres, G. Babnigg, K. Lloyd, R. Jedrzejczak and A. Joachimiak (2014). "Structure and Specificity of Novel Aminopeptidase from Marine Sediment Archaea." 23rd Congress and General Assembly of the International Union of Crystallography, Montreal, Quebec, Canada, Aug. 5–13, 2014.

Steen, A., K. Michalska, G. Chhor, M. Endres, J. Vazin, K. Lloyd, S.W. Wilhelm and A. Joachimiak (2014). "Strategies to Assess the Biochemical Properties of Extracellular Hydrolases in Aquatic Environments." Goldschmidt 2014 Conference, Sacramento, CA, June 8–13, 2014.

Indicates refereed publication

Advanced Computing

2011-213-R3

Deb, S., A. Morandi, K. Pedersen, S. Riemer-Sorensen, D.M. Goldberg and H. Dahle. "Mass Reconstruction Using Particle Based Lensing II Quantifying Substructure with Strong Weak Lensing and X-rays." *Astrophysical Journal*.* (to be published).

Habib, S., V. Morozov, H. Finkel, A. Pope, K. Heitmann, K. Kumaran, T. Peterka, J. Insley, D. Daniel, P. Fasel, N. Frontiere and Z. Lukic (2012). "The Universe at Extreme Scale: Multi-petaflop Sky Simulation on the BG/Q." Supercomputing 12, Salt Lake City, UT, Nov. 10–15, 2012.

Heitmann, K., E. Lawrence, J. Kwan, S. Habib and D. Higdon (2014). "The Coyote Universe Extended: Precision Emulation of the Matter Power Spectrum." *Astrophysical Journal* **780**(1).*

Kwan, J., S. Bhattacharya, K. Heitmann and S. Habib (2013). "Cosmic Emulation: The Concentration-Mass Relation for Wcdm Universes." *Astrophysical Journal* **768**(2).*

Kwan, J., G.F. Lewis and E.V. Linder (2012). "Mapping Growth and Gravity with Robust Redshift Space Distortions." *Astrophysical Journal* **748**(78).*

Shandarin, S., S. Habib and K. Heitmann (2012). "The Cosmic Web, Multi Stream Flows, and Tessellations." *Physical Review D* **85**(8): 083005.*

Upadhye, A., R. Biswas, A. Pope, K. Heitmann, S. Habib, H. Finkel and N. Frontiere (2014). "Large-Scale Structure Formation with Massive Neutrinos and Dynamical Dark Energy." *Physical Review D* **89**(10).*

2011-214-R3

Catlett, C. (2014). "The City of Chicago Technology Plan." Chicago Architecture Foundation, Chicago, IL, June 4, 2014.

Catlett, C. (2014). "Computational Science and Urban Policy." ACM Knowledge Discovery and Data Conference/Urban Computing Workshop, New York, NY, Aug. 24, 2014. (also see 2013-206-R1).

Catlett, C. (2014). "Computational Science and Urban Policy." Annual Meeting of the Coalition for Academic Scientific Computation (CASC), Arlington, VA, Sept. 19, 2014. (also see 2013-206-R1).

Catlett, C. (2014). "Computational Urban Sciences." NCSA Blue Waters Symposium, Urbana, IL, May 13, 2014. (also see 2013-206-R1).

Catlett, C. (2014). "Toward an 'Urban Science'." Urban Sciences Briefing, Washington, DC, July 21, 2014. (also see 2013-206-R1).

Catlett, C. (2014). "Urban Data Science." Big Data and Health Panel (University of Chicago CHESS Conference), Chicago, IL, May 9, 2014. (also see 2013-206-R1).

Catlett, C. (2014). "Urban Science." Symposium on High Performance Computing 2014, Cetraro, Italy, July 11, 2014.

Catlett, C. (2014). "Urban Sciences: Computation and Data Analytics." University of Chicago Urban Imprint, San Francisco, CA, May 14, 2014.

Catlett, C. (2013). "Computation Urban Sciences: Emerging Opportunities." 2nd ACM SIGKDD International Workshop on Urban Computing (UrbComp 2013), ACM-KDD, Chicago, IL, Aug. 11, 2013. (also see 2013-206-R1).

Catlett, C. (2013). "Data Complexity in the Sciences: The Computation Institute." 2013 National Big Data Week, Chicago, IL, Apr. 24, 2013. (also see 2013-206-R1).

Catlett, C. (2013). "Opportunities for Data and Computational Sciences in Present and Future Cities." NCSA 2nd Annual CHANGES Workshop, Chicago, IL, Sept. 10, 2013. (also see 2013-206-R1).

Catlett, C. (2013). "Urban Center for Computation and Data." 2013 Workshop: How Far Can 'Big Data' Take Us Towards Understanding Cities?, Santa Fe, NM, Sept. 20, 2013. (also see 2013-206-R1).

**Indicates refereed publication*

Catlett, C. (2013). "Urban Sciences: Opportunities for High Performance Computing Research." 8th IEEE Conference on eScience, Chicago, IL, Oct. 3, 2012.

Catlett, C. (2013). "Urban Sciences in Chicago." Exploratory Workshop on Energy Policy and Computational Urban Sciences, 8th IEEE Conference on eScience, The University of Chicago Beijing Center, Beijing, China, Jan. 30, 2013. (also see 2013-206-R1).

Catlett, C. (2013). "Urban Sciences in Chicago." Mayor's Innovation Project, Chicago, IL, Aug. 15, 2013. (also see 2013-206-R1).

Catlett, C. (2013). "Urban Security and Risk Management." 14th International Latin American Smart Cities Conference, Quito, Ecuador, Sept. 26, 2013. (also see 2013-206-R1).

Catlett, C. (2013). "Urban Sensing in Chicago." 2013 Workshop on Urban Sensing, Argonne, IL, Aug. 27, 2013. (also see 2013-206-R1).

Catlett, C. (2012). "Importance of Standard Data Exchange and Cyber Security in Smart Cities." International Smart City Workshop: CitiProtocol, Barcelona, Spain, July 17, 2012.

Catlett, C. (2011). "Pervasive Computing and Privacy Research at Argonne National Laboratory." ECE Weekly Colloquium, Illinois Institute of Technology, Chicago, IL, Sept. 30, 2011.

Sankaran, R. and C. Catlett (2012). "Mobile Device and Sensor Work in Chicago." Korea Institute of Energy Technology Evaluation and Planning (KETEP) Workshop on International Collaborative Energy Research & Development Program, Jeju, South Korea, Aug. 30–31, 2012.

Sankaran, R. (2012). "Mobile Device and Sensor Work in Chicago." ETRI USN Meeting, Daejon, South Korea, Aug. 29–31, 2012.

2012-114-R2

Fu, J., M. Min, R. Latham and C.D. Carothers (2013). "Parallel I/O Optimizations for a Massively Parallel Electromagnetic System." SIAM Conference on Computational Science and Engineering, Boston, MA, Feb. 25–Mar. 1, 2013.

Fu, J., R. Latham, M. Min and C. Carothers (2012). "I/O Threads to Reduce Checkpoint Blocking for an Electromagnetics Solver on Blue Gene/P and Cray XK6." Proceedings of the 2nd International Workshop on Runtime and Operating Systems for Supercomputers (ROSS 2012), Venice, Italy, June 29, 2012, ACM, New York, NY, **Article No. 2**.*

Fu, J., M. Min, R. Latham and C. Carothers (2012). "Threading I/O Strategy for Checkpoint/Restart of a Massively Parallel Electromagnetic System." SIAM PP12, Savannah, GA, Feb. 15–17, 2012.

He, Y., M. Min and D. Nicholls. "Spectral Element Method with a Transparent Boundary Operator for Quasi-Periodic Helmholtz Solutions on Rough Structures." *Journal Computational Physics*.* (to be published).

Mametjanov, A., M. Min and B. Norris (2013). "Accelerating Performance of a Petascale Electromagnetic Solver NekCEM with MPI+CUDA." SIAM Conference on Computational Science and Engineering, Boston, MA, Feb. 25–Mar. 1, 2013.

Min, M.S. and P. Fischer (2014). "An Efficient High-Order Time Integration Method for Spectral-Element Discontinuous Galerkin Simulations in Electromagnetics." *Journal of Scientific Computing* **57**(3): 582–603.*

Min, M. (2014). "Hydraulic Modeling for Quantum Absorption Calculation in Plasmonics Based on High-order Spectral Element Discontinuous Galerkin Approach." SIAM Annual Meeting, Chicago, IL, July 7–11, 2014.

Min, M. (2014). "NekCEM: Recent Developments for Electromagnetic Systems Including Drift-diffusion and Quantum Models." Nek5000 Users Meeting, Thessaloniki, Greece, Aug. 21, 2014.

Min, M. (2013). "Exponential Time Integration Methods for Wave-Dominated Problems." AMMCS-2013 Conference, Waterloo, Ontario, Canada, Aug. 26–30, 2013.

Min, M. (2013). "High-order DG Methods: Scalable Algorithms and Performance for Electromagnetics Applications." FEMTEC 2013, the 4th International Congress on Computational Engineering and Sciences, Las Vegas, NV, May 19–24, 2013.

Min, M., J. Fu, A. Mametjanov, H. He and P. Fischer (2013). "Scalable Electromagnetic Solver for Applications in Nanoscale Materials." SIAM Conference on Computational Science and Engineering, Boston, MA, Feb. 25–Mar. 1, 2013.

Indicates refereed publication

Min, M. (2013). "Recent Development on NekCEM/NekLBM Codes for Electromagnetics and Fluids." Second Nek5000 Users Meeting, Zurich, Switzerland, Dec. 8–9, 2012.

Min, M., J. Fu and A. Mametjanov (2012). "Hybrid Programming and Performance for Beam Propagation Modeling." The 11th International Computational Accelerator Physics Conference (ICAP), Rostock-Warnemünde, Germany, Aug. 19–24, 2012.

Min, M., J. Fu and A. Mametjanov (2012). "Hybrid Programming and Performance for Beam Propagation Modeling." Proceedings of the 11th International Computational Accelerator Physics Conference (ICAP2012), FRSAC1, Rostock-Warnemünde, Germany, Aug. 19–24, 2012, *Darmstadt GSI*: 284–286.*

Min, M. and J. Fu (2012). "Massively Parallel, Scalable Algorithms and Softwares for Scientific Computing." 15th SIAM Conference on Parallel Processing for Scientific Computing, Savannah, GA, Feb. 15–17, 2012.

Teng, C., M. Min and J. Wang. "Pseudospectral and Runge-Kutta-Nyström Methods for Second-order Wave Equations: Stable and Accurate Boundary Treatments." *Journal Computational Physics*.* (to be published).

2012-202-R2

Balaprakash, P., D. Buntinas, A. Chan, A. Guha, R. Gupta, S.H.K. Narayanan, A.A. Chien, P. Hovland and B. Norris (2013). "Exascale Workload Characterization and Architecture Implications." 24th International Symposium on Computer Architecture and High Performance Computing (SBAC-PAD 2012), New York, NY, Oct. 24–26, 2012.

Balaprakash, P., D. Buntinas, A. Chan, A. Guha, R. Gupta, S.H.K. Narayanan, A.A. Chien, P. Hovland and B. Norris (2013). "Exascale Workload Characterization and Architecture Implications." 21st High Performance Computing Symposium, 2013 SCS Spring Simulation Multi-Conference (SpringSim'13), San Diego, CA, Apr. 7–10, 2013.

Balaprakash, P., D. Buntinas, A. Chan, A. Guha, R. Gupta, S.H.K. Narayanan, A.A. Chien, P. Hovland and B. Norris (2013). "Exascale Workload Characterization and Architecture Implications." Proceedings of the High Performance Computing Symposium (HPC'13), SCS Spring Simulation Multi-Conference (SpringSim'13), San Diego, CA, Apr. 7–10, 2013, Society for Computer Simulation International, Article 5.

Chien, A. (2012). "Translation Architecture Opportunities." DOE Exascale Research Meeting, Portland, OR, Apr. 17, 2012.

Chien, A. (2012). "Can We Systematically Evaluate and Exploit Heterogenous Accelerators? A 10×10 Perspective." 2012 Symposium on Advanced Accelerators for Height Performance Computing (SAAHPC'12), Argonne National Laboratory, Argonne, IL, July 10–11, 2012.

Gupta, R., P. Balaprakash, D. Buntinas, A. Chan, A. Guha, S.H.K. Narayanan, A.A. Chien, P. Hovland and B. Norris (2013). "An Exascale Workload Study." SC12, Salt Lake City, UT, Nov. 12–16, 2012.

Zhang, J., M. Sinclair II and A. Chien (2013). "Improving Performance Portability in OpenCL Programs." IEEE International Supercomputing Conference (ISC), Liepzig, Germany, June 16–20, 2013.

Zhang, J., M. Sinclair II and A. Chien (2013). "Improving Performance Portability in OpenCL Programs." Proceedings of the 28th International Supercomputing Conference (ISC 2013), Liepzig, Germany, June 16–20, 2013, *Springer Berlin Heidelberg* **7905**(7905): 136–150.*

2013-199-R1

Vázquez-Mayagoitia, A., J.R. Hammond, R.J. Harrison and W.S. Thornton. "Quantum Chemistry Methods with Multiwavelet Bases on Massive Parallel Computers." Annual Reports in Computational Chemistry, Elsevier. **10:** Chapter 1.* (to be published).

Vázquez-Mayagoitia, A. and J.R. Hammond (2013). "DFT and TD-DFT Using Multiresolution Multiwavelet Basis Sets on Petaflop Supercomputers." 15th International Conference on Density Functional Theory and Its Applications (DFT 2013), Durham University, Durham, United Kingdom, Sept. 9–13, 2013.

Indicates refereed publication

2013-206-R1

Catlett, C. (2015). “Creating Integrated Computation and Mathematical Capabilities to Transform the Design, Planning, and Operation of Cities to Achieve Sustainability and Resilience.” Urban Imprint: The Art and Science Shaping Our Cities, Chicago, IL, Nov. 14, 2014.

Catlett, C. (2014). “Computational Science and Urban Policy.” the 20th ACM SIGKDD Conference on Knowledge Discovery and Data Mining, New York, NY, Aug. 24–27, 2014. (also see 2011-214-R3).

Catlett, C. (2014). “Computational Science and Urban Policy.” 2014 Coalition for Academic Scientific Computation Fall Meeting, Arlington, VA, Sept. 17–19, 2014. (also see 2011-214-R3).

Catlett, C. (2014). “Computational Urban Sciences.” NCSA Blue Waters Symposium for Petascale Science and Beyond, Champaign, IL, May 12–15, 2014. (also see 2011-214-R3).

Catlett, C. (2014). “Open Data, Big Computation, and a New Era for Urban Research.” American Association for the Advancement of Science Annual Meeting (AAAS 2014), Chicago, IL, Feb. 7–13, 2014.

Catlett, C. (2014). “Rapid Urbanization in Developing Economies.” Committee on National Statistics, Washington, D.C., Feb. 6, 2014.

Catlett, C. (2014). “Science for Cities.” 7th World Urban Forum: Urban Equity in Development—Cities for Life, Medellin, CO, Apr. 5–11, 2014.

Catlett, C. (2014). “Toward an “Urban Science.” Science and Big Data to Improve Urban Planning, Design, and Policy, Washington, D.C., July 21, 2014. (also see 2011-214-R3).

Catlett, C. (2014). “Urban Data Sciences.” 2014 Big Data and Health, Chicago, IL May 9, 2014. (also see 2011-214-R3).

Catlett, C. (2014). “Urban Imprint: The Art and Science Shaping Our Cities.” Alumni Club of the Bay Area Webcast, San Francisco, CA, May 14, 2014.

Catlett, C. (2014). “Urban Science.” International Advanced Research Workshop on High Performance Computing: From Clouds and Big Data to Exascale and Beyond, Centraro, Italy, July 7–11, 2014.

Catlett, C. (2013). “Big Data and Urban Social Sciences.” ORDCamp, Chicago, IL, Jan. 26, 2013.

Catlett, C. (2013). “Computation Urban Sciences: Emerging Opportunities.” 2nd ACM SIGKDD International Workshop on Urban Computing (UrbComp 2013), ACM-KDD, Chicago, IL, Aug. 11, 2013. (also see 2011-214-R3).

Catlett, C. (2013). “Computational Opportunities in Urban Sciences.” IEEE eScience Conference, Chicago, IL, Oct. 3, 2012.

Catlett, C. (2013). “Data Complexity in the Sciences: The Computation Institute.” 2013 National Big Data Week, Chicago, IL, Apr. 24, 2013. (also see 2011-214-R3).

Catlett, C. (2013). “Interdisciplinary Urban Sciences.” Kickoff Workshop of Urban Sciences Research Coordination Network, Chicago, IL, Feb. 15, 2013.

Catlett, C. (2013). “Opportunities for Data and Computational Sciences in Present and Future Cities.” NCSA 2nd Annual Changes Workshop, Chicago, IL, Sept. 10, 2013. (also see 2011-214-R3).

Catlett, C. (2013). “Urban Center for Computation and Data.” 2013 Workshop: How Far Can “Big Data” Take Us Towards Understanding Cities?, Santa Fe, NM, Sept. 20, 2013. (also see 2011-214-R3).

Catlett, C. (2013). “Urban Sciences in Chicago.” Exploratory Workshop on Energy Policy and Computational Urban Sciences, 8th IEEE Conference on eScience, The University of Chicago Beijing Center, Beijing, China, Jan. 30, 2013. (also see 2011-214-R3).

Catlett, C. (2013). “Urban Sciences in Chicago.” Mayor’s Innovation Project, Chicago, IL, Aug. 15, 2013. (also see 2011-214-R3).

Catlett, C. (2013). “Urban Sciences in Chicago.” Chicago Harris Public Policy Lecture Series, University Club of Chicago, Chicago, IL, Sept. 18, 2013.

Catlett, C. (2013). “Urban Security and Risk Management.” 14th International Latin American Smart Cities Conference, Quito, Ecuador, Sept. 26, 2013. (also see 2011-214-R3).

Indicates refereed publication

Catlett, C. (2013). "Urban Sensing in Chicago." 2013 Workshop on Urban Sensing, Argonne, IL, Aug. 27, 2013. (also see 2011-214-R3).

2013-208-R1

Devoid, S., N. Desai and L. Hochstein (2014). "Poncho: Enabling Smart Administration of Full Private Clouds." Proceedings of the 27th Large Installation System Administration (LISA) Conference, Washington, D.C., Nov. 3–8, 2013, *USENIX Association*: 17–26.*

2013-212-R1

Arsenault, L.F., A. Lopez-Bezanilla, O.A. von Lilienfeld and A.J. Millis (2015). "Machine Learning for Many-body Physics: The Case of the Anderson Impurity Model." *Physical Review B* **90**(15).*

Lopez-Bezanilla, A. and O.A. von Lilienfeld (2014). "Modeling Electronic Quantum Transport with Machine Learning." *Physical Review B* **89**(23).*

Montavon, G., K. Hansen, S. Fazli, M. Rupp, F. Biegler, A. Ziehe, A. Tkatchenko, O.A. von Lilienfeld and K.-R. Müller (2013). "Learning Invariant Representations of Molecules for Atomization Energy Prediction." Proceedings of the Advances in Neural Information Processing Systems (NIPS 2012), Lake Tahoe, NV, Dec. 3–6, 2012, **25**: 449–457.*

Montavon, G., M. Rupp, V. Gobre, A. Vazquez-Mayagoitia, K. Hansen, A. Tkatchenko, K.R. Muller and O. A. von Lilienfeld (2013). "Machine Learning of Molecular Electronic Properties in Chemical Compound Space." *New Journal of Physics* **15**.*

Ramakrishnan, R., P.O. Dral, M. Rupp and O.A. von Lilienfeld (2014). "Quantum Chemistry Structures and Properties of 134 Kilo Molecules." *Scientific Data* **1**: 140022.*

von Lilienfeld, O.A. (2015). "Alchemy and Machine Learning Methods for The Sampling of Chemical Space from First Principles." the 10th Congress of the World Association of Theoretical and Computational Chemists (WATOC 2014), Santiago, Chile, Oct. 5–10, 2014.

von Lilienfeld, O.A. (2013). "First Principles View on Chemical Compound Space: Gaining Rigorous Atomistic Control of Molecular Properties." *International Journal of Quantum Chemistry* **113**(12): 1676–1689.*

2013-213-R1

Boyer, M., J. Meng and K. Kumaran (2013). "Improving GPU Performance Prediction with Data Transfer Modeling." Proceedings of the 3rd International Workshop on Accelerators and Hybrid Exascale Systems (AsHES), Boston, MA, May 20, 2013: 1097–1106.*

Guo, J., J. Meng, Q. Yi, V. Morozov and K. Kumaran (2014). "Analytically Modeling Application Execution for Software-Hardware Co-design " Proceedings of the 2014 IEEE 28th International Parallel & Distributed Processing Symposium (IPDPS), Phoenix, AZ, May 19–23, 2014, *IEEE*: 468–477.*

Joohwan, L., J. Meng and H. Kim (2014). "SESH Framework: A Space Exploration Framework for GPU Application and Hardware Codesign." Proceedings of the 4th International Workshop on Performance Modeling, Benchmarking and Simulation of High Performance Computer Systems (PMBS13) and Supercomputing Conference (SC), Denver, CO, Nov. 17–22, 2013.*

Meng, J., T. Uram, V.A. Morozov, V. Vishwanath and K. Kumaran (2014). "Modeling Cooperative Threads to Project GPU Performance for Adaptive Parallelism." ALCF Technical Report, June 9–11, 2014.

Meng, J., X. Wu, V.A. Morozov, V. Vishwanath, K. Kumaran, V. Taylor and C.W. Lee (2014). "SKOPE: A Framework for Modeling and Exploring Workload Behavior." Proceedings of the 11th Association for Computer Machinery (ACM) Conference on Computing Frontiers (CF), Cagliari, Italy, May 20–22, 2014, *ACM New York, NY* (Article 6).*

Meng, J., V. Morozov, V. Vishwanath and K. Kumaran (2013). "Dataflow-Driven GPU Performance Projection for Multi-Kernel Transformations." Proceedings of the International Conference for High Performance Computing, Networking, Storage, and Analysis (SC 2012), Salt Lake City, UT, Nov. 10–16, 2012, (82).*

**Indicates refereed publication*

Morozov, V., J. Meng, V. Vishwanath, K. Kumaran and M.E. Papka (2013). "Characterization and Understanding Machine-Specific Interconnect." Proceedings of the 12th International Conference on Parallel Computing Technologies (PaCT 2013), St. Petersburg, Russia, Sept. 30–Oct. 4, 2013, *Lecture Notes in Computer Science* **7979**(2013): 90–104.*

Morozov, V., V. Vishwanath, K. Kumaran, J. Meng and M.E. Papka (2013). "Early Experience on the Blue Gene/Q Supercomputing System." Proceedings of the 27th IEEE International Parallel & Distributed Processing Symposium (IPDPS 2013), Boston, MA, May 20–24, 2013: 1229–1240.*

Panwar, L.S., A.M. Aji, J. Meng, P. Balaji and W. Feng (2014). "Online Performance Projection for Clusters with Heterogeneous GPUs." Proceedings of the IEEE International Conference on Parallel and Distributed Systems (ICPADS), Seoul, South Korea, Dec. 15–18, 2013.*

Zhang, Y., P. Balaprakash, J. Meng, V. Morozov, S. Parker and K. Kumaran (2014). "Raexplore: Enabling Rapid, Automated Architecture Exploration for Full Applications." the International Conference for High Performance Computing, Networking, Storage and Analysis (SC14 HPC Matters), New Orleans, LA, Nov. 16–21, 2014.

2014-167-N0

Drewniak, B., F. Chen, R. Jacob and C. Catlett (2014). "Urban Landscapes and Climate Change: Workshop Report." the 11th Symposium on the Urban Environment, American Meteorological Society 94th Annual Meeting, Atlanta, GA, Feb. 2–6, 2014.

Applied Energy and Sustainable Transportation

2012-208-R2

Leong, S.K. and K. Shenai (2013). "Broadband Gallium Nitride (GaN) Power Amplifiers " Gallium Nitride and Silicon Carbide Power Technologies 2. M.D.K. Shenai, N. Ohtani, M. Bakowski, R. Garg. Pennington, NJ, The Electrochemical Society Transactions. **50:** 281–290.*

Megahed, M., A. Bhoj and K. Shenai (2013). "Modeling of SiC CVD Growth Process." Symposium of Gallium Nitride and Silicon Carbide Power Technologies 2 and Electrochemical Society Fall Meeting, Honolulu, HI, Oct. 7–12, 2012.

Pozo Arribas, A., M. Krishnamurthy and K. Shenai (2015). "Accurate Estimation of Switching Losses in SiC Power MOSFET's." *Electro Chemical Society Transactions (ECST)* **64**(7): 283–287.*

Pozo Arribas, A., C.A. Shang, M. Krishnamurthy and K. Shenai (2015). "A Simple and Accurate Circuit Simulation Model for SiC Power MOSFET." *IEEE Transactions on Electron Devices* **62**(2): 449–457.*

Shenai, K., B. Raghothamachar, M. Dudley and A. Christou. "Material Defects and Electrical Power Switching in High-voltage 4H-SiC Power Diodes." *IEEE Electron Device Letters*.* (to be published).

Shenai, K. (2015). "Future Prospects of Wide Bandgap (WBG) Semiconductor Power Switching Devices." *IEEE Transactions on Electron Devices* **62**(2): 248–257.*

Shenai, K. and S. Chattopadhyay (2015). "Optimization of High-voltage Wide Bandgap (WBG) Semiconductor Power Diodes." *IEEE Transactions on Electron Devices* **62**(2): 359–365.*

Shenai, K. (2014). "Manufacturing Challenges in Wide Band Gap (WBG) Power Electronics." *ECS Transactions* **58**(4): 301–310.*

Shenai, K. (2013). "Accurate Design of High-Performance Synchronous Buck DC-DC Power Converters." Proceedings of 2013 IEEE Annual Applied Power Electronics Conference (APEC), Long Beach, CA, Mar. 17–21, 2013: 435–438.*

Shenai, K., J. Wu and Y. Cui (2013). "Electro-Thermal Scaling Constraints in Chip-Scale Power Inductors." Gallium Nitride and Silicon Carbide Power Technologies 2. M.D.K. Shenai, N. Ohtani, M. Bakowski, R. Garg. Pennington, NJ, The Electrochemical Society Transactions. **50:** 367–376.*

Shenai, K., M. Backowski, M. Dudley, R. Garg and N. Ohtani (2013). Gallium Nitride and Silicon Carbide Power Technologies 2. Pennington, NJ, The Electrochemical Society.*

**Indicates refereed publication*

Shenai, K. (2013). "On The De-Rating of 4H-Silicon Carbide (SiC) Power Schottky Barrier Diodes." Gallium Nitride and Silicon Carbide Power Technologies 2. M.D.K. Shenai, N. Ohtani, M. Bakowski, R. Garg. Pennington, NJ, *The Electrochemical Society Transactions*. **50:** 95–102.*

Shenai, K. and S.K. Leong (2013). "Simple and Accurate Physics-Based Compact Circuit Simulation Models for Depletion-Mode Gallium Nitride (GaN) RF Power Transistors." Gallium Nitride and Silicon Carbide Power Technologies 2. M.D.K. Shenai, N. Ohtani, M. Bakowski, R. Garg. Pennington, NJ, The Electrochemical Society Transactions. **50:** 313–322.*

Shenai, K. (2013). "Switching MegaWatts with Power Transistors." *The Electrochemical Society Interface Magazine* **11**(1): 47–53.*

2013-148-R1

Hawkes, E.R., Y. Pei, S. Kook and S. Som (2014). "An Analysis of the Structure of an N-dodecane Spray Flame Using PDF Modelling." Proceedings of Australian Combustion Symposium, the University of Western Austrialia, Australia, Nov. 2013.*

Knox, K.R., A.M.M. Abeykoon, H. Zheng, W.G. Yin, A.M. Tsvelik, J.F. Mitchell, S.J.L. Billinge and E.S. Bozin (2014). "Local Structural Evidence for Strong Electronic Correlations in Spinel $LiRH_2O_4$." *Physical Review B* **88**(17).*

Kodavasal, J., C. Kolodziej, S. Ciatti and S. Som (2015). "CFD Simulation of Gasoline Compression Ignition." Proceedings of the 2014 American Society of Mechanical Engineers (ASME) Internal Combustion Engine Division Fall Technical Conference, Columbus, IN, Oct. 19–22, 2014, **ICEF2014-5591**(V002T06A008): 15 pages.*

Kundu, P., Y.J. Pei, M.J. Wang, R. Mandhapati and S. Som (2015). "Evaluation of Turbulence-Chemistry Interaction Under Diesel Engine Conditions with Multi-flamelet RIF Model." *Atomization and Sprays* **24**(9): 779–800.*

Kundu, P., Y. Pei and S. Som (2014). "Combustion Modeling under Diesel Engine Conditions with Multi-Flamelet RIF Model." Spring Technical Meeting of the Central States Section of the Combustion Institute, Tulsa, OK, Mar. 16–18, 2014.

Liu, W., S. Som, D.Y. Zhou, R. Sivaramakrishnan, D.E. Longman, R.T. Skodje and M.J. Davis (2013). "The Role of Individual Rate Coefficients in the Performance of Compression Ignition Engine Models." 8th U.S. National Combustion Meeting Organized by the Western States Section of the Combustion Institute, University of Utah, Salt Lake City, UT, May 19–21, 2013.

Luo, Z.Y., S. Som, S.M. Sarathy, M. Plomer, W.J. Pitz, D.E. Longman and T.F. Lu (2014). "Development and Validation of an n-Dodecane Skeletal Mechanism Forspray Combustion Applications." *Combustion Theory and Modelling* **18**(2): 187–203.*

Pei, Y., W. Liu, M. Mehl, T. Lu, W.J. Pitz and S. Som (2015). "A Multi-Component Blend as a Diesel Fuel Surrogate for Compression Ignition Engine Applications." Proceedings of the 2014 American Society of Mechanical Engineers (ASME) Internal Combustion Engine Division Fall Technical Conference, Columbus, IN, Oct. 19–22, 2014, **ICEF2014-5625**(V002T06A012): 11 pages.*

Pei, Y., W. Liu, M. Mehl, S. Som, T. Lu and W.J. Pitz (2014). "A Multi-Component Blend as a Diesel Fuel Surrogate for Compression Ignition Engine Applications." Spring Technical Meeting of the Central States Section of the Combustion Institute, Tulsa, OK, Mar. 16–18, 2014.

Pei, Y., E.R. Hawkes, S. Kook, G.M. Goldin and S. Som (2014). "An Analysis of the Structure of Spray A flame using TPDF Modelling." Spring Technical Meeting of the Central States Section of the Combustion Institute, Tulsa, OK, Mar. 16–18, 2014.

Pei, Y., R. Shan, S. Som, M.J. Davis, D.E. Longman and T. Lu (2014). "Global Sensitivity Analysis of a Diesel Engine Simulation with Multi-Target Functions." *SAE International World Congress*: 2014–2001–1117.*

Raju, M., M. Wang, M. Dai, S. Quan, P.K. Senecal, S. Som, M. McNenly and D.L. Flowers (2013). "Towards Accommodating Comprehensive Chemical Reaction Mechanisms in Practical Internal Combustion Engine Simulations." Proceedings of the 8th U.S. National Combustion Meeting Organized by the Western States Section of the Combustion Institute, University of Utah, Salt Lake City, UT, May 19–22, 2013 **3**: 2020–2025.*

Senecal, P.K., E. Pomraning, K.J. Richards and S. Som (2013). "Grid-Convergent Spray Models for Internal Combustion Engine CFD Simulations." *Journal of Energy Resources Technology* **136**(1): 012204.*

**Indicates refereed publication*

Senecal, P.K., E. Pomraning, K.J. Richards and S. Som (2013). "Grid-convergent Spray Models for Internal Combustion Engine CFD Cimulations." Proceedings of ASME 2012 Internal Combustion Engine Division Fall Technical Conference (ASME 2012), Vancouver, British Columbia, Canada, Sept. 23–26, 2012.*

Som, S. (2013). "Simulation of Compression Ignition Engines with Detailed Chemistry and Spray Models." The American Association for the Advancement of Science, Boston, MA, Feb. 14–18, 2013.

Som, S., W. Liu, D.D.Y. Zhou, G.M. Magnotti, R. Sivaramakrishnan, D.E. Longman, R.T. Skodje and M.J. Davis (2013). "Quantum Tunneling Affects Engine Performance." *Journal of Physical Chemistry Letters* **4**(12): 2021–2025.*

Wang, M., M. Raju, E. Pomraning, P. Kundu., Y. Pei and S. Som (2015). "Comparison of Representative Interactive Flamelet and Detailed Chemistry Based Combustion Models for Internal Combustion Engines." Proceedings of the 2014 American Society of Mechanical Engineers (ASME) Internal Combustion Engine Division Fall Technical Conference, Columbus, IN, Oct. 19–22, 2014, **ICEF2014-5522**(V002T06A003): 13 pages.*

Wang, Z., W. Liu, S. Som and D.E. Longman (2014). "Comparison of Different Chemical Kinetic Models for Biodiesel Combustion." Proceedings of the American Society of Mechanical Engineers (ASME) 2013 Internal Combustion Engine Division Fall Technical Conference (ICEF2013), Dearborn, MI, Oct. 13–16, 2013.*

Wang, Z., W. Liu, S. Som and D.E. Longman (2013). "Comparison of Different Chemical Kinetic Models for Biodiesel Combustion." Proceedings of 8th U.S. National Combustion Meeting Organized by the Western States Section of the Combustion Institute, University of Utah, Salt Lake City, UT, May 19–22, 2013, *Curran Associates, Inc.* **1**: 556–566.*

Xue, Q., S. Som, P.K. Senecal and E. Pomraning (2014). "Large Eddy Simulation of Fuel Spray Under Non-Reacting IC Engine Conditions." *Atomization and Sprays* **23**(10): 925–955.*

2014-120-N0

Botterud, A., C. Uckun, P. Thimmapuram, K. Gallagher, E. Constantinescu and J.R. Birge (2015). "Grid Level Energy Storage for Integration of Renewable Energy." The Institute for Operations Research and the Management Sciences (INFORMS) Annual Meeting, San Francisco, CA, Nov. 9–12, 2014.

Botterud, A. (2014). "Energy Storage for the Power Grid: A U.S. Perspective." Workshop on Energy Storage: From Technologies to Grids and Electricity Markets, Porto, Portugal, July 4, 2014.

Li, N., K. Hedman, A. Botterud, C. Uckun and J.R. Birge (2015). "Economic Assessment of Energy Storage in Systems with High Renewable Penetration." The Institute for Operations Research and the Management Sciences (INFORMS) Annual Meeting, San Francisco, CA, Nov. 9–12, 2014.

Biological and Environmental Systems

2012-016-R2

Fierer, N., J. Ladau, J.C. Clemente, J.W. Leff, S.M. Owens, K.S. Pollard, R. Knight, J.A. Gilbert and R.L. McCulley (2014). "Reconstructing the Microbial Diversity and Function of Pre-agricultural Tallgrass Prairie Soils in the United States." *Science* **342**(6158): 621–624.*

Gilbert, J. A. and F. Meyer (2012). "Modeling the Earth's Microbiome, a Real World Deliverable for Microbial Ecology." *ASM Microbe Magazine* **7**(2): 64.*

Larsen, P., N. Scott, A.F. Post, D. Field, R. Knight, Y. Hamada and J.A. Gilbert (2014). "Satellite Remote Sensing Data Predicts Marine Microbial Community Structure and Metabolite Turnover." *ISME Journal* **9**(1): 166–179.*

Larsen, P., Y. Hamada and J. Gilbert (2012). "Modeling Microbial Communities: Current, Developing, and Future Technologies for Predicting Microbial Community Interaction." *Journal of Biotechnology.* **160**(1–2): 17–24.*

Larsen, P.E., S.M. Gibbons and J.A. Gilbert (2012). "Modeling Microbial Community Structure." *FEMS Microbiology Letters* **332**(2): 91–98.*

Larsen, P.E., D. Field and J.A. Gilbert (2012). "Predicting Bacterial Community Assemblages Using MAP, a Novel Bioclimatic Model." *Nature Methods* **9**(6): 621–627.*

Indicates refereed publication

Lax, S., D.P. Smith, J. Hampton-Marcell, S.M. Owens, K.M. Handley, N.M. Scott, S.M. Gibbons, P. Larsen, B.D. Shogan, S. Weiss, J.L. Metcalf, L.K. Ursell, Y. Vazquez-Baeza, W. Van Treuren, N.A. Hasan, M.K. Gibson, R. Colwell, G. Dantas, R. Knight and J.A. Gilbert (2014). "Longitudinal Analysis of Microbial Interaction Between Humans and the Indoor Environment." *Science* **345**(6200): 1048–1052.*

Mason, O.U., N.M. Scott, A. Gonzalez, A. Robbins-Pianka, J. Baelum, J. Kimbrel, N.J. Bouskill, E. Prestat, S. Borglin, D.C. Joyner, J.L. Fortney, D. Jurelevicius, W.T. Stringfellow, L. Alvarez-Cohen, T.C. Hazen, R. Knight, J.A. Gilbert and J.K. Jansson (2014). "Metagenomics Reveals Sediment Microbial Community Response to Deepwater Horizon Oil Spill." *ISME Journal* **8**(7): 1464–1475.*

Scott, N.M., M. Hess, N.J. Bouskill, O.U. Mason, J.K. Jansson and J.A. Gilbert (2014). "The Microbial Nitrogen Cycling Potential is Impacted by Polyaromatic Hydrocarbon Pollution of Marine Sediments." *Frontiers in Microbiology* **5**: 108.*

2012-074-R2

Jastrow, J.D. and C. Liang (2014). "Utility of Chemical and Physical Fractionation Approaches for Assessing the Decomposability of Organic Carbon in Permafrost-Region Soils." Fall Working Group Meeting of the Vulnerability of Permafrost Carbon Research Coordination Network, San Francisco, CA, Dec. 8, 2013.

Kemner, K.M., B. Mishra, E.J. O'Loughlin, M.I. Boyanov, V. Bailey, A. Konopka, J. Jastrow, C. Liang, M. Balasubramanian and R. Gordon (2013). "Investigations of the Physical and Chemical Characteristics of Carbon in the Subsurface and Root Zones to Improve Earth System Modeling of the Biogeochemical Cycling of Carbon." 2013 TES/SBR Joint Investigators Meeting, Potomac, MD, May 14–15, 2013.

Liang, C., M. Steffens, J.D. Jastrow, X. Zhang, D.A. Antonopoulos and I. Kögel-Knabner (2014). "Decoupled Connection between Soil Microbial Community and Organic Geochemical Composition: A Case Study in the Arctic Tundra, North Slope of Alaska." Fall Meeting of the American Geophysical Union, San Francisco, CA, Dec. 9–13, 2013.

Mishra, B., E.J. O'Loughlin, J. Jastrow, M. Balasubramanian and K.M. Kemner (2013). "Non-Resonant Inelastic X-ray Scattering to Analyze Carbon Chemistry in Unaltered Samples." 245th American Chemical Society National Meeting, New Orleans, LA, Apr. 7–11, 2013.

2012-205-R2

Fan, Z.S., J.C. Neff, M.P. Waldrop, A.P. Ballantyne and M.R. Turetsky (2015). "Transport of Oxygen in Soil Pore-water Systems: Implications for Modeling Emissions of Carbon Dioxide and Methane from Peatlands." *Biogeochemistry* **121**(3): 455–470.*

Fan, Z., J.D. Jastrow, C. Liang, R. Matamala and R.M. Miller (2014). "Priming Effects in Boreal Black Spruce Forest Soils: Quantitative Evaluation and Sensitivity Analysis." *PLoS ONE* **8**(10): e77880.*

Fan, Z. and J.D. Jastrow (2013). "Priming Effects in Northern Boreal Forest Soils: A Quantitative Evaluation." American Geophysical Union Annual Meeting, San Francisco, CA, Dec. 3–7, 2012.

Fan, Z., A.D. McGuire, M. Turetsky, J.W. Harden, J.M. Waddington and E. Kane (2013). "Modeling the Response of Boreal Peatlands to Climate Change Using Peatland-DOS-TEM." Terrestrial Ecosystem Model Workshop, Fairbanks, AK, June 17–21, 2013.

Mishra, U., J.D. Jastrow, R. Matamala Paradeda, Z. Fan, B.A. Drewniak, W. Riley and J. Krummel (2014). "Spatial Representation of Soil Properties in Earth System Models." 20th World Congress of Soil Science, Jeju, Korea, June 8–13, 2014.

Mishra, U., J.D. Jastrow, R. Matamala, G. Hugelius, C.D. Koven, J.W. Harden, C.L. Ping, G.J. Michaelson, Z. Fan, R.M. Miller, A.D. McGuire, C. Tarnocai, P. Kuhry, W.J. Riley, K. Schaefer, E.A.G. Schuur, M.T. Jorgenson and L.D. Hinzman (2013). "Empirical Estimates to Reduce Modeling Uncertainties of Soil Organic Carbon in Permafrost Regions: A Review of Recent Progress and Remaining Challenges." *Environmental Research Letters* **8**(3).*

Indicates refereed publication

2012-206-R2

Drewniak, B. and U. Mishra (2014). "Modeling Agriculture Impacts on Soil Organic Carbon under Different Management Practices with the Community Land Model." American Geophysical Union Fall Meeting, San Francisco, CA, Dec. 9–13, 2013.

Drewniak, B.A., U. Mishra, J. Song, J. Prell and V.R. Kotamarthi (2014). "Modeling the Impact of Agricultural Land Use and Management on U.S. Carbon Budgets." *Biogeosciences Discussions* **11**(9): 13675–13698.*

Drewniak, B.A. and U. Mishra (2014). "Soil Organic Carbon Response to Cultivation in the Community Land Model." RCN FORECAST Workshop, Breckenridge, CO, June 11–14, 2014.

Hugelius, G., J. Strauss, S. Zubrzycki, J.W. Harden, E.A.G. Schuur, C.L. Ping, L. Schirrmeister, G. Grosse, G.J. Michaelson, C.D. Koven, J.A. O'Donnell, B. Elberling, U. Mishra, P. Camill, Z. Yu, J. Palmtag and P. Kuhry (2014). "Improved Estimates Show Large Circumpolar Stocks of Permafrost Carbon While Quantifying Substantial Uncertainty Ranges and Identifying Remaining Data Gaps." *Biogeosciences Discussions* **11**(3): 4771–4822.*

Mishra, U., W. Riley, M. Torn, S. Ogle and B. Drewniak (2015). "Predicting Land Use and Climate Change Impacts on Soil Organic Carbon at Regional Scales." Soil Science Society of America Annual Meeting, Long Beach, CA, Nov. 5, 2014.

Mishra, U. and W.J. Riley (2014). "Active-Layer Thickness across Alaska: Comparing Observation-Based Estimates with CMIP5 Earth System Model Predictions." *Soil Science Society of America Journal* **78**: 848–902.*

Mishra, U., J.D. Jastrow, R. Matamala Paradeda, Z. Fan, B.A. Drewniak, W. Riley and J. Krummel (2014). "Spatial Representation of Soil Properties in Earth System Models." 20th World Congress of Soil Science, Jeju, South Korea, June 8–13, 2014.

Mishra, U., J.D. Jastrow, R. Matamala, G. Hugelius, C.L. Ping and G. Michaelson (2014). "Spatial Variability of Surface Organic Horizon Thickness across Alaska." American Geophysical Union Fall Meeting, San Francisco, CA, Dec. 9–13, 2013.

Mishra, U., W.J. Riley and C.D. Koven (2014). "Topographic Controls, Spatial Heterogeneity, and Prediction Accuracies of SOC Stocks across Geospatial and Earth System Models." Soil Science Society of America Meeting, Tampa, FL, Nov. 3–6, 2013.

Mishra, U., W.J. Riley and C.D. Koven (2013). "Assessment of Spatial Heterogeneity, Environmental Controls, and Prediction Accuracy of Soil Organic Carbon Stocks across Geospatial and Earth Systems Models." American Geophysical Union Fall Meeting, San Francisco, CA, Dec. 3–7, 2012.

Mishra, U., J.D. Jastrow, R. Matamala, G. Hugelius, C.D. Koven, J.W. Harden, C.L. Ping, G.J. Michaelson, Z. Fan, R.M. Miller, A.D. McGuire, C. Tarnocai, P. Kuhry, W.J. Riley, K. Schaefer, E.A.G. Schuur, M.T. Jorgenson and L.D. Hinzman (2013). "Empirical Estimates to Reduce Modeling Uncertainties of Soil Organic Carbon in Permafrost Regions: A Review of Recent Progress and Remaining Challenges." *Environmental Research Letters* **8**(3).*

2013-177-R1

O'Loughlin, E.J., T.M. Flynn, J. Koval, S. Owens, K. Arend and D.A. Antonopoulos (2014). "Effects of 2-chloro-6-methylpyridine Concentration on Microbial Community Development During Aerobic Methane Oxidation." 114th General Meeting, American Society of Microbiology, Boston, MA, May 17–20, 2014.

O'Loughlin, E.J., D.A. Antonopoulos, K.M. Kemner, J. Koval, S.L. O'Brien and S. Owens (2014). "Identifying Novel Pathways for Anaerobic Microbial Oxidation of Methane." 5th Annual Argonne National Laboratory Soil Metagenomics Meeting, Bloomington, IL, Oct. 2–4, 2013.

2014-141-N0

Flynn, T.M., J.C. Koval, S.M. Moormann, S.M. Owens, S.L. O'Brien, S. Alvarez-Clare, E.J. O'Loughlin, K.M. Kemner and D.A. Antonopoulos (2014). "Community Level Physiological Profiling of Diverse Environments Reveals Functional and Taxonomic Diversity Within Aerobic, Single Carbon-Source Enrichments." 2014 Ecological Society of America Annual Meeting, Sacramento, CA, Aug. 10–15, 2014.

**Indicates refereed publication*

2014-183-N0

Fang, M., B.A. Albrecht, V.P. Ghate and P. Kollias (2014). "Turbulence in Continental Stratocumulus, Part II: Eddy Dissipation Rates and Large-Eddy Coherent Structures." *Boundary-Layer Meteorology* **150**(3): 361–380.*

Fang, M., B.A. Albrecht, V.P. Ghate and P. Kollias (2014). "Turbulence in Continental Stratocumulus, Part I: External Forcings and Turbulence Structures." *Boundary-Layer Meteorology* **150**(3): 341–360.*

Ghate, V.P., M.A. Miller, B.A. Albrecht and C.W. Fairall (2015). "Thermodynamic and Radiative Structure of Stratocumulus-topped Boundary Layers." *Journal of the Atmospheric Sciences* **72**(1): 430–451.*

2014-187-N0

Biswas, M., J.A. Libera, S.B. Darling and J.W. Elam (2015). "New Insight into the Mechanism of Sequential Infiltration Synthesis from Infrared Spectroscopy." *Chemistry of Materials* **26**(21): 6135–6141.*

2014-188-N0

Buizert, C., Baggenstos, W. Jiang, R. Purtschert, V.V. Petrenko, Z.T. Lu, P. Mueller, T. Kuhl, J. Lee, J.P. Severinghaus and E.J. Brook (2014). "Radiometric ^{81}Kr Dating Identifies 120,000-year-old Ice at Taylor Glacier, Antarctica." Proceedings of the National Academy of Sciences of the United States of America, May 13, 2014, **111**(19): 6876–6881.*

Jiang, W., K. Bailey, Z.T. Lu, P. Mueller, T.P. O'Connor and R. Purtschert (2014). "Ion Current as a Precise Measure of the Loading Rate of a Magneto-optical Trap." *Optics Letters* **39**(2): 409–412.*

Sturchio, N.C., K.L. Kuhlman, R. Yokochi, P.C. Probst, W. Jiang, Z.T. Lu, P. Mueller and G.M. Yang (2014). "Krypton-81 in Groundwater of the Culebra Dolomite Near the Waste Isolation Pilot Plant, New Mexico." *Journal of Contaminant Hydrology* **160**: 12–20.*

Zappala, J.C., K. Bailey, Z.T. Lu, T.P. O'Connor and W. Jiang (2014). "Efficient Generation of Optical Sidebands at GHz with a High-power Tapered Amplifier." *Review of Scientific Instruments* **85**(4): 046104.*

2014-189-N0

Urgun-Demirtas, M., C.J. Arnusch, J.A. Gilbert, S.W. Snyder, J. Dittrich, P. Ignacio-de Leon and K.M. Handley (Accepted). "A Systematic Tool for Development of More Robust 'Smart' Membranes and Energy Efficient Water Treatment Processes." Water and Energy 2015: Opportunities for Energy and Resource Recovery in the Changing World, Washington, D.C., June 8–10, 2015.

2014-193-N0

Ghate, V.P. and M.A. Miller (2014). "Effects of Clouds on Cross-atmospheric Radiative Flux Divergence: Case-studies in Different Cloud Conditions." American Geophysical Union (AGU) Fall Meeting, San Francisco, CA, Dec. 9–13, 2013.

Ghate, V.P., M.A. Miller and B.A. Albrecht (2014). "On the Dynamics and Radiation of Cumulus Topped Marine Boundary Layers." 4th Atmospheric System Research (ASR) Science Team Meeting, Potomac, MD, Mar. 10–13, 2014.

Marquardt-Collow, A., V.P. Ghate, M.A. Miller and L. Trabachino. "A One-year Study of the Diurnal Cycle of Meteorology, Clouds, and Radiation in the West African Sahel Region." *Quarterly Journal of the Royal Meteorological Society*.* (to be published).

Wood, R., M. Wyant, C.S. Bretherton, J. Rémillard, P. Kollias, J. Fletcher, J. Stemmler, S. deSzoeke, S. Yuter, M. Miller, D. Mechem, G. Tselioudis, C. Chiu, J. Mann, E. O'Connor, R. Hogan, X. Dong, M. Miller, V. Ghate, A. Jefferson, Q. Min, P. Minnis, R. Palinkonda, B. Albrecht, E. Luke, C. Hannay and Y. Lin (2014). "Clouds, Aerosol, and Precipitation in the Marine Boundary Layer: An ARM Mobile Facility Deployment." *Bulletin of the American Meteorological Society* **e-View**: 140617093021002.*

**Indicates refereed publication*

Director's Grand Challenge

2013-165-R1

Blaiszik, B., K. Chard, R. Anathakrishnan, S. Tuecke and I. Foster (2015). "Globus Data Publication Services." U.S.—UK Workshop on Materials Theory and Simulation, Argonne National Laboratory, Argonne, IL, Jan. 26, 2015.

Blaiszik, B., K. Chard, H. Pruyne, R. Anathakrishnan, S. Tuecke and I. Foster (2014). "Globus Scientific Data Services Current and Future." Materials Genome Initiative Materials Data Workshop, Air Force Research Laboratory, Dayton, OH, July 15, 2014.

Blaiszik, B., K. Chard, S. Tuecke and I. Foster (2015). "Globus: Research Data Management-as-a-Service." Opportunities in Materials Informatics (OMI), University of Wisconsin-Madison, Madison, WI, Feb. 9, 2015.

Blaiszik, B., K. Chard, S. Tuecke, I. Foster and R. Ananthakrishnan (2014). "Globus Scientific Data Services Current and Future." 2014 Materials Genome Initiative Materials Data Workshop, Dayton, OH, July 15, 2014.

Chen, J., L. Wang and M. Anitescu. "A Parallel Tree Code for Computing Matrix-Vector Products with the Matern Kernel." *ACM Transactions on Mathematical Software*.* (to be published).

Foster, I. (2014). "Networking Materials Data." 2014 International Advanced Research Workshop on High Performance Computing: From Clouds and Big Data to Exascale and Beyond, Centraro, Italy, July 11, 2014.

Foster, I. (2014). "An Architecture for a National Data Service." 1st National Data Service Consortium Workshop, Boulder, CO, June 12–13, 2014.

Foster, I. (2014). "Networking Materials Data." Workshop on Building an Integrated MGI Accelerator Network, Atlanta, GA, June 2014.

Habib, S., A. Pope, H. Finkel, N. Frontiere, K. Heitmann, D. Daniel, P. Fasel, V. Morozov, G. Zagaris, T. Peterka, V. Vishwanath, Z. Lukic, S. Sehrish and W.-K. Liao. "HACC: Simulating Sky Surveys on State-of-the-Art Supercomputing Architectures." *New Astronomy*.* (to be published).

Habib, S. (2014). "HACCing the Universe on the BG/Q." 20th Annual ScicomP 2014 BG Consortium Meeting, Chicago, IL, May 27–30, 2014.

Habib, S. (2014). "Thoughts on Next-Generation Computing and LSST DESC." LLST DESC Dark Energy Science Collaboration Meeting, Philadelphia, PA, June 2014.

Heitmann, K. (2014). "Cosmological Simulations for Large-Scale Sky Surveys." Oak Ridge Leadership Computing Facility (OLCF) Users Meeting, Oak Ridge, TN, July 22–24, 2014.

Heitmann, K., S. Habib, H. Finkel, N. Frontiere, A. Pope, V. Morozov, S. Rangel, E. Kovacs, J. Kwan, N. Li, S. Rizzi, J. Insley, V. Vishwanath, T. Peterka, D. Daniel, P. Fasel and G. Zagaris (2014). "Large-Scale Simulations of Sky Surveys." *Computing in Science & Engineering* **16**(5): 14–23.*

Heitmann, K., E. Lawrence, J. Kwan, S. Habib and D. Higdon (2014). "The Coyote Universe Extended: Precision Emulation of the Matter Power Spectrum." *Astrophysical Journal* **780**(1): 111.* (also see 2011-213-R3).

Kwan, J., S. Bhattacharya, K. Heitmann and S. Habib (2013). "Cosmic Emulation: The Concentration-Mass Relation for Wcdm Universes." *Astrophysical Journal* **768**(2): 123.*

Malik, T., K. Chard and I. Foster (2014). "Benchmarking Cloud-based Tagging Services." 6th International Workshop on Cloud Data Management, 30th IEEE International Conference on Data Engineering, Chicago, IL, Mar. 31, 2014.

Rosenkranz, S. (2014). "Quantitative Analysis of the Diffuse Scattering from a Bilayer Manganite." American Physical Society March Meeting 2014, Denver, CO, Mar. 3–7, 2014.

Wozniak, J.M. (2014). "Studies in Big Data and HPC from X-ray Crystallography." 1st Workshop of the INRIA-Illinois-ANL-BSC Joint Laboratory on Extreme Scale Computing, Sophia Antipolis, France, June 9–11, 2014.

Wozniak, J.M. (2014). "Parallel Scripting for Beamline Science: Connecting Big Data and HPC." 2014 BES Facilities Computing Working Group Technical Meeting, Berkeley, CA, Feb. 20, 2014.

Indicates refereed publication

Wozniak, J.M., T.G. Armstrong, D.S. Katz, M. Wilde and I.T. Foster (2014). "Toward Computational Experiment Management via Multi-language Applications." 2014 ASCR Workshop on Software Productivity for Extreme-Scale Science, Rockville, MD, Jan. 13–14, 2014.

Wozniak, J.M., T.G. Armstrong, S.J. Krieder, K. Maheshwari, M. Wilde and I.T. Foster (2014). "Mega Python: Scalable Inter-language Scripting for Scientific Computing." Super Computer Conference (SC13), Denver, CO, Nov. 18–22, 2013.

Hard X-ray Sciences

2013-111-R1

Holzbauer, J.P. and A. Nassiri (2015). "Thermal Study of a Cryogen-less MgB_2 Cavity." *Nuclear Instruments & Methods in Physics Research Section A—Accelerators Spectrometers Detectors and Associated Equipment* **767**: 407–414.*

Nassiri, A., R. Kustom and T. Proslier (2013). "Cryogen-Free RF System Studies Using Cryocooler-cooled MgB_2 Coated Copper RF Cavities." Proceedings of the 16th International Conference on RF Superconductivity (SRF 2013), Paris, France, Sept. 23–27, 2013.*

2013-168-R1

De Carlo, F., D. Gursoy, F. Marone, M. Rivers, D.Y. Parkinson, F. Khan, N. Schwarz, D.J. Vine, S. Vogt, S.C. Gleber, S. Narayanan, M. Newville, T. Lanzirotti, Y. Sun, Y.P. Hong and C. Jacobsen (2015). "Scientific Data Exchange: A Schema for HDF5-based Storage of Raw and Analyzed Data." *Journal of Synchrotron Radiation* **21**(Pt 6): 1224–1230.*

Gursoy, D., F. De Carlo, X. Xiao and C. Jacobsen (2014). "TomoPy: A Framework for the Analysis of Synchrotron Tomographic Data." 2014 SPIE Optics & Photonics: Developments in X-ray Tomography, San Diego, CA, Aug. 17–21, 2014.

Gursoy, D., F. De Carlo, X. Xiao and F. Jacobsen (2014). "TomoPy: A Framework for the Analysis of Synchrotron Tomographic Data." *Journal of Synchrotron Radiation* **21**(5): 1188–1193.*

Hong, Y.P., S.C. Gleber, T.V. O'Halloran, E.L. Que, R. Bleher, S. Vogt, T.K. Woodruff and C. Jacobsen (2014). "Alignment of Low-dose X-ray Fluorescence Tomography Images Using Differential Phase Contrast." *Journal of Synchrotron Radiation* **21**(Pt 1): 229–234.*

Jacobsen, C.J. (2014). "Big Data at the Advanced Photon Source: Some Order Out of Chaos, and Getting Quick Pictures." Research Data Alliance 4th Plenary Meeting, Amsterdam, The Netherlands, Sept. 22–24, 2014.

Jacobsen, C.J., A. Kastengren and K. Fezzaa (2014). "Imaging at Fast Times: APS Experience and Speculations." Workshop on Scientific Opportunities Using High Repetition Rate X-ray Sources with 1-10 ps Bunch Length, SLAC National Accelerator Laboratory, Menlo Park, CA, Oct. 1–4, 2013.

Jacobsen, C.J. (2014). "The Bionanoprobe at the Advanced Photon Source at Argonne." 2nd 108-SXM Workshop on Scanning X-ray Microscopy, Diamond Light Source, Oxfordshire, UK, Mar. 25, 2014.

Jacobsen, C.J. (2014). "Non-negative Matrix Analysis for Effective Feature Extraction in X-ray Spectromicroscopy." RSC Conference Faraday Discussion 171 Emerging Photon Technologies for Chemical Dynamics, Sheffield UK, July 9–11, 2014.

Jacobsen, C.J. (2014). "Oscillators, X-rays and Global Carbon: Adventures in X-ray Nanofocusing." Colloquium at the University of Illinois Chicago, Chicago, IL, Apr. 2, 2014.

Jacobsen, C. (2014). "Radiation Damage Limits to X-ray Imaging, and Their (Partial) Mitigation." Workshop on Radiation Effects at X-ray Doses from MegaGrays and PetaGrays and Above—the Impact for Science at NSLS-II, NSLS/CFN User Meeting, Brookhaven National Laboratory, Upton, NY, May 21, 2014.

Jacobsen, C.J. (2014). "Scientific Data Exchange: A Flexible HDF5 Schema for Data and Analysis." PaNData ODI Open Workshop (POOW14), Amsterdam, The Netherlands, Sept. 25, 2014.

Jacobsen, C.J. (2014). "Soft X-ray Microscopy and Spectroscopy with Zone Plates." Higher European Research Course for Users of Large Experimental Systems (HERCULES), Grenoble, France, Mar. 14, 2014.

*Indicates refereed publication

Jacobsen, C. (2014). "X-ray Nanofocusing and the MBA Lattice Upgrade." APS/CNM/EMS User Meeting, Advanced Photon Source, Argonne National Laboratory, Argonne, IL, May 13, 2014.

Jacobsen, C. (2014). "X-rays Part 2: Comparison with Electrons, Resolution and Damage, Cryo Ptychography." Workshop on Physical, Engineering and Biological Limits to Brain Measurement, National Science Foundation (NSF), May 31, 2014.

Jacobsen, C.J. (2013). "Cold and in Color: Towards Combining Ptychography with Fluorescence in a Cryogenic Microscope." Real and Reciprocal Space X-ray Imaging, Newport Pagnell, United Kingdom, Feb. 13–14, 2013.

Jacobsen, C.J. (2013). "Simplicity from Complexity: Pattern Recognition Techniques Applied to Soft X-ray Spectromicroscopy." Canadian Light Source 16th Annual Users' Meeting and Related Workshops, Saskatoon, Saskatchewan, Canada, May 2–3, 2013.

Jacobsen, C.J. (2013). "X-ray Microscopy." Higher European Research Course for Users of Large Experimental Systems (HERCULES), Grenoble, France, Feb. 24–Mar. 27, 2013.

Jacobsen, C.J. (2013). "X-ray Microscopy: Combining Imaging and Spectroscopy." RACIRI Summer School on X-ray Science Between Germany, Russia, and Sweden, St. Petersburg, Russia, Aug. 17–25, 2013.

Jacobsen, C.J. (2013). "X-ray Imaging and Microscopy: Methods, Applications, and Detectors." 15th International Workshop on Radiation Imaging Detectors, Paris, France, June 23–27, 2013.

Lerotic, M., R. Mak, S. Wirick, F. Meirer and C. Jacobsen (2014). "MANTiS: A Program for the Analysis of X-ray Spectromicroscopy Data." *Journal of Synchrotron Radiation* **21**(Pt 5): 1206–1212.*

Mak, R., M. Lerotic, H. Fleckenstein, S. Vogt, S.M. Wild, S. Leyffer, Y. Sheynkin and C. Jacobsen (2015). "Non-negative Matrix Analysis for Effective Feature Extraction in X-ray Spectromicroscopy." *Royal Society of Chemistry Faraday Discussions* **171**: 357–371.*

Maser, J., B. Lai, T. Buonassisi, Z. Cai, S. Chen, L. Finney, S.C. Gleber, R. Harder, C. Jacobsen, W. Liu, C. Murray, C. Preissner, C. Roehrig, V. Rose, D. Shu, D. Vine and S. Vogt (2013). "A Next-Generation *In Situ* Nanoprobe Beamline for the Advanced Photon Source." SPIE 2013: Optics & Photonics, San Diego, CA, Aug. 25–29, 2013.*

Wang, S., J. Ward, S. Leyffer, S.M. Wild, C. Jacobsen and S. Vogt (2013). "Unsupervised Cell Identification on Multidimensional X-ray Fluorescence Datasets." Proceedings of the Journal of Synchrotron Radiation (ACM SIGGRAPH 2013) International Conference on Computer Graphics and Interactive Techniques, Anaheim, CA, July 21–25, 2013, *ACM, New York, NY* **88**.*

2014-122-N0

Conway, Z.A., A. Barcikowski, S.M. Gerbick, M.J. Kedzie, M.P. Kelly, J.S. Kerby, S.H. Kim, S.V. Kutsaev, R.C. Murphy, A. Nassiri, P.N. Ostroumov, T.C. Reid, T.L. Smith and A.A. Zholents (2014). "Development and Test Results of a Quasi-waveguide Multi-cell Resonator." 5th International Particle Accelerator Conference (IPAC-14), Dresden, Germany, June 15–20, 2014.

2014-134-N0

Cha, W., S. Hruszkewycz, R. Sichel-Tissot, M.J. Highland, R. Harder, W. Liu, J. Maser and P. Fuoss (2014). "Three-dimensional Bragg Coherent Diffraction Imaging Using Polychromatic X-rays." International Workshop of Phase Retrieval and Coherent Scattering, Evanston, IL, Sept. 2–5, 2014.

2014-184-N0

Shiroyanagi, Y., C. Doose, J. Fuerst, K. Harkay, Q. Hasse, Y. Ivanyushenkov and M. Kasa (2014). "Thermal Analysis of a Superconducting Undulator." Proceedings of the Applied Superconductivity Conference (ASC 2014), Charlotte, NC, Aug. 10–15, 2014.*

Indicates refereed publication

Materials for Energy

2011-217-R3

Krogstad, D.V., S.H. Choi, N.A. Lynd, D.J. Audus, S.L. Perry, J.D. Gopez, C.J. Hawker, E.J. Kramer and M.V. Tirrell (2015). "Small Angle Neutron Scattering Study of Complex Coacervate Micelles and Hydrogels Formed from Ionic Diblock and Triblock Copolymers." *The Journal of Physical Chemistry B* **118**(45): 13011–13018.*

Krogstad, D.V., N.A. Lynd, D. Miyajima, J. Gopez, C.J. Hawker, E.J. Kramer and M.V. Tirrell (2015). "Structural Evolution of Polyelectrolyte Complex Core Micelles and Ordered-Phase Bulk Materials." *Macromolecules* **47**(22): 8026–8032.*

Krogstad, D.V., N.A. Lynd, S.H. Choi, J.M. Spruell, C.J. Hawker, E.J. Kramer and M.V. Tirrell (2013). "Effects of Polymer and Salt Concentration on the Structure and Properties of Triblock Copolymer Coacervate Hydrogels." *Macromolecules* **46**(4): 1512–1518.*

Perry, S.L., Y. Li, D. Priftis, L. Leon and M. Tirrell (2014). "The Effect of Salt on the Complex Coacervation of Vinyl Polyelectrolytes." *Polymers* **6**(6): 1756–1772.*

Priftis, D., K. Megley, N. Laugel and M. Tirrell (2013). "Complex Coacervation of Poly(ethylene-imine)/polypeptide Aqueous Solutions: Thermodynamic and Rheological Characterization." *Journal of Colloid and Interface Science* **398**: 39–50.*

Priftis, D., N. Laugel and M. Tirrell (2013). "Thermodynamic Characterization of Polypeptide Complex Coacervation." *Langmuir: The ACS Journal of Surfaces and Colloids* **28**(45): 15947–15957.*

Priftis, D., R. Farina and M. Tirrell (2012). "Interfacial Energy of Polypeptide Complex Coacervates Measured via Capillary Adhesion." *Langmuir: The ACS Journal of Surfaces and Colloids* **28**(23): 8721–8729.*

Priftis, D. and M. Tirrell (2012). "Phase Behavior and Complex Coacervation of Aqueous Polypeptide Solutions." *Soft Matter* **8**(36): 9396–9405.*

2012-015-R2

Gu, G.S., H.O. Heinonen, H.S. Hong, K.D. Karpeyev, K.M. Kim and N.S. Nakhmanson (2013). "Numerical Simulation of Piezoelectric Vibration Energy Harvester." Finite Element Circus & Rodeo, Baton Rouge, LA, Mar. 8–9, 2013.

Heinonen, O., D. Karpeyev, S. Gu, S.M. Nakhmanson, B. Lee and S. Hong (2013). "Real Space Formulation for Coupled Elastic Problems." CMCSN, Purdue University, West Lafayette, IN, Apr. 15–16, 2013.

Lee, B., S.M. Nakhmanson and O. Heinonen (2014). "Strain Induced Vortex-to-uniform Polarization Transitions in Soft-ferroelectric Nanoparticles." *Applied Physics Letters* **104**(26).*

Lee, B., S.M. Nakhmanson and O. Heinonen (2014). "Two-dimensional Electric Vortices in Soft Ferroelectric Cylindrical Nano-particles." American Physical Society March Meeting, Denver, CO, Mar. 3–7, 2014.

Lee, B., S. Gu, O. Heinonen, D. Karpeyev and S. Nakhmanson (2013). "Polarization 'Doughnut' States in Layered-Oxide Nanostructures." 22nd International Materials Research Congress (IMRC) 2013, Cancun, Mexico, Aug. 11–15, 2013.

Li, D.J., S. Hong, S.Y. Gu, Y. Choi, S. Nakhmanson, O. Heinonen, D. Karpeyev and K. No (2014). "Polymer Piezoelectric Energy Harvesters for Low Wind Speed." *Applied Physics Letters* **104**(1).*

2013-184-R1

Armas, J., M. Rahimi, O. Guzman, J. Whitmer, J. Hernandez-Ortiz and J.J. de Pablo. "Stochastic Simulation of Liquid Crystals at the Mesoscale in an Orthogonal Basis Set." *Journal of Chemical Physics*.* (to be published).

Buchanan, L.E., E.B. Dunkelberger, H.Q. Tran, P.-N. Cheng, C.C. Chiu, P. Cao, D.P. Raleigh, J.J. de Pablo, J.S. Nowick and M.T. Zanni (2014). "Mechanism of IAPP Amyloid Fibril Formation Involves an Intermediate with a Transient β-sheet." Proceedings of the National Academy of Sciences of the United States of America, Nov. 26, 2013, **110**(19285–19290).*

Chiu, C.C., S. Singh and J.J. de Pablo (2013). "Effect of Proline Mutations on the Monomer Conformations of Amylin." *Biophysical Journal* **105**(5): 1227–1235.*

**Indicates refereed publication*

Freeman, G.S., D.M. Hinckley, J.I. Whitmer and J.J. De Pablo. "DNA Shape and Nucleosome Formation: A Critical Paradigm for Molecular Recognition." *Physical Review Letters*.* (to be published).

Freeman, G.S., D.M. Hinckley, J.P. Lequieu, J.K. Whitmer and J.J. de Pablo (2015). "Coarse-grained Modeling of DNA Curvature." *Journal of Chemical Physics* **141**(16): 165103.*

Freeman, G.S., D.M. Hinckley, J.P. Lequieu, J.K. Whitmer and J.J. De Pablo (2015). "DNA Shape Dominates Sequence Affinity in Nucleosome Formation." *Physical Review Letters* **113**(16).*

Hinckley, D.M., G.S. Freeman, J.K. Whitmer and J.J. de Pablo (2014). "An Experimentally-Informed Coarse-Grained 3-Site-Per-Nucleotide Model of DNA: Structure, Thermodynamics, and Dynamics of Hybridization." *Journal of Chemical Physics* **139**(14): 144903.*

Hinckley, D.M., J.P. Lequieu and J.J. de Pablo (2014). "Coarse-grained Modeling of DNA Oligonucleotide Hybridization: Length, Sequence, and Salt Effects." *Journal of Chemical Physics* **141**(3): 035102.*

Hoffmann, K. and J.J. De Pablo). "Systematic Comparison of Force Fields for Prediction of Structure in Disordered Oligopeptides." *PLOS One*.* (to be published).

Hur, S.M., G.S. Khaira, A. Ramirez-Hernandez, M. Mueller, P.F. Nealey and J.J. De Pablo. "Simulation of Defect Reduction in Block Copolymer Thin Films by Solvent Annealing." *ACS Macro Letters*.* (to be published).

Joshi, A.A., J.K. Whitmer, O. Guzman, N. Abbott and J.J. de Pablo (2014). "Measuring Liquid Crystal Elastic Constants with Free Energy Perturbations." *Soft Matter* **10**(6): 882–893.*

Joshi, A.A., J.K. Whitmer, O. Guzman, N.L. Abbott and J.J. de Pablo (2014). "Measuring Liquid Crystal Elastic Constants with Free Energy Perturbations." *Soft Matter* **10**(6): 882–893.*

Li, W., P.F. Nealey, J.J. de Pablo and M. Müller (2015). "Defect Removal in the Course of Directed Self-Assembly is Facilitated in the Vicinity of the Order-Disorder Transition." *Physical Review Letters* **113**(16).*

Liu, C.C., A. Ramirez-Hernandez, E. Han, G.S.W. Craig, Y. Tada, H. Yoshida, H.M. Kang, S.X. Ji, P. Gopalan, J.J. de Pablo and P.F. Nealey (2013). "Chemical Patterns for Directed Self-assembly of Lamellae-Forming Block Copolymers with Density Multiplication of Features." *Macromolecules* **46**(4): 1415–1424.*

Onses, M.S., A. Ramirez-Hernandez, S.M. Hur, E. Sutanto, L. Williamson, A.G. Alleyne, P.F. Nealey, J.J. de Pablo and J.A. Rogers (2014). "Block Copolymer Assembly on Nanoscale Patterns of Polymer Brushes Formed by Electrohydrodynamic Jet Printing." *ACS Nano* **8**(7): 6606–6613.*

Qin, J., G.S. Khaira, Y.R. Su, G.P. Garner, M. Miskin, H.M. Jaeger and J.J. de Pablo (2014). "Evolutionary Pattern Design for Copolymer Directed Self-assembly." *Soft Matter* **9**(48): 11467–11472.*

Qin, J., D. Priftis, R. Farina, S.L. Perry, L. Leon, J. Whitmer, K. Hoffmann, M. Tirrell and J.J. de Pablo (2014). "Interfacial Tension of Polyelectrolyte Complex Coacervate Phases." *ACS Macro Letters* **3**(6): 565–568.*

Ramirez-Hernandez, A., H.S. Suh, P.F. Nealey and J.J. de Pablo (2014). "Control of Directed Self-assembly in Block Copolymers by Polymeric Top Coats." *Macromolecules* **47**(10): 3520–3527.*

Ramirez-Hernandez, A., F.A. Detcheverry, B.L. Peters, V.C. Chappa, K.S. Schweizer, M. Muller and J.J. de Pablo (2013). "Dynamical Simulations of Coarse Grain Polymeric Systems: Rouse and Entangled Dynamics." *Macromolecules* **46**(15): 6287–6299.*

Ramirez-Hernandez, A., M. Muller and J.J. de Pablo (2013). "Theoretically Informed Entangled Polymer Simulations: Linear and Non-linear Rheology of Melts." *Soft Matter* **9**(6): 2030–2036.*

Suh, H.S., A. Ramirez-Hernandez, J. Lee, Y. Ishida, K. Aida, Y. Tada, H. Yoshida, R. Ruiz, W. Chen, J.J. de Pablo and P.F. Nealey. "Directed Assembly of Block Copolymer Films Using Topcoats." *Angewandte Chemie*.* (to be published).

Whitmer, J., A.A. Joshi and J.J. de Pablo. "Adsorption of Ions in Non-polarizable Water Models." *Langmuir*.* (to be published).

Whitmer, J.K., C.C. Chiu, A.A. Joshi and J.J. De Pablo (2015). "Basis Function Sampling: A New Paradigm for Material Property Computations." *Physical Review Letters* **113**: 190602.*

**Indicates refereed publication*

Whitmer, J.K., X.G. Wang, F. Mondiot, D.S. Miller, N.L. Abbott and J.J. de Pablo (2014). "Nematic-Field-Driven Positioning of Particles in Liquid Crystal Droplets." *Physical Review Letters* **111**(22): 227801.*

Whitmer, J.K., A.A. Joshi, T.F. Roberts and J.J. de Pablo (2013). "Liquid-Crystal Mediated Nanoparticle Interactions and Gel Formation." *Journal of Chemical Physics* **138**(19): 194903.*

2013-202-R1

Jorn, R., R. Kumar, D.P. Abraham and G.A. Voth (2013). "Atomistic Modeling of the Electrode-Electrolyte Interface in Li-Ion Energy Storage Systems: Electrolyte Structuring." *Journal of Physical Chemistry C* **117**(8): 3747–3761.*

Knight, C.J., G.E. Lindberg, S. Tse, A.M. Herring, T.W. Witten and G.A. Voth (2014). "Progress Towards a Fundamental Understanding of Charge Transport Mechanisms in Fuel Cell Membranes." 7th Bishop's Lodge Workshop: Materials for Energy Conversion, Santa Fe, NM, Nov. 3–5, 2013.

Sode, O. and G.A. Voth. "Electron Transfer Activation of a Second Water Channel for Proton Transport in [FeFe]-Hydrogenase." *Journal of Chemical Physics*.* (to be published).

Ottochian, A., G. Dezanneau, C. Gilles, P. Raiteri, C. Knight and J.D. Gale (2014). "Influence of Isotropic and Biaxial Strain on Proton Conduction in Y-doped $BaZrO_3$: A Reactive Molecular Dynamics Study." *Journal of Materials Chemistry A* **2**(9): 3127–3133.*

2013-215-R1

Deshmukh, S.A., G. Kamath, D.C. Mancini and S.K.R.S. Sankaranarayanan (2014). "Effect of Methanol/Water Mixtures on the Lower Critical Solution Temperature of Poly(N-isopropylacrylamide)." Proceedings of the MRS Proceedings, Boston, MA, Dec. 1–6, 2013, *Materials Research Society 2014* **1622** (Symposium E — Fundamentals of Gels and Self-Assembled Polymer Systems): 25–30.*

Deshmukh, S.A., G. Kamath, S.K.R.S. Sankaranarayanan and D.C. Mancini (2014). "Effect of Methanol/Water Mixtures on the Lower Critical Solution Temperature of Poly(N-isopropylacrylamide)." 2013 Materials Research Society (MRS) Fall Meeting, Boston, MA, Dec. 1–6, 2013.

Deshmukh, S.A., G. Kamath, D.C. Mancini, S.K.R.S. Sankaranarayanan and W. Jiang (2014). "Meso-scale Simulations of Poly(N-isopropylacrylamide) Grafted Architectures." Proceedings of the MRS Proceedings, Boston, MA, Dec. 1–6, 2013, *Materials Research Society* **1619** (Symposium A — Modeling and Theory-Driven Design of Soft Materials): mrsf13–1619–a1603–1605.*

Deshmukh, S.A., G. Kamath, D.C. Mancini and S.K.R.S. Sankaranarayanan (2014). "Meso-scale Simulations of Poly(N-isopropylacrylamide) Grafter Architectures." 2013 Materials Research Society (MRS) Fall Meeting, Boston, MA, Dec. 1–6, 2013.

Deshmukh, S., G. Kamath, D. Mancini and S.K.R.S. Sankarananayanan (2014). "Multi-Million-Atom Molecular Dynamics Simulations of Polymer Nanoparticle Composites Using Explicit Solvent Treatment." American Physical Society Meeting, Denver, CO, Mar. 3–7, 2014.

Kamath, G., S. Deshmukh, D. Mancini and S.K.R.S. Sankaranarayanan (2014). "All-Atom Molecular Dynamics Simulations of Poly(N-isopropylacrylamide) Grafted Architectures." AIChE Annual Meeting, San Francisco, CA, Nov. 3–8, 2013.

Kamath, G., S. Deshmukh, D.C. Mancini and S.K.R.S. Sankaranarayanan (2014). "Meso-scale Simulations of Poly(N-isopropylacrylamide) Grafted Architectures." 2013 Materials Research Society (MRS) Fall Meeting, Boston, MA, Dec. 1–6, 2013.

Malik, V., K.J. Suthar, D.C. Mancini and J. Ilavsky (2014). "Magnetic-field-dependent Assembly of Silica-coated Magnetite Nanoclusters Probed by Ultra-Small-Angle X-ray Scattering (USAXS)." *Journal of Magnetism and Magnetic Materials* **354**: 70–75.*

Mancini, D., S. Deshmukh, S.K.R.S. Sankarananayanan and G. Kamath (2014). "MD Simulations of PNIPAM Agglomeration and Self-Assembly." Gordon Research Conference on Polymer Physics, Mt. Holyoke College, South Hadley, MA, July 13–18, 2014.

Indicates refereed publication

Mancini, D. and K. Suthar (2013). "Hydrogel-Nanoparticle Composites Synthesized From Nanoparticle Polymer Brushes." Particles 2013 Conference, Dayton, OH, Aug. 5, 2013.

Suthar, K.J. and D.C. Mancini (2014). "Hydrogel-nanoparticle Composites Synthesized from Poly (N-Isopropylacrylamide) Brush Structures." 2013 Materials Research Society (MRS) Fall Meeting, Boston, MA, Dec. 1–6, 2013.

Suthar, K.J., D.C. Mancini and L. He (2014). "Isotope Effect on the Conformation of Linear Poly(N-isopropylacrylamide) Across the LCST Using Small Angle Neutron Scattering." 2013 Materials Research Society (MRS) Fall Meeting, Boston, MA, Dec. 1–6, 2013.

Suthar, K.J., D.C. Mancini and L. He (2014). "Temperature Dependent Conformation Change of Undeuterated and Deuterated Thermo-responsive Linear-polymer Poly(N-isopropylacrylamide) Using Small Angle Neutron Scattering Across LCST." 2013 Materials Research Society (MRS) Fall Meeting, Boston, MA, Dec. 1–6, 2013.

2013-219-R1

Benson, B.A., P.A.R. Ade, Z. Ahmed, S.W. Allen, K. Arnold, J.E. Austermann, A.N. Bender, L.E. Bleem, J.E. Carlstrom, C.L. Chang, H.M. Cho, S.T. Ciocys, J.F. Cliche, T.M. Crawford, A. Cukierman, T. de Haan, M.A. Dobbs, D. Dutcher, W. Everett, A. Gilbert, N.W. Halverson, D. Hanson, N.L. Harrington, K. Hattori, J.W. Henning, G.C. Hilton, G.P. Holder, W.L. Holzapfel, K.D. Irwin, R. Keisler, L. Knox, D. Kubik, C.L. Kuo, A.T. Lee, E.M. Leitch, D. Li, M. McDonald, S.S. Meyer, J. Montgomery, M. Myers, T. Natoli, H. Nguyen, V. Novosad, S. Padin, Z. Pan, J. Pearson, C.L. Reichardt, J.E. Ruhl, B.R. Saliwanchik, G. Simard, G. Smecher, J.T. Sayre, E. Shirokoff, A.A. Stark, K. Story, A. Suzuki, K.L. Thompson, C. Tucker, K. Vanderlinde, J.D. Vieira, A. Vikhlinin, G. Wang, V. Yefremenko and K.W. Yoon (2014). "SPT-3G: A Next-Generation Cosmic Microwave Background Polarization Experiment on the South Pole Telescope." Proceedings of the SPIE—The International Society for Optical Engineering, Montreal, Quebec, Canada, July 23, 2014, **9153** (Millimeter, Submillimeter, and Far-infrared Detectors and Instrumentation for Astronomy VII).*

Chang, C., P. Ade, Z. Ahmed, S. Allen, K. Arnold, J. Austermann, A. Bender, B. Benson, L. Bleem, J. Carlstrom, H.-m. Cho, S. Ciocys, J.-F. Cliche, T. Crawford, A. Cukierman, T. de Haan, M. Dobbs, D. Dutcher, W. Everett, A. Gilbert, N. Halverson, D. Hanson, N. Harrington, K. Hattori, J. Henning, G. Hilton, G. Holder, W. Holzapfel, K. Irwin and R. Keisler (2015). "Low Loss Superconducting Microstrip Development at Argonne National Laboratory." *IEEE Transactions on Applied Superconductivity* **PP**(99): 1-1.*

Wang, G., C.L. Chang, V. Yefremenko, V. Novosad, J. Pearson, R. Divan and J.E. Carlstrom (2015). "Mo/Au Bilayer TES Resistive Transition Engineering." *IEEE Transactions on Applied Superconductivity—ACS 2014 Special Issue* **PP**(99): 1-1.*

2014-121-N0

Sun, Y. (2015). "Discovery Enabled by *in situ* Synchrotron X-ray Techniques." 51st Annual Technical Meeting, Society of Engineering Science (SES 2014), West Lafayette, IN, Oct. 1–3, 2014.

Sun, Y., S. Peng, Z. Li, Y. Ren, J.D. Almer and J.S. Okasinski (2014). "*In situ* Study on the Growth and Transformation of Colloidal Noble Metal Nanocrystals." 2014 Gordon Research Conference on Noble Metal Nanoparticles, South Hadley, MA, June 15–20, 2014.

2014-128-N0

Zhong, X., I. Rungger, P. Zapol and O. Heinonen. "Self-interaction Corrected electronic Structure of Ti_4O_7, TiO_2 and Ti_2O_3." *Physical Review B: Condensed Matter*.* (to be published).

2014-133-N0

Groll, N.R., J.A. Klug, C.Y. Cao, S. Altin, H. Claus, N.G. Becker, J.F. Zasadzinski, M.J. Pellin and T. Proslier (2014). "Tunneling Spectroscopy of Superconducting MoN and NbTiN Grown by Atomic Layer Deposition." *Applied Physics Letters* **104**(9): 092602.*

Klug, J.A., N.G. Becker, N.R. Groll, C. Cao, M.S. Weimer, M.J. Pellin, J. Zasadzinski and T. Proslier (2014). "Heteroepitaxy of Group IV-VI Nitrides by Atomic Layer Deposition." *Applied Physics Letters* **103**(21): 211602.*

**Indicates refereed publication*

2014-139-N0

Wagner, A., P. Zapol, M. Keceli and H. Zhang (2014). "The SIPs Eigensolver for Petascale Applications." 46th Midwest Theoretical Chemistry Conference, Northwestern University, Evanston, IL, June 15–17, 2014.

2014-151-N0

Sichel-Tissot, R., S. Hruszkewycz, M. Highland, W. Cha, R.J. Holt, S.R. Lee, D.D. Koleske and P.H. Fuoss (2014). "X-ray Probes of Local Composition and Structure Near Defects in InGaN Multi-quantum Wells." International Workshop of Phase Retrieval and Coherent Scattering, Evanston, IL, Sept. 2–5, 2014.

Yanguas-Gil, A. (2014). "The Role of Surface Kinetics on Surface Morphology and Defect Evolution during WBG Semiconductor Epitaxy." Workshop on Defects in Wide Band Gaps Semiconductors, University of Maryland, College Park, MD, Sept. 23, 2014.

2014-161-N0

Deshmukh, S., G. Kamath and S.K.R.S. Sankaranarayanan (2014). "Effect of Nanoscale Confinement on Freezing of Modified Water at Room Temperature and Ambient Pressure." *ChemPhysChem* **15**(8): 1632–1642.*

Kamath, G.K., B. Narayanan and S.K.R.S. Sankaranarayanan (2014). "Atomistic Origin of Superior Performance of Ionic Liquid Electrolytes for Al-ion Batteries." *Physical Chemistry Chemical Physics* **16**(38): 20387–20391.*

Kinaci, A., B. Narayanan, M.J. Davis, S. Gray, S. Sankaranarayanan and M. Chan (2015). "Evolutionary Algorithm Search for Global Minimum Structures of Au Nano-Clusters." Materials Research Society Fall Meeting, Boston, MA, Nov. 30–Dec. 5, 2014.

Narayanan, B., A. Kinaci, M. Davis, M. Chan, S. Sankaranarayanan and S. Gray (2015). "Development of Novel Force Field for Gold Nanoclusters." Materials Science and Technology Conference, Pittsburgh, PA, Oct. 12–16, 2014.

Narayanan, B., A. Kinaci, M.J. Davis, M.K. Chan, S. Sankaranarayanan and S.K. Gray (2014). "Development of Force Field for Reactive Interfaces from First Principles." Center for Nanoscale Materials Users Meeting, Argonne National Laboratory, Argonne, IL, May 12–15, 2014.

2014-192-N0

Galli, G. (2014). "Electronic Properties of Aqueous Interfaces: Coupled *ab initio* Molecular Dynamics and GW Calculations." International Center for Materials Research (ICMR) Workshop on *Ab-initio* Description of Charged Systems and Solid/Liquid Interfaces for Semiconductors and Electrochemistry, University of California, Santa Barbara, CA, July 7–11, 2014.

Galli, G. (2014). "Heterogeneous Interfaces: Insights From First Principles Calculations." American Conference on Theoretical Chemistry (ACTC) 2014, Telluride, CO, July 21–24, 2014.

Galli, G. (2014). "Light Absorbers for Photo-electrochemical Energy Conversion: First Principles Calculations." 248th American Chemical Society (ACS) National Meeting, San Francisco, CA, Aug. 10–14, 2014.

Galli, G. (2014). "Photo-excitations in Nanostructured Semiconductors." American Physical Society (APS) March Meeting, Denver, CO, Mar. 3–7, 2014.

Galli, G. (2014). "Predicting Materials for Water Splitting: Condensed Matter Physics Meets Electrochemistry." the 248th American Chemical Society (ACS) National Meeting, Presidential Symposium Photocatalytic Conversion of Water to Hydrogen and Oxygen, San Francisco, CA, Aug. 10–14, 2014.

Galli, G. (2014). "Water at Surfaces: Insights from First Principles Calculations." Water and Aqueous Solutions Gordon Research Conference, Holderness, NH, July 27–Aug. 1, 2014.

Pham, T.A., D. Lee, E. Schwegler and G. Galli (2015). "Interfacial Effects on the Band Edges of Functionalized Si Surfaces in Liquid Water." *Journal of the American Chemical Society* **136**(49): 17071–17077.*

**Indicates refereed publication*

National Security

2013-171-R1

Schabacker, D. and A. Driks (2014). "Enhanced Molecular Attribution Through Proteomic Signatures (EMAPS)." International Microbial Forensics Symposium, Ottawa, Ontario, Canada, Feb. 11–12, 2014.

2013-173-R1

Schaller, R.D. (2014). "Ratiometric Sensing of Bioweapon and Nuclear Threat Agents." National Counterproliferation Center Lab Days, The MITRE Corporation, McLean, VA, Apr. 9, 2014.

Schaller, R.D. (2013). "Probing Energy Migration in Semiconductor Nanocrystals for Sensing and Energy Applications." Telluride Science Research Center, Telluride, CO, June 27, 2013.

2013-178-R1

Bobadilla, A.D., L.E. Ocola, A.V. Sumant, M. Kaminski and J.M. Seminario. "Electrochemical Response of Graphene Ribbons to Europium." *Journal of Physical Chemistry*.* (to be published).

Bobadilla, A., N. Kumar, A. Sumant, L. Ocola, C. Mertz, G. Sandi, M. Kaminski and J. Seminario (2014). "Detection of Uranium and Plutonium by Graphene-Based Nanosensors." American Vacuum Society 60th International Symposium, Long Beach, CA, Oct. 27–Nov. 1, 2013.

Bobadilla, A., L. Ocola, A. Sumant, J.M. Seminario and M. Kaminski (2014). "Electrochemical Response of Graphene Ribbon to Eu (III)." APS/CNM/EMC Users Meeting 2014, Argonne, IL, May 12–15, 2014.

Bobadilla, A., L. Ocola, A. Sumant, J.M. Seminario and M. Kaminski (2014). "Graphene Based Electrochemical Detection of Europium (III)." New Diamond and Nano Carbons Conference, Chicago, IL, May 25–29, 2014.

Bobadilla, A., G. Sandi, L. Ocola, A. Sumant, J. Seminario, M. Kaminski and C. Mertz (2013). "Uranium and Plutonium Detection by Plasmonic Graphene-Based Nanosensors." APS/CNM/EMC Users Meeting, Argonne, IL, May 6–9, 2013.

Mertz, C.J., M.D. Kaminski, I.A. Shkrob, M. Kalensky, V.S. Sullivan and Y. Tsai. "Development of a Field-based Separator for the Rapid Identification of Uranium and Plutonium." *Journal of Radioanalytical and Nuclear Chemistry*.* (to be published).

Nuclear Energy

2013-152-R1

Kun, M., Z. Zhou, Z. Miao, Y. Yun, D. Tung, H.M. Zhang, G. Chen, W. Almer and J.F. Stubbins (2014). "Synchrotron Study on Load Partitioning between Ferrite/Martensite and Nanoparticles of a 9Cr ODS Steel." Proceedings of the 16th International Conference on Fusion Reactor Materials (ICFRM-16), Beijing, China, Oct. 20–26, 2013, **455**(1–3): 376–381.*

Mei, Z.G., M. Stan, A.M. Yacout and J. Yang (2014). "Atomistic Study of the Effects of Point Defects and Xe Atoms on the Thermal Conductivity of UO_2." TMS 2014, San Diego, CA, Feb. 16–20, 2014.

Mei, Z.G. and M. Stan (2014). "First-principles Study of Phase Stability and Thermodynamics of Uranium Nitride." Materials Science & Technology 2013 Conference (MS&T 2013), Montreal, Quebec, Canada, Oct. 27–31, 2013.

Mei, Z.G., M. Stan, A. Yacout and J. Yang (2014). "Thermal Transport in Uranium Dioxide by Atomic Simulations." NuMat Conference 2014, Clearwater, FL, Oct. 27–30, 2014.

Mei, Z.G., M. Stan and A.M. Yacout (2014). "Thermophysical Properties of Uranium Dioxide by First-Principles." 2014 American Nuclear Society (ANS) Annual Meeting and Nuclear Fuels & Structural Materials for Next Generation Nuclear Reactors (NFSM), Reno, NV, June 15–19, 2014.

Mo, K., Y. Miao, Z. Zhou, D. Yun, X. Liu, J. Almer and J.F. Stubbins (2014). "Nanoparticles Loading Behavior Before and After Matrix Necking: An *in situ* Synchrotron Radiation Study in a 9Cr ODS Alloy." 2014 American Nuclear Society (ANS)

**Indicates refereed publication*

Annual Meeting and Nuclear Fuels & Structural Materials for Next Generation Nuclear Reactors (NFSM), Reno, NV, June 15–19, 2014.

Mo, K., D. Yun, W. Mohamed, M. Pellin, J. Almer and A.M. Yacout (2014). "Synchrotron Radiation Study on Steam Oxidation Behavior of Zircaloy-2 with Advanced Coatings." 2014 American Nuclear Society (ANS) Annual Meeting and Nuclear Fuels & Structural Materials for Next Generation Nuclear Reactors (NFSM), Reno, NV, June 15–19, 2014.

Mohamed, W., D. Yun, K. Mo, M. Pellin, M. Billone, J. Almer and A.M. Yacout (2015). "Depth Profile of Oxide Volume Fractions of Zircaloy-2 in High-temperature Steam: An *in situ* Synchrotron Radiation Study." *Journal of Nuclear Materials* **454**(1–3): 192–199.*

Stan, M., D. Yun, Z. Mei, A. Yacout, B. Mihaila and S. Hu (2013). "Microstructural Heterogeneity and Thermal Transport." Pacific Rim International Conference on Advanced Materials Processing (PRICM-8), Waikoloa, HI, Aug. 4–9, 2013.

Yacout, A., M. Mendelsohn, D. Yun and W. Mohamed (2014). "Multilayer ALD Coating of Light Water Reactor Zirconium Alloy Cladding Materials." Multilayers'13, Madrid, Spain, Oct. 1–4, 2013.

Yacout, A.M., M. Pellin and M.C. Billone (2013). "Development and Testing of Nanolaminate Coatings for Conventional LWR Cladding." Proceedings of the LWR Fuel Performance Meeting/Top Fuel 2013, Charlotte, NC, Sept. 15–19, 2013: 847.*

Ye, B., S. Bhattacharya, K. Mo, D. Yun, W. Mohamed, M. Pellin, J. Fortner, Y.S. Kim, G. Hofman and A. Yacout (2014). "80 MeV Xe Irradiation on U-Mo/Al Dispersion Fuel." 19th International Conference on Ion Beam Modification of Materials, Leuven, Belgium, Sept. 14–19, 2014.

Ye, B., Y.S. Kim, G. Hofman, A. Yacout, S. Bhattcharya, K. Mo, D. Yun, W. Mohamed, M. Pellin and J. Fortner (2015). "Xe Irradiation on ZrN-Coated U-Mo/Al Dispersion Fuel." International Meeting on Reduced Enrichment for Research and Test Reactors (RERTR 2014), Vienna, Austria, Oct. 12–15, 2014.

Yun, D., W. Mohamed, B. Ye, M. Kirk, P. Baldo and A. Yacout (Submitted). "*In situ* TEM and Synchrotron Characterization of U-10Mo Thin Specimen Annealed at the Fast Reactor Temperature Regime." *Metallurgical and Materials Transaction A*.*

Yun, D., K. Mo, W. Mohamed, M.J. Pellin and A.M. Yacout (2015). "Irradiation Behavior Study of U-Mo/Al Dispersion Fuel with High Energy Xe." NuMat Conference 2014, Clearwater, FL, Oct. 27–30, 2014.

Yun, D., K. Mo, W. Mohamed, M.J. Pellin and A.M. Yacout (2015). "Modeling Beam Heating and Sample Temperature by High Energy Heavy Ion Irradiation, and Comparison with Experimental Measurements." NuMat Conference 2014, Clearwater, FL, Oct. 27–30, 2014.

Yun, D., J. Wright, J. Terry, K. Mo, R. Xu, W. Mohamed, B. Yei, K. Logan, M. Pellin and A. Yacout (2015). "Study of Xe Ion Beam Irradiated Mo Single Crystal by Synchrotron Extended X-ray Absorption Fine Structure and Microdiffraction." NuMat Conference 2014, Clearwater, FL, Oct. 27–30, 2014.

Yun, D., K. Mo, R. Xu, W. Mohamed, B. Ye, M.J. Pellin and A.M. Yacout (2014). "Characterization of High Energy Xe Ion Damage in U-10Mo Metallic Alloy Fuel with Depth Resolved Synchrotron Microbeam Diffraction." 2014 American Nuclear Society (ANS) Annual Meeting and Nuclear Fuels & Structural Materials for Next Generation Nuclear Reactors (NFSM), Reno, NV, June 15–19, 2014.

Yun, D., K. Mo, R. Xu, W. Mohamed, B. Ye, M.J. Pellin and A.M. Yacout (2014). "Characterization of High Energy Xe Ion Irradiation Effects in Single Crystal Molybdenum with Depth Resolved Synchrotron Microbeam Diffraction." 2014 American Nuclear Society (ANS) Annual Meeting and Nuclear Fuels & Structural Materials for Next Generation Nuclear Reactors (NFSM), Reno, NV, June 15–19, 2014.

Yun, D., W. Mohamed, B. Ye, M. Kirk, P. Baldo and A. Yacout (2013). "Preliminary Assessment of Microstructural Evolution of U-10Mo Thin Specimen Annealed at Typical Fast Reactor Temperature Regime." Proceedings of the American Nuclear Society (ANS) Annual Meeting, Atlanta, GA, June 12–16, 2013: 373.*

2014-177-N0

Tentner, A., E. Merzari and P. Vagendla (2014). "Computational Fluid Dynamics Modeling of Two-Phase Boiling Flow and Critical Heat Flux." Proceedings of the 22nd International Conference on Nuclear Engineering ICONE22, Prague, Czech Republic, July 7–11, 2014, *ASME Proceedings* **4** (ICONE22-30844): V004T010A037.*

Indicates refereed publication

Sustainable Energy Production and Use

2011-210-R3

Kwon, G., G.A. Ferguson, C.J. Heard, E.C. Tyo, C. Yin, J. DeBartolo, S. Seifert, R.E. Winans, A.J. Kropf, J. Greeley, R.L. Johnston, L.A. Curtiss, M.J. Pellin and S. Vajda (2013). "Size-dependent Subnanometer Pd Cluster (Pd_4, Pd_6, and Pd_{17}) Water Oxidation Electrocatalysis." *ACS Nano* **7**(7): 5808–5817.*

Ferguson, G.A., C. Yin, G. Kwon, S. Lee, J.P. Greeley, P. Zapol, B. Lee, S. Seifert, R.E. Winans, S. Vajda and L.A. Curtiss (2013). "Stable Subnanometer Cobalt Oxide Clusters on Ultrananocrystalline Diamond and Alumina Supports: Oxidation State and the Origin of Sintering-resistance." *J. Phys. Chem. C* **116**(45): 24027–24034.*

Other Novel R&D

2014-185-N0

Johnson, C.S. (2014). "Emergence of Na-Ion Battery Technologies." 248th American Chemical Society Meeting, San Francisco, CA, Aug. 10, 2014.

Johnson, C.S. (2014). "Na-ion Batteries: A New Energy Storage Focus." International Society of Electrochemistry Society (ISE) Meeting, Lausanne, Switzerland, Aug. 30, 2014.

Karan, N.K., M.D. Slater, F. Dogan, D. Kim, C.S. Johnson and M. Balasubramanian (2014). "Operando Structural Characterization of the Lithium-Substituted Layered Sodium-Ion Cathode Material P2-$Na_{0.85}Li_{0.17}Ni_{0.21}Mn_{0.64}O_2$ by X-ray Absorption Spectroscopy." *Journal of the Electrochemical Society* **161**(6): A1107–1115.*

Lee, E., S. Sahgong, C.S. Johnson and Y. Kim (2015). "Comparative Electrochemical Sodium Insertion/Extraction Behavior in Layered Na_xVS_2 and Na_xTiS_2." *Electrochimica Acta* **143**: 272–277.*

Lee, E. (2014). "Layered P2/O3 Intergrowth Cathode: Toward High Capacity and High Power Na-Ion Batteries." 17th International Meeting on Lithium Batteries (IMLB) Meeting, Como, Italy, June 10–14, 2014.

Lee, E., J. Lu, Y. Ren, X.Y. Luo, X.Y. Zhang, J.G. Wen, D. Miller, A. DeWahl, S. Hackney, B. Key, D. Kim, M.D. Slater and C.S. Johnson (2014). "Layered P2/O3 Intergrowth Cathode: Toward High Power Na-Ion Batteries." *Advanced Energy Materials* **4**(17).*

Zhou, D., M. Slater, D. Kim, E. Lee, J. Jorne and C.S. Johnson (2014). "SnSb Carbon Composite Anode in a SnSb_C/$NaNi_{1/3}Mn_{1/3}Fe_{1/3}O_2$ Na-Ion Battery." *ECS Transactions* **58**(12): 59-64.*

*Indicates refereed publication

LDRD

Publications and Presentations II

(Arising from LDRD projects completed prior to FY 2014 but produced and/or delivered during FY 2014)

ANNUAL REPORT

2014

2009-070

Pokkuluri, P.R., J. Dwulit-Smith, N.E. Duke, R. Wilton, J.C. Mack, J. Bearden, E. Rakowski, G. Babnigg, H. Szurmant, A. Joachimiak and M. Schiffer (2014). "Analysis of Periplasmic Sensor Domains from Anaeromyxobacter Dehalogenans 2CP-C: Structure of one Sensor Domain from a Histidine Kinase and another from a Chemotaxis Protein." *MicrobiologyOpen* **2**(5): 766–777.*

2009-071

Carneiro, J.-P., F.G. Garcia, J.-F. Ostiguy, A. Saini, R. Zwaska, B. Mustapha and P. Ostroumov (2014). "Transmission Efficiency Measurement at the FNAL 4-Rod RFQ." 27th Linear Accelerator Conference (LINAC14), Geneva, Switzerland, Aug. 31–Sept. 5, 2014.

Martel, I., L. Acosta, R. Carrasco, J.A. Duenas, T. Junquera, A.K. Orduz, A. Peregrin, J.A. Prieto-Thomas, J. Sanchez-Segovia, P.N. Ostroumov, A.C.C. Villari, F. Azaiez, G. de Angelis, M. Lewitowicz and A. Maj (2014). "ECOS-LINCE: A High Intensity Multi-Ion Superconducting Linac for Nuclear Structure and Reactions." 5th International Particle Accelerator Conference (IPAC'14), Dresden, Germany, June 15–20, 2014.

Mustapha, B., M. Alcorta, B.B. Back and P.N. Ostroumov (2014). "Design and Simulation of the Argonne Inflight Radioactive Ion Separator (AIRIS)." 25th North American Particle Accelerator Conference (NA-PAC'13), Pasadena, CA, Sept. 30–Oct. 4, 2014.

Mustapha, B., C.R. Hoffman, B.P. Kay, B.B. Back, P.N. Ostroumov and J.A. Nolen (2014). "An In-Flight Radioactive Beam Separator Design for the ATLAS Facility." 27th Linear Accelerator Conference (LINAC14), Geneva, Switzerland, Sept. 1–5, 2014.

Mustapha, B., S.V. Kutsaev, P.N. Ostroumov and J.A. Nolen (2014). "A Compact Linac Design for an Accelerator Driven System." 27th Linear Accelerator Conference (LINAC14), Geneva, Switzerland, Sept. 1–5, 2014.

Mustapha, B., P.N. Ostroumov and A. Kolomeits (2014). "A Full 3-D Approach to the Design and Simulation of a Radio-Frequency Quadrupole." *Physical Review Special Topics: Accelerators and Beams* **16**: 120101.*

Ostroumov, P.N., A. Barcikowski, Z. Conway, S. Gerbick, M. Kedzie, M.P. Kelly, S. Kim, S. Kutsaev, R. Murphy, B. Mustapha, R. Pardo, D. Paskvan, T. Reid, S. Sharamentov and G. Zinkann (2014). "Upgrade of Argonne's CW SC Heavy Ion Accelerator." 25th North American Particle Accelerator Conference (NA-PAC/13), Pasadena, CA, Sept. 30–Oct. 4, 2013.

Perry, A., C. Dickerson, P.N. Ostroumov and G. Zinkann (2014). "Beam Characterization of a New Continuous Wave Radio Frequency Quadrupole Accelerator." *Nuclear Instruments and Methods in Physics Research Section A: Accelerators, Spectrometers, Detectors and Associated Equipment* **735**: 163–168.*

2009-204

Guest, J.R. (2014). "Exploring Self-assembled Donor-acceptor Heterojunctions at the Atomic Scale: Chirality, Charge Transfer and Reversible Rectification." International Conference on Nanoscience + Technology 2014 (ICN+T2014), Vail, CO, July 20–25, 2014.

Smerdon, J.A., R.B. Rankin, N.C. Giebink, J.W. Cho, L. Gao, O. Suzer, J.P. Greeley, N.P. Guisinger and J.R. Guest (2014). "Exploring Self-assembled Donor-acceptor Heterojunctions at the Atomic Scale: Chirality, Charge Transfer and Reversible Rectification." International Conference on Nanoscience + Technology 2014 (ICN+T2014), Vail, CO, July 20–25, 2014.

Smerdon, J.A., R.B. Rankin, N.C. Giebink, J.W. Cho, L. Gao, O. Suzer, J.P. Greeley, N.P. Guisinger and J.R. Guest (2014). "Exploring Self-assembled Donor-acceptor Heterojunctions at the Atomic Scale: Chirality, Charge Transfer and Reversible Rectification." 2014 International Workshop on Nanoscale Spectroscopy and Nanotechnology, Chicago, IL, July 28–31, 2014.

Zhang, H., J.A. Smerdon, O. Suzer and J.R. Guest (2014). "Development of a 4 K Laser STM for Photophysical Studies at the Atomic Scale." 2014 International Workshop on Nanoscale Spectroscopy and Nanotechnology, Chicago, IL, July 28–31, 2014.

*Note: For information regarding projects listed here, see annual reports from previous years. *Indicates refereed publication*

2009-209

Kopnin, N.B., A.S. Mel'nikov, I.A. Sadovskyy and V.M. Vinokur (2014). "Weak Links in Proximity-superconducting Two-dimensional Electron Systems." *Physical Review B* **89**(8).*

Petković, A. and V.M. Vinokur (2014). "Fluctuation-induced Noise in Out-of-equilibrium Disordered Superconducting Films." *Annals of Physics* **339**: 412-429.*

2009-214

Melikyan, A. and M.R. Norman (2014). "Symmetry of the Charge Density Wave in Cuprates." *Physical Review B* **89**(2): 024507.*

2010-010

Xu, C.Y., J. Singh, J.C. Zappala, K.G. Bailey, M.R. Dietrich, J.P. Greene, W. Jiang, N.D. Lemke, Z.T. Lu, P. Mueller and T.P. O'Connor (2014). "Measurement of the Hyperfine Quenching Rate of the Clock Transition in ^{171}YB." *Physical Review Letters* **113**(3): 033003.*

2010-043

Drake, G., A.A. Paramonov, R.W. Stanek and D.G. Underwood (2014). "A New High-Speed Optical Transceiver for Data Transmission at the LHC Experiments." *Journal of Instrumentation* **9**(01): C01059.*

2010-050

Palacios, E., A. Chen, J. Foley, S.K. Gray, U. Welp, D. Rosenmann and V.K. Vlasko-Vlasov (2014). "Ultra-confined Modes in Metal Nanoparticle Arrays for Subwavelength Light Guiding and Amplification." *Advanced Optical Materials* **2**(4): 394–399.*

2010-063

Park, Y.S., N. Gopalsami and M. Gundeti (2014). "Tactile MEMS-Based Sensor Element for Robotic Surgery." American Nuclear Society Topical Meeting on Decommissioning and Remote Systems, Reno, NV, Jun. 16–18, 2014.

Park, Y.S., J. Martell, P. Dworzanski and T. Elmer (2014). "Frequency-Based Visual Measurement of Suture Strain for Robotic Surgery." American Nuclear Society Embedded Topical Meeting on Decommissioning and Remote Systems, Reno, NV, Jun. 15–19, 2014.

2010-119

Jastrow, J., R. Matamala, Z. Fan, U. Mishra, C.-L. Ping, G. Michaelson, F. Calderon, V. Romanovsky and A. Kholodov (2014). "ANL Terrestrial Ecosystem Science SFA: Soil Carbon Response to Environmental Change." 2014 TES SBR PI Meeting, Potomac, MD, May 6–7, 2014.

Jastrow, J., R. Matamala, K. McFarlane, Z. Fan, R. Porras, M. Torn, T. Guilderson and P. Hanson (2014). "Climatic and Edaphic Effects on Root- and Leaf-litter Carbon Inputs to Temperate Forest Soils." 2014 TES SBR PI Meeting, Potomac, MD, May 6–7, 2014.

Jastrow, J.D., F. Calderon, K. McFarlane, R. Porras, M. Torn, T. Guilderson and P. Hanson (2014). "Climatic and Edaphic Effects on the Turnover and Composition of Mineral-Associated Soil Organic Matter in Temperate Deciduous Forests." American Geophysical Union Fall Meeting, San Francisco, CA, Dec. 9–13, 2013.

*Note: For information regarding projects listed here, see annual reports from previous years. *Indicates refereed publication*

2010-138

Islam, Z. (2014). "Trapped Field Magnets: A New Means to Unrestricted Optical Access for Scattering in High Magnetic Fields." National High Magnetic Field Laboratory, Tallahassee, FL, Jan. 24, 2014.

2010-139

Faria, J.P., J.N. Edirisinghe, J.J. Davis, T. Disz, A. Hausmann, C.S. Henry, R. Olson, R.A. Overbeek, G.D. Pusch, M. Shukla, V. Vonstein and A.R. Wattam (2014). "Enabling Comparative Modeling of Closely Related Genomes: Example Genus *Brucella*." *3 Biotech*.*

Seaver, S.M.D., S. Gerdes, O. Frelin, C. Lerma-Ortiz, L.M.T. Bradbury, R. Zallot, G. Hasnain, T.D. Niehaus, B.E. Yacoubi, S. Pasternak, R.D. Olson, G.D. Pusch, R. Overbeek, R. Stevens, V.d. Crecy-Lagard, D. Ware, A.D. Hanson and C.S. Henry (2014). "PlantSEED: A Resource for High-Throughput Comparison, Functional Annotation, and Metabolic Modeling of Plant Genomes." Proceedings of the National Academy of Sciences of the United States of America, San Diego, CA, Jan. 11–15, 2014.*

2010-156

Fard, H.R., N. Becker, A. Hess, K. Pashayi, T. Proslier, M. Pellin and T. Borca-Tasciuc (2014). "Thermal Conductivity of Er^{+3}:Y_2O_3 Films Grown by Atomic Layer Deposition." *Applied Physics Letters* **103**(193109).*

2010-158

Shui, J., J.S. Okasinski, P. Kenesei, J.D. Almer and D.-J. Liu (2014). "Spatiotemporal Study of Li-O_2 Battery Under Cycling using Microfocused X-ray Diffraction and Tomographic Methods." 2014 APS/CNM/EMC User Meeting, Argonne National Laboratory, IL, May 14, 2014.

Yuan, S., L. Grabstanowicz, G. Goenaga, J. Shui, C. Chen, S. Commet, B. Reprogle and D.J. Liu (2014). "New Approach to High-Efficiency Non-PGM Catalysts Using Rationally Designed Porous Organic Polymers." Proceedings of the 224th Electrochemical Society Meeting, San Francisco, CA, Oct. 27–Nov. 1, 2013, *ECS Transaction* **58**(1): 1671–1681.*

2010-183

Chen, C., J. Deng, Y. Yuan, C. Flachenecker, R. Mak, B. Hornberger, Q. Jin, D. Shu, B. Lai, J. Maser, C. Roehrig, T. Paunesku, S.C. Gleber, D.J. Vine, L. Finney, J. VonOsinski, M. Bolbat, I. Spink, Z. Chen, J. Steele, D. Trapp, J. Irwin, M. Feser, E. Snyder, K. Brister, C. Jacoben, G. Woloschak and S. Vogt (2014). "The Bionanoprobe: Hard X-ray Fluorescence Nanoprobe with Cryogenic Capabilities." *Journal of Synchrotron Radiation* **21**(1): 66–75.* (also see 2010-193).

Yuan, Y., S. Chen, T. Paunesku, S.C. Gleber, W.C. Liu, C.B. Doty, R. Mak, J. Deng, Q. Jin, B. Lai, K. Brister, C. Flachenecker, C. Jacobsen, S. Vogt and G.E. Woloschak (2014). "Epidermal Growth Factor Receptor Targeted Nuclear Delivery and High-resolution Whole Cell X-ray Imaging of Fe_3O_4@TiO_2 Nanoparticles in Cancer Cells." *ACS Nano* **7**(12): 10502–10517.* (also see 2010-193).

2010-185

Shui, J.L., J. Okasinski, C. Chen, J. Almer and D.J. Liu (2014). "In Operando Spatiotemporal Study of Li_2O_2 Grain Growth and Distribution Inside of Operating Li-O_2 Batteries." *ChemSusChem* **7**(2): 543–548.*

2010-188

Koo, B., P. Goli, A.V. Sumant, P.C. dos Santos Claro, T. Rajh, C.S. Johnson, A. Balandin and E.V. Shevchenko (2014). "Toward Lithium-Ion Batteries with Enhanced Thermal Conductivity." *ACS Nano* **8**(7): 7202–7207.*

*Note: For information regarding projects listed here, see annual reports from previous years. *Indicates refereed publication*

2010-190

Kim, J., M. Daghofer, A.H. Said, T. Gog, J. van den brink, G. Khaliullin and B.J. Kim (2014). "Excitonic Quasiparticles in a Spin-orbit Mott Insulator." *Nature Communications* **5**: 4453.*

2010-193

Chen, C., J. Deng, Y. Yuan, C. Flachenecker, R. Mak, B. Hornberger, Q. Jin, D. Shu, B. Lai, J. Maser, C. Roehrig, T. Paunesku, S.C. Gleber, D.J. Vine, L. Finney, J. VonOsinski, M. Bolbat, I. Spink, Z. Chen, J. Steele, D. Trapp, J. Irwin, M. Feser, E. Snyder, K. Brister, C. Jacoben, G. Woloschak and S. Vogt (2014). "The Bionanoprobe: Hard X-ray Fluorescence Nanoprobe with Cryogenic Capabilities." *Journal of Synchrotron Radiation* **21**(1): 66–75.* (also see 2010).

de Jonge, M.D., C.G. Ryan and C.J. Jacobsen (2014). "X-ray Nanoprobes and Diffraction-limited Storage Rings: Opportunities and Challenges of Fluorescence Tomography of Biological Specimens." *Journal of Synchrotron Radiation* **21**(5): 1031–1047.*

Gursoy, D., F. De Carlo, X. Xiao and F. Jacobsen (2014). "TomoPy: A Framework for the Analysis of Synchrotron Tomographic Data." *Journal of Synchrotron Radiation* **21**(Pt 5): 1188–1193.*

Jacobsen, C.J., A. Kastengren and K. Fezzaa (2014). "Imaging at Fast Times: APS Experience and Speculations." Workshop on Scientific Opportunities Using High Repetition Rate X-Ray Sources with 1-10 ps Bunch Length, SLAC, Menlo Park, CA, Oct. 1–4, 2013.

Lerotic, M., R. Mak, S. Wirick, F. Meirer and C. Jacobsen (2014). "MANTiS: A Program for the Analysis of X-Ray Spectromicroscopy Data." *Journal of Synchrotron Radiation* **21**(Pt 5): 1206–1212.*

Yuan, Y., S. Chen, T. Paunesku, S.C. Gleber, W.C. Liu, C.B. Doty, R. Mak, J. Deng, Q. Jin, B. Lai, K. Brister, C. Flachenecker, C. Jacobsen, S. Vogt and G.E. Woloschak (2014). "Epidermal Growth Factor Receptor Targeted Nuclear Delivery and High-resolution Whole Cell X-ray Imaging of Fe_3O_4@TiO_2 Nanoparticles in Cancer Cells." *ACS Nano* **7**(12): 10502–10517.* (also see 2010).

2010-194

Campos, E.F., R. Ware, P. Joe and D. Hudak (2014). "Monitoring Water Phase Dynamics in Winter Clouds." *Atmospheric Research* **147–148**: 86–100.*

Huang, D., E. Campos and Y.G. Liu (2014). "Statistical Characteristics of Cloud Variability. Part 1: Retrieved Cloud Liquid Water Path at Three ARM Sites." *Journal of Geophysical Research-Atmospheres* **119**(18): 10813–10828.*

Ware, R., D. Cimini, E. Campos, G. Giuliani, S. Albers, M. Nelson, S.E. Koch, P. Joe and S. Cober (2014). "Thermodynamic and Liquid Profiling During the 2010 Winter Olympics." *Atmospheric Research* **132–133**: 278–290.*

2010-195

Owens, S., J. Wilkening, J.L. Fessler and J.A. Gilbert (2014). "Metagenomics Chapter." Biofouling Methods. S. Dobretsov, Thomason, J.C., Williams, D.N. Oxford, UK, John Wiley & Sons, Ltd.**:** Chap. 3, Sec. 1.*

Wilke, A., P. Larsen and J.A. Gilbert (2014). "Next Generation Sequencing and the Future of Microbial Metagenomics." Next-generation Sequencing: Current Technologies and Applications. J. Xu, Caister Academic Press**:** Chapter 9.*

2010-197

Mei, Z.G. and M. Stan (2014). "First-principles Study of Phase Stability and Thermodynamics of Uranium Nitride." Materials Science & Technology 2013 (MS&T13), Montreal, Quebec, Canada, Oct. 27–31, 2013.

Mei, Z.G. and M. Stan (2014). "First-principles Study of Thermodynamic Properties of Uranium Dioxide." *Journal of Alloys and Compounds* **603**: 282–286.*

*Note: For information regarding projects listed here, see annual reports from previous years. *Indicates refereed publication*

Mei, Z.G. and M. Stan (2014). "Pressure-induced Phase Transitions in UN: A Density Functional Theory Study." *Journal of Alloys and Compounds* **588**: 648–653.*

Mei, Z.G. and M. Stan (2014). "Pressure-induced Phase Transitions of UN: A Density Functional Theory Study." *Journal of Alloys and Compounds* **588**: 648–653.*

Mei, Z.G., M. Stan and A.M. Yacout (2014). "Thermophysical Properties of Uranium Dioxide by First-Principles." American Nuclear Society/Nuclear Fuels and Structural Materials Annual Meeting (ANS-NFSM 2014), Reno, NV, Jun. 15–19, 2014.

Mei, Z.G., M. Stan and A.M. Yacout (2014). "Molecular Dynamics Study of Thermal Conductivity in Defective Uranium Dioxide." American Nuclear Society/Nuclear Fuels and Structural Materials Annual Meeting (ANS-NFSM 2014), Reno, NV, Jun. 15–19, 2014.

Mei, Z.G., M. Stan, A.M. Yacout and J. Yang (2014). "Atomistic Study of the Effects of Point Defects and Xe Atoms on the Thermal Conductivity of UO_2." TMS Annual Meeting, San Diego, CA, Feb. 16–20, 2014.

Mei, Z.G., A.M. Yacout, Y.S. Kim, G.L. Hofman and M. Stan (2014). "Thermodynamic Stability of ZrN as Diffusion Barriers for UMo/Al Fuel." American Nuclear Society/Nuclear Fuels and Structural Materials Annual Meeting (ANS-NFSM 2014), Reno, NV, Jun. 15–19, 2014.

Stan, M., A. Larzelere, S. Johnson, D. Kothe, T. Allen and A. Siegel (2014). "Miscellaneous: Modeling and Simulation Coordination at DOE Office of Nuclear Energy." Nuclear Energy Advisory Committee Meeting, Washington, D.C., June 5, 2014.

Stan, M., Z.G. Mei, A.E. Thompson and C.M. Wolverton (2014). "EAM Insight into the Phase Stability of Alloys." TMS Annual Meeting San Diego, CA, Feb. 16–20, 2014.

Thompson, A.E., B. Meredig, M. Stan and C. Wolverton (2014). "Interatomic Potential for Accurate Phonons and Defects in UO_2." *Journal of Nuclear Materials* **446**(1-3): 155–162.*

2010-198

Deshmukh, S.A., G. Kamath, D.C. Mancini and S.K.R.S. Sankaranarayanan (2014). "Effect of Methanol/Water Mixtures on the Lower Critical Solution Temperature of Poly(N-isopropylacrylamide)." Proceedings of the 2013 MRS Fall Meeting, Boston, MA, Dec. 1–6, 2013, *Material Research Society Symposium Proceedings* **1622**: 25–30.*

Deshmukh, S.A., G. Kamath, D.C. Mancini and S.K.R.S. Sankaranarayanan (2014). "Effect of Methanol/Water Mixtures on the Lower Critical Solution Temperature of Poly(N-isopropylacrylamide)." 2013 MRS Fall Meeting, Boston, MA, Dec. 1–6, 2013.

Deshmukh, S.A., G. Kamath, D.C. Mancini and S.K.R.S. Sankaranarayanan (2014). "Meso-scale Simulations of Poly(N-isopropylacrylamide) Grafter Architectures." 2013 MRS Fall Meeting, Boston, MA, Dec. 1–6, 2013.

Deshmukh, S.A., G. Kamath, K.J. Suthar, D.C. Mancini and S.K.R.S. Sankaranarayanan (2014). "Non-equilibrium Effects Evidenced by Vibrational Spectra During the Coil-to-Globule Transition in Poly(N-isopropylacrylamide) Subjected to an Ultrafast Heating-cooling Cycle." *Soft Matter* **10**(10): 1462.*

2010-199

Hoefler, T., J. Dinan, D. Buntinas, P. Balaji, B. Barrett, R. Brightwell, W. Gropp, V. Kale and R. Thakur (2014). "MPI + MPI: A New Hybrid Approach to Parallel Programming with MPI Plus Shared Memory." *Computing* **95**(12): 1121–1136.*

Yang, C., W. Bland, P. Balaji and J. Mellor-Crummey (2014). "Portable, MPI-Interoperable Coarray Fortran." ACM SIGPLAN Symposium on Principles and Practice of Parallel Porgramming (PPoPP), Orlando, FL, Feb. 15–19, 2014.

Zhao, X., P. Balaji, W. Gropp and R. Thakur (2014). "MPI-Interoperable Generalized Active Messages." IEEE International Conference on Parallel and Distributed Systems (ICPADS), Seoul, Korea, Dec. 15–18, 2013.

Zhao, X., P. Balaji, W. Gropp and R. Thakur (2014). "Optimization Strategies for MPI-Interoperable Active Massages." IEEE International Conference on Scalable Computing and Communications (ScalCom), Chengdu, China, Dec. 21–22, 2013.

*Note: For information regarding projects listed here, see annual reports from previous years. *Indicates refereed publication*

2010-204

Iacocca, E., O. Heinonen, P.K. Muduli and J. Akerman (2014). "Generation Linewidth of Mode-hopping Spin Torque Oscillators." *Physical Review B* **89**(5).*

2011-012

Benmore, C.J. (2014). "Advanced X-ray Analytical Methods to Understand Structure and Properties and Risk." Discovering & Developing Molecules with Optimal ''Drug-Like'' Properties. **Series Volume 15:** pp. 263–283.*

Benmore, C.J. (2014). "Introducing Levitation Technology for the Production of Amorphous Drugs." 3rd Drug Formulation and Bioavailability Conference, Boston, MA, Jan. 27–29, 2014.

Weber, J.K.R., C.J. Benmore, A.N. Tailor, S.K. Tumber, J. Neuefeind, B. Cherry, J.L. Yarger, Q. Mou, W. Weber and S.R. Byrn (2014). "A Neutron-X-ray, NMR and Calorimetric Study of Glassy Probucol Synthesized using Containerless Techniques." *Chemical Physics* **424**: 89–92.*

2011-023

Haskel, D. (2014). "Recent Progress in High-Pressure Studies of Magnetism using Polarized X-ray Techniques." APS Users Meeting, Argonne, IL, May 12–16, 2014.

Jeffries, J.R., L.S.I. Veiga, G. Fabbris, D. Haskel, P. Huang, N.P. Butch, S.K. McCall, K. Holliday, Z. Jenei, Y. Xiao and P. Chow (2014). "Robust Ferromagnetism in the Compressed Permanent Magnet Sm_2Co_{17}." *Physical Review B* **90**(10).*

Laguna-Marco, M.A., G. Fabbris, N.M. Souza-Neto, S. Chikara, J.S. Schilling, G. Cao and D. Haskel (2014). "Different Response of Transport and Magnetic Properties of $BaIrO_3$ to Chemical and Physical Pressure." *Physical Review B* **90**(1).*

Mardegan, J.R.L., G. Fabbris, L.S.I. Viega, C. Adriano, M.A. Avila, D. Haskel and C. Giles (2014). "Pressure Induced Amorphization and Collapse of Magnetic Order in the Type-I Clathrate $Eu_8Ga_1Ge_{30}$." *Physical Review B* **88**(14): 144105.*

Mardegan, J.R.L., G. Fabbris, L.S.I. Viega, C. Adriano, M.A. Avila, D. Haskel and C. Giles (2014). "High Pressure Studies of Magnetism Using Polarized X-ray Techniques: Present and Future Workshop Extreme Conditions Experiments for Today and at Sirius." LNLS/CNPEM, Campinas, Brazil, March 13–14, 2014.

2011-038

Panwar, L.S., A.M. Aji, J. Meng, P. Balaji and W.-C. Feng (2014). "Online Performance Projection for Clusters with Heterogeneous GPUs." Proceedings of the 19th IEEE International Conference on Parallel and Distributed Systems (ICPADS), Seoul, Korea, Dec. 15–18, 2013.*

2011-060

Lopez-Encarnacion, J.M., K.K. Tanabe, M.J. Johnson and J. Jellinek (2014). "Characterizing Metal Coordination Environments in Porous Organic Polymers: A Joint Density Functional Theory and Experimental Infrared Spectroscopy Study." *Chemistry* **19**(41): 13646–13651.*

2011-063

Li, M.M., L.Y. Wang and J.D. Almer (2014). "Dislocation Evolution During Tensile Deformation in Ferritic-martensitic Steels Revealed by High-energy X-rays." *Acta Materialia* **76**: 381–393.*

Wang, L., M. Li and J. Almer (2014). "*In situ* Characterization of Grade 92 Steel During Tensile Deformation Using Wide Angle and Small Angle X-ray Scattering." TMS Annual Meeting 2014, San Diego, CA, Feb. 16–20, 2014.

Wang, L.Y., M.M. Li and J. Almer (2014). "Investigation of Deformation and Microstructural Evolution in Grade 91 Ferritic-martensitic Steel by *in situ* High-energy X-rays." *Acta Materialia* **62**: 239–249.*

*Note: For information regarding projects listed here, see annual reports from previous years. *Indicates refereed publication*

2011-071

Jiang, Z., Z. Zhong, M.C. Wingert, J. Strzalka, T. Sun, H.H. Wang, J. Wang and R. Chen (2014). "Enhanced Thermal Conductivity in Polymer Nanofibers." Fiber Society Fall 2013 Conference, Clemson, SC, Oct. 23–25, 2013.

Zhong, Z.X., M.C. Wingert, J. Strzalka, H.H. Wang, T. Sun, J. Wang, R.K. Chen and Z. Jiang (2014). "Structure-induced Enhancement of Thermal Conductivities in Electrospun Polymer Nanofibers." *Nanoscale* **6**(14): 8283–8291.*

2011-083

Avci, S., O. Chmaissem, J.M. Allred, S. Rosenkranz, I. Eremin, A.V. Chubukov, D.E. Bugaris, D.Y. Chung, M.G. Kanatzidis, J.P. Castellan, J.A. Schlueter, H. Claus, D.D. Khalyavin, P. Manuel, A. Daoud-Aladine and R. Osborn (2014). "Magnetically Driven Suppression of Nematic Order in an Iron-based Superconductor." *Nature Communications* **5**: 3845.*

Drichko, N., R. Beyer, E. Rose, M. Dressel, J.A. Schlueter, S.A. Turunova, E.I. Zhilyaeva and R.N. Lyubovskaya (2014). "Metallic State and Charge-order Metal-insulator Transition in the Quasi-two-dimensional Conductor κ-(BEDT-TTF)$_2$Hg(SCN)$_2$Cl." *Physical Review B* **89**: 075133.*

Gezo, J., T.-K. Lui, B. Wolin, C.P. Slichter, R. Giannetta and J.A. Schlueter (2014). "Stretched Exponential Spin Relaxation in Organic Superconductors." *Physical Review B* **88**(14): 140504(R).*

Girlando, A., M. Masino, J.A. Schlueter, N. Drichko, S. Kaiser and M. Dressel (2014). "Charge-order Fluctuations and Superconductivity in Two-dimensional Organic Metals." *Physical Review B* **89**(17).*

Lancaster, T., P.A. Goddard, S.J. Blundell, F.R. Foronda, S. Ghannadzadeh, J.S. Moller, P.J. Baker, F.L. Pratt, C. Baines, L. Huang, J. Wosnitza, R.D. McDonald, K.A. Modic, J. Singleton, C.V. Topping, T.A. W. Beale, F. Xiao, J.A. Schlueter, A.M. Barton, R.D. Cabrera, K.E. Carreiro, H.E. Tran and J.L. Manson (2014). "Controlling Magnetic Order and Quantum Disorder in Molecule-Based Magnets." *Physical Review Letters* **112**(20).*

Lang, M., P. Lunkenheimer, J. Muller, A. Loidl, B. Hartmann, N.H. Hoang, E. Gati, H. Schubert and J.A. Schlueter (2014). "Multiferroicity in the Mott Insulating Charge-transfer Salt κ-(BEDT-TTF)$_2$Cu[N(CN)$_2$]Cl." *IEEE Transactions on Magnetics* **50**(6): 2700107.*

Musfeldt, J.L., T.V. Brinzari, J.A. Schlueter, J.L. Manson, A.P. Litvinchuk and Z. Liu (2014). "Pressure-induced Local Lattice Distortions in α-Co[N(CN)$_2$]$_2$." *Inorganic Chemistry* **52**(24): 14148–14154.*

O'Neal, K.R., T.V. Brinzari, J.B. Wright, C. Ma, S. Giri, J.A. Schlueter, Q. Wang, P. Jena, Z. Liu and J.L. Musfeldt (2014). "Pressure-induced Magnetic Crossover Driven by Hydrogen Bonding in CuF$_2$(H$_2$O)$_2$(3-Chloropyridine)." *Scientific Reports* **4**: 6054.*

Tomic, S., M. Pinteric, T. Ivek, K. Sedlmeier, R. Beyer, D. Wu, J.A. Schlueter, D. Schweitzer and M. Dressel (2014). "Magnetic Ordering and Charge Dynamics in κ-(BEDT-TTF)$_2$Cu[N(CN)$_2$]Cl." *Journal of Physics: Condensed Matter* **25**(43): 436004.*

Vaz, M.G., R.A. Cassaro, H. Akpinar, J.A. Schlueter, P.M. Lahti and M.A. Novak (2014). "A Cobalt Pyrenylnitronylnitroxide Single-chain Magnet with High Coercivity and Record Blocking Temperature." *Chemistry* **20**(18): 5460–5467.*

2011-101

Manandhar, K., M. Trenary, S. Otani and P. Zapol (2014). "Dissociation of Trimethylgallium on the ZrB$_2$(0001) Surface." *Journal of Vacuum Science & Technology A* 31(**6**): 061405.*

2011-110

Contalbrigo, M., N. Baltzell, F. Benmokhtar, L. Barion, E. Cisbani, A. El Alaoui, K. Hafidi, M. Hoek, V. Kubarovsky, L. Lagamba, V. Lucherini, R. Malaguti, M. Mirazita, R. Montgomery, A. Movsisyan, P. Musico, D. Orecchini, A. Orlandi, L.L. Pappalardo, S. Pereira, R. Perrino, J. Phillips, S. Pisano, P. Rossi, S. Squerzanti, S. Tomassini, M. Turisini and A. Viticchiè (2014). "The Large-area Hybrid-optics CLAS12 RICH Detector: Tests of Innovative Components." *Nuclear Instruments and Methods in Physics Research Section A: Accelerators, Spectrometers, Detectors and Associated Equipment* **766**: 22–27.*

*Note: For information regarding projects listed here, see annual reports from previous years. *Indicates refereed publication*

2011-129

Drewniak, B.A., U. Mishra, J. Song, J. Prell and V.R. Kotamarthi (2014). "Modeling the Impact of Agricultural Land Use and Management on U.S. Carbon Budgets." *Biogeosciences Discussions* **11**: 13675–13698.*

2011-134

Kalaji, A., S. Skanthakumar, M.G. Kanatzidis, J.F. Mitchell and L. Soderholm (2014). "Changing Hafnium Speciation in Aqueous Sulfate Solutions: A High-energy X-ray Scattering Study." *Inorganic Chemistry* **53**(12): 6321–6328.*

Kalaji, A. and L. Soderholm (2014). "A Novel Nonanuclear Hafnium Oxide-Hydroxide-Sulphate Cluster Crystallized from Aqueous Solution." *Chemical Communications* **50**(8): 997–999.*

Shoemaker, D.P., Y.-J. Hu, D.Y. Chung, G.J. Halder, P.J. Chupas, L. Soderholm, J.F. Mitchell and M.G. Kanatzidis (2014). "*In situ* Studies of a Platform for Metastable Inorganic Crystal Growth and Materials Discovery." *Proceedings of the National Academy of Sciences of the United States of America* **111**(30): 10922–10927.*

2011-147

Flores, B., S. Ciocys, V. Yefremenko, J. Pearson, E. Rozhkova and V. Novosad (2014). "Facile Fabrication of Magnetic Nanomaterials for Biomedical Applications." 2013 Annual Biomedical Research Conference for Minority Students (ABRCMS), Nashville, TN, Nov. 13–16, 2013.

Karapetrov, G., P. Gach, E. Rozhkova and V. Novosad (2014). "Understanding the Cytotoxicity of Permalloy Miscodisks." 2013 American Chemical Society Western Regional Meeting, Santa Clara, CA, Oct. 3–6, 2013.

2011-149

Mak, R., M. Lerotic, H. Fleckenstein, S. Vogt, S.M. Wild, S. Leyffer, Y. Sheynkin and C.J. Jacobsen (2014). "Non-Negative Matrix Analysis for Effective Feature Extraction in X-Ray Spectromicroscopy." *Faraday Discussions* **171**.*

2011-170

Butler, L.G., S. Marathe, L. Assoufid, K. Fezzaa, B. Olatinwo and K. Ham (2014). "Comparison of Stepped and Single-Shot Grating-Based Interferometry for Differential Phase Contrast Imaging of Flame Retardant/Polymer Blends." International Workshop on X-ray and Neutron Phase Imaging with Gratings, Garmisch, Germany, Jan. 21–24, 2014.

Marathe, S., X. Shi, N. Kujala, M. Wojcik, A. Khounsary, J. Qian, A. Macrander and L. Assoufid (2014). "Development of Single Grating X-ray Talbot Interferometer as a Feedback Loop Sensor Element of an Adaptive X-ray Mirror System." SPIE Conference 2014, San Diego, CA, Aug. 17–21, 2014.

Marathe, S., X. Shi, M. Wojcik, N. Kujala, R. Divan, D.C. Mancini, S. Narayanan, A. Sandy, A. Macrander and L. Assoufid (2014). "Characterization of X-ray Beam Coherence Along Multiple Directions Using Checkerboard and Circular Type Phase-grating Interferometers." APS/CNM/EMC Users Meeting, Argonne National Laboratory, Argonne, IL, May 12–15, 2014.

Marathe, S., L. Assoufid, X. Xiao, K. Ham, W.W. Johnson and L.G. Butler (2014). "Improved Algorithm for Processing Grating-Based Phase Contrast Interferometry Image Sets." *Review of Scientific Instruments* **85**(1): 013704.*

Marathe, S., X. Shi, M. Wojcik, N. Kujala, A. Macrander and L. Assoufid (2014). "Single Phase Grating Interferometers for Probing X-ray Beam Coherence Area." Coherence 2014 Conference, Northwestern University, Evanston, IL, Sept. 2–5, 2014.

Marathe, S., X.B. Shi, M.J. Wojcik, N.G. Kujala, R. Divan, D.C. Mancini, A.T. Macrander and L. Assoufid (2014). "Probing Transverse Coherence of X-ray Beam With 2-D phase Grating Interferometer." *Optics Express* **22**(12): 14041–14053.*

Shi, X., S. Marathe, M.J. Wojcik, N.G. Kujala, A.T. Macrander and L. Assoufid (2014). "Circular Grating Interferometer for Mapping Transverse Coherence Area of X-ray Beams." *Applied Physics Letters* **105**(4): 0411161–0411165.*

*Note: For information regarding projects listed here, see annual reports from previous years. *Indicates refereed publication*

Wen, H., A.A. Gomella, A. Patel, S.K. Lynch, N.Y. Morgan, S.A. Anderson, E.E. Bennett, X. Xiao, C. Liu and D.E. Wolfe (2014). "Subnanoradian X-ray Phase-contrast Imaging Using a Far-field Interferometer of Nanometric Phase Gratings." *Nature Communications* **4**: 2659.*

2011-188

Chang, S.H., N. Danilovic, K.C. Chang, R. Subbaraman, A.P. Paulikas, D.D. Fong, M.J. Highland, P.M. Baldo, V.R. Stamenkovic, J.W. Freeland, J.A. Eastman and N.M. Markovic (2014). "Functional Links Between Stability and Reactivity of Strontium Ruthenate Single Crystals During Oxygen Evolution." *Nature Communications* **5**: 4191.*

Lee, J.H., G. Luo, I.C. Tung, S.H. Chang, Z. Luo, M. Malshe, M. Gadre, A. Bhattacharya, S.M. Nakhmanson, J.A. Eastman, H. Hong, J. Jellinek, D. Morgan, D.D. Fong and J.W. Freeland (2014). "Dynamic Layer Rearrangement During Growth of Layered Oxide Films by Molecular Beam Epitaxy." *Nature Materials* **13**(9): 879–883.*

2011-193

Cheng, L., C. Yin, F. Mehmood, B. Liu, J. Greeley, S. Lee, B. Lee, S. Seifert, R.E. Winans, D. Teschner, R. Schlögl, S. Vajda and L.A. Curtiss (2014). "Reaction Mechanism for Direct Propylene Epoxidation by Alumina-Supported Silver Aggregates: The Role of the Particle/Support Interface." *ACS Catalysis* **2014**(4): 32–39.*

2011-199

Chang, K.B., L. Frazer, J.J. Schwartz, J.B. Ketterson and K.R. Poeppelmeier (2014). "The Removal of Copper Vacancies in Cuprous Oxide Single Crystals Grown by the Floating Zone Method." *Crystal Growth & Design* **13**(11): 4914–4922.*

Frazer, L., R. Schaller, K. Chang, J. Ketterson and K. Poeppelmeier (2014). "Third-harmonic Generation in Cuprous Oxide: Efficiency Determination." *Optics Letters* **39**(3): 618–621.*

2011-216

Manoharan, V.S., R. Kotamarthi, Y. Feng and M.P. Cadeddu (2014). "Increased Absorption by Coarse Aerosol Particles Over the Gangetic-Himalayan Region." *Atmospheric Chemistry and Physics* **14**(3): 1159–1165.*

Feng, Y., V.R. Kotamarthi and V.S. Manoharan (2014). "Direct and Semi-direct Radiative Responses to Observation-Constrained Aerosol Absorption Over South Asia." 2013 American Geophysical Union Fall Meeting, San Francisco, CA, Dec. 9–13, 2013.

2012-052

Brik, M.G., C.G. Ma, H.B. Liang, H.Y. Ni and G.K. Liu (2014). "Theoretical Analysis of Optical Spectra of Ce^{3+} in Multi-sites Host Compounds." *Journal of Luminescence* **152**: 203–205.*

Liu, G.K. (2014). "A Degenerate Model of Vibronic Transitions for Analyzing 4f-5d Spectra." *Journal of Luminescence* **152**: 7–10.*

Zhai, D.Y., L.X. Ning, Y.C. Huang and G.K. Liu (2014). "Ce-O Covalence in Silicate Oxyapatites and Its Influence on Luminescence Dynamics." *Journal of Physical Chemistry C* **118**(29): 16051–16059.*

Liu, G., D. Zhai and L. Ning (2014). "f-Elements Photophysics Influenced by Ion-ligand Coordination." 41st International Conference on Coordination Chemistry (ICCC-41), Singapore, Singapore, July 21–25, 2014.

2012-203

Fridlyand, A., S.S. Goldsborough, K. Brezinsky, S.S. Merchant and W.H. Green (2014). "Influence of the Double Bond Position on the Oxidation of Decene Isomers at High Pressures and Temperatures." Proceedings of the Combustion Institute International Symposium on Combustion, San Francisco, CA, Aug. 3–8, 2014, **35**(1): 333–340.*

*Note: For information regarding projects listed here, see annual reports from previous years. *Indicates refereed publication*

2013-114

Jaski, M., R. Dejus, B. Deriy, E. Moog, I. Vasserman, J. Wang, A. Xiao and E. Gluskin (2014). "Fast-switching Variably Polarizing Undulator." 2013 North American Particle Accelerator Conference (NA-PAC 2013), Pasadena, CA, Sep. 29–Oct. 4, 2013.

2013-129

Kim, Y.K., O. Krupin, J.D. Denlinger, A. Bostwick, E. Rotenberg, Q. Zhao, J.F. Mitchell, J.W. Allen and B.J. Kim (2014). "Fermi Arcs in a Doped Pseudospin-1/2 Heisenberg Antiferromagnet." *Science* **345**(6193): 187–190.*

2013-143

Borland, M., G. Decker, L. Emery, V. Sajaev, Y. Sun and A. Xiao (2014). "Lattice Design Challenges for Fourth-Generation Storage Ring Light Sources." *Journal of Synchrotron Radiation* **21**(Pt 5): 912–936.*

*Note: For information regarding projects listed here, see annual reports from previous years. *Indicates refereed publication*

LDRD

Index by Project Number

ANNUAL REPORT

2014

Index by Project Number

2011-210-R3 165
2011-213-R3 48
2011-214-R3 49
2011-217-R3 121
2012-012-R2 3
2012-015-R2 122
2012-016-R2 81
2012-061-R2 4
2012-072-R2 5
2012-074-R2 82
2012-087-R2 7
2012-114-R2 50
2012-180-R2 9
2012-181-R2 11
2012-202-R2 51
2012-204-R2 124
2012-205-R2 83
2012-206-R2 85
2012-208-R2 70
2012-209-R2 125
2013-013-R1 12
2013-016-R1 13
2013-022-R1 15
2013-035-R1 16
2013-036-R1 18
2013-063-R1 19
2013-070-R1 21
2013-080-R1 22
2013-096-R1 24
2013-100-R1 25
2013-111-R1 108
2013-116-R1 26
2013-148-R1 72
2013-152-R1 158
2013-154-R1 74
2013-156-R1 75
2013-165-R1 104
2013-168-R1 109
2013-171-R1 150
2013-173-R1 151
2013-177-R1 86
2013-178-R1 153
2013-184-R1 127
2013-194-R1 88
2013-199-R1 53
2013-202-R1 128
2013-206-R1 54
2013-208-R1 56
2013-212-R1 57
2013-213-R1 59
2013-215-R1 130
2013-216-R1 131
2013-218-R1 60
2013-219-R1 132
2014-004-N0 28
2014-018-N0 29
2014-019-N0 30
2014-023-N0 31
2014-025-N0 32
2014-034-N0 34
2014-046-N0 35
2014-051-N0 37
2014-054-N0 38
2014-077-N0 39

Index by Project Number

2014-081-N0 40
2014-084-N0 42
2014-095-N0 43
2014-108-N0 45
2014-120-N0 77
2014-121-N0 133
2014-122-N0 111
2014-127-N0 113
2014-128-N0 135
2014-129-N0 136
2014-130-N0 138
2014-132-N0 90
2014-133-N0 139
2014-134-N0 114
2014-137-N0 115
2014-139-N0 141
2014-141-N0 91
2014-145-N0 93
2014-151-N0 142
2014-157-N0 94
2014-160-N0 61
2014-161-N0 144
2014-162-N0 95
2014-163-N0 62
2014-166-N0 63
2014-167-N0 64
2014-169-N0 78
2014-174-N0 65
2014-175-N0 117
2014-177-N0 160
2014-181-N0 66
2014-182-N0 67
2014-183-N0 96
2014-184-N0 118
2014-185-N0 167
2014-187-N0 97
2014-188-N0 99
2014-189-N0 100
2014-190-N0 162
2014-191-N0 145
2014-192-N0 147
2014-193-N0 101
2014-194-N0 155

LDRD

Author Index

ANNUAL REPORT

2014

Author Index

Abouimrane, Ali 2012-012-R2 3
Alexeev, Yuri 2013-212-R1 57
Allcock, William 2014-163-N0 62
Almer, Jonathan D. 2013-152-R1 158
Almer, Jonathan D. 2014-121-N0 133
Amine, Khalil 2012-012-R2 3
Anitescu, Mihai 2012-209-R2 125
Antonopoulos, Dionysios A. 2012-074-R2 82
Antonopoulos, Dionysios A. 2013-070-R1 21
Antonopoulos, Dionysios A. 2013-177-R1 86
Antonopoulos, Dionysios A. 2014-141-N0 91
Awschalom, David D. 2014-191-N0 145
Babnigg, Gyorgy 2014-108-N0 45
Babnigg, Gyorgy 2014-157-N0 94
Bair, Raymond 2013-184-R1 127
Beckman, Peter 2014-160-N0 61
Binkowski, Andrew 2014-157-N0 94
Botterud, Audun 2014-120-N0 77
Boyanov, Maxim 2013-070-R1 21
Boyanov, Maxim 2014-162-N0 95
Cai, Zhonghou 2013-036-R1 18
Campos, Edwin 2014-167-N0 64
Cappello, Franck 2014-181-N0 66
Carlstrom, John 2013-080-R1 22
Catlett, Charlie 2011-214-R3 49
Catlett, Charlie 2013-206-R1 54
Catlett, Charlie 2013-218-R1 60
Catlett, Charlie 2014-167-N0 64
Chan, Maria 2014-161-N0 144
Chang, Clarence 2013-080-R1 22
Chang, Clarence 2013-219-R1 132
Chang, Yoon Il 2014-190-N0 162
Chen, Lin X. 2014-046-N0 35
Chen, Xing 2013-156-R1 75
Chen, Xing 2014-169-N0 78
Chen, Zonghai 2014-121-N0 133
Chien, Andrew A. 2012-202-R2 51
Constantinescu, Emil M. 2014-120-N0 77
Conway, Zachary 2014-122-N0 111
Cook, David 2014-132-N0 90
Curtiss, Larry A. 2012-209-R2 125
Darling, Seth B. 2014-187-N0 97
Davis, Michael 2014-161-N0 144
Davis, Michael J. 2013-148-R1 72
De Carlo, Francesco 2013-168-R1 109
de Pablo, Juan J. 2013-184-R1 127
de Pablo, Juan J. 2014-166-N0 63
DeGottardi, Wade 2014-095-N0 43
Demars, Thomas 2014-004-N0 28
Desai, Narayan 2013-208-R1 56
Dixon, David 2014-139-N0 141
Djurcic, Zelimir 2014-023-N0 31
Drewniak, Beth 2014-167-N0 64
Eastman, Jeffrey A. 2014-151-N0 142
Elam, Jeffrey W. 2013-154-R1 74
Elam, Jeffrey W. 2014-133-N0 139
Elam, Jeffrey W. 2014-151-N0 142
Elam, Jeffrey W. 2014-187-N0 97
Ellis, Ross J. 2014-004-N0 28
Erdemir, Ali 2012-072-R2 5
Erdemir, Ali 2013-022-R1 15
Eryilmaz, Osman 2013-022-R1 15
Fan, Zhaosheng 2012-205-R2 83
Fang, Lei 2014-095-N0 43

Author Index (cont.)

Feng, Yan 2014-084-N0 42
Ferrier, Nicola 2014-132-N0 90
Ferrier, Nicola 2014-160-N0 61
Ferrier, Nicola 2014-174-N0 65
Fischer, Paul 2012-114-R2 50
Fischer, Paul 2014-177-N0 160
Fong, Dillon D. 2014-129-N0 136
Foster, Ian T. 2013-165-R1 104
Foster, Ian T. 2013-168-R1 109
Foster, Ian T. 2014-182-N0 67
Fry, Harry 2012-181-R2 11
Fuoss, Paul H. 2014-134-N0 114
Fuoss, Paul H. 2014-151-N0 142
Gallagher, Kevin 2014-120-N0 77
Galli, Giulia 2014-192-N0 147
Garcia Martinez, Marta 2013-148-R1 72
Ghate, Virendra P. 2014-183-N0 96
Ghate, Virendra P. 2014-193-N0 101
Gilbert, Jack A. 2012-016-R2 81
Gilbert, Jack A. 2012-074-R2 82
Gilbert, Jack A. 2014-145-N0 93
Gilbert, Jack A. 2014-189-N0 100
Gog, Thomas 2014-127-N0 113
Gray, Stephen K. 2012-114-R2 50
Gray, Stephen K. 2014-161-N0 144
Gregar, Joseph 2014-121-N0 133
Guest, Jeffrey R. 2013-035-R1 16
Gulotty, Richard 2013-096-R1 24
Guzowski, Leah 2013-218-R1 60
Habib, Salman 2011-213-R3 48
Habib, Salman 2013-165-R1 104
Hamada, Yuki 2014-132-N0 90
Hamada, Yuki 2014-160-N0 61
Harder, Ross J. 2014-134-N0 114
Harder, Ross J. 2014-151-N0 142
Harkay, Katherine 2013-096-R1 24
Heald, Steve 2014-133-N0 139
Heinonen, Olle 2012-015-R2 122
Heinonen, Olle 2012-209-R2 125
Heinonen, Olle 2014-018-N0 29
Heinonen, Olle 2014-128-N0 135
Heinonen, Olle 2014-166-N0 63
Heitmann, Katrin 2011-213-R3 48
Heitmann, Katrin 2014-019-N0 30
Henry, Christopher 2013-194-R1 88
Henry, Christopher 2014-145-N0 93
Hereld, Mark 2014-174-N0 65
Highland, Matthew J. 2013-036-R1 18
Highland, Matthew J. 2014-134-N0 114
Highland, Matthew J. 2014-151-N0 142
Ho Kim, Jung 2014-127-N0 113
Hoffmann, Axel 2013-016-R1 13
Hoffmann, Axel 2014-018-N0 29
Hoffmann, Axel 2014-054-N0 38
Holt, Martin V. 2014-151-N0 142
Hong, Hawoong 2014-081-N0 40
Hong, Seungbum 2013-063-R1 19
Hong, Seungbum 2014-081-N0 40
Hruszkewycz, Stephan O. 2014-134-N0 114
Hruszkewycz, Stephan O. 2014-151-N0 142
Huang, Xianrong 2014-127-N0 113
Ignacio-de Leon, Patricia 2013-156-R1 75
Ivanyushenkov, Yury 2014-137-N0 115
Ivanyushenkov, Yury 2014-184-N0 118

Author Index (cont.)

Jacob, Robert 2014-167-N0 64
Jacobsen, Chris 2013-168-R1 109
Jacobsen, Chris 2014-162-N0 95
Jastrow, Julie 2012-074-R2 82
Jastrow, Julie 2014-162-N0 95
Jedrzejczak, Robert 2014-108-N0 45
Jedrzejczak, Robert 2014-157-N0 94
Jiang, Wei 2014-034-N0 34
Jiang, Wei 2014-188-N0 99
Joachimiak, Andrzej 2013-194-R1 88
Joachimiak, Andrzej 2014-108-N0 45
Joachimiak, Andrzej 2014-157-N0 94
Johnson, Christopher 2014-185-N0 167
Jung, Il Woong 2013-036-R1 18
Kaminski, Michael 2013-178-R1 153
Kariuki, Nancy 2012-180-R2 9
Karpeyev, Dmitry 2012-015-R2 122
Karpeyev, Dmitry 2012-209-R2 125
Karpeyev, Dmitry 2014-128-N0 135
Karpeyev, Dmitry 2014-166-N0 63
Kasa, Matthew 2014-184-N0 118
Keahey, Katarzyna 2014-160-N0 61
Keceli, Murat 2014-139-N0 141
Kemner, Kenneth M. 2012-074-R2 82
Kemner, Kenneth M. 2013-070-R1 21
Kemner, Kenneth M. 2013-177-R1 86
Kemner, Kenneth M. 2014-145-N0 93
Kemner, Kenneth M. 2014-162-N0 95
Klug, Jeffrey 2014-133-N0 139
Knight, Christopher J. 2013-202-R1 128
Koritarov, Tamara 2012-181-R2 11
Kotamarthi, Rao 2014-084-N0 42
Kotamarthi, Rao 2014-167-N0 64
Krause, Theodore 2014-130-N0 138
Krummel, John 2012-206-R2 85
Kumaran, Kalyan 2013-213-R1 59
Kustom, Robert 2013-111-R1 108
Kwok, Wai-Kwong 2014-095-N0 43
Kwok, Wai-Kwong 2014-025-N0 32
Lai, Barry 2014-084-N0 42
Larsen, Peter 2012-016-R2 81
Lee, Jonghun 2014-077-N0 39
Leyffer, Sven 2013-168-R1 109
Leyffer, Sven 2013-206-R1 54
Li, Meimei 2013-152-R1 158
Libera, Joseph 2013-154-R1 74
Lin, Xiao-Min 2014-077-N0 39
Lin, Xiao-Min 2013-035-R1 16
Liu, Di-Jia 2014-051-N0 37
Liu, Di-Jia 2014-130-N0 138
Liu, Wenjun 2014-134-N0 114
Longman, Douglas E. 2013-148-R1 72
Lu, Zheng-Tian 2014-188-N0 99
Mancini, Derrick C. 2013-215-R1 130
Mane, Anil 2013-154-R1 74
Marin, Oana 2014-177-N0 160
Martinez-Moyano, Ignacio 2014-194-N0 155
Martinson, Alex B.F. 2013-100-R1 25
Maser, Jörg 2014-134-N0 114
Matamala, Roser 2012-074-R2 82
Matamala, Roser 2014-132-N0 90
Matveev, Konstantin 2014-095-N0 43
Mertz, Carol 2013-178-R1 153
Merzari, Elia 2014-177-N0 160

Author Index (cont.)

Meyer, Folker 2014-141-N0 91
Michalska, Karolina 2014-108-N0 45
Michalska, Karolina 2014-157-N0..... 94
Miller, Dean 2012-061-R2..... 4
Miller, Jeffery 2014-051-N0 37
Miller, Jeffery 2014-130-N0 138
Miller, R. Michael 2012-074-R2 82
Min, Misun 2012-114-R2..... 50
Mishra, Umakant 2012-206-R2 85
Mootz, Joseph 2014-108-N0 45
Morozov, Vitali 2013-213-R1..... 59
Mueller, Peter 2014-034-N0 34
Munson, Todd 2013-168-R1..... 109
Murphy-Olson, Daniel 2013-208-R1..... 56
Myers, Debbie 2012-180-R2..... 9
Narayanan, Suresh 2013-168-R1..... 109
Narayanan, Suresh 2014-077-N0..... 39
Nassiri, Alireza 2013-111-R1..... 108
Nassiri, Alireza 2014-122-N0 111
Nealey, Paul F. 2013-216-R1.....131
Nocek, Boguslaw 2014-157-N0..... 94
North, Michael 2014-194-N0 155
Novosad, Valentyn 2013-080-R1..... 22
Novosad, Valentyn 2013-219-R1.....132
Nowicki, Tammi 2012-180-R2..... 9
O'Brien, Sarah 2013-070-R1..... 21
O'Brien, Sarah 2014-145-N0 93
O'Brien, Sarah 2014-162-N0 95
O'Loughlin, Edward J. 2012-074-R2 82
O'Loughlin, Edward J. 2013-070-R1..... 21
O'Loughlin, Edward J. 2013-177-R1 86
O'Loughlin, Edward J. 2014-145-N0 93
O'Loughlin, Edward J. 2014-162-N0 95
Obabko, Aleksandr 2014-177-N0..... 160
Ocola, Leonidas 2013-178-R1.....153
Ogata, Craig M. 2014-175-N0.....117
Okasinski, John 2014-121-N0 133
Osborn, Ray 2013-165-R1..... 104
Ostroumov, Peter 2014-122-N0 111
Overbeek, Ross 2013-194-R1..... 88
Paley, Jonathan M. 2014-023-N0 31
Pelliccione, Christopher 2012-087-R2.....7
Pellin, Michael J. 2013-100-R1..... 25
Pellin, Michael J. 2013-116-R1..... 26
Pellin, Michael J. 2013-152-R1..... 158
Pellin, Michael J. 2014-133-N0 139
Pelton, Matthew 2013-035-R1..... 16
Peterka, Thomas 2013-168-R1..... 109
Phatak, Charudatta 2013-063-R1..... 19
Pokkuluri, P. Raj 2013-013-R1..... 12
Proslier, Thomas 2013-080-R1..... 22
Proslier, Thomas 2013-111-R1..... 108
Proslier, Thomas 2014-133-N0 139
Rajh, Tijana 2012-181-R2..... 11
Ramirez, Giovanni 2013-022-R1..... 15
Ratcliff, Laura E. 2013-199-R1..... 53
Reininger, Ruben 2014-162-N0 95
Ren, Yang 2014-121-N0 133
Romero, Nichols A. 2013-199-R1..... 53
Romero, Nichols A. 2014-128-N0 135
Rosenberg, Richard 2014-129-N0 136
Roux, Benoit 2014-161-N0 144
Rozhkova, Elena A. 2013-173-R1 151
Sandy, Alec 2014-077-N0..... 39

Author Index (cont.)

Sankaran, Rajesh 2011-214-R3 49
Sankaran, Rajesh 2014-160-N0 61
Sankaran, Rajesh 2014-167-N0 64
Sankaranarayanan, Subramanian 2014-161-N0 144
Schabacker, Daniel 2013-171-R1 150
Schabacker, Daniel 2013-173-R1 151
Schaller, Richard D. 2013-173-R1 151
Schiffer, Marianne 2013-013-R1 12
Schlepuetz, Christian 2014-133-N0 139
Schwarz, Nicholas 2013-168-R1 109
Seaver, Samuel 2013-194-R1 88
Sereno, Nicholas 2013-096-R1 24
Shenai, Krishna 2012-208-R1 70
Shevchenko, Elena V. 2013-173-R1 151
Singh, Dileep 2012-087-R2 7
Sivaramakrishnan, Raghu 2013-148-R1 72
Snyder, Seth 2014-189-N0 100
Som, Sibendu 2013-148-R1 72
Stacey, Craig 2014-163-N0 62
Stan, Marius 2012-209-R2 125
Stan, Marius 2013-152-R1 158
Stols, Lucy 2013-171-R1 150
Sumant, Anirudha V. 2012-072-R2 5
Sumant, Anirudha V. 2013-096-R1 24
Sumant, Anirudha V. 2013-178-R1 153
Sun, Yugang 2014-121-N0 133
Sydelko, Pamela 2014-194-N0 155
te Velthuis, Suzanne G.E. 2012-204-R2 124
te Velthuis, Suzanne G.E. 2014-054-N0 38
Tentner, Adrian 2014-177-N0 160
Thimmapuram, Prakash 2014-120-N0 77
Timofeeva, Elena V. 2012-087-R2 7
Tirrell, Matthew 2011-217-R3 121
Tischler, Jonathan Z. 2014-129-N0 136
Tuecke, Steven 2014-182-N0 67
Uckun, Canan 2014-120-N0 77
Urgun Demirtas, Meltem 2013-156-R1 75
Urgun-Demirtas, Meltem 2014-189-N0 100
Vajda, Stefan 2011-210-R3 165
Vázquez-Mayagoitia, Álvaro A. 2013-199-R1 53
Vázquez-Mayagoitia, Álvaro A. 2013-212-R1 57
Vázquez-Mayagoitia, Álvaro A. 2014-139-N0 141
Vegendla, Prasad 2014-177-N0 160
Vishwanath, Venkatatram 2013-213-R1 59
Vogt, Stefan 2013-168-R1 109
Vogt, Stefan 2014-084-N0 42
von Lilienfeld, Anatole 2013-212-R1 57
Voth, Gregory A. 2013-202-R1 128
Wagner, Albert 2014-139-N0 141
Wang, Chun-xi 2013-096-R1 24
Wang, Gensheng 2013-080-R1 22
Wang, Gensheng 2013-219-R1 132
Wang, Xiaoping 2012-180-R2 9
Wardle, Kent 2014-177-N0 160
Welland, Michael 2012-015-R2 122
Welp, Ulrich 2014-137-N0 115
Wen, Haidan 2013-036-R1 18
Wild, Stefan 2013-168-R1 109
Wilton, Rose 2013-171-R1 150
Wilton, Rosemarie 2013-013-R1 12
Wilton, Rosemarie 2013-173-R1 151
Winans, Randall 2014-130-N0 138
Wolf, Dieter 2012-209-R2 125
Wu, Man 2014-167-N0 64

Author Index (cont.)

Xia, Fangfang 2013-194-R1 88

Yacout, Abdellatif 2013-116-R1 26

Yacout, Abdellatif 2013-152-R1 158

Yanguas Gil, Angel 2014-133-N0 139

Yanguas Gil, Angel 2014-151-N0 142

Yanguas-Gil, Angel 2013-154-R1 74

Yefremenko, Volodymyr 2013-080-R1 22

Yefremenko, Volodymyr 2013-219-R1 132

Yun, Di 2013-152-R1 158

Zapol, Peter 2014-128-N0 135

Zapol, Peter 2014-139-N0 141

Zapol, Peter 2014-151-N0 142

Zappala, Jake 2014-034-N0 34

Zhang, Yao 2013-213-R1 59

Zholents, Alexander 2014-122-N0 111

Zhong, Xiaoliang 2014-128-N0 135

LDRD

FY 2015 New Start Projects

ANNUAL REPORT

2014

LDRD Projects Begun in FY 2015 (as of March 10, 2015)

Project Number	Project Title	Lead Investigator, Division
2015-015-N0	Detection of Dark Matter Directionality by Means of Columnar Recombination	Richard Talaga, HEP
2015-078-N0	Josephson Plasma Wave-Based Ultra-High-Frequency Electronics	Alexei Koshelev, MSD
2015-091-N0	Next-Generation Natural Gas Adsorbent through Rational Design and Modeling	Di-Jia Liu, CSE
2015-096-N0	Understanding Atomic Scale Uranium Interactions under Severe Accident Conditions	Chris Benmore, XSD
2015-121-N0	Development of Advanced VO2 Nano-Composite Thermochromic Materials for High Performance Smart Windows	Jie Li, NE
2015-124-N0	Incorporating Fungal and Bacterial Community Metabolisms to Improve Carbon Cycle Predictions of Earth System Models	Zhaosheng Fan, BIO
2015-129-N0	Economic and Technical Aspects of Nuclear Energy Competitiveness in the Current U.S. Deregulated Electricity Markets	Francesco Ganda, NE
2015-132-N0	A Novel Reactor for the Continuous Manufacturing of Metal Oxide Particles	Gregory Krumdick, ES
2015-135-N0	Lab-Wide Research Analytics	Ian Foster, CELS
2015-136-N0	Nuclear Materials under Extreme Conditions	Mark Williamson, CSE
2015-139-N0	Implementing a New Extreme-Scale Parallel Programming Model with a Full Sample Application	Barry Smith, MCS
2015-141-N0	Using Hard X-rays to Accelerate the Synthesis of Materials	Peter Chupas, XSD
2015-144-N0	Framework for Integrating Multi-Modal Imaging of Materials for Energy Storage	Doga Gursoy, XSD
2015-145-N0	Understanding Embrittlement in Cast Austenitic Stainless Steels and Stainless Steel Welds	Yiren Chen, NE
2015-147-N0	Development of a Compact 352-MHz/150-kW CW Solid State RF Power Amplifier System for Accelerators	Alireza Nassiri, ASD
2015-149-N0	Integrated Imaging, Modeling, and Analysis of Ultrafast Energy Transport in Nanomaterials	Thomas Peterka, MCS

LDRD Projects Begun in FY 2015 (as of March 10, 2015) (cont.)

Project Number	Project Title	Lead Investigator, Division
2015-150-N0	Unraveling Mesoscale Spatial-Temporal Correlations in Materials Using Coherent X-ray Probes	Alec Sandy, XSD
2015-151-N0	Chemical Vapor Processing for Additive Manufacturing	Jeffrey Elam, ES
2015-152-N0	*In situ* Co-Analysis of Atomic and Electronic Structural Evolution for Materials Synthesis	Hawoong Hong, XSD
2015-153-N0	The VelociProbe: Ultra-High-Resolution Ptychographic Hard X-ray Nanoprobe	David Vine, XSD
2015-154-N0	Integrated Imaging to Understand and Advance Photocatalysis	Jeffrey Guest, NST
2015-157-N0	Sustainable Transportation: Novel Bio-Derived Fuel Additives for Improved Vehicle Efficiency	Samuel Goldsborough, ES
2015-159-N0	Large-Scale Modeling and Simulation for an Adaptive and Resilient Power Grid	Jianhui Wang, ES
2015-161-N0	Ion Beam Figuring with *in-situ* Metrology: Diffraction Limited X-ray Optics and Dynamic Aperture for Three-Dimensional Control of Thin-Film Deposition and Ion-Beam Erosion	Raymond Conley, XSD
2015-164-N0	Next-Generation Mossbauer Spectroscopy	Thomas Toellner, XSD
2015-167-N0	Coherent X-ray Studies of Materials Synthesis and Dynamics	Gregory Stephenson, MSD
2015-168-N0	The Computational Design of New Functional Materials from Complex Transition Metal Oxides	Hyowon Park, MSD
2015-169-N0	Agent-Based Behavioral Modeling of Ebola Spread in Chicago and Other Large Urban Areas	Charles Macal, GSS
2015-170-N0	Biomimetic Approaches for Water Smart Landscapes	Cristina Negri, ES
2015-172-N0	Determining Mechanical Properties of Material Systems Using Parameter-Free Metadynamics	Carolyn Phillips, MCS
2015-173-N0	Isotope Geochemistry via Sn Isotope Fractionation Using Inelastic X-ray Scattering of Synchrotron Radiation	Esen Alp, XSD

LDRD

Argonne Organizations – Abbreviations

ANNUAL REPORT

2014

Argonne Organizations — Abbreviations

ASD..... Accelerator Systems

BIO ..... Biosciences

CELS..... Computer, Environment, and Life Sciences

CSE ..... Chemical Sciences and Engineering

ES ..... Energy Systems

GSS..... Global Security Sciences

HEP..... High Energy Phsyics

MCS..... Mathematics and Computer Science

MSD ..... Materials Science

NE..... Nuclear Engineering

NST..... Nanoscience and Technology

XSD..... X-ray Sciences

U.S. DEPARTMENT OF
ENERGY

Argonne National Laboratory is a U.S. Department of Energy laboratory managed by UChicago Argonne, LLC